



**HAL**  
open science

## **Effect of grape seed extracts and procyanidin B2 on human granulosa cells: cell proliferation and apoptosis, steroidogenesis, oxidative stress and cell signaling**

Alix Barbe, Romain Bazilie, Namya Mellouk, Jérémy Grandhayé, Christelle Ramé, Pascal Froment, Joëlle Dupont

### ► To cite this version:

Alix Barbe, Romain Bazilie, Namya Mellouk, Jérémy Grandhayé, Christelle Ramé, et al.. Effect of grape seed extracts and procyanidin B2 on human granulosa cells: cell proliferation and apoptosis, steroidogenesis, oxidative stress and cell signaling. 51. Annual Meeting of the Society for the Study of Reproduction (SSR), Jul 2018, Nouvelle-Orleans, United States. , 2018, Pathways to Discovery: Signals for Reproduction, Development, & Longevity. hal-02733517

**HAL Id: hal-02733517**

**<https://hal.inrae.fr/hal-02733517>**

Submitted on 2 Jun 2020

**HAL** is a multi-disciplinary open access archive for the deposit and dissemination of scientific research documents, whether they are published or not. The documents may come from teaching and research institutions in France or abroad, or from public or private research centers.

L'archive ouverte pluridisciplinaire **HAL**, est destinée au dépôt et à la diffusion de documents scientifiques de niveau recherche, publiés ou non, émanant des établissements d'enseignement et de recherche français ou étrangers, des laboratoires publics ou privés.



SOCIETY FOR THE STUDY OF REPRODUCTION

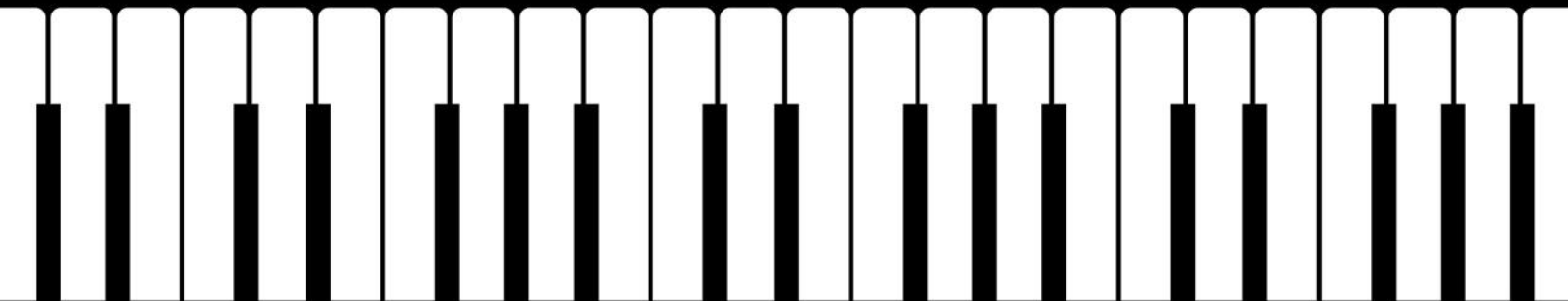
Pathways to Discovery:  
*Signals for Reproduction,  
Development & Longevity*

2018 SSR 51<sup>st</sup> Annual Meeting

Abstracts



Exhibit, Sponsorship, and Support Opportunities



Hilton New Orleans Riverside | New Orleans, Louisiana

## TABLE OF CONTENTS

Invited Speaker Abstracts .....	1-13
Oral and Poster Abstracts.....	14-443

\*\* Abstracts are searchable by author, title and keyword by pressing Ctrl F on your keyboard\*\*

## FOCUS SESSION - INVITED SPEAKER ABSTRACTS

### **The Hippo/YAP Signaling Pathway in Ovarian Granulosa Cell Proliferation, Differentiation and Malignant Transformation.** Cheng Wang, Massachusetts General Hospital

Ovarian granulosa cells are essential for production of fertilizable ovum and secretion of sex hormones. Dysregulation of granulosa cell proliferation, differentiation, or viability can result in subfertility, infertility, or even ovarian malignancy. Despite the rapid progress in our understanding of ovarian follicular development in the last decades, the exact molecular mechanisms underlying the regulation of granulosa cell function are not fully understood. Our recent studies demonstrate that the Hippo/YAP1 pathway, which has been reported to control organ size in many different species, plays a critical role in regulating granulosa cell physiology and pathology. We found that expression of YAP1, the major effector of the Hippo signaling pathway, was tightly associated with granulosa cell proliferation and differentiation. The active form of YAP1 (nuclear YAP1) was highly expressed in proliferative granulosa cells, whereas the inactive form of YAP1 (cytoplasmic YAP1) was detected mainly in terminally-differentiated luteal cells. Knockdown of YAP1 expression or pharmacological inhibition of YAP1 activity in human granulosa cells suppressed cell proliferation and reduced cell survival, suggesting that YAP1 is essential for the proliferation and survival of human granulosa cells. Consistently, injection of verteporfin (a selective antagonist of YAP1) into female CD1 mice inhibited granulosa cell growth, induced granulosa cell apoptosis, and disrupted follicle development, leading to severe subfertility. Similarly, granulosa cell-specific knockout of yap1 resulted in granulosa cell death and follicle atresia, leading to impaired fertility. Ectopic expression of wild-type or constitutively active YAP1 in differentiated human granulosa cells induced dedifferentiation and reprogramming of these cells. Constitutive activation of YAP1 in less-differentiated human granulosa cells resulted in transdifferentiation and malignant transformation of granulosa cells, leading to development of mesenchymal type of ovarian cancer with serous features. In summary, our studies demonstrate that homeostatic YAP1 expression and activation are essential for ovarian granulosa cell proliferation, differentiation and survival. The Hippo/YAP pathway plays pivotal roles in granulosa cell physiology and pathology.

### **Androgens, AR and Theca Cell Function and Dysfunction.** Joanne Richards, Baylor College of Medicine

Ovarian theca cells are essential for normal follicular development and fertility but also contribute to ovarian dysfunction in polycystic ovary syndrome (PCOS), ovarian hyperthecosis and premature ovarian failure (POF)(1). Theca cells are critical, in part, for providing 1) a protective shield around the granulosa cells and oocyte and 2) nutrients, growth regulatory factors and steroid hormones, principally androgens, for granulosa cell survival, growth or differentiation. Theca androgen production is promoted by pituitary LH as well as by insulin, IGF1 and INSL3 that regulate the expression and activity of steroidogenic enzymes, including CYP11A1 and CYP17A1. Theca androgen production is tightly modulated by paracrine factors produced primarily by granulosa cells. These include bone morphogenic proteins (BMPs), activin and estradiol. Women with PCOS are characterized, in part, by ovarian hyperandrogenism. Theca endocrine functions in PCOS women are intrinsically altered leading to elevated expression and activity of CYP17A1, increased production of ovarian-derived androgens and anovulation.

The role of androgens and the androgen receptor (AR, NR3C4) in ovarian follicular development has primarily focused on how they impact granulosa cell functions, whereas the potential impact of androgens and the role of AR on theca and stromal/interstitial cells have been largely overlooked. The oversight is especially evident at the molecular level, despite the fact that mouse and human theca cells express AR, the modulator of AR action co-repressor COUPTF-II/NR2F2 and that NR2F2 is present as a marker of presumptive theca progenitor cells in the XX embryonic gonad at E12.5. A recent theca cell specific androgen receptor knockout (ThARKO) mouse model documents that loss of AR selectively in theca cells prevents excess androgens from promoting a PCOS-like phenotype in an androgen-treated mutant mouse model. This key observation clearly implicates not only elevated theca cell androgens but also theca cell AR and NR2F2 as potential culprits of changes in theca cell functions and changes in the theca/stromal compartment of the ovary, possible contributing to PCOS phenotypes.

The studies conducted herein were undertaken to determine the molecular and cellular events that are altered in theca and stromal cells compared to granulosa cells in mice exposed to androgen excess. Based on previous mouse models of PCOS (24), we used a DHT-treated mouse model and show that this non-aromatizable androgen dramatically alters the gene expression profiles in theca/stromal tissue at 1 week and 2 months post-treatment. Most dramatic is the marked expansion of the theca/stromal ovarian compartment, the intense nuclear staining of AR in this compartment, the co-localization of AR and NR2F2 in theca/stromal cell nuclei and the remarkable induction of vascular cell adhesion molecule 1 (VCAM1) expression in the theca/stromal cells, a known marker of adult Leydig cells. Thus, theca cells exhibit remarkable plasticity in response to elevated androgens.

**The Heat, Steroids, and Protons are Regulators of Sperm Motility.** Polina Lishko, University of California, Berkeley

Ion channels control sperm motility by regulating intracellular ion homeostasis, membrane voltage and help sperm navigate in the female reproductive tract. While intracellular calcium stimulates sperm hyperactivation, intracellular protons inhibit it. Steroid hormone progesterone produced by ovulated egg/cumulus mass promotes calcium influx through sperm ion channel CatSper- an event so central for fertilization that men lacking these channels are infertile. The molecular identities of a proton (Hv1), potassium (Slo1/Slo3) and calcium (CatSper) channels have been described in human sperm. However, the molecular identity of sodium conductance that mediates initial membrane depolarization and, thus, triggers downstream signaling events has yet to be defined. Here, we functionally characterize DSper, the Depolarizing channel of Sperm that bears a hallmark of the temperature-activated channel TRPV4. It is functionally expressed at both mRNA and protein levels, while other temperature-sensitive TRPV channels are not functional in human sperm. DSper currents are activated by warm temperatures and mediate cation conductance, that shares a pharmacological profile reminiscent of TRPV4. Together, these results suggest that TRPV4 activation triggers initial membrane depolarization, facilitating both CatSper and Hv1 gating and, consequently, sperm hyperactivation.

**The Many Faces of a Sperm-Specific Ca<sup>2+</sup> Channel.** Timo Strünker, University of Munster, Germany

CatSper represents the principal Ca<sup>2+</sup> channel in the sperm flagellum of many species. Human CatSper is controlled by voltage and pHi, but also by various ligands of the oviductal fluid that serve as chemical signpost for sperm to spot the egg. We studied the ligand-control of human CatSper and the role of the channel for human sperm navigation.

**Hypothalamic and Pituitary Control of Reproduction.** Lori Raetzman, University of Illinois, Urbana

Endocrine disrupting chemicals (EDCs) are prevalent in the environment and can impair reproductive success by affecting the hypothalamic-pituitary-gonadal (HPG) axis. Critical windows of development are often more sensitive to endocrine disruption and have the ability to induce lasting effects. We have been exploring the impacts of exposure to estrogenic EDCs, such as bisphenol A (BPA), during two critical windows of pituitary development in rodents: embryonic and neonatal. We hypothesized that the changing hormonal milieu of animal as the HPG axis begins to function would alter sensitivity to EDC exposure and the effects may be sex specific as the gonadotrope cells have gene expression differences between males and females after birth. During embryonic development, exposure to environmentally relevant levels of BPA stimulated pituitary proliferation, increased gonadotrope number and affected Lhb and Fshb mRNA levels in a dose-dependent manner, but only in females. In the postnatal pituitary, exposure to BPA or to 17 $\beta$ -estradiol (E2) from postnatal day (PND)0-PND7 did not alter proliferation or gonadotrope number. However, mRNA expression of gonadotrope restricted Lhb, Fshb or Icam5 mRNAs could be suppressed by E2 in vivo and regulated in a sex-specific manner in vitro. BPA at the oral reference dose of 50mg/kg/day suppressed Icam5 in vivo, but did not affect Lhb or Fshb mRNA expression. No effect on expression of these selected gonadotrope genes was observed with 0.05, 0.5, and 50 $\mu$ g/kg/day BPA exposure in vivo. Taken together, these data show that the developing pituitary can be sensitive to BPA exposure in a sex specific manner, depending on the time of exposure. Because of this, it is critical to include pituitary analysis as part of understanding the impact of developmental exposures to BPA on fertility.

**TGF $\beta$  Superfamily Regulation of FSH Synthesis in Mice: Revisiting and Redefining Roles for Activins and Inhibins.** Daniel Bernard, McGill University, Montreal, Canada

Follicle-stimulating hormone (FSH) is produced by gonadotrope cells of the anterior pituitary gland. Following secretion into systemic circulation, FSH binds to its receptor on the plasma membrane of ovarian granulosa cells and testicular Sertoli cells. In females, FSH is essential for the later stages of follicle development and for estradiol production. In males, FSH regulates Sertoli cell number during development and thereby affects spermatogenesis in adulthood. FSH synthesis and secretion are regulated by gonadotropin-releasing hormone from the hypothalamus and by members of the transforming growth factor  $\beta$  (TGF $\beta$ ) superfamily, the activins and inhibins. According to current dogma, activin B is produced by gonadotrope cells and acts in autocrine/paracrine fashion to stimulate transcription of the FSH $\beta$  subunit gene. In contrast, the inhibins are produced in the gonads and act in an endocrine manner to suppress FSH. Specifically, inhibins are thought to act as competitive receptor antagonists, binding to activin type II receptors and hindering activin B action. High affinity inhibin action

is argued to rely on a co-receptor, betaglycan (product of the *Tgfr3* gene). In this lecture, we will provide definitive genetic evidence that activin B does not regulate FSH synthesis in mice. Moreover, we will show that betaglycan functions as a co-receptor for inhibin A, but not inhibin B. These results necessitate the re-writing of current models of TGF $\beta$  superfamily regulation of FSH synthesis.

**The Influence of Maternal Environment on Uterine Natural Killer Cell Function and Placental Development.** Alexander Beristain, University of British Columbia, Vancouver, Canada

In early pregnancy, establishment of the functional layer of the uterus and the early stages of placental development are regulated in part by diverse subsets of uterine immune cells. In particular, a subtype of innate immune cell, called a uterine natural killer (uNK) cell, is thought to play important roles in promoting uterine angiogenesis, blood vessel remodeling, and immunotolerance towards fetal tissue, all while retaining the ability to maintain immunity against potential pathogens. Importantly, uNK cells are highly attuned to their environment, where local decidual factors help shape many of their unique properties. Aberrant conditions in pregnancy, associated with inflammation and/or infection, alter the functional state of uNK cells, promoting uNK cell activation and possibly cytotoxicity. However, the importance of uNK cells in promoting pregnancy health or in contributing to pregnancy disorders is poorly understood. Our work examines the effect of maternal obesity, a condition affecting ~15% of all pregnancies in North America that links with chronic low-grade inflammation and poor pregnancy outcome, on uNK cell biology. We show that maternal obesity in women associates with changes in uNK cell proportions within the maternal-fetal-interface. These cellular changes correlate with impaired uterine artery remodeling. Importantly, maternal obesity associates with a heightened state of uNK activity, defined by altered natural killer receptor expression, and increased rates of degranulation and pro-inflammatory cytokine production. Using a mouse model of maternal obesity, we show that many of these obesogenic effects are conserved, indicating that uterine immunological pathways in early pregnancy are similarly altered in humans and mice. Together, this work addresses how pre-existing obesity affects uNK cell-related processes in early pregnancy. Importantly, this work sheds light into how chronic conditions in pregnancy that associate with poorer outcomes, shape the uterine immune cell environment.

**Mapping the Human Immune Response to Pregnancy, One Cell at a Time.** Brice Gaudilliere, Stanford University

The maintenance of pregnancy relies on a finely tuned immune balance between tolerance to the fetal allograft and protective mechanisms against invading pathogens. Using high-dimensional mass cytometry (CyTOF), we have identified communities of immunological events in maternal blood that precisely time gestation in a term pregnancy and characterized an “immune clock” of pregnancy. Here, we combined the mass cytometry analysis of peripheral immune cell subsets with the high content analysis of circulating plasma factors to identify maternal immunological events that predict the onset labor. A novel cell-signaling Elastic Net (csEN) algorithm was applied to derive an integrated cytomic and proteomic model that accurately predicted the time from sample collection to onset of labor ( $R = 0.91$ , cross-validated  $p = 7.07 \times 10^{-21}$ ). These results provide an analytical framework for future prospective studies identifying immunological events associated with the pathological onset of labor such as in preterm pregnancies.

**The Emerging Role of Progesterone Receptor Membrane Component 1 in Bovine Oogenesis and Early Embryogenesis.** Valentina Lodde, University of Milan, Italy

Improvement of the efficiency of in vitro embryo production in livestock largely depends on the knowledge of basic factors and mechanisms controlling oocytes and early embryos quality. In particular, a deeper knowledge on the function of key players in the process of meiotic and mitotic cell divisions is pivotal to finely modulate in vitro culture systems to recapitulate early stages of mammalian development. In this view, the understanding of Progesterone Receptor Membrane Component 1 (PGRMC1) function in gametes, embryos and ovarian somatic cells have major implications in the field of reproductive sciences, since PGRMC1 is highly expressed in these cells. This protein was initially identified in liver as a progesterone binding protein, which accounts for its name. However, PGRMC1 is expressed in many cell types and has progesterone dependent and independent actions depending in part on its cellular location. In the maturing bovine oocytes PGRMC1 changes its localization dynamically: it associates with the chromosomes at metaphase I and II, while it concentrates between the separating chromosomes during polar body emission. Strikingly, PGRMC1 localization in the maturing oocytes mirrors its localization in ovarian cells undergoing mitosis, particularly at the spindle midzone, suggesting a possible common function in both mitotic and meiotic cell division. Here, we summarize the studies intended to explain the mechanism(s) by which PGRMC1 mediates oocyte and somatic cell division in cattle. By combining the use of immuno-fluorescence microscopy, time lapse fluorescence imaging, flowcytometry, in situ ligation proximity ligation assay, RNA interfering mediated-gene silencing and pharmacological inhibition, we demonstrated that PGRMC1 has a key role during karyokinesis and cytokinesis in both cell types. Finally, recent studies suggesting a possible role of PGRMC1 during early embryo development will be presented.

**SRB-SSR Exchange Lecture: The Effects of Maternal Age and Ovarian Stimulation on Mitochondria and the Follicular environment in Cloned Cattle.** Mark Green, University of Melbourne, Australia

Decreased fertility is a consequence of maternal aging in humans and domestic species. Studies of older females identify numerous responsible factors, including decreased ovarian reserve, altered hormone secretion patterns, diminished ability of oocytes to support early embryo development, and a sub-optimal uterine environment. Coincidentally, there is an established trend for women to reproduce later in life, with the fastest growing proportion of first-time mothers being women over 40 years of age. Ovarian stimulation has become the method of choice to combat reduced fertility, to overcome reproductive diseases and disorders, or to simply improve reproductive outcomes especially associated with increased maternal age. Despite ovarian stimulation regimens being employed, responses and success rates are variable, as increasing maternal age and ovarian stimulation regimens result in a sub-optimal follicular environment, which can comprise oocyte viability and thus the successful establishment of a pregnancy. Determining the relative influence or interdependence of maternal age and stimulation regimens, as well as the underlying cause of infertility, is complicated however, especially in humans. To date, individual studies have focussed on either the genetic contribution, follicular hormone or metabolite concentrations, or cumulus or oocyte gene expression but not all these factors collectively within the same cohort. Equally, no study has investigated mitochondrial DNA (mtDNA) heteroplasmy in individual oocytes that may explain metabolic dysfunction, and little is known about whether the oocyte alters mtDNA copy numbers, mutations and deletions, following ageing or

ovarian stimulation. To gain a more comprehensive understanding of these interactions, we examined the effects of maternal age and ovarian stimulation regimens on all the aforementioned follicular characteristics using a novel bovine model. Our females had the same genetic background but at two different ages; equivalent to women in their mid-twenties or in their late-thirties. All females were subjected to repeated rounds of varying severities of ovarian stimulation regimens and samples collected for analyses. We have utilized these data to establish diagnostic oocyte quality markers and to postulate potential new approaches that may avoid negative effects on the follicular environment and improve upon the current ovarian stimulation methods. Ultimately, use of this knowledge may therefore provide approaches to optimize the fertility and success rates of older females. These studies were supported by grants from Fertility Associates Ltd, The Pearce Trust, Nuture Foundation NZ, Auckland Medical Research Foundation, The Fertility Society of Australia, and AgResearch Ltd New Zealand.

**Of Cows and Humans: Mir-96 Promotes Luteal Cell Survival and Progesterone Production.** Xavier Donadeau, University of Edinburgh, UK

MiRNAs play central roles in post-transcriptional regulation of cell differentiation processes across body tissues, however information on the involvement of miRNAs in corpus luteum development is still limited. A detailed understanding of the mechanisms regulating luteal development is critical as luteal insufficiency has been associated with pregnancy loss in different species. Information is particularly limited in humans due to the reduced availability of healthy ovarian tissues for study. In that regard, monovular species such as cattle can provide extremely valuable insight, particularly compared to common rodent models with much more distinct ovarian physiology. Our studies have been aimed at characterizing the changes in miRNA expression associated with the follicular-luteal transition in the monovular ovary in order to identify key miRNA species involved in this process. Through transcriptome analyses of bovine tissues we found that two miRNA clusters, miR-183-96-182 and miR-212-132, are dramatically upregulated in the early corpus luteum relative to the mature, ovulatory-size follicle. Loss-of-function analyses showed that miR-96 promotes cell survival in both bovine luteal cells and human luteinized granulosa cells (hLGCs), as well as promoting progesterone but not estradiol production in cultures of hLGCs. In contrast, miR-132 has relatively limited effects on either bovine or human cells. Moreover, we identified that miR-96 targeting of FOXO1 mediates the effects on luteal cell survival and steroidogenesis. I will present these and other data demonstrating the value of using the bovine model for identifying candidate mechanisms involved in functional regulation of the corpus luteum in monovular species.

**Thrombospondin-1 at the Crossroads of Corpus Luteum Fate Decisions.** Rina Meidan, The Hebrew University of Jerusalem, Israel

Thrombospondin-1 (THBS1) affects corpus luteum (CL) regression. It is induced by PGF2 $\alpha$  in a luteal-stage specific manner and acts as a natural anti-angiogenic, pro-apoptotic compound. THBS1 is a large multi-modular matrix protein, exerting its biological activities through diverse mechanisms. Within the THBS family, THBS1 and THBS2 are closely related in terms of their domain organization and degree of sequence identity. THBSs are expressed in both luteal steroidogenic and endothelial cells, and like in vivo, they are significantly stimulated by PGF2 $\alpha$  in these cell types, in vitro. On the other hand,

luteinization by LH and insulin decreased the expression of THBS1 and THBS2, together with their CD36 receptor. In vivo, FGF2 and THBSs exhibit the most divergent profile of induction by PGF2 $\alpha$ , FGF2 dominated the early luteal phase while THBS1, CL regression, suggesting that they are inversely regulated. Our studies demonstrated that these two factors are indeed antagonistic functionally and transcriptionally. THBS1 reduced luteal cell numbers and promoted apoptosis by activation of caspase-3. In contrast, FGF2 reduced basal and THBS1-induced caspase-3 levels. Consistent with these findings, siRNA silencing of THBS1 in luteal cells reduced the levels of active caspase-3 and improved the survival of cells when challenged with apoptotic compound staurosporine. Besides THBS1, TGFB1 and SERPINE1 were similarly induced in the regressing CL. Interestingly, these key PGF2 $\alpha$ -induced luteolytic genes were significantly downregulated by the pregnancy recognition signal, IFNT, suggesting that it may exert anti-luteolytic effects in bovine CL. Luteolytic gene products can act in concert to promote vascular instability, apoptosis, and matrix remodeling during luteal regression.

**Genetics of Meiotic Recombination and Fertility in Mouse and Human.** Jeremy Wang, University of Pennsylvania

Meiotic recombination enables the reciprocal exchange of genetic material between parental homologous chromosomes and ensures faithful chromosome segregation during meiosis in sexually reproducing organisms. This process relies on the complex interaction of DNA repair factors and many steps remain poorly understood in mammals. Meiotic defects can lead to sterility. Here I will present our studies of single stranded DNA (ssDNA)-binding proteins in meiotic recombination. Replication protein A (RPA) is an ssDNA-binding heterotrimeric protein complex of RPA1, RPA2, and RPA3. MEIOB is a meiosis-specific homologue of RPA1. Like RPA1, MEIOB binds to ssDNA. In addition, we find that MEIOB forms a heterodimer with SPATA22, another meiosis-specific protein, through defined interacting domains. A high-throughput screening assay has been developed for identifying small molecule inhibitors of MEIOB-SPATA22 interaction for the purpose of male contraception. The MEIOB/SPATA22 heterodimer colocalizes and interacts with RPA. Despite the requirement of RPA for DNA replication and DNA damage repair, its physiological role in meiotic recombination remains mysterious. I will discuss our strategy to uncover the role of RPA1 in mammalian meiosis. A mutation in MEIOB has been identified in infertile men. We have generated knockin mice to validate human mutations and find differences between human and mouse phenotypes. Genetic studies of factors involved in meiotic recombination provide a mechanistic understanding of the critical meiotic recombination process, help to elucidate the etiology of infertility in humans, and identify protein targets for male contraception.

**Germline Exposure to our Chemical Landscape: Assessing Effects and Mechanisms of Function in *C. elegans*.** Monica Colaiacovo, Harvard Medical University

Failure to achieve accurate chromosome segregation during meiosis results in aneuploidy and can lead to infertility, stillbirths, miscarriages and birth defects such as Down syndrome. Although exposure to environmental chemicals, such as plasticizers and pesticides, has been linked to aneuploidy and infertility in mammals, the identification of mechanisms by which these exposures impact meiosis has proven challenging. Utilizing the nematode *C. elegans*, which is a genetically tractable system that shares a high degree of conservation of its genes and biological processes with humans, we successfully

completed a high-throughput screen to identify chemicals leading to aneuploidy. We screened 46 chemicals, including pesticides and phthalates that are highly prevalent in our environment, at concentrations ( $\leq 100$  mM) correlating well with mammalian reproductive endpoints. We identified several chemicals that led to increased chromosome nondisjunction and subsequent analysis of a subset of these revealed meiotic defects, providing further validation for use of this screening strategy to identify exposures impacting meiosis. Specifically, analysis of dibutyl phthalate (DBP), a likely endocrine disruptor and frequently used plasticizer, as well as the pesticides permethrin and 2-(thiocyanomethylthio) benzothiazole (TCMTB), revealed alterations in germline chromosome morphogenesis following a 24-hour exposure starting at the L4 stage, when the germline is fully formed, compared to vehicle alone (DMSO). This was not due to alterations in mitotic proliferation or meiotic progression, as indicated by normal SUN-1 phosphorylation. There were also no detectable defects in chromosome synapsis, as indicated by immunostaining for structural components of the synaptonemal complex. Instead, we observed a p53/CEP-1-dependent increase in germ cell apoptosis and increased phosphorylated CHK-1 signal at late pachytene, both indicative of the activation of a DNA damage checkpoint. We hypothesize that this is partly due to altered DNA double-strand break (DSB) formation and/or repair, as indicated by elevated levels of RAD-51 foci (a protein involved in strand invasion and exchange during DSB repair). We also observed chromosome fragments and evidence of chromatin bridges in oocytes at diakinesis following these chemical exposures, indicating that elevated germ cell apoptosis was not sufficient to remove all nuclei carrying unrepaired recombination intermediates. Live imaging of the first embryonic cell division revealed that these exposures result in defects in chromosome alignment at the metaphase plate, formation of chromatin bridges and spindle abnormalities. Quantitative RT-PCR analysis suggests that germline-specific altered expression of conserved DSB repair and histone methyltransferase genes may account for the germline defects observed following DBP exposure. Taken together, our studies in *C. elegans* are allowing for the rapid identification of chemicals resulting in aneuploidy and providing novel insights into the mechanisms by which these exposures affect meiosis.

**Placental Phenotype and Insulin-like Growth Factor-2 Signaling: Resource Allocation to Fetal Growth.** Amanda Sferruzzi-Perri, University of Cambridge, Cambridge, UK

During pregnancy, the fetus requires nutrients and oxygen supplied by the mother to grow and develop. However, the mother also requires sufficient resources to support the pregnancy and the subsequent lactation. Failure to appropriately regulate resource allocation between the mother and fetus can lead to complications during pregnancy with immediate and life-long consequences for maternal and offspring health. The placenta is central to the allocation of resources during pregnancy as it supplies all the nutrients and oxygen required for fetal growth and secretes hormones that facilitate maternal allocation of resources to the fetus. In this presentation I will describe to you our findings in the mouse, which highlight the importance of insulin-like growth factor (IGF)-2 in regulating materno-fetal resource allocation, via its control of placental development and function during physiological and environmentally-challenged pregnancies. By understanding the role of IGF2 in regulating the allocation of resources between the mother and fetus, the work presented hopes to provide novel insight into the aetiology of pregnancy complications and programming mechanisms.

**Gassing the Utero-placental Vasculature and Preeclampsia: An Emerging Role of H<sub>2</sub>S.** Dongbao Chen, University of California, Irvine

Once conceived, a woman's cardiovascular system undergoes dramatic structural and functional remodeling to accommodate the circulatory demands of the growing fetus, resulting in profound dilation of the uterine and placental circulations, exemplified by dramatic rises in uteroplacental blood flow (UBF) in late pregnant vs. nonpregnant state. UBF is rate-limiting for pregnancy health because: 1) it carries out the bi-directional maternal-fetal exchanges of gases (i.e., O<sub>2</sub> and CO<sub>2</sub>), provides the sole nutrient support for fetal and placental growth, and excludes placental and fetal wastes and 2) insufficient rise in UBF during pregnancy results in preeclampsia and intrauterine growth restriction (IUGR), not only raising the morbidity and mortality of both the fetus and the mother during pregnancy but also putting the mother and her neonate into significantly higher risk to cardiovascular and other metabolic diseases later in life. The hitherto study of uteroplacental dilation during pregnancy has been dominated by work on the role played by the gaseous vasodilator nitric oxide (NO). Enhanced uterine artery (UA) endothelium NO production has been identified as a leading mechanism for mediating pregnancy-associated and agonist (estrogens and VEGF, etc.) -stimulated UA dilation and maternal-fetal interface angiogenesis, two critical mechanisms for mediating rise in UBF; however, prolonged inhibition of NO only modestly decreases baseline UBF during the third trimester of ovine pregnancy and ~65% estrogen-induced acute rise in UBF, definitely demonstrating that mechanisms in addition to endothelium NO exist to regulate uterine hemodynamics. Endogenous hydrogen sulfide (H<sub>2</sub>S) is another gaseous vasodilator that is mainly produced by metabolizing L-cysteine via cystathionine β-synthase (CBS) and cystathionine γ-lyase (CSE). We have recently identified for the first time that: 1) pregnancy significantly augments UA H<sub>2</sub>S production in rats, ewes, and women, which is stimulated by exogenous and endogenous estrogens and VEGF via selectively upregulating endothelium and smooth muscle CBS but not CSE expression and 2) augmented UA H<sub>2</sub>S contributes to pregnancy-associated and agonist-stimulated uterine vasodilation. We report here that UA endothelium and smooth muscle CBS but not CSE protein is significantly reduced in a rat model of preeclampsia induced by reduced uterine perfusion pressure (RUPP). Inhibition of CBS/H<sub>2</sub>S decreased UBF in rats in vivo, whereas administration of H<sub>2</sub>S donor partially rescued preeclampsia-like symptoms (i.e., hypertension, proteinuria, and IUGR, etc.) in RUPP rats. Myometrial artery endothelium and smooth muscle CBS, but not CSE, protein expression is significantly downregulated in preeclamptic vs. normotensive women. We also have reported that human trophoblast-derived H<sub>2</sub>S stimulates placental artery endothelial cell angiogenesis in vitro. Thus, our findings allow us to conclude that endothelium and smooth muscle CBS/H<sub>2</sub>S is a new gaseous pathway critical for uterine and placental hemodynamic regulation and altering UA CBS-H<sub>2</sub>S pathway may offer new therapeutic means for clinical management of hypertension-related pregnancy complications like preeclampsia and IUGR in women (Supported by NIH RO1 70562 and RO1 HL134779).

**Immune Checkpoint Blockade: A Hopeful Revolution for Gynecologic Cancers.** Whitfield Growdon, Massachusetts General Hospital, Boston

The advent of immune checkpoint inhibitors has revolutionized oncology care in many solid tumors. These therapies constitute one of the great innovations that has not only prolonged life with cancer but has cured patients once thought to have no therapeutic options. This class of therapeutic antibody acts

to block interactions of key immune checkpoint proteins such that cytotoxic T-cells no longer tolerate the cancer cell, but recognize tumors as foreign and mount an anti-tumor response. Response to checkpoint inhibition has been linked to an increased tumor mutational burden that likely leads to more 'non-self' antigen and the expression of specific immune checkpoint proteins, such as PD-L1. Checkpoint inhibitors that antagonize the PD-L1/PD-1 interaction have become approved in numerous solid tumors and importantly, have attained a tissue agnostic approval for use in all tumors that harbor microsatellite instability (MSI) due to mismatch repair deficiency. Outside of MSI tumors, the role of these potent therapies has not been clearly elucidated in gynecologic cancers. This review will chronicle the success of checkpoint immune therapy, the biomarkers that have emerged, and examples current laboratory and clinical trial strategies propounded to best understand how these therapies can be utilized in ovarian, endometrial, cervical vaginal and vulvar cancers. Endometrial cancer will be highlighted as a tumor that innately harbors molecular attributes that have been associated with response to immune checkpoint inhibition. The experience with gynecologic malignancies highlights the emerging concept that combination approaches with other immune modulators, anti-angiogenic agents and DNA repair pathway inhibitors may be required to attain the durable responses and cure more women.

**Insights into Immune Dysfunction in Endometriosis.** Chandrakant Tayade, Queen's University, Kingston, Canada

Endometriosis is a chronic inflammatory, estrogen-dependent disease characterized by growth of endometrial tissue outside of the uterine cavity. Although the etiology of endometriosis remains largely unknown, the most widely accepted theory is that of retrograde menstruation, whereby endometrial tissue is refluxed into the fallopian tubes and peritoneal cavity during menstruation. This does not explain, however, why 76-90% of women experience retrograde menstruation, while only 6-10% develop endometriosis. Research in our laboratory has shown that endometriosis patients have immunological dysfunction, which facilitates endometriotic lesion growth within the peritoneal cavity and ultimately perpetuates disease symptoms. In this presentation, I will discuss the unique endometriotic lesion microenvironment and how interplay between adaptive and innate immune cells with stromal and epithelial compartments of endometriotic lesions are regulated by inflammatory pathways.

**Endocrine Disrupting Activity Associated with Chemicals Used in Hydraulic Fracturing for Natural Gas and Oil.** Susan Nagel, University of Missouri, Columbia

Unconventional oil and gas (UOG) extraction combines directional drilling with hydraulic fracturing "fracking" to release oil and natural gas from previously inaccessible reserves. Fracking involves the injection of millions of gallons of water, chemicals and sand under high pressure to fracture underground rock. Billions of gallons of wastewater containing fracking and naturally occurring chemicals are produced each year. We measured the endocrine disrupting potential of 23 UOG chemicals and found antagonism for one or more of the estrogen, androgen, glucocorticoid, thyroid hormone, and progesterone receptors for 23 chemicals. An equimass mixture of these chemicals showed less than additive activity for androgen and glucocorticoid receptors, additive activity for the progesterone and estrogen receptors and more than additive activity for the thyroid hormone receptor.

We assessed adult outcomes following developmental exposure via maternal drinking water to a mixture of these 23 UOG chemicals at four doses in two different exposure windows in C57Bl6 mice. We found overlapping and distinct outcomes in mice following a prenatal (gestation day 11 to 19) versus a combined prenatal and postnatal exposure window (gestation day 1 to postnatal day 21). Body weight was increased in male weanlings after prenatal exposure and decreased with combined prenatal and postnatal exposure, however body weight changes did not persist into adulthood. Male offspring with prenatal exposure had reduced caudal sperm counts at 30 and 300  $\mu\text{g}/\text{kg}$  mixture per day, increased testes weights at 3 and 3000  $\mu\text{g}/\text{kg}$  and altered serum testosterone concentrations at 300 and 3000  $\mu\text{g}/\text{kg}$ . On the contrary, male offspring with combined exposure had increased caudal sperm and decreased apoptosis at 150  $\mu\text{g}/\text{kg}$  per day, increased motility at 1.5, 15 and 150  $\mu\text{g}/\text{kg}$  per day, and decreased testes weight at 15  $\mu\text{g}/\text{kg}$  per day. In females, prenatal exposure to oil and gas operation chemicals suppressed pituitary hormone concentrations across experimental groups (prolactin, LH, FSH, and others), altered body, uterine, ovary, and heart weights, and folliculogenesis, and the combined pre and postnatal exposure altered body composition, energy expenditure and behavior. In a mouse follicle culture system, the 23-mix (7.5  $\mu\text{M}$ ) significantly inhibited follicle growth at 96 h compared to control (n=3 separate cultures). However, it did not significantly affect progesterone production by antral follicles. These and other ongoing studies are aimed at identifying the underlying mechanisms for these effects. Taken together, these data suggest that developmental exposure to UOG chemicals at potential environmentally relevant levels may have negative impacts on development, reproduction, behavior and metabolism.

## FOCUS SESSION - INVITED SPEAKER ABSTRACTS

**A Novel Atypical Centriole in Animal Spermatozoa Functions in the Zygote.** Tomer Avidor-Reiss, Emily L. Fishman, Kyoung Jo, Quynh P.H. Nguyen, Dong Kong, Rachel Royfman, Anthony R. Cekic, Sushil Khanal, Ann L. Miller, Calvin Simerly, Gerald Schatten, Jadranka Loncarek, and Vito Mennella

One of the last major unidentified pathways during fertilization in humans, other mammals, and insects is the precise way in which the centrosome (the cell's dominant microtubule-organizing center) of the zygote is inherited. In contrast to the biparental merging of the sperm and egg nuclei at the onset of reproduction, as well as the unimaternal inheritance of the egg mitochondria, the exact mode of centrosome inheritance is yet not understood. Without DNA as reliable fiduciary markers, accurate tracking of the centrosome had not been possible, since many of its proteins are transient residents.

We previously found that insect (flies and beetles) sperm centrioles have in additions to their typical centriole that form the sperm tail also an atypical centriole (the Proximal Centriole Like or PCL) that lacks microtubules but is essential for fertility. We, therefore, hypothesized that animal spermatozoa have a combination of typical and atypical centrioles that are necessary for zygote function.

Recently, we found that the sperm centrosome of human and other mammal is composed of a novel atypical centriole made of splayed microtubules (distal centriole, DC) surrounding bars of centriole luminal proteins, a typical barrel-shaped centriole (the proximal centriole, PC), and the surrounding specialized matrix (the pericentriolar material, PCM). The atypical centriole is formed during spermiogenesis by differential reduction and enrichment of specific types of centrosomal proteins. In vivo and in vitro investigations found that the atypical DC is capable of recruiting PCM, forming a centrosome that nucleates a microtubules aster, templating a new centriole, and localizing to the spindle pole during the first mitosis. This now enables, for the first time, tracing of proteins contributed by the human sperm during fertilization, which both solves a fundamental mystery and affords new strategies for infertility diagnostics and male contraceptive approaches.

**Ovine Sex-sorted Semen - Post Thaw Quality and Field Fertility.** C. Gonzalez-Marin, M. Stiaque, J. Hepburn, J. F. Moreno, and R. Vishwanath

Sexing Technologies has performed numerous experiments in the last few years with the objective of developing a commercial ovine sex-sorted semen product.

Laboratory evaluations were performed on semen from 2 rams. Each ejaculate was split in two aliquots and processed in one of two methods: Non-sorted (conventional) or Sex-sorted. Conventional (CONV) semen was processed at 60 million cells per straw at the Animal Breeding Services laboratory (ABS, New Zealand). Sex-sorted semen was processed using flow cytometry (Genesis™ sperm sorting systems) at a gender purity of 92% at the Sexing Technologies laboratory (New Zealand). After sorting, sperm was divided in four and processed as fresh semen at 1 million (Fresh1M) and 2 million cells per dose (Fresh2M), and as cryopreserved semen at 3 million cells per pellet (Cryo3M) and 6 million cells per straw (Cryo6M).

Percent visual sperm motilities were analyzed after final dilution (0 h) and after 24 h of incubation at 18°C for sex-sorted fresh semen. For cryopreserved semen, visual motilities were assessed after thawing

(0 h) and after 3 h incubation at 37°C. No differences ( $P < 0.05$ ) were found in percent total motile between Fresh1M and Fresh2M at 0 h ( $73.0 \pm 3.0\%$  vs  $73.0 \pm 3.0\%$ ) or after 24 h of incubation ( $71.0 \pm 3.5\%$  vs  $71.0 \pm 3.5\%$ ). Cryo3M sperm motilities were lower than those of fresh semen, but they were significantly higher than CONV at 0 h ( $68.5 \pm 4.9\%$  vs  $60.8 \pm 7.9$ ) and 3 h ( $63.0 \pm 2.8\%$  vs  $48.3 \pm 12.0\%$ ). Percent motile sperm was the lowest in Cryo6M at 0 h ( $49.5 \pm 5.7\%$ ) and 3 h after incubation ( $43.0 \pm 2.8\%$ ).

The fertility of each treatment was assessed after laparoscopic artificial insemination (LAI) of a total of 285 synchronized East Friesian ewes.  $57 \pm 4$  ewes were inseminated per treatment. No statistical differences ( $P < 0.05$ ) were found in the percentage of ewes lambing after insemination between sex-sorted and conventional semen. Numerically, pregnancy scores were higher for Cryo6M (56%) followed by Fresh2M (44%), CONV (42%), Fresh1M (36%) and Cryo3M (33%).

This study demonstrates that sex-sorted ram sperm are equally fertile to conventional. In fact, Cryo6M and Fresh2M presented numerically superior fertility when used in LAI than CONV sperm inseminated at higher concentrations. On the other hand, Cryo6M presented numerically higher conception rates than Cryo3M, this was also true for Fresh2M compared to Fresh1M, which could indicate a dose effect. The overall results are promising for the commercialization of the sex-preselection technology in sheep, and the fact that fresh or cryopreserved sex-sorted sperm, and cryopreserved sperm in straws or pellets presented no differences in fertility, would ensure flexibility and ease of use in the field once the product is commercialized. More field trials are needed to determine optimal synchronization protocols and minimum sperm per insemination when using sex-sorted sheep semen, which would allow continuous success in the field and a decrease in the cost per dose.

#### **Punicalagin is Beneficial for Spermatogenesis in Male New Zealand White Rabbits.** Mehmet Sukru Gulay, and Ozlem Yildiz Gulay

Taking into account that punicalagin (PUN) is a very powerful antioxidant; the current study evaluated the potential positive effects of oral PUN on spermatological parameters of male New Zealand White rabbits. A total of 24 male bucks was housed individually and trained for semen collection for 2 weeks before the experiment. After the training, rabbits were assigned into 4 groups and received daily gavages of 0, 1, 2, and 10 mg/kg PUN in tap water for 9 weeks. Doses were adjusted weekly according to the animals' weight. Libido was also evaluated during semen collection. Semen was collected once a week from each rabbit and samples at d 1 and 63 of the experiment were analyzed separately. The PROC GLM procedure and Dunnett post hoc analysis were used for statistical evaluations. At the end of the experiment, the rabbits were euthanized and weights of testes, epididymides and accessory sex glands as a whole was recorded. Initial values (ejaculate volume, ejaculate weight, ejaculate pH, sperm concentration, percent progressive motility, and seminal plasma protein levels) tested at d 1 were similar among the groups. There were also no differences in ejaculate volume, ejaculate weight, ejaculate pH and seminal plasma protein levels at the end of the experiment ( $P > 0.1$ ). Libido and weights of reproductive organs were not affected by the treatments ( $P > 0.1$ ). However, sperm concentrations ( $P < 0.01$ ) and percent progressive motility ( $P < 0.04$ ) were significantly improved, especially for bucks in 2 and 10 mg/kg PUN groups. Thus, the current study suggested that as low as 2 mg/kg PUN per day can be beneficial for spermatogenesis and motility in male rabbits. This project was supported by TÜBİTAK (project no: 116O027).

**Spatial and Temporal Resolution of ORC4 Fluorescent Variants Reveals Structural Requirements for Maintaining Higher Order Self-association and Pronuclei Entry.** Hieu Nguyen, Brandon Nguyen, Thien P Nguyen, W. Steven Ward, and Nicholas G. James

DNA licensing is an essential step in replicating DNA during cell division. The Origin Replication Complex (ORC), which is composed of six proteins ORC1-6, are responsible for initiating licensing at replication origins and recruits of adaptor molecules necessary to form the blank. Previously, we reported that ORC4 polar body extrusion (PBE) in addition to DNA licensing. Herein we utilized lifetime and fluctuation microscopy on two fluorescent constructs of ORC4, ORC4-eGFP and ORC4-FIAsH, to examine its spatial dynamics during oocyte activation. Our results demonstrated that expression of ORC4-eGFP failed to form large, cage like structures around chromosomes during anaphase II while the FIAsH labeled variant clearly showed higher order self-association. Interestingly, both variants were found in the pronuclei indicating no loss in DNA licensing function. Our results demonstrate that fusion of ORC4 C-termini to eGFP prevents higher order oligomerization needed for cage formation during PBE; thereby we described a possible ORC4 construct, namely ORC4 with a FIAsH sequence at site Cys-Cys-Pro-Gly-Cys-Cys, which allows for site-specific labeling and minimal background signal from nonspecific binding within live embryos. This work also represents the first step towards establishing a transgenic mouse model expressing endogenous levels of a trackable variant of ORC4.

**Expression Pattern of the Histone H3 Lysine 36 Methyltransferase, SETD2, in Porcine Oocytes and Embryos.** Dong Il Jin, Tao Lin, Yun Fei Diao, Xiaoxia Li, Reza K. Oqani, Jae Eun Lee, and So Yeon Kim

SETD2 is a histone H3 lysine 36 (H3K36)-specific methyl-transferase that may play important roles in active gene transcription in human cells. However, its expression and roles in porcine oocytes and preimplantation embryos are not well understood. In this study, we determined SETD2 expression in porcine oocytes and preimplantation embryos derived from in vitro fertilization (IVF), parthenogenetic activation (PA) and somatic cell nuclear transfer (SCNT) by immunofluorescence using specific antibodies and laser scanning confocal microscopy. The SETD2 signal was observed in non-surrounded nucleolus (NSN)-stage oocytes, but not in surrounded nucleolus (SN)-, metaphase I (MI)- or metaphase II (MII)-stage oocytes. The SETD2 signal was detectable in sperm, but it was lost after in vitro fertilization. Thereafter, it became detectable at the 2-cell stage of IVF embryos, peaked at the 4-cell stage, when porcine embryonic gene activation occurs, and remained to the blastocyst stage. Similar to the pattern found in IVF embryos, the SETD2 signal was not detected in 1-cell-stage PA embryos, but it was detected at the 2-cell stage and maintained to the blastocyst stage. Unlike IVF and PA embryos, SCNT embryos did not lose the SETD2 signal at the 1-cell stage, and the signal was detectable throughout embryonic development. Overall, these data indicate that SETD2 could be related to embryonic gene activation in porcine preimplantation embryos, and that aberrant SETD2 expression in 1-cell-stage porcine SCNT embryos may contribute to the reprogramming errors seen in these embryos and the low efficiency of somatic cell cloning.

**Spix Yellow-Toothed Cavy Embryos Have Potential to Produce Steroid Hormones at 7 Days of Gestation.** Franceliusa Delys de Oliveira, Paulo Ramos Silva Santos, Moacir Franco de Oliveira, and Antônio Chaves de Assis Neto

The objective was to determine steroidogenic capabilities of spix yellow-toothed cavy embryos (*G. spixii*) early in the embryonic period. Embryos were collected on Days 7, 8, 10, and 15 of gestation; some were fixed in 4% paraformaldehyde for morphological and immunohistochemical analysis (P450arom, P450c17, and P450scc), whereas others had RNA extracted to determine expression of genes encoding these enzymes. In addition, maternal ovaries, livers and adrenals were collected as control tissues (for immunochemistry) and to determine hormonal dynamics in the maternal unit during pregnancy. All three maternal tissues had positive staining for aromatase, whereas P450c17 and P450scc were only detected in maternal adrenal glands and liver, respectively, although none of the embryos stained for any of these three enzymes. Based on qPCR reactions, CYP11, CYP17, and CYP19 genes were expressed in all embryos (except the CYP11 gene was not detected at Day 8). Expression of these three genes was high at Day 7, lower on Days 8 and 10, and highest on Day 15. In conclusion, spix yellow-toothed cavy (*Galea spixii*) embryos expressed steroidogenic genes during the post-implantation period, indicating they have the potential to produce steroid hormones. This work was supported by grants from Sao Paulo Research Foundation/FAPESP (12/112178) and and by National Council of Scientific Researches (Process number 442631/20146).

**Social Transmission of Maternal Behavior by Oxytocin.** Ioana Carcea, Rumi Oyama, Joyce Mendoza, Naomi Lopez, Daniel Ramos, and Robert C. Froemke

In mammals, an important aspect of successful reproduction is represented by the quality of care for offspring during the post-natal period. In many species, including laboratory mice, this responsibility is shared with con-specifics, in a process called alloparenting. How is alloparenting acquired in mice? Our lab showed recently that inexperienced virgin female mice can start responding maternally to pup distress calls - by retrieving isolated pups to the nest - after being co-housed with an experienced dam (mother) and her pups for three to seven days. These behavioral responses result, in part, from enhancements in cortical representation of pup distress calls. To understand how the co-housing experience modulates activity in neural circuits to induce cortical plasticity and acquisition of maternal behavior, we built a system to continuously record synchronized behavioral and neuronal data throughout co-housing. With this system, we identified two spontaneous behaviors for the social transmission of maternal care in virgin mice. First, dams self-generate pup retrievals during co-housing with the virgin mouse. Virgins that are exposed to repeated episodes of dam retrievals can start retrieving themselves, even outside of the co-housing context. Second, dams chase the virgins into the nest where they would spend more time caring for pups. To understand how these spontaneous dam behaviors might contribute to plasticity in virgins, we recorded single-unit neuronal data from the paraventricular nucleus of the hypothalamus (PVN), which contains the majority of oxytocinergic neurons. Oxytocin, a peptide important for social bonding and for maternal care, can induce cortical synaptic plasticity. We find that interactions with a dam increase PVN firing and the potential release of oxytocin in virgin mice. This leads to suppression of inhibitory neurons in the auditory cortex, which consequently leads to increased responses and plasticity in excitatory neurons. Pharmacogenetic

suppression of oxytocin neuron activity during co-housing prevents the acquisition of pup care in virgins, indicating an essential role for oxytocin in enabling maternal behavior during the co-housing procedure.

**Prenatal Exposure to Di(2-ethylhexyl) Phthalate Causes Differential Gene Expression in the F3 Generation Ovaries of Mice.** Saniya Rattan, Emily Brehm, Liying Gao, CheMyong Ko, and Jodi A. Flaws

Di(2-ethylhexyl) phthalate (DEHP) is a plasticizer found in polyvinyl chloride products such as plastic food containers, medical equipment, and building materials. DEHP also is a ubiquitous environmental contaminant and a known endocrine disrupting chemical. Our laboratory has previously shown that prenatal DEHP exposure disrupts ovarian functions and female fertility in a transgenerational manner. However, little is known about the underlying mechanism by which prenatal exposure to DEHP impacts ovarian functions and fertility in female mice across three generations. Therefore, this study investigated the changes in gene expression in the ovary from female mice prenatally and ancestrally exposed to DEHP in the F1, F2, and F3 generations. Pregnant CD-1 mice (F0 generation) were orally dosed with corn oil (vehicle control) or DEHP (20 µg/kg/day) daily from gestation day 10.5 until birth (7-28 dams/treatment group). Pups born to these dams were considered the F1 generation. F1 females were mated with untreated males to obtain the F2 generation, and F2 females were mated with untreated males to produce the F3 generation. On postnatal day 21, female pups from the F3 generation were euthanized and ovaries were removed and frozen in liquid nitrogen. Total mRNA was extracted and subjected to next generation RNA sequencing (RNA-seq) to identify differentially expressed genes in the ovary. The Database of Annotation, Visualization, and Integrated Discovery Bioinformatics resource was utilized to functionally analyze the genes. These approaches led us to identify 104 genes that are upregulated and 73 genes that are downregulated by ancestral exposure to DEHP. Further, pathway analysis reveals that the PI3K-AKT, cyclins and cell cycle regulation, and extra-cellular matrix receptor interaction pathways are altered in the F3 ovaries. Functional annotation gene clustering analysis suggests that ancestral exposure to DEHP also causes differential expression of genes important for positive regulation of cell proliferation (21 genes), negative regulation of apoptotic processes and cell death (24 genes), cellular response to hormone stimulus (14 genes), and organ morphogenesis (17 genes). Collectively, these data indicate that ancestral DEHP exposure causes transgenerational changes in the expression of genes and pathways in the ovary that are important for ovarian functions and fertility. Further, these data provide an important foundation for identifying differentially expressed genes and their related pathways in the F3 generation of DEHP-exposed ovaries. Supported by NIH P01 ES022848, EPA RD-83459301, T32 ES007326, and the Billie A. Field Fellowship.

**Transient Inhibition Of P53 Homologs Protects Ovarian Function From Two Distinct Apoptotic Pathways Triggered by Anti-Cancer Therapies.** So-Youn Kim, Devi Nair, Megan Romero, Vanida A. Serna, Anthony J. Koleske, Teresa K. Woodruff, and Takeshi Kurita

Platinum-based chemotherapies can result in ovarian insufficiency by reducing the ovarian reserve, a reduction believed to result from oocyte apoptosis via activation/phosphorylation of TAp63 by kinases including ABL1 and CHEK2. Here we demonstrate that cisplatin (CDDP) induces oocyte apoptosis through a novel pathway and that temporary repression of this pathway fully preserves ovarian function in vivo. We establish ABL1 and ABL2 are dispensable for damage-induced apoptosis. Instead, CDDP

activates TAp63 through the ATR>CHEK1 pathway independent of TAp63 hyper-phosphorylation, whereas X-irradiation activates the ATM>CHEK2>TAp63-hyper-phosphorylation pathway. Furthermore, oocyte-specific deletion of Trp73 partially protects oocytes from CDDP but not from X-ray, highlighting the fundamental differences of two pathways. Nevertheless, co-treatment with a dual inhibitor for CHEK1/CHEK2 fully preserves fertility in female mice against CDDP as well as X-rays. Our current study establishes the molecular basis and feasibility of fertility-preserving adjuvant therapies against gonadotoxic therapeutics in female.

### **PGE2 Up-regulates FGF2 via Novel Cyclic AMP-dependent Mechanism in Bovine Granulosa Cells.**

Ketan Shrestha and Rina Meidan

PGE2 is essential for ovulation and reproductive success. During the periovulatory period, the profiles of PGE2 and fibroblast growth factor-2 (FGF2) coincide; moreover, both compounds are synthesized by granulosa cells (GCs) in response to LH. Thus, we examined here whether PGE2 could directly stimulate FGF2 production in GCs and if so, to determine its mode of action. Epregeulin (EREG), a known PGE2 target in GCs was studied alongside with FGF2 to better understand the signaling pathways triggered by PGE2. PGE2 rapidly induced FGF2 and EREG by 3h, with upregulation gradually subsiding until 24h. Suppressing endogenous PGE2 levels by PTGS2-silencing, reduced FGF2 mRNA and protein levels, further verifying that endogenous PGE2 is necessary for FGF2 production in GCs. We also observed that PGE2 elevated GCs' numbers; this effect was significantly abolished in the presence of FGF receptor1 inhibitor (PD173074), demonstrating that FGF2 mediated PGE2 action on GCs' proliferation. Next we investigated which of the PGE2 receptors (PTGERs) reproduce PGE2 actions on FGF2 and EREG. Using the four PTGERs agonists, only PTGER2 agonist (butaprost) mimicked PGE2 effects, up-regulating FGF2 and EREG. PGE2 and butaprost incubated for 30-60 minutes, increased cAMP levels in GCs' culture media, confirming PTGER2-dependent activation of Gas protein. Exploring cAMP-dependent downstream signaling pathway, we found that PKA-inhibitor (H-89) reduced EREG stimulated by either PGE2, butaprost or forskolin (adenylyl cyclase activator), however FGF2 remained unaffected. Therefore, we examined the involvement of another cAMP effector which is independent of PKA, i.e. EPAC (exchange protein directly activated by cAMP). The two isoforms; EPAC1 and EPAC2 were identified in GCs. EPAC-activator (8pCPT-AM) dose-dependently induced FGF2 and EREG, while EPAC inhibition by ESI09 (inhibiting both EPACs) reduced butaprost or 8pCPT-AM induction of both genes. The functional importance of the two EPAC isoforms was further examined using specific siRNAs. These siRNAs significantly knockdown their respective EPAC form. In EPAC1- and EPAC2-silenced GCs, levels of forskolin-induced FGF2 and EREG were significantly decreased, in agreement with effects observed using ESI09. There was a stronger inhibitory effect on these two genes with EPAC1 silencing than that of EPAC2. Importantly, FGF2 was more strongly inhibited as compared to EREG 48 and 72h post-transfection. In agreement with experimental data, Genomatix-MatInspector identified more CREB binding sites in EREG's promoter than in FGF2's (7 vs. 3) and higher number of Ras responsive element binding-1 (implicated in EPAC actions) in FGF2 than EREG (5 vs. 2).

This study shows a novel action of PGE2 acting via PTGER2 in GCs, i.e. stimulation of FGF2. It unraveled PTGER2-cAMP signaling pathways in these cells, demonstrating that FGF2 induction utilizes EPACs and is PKA-independent while EREG activation employs primarily PKA pathway and, to a lesser extent, EPACs.

PGE2-elevated FGF2 can act on GCs to promote cell survival and on endothelial cells to enhance their proliferation during angiogenesis.

**Interferon-tau Facilitates Anti-apoptotic and Proangiogenic Actions in Bovine Luteinized Granulosa Cells.** Raghavendra Basavaraja, Senasige Thilina Madusanka, Svetlana Farberov, Milo Wiltbank, and Rina Meidan

Interferon-tau (IFNT), a member of cytokine family, serves as maternal recognition of pregnancy signal in ruminant species. During early pregnancy, there is expression of IFNT stimulated genes (ISGs) in peripheral tissues including the corpus luteum (CL) indicating that, in addition to local uterine actions, IFNT also has endocrine effects. Furthermore, endocrine delivery of IFNT in ewes, was previously found to protect the CL from PGF2 $\alpha$ -induced luteolysis and stimulated cell survival genes. We have reported that IFNT treatment enhanced bovine luteal endothelial cells (LECs) survival and reduced luteolytic genes. Here we examined whether IFNT also directly affects large luteal cells, a major contributor to progesterone output from the CL. To that end, granulosa cells isolated from healthy large bovine follicles were luteinized using 2  $\mu$ g/ml insulin and 10  $\mu$ M forskolin. Luteinized granulosa cells (LGCs) provide an in-vitro model for large luteal cells. Recombinant ovine IFNT (roIFNT) stimulated ISGs (MX2, ISG15 and OAS1) and interferon associated genes (STAT1 and IRF9). Silencing of IRF9 markedly reduced 50% of ISGs mRNA levels induced by IFNT. We also observed a rapid and transient induction of STAT1 phosphorylation as well as total STAT1 protein (4.5 fold;  $p < 0.025$ ) at 36h; demonstrating direct roIFNT-dependent responses in LGCs. IFNT (1ng/ml for 24h) significantly elevated angiogenesis-related genes such as platelet derived growth factor B (PDGFB; 7.3 fold), its alpha receptor (PDGFAR; 1.4 fold) and matrix metalloproteinase 9 (MMP9; 1.4 fold) in LGCs. Importantly, IFNT also significantly and dose-dependently upregulated the mRNA and protein of basic fibroblast growth factor (FGF2). FGF2 is a major luteal angiogenic factor and was also shown to promote LGCs survival. Indeed, we found that FGF2 increased viable number of LGCs after 48h of incubation. IFNT had similar effects, however while FGFR1 inhibitor (PD173074), significantly abolished FGF2 actions, it only partially inhibited IFNT induced LGCs survival. In addition to the elevation in pro-angiogenic genes, IFNT markedly and significantly reduced thrombospondin-2 (THBS2; 7.2 fold). THBS2 and THBS1 are potent apoptotic factors elevated in the CL during PGF2 $\alpha$ -induced regression. It was interesting to note that IFNT abolished the pro-apoptotic actions of THBS1 (on cell viability and cleaved caspase-3). The anti-apoptotic actions of IFNT were further demonstrated in the upregulation of survival proteins such as X-linked inhibitor of apoptosis protein (XIAP; 2 fold), myeloid cell leukemia 1 (MCL1) and inhibition of pro-apoptotic proteins such as poly [ADP-ribose] polymerase 1 (PARP1) and gamma H2A histone family, member X (gamma-H2AX). Cell apoptosis triggered by Fas ligand was also reduced (4 fold) by IFNT in LGCs. In conclusion, IFNT acts on bovine LGCs by stimulating ISGs via STAT1-IRF9 dependent pathway. Promoting factors such as MMP-9, PDGFB and FGF2, while inhibiting THBS2, IFNT acts to support angiogenic responses in the CL of early pregnancy. Findings reported here also portray IFNT is an important survival factor for LGCs, as previously shown for LECs. Together these effects may contribute to IFNT induced CL maintenance and function during early pregnancy.

**Hormonal Regulation of CLCA1 in the Macaque Cervix.** Jessenia L. Chavez, Corinne Wilcox, Emily Mishler, Addie Luo, and Ov D. Slayden

Our goal is to investigate new targets for contraception. Low-dose progestin-only contraceptives do not reliably block ovulation and are believed to act by thickening cervical mucus to prevent sperm passage. Mucus rheology is controlled by the dynamic interaction of mucins, mucin biochemical modifications, hydration, and salt concentrations (e.g. Na<sup>+</sup>, Ca<sup>2+</sup>), which are regulated by membrane ion channels such as the cystic fibrosis transmembrane regulator (CFTR). The calcium-activated chloride channel regulator (CLCA) family of genes encode membrane-associated and secreted proteins that increase mucus production by airway and intestinal epithelia. We hypothesized that CLCA1 should be hormonally regulated and correlate with periods of heightened cervical mucus secretion. To test this hypothesis we characterized the effect of estradiol (E2) and progesterone (P) on CLCA1 in the macaque. Adult female rhesus macaques (*Macaca mulatta*) were ovariectomized and treated sequentially with E2 and then E2 plus P to create 28-day artificial menstrual cycles. Reproductive tracts were collected on cycle day (D) 3 (E2 only for 3 days; n=4); D14 (proliferative; E2 only; n=5); D15 (E2 + 1 day of P; n=5); D17 (early secretory; E2 + 3 days of P; n=5); D21 (mid-secretory; E2 + 7 days of P; n=4) and D28 (late-secretory; E2 +14 days of P; n=5). Samples containing mid-cervix epithelium and lamina propria were archived for RNA isolation and immunohistochemistry (IHC). RNA was reverse transcribed and analyzed by real-time PCR with macaque-specific primers and probes (NCBI reference sequence: NM\_001032912.1). A subset of samples were also analyzed by Affymetrix GeneChip® Rhesus Macaque Genome Arrays, and analyzed with Transcriptome Analysis Console (Applied Biosystems). Transcript expression was statistically interrogated by one-way ANOVA. Paraffin-embedded sections (5µm) were stained by IHC with CLCA1-specific antibodies (Abcam ab180851). Results were correlated with previous *in vivo* assessments of mucus secretion. We report that CLCA1 was minimal at the end of the secretory phase immediately preceding menstruation and maximal after 14 days E2 treatment. Peak levels coincides with maximal mucus secretion in this species. CLCA1 expression decreased significantly.

**A Novel Atypical Sperm Centriole Functions in Human Fertilization.** Emily L. Fishman, Kyoung Jo, Quynh P.H. Nguyen, Dong Kong, Rachel Royfman, Anthony R. Cekic, Sushil Khanal, Ann L. Miller, Calvin Simerly, Gerald Schatten, Jadranka Loncarek, Vito Mennella, and Tomer Avidor-Reiss

During fertilization, the zygote inherits most of its organelles from the egg, but the sperm is responsible for delivering the one of the cell's most critical organelles – the centrosome. Typical centrosomes include a pair of centrioles that are responsible for orchestrating cell division and nucleating a cilium. Abnormal centriole number can lead to cancer, blindness, microcephaly, and other devastating diseases, so centriole number is highly regulated. A single centriole gives rise to exactly one daughter centriole during centriole duplication, thus ensuring that each cell, with two centrioles, duplicates and divides, to produce two daughter cells, each with exactly two centrioles. Because the centrosome duplication program is so highly regulated, it is surprising that the number and origin of centrioles in the zygote is unclear. The egg does not contain any centrioles, and it is thought that human sperm contains only one centriole. This creates a dogma in which the sperm contributes a single centriole, which somehow must supply the zygote with the correct number of centrioles in order to divide, and in order to provide all the future somatic cells of the child with two centrioles. Such an event, where the dividing zygote creates

four centrioles from one, contradicts the known centrosome duplication pathway, creating a fundamental mystery in biology.

A similar conundrum existed in insects until only recently when our lab discovered that the sperm of both *Drosophila* and *Tribolium* possess, in addition to the known centriole, an unknown, atypical centriole. This atypical centriole deviates from the typical, nine-fold symmetric microtubular structure, but possesses centriolar proteins, resides at the expected position for a sperm centriole, is inherited into the zygote upon fertilization, and is essential for early embryo development. These discoveries suggest that centriole number is conserved, while sperm centriole structure is more diverse.

These discoveries poised us to challenge the idea that human sperm has only one centriole. Using a range of techniques, including confocal microscopy, electron microscopy, super-resolution microscopy, *in vitro* assays, and *in vitro* fertilization, in humans and in bovine, we have determined that non-murine mammalian sperm contain, in addition to the known typical barrel shaped centriole (the proximal centriole, PC) and the surrounding specialized matrix (the pericentriolar material, PCM), an atypical centriole. This atypical centriole is made of rods of centriole luminal proteins surrounded by splayed microtubules (distal centriole, DC). The DC rods form during spermatogenesis through a series of protein reductions and enrichments, in a process we have termed centriole remodeling. The atypical DC is inherited into the zygote, recruits PCM, acts as a platform for the formation of a daughter centriole, and resides at the spindle pole during the zygote's first mitosis. This work shows, for the first time, a second, atypical, centriole, that functions in the zygote, in human sperm. This has major implications for the investigation of diagnostics and therapeutic strategies for male infertility and early embryo developmental defects.

**Lotus Root Stabilizes Radical Spoke Complex by Interacting with dRSPH3 During Sperm Elongation in *Drosophila*.** Ya Wang, Rui Xu, Yiwei Cheng, Haowei Cao, Xuejiang Guo, Mingxi Liu, Juan Huang, and Jiahao Sha

Cilia plays important roles in vital process. Disorder in ciliogenesis could cause many serious diseases, such as PCD, polycystic kidney disease, infertility, blindness and tumor. However, little is known about how its assemble is regulated. Flagella is a special type of cilia which could help cells move. Sperm, for example, could swim to the oviduct ampulla and bind oocyte with the help of flagella. Here we report a novel protein, Lotus root (Lr/CG10014), which is mainly localized in the sperm flagellum radical spoke, and also in the individualization complex (IC), and is essential for spermatogenesis in *Drosophila*. Loss of Lr results in no mature sperm in seminal vesicles, asynchronous IC, and "9+2" structure defects in flagella. We also found that Lr can interact with dRSPH3, a radial spoke protein, and maintain its stabilization during sperm elongation. Besides, Lr can recruit dRSPH3 from nuclear to cytoplasm in S2 cells. In both of these processes, the PKA superfamily domain of Lr is indispensable. dRSPH3 only localized in the sperm flagellum, however, its mutant showed similar phenotypes as Lr mutant, such as sterile, asynchronous IC and loss of central paired microtubules. Loss of function of another two radical spoke proteins, dRSPH1 and dRSPH9, cause same phenotypes as dRSPH3 mutant. They can interact directly with dRSPH3 and compete with Lr in recruiting dRSPH3 in S2 cells. We also detected the phosphorylation state of the Lr mutant testis by MS and found that the phosphorylation of many proteins is affected, and the affected proteins indicate that Polo might be a candidate kinase that cause the change. These data showed that Lr plays an important role in regulating the assemble of radical

spoke by recruiting and stabilizing dRSPH3 to microtubule A to form the “9+2” structure of axoneme. These studies reveal a new mechanism of ciliogenesis during spermiogenesis. This research was supported by the National Key R&D Program of China (2017YFA0103803).

**DPEP3/SPAG4/RSPH9 Complexes are Required for Remodeling of Nucleus in Post Meiotic Male Germ Cells.** Yunfei Zhu, Xiaodan Shi, Yiqiang Cui, Mingxi Liu, and Jiahao Sha

Spermatogenesis is an extremely complicated process in mammals. During the final stage, spermatids undergo a complex restructuring program in which the circular sperm nucleus extends to be a polar structure; DNA is tightly packed; lamin composition and structure are changed, and the nuclear pore complex is eliminated. Dynamical changes of structures between manchette and nucleus plays an extremely important role in the remodeling process of spermatid nucleus. Spag4 has been reported as a sperm-specific expression gene in sperm deformation process. However, the mechanism of manchette and nucleus anchor and the direct role of manchette in nucleus remodeling remains unknown. In this study, we explored the effects and mechanisms of Spag4 in spermatogenesis. With CRISPR/Cas9 technique, 2 domain mutation of Spag4 models were built. Abnormal deformation in the homozygous mouse spermatogenic lumen of the SPAG4 carboxy-terminal mutation (hereinafter referred to as SPAG4-ΔC) model was found. Co-immunoprecipitation showed that SPAG4 interacted with DPEP3 and RSPH9 in testis, but not SPAG4-ΔC. Immunostaining of sperm revealed the co-localization of DPEP3 and RSPH9 in manchette of spermatid. Moreover, DPEP3 can not be recruited to the opposite spermatid poles and RSPH9 attached to manchette instead of the opposite spermatid poles in SPAG4-ΔC mice. C terminal mutant of SPAG4 disturbed the localization of SPAG4 in the opposite spermatid poles, blocking the recruit of DPEP3, and blocking the anchor of RSPH9 to nucleus membrane, which caused abnormal remodeling of nucleus and the formation of “mushroom head” sperms.

**Long-Term Effects of Lactocrine Deficiency on the Global Porcine Endometrial Transcriptome and the Microrna-Mrna Interactome at Pregnancy Day 13.** Ashley F. George, Teh-Yuan Ho, Nripesh Prasad, Brittney N. Keel, Jeremy R. Miles, Jeffrey L. Vallet, Frank F. Bartol, and Carol A. Bagnell

Through lactocrine mechanisms, bioactive factors are transferred from mother to offspring as a specific consequence of nursing to support development. A large, long-term study in pigs showed that minimal colostrum consumption on the day of birth [postnatal day (PND) 0], reflected by low serum immunoglobulin immunocrit (iCrit) values, was associated with reduced live litter size when the lactocrine deficient piglets reached adulthood. Thus, reproductive performance of female pigs that do not receive sufficient colostrum from birth is permanently impaired. Whether neonatal lactocrine deficiency ultimately affects patterns of uterine endometrial gene expression as a mechanism for reduced litter size is unknown. Therefore, objectives were to identify effects of PND 0 lactocrine deficiency on the porcine endometrial mRNA and microRNA transcriptome during the peri-attachment period of pregnancy (pregnancy day 13). At birth, serum iCrit ratios were used to assign gilts into high ( $0.115 \pm 0.01$ ;  $n = 8$ ) or low ( $0.033 \pm 0.01$ ;  $n = 7$ ) iCrit groups. At puberty, following one normal estrous cycle, gilts were mated by artificial insemination. On pregnancy day 13, gilts were euthanized, pregnancy confirmed, and endometrium collected. Total endometrial RNA was extracted and used to create cDNA libraries. Libraries were barcoded individually and paired-end mRNAseq (25 million reads) and

microRNAseq (15 million reads) were performed using an Illumina HiSeq 2500. Raw reads were mapped to the Sscrofa 11.1 genome build and mature microRNAs were annotated with miRBase release 21. Differentially expressed mRNAs and microRNAs, based on fold change ( $\geq \pm 1.5$ ,  $P < 0.05$ ), were identified with respect to neonatal iCrit groups (high versus low iCrit). Expression of selected genes was validated using quantitative PCR. No differences in ovulation rate, uterine length, uterine wet weight, or embryo recovery were observed on pregnancy day 13 in high compared to low iCrit gilts. However, 1157 endometrial mRNAs were differentially expressed, including 562 genes that decreased and 595 genes that increased in expression in high versus low iCrit gilts. Included were genes involved in prostaglandin signaling, uterine receptivity and remodeling, conceptus attachment, immune response, and membrane transport. Bioinformatic analyses identified neonatally lactocrine-sensitive biological processes at pregnancy day 13 including immune response, extracellular matrix remodeling, and cell transport. Six differentially expressed endometrial microRNAs were identified, including miR-129a-3p, miR-7135-5p, miR-371-5p, miR-338, miR-365-5p, and miR-144. Their expression was increased in high versus low iCrit gilts. Integrated microRNA-mRNA analyses, conducted in silico, predicted that five of the six differentially expressed endometrial microRNAs were likely to target 62 of the 1157 differentially expressed mRNAs. Predicted microRNA-mRNA interactions were associated with biological processes similar to those observed for mRNAseq data alone, including those related to development and regulation of cellular functions, such as cell motility. Results indicate that lactocrine deficiency from birth has long-term consequences for endometrial function as reflected by changes in the endometrial transcriptome during early pregnancy. Effects of insufficient colostrum consumption on endometrial function may contribute to the previously observed reduced litter size in adulthood. [Support: USDA-NIFA 2013-67016-20523; NSF-EPS-158862. USDA is an equal opportunity provider and employer].

### **Ablation of Ggnbp2 Impairs Meiotic DNA Double Strand Break Repair During Spermatogenesis in Mice.**

Kaimin Guo, Yan He, Lingyun Liu, Zuowen Liang, Xian Li, Hongliang Wang, and Zhenmin Lei

Impairment of spermatogenesis is a common cause of male infertility which can occur at several stages, including at proliferation and differentiation of spermatogonia, at meiotic divisions of spermatocytes and at transformation of haploid spermatids. Gametogenetin binding protein 2 (GGNBP2) is a highly conserved zinc finger protein expressing abundantly in spermatocytes and spermatids in human and mouse testes. We previously discovered that Ggnbp2 resection caused dramatic structural defects during spermatid metamorphosis and resulted in a complete absence of mature spermatozoa in mice. However, whether GGNBP2 affects meiotic progression of spermatocytes during spermatogenesis remains to be established. In this study, flow cytometric analyses showed that a significant decrease in haploid, while an increase in tetraploid spermatogenic cells in both 30- and 60-day old Ggnbp2 knockout testes compared to that of wild-type littermates. In spread spermatocyte nuclei, Ggnbp2 loss increased DNA double strand breaks (DSB), compromised DSB repair and reduced crossovers. Further investigations demonstrated that GGNBP2 co-immunoprecipitated with gametogenetin (GGN), a testis-enriched protein known to play a role in DSB repair during spermatogenesis. Immunofluorescent staining revealed that both GGNBP2 and GGN had the same subcellular localizations in spermatocyte, spermatid and spermatozoa. Ggnbp2 loss suppressed Ggn expression and diminished nuclear accumulation of GGN. Furthermore, deletion of either Ggnbp2 or Ggn in immortalized mouse spermatocytes (GC-2spd cells) inhibited their differentiation into haploid cells in vitro. Overexpression of Ggnbp2 in Ggnbp2 null but not in Ggn null GC-2spd cells partially rescued the defect coinciding with a

restoration of Ggn expression. The results indicate that GGNBP2 plays a role in DSB repair during meiotic progression of spermatocytes, which is likely mediated by its interaction with GGN. These data together with our previous findings suggest that spermatogenic arrest in Ggnbp2 knockout males may occur at meiosis of spermatocytes and is aggravated during differentiation of spermatids, which leads to an azoospermic phenotype.

**Fipronil Has Detrimental Effects on Meiotic Maturation in Porcine Oocytes.** Wenjun Zhou, Ying-Jie Niu, Zheng-Wen Nie, Kyung-Tae Shin, and Xiang-Shun Cui

Fipronil is a widely used and highly effective phenylpyrazole pesticide, its metabolites have detrimental effects on mammalian blood and nerve cells and spermatogonia causing increased level of ROS and DNA damage. However, studies on the effect of fipronil on the female mammalian reproductive system have hardly reported, especially on oocytes. In this study, effect of fipronil on the meiotic maturation of porcine oocytes was investigated. The results showed that cumulus cell expansion was significantly inhibited and more oocytes were arrested at GV stage when treated with 100  $\mu$ M fipronil. The apoptosis and autophagy activities were significantly enhanced in 100  $\mu$ M fipronil treatment group compared to control. Meanwhile, the fipronil caused a significant increased ROS level and more severe DNA damage inside the oocytes. In the 100  $\mu$ M fipronil group, the mitochondrial membrane potential and expression level of BCL-xL mRNA were significantly dropped and the cytochrome C was released from the mitochondria in the 100  $\mu$ M fipronil treated group. Furthermore, the result showed a significantly delayed increase of MPF activity during GVBD in the fipronil treatment group, which was also consistent with the lag of cyclin B1 degradation. In conclusion, the fipronil causes apoptosis and cell cycle arrest in the porcine oocyte during meiotic maturation through induction of ROS level and DNA damage. It suggests that the fipronil inside the environment and contaminated farm products may have potential detrimental effects on the female mammalian reproductive system.

**Genotypic Differences in Placental Development During Late Gestation Between Chinese Meishan and White Crossbred Gilts in Response to Intrauterine Crowding.** Jeremy R. Miles and Jeffrey L. Vallet

The porcine placenta is classified as non-invasive, epitheliochorial in which hemotrophic (i.e., capillary) exchange is maximized during late gestation via modification of the folded bilayer consisting of an intact uterine epithelium and trophoctoderm embedded in loose stroma that increases in width and complexity. Histotrophic (i.e., glandular) exchange occurs via placental areolae juxtaposed to the uterine glandular epithelium. The objective of this study was to evaluate placental development during late gestation between prolific Chinese Meishan (MS) and White crossbred (WC) gilts following intrauterine crowding. To induce intrauterine crowding, similar aged MS (n = 7) and WC (n = 5) gilts were unilaterally hysterectomized-ovariectomized at approximately 60 days of age and allowed to recover prior to breeding (0.38) in uterine capacity, fetal survival, fetal and placental weights or placental efficiency (fetal to placental ratio). In contrast, allometric growth relationship between fetal and placental weights was decreased (P = 0.01) in MS gilts compared to WC gilts indicating a greater fetal sparing effect within the MS breed. The width of the folded bilayer was greater (P < 0.01) in placentas from WC gilts compared to MS gilts, irrespective of fetal size. Placentas from small fetuses had greater (P < 0.01) folded bilayer width compared to placentas from large fetuses, irrespective of gilt

breed. The stromal width was greater ( $P < 0.01$ ) in placentas from large fetuses compared to small fetuses, but stromal width was not different ( $P = 0.29$ ) between breeds. However, the difference between stromal width in placentas between small and large littermate fetuses was greater ( $P = 0.05$ ) in WC gilts compared to MS gilts suggesting limited response to fetal crowding in MS gilts. There was a breed by size interaction ( $P < 0.01$ ) for areolae density in which placentas from large MS fetuses had greater areolae density compared to small MS fetuses. However, the density of areolae and total number of areolae were greater ( $P < 0.01$ ) in either small or large MS fetuses compared to WC fetuses illustrating greater histotrophic exchange in MS placentas compared to WC placentas. These results demonstrate altered placental development during late gestation in MS pregnancies corresponding to less sensitive response to intrauterine crowding. \*USDA is an equal opportunity provider and employer.

**Post-Transcriptional Regulation by FXR1 and IGF2BP2 Can Be New Insights and Potential Druggable Mechanisms in Ovarian Cancer.** James A. MacLean II, Nikola Sekulovski, Sambasiva R. Bheemireddy, Hiroshi Okuda, Kyle N. Plunkett, Zhifeng Yu, Martin M. Matzuk, and Kanako Hayashi

Aberrant canonical WNT/CTNNB1 signaling has been reported in ovarian cancer and is a critical mediator of malignant transformation. We have previously reported the therapeutic potential of inhibition of the WNT7A/CTNNB1-FGF1 axis in ovarian cancer. Specifically, an FDA-approved minimally toxic, and an affordable drug, niclosamide, most efficiently abrogated WNT7A/CTNNB1 signaling in our ovarian cancer model. However, niclosamide has been identified by many high-throughput screening platforms as a potential effective compound for several cancer types targeting multiple signaling pathways. The goal of the current study was to understand the core functions in multiple signal transduction mechanisms altered by niclosamide in ovarian cancer. We first identified target proteins that niclosamide directly binds to within ovarian cancer cells using biotinylated niclosamide as affinity reagents. After biotinylation of niclosamide, we performed affinity purification (pull-down) and mass spectrometry analysis (liquid chromatography tandem mass spectrometry, LC-MS/MS) to identify putative target proteins from high-grade serous ovarian cancer (HGSOC) cell lysate directly associated with niclosamide. The obtained MS/MS spectra were matched against the human RefSeq database and a total of 2395 proteins were identified. Of these, 295 proteins had a  $> 1.5$ -fold binding affinity with biotinylated niclosamide vs. unlabeled niclosamide (which was used as a negative control).

Interestingly, 56 of the 295 proteins are known RNA binding proteins (RBPs). We chose two RBPs (FXR1 and IGF2BP2) for further analysis, as both have been recently identified as oncogenes, and are located in 3q26-29, which includes frequent genomic alteration with PIK3CA, PRKCI, ECT2, SOX2, and TP63 in lung squamous cell carcinoma and other cancers. A significant correlation in which high-expression of FXR1 or IGF2BP2 was associated with reduced survival of ovarian cancer patients by log-rank test ( $P=0.0276$  or  $P=0.0039$ , respectively). Because FXR1 and IGF2BP2 are closely located in 3q28 and 3q27.2, respectively, amplification of both genes is significantly correlated in ovarian cancer ( $P < 0.001$ ) according to the cBioPortal for Cancer Genomics. Knockdown of FXR1 or IGF2BP2 in ovarian cancer cells resulted in significantly reduced cell viability, adhesion, and invasion. These results suggest that both RBPs, FXR1 and IGF2BP2, are direct targets of niclosamide and could have critical functions that drive multiple oncogenic pathways in ovarian cancer.

**Human Globozoospermia-Related Gene Spata16 is Required for Sperm Formation Revealed by CRISPR/Cas9-Mediated Mouse Models.** Yoshitaka Fujihara, Asami Oji, Tamara Larasati, Kanako Kojima-Kita, and Masahito Ikawa

A recent genetic analysis of infertile globozoospermic patients identified causative mutations in three genes: a protein interacting with C kinase 1 (PICK1), dpy 19-like 2 (DPY19L2), and spermatogenesis associated 16 (SPATA16). Although mouse models have clarified the physiological functions of Pick1 and Dpy19l2 during spermatogenesis, Spata16 remains to be determined. Globozoospermic patients carried a homozygous point mutation in SPATA16 at 848G→A/R283Q. We generated CRISPR/Cas9-mediated mutant mice with the same amino acid substitution in the fourth exon of Spata16 to analyze the mutation site at R284Q, which corresponded with R283Q of mutated human SPATA16. We found that the point mutation in Spata16 was not essential for male fertility; however, deletion of the fourth exon of Spata16 resulted in infertile male mice due to spermiogenic arrest but not globozoospermia. This study demonstrates that Spata16 is indispensable for male fertility in mice, as well as in humans, as revealed by CRISPR/Cas9-mediated mouse models.

This work was supported by Eunice Kennedy Shriver National Institutes of Child Health and Human Development grants R01HD088412 and P01HD087157.

**Impact of Seasonality and Storage of Semen on Epigenetics in Swine Placenta and Fetal Livers.** Lea A. Rempel, Megan M. Krautkramer, John J. Parrish, and Jeremy R. Miles

Epigenetics includes the study of external factors that can influence the expression of genes by altering accessibility of DNA through methylation and histone modification. To investigate the influence of: season (semen collection and breeding), absolute sperm head-shape change, and semen storage on placental and fetal tissues (45d gestation); 83 pregnancies ( $n \leq 5$  litters per group) generated in the summer or winter using boar semen from either least or most sperm head-shape change between June and August, collected during cool or warm seasons and stored either as cooled-extended or cryopreserved. Correlation of methylation activity within tissues were assessed with relative quantitative expression of candidate genes with differentially methylated regions using Pearson's Correlation. Effects upon relative expression were evaluated using the Mixed procedure of SAS. Ratio of 5-methylcytosine to 5-hydroxymethylcytosine activity (5mC:5hmC) was lower ( $P < 0.05$ ) in placenta versus fetal liver. Within tissue, fetal liver had a lower ( $P < 0.05$ ) ratio from summer matings, while placental tissues were least ( $P < 0.05$ ) during winter matings. There was a negative ( $P < 0.05$ ) relationship between 5mC:5hmC and placental relative expression of CDH1 (-0.17) and GNAS (-0.30). No correlations were detected between 5mC:5hmC and fetal liver relative expression. Relative expression of CDH1 tended ( $P < 0.10$ ) to be greater in placenta generated from cryopreserved semen versus cooled-extended semen and tended ( $P < 0.10$ ) to be greater in pregnancies from semen collected during cool periods versus warm periods. Relative expression of placental GNAS was greatest ( $P < 0.05$ ) in pregnancies derived from semen collected during cool periods used in winter matings, least ( $P < 0.05$ ) from semen collected during cool periods used in summer matings, and intermediate from semen collected during warm seasons regardless of mating season. Cryopreserved semen yielded greater ( $P < 0.05$ ) placental relative expression of GNAS. Placental MEST and RHOBTB3 tended ( $P < 0.10$ ) to have greater relative expression from pregnancies generated using semen collected during cool periods used during winter matings. Relative expression of GNAS and HGF within fetal liver was greater ( $P < 0.05$ )

from pregnancies generated from winter matings. Pregnancies generated from semen with the least amount of sperm head-shape change and winter matings had the greatest ( $P < 0.05$ ) relative expression of fetal liver CDH1, those derived from semen with most head-shape change and winter matings were intermediate, and relative expression of fetal liver CDH1, was least ( $P < 0.05$ ) from summer matings, regardless of sperm head-shape change. A lower 5mC:5hmC suggests increased gene transcript activity and was apparent in the current study within placental tissues. Seasonality of; semen collection, mating, and effect on sperm head-shape change had an influence on expression of genes with known differentially methylated regions from embryonic and extraembryonic tissues. To increase our understanding of external influences on epigenetics of the placenta, future studies will examine the seasonal effects of semen collection, storage, and mating on gene expression within the epigenetic chromatin enzymes modification network. USDA is an equal opportunity provider and employer.

**Sin3a is Indispensable for the First Lineage Specification in Preimplantation Embryos.** Panpan Zhao, Han Wang, Tong Liu, and Kun Zhang

Laboratory of Mammalian Molecular Embryology, Institute of Dairy Science, College of Animal Sciences, Zhejiang University, Hangzhou, Zhejiang 310058, P. R. China; Correspondence: kzhang@zju.edu.cn

Sin3a is a scaffold component of the Sin3a/Hdac1 complex that is known for its transcriptional repression activity. Conventional knockout of Sin3a results in early embryonic lethality, suggesting its critical role during early embryonic development. However, the concrete function and regulatory mechanism of Sin3a during preimplantation development remains unclear. Morphologically, Sin3a knockdown (KD) embryos fail to develop to blastocyst stage with the majority arrested at morula stage. Sin3a KD also results in reduced cell numbers, which was observed from early morula stage. The first lineage specification take place in late morula and give rises to inner cell mass (ICM) and trophectoderm (TE). To determine if Sin3a deficiency affect this developmental event, critical lineage markers of ICM (Oct4, Nanog) and TE (Cdx2) were examined. Gene profiling analysis show that both Cdx2 and Nanog were significantly reduced while Oct4 is not changed in Sin3a KD embryos. Indeed, immunofluorescence (IF) analysis confirmed that Cdx2 and Nanog were decreased obviously and Oct4 is stable in Sin3a KD embryos. To determine if Sin3a is required for the enzymatic activity of the histone deacetylases in Sin3a complex, a selected acetylated histone was monitored. IF results show that histone H4 lysine 5 acetylation (H4K5ac) was enhanced as predicted. Previous evidence shows there are direct physical interactions between Sin3a complex components and DNA modifiers, including DNMT1. To determine if Sin3a is involved in the regulation of genome-wide DNA methylation during preimplantation embryos, IF against 5-methylcytosine (5mc) and 5-hydroxymethylcytosine (5hmc) was analyzed. Results indicate 5mc was markedly increased and 5hmc was not changed in KD group. Furthermore, we also documented that Histone H3 lysine 9 dimethylation (H3K9me2) level was dramatically decreased. Collectively, our results suggest Sin3a is functionally required for the first lineage specification and involved in the regulation of proper epigenetic modifications in preimplantation embryos.

**FecB Mutation Affects Ovarian DNA Methylome in Small Tail Han Sheep.** Lingli Xie, Xiangyang Miao, Qingmiao Luo, Huijing Zhao, and Xiaoyu Qin

FecB gene, a mutant of BMPR-1B identified in Booroola Merino, was the first found prolificacy gene in sheep, and leads to increased ovulation rate and litter size. The mechanisms that how fecB affects sheep fecundity have not been revealed clearly. Small Tail Han sheep is a typical hyperprolificacy sheep bred in China, and our previous studies have explored the ovarian gene expression difference between Han sheep with homozygous FecB mutant (HanBB) and Han sheep with wildtype BMPR-1B (Han++). DNA methylation is an epigenetic mechanism to regulate gene expression in gametogenesis and embryogenesis, and we have proved the DNA methylation takes part in the gene expression difference between HanBB sheep and a relative low prolific Dorset sheep. In the present study, we examined the difference of DNA methylation patterns between HanBB and Han++ sheep, successfully identified several differentially methylated genes involved in GnRH signaling pathway. Our findings provide a novel insight of FecB gene induced sheep hyperprolificacy.

**FecB Mutation Affects Ovarian DNA Methylome in Small Tail Han Sheep.** Lingli Xie, Xiangyang Miao, Qingmiao Luo, Huijing Zhao, and Xiaoyu Qin

FecB gene, a mutant of BMPR-1B identified in Booroola Merino, was the first found prolificacy gene in sheep, and leads to increased ovulation rate and litter size. The mechanisms that how fecB affects sheep fecundity have not been revealed clearly. Small Tail Han sheep is a typical hyperprolificacy sheep bred in China, and our previous studies have explored the ovarian gene expression difference between Han sheep with homozygous FecB mutant (HanBB) and Han sheep with wildtype BMPR-1B (Han++). DNA methylation is an epigenetic mechanism to regulate gene expression in gametogenesis and embryogenesis, and we have proved the DNA methylation takes part in the gene expression difference between HanBB sheep and a relative low prolific Dorset sheep. In the present study, we examined the difference of DNA methylation patterns between HanBB and Han++ sheep, successfully identified several differentially methylated genes involved in GnRH signaling pathway. Our findings provide a novel insight of FecB gene induced sheep hyperprolificacy.

**Effects of Melatonin on Cells Survival of Equine Cumulus Cells During Oocyte Maturation in Vitro.**

Lauro E. Contreras-Navarro, Hilda M. Guerrero-Netro, Ana M. Boeta-Acosta, Rodrigo González-López, Christopher A. Price, and Mouhamadou Diaw

Melatonin is a hormone produced by the pineal gland. Melatonin regulates the sleep cycle and acts on the reproductive system, especially in seasonal species like horses. In cows, melatonin increases oocyte nuclear maturation, cumulus cells expansion and alter mitochondrial distribution patterns. In pigs, melatonin increased nuclear and cytoplasmic maturation during oocyte in vitro maturation. In mice oocytes, melatonin can significantly reduce oxidative stress and as a result, delay apoptosis. In horses, melatonin receptor MT1 is present in the corpus luteum and follicles. However, the exact role of melatonin in modulating reproduction of mares is not fully understood, especially its effects on oocytes and cumulus cells. Our objective was to assess the effects of melatonin on cell survival of cumulus cells during oocyte in vitro maturation.

Mare ovaries were obtained during the breeding season from a local slaughterhouse, independently of the stage of the estrous cycle and transported to the laboratory at 22°C. Cumulus-oocyte-complexes were obtained from follicles smaller than 30mm as previously described by Carnevale et al. 2016. Cumulus-oocyte complexes were matured in vitro in the presence of FSH and with or without three different doses of melatonin 10, 100 and 1000ng/ml for 30 hours. After maturation, oocytes were denuded by pipetting using PBS. Apoptosis in cumulus cells was measured by Annexin V flow cytometry. Additionally, levels of caspase 3 were measured in oocytes by immunofluorescence at different time points of maturation (10 and 20h). All experiments were performed in triplicate.

Treatment with 10 ng/ ml of melatonin significantly reduced the percentage of early apoptotic cells and increased the percentage of live cells but, it did not affect the percentage of apoptotic cells. Other doses of melatonin (100 and 1000ng/ml) had no effects on cumulus cell survival compared to the control. These results were confirmed by the levels of caspase 3. A dose of 10 ng/ml significantly reduced the levels of caspase 3 at both time points (10 and 20h), while higher doses did not affect caspase 3 levels. Taken together, these results suggest a positive effect of low doses of melatonin on cumulus cell but, these roles may vary according to the dose. This work was supported by Fonds en Santé Équine (FSÉ), Faculté de Médecine Vétérinaire, Université de Montréal, a donation from Zoetis and by CONACYT.

**Dacarbazine Depletes the Ovarian Reserve in Mice and Depletion is Enhanced with Age.** Amy Winship, Monika Bakai, Urooza Sarma, Seng Liew, and Karla Hutt

**Background** It is well-established that chemotherapies damage germ cells in a drug class and age-dependant manner. Primordial follicle oocytes are the precursors of all mature ovulatory oocytes. Their accelerated depletion in young females receiving anti-cancer treatments may lead to infertility and premature menopause. Dacarbazine is a non-classical alkylating agent, commonly administered to young patients for the treatment of malignant melanoma, sarcoma, neuroblastoma and Hodgkin's lymphoma, among other cancers. It is the current clinical recommendation that dacarbazine-containing chemotherapy regimens have a low-risk of causing ovarian toxicity and that fertility preservation should not be considered. However, its effects on the ovary have been poorly characterised. Herein, we assessed the impact of dacarbazine on the ovary in reproductively young and aged mice.

**Materials and Methods** 8 week and 6 month old C57BL/6J mice were administered intravenously with dacarbazine (130mg/kg), or saline vehicle control on day (d)0 and d7, then sacrificed 12 hours (h), or 14d following final treatment (n=5/group). One ovary per animal was used to quantify follicle numbers using stereology. Serum anti-Müllerian hormone (AMH) concentrations were assayed by ELISA. Corpora lutea and ovarian volume were quantified. Estrous cyclicity was monitored for 14d by vaginal cytology. At 12h, histological markers of follicle atresia (TUNEL, cleaved caspase-3), proliferation (pH3), DNA damage ( $\gamma$ H2AX) and ovarian tissue fibrosis (Picrosirius red) were assessed. Statistical analysis was performed using student's t-test, or ANOVA and differences considered significant when  $p < 0.05$ .

**Results** In reproductively young mice, dacarbazine had no impact on primordial follicle numbers at 12h following final treatment, versus control, but resulted in a significant 36% reduction at 14d ( $p < 0.05$ ). Depletion was enhanced with age in mice, with a 24% ( $p < 0.05$ ) and 36% ( $p < 0.01$ ) reduction at 12h and 14d after final dacarbazine treatment. In both age groups, atretic antral follicle numbers were increased at 12h ( $p < 0.05$ ), culminating in reduced total healthy antral follicles at 14d ( $p < 0.05$ ) in

response to dacarbazine. Despite this, serum AMH concentrations, estrous cyclicity and total number of corpora lutea (indicative of ovulation) remained unchanged between treatment groups, at both ages. Histological analysis showed a significant increase in TUNEL positive antral follicles in response to dacarbazine treatment in both age groups 12h after treatment ( $p < 0.05$ ). However, there were no differences in the number of cleaved caspase-3 positive (apoptotic),  $\gamma$ H2AX positive (DNA damaged), or pH3 positive (proliferative) follicles in response to dacarbazine chemotherapy.

Conclusions Dacarbazine administration reduced the ovarian reserve of primordial follicles in mice. Furthermore, depletion was enhanced with age. We observed an acute reduction in growing antral follicles in response to dacarbazine, although this was not sufficient to disrupt AMH serum levels, estrous cycling, or ovulation. These findings have important clinical implications, since female cancer patients may present with normal menstrual cycles and AMH levels following chemotherapy, despite having a diminished ovarian reserve. Importantly, as reduced ovarian reserve can ultimately result in early loss of fertility and premature menopause, our data contradict current clinical advice and suggest that counselling and fertility preservation should be considered for young female patients prior to dacarbazine treatment.

**Genome-wide Epigenome Analysis and Genome Editing Identified a Novel Enhancer Region for IGF–Binding Protein-1 (IGFBP-1) Expression in Human Endometrial Stromal Cells Undergoing Decidualization.** Isao Tamura, Haruka Takagi, Yuichiro Shirafuta, and Norihiro Sugino

Introduction: Decidualization is the process that human endometrial stromal cells (ESCs) differentiate into decidual cells by progesterone. We have previously shown that decidualization causes a genome-wide increase in the levels of acetylation of histone-H3 Lys-27 (H3K27ac), which is an active enhancer mark. These regions are mainly observed in the distal gene regions, which are more than 3 kb up or downstream of gene transcription start sites. Insulin-like growth factor–binding protein-1 (IGFBP-1) is a specific decidualization marker and has increased H3K27ac levels in its distal upstream region (-4701 bp to -7501 bp), suggesting that this region is a novel enhancer region involved in IGFBP-1 expression during decidualization. In this study, we identified a novel enhancer region for IGFBP-1 expression by a genome-wide epigenome analysis of ESCs and genome editing. We also examined how transcription factors and coactivators regulate IGFBP-1 expression through the activation of the enhancer region during decidualization.

Methods and Results: This study was approved by IRB of Yamaguchi University. ESCs isolated from the proliferative endometrial tissue were incubated with or without dibutyryl-cAMP (cAMP, 0.5 mM) for 4 days to induce decidualization. We tested the hypothesis that the region we focused on is an IGFBP-1 enhancer by using a luciferase reporter gene construct containing this IGFBP-1 upstream region. cAMP increased luciferase expression, indicating that decidualization increased the transcriptional activity from the IGFBP-1 upstream region. To test the endogenous function of the enhancer region in regulating IGFBP-1 expression, we established cell lines in which the IGFBP-1 enhancer region was deleted from its endogenous locus by CRISPR/Cas9 editing. Deletion of this region significantly reduced IGFBP-1 expression, confirming its endogenous role as an IGFBP-1 enhancer. We also investigated the involvement of transcription factors in the activation of the enhancer region. A ChIP assay revealed that cAMP increased the recruitment of the transcriptional regulators CCAAT enhancer–binding protein  $\beta$  (C/EBP $\beta$ ) and forkhead box O1 (FOXO1) to the IGFBP-1 enhancer. We also examined the recruitment of

p300 by decidualization because it is a transcription coactivator that has histone acetyltransferase (HAT) activities and induces H3K27ac. cAMP increased the recruitment of p300 to the enhancer region. The effect of cAMP on the changes of chromatin structure in the IGFBP-1 enhancer region were examined by FAIRE (formaldehyde-assisted isolation of regulatory elements)-qPCR. cAMP opened the chromatin structure of the enhancer region. Of note, C/EBP $\beta$  knockdown inhibited the stimulatory effects of cAMP on the levels of H3K27ac, chromatin opening, and p300 recruitment at the IGFBP-1 enhancer. These results indicate that C/EBP $\beta$  acts as a pioneer factor initiating the process of chromatin remodeling to activate the enhancer region.

Conclusions: We identified a novel enhancer region for IGFBP-1 expression by a genome-wide epigenome analysis and genome editing in ESCs. This enhancer region is activated by the recruitment of C/EBP $\beta$  and FOXO1 to up-regulate IGFBP-1 expression. Especially, C/EBP $\beta$ , cooperating with p300, increases H3K27ac levels and opens the chromatin structure of the enhancer region. Our work shows a novel molecular mechanism by which IGFBP-1 expressions is induced during decidualization in human ESCs.

**Depletion of the Orphan Nuclear Receptor Nr5a2 Affects Early Folliculogenesis.** Marie-Charlotte Meinsohn, Olivia Eilers Smith, Anthony Estienne, Raj Duggavathi, and Bruce D Murphy

The orphan nuclear receptor Nr5a2, also known as Lrh-1, is required for fertility, as its specific depletion in granulosa cells results in impaired cumulus expansion, ovulation and luteinization. As a result, these mice are infertile. We previously shown that Nr5a2 is essential for granulosa cell proliferation. Based on these results, we hypothesized that Nr5a2 could act as early as follicular formation and in the follicular development process. We generated granulosa-specific knockout mice (Nr5a2f/fAmhr2Cre/+; cKO) with Nr5a2 depletion linked to the transcription of Amhr2 in granulosa cells of all follicles from primary follicles forward and in corpora lutea. Because Amhr2 has been reported to be expressed in granulosa cells as early as postnatal day 13 (PND13), immature PND13 ovaries from cKO and control mice were collected and fixed in 10% formalin, or snap-frozen for RNA extraction purposes. Our first objective was to determine whether the number of primary follicles was affected by the depletion of Nr5a2. Paraffin slides of fixed ovaries were stained with eosin and hematoxylin and primordial and primary follicles enumerated. Remarkably, we showed a significantly higher number of primordial follicles in the cKO mice, with more than five-fold more primordial follicles compared to the controls. The absence of activation of these primordial follicles was confirmed by PCNA immunofluorescence that showed no incorporation in granulosa cells. Given this phenotype at PND13, we decided to look at the effects of depletion of Nr5a2 at PND4, end of the invasion of pre-granulosa cells into the oocyte nests. A drastic increase in the number of oocytes in the cKO mice led to investigation of the mechanisms by which the depletion of Nr5a2 had an impact on the early stages of folliculogenesis. We assessed the quantity of transcripts for key genes involved in the formation of primordial follicles and in their transition to the primary stage. Quantitative PCR analysis of PND4 CON and cKO ovaries indicated that Nr5a2 transcript abundance was significantly downregulated, as it was for Amh, its receptor Amhr2, and Foxl2. The mRNA for the granulosa cells expressed transcription factors Kitl and Notch2 were also deregulated. As it is well known that granulosa cell-oocyte communication is key for a successful follicle development, we therefore quantified oocytes expressed genes including Figla, cKit, Gdf9 and Foxo3. We found that they were all significantly upregulated. Finally, we measured apoptosis and autophagy related genes

such as Mcl1, Bcl2l1 by qPCR and Cleaved Caspase 3 by immunofluorescence. Pro-survival genes Mcl1 and Bcl2l1 were upregulated in the cKO mice while pro-apoptotic Cleaved Caspase 3 immunofluorescence showed a significantly decreased signal. The mechanisms involved are currently being confirmed and explored further by RNA sequencing. We conclude that Nr5a2, functioning via multiple mechanisms, plays a key role in the activation of primordial follicles, their consequent progression to the primary state and their survival.

### **The Effects of Acute Exposure to Di(2-Ethylhexyl) Phthalate and Diisononyl Phthalate During**

**Adulthood on Female Reproduction.** Catheryne Chiang, Saniya Rattan, Emily Brehm, Liying Gao, Daryl D. Meling, and Jodi A. Flaws

Di(2-ethylhexyl) phthalate (DEHP) is used as a plasticizer in several consumer products such as baby toys, food containers, carpeting, and medical devices. It can be absorbed via ingestion, inhalation, and dermal contact and can enter multiple tissues in the body. Because DEHP is so widely used and readily leaches from products, it is a ubiquitous environmental contaminant that humans are exposed to on a daily basis. Concerningly, DEHP has also been shown to have endocrine disrupting capabilities, and compounding this concern is a lack of knowledge of the effects of DEHP on the ovary. Recognizing the reported negative effects of DEHP, some manufacturers have elected to replace DEHP with other plasticizers. However, often even less is known about these DEHP replacements than is known about DEHP itself. One such replacement, diisononyl phthalate (DiNP), is a rising human toxicant and has been detected in increasing levels over the years in human urine samples. Thus, this study tested the hypothesis that adult exposure to DEHP or DiNP negatively affects female reproductive health. To test this hypothesis, adult female CD-1 mice (age 39-40 days) were orally dosed with either vehicle control (corn oil), DEHP (20 or 200  $\mu\text{g}/\text{kg}/\text{day}$  or 20 or 200  $\text{mg}/\text{kg}/\text{day}$ ), or DiNP (20 or 100  $\mu\text{g}/\text{kg}/\text{day}$  or 20 or 200  $\text{mg}/\text{kg}/\text{day}$ ) for 10 days. Immediately following completion of dosing, some mice were euthanized in diestrus and ovaries, uteri, and livers were collected and weighed. Additional mice were paired with untreated male mice immediately following dosing for breeding trials. Mice were allowed to deliver their pups and litter data were analyzed. Additionally, 3 months following dosing, the same mice that underwent breeding trials were vaginally lavaged daily for two weeks to assess their cyclicity. DEHP and DiNP did not affect the overall body weight, ovarian weight, or liver weight of mice collected immediately after dosing. However, 200  $\mu\text{g}/\text{kg}/\text{day}$  and 20 and 200  $\text{mg}/\text{kg}/\text{day}$  DEHP significantly reduced uterine weight compared to controls ( $p \leq 0.05$ ). In the breeding trials, females treated with 20  $\text{mg}/\text{kg}/\text{day}$  DEHP had pups that weighed more on average at birth than pups from control females ( $p = 0.053$ ). After 3 months, DiNP significantly decreased the time females spent in proestrus (20  $\mu\text{g}/\text{kg}/\text{day}$ , 200  $\text{mg}/\text{kg}/\text{day}$ ,  $p \leq 0.05$ ) and increased the time females spent in metestrus and diestrus compared to controls (100  $\mu\text{g}/\text{kg}/\text{day}$ , 200  $\text{mg}/\text{kg}/\text{day}$ ,  $p \leq 0.05$ ). DEHP also moderately decreased the time females spent in proestrus compared to controls (200  $\text{mg}/\text{kg}/\text{day}$ ,  $p = 0.087$ ). These data show that DEHP exposure reduces uterine weight and increases pup weight immediately following dosing, and it alters cyclicity after 3 months post-dosing. Additionally, exposure to DiNP, a common DEHP replacement, significantly disrupts estrous cyclicity following 3 months post-dosing, showing that acute exposure to DiNP can have long lasting effects on reproductive outcomes after exposure has stopped. Supported by R56 ES 025147 (JAF) and T32 ES 007326 (CC).

### **Neuropeptide Y Regulates Proliferation and Apoptosis in Ovarian Granulosa Cells During Follicular Development.** Yoko Urata

Ovarian follicular development is regulated by hormonal, intraovarian and immunological factors. Only one follicle within the cohort of follicles recruited for development is selected to mature and to ovulate, and the remaining follicles become atretic as their cells undergo apoptosis. This selection mechanism is not completely understood. Neuropeptide Y (NPY) is expressed in the central nerve system and peripheral nerves, and is associated in various processes including brain activity, stress adaptation, metabolism, obesity and immune regulation. Polycystic ovarian syndrome (PCOS) is associated with follicle growth arrest and higher serum NPY level compared with non-PCOS. Although NPY regulates proliferation and apoptosis in luteinized granulosa cells, its function in folliculogenesis is unclear. The overall objective of this study was to examine the expression and role of NPY and its receptors during ovarian follicular development. We hypothesized that NPY is expressed predominantly in granulosa cells and regulates granulosa cell fate during folliculogenesis. Immunohistochemical studies on the expression of NPY and its receptors in follicle cells at different stages of development in the immature Sprague Dawley rats (21-days of age) and following eCG treatment (10 IU/rat; ip) indicate that NPY protein expression was higher in early antral follicles than in preantral and antral follicles, and was more intense in antral granulosa cells than in cumulus cells, mural granulosa cells and theca cells. NPY receptors in the follicles increased with follicular development. Npy mRNA abundance in isolated granulosa cells (determined by real-time PCR) was higher from early antral follicles than from antral follicles (n = 5 per group). Addition of recombinant NPY (10<sup>-10</sup> M) to cultured granulosa cells increased Ki67-positive but decreased TUNEL-positive granulosa cells from early antral follicles. In contrast, NPY reduced Ki67-positive and increased TUNEL-positive cells from antral follicles. NPY did not alter both Ki67- and TUNEL positivity in granulosa cells from preantral follicles. These results indicate that NPY regulates granulosa cell proliferation and apoptosis in a follicular stage-dependent and autocrine manner. This research was supported by a grant from the Canadian Institutes of Health Research.

### **Improvement of Icsi Outcome using Spermatozoa Selected by Thermotaxis.** Serafín Pérez-Cerezales, Ricardo Laguna-Barraza, María Jesús Sánchez-Calabuig, Esther Cano-Oliva, Francisco Javier de Castro-Pita, Luis Montoro-Buils, Eva Pericuesta, Raúl Fernández-González, and Alfonso Gutiérrez-Adán

In mammals, from a whole ejaculate only a small number (~tens or hundreds) of spermatozoa migrates toward the oviduct. Thus, in mouse only few dozen reach the ampulla, where the fertilization occurs. We have previously demonstrated that during this transit there is a strong positive selection of those spermatozoa containing high chromatin integrity. This selection is bypassed when some artificial reproductive techniques (ART) are used, such as in vitro fertilization or intracytoplasmic sperm injection (ICSI), and could explain in part their low success when applied in fertility treatments. Here, we tested the use of thermotaxis, a sperm guidance mechanism proposed to operate along the oviduct, for selecting high quality spermatozoa. We show that mouse, stallion and human spermatozoa separated by 1 hour of positive thermotaxis in vitro possess significantly less fragmented DNA than the spermatozoa that did not respond to thermotaxis. We also demonstrate that the use of mouse spermatozoa separated by thermotaxis, in contrast to swim-up separated spermatozoa (control), significantly improves the outcome of the ICSI by increasing the percentage of embryos reaching blastocysts stage (73 ± 4% vs 41 ± 6% respectively). Furthermore, after transfer to pseudopregnant females, the

blastocysts derived from thermotactic spermatozoa implanted in higher percentage than the control ( $77 \pm 9$  vs  $43 \pm 18\%$  respectively). In addition, we found that the transfer of 2-cell embryos generated with thermotactic spermatozoa produced higher percentage of implantations than the control ( $69 \pm 8\%$  vs  $22 \pm 6\%$  respectively) as well as higher number of pregnancies to term (5 and 13 pregnancies to term out of 24 transfers per group for swim-up-ICSI and thermotaxis-ICSI respectively). Thus, we suggest thermotaxis as one of the main mechanisms of sperm selection in vivo as well as we claim its possible use in human clinic as a method for separating high quality spermatozoa previous to their use in ART.

### **A Mathematical Model to Simulate and Predict the Influence of Glucose Metabolism on the Bovine Estrous Cycle.** Julia Ploentzke, Mohamed Omari, and Susanna Roebnitz

Nutrition impacts reproductive performance in dairy cows and other species. In the present study we explore the dynamic, mechanistic interaction between energy metabolism, in particular glucose metabolism and the estrous cycle with an ordinary differential equation model. For this purpose two before published models were coupled via Insulin and IGF-1. The coupled model describes how the glucose content in feed affect the reproductive hormones and follicular development over time. Model simulations reproduce clinical study findings in non-lactating and lactating cows. Furthermore we simulate numerical experiments by varying the amount of DMI and the glucose content in DMI. The simulation results are validated with clinical study findings. With the validated model we aim to address interdisciplinarily open questions and hypothesis.

### **Development of a Novel Reporter Cell Line to Map the Human Decidualization Genetic Network.**

Meade Haller, Yan Yin, and Liang Ma

Background: Failure of embryo implantation accounts for a significant percentage of pregnancy failure during both natural pregnancy and in vitro fertilization procedures. Exquisitely coordinated interactions between the competent blastocysts and the receptive uterus require the precise interplay between hormonal, growth factor, and intercellular signaling. Decidualization, the rapid proliferation and differentiation of fibroblast-like endometrial stromal cells into epithelioid-like decidual cells, is an integrated part of the implantation process. Decidualized cells later become part of the decidual tissue that surrounds the implanting conceptus. Decidualization defects can directly lead to implantation failure. In addition, early decidualization defects commonly result in unhealthy pregnancies due to defects in placentation, decreased intrauterine fetal growth, and early parturition leading to pre-term birth. Objective & Methods: Up to now, the process of decidualization has not been systematically studied at the genetic level due to the lack of a suitable high-throughput screening tool. Here we describe the generation of a novel immortalized human endometrial stromal cell line that contains a YFP-fluorescent readout of the decidualization response under the control of the prolactin promoter, hESC-PRLY cells. Upon stimulation with hormone cocktail, high throughput imaging and quantification reveals that the measurement of (YFP intensity x cellular area) is reliably induced 10 fold. Using this cell line, we are currently performing a genome-wide siRNA library screen to identify previously unrecognized genes required for decidualization, as well as genes whose purpose is to actively inhibit the process. Each gene is targeted with three independent siRNA constructs, and those genes which increase or decrease hormone response relative to scramble transfected cells by at least 2 standard

deviations (approximately 40%) using at least two of the three constructs will be further assessed. Results: As the screen continues to identify new hits, gene ontology analysis has already revealed several significant molecular pathways not previously recognized as decidualization modulators. From this screen we will identify candidate transcription factors required for decidualization and generate a temporal induction map outlining the transcription factor cascade required for decidualization. Additionally, we have developed a clone of the hESC-PRLY cells that constitutively expresses Cas9, allowing for the validation of knockdown hits using organoid-based independent knockout models for each hit via the transfection of targeted guide RNAs. Conclusions: Developing a high-throughput tool to prospectively assess the role of each human gene in the process of decidualization has already markedly improved our understanding of the molecular pathways underlying this process. Using this novel cell line and its derivatives as tools, we can now thoroughly map the genetic components of the decidualization network. These findings will aid in the development of patient-specific treatments for recurrent pregnancy loss, subfertility and infertility due to decidualization defects.

**The Exosome-Mediated Role of Plasma Gelsolin in Immune Cell Regulation In Ovarian Cancer Chemoresistance.** Meshach Asare-Werehene, Chen-Tzu Chiu, Wesker Lee, Laudine Communal, Mohammad R. Abedini, Pei-Wen Wang, Arkadiy Reunov, Euridice Carmona, Dylan Burger, Dar-Bin Shieh, Anne-Marie Mes-Masson, and Benjamin K Tsang

Ovarian Cancer (OVCA) is the most lethal gynecological cancer, due predominantly to late diagnosis, recurrence and chemoresistance. Although combined surgical debulking and chemotherapy is an important treatment strategy, chemoresistance remains a major challenge to successful long term therapeutic success. The responsiveness of cancer cells to chemotherapy is dependent on its microenvironment. Tumour-derived soluble factors and extracellular vesicles (exosomes) down-regulate T lymphocytes which influence the responsiveness of cancer cells to chemotherapy. Exosomes are membrane bound vesicles that transport biologically active proteins, nucleic acids and fatty acids to recipient cells in order to modulate their functions. Plasma gelsolin (pGSN), a soluble isoform of GSN expressed from the same GSN gene, has been shown to interact with integrin; however, its role in chemoresistance is yet to be explored. We have demonstrated previously that elevated circulatory levels of pGSN in head-and-neck and oral squamous cell carcinoma (OSCC) patients are significantly associated with chemoresistance and tumour recurrence respectively. These findings led us to hypothesize that exosomes containing pGSN (Ex-pGSN) regulate OVCA responsiveness to cisplatin (CDDP) through T cell modulation. Our recent mechanistic studies have shown that pGSN, is likewise highly expressed in chemoresistant OVCA cells than in its chemosensitive counterparts. pGSN, secreted and transported via exosomes, up-regulates HIF-1 $\alpha$ -mediated GSN expression in chemoresistant OVCA cells in an autocrine manner, confers cisplatin resistance in otherwise chemosensitive OVCA cells and induces apoptotic cell death in T lymphocytes. Chemoresistant cells also adopt a peripheral secretion mechanism to release Ex-pGSN as well as platinum in order to survive CDDP-induced apoptosis. Our recent immunolocalization studies on 213 high grade serious ovarian tumors indicate that pGSN expression hinders the prognostic impact of tumour infiltrating T cells and TCGA microarray data of 489 HGSC analysis shows a significant positive correlation with CD4 T cells but not CD8 T cells in the tumor microenvironment raising a possibility that pGSN could mediate T helper 2 response as well as down-regulate CD8+ T cells function. Exogenous pGSN and chemoresistant OVCA cell-derived exosomes reduced proliferation and induced cell death in CD8+ T cells but not CD4+ T cells. These effects were not

observed with chemosensitive OVCA cell-derived exosomes. Naïve CD4+ T cells were also preferentially polarized into T-helper 2 and T-regulatory cells which were evident by increased secretion of IL-4 and TGF- $\beta$ . In summary, pGSN regulates OVCA responsiveness to CDDP by regulating its own gene expression in an autocrine manner and downregulating T cell functions in a paracrine manner. These findings will support the immunosuppressive role of pGSN in the ovarian tumour microenvironment and chemoresistance as well as provide a novel target for treatment modalities (Support by grants from the Canadian Institutes of Health Research, Ovarian Cancer Canada and the Ministry of Science and Technology of Taiwan).

**Involvement of Specific Akt Isoforms in The Decidualization Mechanisms of the Mouse Uterus.** Pascal Adam, François Fabi, Francis Demontigny, Laurence Tardif, Sophie Parent, and Eric Asselin

North American couples find it increasingly difficult to conceive; unsurprisingly, infertility is a rising problem that currently touches 16% of couples trying to conceive. Many factors can contribute to this condition, which is thought to mainly arise from dysregulation in the maternal-embryonal communication mechanisms. Successful implantation, by which the embryo invades the maternal endometrium, necessitates an extraordinarily well-coordinated interaction between both the embryonic and maternal cells. In order to achieve this process, the endometrium is required to be fully prepared and receptive for implantation; this "window of implantation" is dependent on the process of decidualization. Under the effect of progesterone, estrogen and cyclic AMP, the endometrial stromal cells undergo fundamental phenotypical changes, transitioning from fibroblasts to epithelial, secretory, glycogen-filled cells. During this process, many signaling pathways involved in proliferation and apoptosis such as PI3K/Akt are modulated. It has been previously demonstrated that the activity of Akt is regulated during decidualization, but little is known about its implication in cell survival, apoptosis and glycogen synthesis. Three isoforms of Akt have been identified and it is well recognized that they have distinct physiological and pathological roles. We hypothesize that this is also the case during decidualization and the pregnancy onset.

The aim of this study is to investigate the role of each specific Akt isoform regulation during the in vivo mouse decidualization process. Previous in vitro results obtained in our lab using Human Immortalized Endometrial Stromal Cells (HIESC) suggest that the decrease expression and activity of specific Akt isoforms is necessary for the decidualization process to successfully occur. Therefore, we developed a novel endometrial-targeted mouse model with simple and combined KO of each Akt isoforms using the PR-Cre mouse model. By artificially inducing mouse uterine decidualization, the specific cellular localization, the expression and the activation of each Akt isoforms and their downstream targets was investigated during this process in order to evaluate the regulation of PI3K/Akt pathway.

Our results suggest that the downstream targets activity of p70S6K, I $\kappa$ B $\alpha$  and FOXO1 is regulated in a Akt isoform specific manner during decidualization that could reveal distinctive role of each isoform during this biological process. Moreover, differences in morphological aspects of the uterus and average mouse litter number has been observed depending of the KO genotype. Thus, it is clear that the PI3K/Akt pathway has an important role in fertility. Further studies will allow us to understand the precise signaling mechanisms by which this pathway is regulated and will lead to a better understanding of the cellular and molecular aspects of infertility. This research was supported by the Natural Sciences and Engineering Research Council of Canada (NSERC) (238501-01).

**Prenatal Exposure to a Phthalate Mixture Alters Sex Steroid Hormones in the F1, F2, and F3 Generations of Female Mice.** Emily Brehm, Changqing Zhou, Liying Gao, and Jodi A. Flaws

Phthalates are a group of synthetic chemicals ubiquitously used in a large variety of consumer products, including personal care products, medical tubing, and plastic products. Phthalates are known endocrine disrupting chemicals, and previous studies have shown that phthalates affect female reproduction. These previous studies have mainly focused on single phthalate exposure, however, humans are exposed daily to mixtures of chemicals including phthalates. Previously, our laboratory developed a phthalate mixture made of 35% diethyl phthalate, 21% di(2-ethylhexyl) phthalate, 15% dibutyl phthalate, 15% diisononyl phthalate, 8% diisobutyl phthalate, and 5% benzylbutyl phthalate that mimics human exposure. We tested the effects of prenatal exposure to this mixture on reproductive outcomes in the F1, F2, and F3 generations of female mice and found that it impaired reproductive outcomes by increasing uterine weight, altering anogenital distance, inducing enlarged cystic ovaries, disrupting estrous cyclicity, and causing fertility complications in multiple generations. Many of these impaired reproductive outcomes could be due to abnormal sex steroid hormone levels. However, it is not known whether the phthalate mixture affects sex steroid hormones in females. Thus, we tested the hypothesis that prenatal exposure to a phthalate mixture alters sex steroid hormones in a multi- and transgenerational manner in female mice. Pregnant CD-1 dams were orally dosed with vehicle control (tocopherol-stripped corn oil) or a phthalate mixture (20 and 200  $\mu\text{g}/\text{kg}/\text{day}$ , 200 and 500  $\text{mg}/\text{kg}/\text{day}$ ) daily from gestational day 10 to birth. Adult F1 females born to these dams were used to generate the F2 generation by mating them with unexposed males and adult F2 females were used to generate the F3 generation by mating them with unexposed males. On postnatal days (PNDs) 21 and 60, female pups from each litter were euthanized and sera were collected to measure estradiol, progesterone, and testosterone levels. At PND 21, prenatal phthalate mixture exposure decreased estradiol and testosterone levels, but did not affect progesterone levels in the F1 generation. At PND 60, phthalate mixture decreased estradiol, progesterone, and testosterone levels in the F1 generation. Further, ancestral phthalate mixture exposure increased estradiol levels at PND 60 in the F2 generation. Lastly, ancestral phthalate mixture exposure did not affect hormone levels at PND 21, but it increased estradiol levels and decreased progesterone and testosterone levels at PND 60 in the F3 generation. Overall, these data suggest that prenatal exposure to an environmentally relevant phthalate mixture induces some multi- and transgenerational effects on sex steroid hormone levels in female mice. Supported by NIH P01 ES022848 and EPA RD-83459301.

**Synergy of Paracrine Signaling in Early-Stage Mouse Ovarian Follicle Development in Vitro.** Hong Zhou, Joseph T. Decker, Melissa M. Lemke, Claire E. Tomaszewski, Lonnie D. Shea, Kelly B. Arnold, and Ariella Shikanov

Paracrine signals, such as soluble cytokines and extracellular matrix cues, are essential for the survival and development of multicellular ovarian follicles. While it is well established that hydrogel-based culture systems successfully support the growth of late-stage ovarian follicles for fertility preservation, growing small, early-stage ovarian follicles still proves to be challenging. We hypothesized that paracrine factors secreted from neighboring follicles may be crucial for improving the survival of early-stage follicles in vitro. To test our hypothesis, we investigated the bi-directional crosstalk of the paracrine signals, such as cell-secreted cytokines and transcription factors (TFs), in follicles encapsulated in

alginate in groups of five (5X) and ten (10X). The differential profiles of transcription factor dynamic activity and secretome during folliculogenesis were analyzed using TRanscriptional Activity Cellular aRay (TRACER) and data-driven multivariate modeling approach. This is the first report of our novel systems-level, integrated experimental approach that captured the complexity of signaling pathways that lead to successful ovarian follicle development in vitro. Applied for the first time in large growing organoids, the analysis of TRACER and secreted cytokines revealed critical early interactions between cytokines and TFs which correlated with the observed phenotypical and functional differences between follicles cultured in groups of five and ten. We identified unique signatures of synergism between ovarian follicles during early-stage development, leading to successful follicle development. The discovered novel synergism is a significant step forward towards understanding the underlying mechanisms that dictate the relationship between the extracellular microenvironment and downstream effects on individually cultured primary follicle in vitro. Correlations of TRACER, cytokine, and hormone results with confirmation in phenotype and functionality changes serve as a useful in vitro model in which to molecularly dissect media components and their effects on folliculogenesis across species in vitro. This strategy show great potential in developing new in vitro eIVFGs and the molecular-level understanding that may ultimately enable the development of cell-free, serum-free media for follicles at all developmental stages across species. These findings bring us closer to understanding of mechanisms underlying the downstream effects of interactions between the extracellular microenvironment and early-stage folliculogenesis in vitro.

**Ablation of TRP53, PTEN and CDH1 with RB Inactivation in Ovarian Surface Epithelium Induces Ovarian Cancer Transformation and Metastasis.** Mingxin Shi, Nikola Sekulovski, Allison Whorton, Marilène Paquet, James A. MacLean II, Yurong Song, Terry Van Dyke, and Kanako Hayashi

Ovarian cancer (OvCa) is a poorly understood disease associated with high lethality. While several molecular mutations/alterations have been confirmed in human primary tumors and characterized in animal models, the mechanism of initiation and progression of OvCa still remains unclear. In this study, we examined a quadruple combination of pathway perturbations including TRP53, RB, PTEN and CDH1 (E-cadherin) in the mouse ovary. To specifically characterize the cancer-promoting events in the ovarian surface epithelium, Amhr2-Cre was used to ablate floxed alleles of Trp53, Pten and Cdh1, which were crossed with TgK19GT121 mice, that can Cre-dependently inactivate RB, and its functionally redundant proteins RBL1 (p107) and RBL2 (p130), in KRT19 (cytokeratin 19) expressing cells. At 1.5-2 months of age, mice with conditional ablation/inactivation of TRP53, PTEN, CDH1 and RB (Trp53d/d Pten/d Cdh1d/d TgK19GT121) showed serous micropapillary carcinomas originating from the ovarian surface epithelium. At 2-3 months, serous micropapillary carcinomas invaded into the ovary. At 3 months, no evidence of metastasis to the peritoneal cavity and distant organs was observed in Trp53d/d Pten/d Cdh1d/d TgK19GT121 mice. However, by 4-6 months, these all exhibited clearly defined serous carcinomas with abundant cell proliferation and angiogenesis in the ovary. Furthermore, these tumors were also WT1 positive, and the tumors in 6-month old mice were highly aggressive and disseminated within the peritoneal cavity creating a peritoneal carcinomatosis. We also observed ascites fluid accumulation in Trp53d/d Pten/d Cdh1d/d TgK19GT121 mice starting at 4 months of age. Trp53d/d Pten/d TgK19GT121 mice (without CDH1 ablation) also showed serous micropapillary carcinomas at 3-6 months of age. However, we did not observe any ascites fluid accumulation in Trp53d/d Pten/d TgK19GT121 mice. Interestingly, Trp53d/d Pten/d Cdh1d/d mice (without RB inactivation) exhibited

abnormal uterine phenotype with apparently normal ovarian morphology. Some of these mice exhibited lesions that were similar to endometrial adenocarcinoma described in humans. Kaplan-Meier analysis revealed that the survival time of Trp53d/d Ptend/d Cdh1d/d TgK19GT121 and Trp53d/d Ptend/d TgK19GT121 mice was significantly reduced (P 80-90% of mice had died (or were euthanized due to tumor burden) by 6.5 months of age. In summary, ablation/inactivation of TRP53, RB and PTEN in ovarian surface epithelium initiates serous carcinomas, and additional ablation with CDH1 accelerates tumor dissemination and ascites fluid accumulation enhancing peritoneal carcinomatosis.

**Heat-induced Perturbations in Gap Junction Transfer are Associated with Accelerated Chromatin Condensation in Maturing Bovine Cumulus-Oocyte Complexes.** Kelly Campen, Chelsea Abbott, Louisa Rispoli, Rebecca Payton, Arnold Saxton, and Lannett Edwards

Heat-stressed bovine oocytes undergo germinal vesicle breakdown earlier than non-stressed counterparts which likely contributes to reduced developmental competence after fertilization. Meiotic resumption is coincident with uncoupling of gap junctions that connect the surrounding cumulus cells to the oocyte and to one another. The objective of our study was to determine whether heat stress exposure at the onset of maturation affects cumulus-oocyte complex gap junction communication. Bovine cumulus-oocyte complexes underwent in vitro maturation for 4 h at 38.5°C (control) or at an elevated temperature of 40.0, 41.0 or 42.0°C. Impact on gap junction communication was assessed by examining the transfer of the fluorescent dye calcein from the cumulus to the oocyte. Thereafter, oocyte meiotic progression was evaluated by staining with Hoechst 33342 and scoring based on chromatin configuration. A score of one indicated diffuse chromatin taking up 20-30% of the oocyte surface, scores of two or three indicated condensing chromatin at varying stages, a score of four indicated a single mass of condensed chromatin, whereas a score of five denoted prometaphase I where individual chromosomes were apparent. Heat stress exposure impaired transfer of the calcein dye from the cumulus cells to the oocyte ( $P < 0.0001$ ). Specifically, maturation at 41.0 or 42.0°C reduced dye transfer in cumulus-oocyte complexes by 48 and 40% respectively; dye transfer was similar in control and 40°C treated-oocytes. Subsequent staining with Hoechst revealed oocytes matured at 41.0°C or 42.0°C had higher mean chromatin scores (i.e., advanced condensation;  $P < 0.0001$ ). Average chromatin score of 40°C treated-oocytes was similar to the controls. Application of a gap junction inhibitor, carbenoxolone, reduced calcein dye transfer to the oocyte by approximately 90% ( $P < 0.0001$ ) and accelerated chromatin condensation to a similar extent as observed with heat stress exposure. Subsequent efforts to examine cyclic guanosine monophosphate (cGMP) levels in denuded oocytes and their associated cumulus cells after maturing cumulus-oocyte complexes at 38.5 or 41.0°C for 4 h showed no impact on this important molecule. Findings described herein identify novel cumulus cell components affected by heat stress exposure which may explain, in part, heat-induced hastening of the onset of meiotic progression. This project was supported by Agriculture and Food Research Initiative Competitive Grant no. 2016-67015-24899 from the USDA National Institute of Food and Agriculture.

**Bisecting GlcNAc, the Molecular Epitope of an Anti-sperm Auto-antibody, Ts4 : Its Morphological Characteristics and Identification of the Candidate Glycoprotein(s) Possessing the Sugar Moiety in Mice.** Risako Oda, Hiroshi Yoshitake, Saiko Kazuno, Yoshiki Miura, Takashi Ueno, Mayumi Sakuraba, Kenji Takamori, Akiko Hasegawa, Hiroshi Fujiwara, Satoru Takeda, and Yoshihiko Araki

Glycosylation, one of the most pivotal post-translational processes, is believed to result in changes of the biological functions of glycoproteins. Among N-linked OS structures on glycoproteins, bisecting N-acetylglucosamine (GlcNAc), has recently been associated with cancer progression and metastasis. However, significant heterogeneity and the complex nature of OS chains hampers the elucidation of their exact functions. We previously established a mouse anti-sperm monoclonal antibody (mAb), Ts4, and demonstrated that the mAb is reactive with a specific sugar moiety of glycoproteins containing agalacto-biantennary N-glycan with bisecting GlcNAc carrying fucose residues. Ts4 is an autoantibody, originally generated using splenocytes from immunologically naïve male aged mice, by screening for immunoreactivity against the acrosomal region of epididymal spermatozoa. Fluorescent studies using frozen sections fixed with 4% paraformaldehyde (PFA) demonstrated Ts4 reactivity against epididymal spermatozoa, mature testicular germ cells, and early embryo, but not with ovaries nor other somatic cells of major organs. In mature testicular germ cells, Ts4 showed immunoreactivity to a germ cell specific glycoprotein, TEX101, whereas the mAb immunoreacted to alpha-N-acetylglucosaminidase in the acrosomal region of cauda epididymal spermatozoa. In addition, Ts4 has an inhibitory effect on fertilization in vitro. Since distribution of the Ts4-epitope OS is observed only in reproduction-related regions as described above, the Ts4-reactive bisecting GlcNAc may have roles in the reproductive process. To clarify the distribution of glycoproteins having Ts4-reactive OS chain more precisely, we investigated the molecular expression of the Ts4-epitope using a morphological approach, and identified candidate glycoprotein(s) by immunoprecipitation (IP) combined with liquid chromatography (LC)-tandem mass spectrometry analysis (MS/MS). As an initial step, we used Bouin's solution for organ fixation, because Ts4 is compatible with high preservation fixation. However, immunofluorescent studies using Bouin-fixed sections revealed that Ts4 reacts with testes, ovaries and somatic cells from the embryonic stage through to mature mice, differing from the results of fixation in PFA. These results imply that the nature of Ts4-reactive OS structure in situ (epitope-exposure on the section) may be altered depending on the fixation conditions. Western blot analyses revealed that Ts4 immunoreactivity was observed against a protein with an apparent molecular mass of 65 kDa in testicular samples from 1 to 29 day-post-partum, unlike mature testicular lysates. To identify the Ts4-reactive 65 kDa molecule in immature testes, LC-MS/MS was performed after IP using Ts4. Of the candidate molecules detected, we identified CD73 as an associated protein with Ts4. CD73, otherwise known as ecto-5'-nucleotidase, is a GPI-anchor glycoprotein involved in the mechanism of tumor immune escape, through the production of extracellular adenosine by dephosphorylating AMP. Moreover, adenosine is reported to have a role in capacitation and regulation of germ cell proliferation. Although no direct evidence was shown at present, the bisecting GlcNAc recognized by Ts4 on CD73, may play a role in regulating the early development of germ cells in male gonadal organ. (Supported in part by Grants-in Aid for General Scientific Research Nos. 25462575, 26293358, 16K11111, 17K19734 from the Minister of Education, Culture, Sports, Science & Technology, Japan, and a grant from AMED-CREST, AMED, No. 17gk0110024h0001)

**DNA Methylome Profiling of Cumulus Granulosa Cells Reveals Altered Methylation of Genes Regulating Vital Ovarian Functions in Polycystic Ovary Syndrome (PCOS).** Pooja Sagvekar and Srabani Mukherjee

Polycystic ovary syndrome (PCOS), one of the leading causes of anovulatory infertility is characterised by ovarian, neuroendocrine and metabolic perturbations in women of reproductive age-group. With a global prevalence of 6-15%, it features the presence of multiple ovarian cysts on ultrasonography, irregularity or absence of menses, insulin resistance and hyperandrogenemia. Apart from genetic predisposition, collateral epigenetic repercussions arising due to physiological cross-talk with alterations in the external environmental milieu and changing lifestyles are said to have a substantial impact on PCOS development. These changes necessitate the study of tissue-specific epigenetic alterations in this disorder. The current study lays emphasis on plausible epigenetic transitions occurring in cumulus granulosa cells (CGCs) of women with PCOS. To investigate epigenetic dysregulation associated with this disease, we carried out 'methyl-capture sequencing' (MC-Seq) based whole DNA methylome profiling, so as to identify locus-specific alterations in the methyl-CpG signatures of CGCs obtained from 3 women with PCOS and 3 age-BMI matched, regularly menstruating controls. Paired-end, next generation bisulfite sequencing approach (NGS) was employed to sequence these samples on Illumina HiSeq 2500® platform. Data were analysed using the Bismark methyl analysis tool. Enrichment and annotation of both hypo and hyper methylated sites was carried out for CpG-sites within 10kb upstream of annotated transcription start sites and transcription end sites each. Pyrosequencing and/or direct bisulfite sequencing by Sanger's method were performed to further validate the methylation status of few differentially methylated genes relevant to ovarian function in CGCs of 17 controls and 17 women with PCOS. Additionally, relative transcript expression levels of these genes, and of maintenance and de novo DNA methyltransferases (DNMT1, DNMT3A, DNMT3B), and ten eleven translocation methylcytosine dioxygenases (TET1, TET2, TET3) were evaluated by quantitative real time PCR (qPCR) using Taqman chemistry. Our methyl-seq data revealed a total of 6486 CpG-sites associated with 3840 genes linked with Wnt signaling, integrin and endothelin signalling, G-protein receptor signaling, angiogenesis and chemokine/ cytokine mediated inflammation pathways to be significantly enriched in PCOS. Of these, a total of 3509 CpG-sites representing 1777 genes were found to be hypomethylated while 2977 CpGs associated with 2063 genes were identified as hypermethylated in PCOS. Altered methylation was also noted in several non-coding RNAs regulating vital ovarian functions that are impaired in PCOS. Genes such as androgen receptor (AR), oxidized low density lipoprotein receptor (OLR1), hyaluronan and proteoglycan link protein 1 (HAPLN1), tumor necrosis factor (TNF $\alpha$ ) etc. were differentially methylated, and their transcript expression levels were found to be altered in PCOS. Moreover, the DNMT and TET transcript expression levels were altered in CGCs of these women. Our study findings suggest that the DNA methylation and demethylation machineries are altered in ovaries of women with PCOS, leading us to confer that epigenetic alterations play a crucial role in etiopathogenesis of this complex disorder. Research supported by DST (EMR/2015/001014), ICMR and DAE-BRNS (20150537B01RP01318-BRNS) grants, Govt. of India.

### **Bull Spermatozoa Kinetics is Enhanced by Using Reduced Sperm Number Following Single Layer**

**Colloid Centrifugation Before Freezing.** Alicio Martins Jr., Fernanda Nunes Marqui, Tairini Erica da Cruz, Camila de Paula Freitas Dell' Aqua, Tatiana Issa Uherara Berton, Diego Gouvêa de Souza, and José Antonio Dell' Aqua Júnior

Sperm selection using single layer centrifugation (SLC) has been routinely used in human and equine reproduction before artificial insemination with fresh semen. Recently, this technique also proved to be useful for recovery of bull spermatozoa before freezing. This study aimed to investigate the effects of reduced sperm number per insemination dose derived from selected sperm through SLC before freezing on frozen/thawed sperm movement. Eighteen ejaculates of three Nelore bulls (from six replicates) were collected and only sperm samples with motility  $\geq 60\%$ , concentration  $\geq 1$  billion spermatozoa/ml and total and minor defects  $\leq 30$  and  $10\%$ , respectively, were used. Then, ejaculates were pooled and divided into unselected sperm and selected sperm groups, respectively, with 24 and 12 millions of spermatozoa/straw. Unselected sperm samples were diluted in commercial freezing extender and kept at  $30^\circ\text{C}$  in water bath until cooling and freezing. At the same time one billion of spermatozoa (volume varying from 0.5 to 0.7 ml) was layered on top of 9-ml column of colloidal silane-coated silica particles (Percoll Plus at concentration of 70%) and subjected to centrifugation in 15-ml centrifuged tubes for 13 min at  $839 \times g$  at room temperature. After that, the supernatant was removed and the resulted sperm pellet was immediately diluted in freezing extender to adjust the spermatozoa concentration as mentioned above. Then, all semen samples were cooled for 5 h at  $4^\circ\text{C}$ , filled in 0.50 ml French straws, and frozen in a programmable freezing machine. After the storage period sperm samples were thawed in water bath at  $37^\circ\text{C}/30$  s and immediately evaluated using a computer assisted sperm analyzer. The following spermatoc characteristics were assessed: total motility (TM, %), progressive motility (PM, %), curvilinear velocity (VCL,  $\mu\text{m}/\text{s}$ ), straight line velocity (VSL,  $\mu\text{m}/\text{s}$ ), average path velocity (VAP,  $\mu\text{m}/\text{s}$ ), amplitude of lateral head displacement (ALH,  $\mu\text{m}$ ), beat cross frequency (BCF, Hz), linearity (LIN, %), and straightness (STR, %), and wobble (WOB, %). ANOVA and Tukey's test were used for statistical analysis, with values expressed as mean  $\pm$  standard deviation, and  $P < 0.05$  taken as significant. Results for TM ( $69.1 \pm 6.2$ ), PM ( $61.6 \pm 7.1$ ), LIN ( $70.0 \pm 0.04$ ), STR ( $88.0 \pm 0.05$ ), and WOB ( $80.0 \pm 0.04$ ) were higher in the selected sperm group ( $P < 0.05$ ) than in the unselected sperm (values of  $57.0 \pm 4.4$ ,  $44.3 \pm 2.6$ ,  $55.0 \pm 0.03$ ,  $79.0 \pm 0.02$ , and  $68.0 \pm 0.03$ ), respectively. No difference was found between groups for VCL, VSL, and VAP, but ALH was lower in the selected sperm ( $1.37 \pm 0.1$ ) than in the unselected sperm ( $1.81 \pm 0.12$ ). Bull sperm samples yielded with reduced spermatozoa number after SLC prior to freezing greatly improved the major sperm kinetics parameters. Although only the spermatozoa kinetics parameters were taking into consideration for analysis, the approach described here lends encouragement to optimize the sperm inseminating doses in the bovine frozen semen industry. Acknowledgements: FAPESP (grant # 2015/20986-3), Tairana Artificial Insemination Station, Botupharma, Master Fertility Animal Reproduction, Brazil.

### **Comparative Analysis of the MicroRNA Transcriptome Between Yak and Cattle Provides Insight Into High-Altitude Adaptation.**

Jiuqiang Guan, Keren Long, Jideng Ma, Mingzhou Li, and Xiaolin Luo

Extensive and in-depth investigations of high-altitude adaptation have been carried out at the level of morphology, anatomy, physiology and genomics, but few investigations focused on the roles of microRNA (miRNA) in high-altitude adaptation. We examined the differences in the miRNA

transcriptomes of two representative hypoxia-sensitive tissues (heart and lung) between yak and cattle, two closely related species that live in high and low altitudes, respectively. In this study, we identified a total of 808 mature miRNAs, which corresponded to 715 pre-miRNAs in the two species. The further analysis revealed that both tissues showed relatively high correlation coefficient between yak and cattle, but a greater differentiation was present in lung than heart between the two species. In addition, miRNAs with significantly differentiated patterns of expression in two tissues exhibited co-operation effect in high altitude adaptation based on miRNA family and cluster. Functional analysis revealed that differentially expressed miRNAs were enriched in hypoxia-related pathways, such as the HIF-1 $\alpha$  signaling pathway, the insulin signaling pathway, the PI3K-Akt signaling pathway, nucleotide excision repair, cell cycle, apoptosis and fatty acid metabolism, which indicated the important roles of miRNAs in high altitude adaptation. These results suggested the diverse degrees of miRNA transcriptome variation in different tissues between yak and cattle, and suggested extensive roles of miRNAs in high altitude adaptation.

**Follistatin Supplementation During in Vitro Embryo Culture Improves Developmental Competence of Bovine Embryos Produced Using Sex Sorted Semen.** Mohamed Ashry, KyungBon Lee, Joseph K. Folger, Sandeep K. Rajput, and George W. Smith

Using sex sorted semen to produce offspring of desired sex is associated with reduced developmental competence and lower fertility rates. Previous studies in our laboratory have shown that follistatin (TGF-beta superfamily binding protein) supplementation during in vitro embryo culture increases many indices of embryonic developmental competence, including early cleavage rate and the percentage of embryos that reach blastocyst stage. We have also observed that the positive effects of follistatin are associated with increases in indices of SMAD signaling as well as activation of the AKT pathway. Since embryos produced with sex sorted semen have decreased developmental competence in vitro, we hypothesized that follistatin supplementation will restore in vitro development rates in embryos produced with sex sorted semen and that the increase in developmental capacity will be associated with changes in follistatin regulated pathways. To test these hypotheses, IVF was done using frozen-thawed X-sorted bovine spermatozoa from three different bulls (bull A, B or C), and a control group that was fertilized with unsorted frozen-thawed semen. Follistatin (minimum effective dose from previous studies; 10 ng/ml) was supplemented during the initial 72 h of in vitro embryo culture, then 8-16 cell embryos were isolated, washed and cultured in fresh media without follistatin until day 7. Effects of exogenous follistatin supplementation on early cleavage (30 hpi), total cleavage (48 hpi), development to 8-16 cell (72 hpi) and d7 blastocyst rates were recorded. Gene expression analysis of cell lineage markers (CDX2, NANOG) and downstream targets of SMAD signaling (CTGF, ID2, ID3) by qRT-PCR was performed on blastocysts, whereas, Western blot analysis for phosphorylated (p) AKT-Ser473 and pAKT-Thr308 was performed on embryos collected 10 h after follistatin supplementation. Exogenous follistatin supplementation restored the in vitro developmental competence of embryos produced with sex sorted semen to the levels of control embryos produced with unsorted semen, and comparable results were obtained using sorted semen from three different bulls. The mRNA abundance for SMAD signaling downstream target genes, CTGF (SMAD 2/3 pathway) and ID2 (SMAD 1/5 pathway), was lower in blastocysts produced using sex sorted versus unsorted semen, but mRNA levels for CDX2, NANOG, ID1 and ID3 were similar in both groups. Follistatin supplementation restored CTGF and ID2 mRNA in blastocysts produced using sex sorted semen to levels seen in control embryos. Moreover, levels of

pAKT (Ser-473 and Thr-308) were similar in embryos derived from sex sorted and unsorted semen, but follistatin treatment increased pAKT levels in both groups. Taken together, results demonstrated that follistatin improves in vitro development of embryos produced with sex sorted semen and such effects are associated with enhanced indices of SMAD signaling. (Supported by NIH grant R01HD072972 and by Michigan State University AgBioResearch).

**Treatment with Pigment Epithelium-Derived Factor (PEDF) Reverses the Impaired Inflammatory and Angiogenic Balance in Ovaries of PCOS-Induced Mice.** Irit Miller, Hadas Bar-Joseph, Ido Ben-Ami, and Ruth Shalgi

Polycystic ovary syndrome (PCOS) is the most common endocrine disorder, affecting 5-15% of women of reproductive age; thus being a prevalent cause of female infertility. Inflammation, angiogenesis and hyperandrogenism are considered hallmarks of PCOS; however, the relationship among the three is not well understood. Ovaries of patients with PCOS have increased expression of VEGF and cytokines such as IL6 and IL8. This overproduction is suggested to be responsible for the development of ovarian hyperstimulation syndrome (OHSS), and is frequently seen in PCOS patients. We have previously shown that PEDF, an endogenous potent anti-angiogenic and anti-inflammatory factor, restores the impaired angiogenic-inflammatory balance, which governs OHSS. Moreover, data from our in-vitro PCOS model of human granulosa cells (GC) have shown that dihydrotestosterone (DHT) caused an increase in the levels of IL6 and IL8 concurrently with a decrease in PEDF level. The aim of the current study was to evaluate the role of PEDF and its therapeutic potential in the in-vivo PCOS mice model. For establishing PCOS-mice model, pregnant female mice were treated with DHT on days 16 -18 of pregnancy, thus causing PCOS-like abnormalities in the female offspring. To test PEDF therapeutic abilities in OHSS and PCOS-mice, we injected recombinant-PEDF (rPEDF; 2 mg/kg) S.C. and recorded changes in gene expression and OHSS-parameters. Gene analysis of mice primary GC (mpGC) showed that the levels of IL6 and VEGF in PCOS-mice were higher than in control mice ( $P < 0.05$ ). mpGC of PCOS-mice treated with rPEDF (PCOS+rPEDF) showed a decrease in the excess expression of IL6 and VEGF mRNA compared to PCOS-mice. No change in the expression of PEDF mRNA was detected; though the ratios of PEDF/IL6 and PEDF/VEGF were significantly lower in mpGC of PCOS-mice than in mpGC of PCOS+rPEDF mice ( $P < 0.05$ ). Interestingly, similar to PCOS patients, mpGC of PCOS-mice expressed elevated level of AMH mRNA, higher than control mice ( $P < 0.05$ ); the level of AMH mRNA in mpGC of PCOS+rPEDF mice was similar to that of control mice. To examine PEDF therapeutic abilities, we tested six experimental groups – control superovulated mice "A"; OHSS-induced mice "B"; OHSS-induced PCOS-mice "C"; OHSS-induced PCOS-mice treated with rPEDF "D"; superovulated PCOS-mice "E" and superovulated PCOS-mice treated with rPEDF "F". Induction of OHSS resulted in an increase in all OHSS parameters: significant gain of body weight, increased ovarian weight and an increase in protein leakage into the abdominal cavity of groups "B" and "C", compared to control mice ("A";  $P < 0.05$ ). Interestingly, mice in group "E" exhibited similar OHSS symptoms as those in group "B" ( $P < 0.05$ ). Treatment with rPEDF alleviated the severity of all OHSS parameters significantly, both in mice of groups "D" and "F" (compared with "C"; "D" respectively  $P < 0.05$ ). Our data suggest that intra-ovarian impaired androgens-angiogenic-inflammatory balance is part of a local regulatory loop, which disrupts the expression of GC genes in PCOS, but may be restored by rPEDF treatment. Moreover, our PCOS-mice are predisposed to develop OHSS; thus, they may serve as a suitable research model, which reflects the clinical condition.

**FSH Stimulated Bovine Granulosa Cell Steroidogenesis Involves Both Canonical and Non-Canonical WNT Signaling.** Joseph K. Folger, Mohamed Ashry, Sandeep K. Rajput, and George W. Smith

Although the key roles of gonadotrophins in follicular development are well established, the molecular mechanisms are not fully understood. FSH regulation of aromatase and subsequent estradiol production relies on the transcription co-factor,  $\beta$ -catenin, a key effector of WNT signaling. The WNT signaling system is composed of multiple ligands, known as WNT proteins, and multiple receptor proteins, known as Frizzled proteins, that can signal through both canonical ( $\beta$ -catenin dependent) and non-canonical ( $\beta$ -catenin independent) pathways. Our previous studies demonstrated that treatment with the canonical WNT inhibitor, IWR-1, reduced FSH induced bovine granulosa cell estradiol production. Therefore, we hypothesized that both canonical and/or non-canonical WNT ligands modulate FSH stimulated estradiol production in vitro. To test this hypothesis, we used our well established 6-day granulosa cell culture system to examine the effects of specific WNT ligands on FSH stimulated estradiol production in the absence of endogenous WNT production. After initial experiments to determine the maximally inhibitory dose of LGK-974, a specific PORCN inhibitor that prevents acetylation of endogenous WNT ligands and inhibits secretion, granulosa cells were cultured in the presence of FSH, LGK-974 and increasing concentrations of either WNT2B (a canonical WNT ligand) or WNT5A (a non-canonical WNT ligand). After 6 days of culture, estradiol concentrations in media and the abundance of proteins that are indices of activation of the canonical WNT pathway (CTNNB1) and the non-canonical WNT pathway (phosphorylated (p) LEF1, pJNK and pP38) were determined.

Results demonstrated that LGK-974 was able to inhibit FSH stimulation of estradiol production and abundance of proteins linked to canonical and non-canonical WNT pathway activation. Supplementation with the canonical ligand WNT2B had no effect on FSH stimulated estradiol production from LGK-974 treated cells but rescued the inhibitory effects of LGK-974 on abundance of CTNNB1 (canonical pathway) but not pLEF1, pJNK or pP38 (non-canonical pathway). In contrast, WNT5A treatment rescued FSH stimulated estradiol production and restored indices of activation of both the canonical (CTNNB1 levels) and non-canonical (pLEF1, pJNK and pP38 abundance) WNT signaling pathways in LGK-974 treated bovine granulosa cells. Taken together these results suggest that both canonical and non-canonical WNT pathway activation is linked to FSH stimulation of estradiol production by bovine granulosa cells. Supported by Agriculture and Food Research Initiative Competitive Grant no. 2016-67015-24898, USDA National Institute of Food and Agriculture.

**Effect of Lipopolysaccharide (LPS) Treatment on Gap Junctional Intercellular Communication in Ovine Luteal Endothelial Cells (OLENDO).** Aykut Gram, Anna T. Grazul-Bilska, Alois Boos, and Mariusz P. Kowalewski

Gram-negative bacteria, especially *E. coli*, having a lipopolysaccharide (LPS)-containing outer cell wall, are a common cause of clinical metritis and mastitis in humans and livestock. By its accumulation in follicular fluid, LPS initiates inflammatory reactions following recognition by cell surface Toll-like receptors (TLR2 and, predominantly, TLR4) in the ovary. Subfertility results due to disrupted follicular growth and ovarian cyclic activity, associated with decreased intrafollicular and circulating concentrations of steroid hormones. Accordingly, altered levels of steroidogenic factors, e.g., STAR and HSD3B have recently been shown in the corpus luteum (CL) of LPS-treated cows. Luteal expression of both TLR2 and TLR4 was detected in luteal and endothelial cells in the bovine CL. Interestingly, LPS

treatment did not affect STAR and HSDB3B expression in primary luteal cells isolated from bovine CL or in a luteinized granulosa KK1 cell line. Consequently, we hypothesized that different cellular components of the CL, in particular endothelial cells, might be predominantly involved in initiating inflammatory responses to LPS in the CL. However, the underlying molecular and cellular mechanisms remain unknown.

In order to address our hypothesis, a model cell line has been created using ovine luteal microvascular endothelial (OLENDO) cells. Cells were isolated using Griffonia (Bandeiraea) Simplicifolia Lectin I (BSL-I)-coated magnetic tosylactivated beads (Dynabeads M-450) and immortalized at p = 0 by transfecting them with a plasmid vector expressing the large T-antigen of Simian Vacuolating Virus 40 (pSV40Tag), maintained in Endothelial Cell Growth Media/Media 2 (PromoCell), and characterized. Stable genomic incorporation of the SV40Tag-protein was verified by immunofluorescence and western blot analyses. The endothelial character of OLENDO cells was verified using an acetylated fluorescently-labelled low-density lipoprotein (LDL) uptake assay, BSL-I lectin and VEGFR2 immunofluorescent staining. No staining was detected for markers of other cells, e.g., fibroblasts (COL1) and luteal cells (STAR). The OLENDO cells maintained their morphological cobblestone appearance, tube formation abilities and expression of several gap junctional protein connexins (e.g., Cx37, Cx40 and Cx43) for more than 30 passages. Importantly, OLENDO cells stably expressed TLR2 and TLR4. In experiments using OLENDO cells, LPS-treatment (concentrations 1, 10 and 100ng/ml) disrupted in vitro formation of capillary-like structures in a dose-dependent manner, without affecting the viability and proliferation of cells. The functionality of junctional intercellular communication in LPS-treated cells was assessed by using the scrape loading/dye (Lucifer yellow) transfer technique. Transmission of the dye was strongly inhibited by LPS. Moreover, the expression and cellular localization of Cx43, known for its importance in regulating cell-to-cell communication in endothelial cells, was assessed. This led us to one of the most interesting findings of our in vitro study, which is LPS-induced cellular internalization, and thereby, alteration of Cx43 function. Cumulatively, using immortalized OLENDO cells, we have established a useful in vitro tool for investigating luteal vascular functions. The results obtained support our hypothesis and clearly indicate that LPS disrupts capillary morphogenesis and endothelial barrier function, possibly in association with altered gap junctional intercellular communication mediated particularly by Cx43 and possibly by other Cxs.

**Effect of L-carnitine Supplementation on the in Vitro Production of Bovine Embryos.** Diego F. Carrillo-Gonzalez, Nérida Rodríguez-Osorio, Charles R. Long, and Juan G. Maldonado-Estrada

In vitro embryo production is a valuable tool for basic and clinical research and for accelerating genetic improvement in livestock, in combination with other biotechnologies such as semen sexing, genetic editing and cloning. However, in vitro embryo production is limited by suboptimal culture conditions, leading to low yields, decreased embryo viability and cryotolerance. L-carnitine works mainly as a carrier of free fatty acids from the cytosol to the mitochondria for beta-oxidation, increasing mitochondrial activity and intracellular ATP content. The aim of this study was to evaluate the effects of L-carnitine on mitochondrial activity, reactive oxygen species (ROS), Reduced glutathione (GSH), and lipid droplet content during in vitro oocyte maturation and in vitro culture of bovine embryos. Oocytes collected post-mortem were matured with or without L-carnitine (3.8mM), fertilized and presumptive zygotes were cultured for 66 hpi. Embryos from each group were then subdivided in two new groups to evaluate

L-carnitine supplementation on culture (1.5 mM) until day 8. Oocyte maturation was evaluated based on cumulus expansion; cleavage and blastocyst rates were determined on the initial number of oocytes. Mitotracker green and Nile red dye were used to assess mitochondrial activity and lipid droplet content. Reduced glutathione and ROS were measured using monochlorobimane and dihydrofluorescein diacetate staining respectively. Overall, 408 oocytes, for the control group, and 436, for the treatment group, were evaluated in 13 replicates. The results were subjected to analysis of variance and Tukey test. Cumulus expansion was significantly higher in the L-carnitine group ( $87,11\% \pm 5,3$ ) compared to control group ( $77,71 \pm 10,1$ ) ( $P < 0.05$ ). However, no differences were found in lipid droplet content, mitochondrial activity, GSH, and ROS activity. Moreover, L-carnitine supplementation during embryo culture did not affect cleavage (day 2), blastocyst (days 7 and 8), and hatching (day 9) rates. These results suggest that L-carnitine supplementation during bovine in vitro embryo production improves oocyte maturation, with no overt effect on the developmental rate of the embryos, their mitochondrial activity, lipid content, GSH and ROS levels.

#### **What Does the Unique Pattern of Bovine Sertoli Cell Proliferation Tell Us?** Kimberly Miller and Trish Berger

Sertoli cells line the seminiferous tubules in the testes and play a key role in spermatogenesis. Two waves of Sertoli cell proliferation are recognized in humans, boars, and rhesus monkeys, suggesting that other mammals would exhibit a similar pattern of Sertoli cell proliferation. Laboratory rats and mice lack the two waves of proliferation, but the period of time between birth and puberty is very short in these species. This suggests that the two waves of proliferation might overlap in laboratory rodents, if both waves exist. Our objective was to characterize the pattern of bovine Sertoli cell proliferation between birth and puberty. While the assumption was that cattle have a similar pattern of proliferation to other long-lived mammals, the precise timing of proliferation was largely unknown as previously determined numbers did not clearly distinguish between proliferation and tissue growth. Six groups ( $n = 8$  per group) of Hereford/Angus crossbred bulls were castrated at ages 1, 2, 3, 4, 5, or 6 months. Utilizing immunohistochemical labeling with GATA-4 and quantitative morphometry, the total number of Sertoli cells per testis was characterized by multiplying the density of Sertoli cells by the weight of the testis. Sertoli cell number increased linearly between one and five months of age ( $p < 0.001$ ,  $r = 0.77$ ). The total number of Sertoli cells was similar at five and six months of age, indicating Sertoli cell numbers had reached a plateau. At five months of age, 75% of bulls demonstrated obvious lumen formation with 25% having lumens apparent in all tubules. As only immature Sertoli cells proliferate, the appearance of lumens in the seminiferous tubules at five months of age indicated that Sertoli cell differentiation had occurred and proliferation had ceased. Bulls have a single postnatal, prepubertal interval of Sertoli cell proliferation. Although Sertoli cell number more than quadrupled between 2 and 5 weeks of postnatal age in the boar, this is roughly halfway between gonadal differentiation and puberty. With the longer gestation interval, the halfway interval between gonadal differentiation and puberty occurs in utero in the bovine. Hence, the first postnatal wave of Sertoli cell proliferation in the pig may correspond to a prenatal interval of proliferation in the bovine. The pattern of postnatal Sertoli cell proliferation in the bull differs from that of the boar. Research supported by the UC Davis FAPESP Joint Project.

**Dysregulation of Glucose Transporter 1 and Insulin Receptor Substrate 1 in the Eutopic and Ectopic Endometrium of Macaques with Endometriosis.** Fangzhou Luo and Ov Slayden

Endometriosis is a disorder in women and menstruating nonhuman primates where endometrium-like tissues are present outside the uterine cavity. Patients with endometriosis are reported to have a higher rate of chronic inflammation that can lead to impaired endometrial function. Neutrophil granulocytes are the most abundant leukocytes in circulation, but their abundance is minimal in the endometrium, except during menstruation. Chronic inflammation stimulates the recruitment of neutrophils. Neutrophils generate reactive oxygen species (ROS) during phagocytosis, which creates a heightened inflammatory response. ROS are a stimulant for local hypoxia, which features increased glucose transport and altered cell metabolism. Our working hypothesis is that the endometrium of subjects with endometriosis is in a pro-inflammatory state that promotes the recruitment of leukocytes, altered glucose uptake and metabolism. To explore this hypothesis we assessed expression and immunolocalization of Granulocyte Colony Stimulating Factor (CSF3), Glucose Transporter 1 (GLUT1), and the signaling adapter protein Insulin Receptor Substrate 1 (IRS1) in the endometrium of macaques with induced endometriosis. For comparison, we also assessed these targets in the induced lesions. Adult cycling rhesus macaques (*Macaca mulatta*) were treated with Silastic capsules releasing estradiol E2 and then E2 plus progesterone (P) to stimulate artificial 28-day menstrual cycles. Endometriosis was induced in the artificially cycled animals by seeding of menstrual tissue 72 hours following P withdrawal, concordant with day one of menstruation (n=5). Healthy endometrial tissue was collected from artificially cycled controls (n=5). Quantitative real-time RT-PCR (Q-RT-PCR) was used to detect CSF3, GLUT1 and IRS1 transcript. Immunohistochemistry was validated to localize CSF3, GLUT1, and IRS1 in paraffin embedded tissue sections. Results showed that CSF3 and Glut1 mRNA increased significantly and IRS1 transcript decreased significantly in the endometrium of animals with endometriosis compared to the endometrium of animals without endometriosis. Glut1 is increased and IRS1 decreased in ectopic endometrium. In normal endometrium, CSF3-specific staining was localized to stromal cells in the shedding functionalis during menstruation. In normal endometrium, minimal staining was observed in the proliferative and mid secretory phase of the cycle. However, in monkeys with induced endometriosis, endometrial CSF3 staining was stronger in the stromal cells close to the luminal epithelium and the basal membrane of glandular epithelium during the proliferative phase of the cycle. Intense CSF3 staining was also observed in ectopic lesions. Elevated Glut1 staining was localized to the glandular epithelium in the shedding functionalis zone in disease-free menstruating uterus and decidualized stroma, but was more restricted to the red blood cells during other phases of the cycle. Animals with endometriosis displayed a significant increase in the number of Glut1-positive erythrocytes and an increased eutopic and ectopic stromal cell expression in all phases. A significant decrease of IRS1 staining was seen in endometriosis, but when there was discernible IRS1 staining, GLUT1 expression was confined to the blood vessel. We conclude that increased Glut1 and reduced IRS1 is consistent with the pro-inflammatory and potentially hypoxic conditions induced by the migrated granulocytes. Selectively targeting Glut1 or enhancing IRS1 may modulate these conditions and reduce leukocyte recruitment in the endometrium of subjects with endometriosis. Supported by NICHD U54 HD055744; OD011092.

**Inflammatory Microenvironment Established Between Endometriotic Cells and Macrophages Can Be a Druggable Target for Endometriosis.** Nikola Sekulovski and Kanako Hayashi

Endometriosis is a common gynecological disease, which causes chronic pelvic pain, dysmenorrhea, dyspareunia, irregular uterine bleeding and infertility in women of reproductive age. As current treatment options such as hormone therapies along with laparoscopic surgery for endometriosis are inefficient and plagued by side effects, a critical need exists to characterize mechanistic targets and develop new and effective treatments for endometriosis. We have recently reported that an FDA-approved anthelmintic drug, niclosamide, reduces growth and progression of endometriosis-like lesion, as well as inflammatory signaling including NF $\kappa$ B and STAT3 using mice as a model. Niclosamide treatment did not disrupt ovarian and uterine function. In this study, we examined further inhibitory mechanisms by which niclosamide affects endometriotic lesions using an endometriotic cell line, 12Z, and macrophages differentiated from a monocytic THP-1 cell line. Comparable to the *in vivo* findings, niclosamide dose dependently reduced 12Z cell proliferation and STAT3 activity, and increased both cleaved caspase-3 and cleaved PARP. To resemble the inflammatory microenvironment in endometriotic lesions, we exposed 12Z cells to macrophage conditioned media (CM). Macrophages were differentiated from THP-1 cells using Phorbol 12-myristate 13-acetate (PMA) as M0, and then M0 macrophages were further activated into M1 or M2 using LPS/IFN $\gamma$  or IL4/IL13, respectively. CM from M0, M1 or M2 cultures increased 12Z cell proliferation. This effect was blocked by niclosamide, and proliferation returned to that of control media from cells treated with niclosamide alone. To assess proteins targeted by niclosamide in 12Z cells, CM from 12Z cells cultured with M0, M1 or M2 with/without niclosamide were analyzed by cytokine/chemokine antibody array kits. CM from M0, M1 and/or M2 stimulated the secretion of ANG, ANGPT2, BDNF, BSG, CCL2, CCL5, CCL12, CCL17, CCL19, CCL22, CHI3L1, CST3, CXCL11, CXCL8, CXCL12, CXCL17, FGF2, GDF15, ICAM1, IGFBP3, IL4, IL10, IL11, IL17A, IL22, LCN2, PDGFA, RARRES2, VCAM1 from 12Z cells. Specifically, M2 CM increased ANG, ANGPT2, BDNF, CCL5, CCL17, CST3, CXCL11, CXCL12, ICAM1, IGFBP3, IL10, IL11, IL17, LCN2, PDGFA, THBS1, VCAM1. Production of most of these secreted cytokines/chemokines in 12Z cells was inhibited by niclosamide. Based on the stimulation of protein secretion by M0, M1 and/or M2 macrophages and inhibition by niclosamide, we have selected CCL5, CXCL12, IL22, MDK, and THBS1 for further analysis. When we knocked down each gene in 12Z cells using siRNA, 12Z cells exhibited reduced proliferative activity. These results indicate that niclosamide can inhibit the inflammatory microenvironment established between endometriotic cells and macrophages by targeting STAT3 signaling. Furthermore, cytokines/chemokines stimulated by macrophages and targeted by niclosamide have critical functions in endometriotic cells. Supported by NIH/NICHD, R21HD092739.

**Super-Resolution Imaging of Live Sperm Reveals Specific Dynamic Changes of the Actin Cytoskeleton During Acrosomal Exocytosis.** Ana Romarowski, Angel G Velasco Felix, Maria G Gervasi, Xinran Xu, Paulina Torres Rodriguez, Guillermina M Luque, Claudia Sanchez-Cardenas, Hector V Ramirez-Gomez, Diego Krapf, Pablo Visconti, Dario Krapf, Adan Guerrero, Alberto Darszon, and Mariano Buffone

Acrosomal exocytosis is an absolute requisite for fertilization in mammals. This complex exocytic process is controlled by several players including changes in the actin cytoskeleton. Most studies to evaluate actin polymerization (formation of filamentous actin or F-actin) in mammalian sperm were performed using phalloidins, which are toxic and not capable of crossing the cell plasma membrane. As a result, it is

not possible to use this approach to study this dynamic process in real time using live cells. SiR-actin is a novel membrane permeable fluorescent probe that binds to actin filaments in vivo. Using this new tool, we aimed to examine actin polymerization dynamics in live mouse sperm. We observed by image-based flow cytometry a capacitation-induced increase in polymerized actin levels ( $n=12$ ,  $p < 0.05$ ). We found 6 F-actin structures within the sperm head: perforatorium, lower acrosome, upper acrosome, ventral, septum and neck. The same structures were also observed when we used sperm from transgenic mice expressing LifeAct-EGFP, supporting our in vivo observations using SiR-actin. A six positions binary code was used to analyze their possible combination present in the sample. The proportion of five of the structures combinations statistically changed with capacitation ( $n=3$ , analyzed cells=600,  $p < 0.05$ ). We were able to observe in great detail these F-actin structures using super-resolution microscopy. We evaluated the dynamic actin cytoskeletal changes at the onset of acrosomal exocytosis, by labelling sperm with SiR-actin and FM4-64 (a marker of acrosomal exocytosis). Interestingly, we found that in all sperm that possessed the septum or the lower acrosome F-actin structure, the actin cytoskeleton depolymerized in those regions prior to ionomycin induced acrosomal exocytosis, while the rest of the F-actin structures remained unchanged or were lost after exocytosis occurred. Thus, we have simultaneously visualized actin dynamics and acrosomal exocytosis by super-resolution in vivo and demonstrated for the first time that actin depolymerization occurs in specific regions of the sperm head during the acrosomal exocytosis. Our work emphasizes the utility of live-cell nanoscopy for the study of sperm ultra-structures, given that these imaging capabilities will undoubtedly impact the search for mechanisms that underlie basic sperm functions. Research supported by NIH-RO1TW008662, Eunice Kennedy Shriver National Institute of Child Health and Human Development, NIH-RO1HD38082, PICT 2015-2294, National Science Foundation 1401432 and Red de Macrouiversidades.

**Transcriptomic Analysis Reveals that Genes Related to Oxidative Phosphorylation are Downregulated in Embryos Obtained with Frozen Thawed Sperm.** J. M. Ortiz, M. C. Gil, C. Ortega, and F. J. Peña

Equine embryos were harvested by uterine flush snap frozen in LN and stored at  $-80^{\circ}\text{C}$ . RNA was isolated using the kit PicoPure™ RNA Isolation Kit. Libraries were built for RNA-seq analysis in an IonTorrent next-generation sequencer. The raw reads were aligned to a horse transcriptome generated using ENSEMBL (Equ Cab 2 ). Then, custom scripts were used to transform BAM reads into transcript counts, and RPKM scores for each gene were retrieved. To obtain statistically significant gene expression differences first, we calculated the random RPKM differences between two conditions by permutation of the RPKM gene scores. Then we chose the genes whose expression difference between the two conditions was higher than in 99% (P AGL2017-83149-R).

**Suppressing Inflammatory Responses in Endometrial Lesions by Reducing the Secretion of Cytokines and Chemokines.** Allison Whorton, Nikola Sekulovski, Tomoki Tanaka, Yasushi Hirota, James A. MacLean II, Mingxin Shi, J. Ricardo Loret de Mola, Kathleen Groesch, Paula Diaz-Sylvester, Teresa Wilson, Liliana Palencia, Andrea Braundmeier-Fleming, and Kanako Hayashi

Endometriosis affects 6-10% of women of reproductive age, and approximately 50% of affected women experience severe chronic pelvic pain and infertility. Because endometriosis is an estrogen-dependent disease, the most widely used medical drugs are oral contraceptives, GnRH agonists and progestins,

which suppress ovarian function and subsequently reduce pelvic disease and associated pain. However, these hormonal treatments are often of limited efficacy, elicit side-effects, and temporarily inhibit fertility. Additionally, these treatments are ineffective long-term, ultimately resulting in high recurrence rates. Therefore, it is necessary to identify new therapeutic targets and effective drug(s) that improve current treatment. Recently, we have reported that a FDA-approved anthelmintic drug, niclosamide, reduces growth and progression of endometriosis-like lesions, as well as inflammatory signaling including NF $\kappa$ B and STAT3 using a mouse model. Several genes related to inflammatory responses, WNT, and MAPK signaling were shown to be downregulated by niclosamide. Niclosamide treatment does not disrupt ovarian or uterine function including estrous cycles, ovulation, pregnancy rate, gestational length and litter size. In order to better understand the effects of niclosamide, we used primary human endometriotic stromal cells (hESC), isolated from endometriomas from consenting subjects who underwent laparoscopic surgery for endometriosis. Similar to our in vivo findings, niclosamide dose-dependently suppressed hESC proliferation; furthermore, addition of estradiol-17 $\beta$  did not change the effects of niclosamide. Niclosamide inhibited STAT3 activation in hESC. To mimic the actual inflammatory microenvironment of endometriosis, we exposed hESC to macrophage conditioned media (CM). Macrophages were differentiated using granulocyte-macrophage colony-stimulating factor (GM-CSF) or macrophage-CSF (M-CSF) from monocytes isolated from primary blood mononuclear cells (PBMC). Activation of the macrophages was achieved using LPS, IFN $\gamma$ , IL-4, IL-10 and/or IL-13. During the exposure of hESC to CM, cells were treated with niclosamide (control cultures were treated with vehicle). Using proteome human chemokine and cytokine array kits, we analyzed the hESC secretion of over 100 chemokine and cytokines. Subsequent treatment with CM from macrophage cultures stimulated hESC to secrete: ADIPOQ, CD40LG, CCL5, CCL7, CCL17, CCL18, CCL20, CCL22, CXCL5, CXCL9, CXCL10, CXCL11, CXCL17, FASLG, FGF2, FGF7, HAVCR2, IL1RL1, IL3, IL4, IL5, IL6, IL6ST, IL22, IL23, MMP9, PECAM1, PDGFA, PLAUR, RBP4, VEGF, and XCL1. Production of most of these secreted cytokines/chemokines was abrogated by niclosamide. Collectively, niclosamide treatment can potentially improve the microenvironment surrounding endometriotic lesions in vivo with minimal cytotoxic and hormonal effects. Supported by NIH/NICHD, R21HD092739.

**Knockout analysis of Oocyte-Specific Multi-Copy Gene, Oog1.** Yuka Miki, Satoshi Tsukamoto, Hiroshi Imai, and Naojiro Minami

Sex-specific genes in germ cells contribute to maintain the sex identity of germ cells. The hierarchy in the control of sex-specific genes ensures proper sex-specific germ cell development. Oog1 is an oocyte-specific gene and seems to function as a transcription factor during meiosis. In Oog1-knockdown (KD) oocytes, sperm-specific genes such as Tektin2 (Tekt2), Tudor Domain Containing 6 (Tdrd6), Kelch Like Family Member 5 (Klhl5) and Transition Protein 2 (Tnp2) were upregulated and oocyte-specific linker histone H1foo was downregulated, suggesting that Oog1 suppresses sperm-specific genes and activates oocyte-specific genes in oocytes to maintain the female sex. Significant phenotype, however, is not observed in Oog1-knockdown mice. We thought that knock out (KO) analysis is more effective because any mRNA is not produced. We tried to produce Oog1-knockout mice using CRISPR/cas9 system. It is challenging because Oog1 has 5 copies. We have knocked out some of all 10 alleles using three kinds of gRNAs shared by all 5 copies. Two gRNAs are on the exon 3 and the other is on the exon 4. Each gRNA binding region contains restriction enzyme recognition site, AseI, AclI or SspI. If the region has been knocked-out, the restriction enzyme can not digest the region. Five pairs of PCR primers specific to each

copy were designed to amplify only targeted copies. Even though 5 copies share high homology, these copy-specific primers mainly amplify targeted copies. Fifty percentages of TA cloning products successfully have the targeted Oog1 copy. After PCR with these primers, the PCR products were digested by AseI, AclI or SspI to select CRISPR/Cas9 mediated mutation of each Oog1 copy. The result of restriction enzyme treatment indicates that 3 copies are knocked out in one male mouse line (#1), and 2 other copies are knocked out in another line (#2). All 5 copies are mutated in the third line (#3). We next intend to generate KO female mice with all alleles mutated by mating these CRISPR/Cas9 transgenic mouse lines and examine the detail function of Oog1.

### **The Cell Type-Specific Expression of Lhcgr in Mouse Ovarian Cells During Follicular Development**

**Process: Evidence for a DNA-Demethylation Dependent Mechanism.** Tomoko Kawai, S. A. Masudul Hoque, JoAnne S. Richards, and Masayuki Shimada

During follicular development, ovarian somatic cells proliferate and then differentiate: mural granulosa cells attach to follicular basal lamina and cumulus cells directly surround the oocyte. Mural granulosa cells in preovulatory follicles express the LH receptor (Lhcgr) and in response to the LH surge terminally differentiate into luteal cells. In contrast, cumulus cells do not luteinize, in part, because cumulus cell functions and Lhcgr expression are suppressed by oocyte-secreted factors. In this study, we investigated whether the cell type specific differentiation and expression of Lhcgr in mural granulosa cells compared to cumulus cells is regulated by DNA-methylation of the Lhcgr promoter. Granulosa cells and cumulus cells were collected from control or eCG-treated immature mice and prepared for gene expression qPCR analyses or bisulfite sequence analyses. In granulosa cells, methylation of CpG islands within the Lhcgr promoter region decreased significantly when immature mice were treated with eCG whereas methylation of the Lhcgr promoter remained high in cumulus cells. RA levels are significantly increased in granulosa cells but not in cumulus cells of eCG-injected mice. When mice were by co-injected with a retinoic acid (RA) synthase inhibitor, 4-methylpyrazole, and eCG, demethylation of Lhcgr promoter region and Lhcgr mRNA expression in granulosa cells were significantly blocked. To determine the underlying mechanisms by which RA levels increase in granulosa cells but not in cumulus cells, the expression of genes involved in RA synthesis and degradation were examined by qPCR. In granulosa cells, genes encoding enzymes controlling RA synthesis were induced whereas a gene involved in RA degradation, Cyp26b1, was down-regulated by eCG. In cumulus cells, Cyp26b1 expression was significantly higher as compared with that in granulosa cells, suggesting that RA is rapidly and selectively degraded in cumulus cells and that this impacts DNA-methylation of the Lhcgr promoter region.

Interestingly, co-culture of GV stage oocytes with granulosa cells significantly increased DNA methylation of the Lhcgr promoter and Cyp26b1 expression. When cumulus oocyte complexes (COCs) were cultured with RA, demethylation of Lhcgr promoter region and Lhcgr expression were significantly induced in cumulus cells. Similar changes were observed in cumulus cells of COCs treated with SMAD inhibitor, SB431542, suggesting that oocyte-secreted factors activate a SMAD pathway leading to the induction of Cyp26b1, rapid degradation of RA and methylation of the Lhcgr promoter. One possible mechanism by which RA regulates demethylation of the Lhcgr promoter in granulosa cells is by suppressing DNA methyltransferase (Dnmt1) expression. Reduced methylation of Lhcgr promoter region was also suppressed when granulosa cells were cultured with a cell cycle inhibitor, aphidicolin. Thus, demethylation of the Lhcgr promoter region appears dependent on the failure of methylation related to

both cell proliferation and reduction of DNMT1 in granulosa cells. In summary, our results show SMADs→ Cyp26b1↓ RA↓ DNMT1↓ Lhcgr methylation→ Lhcgr expression that the induction of RA in granulosa cells but not in cumulus cells impacts cell type specific DNA methylation patterns. Oocyte-secreted factors acting via SMADs are associated with the epigenetic regulation of follicular somatic cells.

**The Role and Regulation of Peroxisome Proliferator-Activated Receptor Gamma Coactivator 1-Alpha (PGC1 $\alpha$ ) in Decidualization of Human Endometrial Stromal Cells.** Haruka Takagi, Isao Tamura, Yuichiro Shirafuta, and Norihiro Sugino

Introduction: Decidualization is the process that endometrial stromal cells (ESCs) differentiate into decidual cells by progesterone. During this process, a number of genes are up-regulated by the activation of various transcription factors. Peroxisome proliferator-activated receptor gamma coactivator 1-alpha (PGC1 $\alpha$ ) is a transcriptional coactivator that regulates the expression of genes involved in mitochondrial energy metabolism, glucose metabolism and fatty acid oxidation. The roles of PGC1 $\alpha$  in reproductive organs have been reported, e.g. upregulation of steroidogenesis of ovarian granulosa cells or activation of energy metabolism of testicular sertoli cells. PGC1 $\alpha$  is also expressed in human ESCs and its expression increases with decidualization. However, the function of PGC1 $\alpha$  in the endometrium is still unclear. The present study was undertaken to investigate the involvement of PGC1 $\alpha$  in the regulation of decidualization. Materials and methods: This study was approved by IRB of Yamaguchi University. (1) PGC1 $\alpha$  protein expression in the human endometrium was examined by immunohistochemistry. (2) ESCs isolated from the proliferative endometrial tissue were incubated with or without dibutyryl-cAMP (cAMP, 0.5 mM) for 4 days to induce decidualization and PGC1 $\alpha$  mRNA expression was examined by qPCR. Decidualization was evaluated with the mRNA expressions of IGF-binding protein-1 (IGFBP-1) and prolactin (PRL), which are recognized as specific markers of decidualization. To investigate the role of PGC1 $\alpha$  in decidualization, PGC1 $\alpha$  was knocked down by siRNA and expressions of IGFBP-1 and PRL were examined in the presence or absence of cAMP. (3) To investigate the mechanism by which PGC1 $\alpha$  is up-regulated by cAMP, we focused on C/EBP $\beta$  that regulates many gene expressions during decidualization. C/EBP $\beta$  was knocked down by siRNA and PGC1 $\alpha$  expression was examined in the presence or absence of cAMP. (4) Because public ChIP-sequence data of other cell lines shows the existence of C/EBP $\beta$  binding site in the enhancer region of PGC1 $\alpha$  gene, the C/EBP $\beta$  binding to this enhancer region was examined by ChIP assay. (5) To examine the enhancer activity of the enhancer region in the second intron of PGC1 $\alpha$  gene, luciferase assay was performed. (6) To test the endogenous function of the PGC1 $\alpha$  enhancer region on PGC1 $\alpha$  expression, the endogenous PGC1 $\alpha$  enhancer region was deleted by CRISPR/Cas9 system in HepG2 cells. Results: (1) PGC1 $\alpha$  protein was expressed in stromal cells in the late proliferative phase endometrium, and its expression increased in those in the late secretory phase. (2) cAMP increased PGC1 $\alpha$  expression with the induction of IGFBP-1 and PRL. Knockdown of PGC1 $\alpha$  significantly inhibited cAMP-induced expressions of IGFBP-1 and PRL. (3) Knockdown of C/EBP $\beta$  decreased cAMP-induced PGC1 $\alpha$  expression. (4) cAMP increased the C/EBP $\beta$  binding to the PGC1 $\alpha$  enhancer region. (5) cAMP increased luciferase activities of the PGC1 $\alpha$  enhancer region. (6) PGC1 $\alpha$  mRNA levels were significantly inhibited by the deletion of the PGC1 $\alpha$  enhancer region. Conclusions: PGC1 $\alpha$  is an important transcription factor regulating decidualization in human ESCs. C/EBP $\beta$  is an upstream gene that regulates PGC1 $\alpha$  expression by binding to the novel enhancer region.

**Embryotropic Effects Of VEGF on in Vitro Produced Porcine IVF Embryos.** Dibyendu Biswas, Kyoung-Ha So, Gab-Sang Lee, and Sang-Hwan Hyun

Several published studies recently suggested that supplementation of vascular endothelial growth factor (VEGF) in IVM/IVC medium had beneficial effects on porcine embryos development in vitro, however, underlying molecular signaling mechanism nevertheless clear. The aim of the current study was to evaluate the molecular signal of embryos development throughout in vitro culture with VEGF of porcine embryos. In vitro matured porcine oocytes were utilized in this study and after fertilization the zygotes were cultured with 5ng/ml VEGF supplemented with and/or without FBS on day-4 until day-7. Real time qPCR was applied to confirm the expression pattern of apoptosis and oxidative stress related genes of day-7 blastocyst (BL). Early stage of apoptosis was measured by Annexin-V assay of day-2 and day-7 embryos. In these study, it had been found that addition of VEGF throughout the culture period mimics the embryo development and it absolutely was significant ( $p < 0.05$ ) than control and also either in presence or absence of FBS on day-4. Supplementation of VEGF in absence of FBS significantly ( $p < 0.05$ ) increased the early BL formation but addition of FBS on day-4 significantly ( $p < 0.05$ ) increased the hatched blastocyst formation either in presence or absence of VEGF. However, supplementation of VEGF in presence of FBS synergistically increased the expanded BL formation compared to only FBS supplementation. The average total cells number per BL was significantly higher in VEGF supplemented group in absence of FBS but supplementation of FBS synergistically increased the cell number in presence of VEGF. Reactive oxygen species (ROS) accumulation was significantly ( $p < 0.05$ ) reduced in VEGF treated BL in presence and/or absence of FBS. On the other hand, mRNA expression of caspase-3 was significantly ( $p < 0.05$ ) reduced in presence of VEGF compared to embryo culture with or without FBS. Moreover, mRNA expression of Bcl-2 was significantly ( $p < 0.05$ ) higher in VEGF treated embryos without supplemented of FBS. However, mRNA expression of Nrf-2 was significantly higher in VEGF treated BL in absence and/or presence of FBS supplementation. On day-2, the viable embryos ( $44.06 \pm 3.94\%$ ) and blastomeres ( $67.18 \pm 3.60\%$ ) were significantly ( $p < 0.0001$ ) higher in VEGF treated BL compared to control. On the other hand, early apoptotic embryos ( $55.94 \pm 3.94$ ) and blastomeres ( $23.23 \pm 4.22$ ) were significantly ( $p < 0.0001$ ) lowered in VEGF treated group than control. On day-7 BL, early apoptotic cells were significantly ( $p < 0.05$ ) lowered in VEGF treated BL in presence and/or absence of FBS. These results recommended that the supplementation of VEGF during in vitro culture of porcine IVF embryos increased the developmental potential by increased expression of Nrf-2 signal that reduced the ROS production and reduced programmed cell death process throughout in porcine IVF embryos.

**Acknowledgments:** This work was supported, in part, by a grant from the Global Research and Development Center (GRDC) Program through the NRF funded by the Ministry of Science and ICT (2017K1A4A3014959), the Korea Research Fellowship Program through the National Research Foundation of Korea (NRF) funded by the Ministry of Science and ICT (NRF-2015H1D3A1066175, NRF-2017R1A2B4002546), South Korea.

### **Epididymal Spermatozoa for in Vitro Fertilization of Bovine Oocytes: Reduction in Co-Incubation Time.**

Andrielle Thainar Mendes Cunha, Gabriela Oliveira Fernandes, Felipe Manoel Caixeta, José Oliveira Carvalho, and Margot Alves Nunes Dode

Epididymal spermatozoa and their use in assisted reproductive technologies, such as in vitro embryo production (IVEP), have an important role in the multiplication of genetic material from sires that die suddenly and/or have acquired reproductive failure. However, in order to establish an appropriate procedure to use those sperm in IVEP in bovines, a better knowledge about their physiological behavior facing the events involved in IVEP is needed. The aim of this study was to evaluate different sperm-oocyte co-incubation times when epididymal (EP) spermatozoa are used for bovine IVEP. A pool of EP and ejaculated (EJ) cryopreserved spermatozoa, recovered from seven Gir bulls through electroejaculation and followed by bilateral orchietomy were used. The pool of EJ group was considered the control and were selected in Percoll gradient 45%-90% (GE Healthcare Bio Science, Uppsala, Sweden), and EP group were selected in PureSperm gradient 40%-80% (Nidacon Laboratories AB, Gothenborg, Sweden). Four groups were formed based on sperm-oocyte co-incubation time: EJ sperm co-incubated with oocytes per 18 h, control group (EJ18); EP sperm co-incubated with oocytes per 6 h (EP6); EP sperm co-incubated with oocytes per 12 h (EP12) and EP sperm co-incubated with oocytes per 18 h (EP18). After selection, sperm samples were co-incubated with a total of 627 cumulus-oocyte-complexes (COC's) in fertilization medium in a 5 replicates experiment. After fertilization embryos were evaluated on day (D) two (D2), for cleavage and on D6 and D7 for blastocyst rates. At D7 expanded blastocysts were assessed for a total and apoptotic cell number using the Transferase desoxynucleotidil Terminal dUTP (TUNEL) test. Embryo development data were analyzed using Chi-square (mean±SD;  $P \leq 0.05$ ) and TUNEL data by Tukey using Prophet 5.0 ( $P \leq 0.05$ ). No differences ( $P > 0.05$ ) were observed among treatments for cleavage (EJ18=78.0%; EP6=74%; EP12=77% and EP18=82%) or blastocyst rate on D6 (EJ18=23%; EP6=24%; EP12=21% and EP18=23%) and D7 (EJ18=42%; EP6=38%; EP12=40% and EP18=46%). In addition, neither the blastocyst rate at D6 or the kinetics of embryos development varied among treatments ( $P > 0.05$ ). The mean of total number of cells and the percentage of apoptotic cells were also similar between EJ18 (158;4.0%), EP6 (174;4.0%) EP12 (164; 4.2%) and EP18 (173;4.0%) treatments. These results suggested time required for bovine EP spermatozoa to fertilize in vitro matured oocytes is less than the time needed for EJ spermatozoa. Therefore, sperm-oocyte co-incubation time can be reduced for 6 h without affecting embryo production and embryo quality.

### **Prenatal Exposure to Bisphenol a Analogues, BPE And BPS, Impact on Male and Female Reproductive Functions in Mice.** Mingxin Shi, Nikola Sekulovski, James A. MacLean II, and Kanako Hayashi

Bisphenol (BP) A has been well-known as an endocrine disruptor that affects development and function of the reproductive system and causes fertility problems. Due to its toxic effects in humans, structurally similar analogues such as BPS have been used as alternatives for BPA. In this study, we examined whether prenatal exposure to BPE and BPS negatively impacts male and female reproductive functions using mice as a model. CD-1 mice (F0) were orally exposed to control treatment (corn oil), BPA, BPE and BPS (0.5, 20 or 50  $\mu\text{g}/\text{kg}/\text{day}$ ) from gestational day 11 (GD11) to birth. In F1 males, sperm counts were significantly reduced by BPA, BPE or BPS on postnatal day (PND) 60, and only BPE or BPS exposure exhibited reduced sperm motility. Exposure to BPA, BPE or BPS disrupted the progression of germ cell development, as morphometric analyses exhibited an abnormal distribution of the stages of

spermatogenesis. BPS (50 µg/kg/day) increased the level of serum estradiol-17β in adult males. On PND12, BPE or BPS significantly increased TUNEL positive cells in neonatal testis, following disruption of the expression of apoptosis, autophagy and oxidative stress related factors. The expression of methyltransferases for DNA methylation and histone modification was also affected by prenatal exposure to BPA, BPE or BPS in neonatal testis, suggesting epigenetic regulation is altered. In F1 females, vaginal opening as the age of puberty was detected 1-2 days earlier than controls in BPA, BPE or BPS groups. Following vaginal opening, mice from BPA, BPE or BPS exposure showed irregular estrous cyclicity with several days in estrus and diestrus. When females were mated with normal males at 3, 6 and 9 months, mice at 6 and 9 months took longer time to exhibit vaginal plugs. Especially, a few mice at 6 months and further increased number of mice at 9 months with no plug were observed in all BP groups, leading to reduction of successful pregnancy at older ages. We also observed loss of pregnancy after mice received the plug, and increased parturition and nursing issues of mice in all BP groups at 9 months. Additionally, serum testosterone levels were significantly increased by BPE or BPS at 9 months. On PND4, follicular development has already been altered by BP exposure. BPA or BPE exposure increased germ cells to remain in nests, and BPA, BPE or BPS decreased primary and/or secondary follicles. In summary, these results suggest that prenatal exposure at physiologically relevant doses to BPA analogues, BPE and BPS, affects male and female reproductive functions probably due to spermatogenic defect and folliculogenesis in the developing testis and ovaries, respectively.

#### **Effects of Single Layer Colloid Centrifugation and Insemination Dose with Reduced Spermatozoa Number on Bull Sperm Membrane Integrity and Conception Rate after Timed Artificial Insemination.**

Alicio Martins Jr., Tairini Erica da Cruz, Fernanda Nunes Marqui, Camila de Paula Freitas Dell' Aqua, Tatiana Issa Uherara Berton, Fernando Franco Polizel, and José Antonio Dell' Aqua Júnior

Sperm membrane integrity plays an important role in maintaining the spermatozoa movement and their fertilizing ability. However, as well known, spermatozoa can keep moving even when carrying plasma and/or acrossomal membrane damages. The purpose of this study was to verify the influence of reduced spermatozoa number per insemination dose from ejaculates derived from single layer centrifugation (SLC) on post-thawing sperm membrane integrity and conception rate after timed artificial insemination (TAI). Semen of three Nellore bulls (six ejaculates of each one) was collected at Artificial Insemination Station. After routine work evaluations, the pooled sperm samples (three ejaculates per collection) were divided into unselected sperm group, in which semen was immediately diluted in freezing extender (24 x 10<sup>6</sup> sperm/straw) and in the selected sperm group with doses adjusted to a final concentration of 12 x 10<sup>6</sup> sperm/straw. Selected spermatozoa were obtained through SLC with silane-coated silica particle solution (Percoll Plus). One billion of spermatozoa was placed on top of 9-ml column of 70% colloid (in 15- ml centrifuge tubes) and then, centrifuged at 830 x g for 13 min at room temperature. The supernatant was discarded, the sperm pellet counted and diluted as mentioned above. Following frozen-thawed sperm samples of both groups were assessed simultaneously for plasma and acrossomal membrane integrity (PAMI) and translocation of phosphatidylserine (TPS) using propidium iodide, fluorescein isothiocyanate conjugated with *Pisum sativum* agglutinin and annexin V, whereas YO-PRO-1 dye was employed to detect plasma membrane destabilization (PMD). A cell-permeate nuclear counterstain was used throughout the staining protocols. Ten thousand gated-events were analysed per sample through use of flow cytometer. A total of 130 inseminations were performed in Nellore and crossbred Nellore cows synchronized in an 11-day

protocol based on estradiol, progesterone, PGF2 $\alpha$  and equine chorionic gonadotropin. Conception rate (CR) was determined by ultrasound 38 days after TAI. Data was analyzed through use of ANOVA, Tukey's test and logistic regression (least squares means, GLIMMIX of SAS) with  $P < 0.05$  considered as significant. There was significant difference ( $P < 0.05$ ) between unselected and selected groups for PAMI ( $53.8 \pm 1.7$  vs.  $38.8 \pm 2.1\%$ , respectively). Higher percentage of intact cells ( $P < 0.05$ ) with no TPS ( $54.9 \pm 1.64$  vs.  $34.8 \pm 1.8$ , respectively) and without PMD ( $52.6 \pm 1.5$  vs.  $31.2 \pm 2.1$ , respectively) were observed in the unselected sperm in comparison to selected sperm group. Despite the increased proportions of spermatic membranes changes detected in the selected sperm group, CR (preliminary data, one of two random replicates) was similar between unselected and selected sperm groups with values of 60.9% (39/64) and 68.2% (45/66), respectively. In short, insemination doses with reduced spermatozoa number obtained through SLC even exhibiting higher sperm membrane damage did not negatively influenced the CR. Moreover, these findings open horizons to further investigations that lead to the establishment of reliable spermatic standards, avoiding the use of questionable frozen bull semen in artificial insemination programs. Acknowledgements: FAPESP (grant 2015/20986-3), Tairana Artificial Insemination Station and Botupharma, Brazil.

**Regulation of Human Follicle-Stimulating Hormone  $\beta$  Expression (FSHB) by Activins, SMAD4, and FOXL2 in Pituitaries of Transgenic Mice.** Luisina Ongaro, Gauthier Schang, T. Rajendra Kumar, Mathias Treier, Chu-Xia Deng, and Daniel J. Bernard

Follicle-stimulating hormone (FSH) is an essential regulator of fertility in female mammals. The hormone is synthesized by pituitary gonadotrope cells in response to GnRH stimulation from the hypothalamus and/or to activins (or related ligands) in the pituitary. Activin signaling is initiated upon ligand binding to complexes of type I/type II receptor serine/threonine kinases, which phosphorylate SMAD proteins. Complexes of SMAD3 and SMAD4 accumulate in the nucleus where they bind the proximal promoter of the FSH $\beta$  subunit gene (*Fshb*) in combination with forkhead box L2 (FOXL2). Female mice with conditional deletions of *Smad4* and *Foxl2* in combination in gonadotropes are FSH deficient and sterile. It is presently unclear whether human FSHB expression is regulated by activins and, if so, by similar mechanisms. Human FSHB promoter-driven reporters are poorly responsive to activins in immortalized murine gonadotrope cells and SMAD/FOXL2 cis-regulatory elements identified in murine *Fshb* are not perfectly conserved in human FSHB. To determine a potential role for activin signaling in human FSHB expression, we employed a mouse model in which mice harbor a 10-kb human FSHB transgene (hereafter hFSHB+), and express the corresponding mRNA and protein specifically in gonadotrope cells. We cultured pituitaries from hFSHB+ mice and measured both murine *Fshb* and the human FSHB mRNA levels under a variety of conditions. As expected, murine *Fshb* mRNA expression was stimulated by exogenous activin A or B in cultures from hFSHB+ mice. Basal *Fshb* mRNA levels were greatly reduced by the activin antagonist, follistatin-288, or the activin type I receptor inhibitor, SB431542, demonstrating an essential role endogenous activin-like signaling in murine *Fshb* expression in this culture system. Activins stimulated and the inhibitors similarly attenuated human FSHB mRNA levels in hFSHB+ pituitary cultures, though the effects were smaller when compared to those with murine *Fshb*. The weaker response of human FSHB, especially to the inhibitors, suggested that there may be differences in FSHB vs. *Fshb* mRNA stability. Indeed, after treatment with actinomycin D (a transcription inhibitor), murine *Fshb* levels were reduced by 60% or more after 6 h. In contrast, human FSHB mRNA levels were largely unaffected in the same time frame. Whether this reflects differences in gene copy number or inherent

differences in mRNA stability between the two species is not yet clear. Finally, we assessed whether FOXL2 and SMAD4 regulate human FSHB expression by crossing hFSHB+ transgenic mice with animals carrying floxed alleles for Foxl2 and Smad4. We cultured their pituitaries and transduced them with control or Cre-expressing adenoviruses. Ablation of FOXL2 and SMAD4 with Cre strongly impaired basal and activin-stimulated murine Fshb and human FSHB mRNA expression. Collectively, the data indicate that the human FSHB gene is activin responsive in pituitaries of transgenic mice, and that its expression is dependent on FOXL2 and SMAD4. These results suggest that mechanisms of Fshb/FSHB regulation may be conserved between mice and humans. Research supported by CIHR MOP-133394 to DJB and Ferring PDF Scholarship to LO.

**DNA Methylomes of Bovine Gametes and in Vivo Produced Preimplantation Embryos.** Jiang Z., Lin J., Dong H., Zheng X., Marjani S.L., Duan J., Ouyang Z., Chen J., and Tian X.C.

DNA methylation is an important epigenetic modification that undergoes dynamic changes in mammalian embryogenesis, during which both parental genomes are reprogrammed. Despite the many immunostaining studies that have assessed global methylation, the gene-specific DNA methylation patterns in bovine preimplantation embryos are unknown. Using reduced representation bisulfite sequencing, we determined genome-scale DNA methylation patterns of bovine sperm and individual in vivo developed oocytes and preimplantation embryos. We show that: 1) the major wave of genome-wide demethylation was completed by the 8-cell stage; 2) promoter methylation was significantly and inversely correlated with gene expression at the 8-cell and blastocyst stages; 3) sperm and oocytes have numerous differentially methylated regions (DMRs) - DMRs specific for sperm were strongly enriched in long terminal repeats (LTRs) and rapidly lost methylation in embryos, while the oocyte-specific DMRs were more frequently localized in exons and CpG islands (CGIs) and demethylated gradually across cleavage stages; 4) a unique set of DMRs were found between in vivo and in vitro matured oocytes; and 5) differential methylation between bovine gametes was confirmed in some but not all known imprinted genes. Our data provide insights into deciphering the complex epigenetic reprogramming of bovine early embryos and will serve as an important model for investigating human development and the evolutionary and regulatory roles of DNA methylation.

**PINK1 Regulates Mitochondrial Morphology via Mitochondrial Fission in Porcine Preimplantation Embryos.** Ying-Jie Niu, Kyung-Tae Shin, Zheng-Wen Nie, Wenjun Zhou, and Xiang-Shun Cui

PINK1 selectively locates to the outer membrane of impaired mitochondria and promotes their autophagy. PINK1 regulates mitochondrial dynamics through promoting mitochondrial fission in *Drosophila* and has a role in Parkinson's disease. Mitochondrion is an important organelle in mammalian preimplantation embryos, but few studies focus on the mitochondrial dynamics during preimplantation embryo development. To investigate whether PINK1 are required for mitochondrial dynamics in porcine preimplantation embryos, gene knockdown and inhibitors were engaged in the present study. The results showed that the blastocyst formation was compromised significantly ( $42.9 \pm 1.9\%$  vs.  $36.2 \pm 1.4\%$ ,  $p < 0.01$ ) after PINK1 knockdown. Furthermore, knockdown of PINK1 induced mitochondrial elongation ( $1.93 \pm 0.06 \mu\text{m}$  vs.  $3.03 \pm 0.09 \mu\text{m}$ ,  $p < 0.001$ ) and mitochondrial copy number reduce ( $1.01 \pm 0.07$  vs.  $0.80 \pm 0.04$ ,  $p < 0.05$ ). The mitochondrial quality and oxidative stress was estimated by staining with

5,5,6,6'-tetrachloro-1,10,3,30-tetraethyl-imidacarbocyanine iodide (JC-1), 20,70-dichlorodihydrofluorescein diacetate (H2DCF-DA). The results showed that the total ROS ( $10.79 \pm 0.97$  vs.  $20.46 \pm 1.86$ ,  $p < 0.001$ ) and mitochondrial derived ROS ( $6.69 \pm 0.71$  vs.  $13.06 \pm 3.07$ ,  $p < 0.05$ ) was observably increase, but the mitochondria were seriously depolarized. In addition, both of the autophagy ( $9.17 \pm 4.01$  vs.  $32.57 \pm 7.35$ ,  $p < 0.05$ ) and apoptosis ( $6.80 \pm 1.18\%$  vs.  $18.00 \pm 3.21\%$ ,  $p < 0.01$ ) were significantly increase after mitochondrial elongation. In conclusion, these data suggest that PINK1 promotes mitochondrial fission in porcine preimplantation embryos.

**Molecular Mechanism of Thiamethoxam Toxicity on Early Embryonic Development in Pigs.** Zheng-Wen Nie, Ying-Jie Niu, Wenjun Zhou, Kyung-Tae Shin, and Xiang-Shun Cui

Thiamethoxam (TMX) is a neonicotinoid insecticide. It has specific high toxicity to insects. So far, residues of TMX has been detected in rice hull, bran, and polished rice grains, and the quantified values are greater in hull and in rice bran. Early embryo quality is vital for fertility. Overmuch production of ROS can override an embryo's antioxidant defenses producing oxidative stress that triggers apoptosis, necrosis and/or permanent DNA-damage response (DDR) in the developing early embryo. Relative study points that TMX hepatotoxicity is significant to mammals in acute test, but it is unknown on accumulated chronic toxicity to early embryo development of mammals. Therefore, it is necessary to make it clear. We obtained porcine embryos by parthenogenetic activation of MII oocytes, cultured them in PZM-5 medium with or without TMX for 7 days. We found expanding and hatch of blastocysts treated with TMX decreased by 21.73% and 16.71% compared with control, respectively. With 5-bromo-2-deoxyuridine (BrdU) incorporation, the rate of cell proliferation decreased by 44.33% compared with expand blastocyst of control. With fluorescent staining, increased ROS ( $1.00$  vs  $1.73 \pm 0.27$ ) and  $\gamma$ H2AX ( $8.16\% \pm 1.26$  vs  $33.52\% \pm 2.82$ ) occurred in TMX group. Real-time reverse-transcription polymerase chain reaction showed that increased mRNA of *sod1* ( $1.00$  vs  $1.47 \pm 0.03$ ) and decreased transcription of *mnsod* ( $1.00$  vs  $0.38 \pm 0.21$ ) and *gpx1* ( $1.00$  vs  $0.20 \pm 0.08$ ). Activity of MPF was reduced by 31.41% in expanding blastocysts with CDK1 kinase assay kit. In conclusion, the present results suggest that TMX inhibits blastocysts expanding and hatching by ROS-induced G2 checkpoint activation, which inhibits activation of MPF and cell cycle in porcine blastocysts.

**Effects of Downregulating YAP1 Transcripts by RNA Interference on Early Development of Porcine Embryos.** Natsuko Emura, Kazuki Takahashi, Senga Toma, Shuto Minagawa, Yuriko Saito, Tsutomu Hashizume, and Ken Sawai

In mammalian development, the first visible cell lineage segregation occurs during the transition from the morula to blastocyst stage. The blastocyst consists of two types of cells; inner cell mass (ICM) and trophoctoderm (TE). ICM is pluripotent and eventually gives rise to the fetus and additional extraembryonic tissues. In contrast, TE is involved in implantation and form extraembryonic tissues, including placenta. These ICM and TE fates are established at the morula stage. In murine morula stage embryos, the inside cells express Oct-4 and Sox2, which contribute to pluripotent regulation and develop into ICM. On the other hand, the outside cells differentiate into TE through Cdx2 expression. It is well known that Tead4 is an important factor for TE differentiation and induces Cdx2 expression. Recent reports have shown Hippo Pathway modulates Tead4 function by preventing nuclear

accumulation of Yap1, which is a Tead4 coactivator, in the inside cells. In the outside cells, Yap1 can accumulate in the nucleus and form a complex with Tead4 to activate Cdx2. In addition, there is a mutual antagonism between Oct-4 and Cdx2, and Tead4 downregulates Sox2 expression. In previous research, we identified TEAD4 is essential for the development of the morula to the blastocyst stage in porcine embryos. Thus, like the situation in murine embryos, YAP1 may have an important role in the segregation of TE lineage in porcine embryos. However, YAP1 functions of porcine embryos have not been investigated. This study examined the gene transcript and protein expression patterns of YAP1 and attempted to elucidate the functions of YAP1 during porcine preimplantation development using RNA interference. In vitro matured oocytes were inseminated for 10 h, and then specific YAP1 siRNA or nonsilencing siRNA (control siRNA) duplexes were injected into the cytoplasm of each embryo. Some embryos were not injected with siRNA as the control. Porcine embryos injected with or without siRNA were cultured for 5 days. YAP1 mRNA levels were high in matured oocytes and 1-cell stage embryos, and were downregulated following 2~4-cell stages. Nuclear localization of the YAP1 protein was detected in the morula and TE of the blastocyst. At the 16-cell stage, YAP1 expression level in the embryos injected with YAP1 siRNA was reduced significantly ( $P < 0.01$ ) compared with control siRNA injected and uninjected embryos. On day 5, the blastocyst developmental rate of YAP1 siRNA injected embryos (0.5%) was significantly ( $P < 0.05$ ) lower than those of uninjected embryos (20.4%) and control siRNA injected embryos (15.9%). The YAP1 downregulation by specific siRNA injection resulted in a significant ( $P < 0.05$ ) increase in OCT-4 and SOX2 expression levels at the 16-cell stage. These findings suggest that YAP1 contributes to TE segregation through downregulation of OCT-4 and SOX2. Our results indicated that YAP1 is essential for blastocyst formation and functionalization of TE lineage of porcine embryos.

**Elastographic Assessment of Uterine Contractility and Subendometrial Vasculature as Prognostic Factors for Successful Pregnancy in IVF Patients: A Pilot Study.** Han Moie Park, Hye Nam Lee, and Woo Sik Lee

Good-quality embryos and optimal intrauterine environment are the basic determinants of success for embryo transfer and the whole IVF—embryo transfer procedure. Implantation and pregnancy rates are inversely correlated with the frequency of uterine contractions. To evaluate whether uterine contractility elastography based on the analysis of tissues deformation induced by mechanical distortion, such as blood pulse at each heartbeat, subendometrial vasculature measurement by 3-dimensional Ultrasound with power Doppler angiography and clinicopathological factors are associated with successful pregnancy in IVF patients. Thirty-four volunteer women scheduled for embryo-transfer in IVF between August 2017 and December 2017. two-dimensional sagittal uterus elastography was recorded for 300 seconds, the elasticity index, defined as the mean ratio of elastographic measurements between endometrial area and subendometrial area was computed. Uterine contractility frequency, endometrial thickness, and volume were measured. Also, subendometrial 3-dimensional ultrasound and power Doppler angiography were performed to examine the vascularization index (VI), flow index (FI), and vascularization-flow index (VFI). The subendometrial FI was significantly increased in pregnant women on ET day (SMD, 0.30; 95% CI, 0.08, 0.52;  $P = .007$ ). The elasticity index was higher in pregnant women (2.1 1.5 vs 1.0 0.5). Significantly, FI and elasticity index had relationship ( $p < 0.05$ ; OR=48.33), less echogenic endometrium, high endometrial thickness (>6mm; OR=21.1) on ET day were also predictive of pregnancy after ET. The present results suggest that Uterine contractility and subendometrial

vasculature measurement by 2D and 3D ultrasound with power Doppler as non-invasive technique can be used to assess to evaluate intrauterine environment for successful pregnancy in IVF patients.

**Attenuated Expression of Kruppel-like Factor 5 in the Decidua of Women Who Experience Sporadic Miscarriage.** Kaiyu Kubota, Junya Kojima, and Hirotaka Nishi

Early clinical miscarriage is a common complication of early pregnancy, and its incidence is approximately 15% of all conceptions. Two or three consecutive miscarriages, which is referred as recurrent miscarriage, is rare. However, sporadic miscarriage occurs even in fertile women, as many women who experience sporadic miscarriage have delivered before, or can become pregnant and deliver a live baby within a few years. Chromosomal abnormalities are thought to be the major cause of fetal malformations, whereas insufficient uterine adaptation for either embryonic implantation or fetal development may also be very important particularly in cases in which healthy embryos are compromised by improper surroundings. To understand the mechanism of sporadic miscarriage, in this study we compared the expression levels of genes in the decidua of women who experience sporadic miscarriage in the first trimester of pregnancy with those from selected abortions. Decidual samples were collected with informed consent from patients without genetic aberrations, autoimmune disorders, clinical genital infections or any other systemic diseases. Candidate decidual genes were selected from genes critical for decidualization, which were identified from various transgenic mouse studies. Among them, transcription factor kruppel-like factor 5 (KLF5) expression was significantly lower in the decidua of women experiencing sporadic miscarriage, at both the transcriptional and translational levels determined by quantitative RT-PCR, western blot, and immunohistochemistry analyses. To further analyze the function of KLF5 in the human endometrium, we utilized a primary human endometrial stromal cell (pHESC) culture model together with the lentivirally transduced shRNA-mediated knockdown strategy. pHESCs were induced to differentiate by treatment with 250  $\mu$ M 8-br-cAMP for 3 days, and KLF5 expression was found to increase together with pHESC decidualization, consistent with the in vivo results. Two different shRNAs targeting the human KLF5 gene were each successfully introduced into pHESCs and knockdown efficiency was confirmed by western blot analysis. Knockdown of KLF5 significantly decreased the expressions of decidual markers prolactin, and insulin-like growth factor binding protein 1 in decidualized pHESCs indicating that KLF5 is necessary for human endometrial stromal decidualization. Our results suggest that in patients who experience miscarriage, lower expression of KLF5 results in insufficient decidual differentiation of the endometrium, leading to pregnancy loss. On the other hand, there are multiple etiologies of miscarriage. Therefore, in some cases, the compromised expression of KLF5 might just be a result of miscarriage occurring by the other triggers. In conclusion, we identified that KLF5 expression is attenuated in the decidua of women with sporadic miscarriage. Because we also demonstrated that KLF5 plays a crucial roles in human endometrial decidualization, KLF5 might be involved in the onset and/or pathophysiology of miscarriage. These findings shed light on the future identification of diagnostic markers and the development of clinical treatments for sporadic miscarriage.

**Low Oxygen Level Affects Steroidogenesis, Cell Proliferation, and Stimulates Early Luteinization Associated Changes in Bovine Granulosa Cells.** Vijay S. Baddela, Arpna Sharma, Torsten Viergutz, Dirk Koczan, and Jens Vanselow

In ovarian follicles, the granulosa cell layer is devoid of direct blood supply because of a blood-follicle barrier, which exerts a natural low oxygen micro-environment to the inner follicular cells. As the diameter of an ovarian follicle greatly increases during follicular development, oxygen concentration might continuously decrease in the follicular fluid and reaches lowest levels in (pre)ovulatory follicle. Moreover, a hand full of earlier studies have reported that oxygen concentration in reproductive tissues, including follicular fluid, is between 1 - 5%, which is far less than the atmospheric oxygen concentration (21%) that is generally used in regular cell culture experiments. Therefore, the present study was designed to investigate the granulosa cell (GC) function at physiological low oxygen condition using our estrogen-active bovine GC culture model. GC were aspirated from the ovaries, obtained from a local abattoir, and cultured at atmospheric oxygen concentration in FSH and IGF1 supplemented serum-free media for six days while the spent media was replaced every 2 days. On the sixth day, after the exchange of hormone supplemented media, GC were subjected to normal (21%) and low oxygen (1%) conditions, separately, for 48 hrs. The viability of GC was not found to be affected at low oxygen condition compared to normal oxygen condition, as evident from the flow cytometry analysis. Hormone estimation by radioimmunoassay revealed that production of estradiol and progesterone was significantly reduced at low oxygen condition. This was further confirmed by the qPCR analysis of key genes, CYP19A1, FSHR, and LHCGR, associated with GC function. To understand the genome-wide gene expression changes, microarray analysis was performed using Affymetrix's Bovine Gene 1.0 ST Arrays. It resulted in the identification of 1104 differentially regulated genes ( $|FC| > 2$  or  $< -2$ ;  $p < 0.05$  and  $FDR < 0.05$ ), in which 505 were upregulated and 599 were downregulated at low oxygen conditions. Pathway analysis using Ingenuity pathway analyzer (IPA) has identified 36 significantly affected ( $p < 0.05$ ) canonical pathways. Importantly, pathways like "Estrogen-mediated S-phase Entry" and "Cyclins and Cell Cycle Regulation" were found to be greatly affected under low oxygen conditions. To validate this effect, GC were cultured as mentioned above and subjected to cell cycle analysis, after fixing followed by staining the nucleus with propidium iodide, using flow cytometry. The results indicate that GC were significantly arrested at the G0/G1 phase of the cell cycle with a significantly fewer number of cells undergoing the DNA replication (S phase) process. This was further confirmed by the expression analysis of marker genes of cell proliferation, PCNA, and CCND2. Further, upregulation of multiple LH induced early genes (VNN2, RGS2, and VEGFA) was also detected in GC cultured at low oxygen condition. Overall, all these findings intuitively indicate that a low oxygen level, could stimulate early luteinization in bovine granulosa cells and, is plausibly an essential feature of (pre)ovulatory follicles for the formation of a functional corpus luteum. Funding: This research was supported by Alexander von Humboldt Foundation, Bonn, Germany.

**Evaluation of the Ion Channel Functions in Phasic Spontaneous Contraction and Characterization of Ca<sup>2+</sup> Oscillation in Cultured Smooth Muscle Cells in Bovine Oviduct.** Yuki Yamamoto, Maho Kurokawa, Taiji Ogawa, and Koji Kimura

[Introduction] Phasic spontaneous contraction of mammalian oviducts is essential for the transport of gametes and embryos. Previous studies have demonstrated that spontaneous membrane depolarization

of "pacemaker" cells, the endogenous generator for contraction, induces Ca<sup>2+</sup> increase in myocytes resulted in muscular contraction in the hearts and intestines. Some studies have detected potential pacemakers expressing marker proteins for an intestinal pacemaker in mouse oviduct. However, such marker proteins were not detected in bovine oviduct in our previous study. This study aimed to clarify the basic mechanism of spontaneous contraction to identify the pacemaker in bovine oviduct.

[Materials and Methods] Isthmic tissues of bovine oviduct were used for the following experiments. Experiment 1: The effects of ion channel and gap junction blockers on the spontaneous contraction were investigated using Magnus system. Target factors were as follows; 1) voltage-dependent Ca<sup>2+</sup> channels (VDCC) and the receptors responsible for Ca<sup>2+</sup> release from endoplasmic reticulum (IP3R and RyR) as Ca<sup>2+</sup> source, 2) Na<sup>+</sup> and Cl<sup>-</sup> channel as a depolarization initiator, 3) voltage-dependent K<sup>+</sup> channel (VDKC) and Ca<sup>2+</sup>-activated K<sup>+</sup> channels (BK and SK channels) as re-/hyper-polarization regulators, and 4) gap junction-mediated propagation of depolarization to neighboring cells. Experiment 2: Culture methods of oviduct smooth muscle cells (SMCs) were examined to observe intercellular Ca<sup>2+</sup> signaling as an indicator of SMC activity. Immunohistochemistry for smooth muscle actin was carried out to identify SMCs on the culture plate. Intracellular Ca<sup>2+</sup> was visualized by Fluo4.

[Results and Discussion] Experiment 1: 1) The VDCC blocker decreased amplitude of contraction resulting in the loss of contraction. Co-inhibition of both IP3R and RyR decreased the number and amplitude. These results indicate that Ca<sup>2+</sup> influx via VDCC or release from endoplasmic reticulum is necessary for spontaneous contraction. 2) Na<sup>+</sup> channel blocker did not affect contraction, whereas Cl<sup>-</sup> blockers decreased the frequency of contraction. It is suggested that the Cl<sup>-</sup> channel is involved in the initiation of depolarization. 3) A blocker of the VDKC decreased the number and amplitude. BK channel blocking decreased the number of contraction, although BK and SK channel blockers increased the amplitude. These results suggest VDKC and Ca<sup>2+</sup>-activated K<sup>+</sup> channels are involved in the regulation of re-/hyper-polarization. 4) A blocker of gap junction suppressed contraction, suggesting that depolarization propagates via gap junctions. Experiment 2: When the extent of the area covered by smooth muscle actin positive cells exceeded 90% (90% confluence), spontaneous Ca<sup>2+</sup> oscillation was observed in the cells after reached confluent, but not at 70% confluence. This result indicates that spontaneous activity of pacemaker cells and SMCs can be observed in culture, and that cell-to-cell contact is required for the initiation of Ca<sup>2+</sup> oscillation. Ca<sup>2+</sup> oscillation was observed in groups of cells, with neighboring cells oscillating in synchrony in some regions, and not in synchrony in other regions. Our aim in future is to identify the pacemaker in bovine oviduct using this method.

### **Cryopreservation of Male and Female Gonial Cells in the Critically Endangered Cyprinid *Gnathopogon caerulescens*.** Tatsuyuki Takada, Ikuo Tooyama, Yasuhiro Fujioka, Noriyoshi Sakai, and Shogo Higaki

Natural stocks of endemic fish have decreased rapidly over recent decades. As rapid recovery of their population is not easy, ex situ cryopreservation of their genetic materials is of increasing importance before its extinction. However, studies on cryopreservation of gonial cells in fish were limited. We therefore investigated the cryopreservation of spermatogonia and oogonia in the critically endangered cyprinid *Gnathopogon caerulescens* using slow-cooling (freezing) and rapid-cooling (vitrification) methods. We examined the testicular cell toxicities and glass-forming properties of the five cryoprotectants; ethylene glycol (EG), glycerol (GC), dimethyl sulfoxide (DMSO), propylene glycol (PG), and 1,3-butylene glycol (BG), and determined cryoprotectant concentrations that are suitable for

freezing and vitrification solutions, respectively. Subsequently, we prepared the freezing solutions of EG, GC, DMSO, PG, and BG at 3, 2, 3, 2, and 2 M and vitrification solutions at 7, 6, 5, 5, and 4 M, respectively. Following the cryopreservation of the testicular cells mainly containing early-stage spermatogenic cells (e.g. spermatogonia and primary spermatocytes), cells were cultured for 7 days and immunohistochemically stained against germ cell marker protein Vasa. Areas occupied by Vasa-positive cells indicated that vitrification led to better survival of germ cells than the freezing method, and the best result was obtained with 5 M PG; about 50% recovery of germ cells following vitrification. Prolonged culture resulted differentiation of EdU incorporated sperm. In the case of ovarian cells containing oogonia and stage I, II, and IIIa oocytes, vitrification with 5 M DMSO resulted the best survival of oogonia, with equivalent cell numbers to those cultured without vitrification. In addition, proliferation of oogonia and early differentiation was observed by EdU incorporation and morphological observation, respectively, in in vitro culture. The present data suggest that male and female gonial cells of the endangered species *G. caerulescens* can be efficiently cryopreserved using suitable cryoprotectants for spermatogonia and oogonia, respectively.

**Role of Rab11a in Docking of Cell Adhesion Molecules in Endometrial Epithelial Cells.** Ruchi Kakar-Bhanot, Krupanshi Brahmabhatt, Bhagyashree Chauhan, Rajendraprasad Katkam, Tahir Bashir, Harshawardhan Gawde, Niranjana Mayadeo, Uddhav Chaudhari, and Geetanjali Sachdeva

The human endometrium permits blastocyst adhesion only during days 20-24 of the menstrual cycle; a period defined as 'Window of Implantation'. This fetomaternal interaction is facilitated by Cell Adhesion Molecules (CAMs) expressed by uterine and embryonic cells. Optimal expression as well as appropriate localization of CAMs, such as integrins, mucins, cadherin etc., are pre-requisites for successful pregnancy. Microarray and proteomics approaches have identified a number of CAMs vital for embryo-endometrial interactions; however, cell surface distribution of these molecules in endometrial epithelial cells has not been investigated in detail. Rab GTPase mediated trafficking machinery is one of the mechanisms regulating the abundance of adhesion molecules on the cell surface. Rab11a, one of the Rab GTPases, functions in recycling of receptors to the cell surface and also in the exocytosis of biosynthetic cargo. We hypothesize that Rab11a mediated trafficking mechanisms govern the surface abundance of these CAMs (Integrin  $\alpha V\beta 3$  and E-cadherin) in endometrial epithelial cells and determine the outcome of embryo-endometrial interactions. For this, we generated Rab11a knockdown stable clones of Ishikawa (an endometrial epithelial cell line). These Rab11a deficient clones were assessed for surface localization of Integrin  $\alpha V\beta 3$  and E-cadherin. The cell surface abundance of Integrin  $\alpha V\beta 3$  in Rab11a knockdown clones was significantly ( $p < 0.01$ ) lower despite no alteration in the total expression. Rab11a knockdown cells also exhibited significantly ( $p < 0.01$ ) reduced adhesiveness towards trophoblastic JAr spheroids suggesting impaired embryo-endometrial interaction. When assessed for E-cadherin expression, it was found to be significantly ( $p < 0.001$ ) reduced in Rab11a knockdown clones though the transcript levels remained unaltered. Golgi membrane extracts demonstrated significantly ( $p < 0.05$ ) reduced levels of E-cadherin protein in Rab11a knockdown clones implying a defect in the biosynthetic pathway. Lysosomal membrane extracts also displayed significantly ( $p < 0.05$ ) reduced levels of E-cadherin protein ruling out the possibility of increased degradation, suggesting some post transcriptional modifications. Also, Rab11a knockdown clones displayed increased presence of stress fibres and a higher migratory potential indicating a loss of "epithelial-ness". Further, endometrial Rab11a expression did not alter between pre-receptive and receptive phase tissues from

fertile women. Interestingly, mid-secretory phase endometrial samples from women with unexplained infertility were found to have reduced expression of Integrin  $\beta 3$ , E-cadherin as well as Rab11a ( $p < 0.05$ ), thereby suggesting a possibility that the expression of these molecules could be regulated indirectly by Rab11a in infertile women. Overall, the study demonstrates the relevance of Rab11a in endometrial adhesiveness and cohesiveness.

**Sildenafil Ameliorates Aging-Induced Changes in Rat Testis.** Tatjana Kostic, Srdjan Sokanovic, Ivan Capo, Marija Medar, and Silvana Andric

NO-cGMP signaling pathway has been implicated in reduction of testicular steroidogenesis during aging. Here we analyzed the effect of PDE5 inhibition on old testicular phenotype formation. The old phenotype exhibited low testosterone and increased nitrite levels in circulation, increased cGMP accumulation in testicular interstitial fluid (TIF), progressive atrophy of testicular seminiferous tubules and enlargement of interstitial area followed by rise in blood vessel density and slight increase in the number of Leydig cells and macrophages. Leydig cells have reduced steroidogenic capacity, increased MAP kinases expression (MEK, ERK1/2, JNK) and antiapoptotic PRKG1 and AKT, suggesting increased proliferation/survival and accumulation of senescent Leydig cells in testis. In 12 month-old rats, a long-term treatment with sildenafil (PDE5 inhibitor) normalized testosterone/nitrite levels in circulation and cGMP accumulation in TIF; improved Leydig cell steroidogenic capacity; decreased MEK, ERK1/2 and PRKG1 expression; prevented an increase in the Leydig cells number and atrophy of seminiferous tubules leading to histological appearance of young rat testes. In 18 month-old rats, long-term PDE5 inhibition partially recovered testosterone and nitrite levels in serum; normalized PRKG1 expression without effect on MEK and ERK1/2; and slowed down Leydig cell and macrophage accumulation and regressive tubular changes. Culturing of primary Leydig cells from aged rats in presence of PDE5-inhibitor stimulated steroidogenic and MAPK gene expression. Taking together, results indicate that cGMP targeting alter both steroidogenesis and signaling pathways associated with cell proliferation/survival. The long-term PDE5 inhibition improves testicular steroidogenesis and slows-down regressive changes in testes during aging.

**Spermatic Kinetics of Bovine Semen Cryopreserved in Extender Supplemented with Iodixanol.**

Fernanda Nunes Marqui, Alicio Martins Jr., Tairini Érica Cruz, Tatiana Issa Uherara Berton, Diego Gouvêa Souza, José Antônio Dell'Aqua Júnior, and Eunice Oba

Although the cryopreservation of bovine spermatozoa is an efficient technique, several investigations have been addressed to identify the additive effect of different compounds after adding to the freezing extender. Iodixanol, a polysucrose substance, appears to maintain spermatozoon membrane integrity and their motility after freezing/thawing process. Thus, the goal of this study was to verify the effects of different concentrations of iodixanol added to the freezing extender on post-thawed bull's sperm kinetics parameters. Ejaculates ( $n = 18$ ) of three Nellore bulls were collected by artificial vagina and after routine evaluation (sperm motility, concentration and morphology) were pooled. Then, sperm samples were diluted in commercial freezing extender, based on egg yolk and 7% of glycerol, supplemented with iodixanol at concentrations of 0% (control group), 2.5%, 5%, and 10%, consisting the groups I2.5, I5, and I10, respectively. Dilution was done to adjust the sperm number to 60 million/ml. Subsequently, semen

samples were cooled for 5 h at 4°C, filled in 0.50 ml straws and frozen in a programmable freezer machine. After that, the straws were stored in liquid nitrogen until sperm evaluations, which were performed by thawing the samples in water bath at 37°C/30s. The spermatoc kinetics was assessed using computer assisted sperm analyzer. Total motility (TM, %), progressive motility (PM, %), curvilinear velocity (VCL,  $\mu\text{m/s}$ ), straight line velocity (VSL,  $\mu\text{m/s}$ ), average path velocity (VAP,  $\mu\text{m/s}$ ), amplitude of lateral head displacement (ALH,  $\mu\text{m}$ ), beat cross frequency (BCF, Hz), linearity (LIN, %), straightness (STR, %), and wobble (WOB, %) were analyzed. ANOVA and Tukey's test were used to identify statistical differences (values expressed as mean  $\pm$  standard deviation) with  $P < 0.05$  taken as significant. Higher ( $P < 0.05$ ) total sperm motility was observed for I10 ( $72.03 \pm 10.4$ ) than for I2.5 ( $49.5 \pm 0$ ). However, I10 showed lower VCL and ALH ( $111.2 \pm 1.9$  and  $1.4 \pm 0.06$ , respectively) than I2.5 ( $122.4 \pm 3.5$  and  $1.63 \pm 0.1$ ) and control group ( $130.1 \pm 5.3$  and  $1.71 \pm 0.06$ , respectively). VSL and VAP were higher in control ( $70.4 \pm 1.9$  and  $88.7 \pm 2.8$ , respectively) than for I10 ( $62.8 \pm 2.5$  and  $78.7 \pm 1.2$ ), I5 ( $65.5 \pm 1.0$  and  $82.9 \pm 1.1$ ) and I2.5 ( $65.3 \pm 0.8$  and  $83.0 \pm 2.0$ ). On the other hand, the percentage of PM, LIN, STR and WOB did not differ among groups. Based on the overall sperm kinetics parameters evaluated, the highest concentration of iodixanol increased significantly total sperm motility in comparison to the lower concentration, having no apparent deleterious effect on spermatozoa. However, further tests aiming using fluorescent probes in flow cytometry are in progress and can provide additional information on sperm viability. Acknowledgements: CAPES, Tairana Artificial Insemination Station, Botupharma and Master Fertility Animal Reproduction, Brazil.

**Insulin/IGF1 Signalling Regulates Expression of the Key Markers of Mitochondrial Biogenesis in Steroidogenic Cells of Prepubertal Testis, but Not Ovaries.** Silvana Andric, Sava Radovic, Isidora Starovlah, Serge Nef, and Tatjana Kostic

Controlled changes in mitochondrial biogenesis and morphology are required for cell survival and homeostasis, but the molecular mechanisms are largely unknown. Here, the male and female prepubertal mice (P21) with insulin and IGF1 receptors deletion in steroidogenic tissues (*Insr/Igf1r*-DKO) were used to investigate transcription of the key regulators of mitochondrial biogenesis (*Ppargc1a*, *Ppargc1b*, *Pparg*, *Nrf1*, *Tfam*) in Leydig cells, ovaries and adrenals. The mitochondrial architecture markers (*Mfn*, *Mfn2*, *Opa1*) were followed in Leydig cells. Results showed that expression of PGC1, the master regulator of mitochondrial biogenesis and integrator of environmental signals, as well as its downstream target *Tfam*, significantly decreased in androgens-producing Leydig cells. This was followed with reduction of *Mtnd*, the core subunit belongs to the minimal assembly required for catalysis. Transcription of mitochondrial markers remained unchanged in ovaries. Differently, in adrenals, the pattern of transcripts for mitochondrial biogenesis markers was the same in both sexes, and opposite from Leydig cells. The level of transcripts for markers of mitochondrial architecture (*Mfn1*, *Mfn2*) significantly increased in Leydig cells from *Insr/Igf1r*-DKO. This was followed with dramatic changes in mitochondrial morphology, suggesting that the mitochondrial phase of steroidogenesis could be affected. Indeed, basal and pregnenolone stimulated progesterone productions (taking place in mitochondria) in Leydig cells from *Insr/Igf1r*-DKO decreased more than androgens production and were barely detectable. Our results are the first to show that *INSR* and *IGF1R* are important for mitochondrial biogenesis in gonadal steroidogenic cells of prepubertal males, but not females, serving as important regulators of mitochondrial architecture and biogenesis markers in Leydig cell.

### **Ubiquitination Regulate Spermiation Through Degradation of Apical Ectoplasmic Specialization.**

Mingxi Liu, Jinyuan Wan, Xin Zhang, Yueshuai Guo, Xuejiang Guo, and Jiahao Sha

Spermatogenesis is a highly complicated process of germ cell division and differentiation which finally produce spermatozoa. Spermatozoa need to be released from seminiferous epithelium, then enter into epididymis for further maturation and to gain mobility. The process of spermatozoa release is called spermiation, disability of spermiation can induce azoospermia. The morphological and ultrastructural events associated with spermiation shows dynamic changes, including: the remodeling of the spermatid nucleus, removal of Sertoli cell ectoplasmic specialization (ES) junctions and retraction of Sertoli cell cytoplasm. The apical ES junctions present the dynamic changes in order, and they are the basic structures of spermiation. However, how does the composition of ES junction change during spermiation and whether there is a 'switch' molecular controlling this process. In eukaryotes, there are two proteolytic routes, the autophagy and ubiquitin-26S proteasome system (UPS). In this study, we found proteasome inhibitor impaire spermiation. We screened 616 E3 ubiquitin ligases base on testicular expression pattern, and test interaction between testicular E3 ubiquitin ligases with ES junction protein. We found that Espin binding E3 ubiquitin ligases (EbEULs) specifically recognize ES junction protein Espin. Gene knockout models of EbEULs reveal that EbEUL1 -null male mice were infertile and failure of spermiation, with normal hormone level. We generated germ cells (EbEUL1 F/F Stra8-Cre) and Sertoli cells (EbEUL1 F/F AMH-Cre) conditional KO mice, respectively, and found germ cells conditional KO mice showed similar phenotypes to the EbEUL1 -/- mice only. To elucidate how EbEUL1 regulates ESPIN in testis, we generated anti-EbEUL1 antibody. Co- immunoprecipitation assay reveal that EbEUL1 interact with SKP1, and suggesting that EbEUL1 was involved in E3 ligase SCF EbEUL1 complex in testis. And in EbEUL1 -/- mice testis, the poly-ubiquitination level of Espin was decreased, thus, leading to the reduction of the degradation of protein. Collectively, these data revealed EbEUL1 could ubiquitinate Espin and regulate its degradation process. These results demonstrated that EbEUL1 is an 'on-off' of spermiation and provide theoretical basis for infertility treatment and male contraceptives development.

### **Heparan Sulfate Proteoglycan Sulfation Regulates Uterine Differentiation and Signaling during Embryo Implantation.**

Yan Yin, Adam Wang, Li Feng, Yu Wang, Hong Zhang, Ivy Zhang, Brent Bany, and Liang Ma

To prepare for embryo implantation, uterus must undergo a series of reciprocal interactions between the uterine epithelium and the underlying stroma, which are orchestrated by ovarian hormones. During this process, multiple signaling pathways are activated to direct cell proliferation and differentiation, which render the uterus receptive to the implanting blastocysts. One important modulator of these signaling pathways is the cell surface and extracellular matrix macromolecules, heparan sulfate proteoglycans (HSPGs). HSPGs play crucial roles in signal transduction by regulating morphogen transport and ligand binding. In this study, we examine the role of HSPG sulfation in regulating uterine receptivity by conditionally deleting N-deacetylase/N-sulfotransferase 1 gene (Ndst1) in the mouse uterus using the Pgr-Cre driver, on a Ndst2- and 3-null genetic background. Although development of the female reproductive tract and subsequent ovarian function appear normal in Ndst triple knockout females, they are infertile due to implantation defects. Embryo attachment appears to occur but the uterine epithelium at the site of implantation persists rather than disintegrates in the mutant. Uterine epithelial cells continued to proliferate past day 4 of pregnancy accompanied by elevated Fgf2 and Fgf9

expression, while uterine stroma failed to undergo decidualization, as evidenced by lack of Bmp2 induction. Despite normal Indian Hedgehog (Ihh) expression, transcripts of Ptch1 and Gli1, both components as well as targets of the Hh pathway, were detected only in the subepithelial stroma, indicating altered Hh signaling in the mutant uterus. Taken together, these data implicate an essential role for HSPGs in modulating signal transduction during mouse implantation.

**Upregulation of microRNA Expression in Bovine Granulosa and Endothelial Cells Due to Recombinant VEGF and TSP-1 Treatment.** Allyssa Hooper and Jim Petrik

Cystic ovarian disease (COD) is a major contributor to infertility in cattle, with 30% of cows developing ovarian cysts during a given lactation and becoming anovulatory. The cause of COD has remained elusive and is thought to be multifactorial, with angiogenic and genetic contributions proposed. There is an increasing body of work suggesting that microRNAs (miRNAs) may be involved in a number of ovarian-based reproductive disorders. Changes in miRNA expression can affect a multitude of genes and may be important regulators of the dynamic processes involved in each ovarian cycle. We hypothesize that miRNAs are integral to the regulation of critical ovarian processes such as angiogenesis and follicular development and that altered miRNA expression contributes to the onset and progression of ovarian dysfunction and reproductive disorders. Based on this hypothesis, we have identified eight miRNAs (miR-15a, -18a, -20a, -21, -29a, -126, -132, Let7a) that have been shown in the literature to target vascular endothelial growth factor (VEGF), a pro-angiogenic factor, or thrombospondin-1 (TSP-1), an anti-angiogenic factor, both of which play a role in angiogenesis and folliculogenesis. The objective of this study is to determine which of our selected miRNAs are involved in regulating VEGF and TSP-1 in the ovary in vitro. We treated three different cell lines – bovine granulosa cells (BGCs), spontaneously immortalized rat granulosa cells (SIGCs), and bovine aortic endothelial cells (BAECs), with a recombinant VEGF or TSP-1 analog in order to artificially enhance their expression levels (n=3 per treatment group). We then isolated RNA and performed qPCR to analyze miRNA expression patterns. The results using a 2-way ANOVA with Tukeys post-hoc showed a significant increase in miR-15a ( $p < 0.0001$ ), miR-29a ( $p < 0.001$ ), miR-126 ( $p < 0.0001$ ), and miR-132 ( $p < 0.05$ ) in the BAECs treated with recombinant VEGF as well as a significant increase in miR-132 ( $p < 0.01$ ) in BAECs treated with recombinant TSP-1. These results suggest that miR-15a, -29a, -126, and -132 may regulate VEGF and TSP-1 in bovine ovarian cells, respectively. In order to study these miRNAs further, we will treat these cell lines with miRCURY® LNA® miRNA mimics in order to enhance miR-15a, -29a, -126, and -132 expressions. We will then analyze expression levels of their targets, VEGF and TSP-1 through qPCR, Western Blot, and immunofluorescence. By studying miRNA expression in vitro, we will be able to identify which miRNAs are involved in regulating ovarian angiogenesis and folliculogenesis, which will allow us to further study these miRNAs in vivo. This research will ultimately lead to a better understanding of ovarian dysfunction, reproductive disorders, and infertility in cattle. This research was supported by The Natural Sciences and Engineering Research Council.

### **Exposure to Endocrine Disrupting Chemicals and High Fat Diet During Early Pregnancy Affects**

**Placental Development.** Athilakshmi Kannan, Liying Gao, Jodi A. Flaws, Milan K. Bagchi, and Indrani C. Bagchi

Phthalates are synthetic endocrine disrupting chemicals (EDCs) that are found in numerous consumer products. Di(2-ethylhexyl) (DEHP), one of the common phthalates, is found ubiquitously in the environment. Despite constant exposure to phthalates, the impact of their exposure on placental development and function is not well understood. We recently conducted studies in which pregnant mice were exposed to an environmentally relevant level of DEHP during early gestation to analyze the effect of this exposure on placental development. Our results indicate that exposure to DEHP causes disruption of labyrinth vasculature and impairs differentiation and segregation of trophoblast cells in the placental labyrinth layer, indicating a defect in placental development. Previous studies indicated that DEHP and its metabolites interact with members of the peroxisome proliferator-activated receptor (PPAR) family. Indeed, the observed DEHP-mediated defects in placentation are strikingly similar to those displayed by PPAR $\gamma$ -null mice. PPAR $\gamma$ , a ligand-activated transcription factor, is abundantly expressed in all trophoblast subtypes and is required for proper placental function. In the absence of PPAR $\gamma$ , the labyrinthine trophoblast precursors fail to undergo terminal differentiation, causing a defect in permeation of blood vessels and compromised maternal-fetal exchanges leading to early embryonic death. We observed similar phenotypic defects in the placenta upon exposure to DEHP. Our studies further revealed dysregulated expression of PPAR $\gamma$  target genes in the placenta in response to DEHP exposure. Interestingly, when mice were exposed to DEHP and fed high fat diet during pregnancy, the placental defects, including terminal differentiation of labyrinthine trophoblast cells and vascularization of the placenta, were exacerbated. Feeding high fat diet alone without DEHP exposure, however, did not adversely affect placental development. Collectively, these results indicate that phthalates and high fat diet disrupt PPAR $\gamma$ -dependent signaling pathways in the placenta to severely affect its development during pregnancy.

This research was supported in part by NIH P01ES022848 and EPA RD-83459301 (JAF).

### **In Utero Exposure to Endocrine Disrupting Chemicals Results in Pregnancy Complications in Multiple**

**Generations.** Arpita Bhurke, Athilakshmi Kannan, Emily Brehm, Saniya Rattan, Jodi A. Flaws, Milan K. Bagchi, and Indrani C. Bagchi

Emerging evidence suggests that environmental exposures during fetal development can have long-lasting health consequences later in life. To date, studies have not addressed the effects of early life exposures on uterine function and establishment of pregnancy in the subsequent generation of female offspring. Thus, we conducted studies in which pregnant mice (F0) were exposed to environmentally relevant levels of di(2-ethylhexyl) phthalate (DEHP), an endocrine disrupting chemical (EDC), and analyzed the effects of this exposure on the reproductive health of F1, F2, and F3 female mice. Our studies revealed that DEHP exposure of pregnant mice (F0) mice leads to subfertility in F1-F3 females. In humans and rodents, pregnancy is established when the embryo attaches to the uterine epithelium, invades the underlying stroma and promotes differentiation of the stromal cells to decidual cells, which support embryo growth and survival until placentation. In both species, these events are acutely dependent on a timely balance of steroid hormones estrogen (E) and progesterone (P). While E acts as a mitogen by promoting epithelial proliferation, P inhibits this process to promote differentiation, and

renders the epithelium competent for embryo attachment. Thus, dysregulated steroid hormonal signaling with a dominance of E over P adversely affects implantation and establishment of pregnancy. Interestingly, DEHP exposure markedly enhances the proliferation of uterine epithelial cells, raising the possibility that exposure to this EDC influences steroid signaling mechanisms. Our previous studies have shown that HAND2, a transcription factor, is a key mediator of the anti-proliferative effects of P in the uterus. Consistent with this observation, knockout mice harboring a deletion of Hand2 in the uterus exhibit enhanced E-dependent signaling, implantation failure and infertility. HAND2 is also expressed in human uteri. Remarkably, we found that the HAND2 locus is prone to DNA hypermethylation in the human genome, which leads to the silencing of this gene and is strongly associated with uterine hyperplasia. We found that HAND2 expression is markedly suppressed in the uteri of F1-F3 females following DEHP exposure, raising the possibility that DEHP induces alteration in DNA methylation, thereby affecting the expression of uterine genes including Hand2. Our studies further revealed that DEHP exposure leads to dysregulated expression of a key histone mark, H3Lys27me3, in uterine cells of F1-F3 females. Based on these data, we hypothesize that in utero DEHP exposure alters DNA methylation and histone code to affect uterine gene expression. This altered gene expression modifies the intrinsic responsiveness of uterine cells to proliferation and differentiation signals, triggering implantation failure and pregnancy loss in multiple generations.

This research was supported in part by NIH P01ES022848 and EPA RD-83459301 (JAF). AB was supported by the Environmental Toxicology Fellowship.

**Biomimetic Hydrogel Supports the Development of Murine Primary Ovarian Follicles Co-cultured with Adipose Derived Stem Cells.** Claire Tomaszewski, Elizabeth Constance, Hong Zhou, and Ariella Shikanov

In vitro culture of ovarian follicles that result in fertilizable oocytes can preserve fertility in women facing primary ovarian insufficiency resulting from chemotherapy treatment or other reproductive pathologies. Previous culture systems have successfully utilized biomaterials, such as alginate, to encapsulate and culture immature mouse ovarian follicles to yield live, fertile offspring. Alginate, however, is not degradable on the time scale of follicle culture and therefore may exert significant compressive force to the expanding follicles, especially in large species. Contrary to alginate, poly(ethylene glycol) (PEG) is a biocompatible synthetic polymer with tunable physical properties, including varying stiffness and biological activity, such as sensitivity to cell-secreted proteases and extracellular matrix (ECM) sequestering sequences. As a result, PEG hydrogels degrade in response to plasmin and matrix metalloproteases (MMPs), thereby creating space for follicular expansion without exerting a compressive force. We have reported earlier that PEG hydrogels formed with plasmin sensitive crosslinkers enabled in vitro encapsulation and maturation of mouse secondary ovarian follicles (140 – 150  $\mu\text{m}$ ). However, further innovations are required to promote the survival and maturation of smaller, early-stage follicles. In this report, we investigated the co-encapsulation of mouse primary and early secondary ovarian follicles (90 – 110  $\mu\text{m}$ ) with adipose derived stem cells (ADSCs). Accepted approaches utilize feeder cells to promote the undifferentiated growth of embryonic stem cells (ESCs), and similarly, co-encapsulated ADSCs provide critical paracrine factors necessary for early-stage follicle survival and maturation. The paracrine factors from ADSCs significantly improved the survival and maturation of the early-stage follicles cultured in vitro via bidirectional crosstalk. Additionally, ADSC-driven degradation of the dual-functional crosslinker allows for greater follicle expansion at the start of culture when follicle-

secreted plasminogen activator levels are low. Preliminary data shows that survival rate of follicles increased to 54% when co-cultured with ADSCs from 36% when single follicles were cultured in ADSC conditioned medium (CM), and 33% when cultured alone in regular medium. Follicles co-cultured with ADSCs also showed improved growth to a final diameter of 222  $\mu\text{m}$  from 203  $\mu\text{m}$  in CM and 167  $\mu\text{m}$  when cultured alone. Co-culture of ADSCs with early stage follicles in a dual-functional PEG hydrogel improved follicle growth and survival through soluble paracrine factors and enhanced degradation for follicle expansion. The use of the biocompatible and biodegradable PEG hydrogels offers a xeno-free culture system that could be used to culture large species and human follicles. Moreover, ADSCs can be derived in a patient specific way in clinical settings, therefore making this approach highly translational.

This research was supported by NSF CAREER to A.S. (#1552580)

### **Dysregulated Androgen-Induced Exosomal Release of Mir-379-5p Determines Granulosa Cell Fate.**

Reza Salehi

Androgen promotes both follicular growth and atresia in a follicular stage-dependent manner. MicroRNAs (miRNAs) repress gene expression by targeting the 3' UTR of specific mRNAs and are differentially expressed in DHT-induced PCOS rats. Exosomes are bioactive vesicles with an important role in intercellular communication in the ovarian microenvironment. However, how exosomal miRNAs are involved in ovarian cell fate determination is not well understood.

My overall hypothesis is androgen regulates exosomal content of miRNAs in a follicular stage-dependent manner, a process which determines granulosa cell fate. Our specific objectives are to determine: (1) the regulation of granulosa cell-extracellular vesicle release (exosomes and microvesicles) by androgen, (2) if androgen regulates cellular and extracellular content of miRNAs in granulosa cells, and (3) whether the regulation of these processes is follicular stage-dependent. Preantral follicles (PAF; DES-primed rats) and antral follicles (AF; PMSG-primed rats) were cultured without and with DHT (1  $\mu\text{M}$ ; 24 & 36h) and exosomes and microvesicles were isolated from spent media by differential centrifugations and characterized by nanoparticle tracking analysis. Cellular and extracellular content of several candidate miRNAs (rno-let-7d-5p and -3p, rno-mir-24-5p and 3p, rno-mir-9-5p and 3p and rno-mir-379-5p and 3p) were assessed (Taqman miRNA assay) in PAF and AF GC treated with DHT in vitro.

DHT treatment for 36h reduced microvesicle concentration at both PAF and AF GC conditioned media, but reduced GC exosome secretion in AF but not PAF. The ratio of microvesicles to exosome was reduced 36h post-DHT treatment in PAF GC. DHT reduced PAF GC rno-mir-379-5p content and increased its content in exosome but not in microvesicles. rno-mir-379-5p was not detectable in extracellular vesicle-depleted conditioned media, supporting the notion that its transport is primarily via exosomes. DHT had no influence on the cellular and extracellular content of rno-mir-379-5p in AF, nor those of rno-mir-379-3p, rno-let-7d-5p and -3p, rno-mir-24-5p and 3p, rno-mir-9-5p and 3p in PAF and AF. Studies with miRNA mimic and inhibitor suggested phosphoinositide-dependent kinase-1 (PDK1) as a downstream target of rno-mir379-5p. The increased release of exosomal rno-mir-379-5p in DHT treated-PAF GC is associated with increased cellular content of PDK1, P-PDK1, P-AKT/AKT ratio and MCM2 (a cell proliferation marker) but not in AF GC. Inhibition of exosome release in PAF GC with GW4869, exosome release inhibitor, resulted in increased cellular content of rno-mir-379-5p, reduced that of PDK1 and MCM2 in the presence of DHT, indicating exosomal release of rno-mir-379-5p is a

regulatory mechanism for PDK1 cellular content and proliferation. Studies with rno-mir-379-5p mimic and inhibitor further confirmed rno-mir-379-5p reduces PAF GC proliferation (MCM2). DHT treatment reduced proliferation of AF GC (MCM2). Conversely, the inhibition of cellular rno-mir379-5p using miRNA inhibitor rescued proliferation ability in AF GC treated with DHT. These findings suggest that increased exosomal release of mir-379-5p from GC in response to androgenic stimulation is a survival mechanism specific for the preantral stage of follicle development (Supported by a grant from CIHR and the Lalor Foundation Postdoctoral Fellowship).

**Ovulation Failure in Mice Lacking Granulosa Cell Insulin Receptors.** Nikola Sekulovski, Mingxin Shi, Allison Whorton, Kanako Hayashi, and James A. MacLean

Insulin signaling is crucial for the development of preovulatory follicles and progression through the antral stage. It has been shown that *Igf1r*<sup>-/-</sup> mice have impaired folliculogenesis due to defective FSH responsiveness in the mouse ovary. Also, as previously published female mice with a conditional knockdown of IGF1R in granulosa cells (GCs) are sterile, have smaller ovaries than those of control animals and contain no antral follicles even after gonadotropin stimulation, suggesting that folliculogenesis is strongly regulated by IGF1R. The lack of antral follicles correlates with a significant decrease in serum estradiol levels. Consequently, the GCs of the knockout mice express lower levels of preovulatory markers including aromatase and luteinizing hormone receptor. For our initial study, we employed *Pgr*-Cre knock-in mice to simultaneously delete floxed alleles for both *Igf1r* and *Insr*. Ablation of both receptors eliminate potentially redundant signaling actions, with the *Pgr* promoter initiating knockout in granulosa cells after FSH response has initiated follicle growth. These mice show complete sterility, reduced number of ovulated oocytes, displayed significantly fewer corpora lutea (CLs), abnormal CL morphology, and occasional cysts when compared to their single knockout and wildtype littermates. Follow up analyses show that like the double knockout, either single receptor knockout mice have reduced progesterone serum levels at 24h and 48h post eCG 48h/hCG treatment. This decline was linked to reduced expression of steroidogenesis enzymes: *Star* and *Cyp11a1*, by 98% and 72% respectively in superovulated double knockout mice at 12h post hCG. Ovaries from double knockout mice exhibit trapped oocytes in luteinized follicles reminiscent of *Pgr*-null mice. We observed a 6.5-fold reduction of *Pgr*, and a 5-fold reduction of *Adamts1* compared to control littermates, supporting failed *Pgr* signaling as a contributing factor in impaired ovulation. To identify additional potentially novel factors downstream of insulin signaling we performed RNA sequencing. After GSEA analyses, one of the main groups of significantly changed genes were part of the CAGGTG\_E12\_Q6 gene set (FDR=1.17x10<sup>-27</sup>), this set contains genes having at least one occurrence of the transcription factor 3 (TCF3) consensus binding motif. This suggests insulin receptor signaling may coordinate multiple downstream genes via altering TCF3 levels. Reduced expression in the double knockout mouse ovaries was verified for several putative TCF3 targets including *Scg2*, *Slco2a1*, *Slc39a14*, *Slc7a11*, and *Vcan* by quantitative real-time RT-PCR (qPCR). Additional genes of interest from our RNA-seq, with established ties to ovulation, were confirmed as downregulated including: *Adam23*, *Arnt1*, *Efh1*, *Epha4*, *Ereg*, *Hs6st1*, *Hspe1*, *Idh1*, *Il1r1*, *Il1r2*, *Pam*, and *Plxnd1*. Collectively, these results highlight the importance of growth factors of the insulin family, specifically in the periovulatory window, opening new lines of investigation for factors critical for ovulation. Supported by SOM Seed Grant 505144.

### **Evaluation of Equine Endometrium During Maternal Recognition of Pregnancy Utilizing RNA**

**Sequencing.** Kristin Klohonatz, Alma Islas-Trejo, Juan Medrano, Ann Hess, Stephen Coleman, Milton Thomas, Gerrit Bouma, Jason Bruemmer

Equine maternal recognition of pregnancy (MRP) is a process whose signal remains unknown. During MRP the conceptus and endometrium communicate to attenuate prostaglandin F<sub>2</sub>α (PGF) secretion thus sparing the corpus luteum and maintaining progesterone production. Recognition of a mobile and viable conceptus by the endometrium is critical prior to days 14-16 post-ovulation (PO). Between days 14-16 PO in the non-pregnant mare, endometrium produces PGF, which initiates luteolysis. Previous gene expression analyses have failed to robustly reveal possible candidates involved in MRP. Therefore, we evaluated equine endometrial gene transcripts via RNA Sequencing during MRP. The objective of this study was to evaluate endometrial gene expression changes based upon pregnancy status. This experiment utilized a cross-over design with each mare serving as a pregnant and non-mated control on days 9, 11, and 13 PO (n=3/day). Mares were randomly assigned to a collection day and each provided endometrial samples for a pregnant and non-mated cycle. Pregnancy was confirmed by terminal uterine lavage at the time of endometrial biopsy. Biopsy samples were snap frozen and stored until RNA isolation. Total RNA was isolated with Tri Reagent. Libraries were prepared using the Illumina TruSeq RNA Sample Preparation kit and sent to the University of California-Berkeley for RNA-Sequencing. Reads were mapped and annotated using CLC Genome Workbench. Annotation details were based on Ensembl and NCBI models combined with publicly available RNA-Seq data. Expression values for genes and transcripts were summarized as reads per kilobase per million reads (RPKM). All transcripts considered for analysis were present in all three samples from a group with an RPKM > 0.25. Differential gene expression was analyzed with SAS via student's paired t-test for comparing pregnancy status within and across days following calculation and application of the Benjamini-Hochberg correction for multiple testing (P < 0.05 was considered significantly differentially expressed). On day 9, 11 and 13 there were 1296, 1647 and 1497 genes and 1579, 2010 and 1808 corresponding transcripts, respectively. Across all three days, 8 genes and 9 corresponding transcripts were only present in samples from non-pregnant mares and 9 genes and 10 transcripts were present in samples from pregnant mares. Interestingly, among the 17 uniquely expressed genes confirmed by PCR, CATSPERD\_1 was present only in endometrial biopsies from pregnant mares, but it has never been described in the endometrium from any species. Further analysis is being completed to understand the localization and function of CATSPERD in endometrium. These findings imply that transcript variants differ between endometrium from pregnant and non-pregnant mares as well as over the time of MRP.

**Sexually Dimorphic Epigenetic Profile of the Inner Cell Mass in the Mouse Embryo.** Elena Ruggeri, Annemarie Donjacour, Xiaowei Liu, and Paolo Rinaudo

Blastocysts conceived by in vitro fertilization (IVF) have a high male to female sex ratio, with female embryos having a higher apoptosis rate and are more vulnerable. Furthermore, up to one third of genes are differentially expressed between male and female blastocysts. Prior studies have found a sexually dimorphic effect of IVF on both phenotype and metabolite expression, indicating a sex dependent sensitivity of the embryo and adult to the environmental stress added by the use of IVF. These changes in gene expression may be due to an asymmetrical distribution of epigenetic marks between male and female embryos. The primary objective of our study was to determine if preimplantation embryo

manipulation is associated with DNA methylation and histone changes in a sex dependent fashion. We compared DNA methylation using whole genome bisulfite sequencing (WGBS) in the inner cell mass of male and female mouse blastocysts conceived in vivo or in vitro. Mouse blastocysts were obtained from CF-1 females crossed with B6D2F1 males and utilized for in vitro fertilization or flushed out of the uterus. IVF was performed using KSOM with amino acids and 5% O<sub>2</sub>. Blastocysts were collected (IVF and in vivo) and immune-surgery performed isolating ICM and trophectoderm (TE) cells. DNA was isolated from the TE cells and was utilized in quantitative real time PCR for sexing, specifically evaluating X-chromosome gene lysine-specific demethylase 5 (kdm5c) and the corresponding Y-chromosome gene (Kdm5d). Pooled ICM of male and female blastocysts (n=15/group, 2 replicates/group) were utilized for whole genome bisulfite sequencing (WGBS). Methyl-MaxiSeq was used for WGBS and sequenced on the Illumina HiSeq4000. Reads were mapped to the mouse genomes (mm9) using Bismark and differentially methylated regions (DMR) identified using BSSEQ Bioconductor package in R. DMR were functionally characterized using Genomic Regions Enrichment of Annotations Tool (GREAT). There were 3093 differentially CpG methylated regions (DMR: 1531 hypomethylated and 1562 hypermethylated) between male and female ICMs. The majority of DMR were located between 5 and 500 kb from the transcription start site (TSS) and approximately 50% were located in the body of the genes. The hypomethylated regions, corresponded to genes whose function was involved in posttranscriptional regulation of gene expression, microtubule-based process, nucleoside triphosphate metabolic process, ribonucleoside triphosphate metabolic process, purine nucleoside triphosphate metabolic process, and nucleoside triphosphate catabolic process. The hypermethylated regions, were in proximity of genes whose function was negative regulation of myoblast differentiation, extracellular matrix organization, extracellular structure organization, regulation of myotube differentiation, and UDP-glucose metabolic process. This is the first report of global DNA methylation changes in isolated ICMs of male or female blastocysts. The candidate genes identified as being differentially methylated in ICM of male and female embryos can elucidate the phenotypic alterations noted in adult animals.

**Effects of IGF-1 on Markers of Follicle Development in the Hen.** Laurie Francoeur, Jasmine Kannampuzha-Francis, and Patricia Johnson

In laying hens, follicle selection is very organized and results in a well-defined hierarchy; in contrast, broiler breeder hens fed ad libitum (FF) have excessive ovarian follicular development that often results in multiple ovulations. This tendency causes erratic patterns of lay and reduces productivity. Evidence in the literature as well as in our data indicates that selection for increased growth rates in broiler chickens has altered the growth hormone/insulin-like growth factor I (GH/IGF-1) axis, resulting in higher production of liver IGF-1 and increased bioavailability of circulating IGF-1 in FF broiler hens. The IGF-1 receptor (IGF-1R) is present in granulosa cells and increases with size of follicles. While IGF-1 has been shown to influence granulosa cell proliferation and progesterone production in chickens, its effects on other markers of follicle selection have not yet been examined in the hen. Moreover, although the expression of IGF-1R has not been identified in the hen oocyte thus far, IGF-1 could potentially exert a direct effect on the oocyte.

In Experiment 1, we investigated the effect of IGF-1 on mRNA expression of FSH receptor (FSHR), anti-mullerian hormone (AMH), and steroidogenic acute regulatory protein (StAR) in cultured granulosa cells. Follicles were removed from commercial Single-comb White Leghorn hens (n=7) with consistent laying

patterns. Granulosa cells from 3-5 and 6-8 mm follicles were removed and pooled within hen according to size. Cells (2-3 million cells/well) were allowed to attach for 24 hours in a 6-well culture plate, then cultured in Medium 199 + 0.1% BSA and human recombinant IGF-1 (0, 25, or 200 ng/ml) for an additional 24 hours in the presence or absence of FSH (10 ng/ml). Parallel 96-well plates were set up to estimate cell proliferation. Using qPCR, mRNA expression of AMH, FSHR, and StAR was quantified. IGF-1 did not have a significant effect on any of the targets nor on granulosa cell proliferation from 3-5 or 6-8 mm follicles. In granulosa cells from 3-5 mm follicles, FSH significantly increased StAR and decreased AMH expression ( $p < 0.01$ ). Moreover, granulosa cells from 3-5 mm follicles had significantly higher expression of FSHR and AMH than those of 6-8 mm follicles ( $p < 0.01$ ). In Experiment 2, to investigate whether there could be a direct effect of IGF-1 on the oocyte, we evaluated the mRNA expression of IGF-1R and bone morphogenetic protein 15 (BMP15) in granulosa cells and ooplasm of 3 and 5 mm follicles ( $n=8$  hens) using qPCR. IGF-1R and BMP15 were found to be more abundant in 3 mm follicles compared to 5 mm follicles ( $p < 0.01$ ). In 3 mm follicles, the mRNA for IGF-1R ( $p=0.05$ ) and BMP15 ( $p < 0.01$ ) was significantly higher in ooplasm compared to granulosa cells, however, there was no difference between granulosa cells and ooplasm for either IGF-1R or BMP15 expression in 5mm follicles. These findings suggest that IGF-1 may be acting on the oocyte to indirectly affect granulosa cell function.

This project was supported by Agriculture and Food Research Initiative Competitive Grant no. 2017-67015-26453 from the USDA National Institute of Food and Agriculture

**Maternal Obesity in Sheep Increases Aortic Collagen: Elastin Ratio and Hypertension.** Chris L. Pankey, Peter W. Nathanielsz, and Stephen P. Ford

According to the World Health Organization, cardiovascular diseases (CVD) are the world's greatest killer, accounting for 31% of all global deaths. Obesity and hypercaloric diet are amongst the greatest risk factors for CVD, and accumulating evidence suggests that maternal obesity during gestation programs adverse cardiovascular development, leaving offspring susceptible to CVD. Therefore, we hypothesized that diet induced obesity during gestation would result in adverse cardiovascular development in offspring. To test this hypothesis, multiparous rambouillet/columbia cross ewes were fed a highly palatable diet at either 100% (CON), or 150% (OB) of National Research Council recommendations from 60 days prior to conception, until necropsy at day 135 (90%) of gestation (CON:  $n=7$ , OB:  $n=6$ ), or through term (CON:  $n=15$ , OB:  $n=10$ ). Ewes were either sedated with ketamine and necropsied following exsanguination under isoflurane inhalation general anesthesia, or allowed to lamb unassisted. For necropsied animals, fetal aortas were removed, placed in 4% paraformaldehyde, and paraffin embedded. 5  $\mu$ m sections were deparaffinized, and stained using Van Geison, Masson Trichrome, and hematoxylin and eosin staining protocols. Stained sections were imaged using a 4x objective on an Olympus BX51 using a Qimage Retiga EXi camera. Color deconvolution of all images was accomplished using ImageJ software, and mean intensity of elastin (Colour 2 image - red) and collagen (Colour 2 image -blue) expression were determined using the measure command. Optical Density (OD) was determined using  $OD = \log_{10}(\text{mean intensity}/\text{max intensity})$ , where max intensity = 255 (for 8 bit image). For lambs, F1 morphometrics were recorded at birth, and blood pressures (BP) were recorded via auricular artery catheterization using an invasive blood pressure monitor at 2.5 months of age. Birth weight did not differ between CON and OB lambs ( $5.1 \pm 0.2$  vs  $4.9 \pm 0.2$  Kg, respectively). Systolic BP was greater ( $p < 0.03$ ) in OB than CON lambs ( $107.9 \pm 3.4$  vs  $101.2 \pm 1.5$  mmHG, respectively), while diastolic

BP did not differ ( $82.0 \pm 2.5$  vs  $84.3 \pm 3.1$  mmHg, respectively). There were no differences between OB and CON lambs in heart rate ( $136.9 \pm 7.41$  vs.  $127.5 \pm 6.3$  bpm, respectively). Aortic wall thickness was greater ( $p < 0.05$ ) in OB than CON fetuses ( $754.1 \pm 56$  vs.  $610.5 \pm 51$   $\mu$ m, respectively). Masson trichrome staining showed a tendency ( $p < 0.07$ ) for increased OD of collagen ( $0.107 \pm 0.01$  vs.  $0.128 \pm 0.009$  A.U. for CON and OB fetuses, respectively), and Van Gieson staining showed decreased ( $p < 0.05$ ) OD of elastin ( $0.062 \pm 0.005$  vs.  $0.048 \pm 0.003$  A.U. for CON and OB, respectively) in fetal aorta sections. Consequently, OB fetal aortas had higher ( $p < 0.02$ ) collagen to elastin ratios than CON fetal aortas ( $2.74 \pm 0.34$  vs.  $1.85 \pm 0.18$ , respectively). These findings suggest that maternal obesity programs altered vascular development by late gestation. An increased collagen:elastin ratio suggests decreased compliance in the aorta, which has been linked to systolic hypertension. Previous studies demonstrate that increased aortic collagen:elastin ratio is in response to hypertension as a protective mechanism, suggesting that blood pressure may also be elevated during gestation. Hemodynamics are established as a primary determinant of cardiovascular development, thus, future studies focusing on hemodynamics are imperative to determine the developmental consequences from maternal obesity.

### **Let7 miRNA are Abundant in the Bovine Corpus Luteum and Regulate Cellular Metabolic Functions.**

Vijay S. Baddela, Camilla K. Hughes, and Joy L. Pate

Let-7 miRNA constitute an abundantly expressed miRNA family in both male and female gonads among many animal species. This was confirmed by miRNA sequencing data from the corpus luteum (CL) of both cyclic and pregnant cows. Yet, the studies describing the let-7 isomirs and their genome-wide biological functions have not been performed in eukaryotes. Therefore, the present study was designed to identify let-7 isomirs and to determine the targets of the abundantly expressed let-7 miRNAs. Analysis of miRNA sequencing data from Day 17 CL ( $n = 4$  cyclic and 4 pregnant) indicated the presence of eleven different let-7 miRNA (bta-let-7b, bta-let-7a-3, bta-let-7f-1, bta-let-7c, bta-let-7e, bta-let-7g, bta-let-7d, bta-let-7f-2, bta-let-7i, bta-let-7a-1, bta-let-7a-2), which together constituted 87% and 86% of total annotated miRNA reads in CL of pregnant and cyclic cows, respectively, indicating the substantial contribution of let-7 miRNA in the miRNome of the CL. Isomir classification was performed using sRNAbench tool. In this, all let-7 reads were classified into 8 different mature let-7 miRNAs (let-7a-5p, let-7b, let-7c, let-7d-5p, let-7e, let-7f, let-7g, and let-7i) and all of them were found to be present in six different isomir forms, which included canonical sequences, 3' trims, 3' elongations, 5' trims, 5' elongations and MV (reads with multiple nonlinear changes). This further revealed that the canonical reads of let-7a-5p and let-7b were the top two abundant miRNA sequences in the CL. Biotinylated let-7a-5p, let-7b and a scrambled miRNA control were transfected into cultured luteal cells obtained from midcycle bovine CL. The captured mRNA were pulled down using streptavidin magnetic beads and sequenced via Illumina MiSeq platform. Results indicated that 24 (12 nuclear and 12 mitochondrial) and 12 (2 nuclear and 10 mitochondrial) annotated mRNA were significantly enriched as targets of let-7a-5p and let-7b, respectively, compared to control. All the targets that were pulled down by let-7b were also found amongst the targets of let-7a, indicating the similar biological functions for let-7a-5p and let-7b miRNA, likely because let-7a-5p and let-7b differ in only one nucleotide at the 3' end. Notably, 9 out of 12 nuclear genome-derived pull-down targets were found to be predicted targets of let-7 miRNA in at least one of the target prediction programs used (Targetscan, MicroT-CDS, Tarbase, IPA, and miRanda). Further, the probable let-7 binding sites in all pull-down mRNA were identified using sTarMir tool (<http://sfold.wadsworth.org/cgi-bin/starmir.pl>). In pathway analysis (Ingenuity Pathway Analysis,

Qiagen), nuclear-derived targets were found to be involved in actin filament organization, cellular adhesion, glycolysis, antiviral response, and growth hormone signaling. As expected, the mitochondrial targets are involved in oxidative phosphorylation. Overall, the current results clearly suggest that let-7 miRNA could be important regulators of luteal function by regulating multiple nuclear and mitochondrial genes that might be essential for luteal homeostasis. Funding: This project was supported by Agriculture and Food Research Initiative Competitive Grant no. 2012-67015-30212 from the USDA National Institute of Food and Agriculture.

**Gonadotropin-Dependent Neuregulin-1 $\beta$  Signaling Attenuates TNF $\alpha$  Induced Rat Granulosa Cell Apoptosis.** Indrajit Chowdhury, Saswati Banerjee, Wei Xu, Sameer Mishra, and Winston E Thompson

Epidermal growth factors (EGFs) serves as gonadotropins-mediator throughout folliculogenesis, and are involved in various crosstalks through autocrine–paracrine mechanisms. Our studies have shown that neuregulin1 $\beta$  (NRG1 $\beta$ ), a member of the EGF family of proteins, is gonadotropin dependent differentially regulated in granulosa cells (GCs) and theca cells, and secreted in rat ovarian follicular fluid (FF). NRG1 $\beta$  acts as a survival factor through trans-membrane bound tyrosine kinase receptors (ErbB2 and ErbB3) during follicular development. However, the detailed mechanisms associated with the interplay of NRG1 $\beta$  and its receptors in GC in the presence of gonadotropins is not known. Therefore, we examined the role and action of NRG1 $\beta$  and its receptors in the gonadotropin signaling pathway that impacts GCs survival and inhibition of inflammatory cytokine productions. In order to confirm that Luteinizing hormone (LH)- dependent expression of NRG1 $\beta$  is anti-inflammatory, we employed siRNA interference to knock-down endogenous NRG1 $\beta$  in GCs collected from 25 days-old immature female rats treated with pregnant mare's serum gonadotropin (PMSG). Cell morphology was monitored by phase contrast microscopy revealed that GCs were fibroblastic in appearance in vitro in serum free medium (scrambled shRNA treated GCs). In the presence of LH, they present altered cellular appearance with an epithelioid morphology, characteristics of highly differentiated GCs. Whereas, GCs transfected with siRNA for NRG1 $\beta$  and treated with LH revealed fibroblastic morphology indicative of no cellular differentiated phenotype. Furthermore, knock down of NRG1 $\beta$  in GCs treated with LH showed increased levels of tumor necrosis factor- $\alpha$  (TNF $\alpha$ , an inflammatory cytokine) production, and enhanced GCs sensitivity to induction of apoptosis. Further studies revealed that GCs treated with exogenous TNF $\alpha$  promoted apoptosis in a dose and time-dependent manner in GCs. However, the effects of TNF $\alpha$  are attenuated in presence of exogenous NRG1 $\beta$  in a dose and time-dependent manner. Next, under these experimental conditions, immunoblot studies were performed to examine the expression of selective anti-apoptotic proteins Bcl2 and Bclxl, and ErbB2-ErbB3-PI3K-Akt signaling pathway. These studies indicated that exogenous TNF $\alpha$  treatment in presence of NRG1 inhibit apoptosis through increased levels of the anti-apoptotic proteins Bcl2 and Bclxl, and activation of ErbB2-ErbB3-PI3K-Akt signaling pathway. Collectively, these studies provide new insights on the gonadotropins-dependent activation of NRG1 $\beta$ -mediated anti-apoptotic mechanism in GCs through ErbB3-ErbB2-PI3K-Akt $\rightarrow$ Bcl/Bcl-xL pathway and may have important clinical implications.

Acknowledgements: This study was supported in part by National Institutes of Health Grants 1S3GM113751 and G12RR03034. This research was conducted in a facility constructed with support from the Research Facilities Improvement Grant C06RR018386 from the National Institutes of Health National Center for Research Resources.

**Glutamine Supplementation Enhances Development of in Vitro-Produced Porcine Embryos and Increases Leucine Consumption from the Culture Medium.** Paula Chen, Bethany Redel, Lee Spate, Tieming Ji, Shirley Rojas Salazar, and Randall Prather

Improper nutrient composition of culture medium is one of several factors contributing to reduced viability of in vitro-produced embryos. Specifically, glutamine (Gln) is a crucial amino acid for preimplantation embryos as it supports proliferation and is involved in many biosynthetic pathways. Previous transcriptional profiling revealed several upregulated genes related to Gln transport and metabolism in in vitro-produced porcine blastocysts compared to in vivo-produced counterparts, indicating a possible deficiency in the culture medium. The objective of this study was to determine the effects of Gln supplementation as a free amino acid or as the L-alanyl-L-glutamine dipeptide, GlutaMAX, on in vitro-produced porcine embryo development, gene expression, and metabolism. After fertilization and culture for 28 h, cleaved embryos were selected, and equal numbers were placed into the following treatments: MU2 with 1 mM Gln (control), MU2 with 3.75 mM Gln (+Gln), MU2 with 3.75 mM GlutaMAX (+Max), or MU2 with 3.75 mM alanine (+Ala). Percentage developed to the blastocyst stage and total cell number were recorded. Expression of message for glutamine and glutamate transporters (SLC1A1, SLC1A5, SLC7A5) and enzymes related to glutamine metabolism (GLS, GLUD1, ASNS, GPT2, PSAT, PYCR1) were analyzed by real-time PCR. A metabolomics analysis of spent culture medium was conducted to determine the effects of glutamine supplementation on production or consumption of metabolites in the medium. Lastly, mitochondrial function was assessed by expression of IMMT, SSBP1, PAM16, and PINK1 and JC-10 staining to determine mitochondrial membrane potential. All analyses were performed on day 6 blastocysts with at least 4 biological replicates. Data were analyzed for normality by a Shapiro-Wilk test, and differences between means were detected by one-way ANOVA followed by Fisher's LSD test ( $P < 0.05$  was considered significant). Embryos cultured with +Gln or +Max had increased development to the blastocyst stage ( $68.9 \pm 2.7\%$  or  $70.7 \pm 3.5\%$  vs  $58.9 \pm 2.6\%$ , respectively) and total cell number ( $51.5 \pm 2.1$  or  $52.3 \pm 2.5$  vs  $41.1 \pm 2.5$ , respectively) compared to the control. Expression of SLC1A1 and SLC7A5 were decreased in embryos cultured with +Gln or +Max, indicating alleviation of amino acid deficiencies. In agreement with the mechanism of SLC7A5 transport, metabolomics analysis revealed increased production of glutamine and glutamate from embryos cultured with +Max and increased consumption of leucine by those cultured with +Gln or +Max. Expression of GLS, which encodes an enzyme for glutamine catabolism, was increased in embryos cultured with +Gln and tended ( $P = 0.06$ ) to be increased in embryos cultured with +Max. Expression of enzymes involved in nonessential amino acid biosynthesis (ASNS, PYCR1) were decreased in embryos cultured with +Gln or +Max. Furthermore, expression of mitochondrial-related genes (IMMT, SSBP1, PAM16) were increased in embryos cultured with +Gln or +Max, and mitochondrial membrane potential (JC-10 staining) was increased in embryos cultured with +Max compared to the control. Culture with +Gln or +Max corrects amino acid transporter expression, increases leucine consumption from the medium, and enhances mitochondrial function to improve in vitro-produced porcine embryo development. This research was supported by Food for the 21st Century and R01HD080636.

**Neonatal Inhibition of a Mesenchymal Progenitor Cell by MIS/AMH Disrupts Uterine Development and Results in Infertility.** H. Duygu Saatcioglu, Motohiro Kano, Li Hua Zhang, Nicholas Nagykerly, Rana Suliman, Jenifer Hsu, Dan Wang, Guangping Gao, Mary Sabatini, Alessandro Alessandrini, Patricia Donahoe, and David Pepin

Mullerian Inhibiting Substance Receptor-2 (Misr2) is expressed in the mesenchyme surrounding the Mullerian duct epithelium during the early fetal urogenital ridge development of both sexes. In male embryos, secretion of MIS (Mullerian Inhibiting Substance), the ligand of Misr2, by the embryonic testes causes regression of the Mullerian duct. Misr2 expression perdures in developing female Mullerian ducts; however, the role of Misr2 in neonatal uterine development remains unknown. The mesenchymal progenitor cells of the Mullerian duct are thought to give rise to the two main layers of the uterus after birth: endometrium and myometrium, both of which play crucial roles in menstrual cycle, pregnancy, and labor. Therefore, genes affecting early development of these uterine layers may be of importance to female infertility.

We confirmed that Misr2 expression is high and restricted to a subset of mesenchymal cells directly adjacent to the Mullerian ductal epithelium during early uterine development. To study the effect of MIS on the neonatal development and differentiation of these Misr2+ uterine mesenchymal cells, we treated rat pups with adeno-associated viral vectors to deliver MIS (MISR2 ligand) continuously starting from day 1 and analyzed their uteri at various time points. Surprisingly, the Misr2+ mesenchymal cells remain susceptible to inhibition by MIS in neonatal rats, with treatment resulting in significantly smaller uteri ( $n>3$ ,  $p=0.0047$ , day 15), underdeveloped endometrial stromal layer ( $n>2$ , at day 6, 10, 20, and 45) and glandular defects ( $n>2$ , at day 20 and 45), but does not prevent the formation of myometrium ( $n>3$ ).

As a result of these developmental defects, treated rats were completely infertile, even when treatment was restricted to just the first 6 days of development using recombinant MIS protein (daily dose: 3mg/kg;  $n=3$ , postnatal day 1 until day 6,  $p=0.0114$ ). These results confirm that MIS can inhibit normal endometrial differentiation of uterine cells postnatally, at a time when MIS production in the ovary begins.

We further characterized the differentially expressed genes of the developing uteri in response to MIS by RNA-sequencing with droplet-based microfluidics (InDrop). We uncovered new sets of genes that are regulated by MIS in the uterus. 1) Genes uniquely present in the MIS-treated uteri expressed by an inhibited mesenchymal progenitor cell population (Bambi, Hdac4, Misr2, Smad6), 2) Early differentiating endometrial stromal genes which are expressed by a population of cells (present in controls) that is prevented from developing under MIS treatment (Vcan, Col3a, Bmp7). 3) Unique markers of (Misr2-) epithelial ductal cells, which are indirectly disrupted by MIS treatment (Acsn3, Id3, Msx2). These previously unidentified gene signatures represent important developmental pathways, which when disrupted neonatally have profound consequences on the later development of the uterus.

**Four Years of Combined Hyperandrogenemia and Western-Style Diet Impairs Metabolic and Reproductive Function in Young Female Rhesus Macaques.** Cecily V. Bishop, Diana Takahashi, Emily Mishler, Ov Slayden, Richard L. Stouffer, and Cadence True

Polycystic ovary syndrome (PCOS), is a leading cause of infertility in reproductive-age women associated with elevated androgen levels (hyperandrogenemia), obesity and insulin resistance. Both hyperandrogenemia and obesity are associated with reproductive dysfunction, making it unclear which of these factors drives subfertility in PCOS patients. A nonhuman primate model of hyperandrogenemia with and without obesity was developed by chronically exposing female rhesus macaques beginning at puberty to either mildly elevated testosterone (T via silastic implants, ~4-fold elevation), a western-style diet (WSD), or the combination (T+WSD) in a 2 by 2 factorial design to determine the individual and combined effects of treatment on metabolic and reproductive health. Macaques (n=9-10/group), including age-matched controls (C), received 4 years of treatment through the current evaluations. Previous studies after 3 years of treatment demonstrated reduced fertility in the T, WSD and T+WSD groups related to the degree of metabolic dysfunction [PMID: 29401269]. By 4 years of treatment, the T+WSD had the worst metabolic outcomes, including increased body weight (overall effect of WSD  $p=0.004$ , interaction T by WSD  $p < 0.03$ ) and body mass index (BMI; T  $p=0.02$ , WSD  $p=0.003$ ) compared to other groups. The percent body fat was greater in WSD and T+WSD groups (WSD  $p=0.0005$ ). In addition, the T+WSD group had increased percentage of fat in the android region (WSD  $p=0.0003$ ) compared to C and T groups, which correlates with insulin resistance in humans. Consumption of WSD was associated with increased fasting insulin levels (WSD,  $p=0.01$ ) as well as increased glucose area under curve (AUC) and insulin secretion during an intravenous glucose tolerance test (ivGTT; WSD  $p < 0.0001$ , interaction T by WSD  $p=0.04$ ; WSD  $p=0.01$ ). Number and length of menstrual cycles were analyzed in the middle of the macaque breeding season during the fifth year on treatment (October-February). The WSD was associated with fewer menstrual cycles in WSD and T+WSD groups (WSD  $p=0.04$ ), possibly due to slightly longer menstrual cycles ( $37\pm 5$  and  $34\pm 3$  days) compared with C and T groups ( $32\pm 3$  and  $31\pm 1$  days). Number of menstrual cycles negatively correlated ( $R^2 = -0.45$ ,  $p=0.003$ ), whereas menstrual cycle length positively correlated ( $R^2 = 0.3$ ,  $p=0.056$ ), with glucose AUC during ivGTT. These data suggest that exposure to hyperandrogenemia in the presence of an obesogenic diet drives metabolic dysfunction in young women with PCOS. However, metabolic changes induced by chronic consumption of the WSD alone have a subtle impact on menstrual cycle regularity. Since macaque females vary in their sensitivity to an obesogenic diet, the correlations between menstrual cycle disruption and uncontrolled glucose clearance reflects a link between reproductive and metabolic dysfunction in primates. These females are still relatively young (similar to ~21-year old women) and therefore effects of hyperandrogenemia and WSD/obesity on reproductive and metabolic dysfunction may worsen as treatments continue, especially as they reach similar ages to women with PCOS presenting for infertility therapy (late 20's - early 30's). Supported by NIH P50 HD071835 (NCTRI/RLS), and P51 OD011092 (ONPRC).

**Use of Synthetic Polymers Improves the Quality of Vitrified Caprine Preantral Follicles in the Ovarian Tissue.** Ana Paula Ribeiro Rodrigues, Diego Alberto Montano Vizcarra, Yago Pinto da Silva, Jamilly Bezerra Bruno, Danielle Cristina Calado de Brito, Luciana Mascena Silva, Maria Luana Gaudêncio dos Santos Morais, José Ricardo de Figueiredo, and Mary B. Zelinski

The aim of this study was to evaluate whether the addition of non-permeating, synthetic polymers to the vitrification solution affected follicular morphology and development, reactive oxygen species (ROS) levels and the expression of Ki-67, Aquaporin 3 (AQP3) and cleaved Caspase-3 proteins in ovarian tissue of the caprine species. Caprine ovaries were fragmented and randomly distributed among the groups. Two fresh fragments were immediately fixed (Fresh Control) for morphological evaluation, while other two were in vitro cultured for 7 days (Cultured Control) and then fixed as well. The remaining fragments were distributed in two different vitrification groups: Vitrified Group (Vitrified), when the fragments were fixed after vitrification and Vitrified/ Cultured Group (Vitrified/Cultured), when they were fixed after vitrification and in vitro culture for 7 days. Each group was composed of 4 different vitrification treatments (2 fragments/treatment/group): 1) Vitrification with the addition of sucrose (SUC); 2) Vitrification with the addition of SuperCool X-1000 0.2 % (X-1000); 3) SuperCool Z-1000 0.4 % (Z-1000) or 4) with PVP K-12 0.2 % (PVP), totaling four experimental treatments. Medium was collected at Day 1 and Day 7 of in vitro culture for ROS levels analysis. Also, Fresh Control, Cultured Control, Sucrose and SuperCool X-1000 were destined to immunohistochemical detection of Ki-67, AQP3 and cleaved Caspase-3 proteins. Morphologically, the treatment with SuperCool X-1000 showed no significant difference with the Fresh Control group and was superior to the other treatments. All vitrified and in vitro cultured treatments maintained the percentage of developing follicles similar to the Fresh Control, except the one vitrified with SuperCool Z-1000. Only the Fresh Control showed Ki-67-positive granulosa cells, indicative of proliferation. After the cleaved caspase-3 analysis, the SuperCool X-1000 treatment showed the lowest percentages of GIII staining intensity follicles, while Cultured Control treatment showed the highest. Also, a positive correlation was found between the percentages of degenerated follicles and the percentages of GIII staining intensity follicles. The highest percentages of strong (+++) AQP3 immunostaining intensity were found in the SuperCool X-1000 treatment. There were no significant differences in the ROS levels between day 1 and day 7 or among treatments at day 7. We have demonstrated that the vitrification with the synthetic polymer SuperCool X-1000 followed by in vitro culture for 7 days maintained the follicular morphology similar to the observed in the Fresh Control.

**Live Birth of a Pashmina Goat Kid After Transfer of Handmade Cloned Blastocysts.** Maajid Bhat, Firdous Khan, Hilal Yaqoob, Hilal Khan, Mujeeb Fazili, Nazir Ganai, and Riaz Shah

The aim of the present study was to establish a continuous culture medium and culture system for the successful hand made cloned embryos. Abattoir derived oocytes were in vitro matured, after maturation the oocytes were enucleated and fused with the somatic cells derived from adult Pashmina goat. The reconstructs were activated by Calcium ionophore- DMAP procedure. The embryos were distributed in either of the two experimental groups. In Experiment 1, the embryos were distributed in either of the following culture media (i) G1.G2 (ii) mSOF (iii) RVCL (iv) EDM, and cultured for 7 days. The cleavage rates in G1.G2 and RVCL were higher than mSOF and EDM (86.84%, 82.44% vs. 77.30% and 68.82%), respectively. The blastocyst rates were higher in RVCL than mSOF, EDM and G1.G2 (15.01% vs. 10.53%

vs. 4.92% vs. 2.22%), respectively. In experiment 2, the embryos were cultured in different culture systems (i) FS (ii) WID (iii) WOW (iv) Microdrop (v) Hanging drop, for 7 days. The cleavage rates in FS and WID were higher than WOW, Microdrop and hanging drop (84.34% and 81.26% vs. 73.60%, 73.55% and 70.38), respectively. The blastocyst rates were higher in WID than WOW, Microdrop, hanging drop and FS systems (21.65% vs. 13.72%, 11.57%, 10.94% and 3.92%), respectively. Out of the three pregnancies established on day 40, one resulted in the delivery of a healthy Pashmina Kid. To our knowledge this is the first report of a cloned Pashmina kid produced through hand made cloning technique from abattoir derived oocytes.

**The Expression of Post-Transcriptional Regulator Lin28 During Porcine Testicular Development.** Jae-Seok Woo, Keon Bong Oh, Sun-A Ock, Sung June Byu, Lee Hwi-Cheul, Yang Hyeon, Gi-Sun Im, Wootae Ha, and Hyuk Song

The Lin28 is known as post-transcriptional regulator for pluripotency in mice embryonic stem cells and spermatogonial stem cells. However, the expression of Lin28 have not identified yet in pig. Thus, we analyzed the expression of Lin28 during developmental stages of porcine testis. Briefly, the porcine testis were obtained from 5, 60, 90, 120, 150 days old crossbred pig with approved guideline from the Institutional Animal Care (No. NIAS2015-120). Immunohistochemistry were performed to identify the specific expression of Lin28 in porcine testis. In post-natal stage before puberty, the Lin28 expression was observed only in spermatogonial stem cells of porcine testis. After puberty, the Lin28 expression was observed in several types of differentiated cells. Additionally, these types of differentiated cells were analyzed by multiple staining with C-kit, Scp3, and Acrosin. The Lin28-positive expression was observed in C-kit-negative cells but some of Lin28-positive cells were also positive to Scp3 and Acrosin. Conclusively, the expression of Lin28 was observed at spermatogonial stem cells in the pre-pubertal testis, but it was also observed at differentiated cells after puberty. Therefore, the Lin28 could be a useful marker for spermatogonial stem cells in pre-pubertal stage of porcine testis and can be used to understand spermatogenesis in adult porcine testis. This work was carried out with the support of "Cooperative Research Program for Agriculture Science & Technology Development (Project No. PJ01094403)" Rural Development Administration, Republic of Korea. (Key words: porcine, puberty, testicular, spermatogonial stem cell, Lin28)

**Sensitivity to Luteinizing Hormone of Bovine Luteal Steroidogenic Cells in Various Culture Methods with Collagen.** China Maruo, Kazuhisa Hashiba, Daisuke Watanabe, and Koji Kimura

In mammals, the corpus luteum (CL) is an essential endocrine organ for the establishment and maintenance of pregnancy. It has been reported that luteal cells are surrounded by extracellular matrix (ECM), which is a supramolecular structure present outside cells and is involved in tissue remodeling, signal transduction, and others. ECM in CL has important roles in luteal formation, development, and vascularization. Collagen type I is a major luteal component of the ECM and its content changes during the estrous cycle. However, since monolayer culture of luteal cells, which is a common cell culture method, does not include collagen, the function of luteal cells cultured with collagen is yet to be analyzed.

In the first experiment in this study, we examined how collagen of bovine luteal steroidogenic cells (LSCs) affects progesterone (P4) production and the mRNA expression of luteinizing hormone receptor (LH-R), when LSCs are cultured on or in collagen gel. Ovaries were collected from cows at a local slaughterhouse. Bovine mid-stage LSCs (days 8–12 after ovulation;  $1 \times 10^4$  cells/well) were cultured on plastic dishes (monolayer culture), on collagen type I gel (culture on collagen gel), or in collagen type I gel (collagen gel-embedded culture). LSCs were cultured in culture medium, D-MEM/Ham's F-12 containing 5% calf serum. After 5 days of culture, the medium was replaced with D/F medium without phenol red containing 0.1% BSA, sodium selenite, and holo-transferrin and was exposed to luteinizing hormone (LH; 10 ng/ml) for 24 h. At the end of culture, the supernatant and cells were collected. P4 production in the supernatant was measured by enzyme immunoassay. The expression of LH-R mRNA was examined by RT-PCR.

There are two types of collagen structures. One is a three-dimensional structure, such as collagen gel, and the other is a planar structure, such as collagen coating. In the second experiment here, we examined how the structure of collagen of LSCs affects P4 production and the mRNA expression of LH-R. For this, bovine mid-stage LSCs were cultured on plastic dishes, collagen type I gel (culture on collagen gel) or collagen type I-coated dishes (culture on collagen-coated dishes). The time course of the culture, the method of measuring P4 production, and the expression of LH-R were the same as in the first experiment.

In the first experiment, treatment with LH significantly induced P4 production in the monolayer culture ( $P < 0.05$ ), but not in the culture on collagen gel and embedded collagen culture. The expression of LH-R mRNA was significantly lower in the culture on collagen gel and embedded collagen gel culture than in the monolayer culture ( $P < 0.05$ ). In the second experiment, treatment with LH significantly induced P4 production in culture on collagen-coated dishes ( $P < 0.05$ ), as well as in monolayer culture. However, when LSCs were cultured on collagen gel, the expression of LH-R significantly decreased, resulting in insensitivity to LH. These results suggest that the sensitivity of bovine LSCs to LH was affected by the structure of collagen rather than its presence in the culture.

**Effect of Dietary N-3 Polyunsaturated Fatty Acid Supplementation on the Expression of Genes in Progesterone Synthesis in the Corpus Luteum of Doe (*Capra Hircus*).** Ravjibhai Chaudhari, Ajit Singh Mahla, Amit Khatti, Sanjay Kumar Singh, Harendra Kumar, and Narayanan Krishnaswamy

Effect of dietary n-3 polyunsaturated fatty acid supplementation on the expression of genes in progesterone synthesis in the corpus luteum of doe (*Capra hircus*)

Ravjibhai K Chaudhari, Ajit Singh Mahla, Amit Khatti, Sanjay Kumar Singh, Harendra Kumar, Narayanan Krishnaswamy. College of veterinary science and animal husbandry, Sardarkrushinagar Dantiwada Agricultural University, Sardarkrushinagar, Dantiwada, Gujarat, India; Division of Animal Reproduction, ICAR-Indian Veterinary Research Institute, Izatnagar, Bareilly, Uttar Pradesh, India

Dietary n-3 polyunsaturated fatty acid (PUFA) modulates not only endometrial prostaglandin production but also ovarian steroidogenesis in the ruminants. Recently, we reported that dietary fish oil (FO) rich in n-3 eicosapentaenoic acid (EPA) and docosohexaenoic acid (DHA) increased the diameter of developing

corpus luteum (CL) without influencing the peripheral progesterone (P4) in the doe. Accordingly, we studied the modulation of transcripts involved in the P4 synthesis. Cycling does (n=12) of Rohilkhand region were divided into two equal groups and fed an isocaloric diet supplemented with either FO containing 26 % n-3 PUFA or palm oil (PO) at the rate 0.6 mL/kg body weight for 55-57 days. Estrus was synchronized by two injections of PGF2 $\alpha$  analog and laparotomy was done to collect luteal tissue on day 16 post-estrus. Expression of genes involved in the P4 pathway biosynthesis was done on the cDNA using real-time PCR. The relative mRNA expression of steroidogenic acute regulatory protein (STAR) was nearly decreased by 2 fold (P < 0.05, while 3-beta-hydroxysteroid dehydrogenase (HSD3B) was increased by 1.13 fold (P < 0.05) in the FO than that of PO group. The expression of cholesterol side cleavage enzyme (CYP11A1) was not modulated. Moderate downregulation of STAR, which is the rate limiting protein, indicated that dietary FO rich in n-3 EPA and DHA would decrease luteal P4 synthesis. The study was funded by The Department of Biotechnology, Ministry of Science and Technology, India vide grant No.45613140115.

**Is Resistin Engaged in the Regulation of Seasonality of Reproduction in Sheep?** Dorota A. Zięba, Weronika Biernat, Katarzyna Kirsz, and Małgorzata Szczęśna

Relationships between energy metabolism and fertility have been observed in many species. However, there are several metabolic signaling pathways, including those involving the adipokine resistin, that have not been fully explored. Work in cattle and rodents has shown that resistin, in addition to its roles in insulin resistance and inflammation, is involved in the regulation of gonadal and testicular steroidogenesis and gametogenesis. However, its role in the regulation of reproductive processes in other species such as the seasonal breeding sheep is unknown. Herein, we tested the hypothesis that resistin can influence secretion of anterior pituitary hormones and leptin and that its effect is dependent on the length of the day in ewes. Thirty ewes of the Polish Longwool breed, a breed that exhibits strong seasonal reproduction, were ovariectomized with estrogen replacement using subcutaneously inserted estradiol implants. Ewes were fed *ad libitum* and housed in natural photoperiod (longitude: 19°57' E, latitude: 50° 04' N). Intravenous treatments consisted of control or recombinant bovine resistin (rbresistin) in saline: 1) Control (saline; n = 10), 2) Low resistin (1.0  $\mu$ g/kg BW; n = 10), and 3) High resistin (10.0  $\mu$ g /kg BW; n= 10). Experiments were conducted during both short (SD) and long days (LD). Blood samples were collected every 10 minutes during 4 h. Blood plasma concentrations of FSH, LH, and leptin were assayed using RIA and ELISA kits. A season x dose interaction was observed for all hormonal variables measured. Greater concentrations (P < 0.001) of LH and FSH were observed during SD compared for LD in all groups. During SD, the High dose (10  $\mu$ g/kg BW) decreased (P < 0.001) basal LH and amplitude (P < 0.05) of LH pulses and increased (P < 0.001) circulating concentrations of FSH. However, the lower dose of resistin decreased (P < 0.001) FSH concentrations compared to Controls. During LD, both the Low and High resistin doses increased mean concentrations of LH (P < 0.001 and P < 0.05, respectively) and FSH (P < 0.001). Resistin infusion decreased (P < 0.001) mean circulating concentrations of leptin in a dose-dependent manner during both seasons. However, leptin concentrations were greater during LD compared to SD. These results demonstrate for the first time that resistin is involved in the regulation of pituitary gonadotropin secretion and this effect is differentially mediated during LD and SD. Moreover, resistin appears to also modulate metabolic signaling hormones such as leptin. Further studies are underway to clarify the potential roles of resistin

in modulating central leptin sensitivity, as well as effects on secretion of prolactin and growth hormone. Research supported by National Science Centre, Poland - NCN 2015/19/B/NZ9/01314 to DAZ.

**Cryoprotectant Effect of Iodixanol on Bovine Sperm Kinetics..** Fernanda Nunes Marqui, Alicio Martins Jr., Tairini Erica Cruz, Tatiana Issa Uherara Berton, Diego Gouvêa Souza, José Antônio Dell'Aqua Júnior, and Eunice Oba

Iodixanol, a nontoxic solution, has been used as a density gradient medium to isolate viable spermatozoa as well as a cushioned substance to protect sperm during centrifugation. However, there are few studies on its addition in freezing extender and, to our knowledge, this is the first report of added iodixanol as a single cryoprotectant for bovine semen cryopreservation. Therefore, a pool of ejaculates from three Nelore bulls (n=18) was extended in a commercial freezing medium (egg yolk-sugar based) plus 7% glycerol (control) and in the same extender, but with 3.5% of glycerol and 3.5% of iodixanol or devoid of glycerol plus 7% of iodixanol. Only ejaculates with total motility  $\geq 60\%$ , vigor  $\geq 3$ , concentration  $\geq 1$  billion of spermatozoa/ml and major and minor defects  $\leq 10\%$  and  $< 20\%$ , respectively, were selected for this study. After dilution (60 million of spermatozoa/ml), the semen samples were cooled at  $4^{\circ}\text{C}$  for 5h, filled in 0.5 ml straws and frozen in a programmable freezer machine, according to the follow temperature/time curve: from  $4^{\circ}\text{C}$  to  $-10^{\circ}\text{C}$  ( $5^{\circ}\text{C}/\text{min}$ ),  $-10^{\circ}\text{C}$  to  $-100^{\circ}\text{C}$  ( $40^{\circ}\text{C}/\text{min}$ ) and from  $-100^{\circ}\text{C}$  to  $-140^{\circ}\text{C}$  ( $20^{\circ}\text{C}/\text{min}$ ), in a total of 8 min. The straws were stored in liquid nitrogen and at the moment of evaluation, they were thawed in water bath a  $37^{\circ}\text{C}/30\text{s}$ . A computer assisted sperm analyzer was used to assess the sperm samples for the following kinetic parameters: total motility (TM, %), progressive motility (PM, %), curvilinear velocity (VCL,  $\mu\text{m}/\text{s}$ ), straight line velocity (VSL,  $\mu\text{m}/\text{s}$ ), average path velocity (VAP,  $\mu\text{m}/\text{s}$ ), amplitude of lateral head displacement (ALH,  $\mu\text{m}$ ), beat cross frequency (BCF, Hz), linearity (LIN, %), straightness (STR, %) and wobble (WOB, %). ANOVA and Tukey's test were used for statistical analysis with results expressed as mean  $\pm$  standard deviation (data of six replicates).  $P < 0.05$  was considered significant. Total and progressive motility were higher ( $P < 0.05$ ) in control group ( $63.3 \pm 8.4$  and  $51.5 \pm 4.9$ , respectively) than for samples frozen in glycerol + iodixanol ( $47.5 \pm 4.7$  and  $36.9 \pm 2.8$ ) and for those with iodixanol alone ( $5.4 \pm 1.6$  and  $4.05 \pm 1.5$ ). Furthermore, the control group showed higher VCL ( $130.1 \pm 5.3$ ), VSL ( $70.4 \pm 1.9$ ), VAP ( $88.7 \pm 2.8$ ) and ALH ( $1.1 \pm 0.06$ ) compared to glycerol + iodixanol ( $100.5 \pm 2.9$ ,  $60.7 \pm 1.6$ ,  $71.3 \pm 7.2$  and  $1.3 \pm 0.02$ , respectively) and iodixanol ( $94.9 \pm 1.2$ ,  $58.2 \pm 2.5$ ,  $72.8 \pm 2.3$  and  $1.2 \pm 0.1$ , respectively). However, LIN and WOB were significantly lower in control group ( $0.55 \pm 0.01$  and  $0.69 \pm 0.01$ , respectively) than for the other two groups. Values of BCF and STR were similar between groups. Thus, it be concluded that iodixanol as a single cryoprotectant, under these experimental conditions, reduced significantly the bovine spermatozoa motility after freezing and thawing process. Further tests, including sperm membrane integrity, mitochondrial membrane potential and lipid peroxidation might provide relevant contributions on the factors involved in decreasing motility after the cryopreservation procedure. Acknowledgements: CAPES, Tairana Artificial Insemination Station, Botupharma and Master Fertility Animal Reproduction, Brazil.

**The Use of Pentoxifylline to Improve the Motility of Cryopreserved Equine Spermatozoa.** Byoung-Chul Yang, Jun-Kyu, Son, Nam-Young Kim, Jae-Hoon Woo, Sang-Min Shin, Sung-Woo Kim, Moon-Cheol Shin, and Ji Hyun Yoo

In Jeju Island in Republic of Korea, Jeju native stallion is designated as a national treasure and protected. In addition, there have been efforts to use them as racing horses and road riders. Spermatozoa should be frozen in order to use them for the improvement of Jeju native stallion by artificial insemination. However, there is a great variation in survival rate of spermatozoa after freezing and thawing in Jeju male horses. Therefore, it is necessary to freeze the spermatozoa to obtain stable semen with good vitality after freezing and thawing. In this study, mobility, survival rate, and cytotoxicity of frozen-thawed spermatozoa were evaluated depending on pentoxifylline levels (4 mM, 8 mM and 16 mM) in order to improve the properties of frozen semen of Halamma(Thoroughbred×Jeju native stallion). The addition of pentoxifylline, a phosphodiesterase inhibitor, has been reported to prevent early acrosome reaction in sperm, increase fertility and inhibit free radicals (Henkel et al., 2003). When the semen was frozen-thawed and incubated at 37 ° C for 30 minutes, the progressive motility of spermatozoa was 53.25±2.87 and 50.28±2.14 in pentoxifylline 4 mM and 8 mM treatment respectively. This was significantly higher than that of pentoxifylline 16 mM in the control and 41.27±2.82 and 40.09±5.15, respectively ( $p < 0 .05$ ). Progressive fast motility also showed significantly higher levels of pentoxifylline 4mM and 8mM than the control and 16mM treatments ( $p < 0 .05$ ). The total motility of the sperm cultured at 37 ° C for 1 hour after freeze-thawing was 68.96±1.64 and 67.90±6.72 in 4 mM and 8 mM of pentoxifylline, respectively, which were significantly higher than those of control and 16 mM treatment( $p < 0 .05$ ). These results indicate that the treatment with pentoxifylline 4mM and 8mM was more effective in increasing sperm motility than the control. Further studies are required to determine whether pentoxifylline affects not only sperm freezing but also pregnancy rate through the artificial insemination using frozen-thawed sperm from Jeju native stallion.

**Blastocyst-induced Changes in the Bovine Endometrial Transcriptome.** Claudia Passaro, Desmond Tutt, John A. Browne, Gry B. Boe-Hansen, Trudee Fair, and Patrick Lonergan

In a previous study from our group, we used an endometrial explant as an ex-vivo model to investigate the local response of the endometrium when exposed to embryos. This model allowed us to identify changes in the transcripts abundance of several interferon-tau (IFNT)-stimulated genes (ISGs) following 6 h co-culture with Day 8 blastocysts. Using the same model, the objectives of this study were (i) to investigate if upregulation of the five candidate ISGs in the endometrium in response to exposure to Day 8 embryos in vitro was specific to the blastocyst stage; (ii) to test if direct contact is required between embryos and the endometrial surface to stimulate endometrial gene expression; and (iii) to test if changes in endometrial gene expression can be induced by blastocyst-conditioned medium. Bovine uteri in the mid-luteal phase were collected at a local abattoir and 4-mm intercaruncular endometrial explants were taken from the ipsilateral horn. In Experiment 1, endometrial explants were exposed for 6 h to medium alone (Control) or to 20 denuded oocytes, 2-cell embryos, Day 5 morulae or Day 8 blastocysts. In Experiment 2, explants were cultured for 6 h with medium alone (Control) or with Day 8 blastocysts in a cell culture insert (no direct contact) or on a polyester mesh (direct contact). In Experiment 3, endometrial explants were cultured for 6 h in medium (Control) or in blastocyst-conditioned medium (BCM). In all experiments, following incubation, explants were snap frozen and

stored at  $-80^{\circ}\text{C}$  until RNA extraction, reverse transcription and quantitative PCR analysis. Culture of endometrial explants with Day 8 blastocysts for 6 h caused a significant ( $P < 0.01$ ) upregulation of five candidate ISGs (MX1, MX2, OAS1, ISG15, RSAD2). Exposure of explants to oocytes, 2-cell embryos or Day 5 morulae did not alter the relative abundance of any of the transcripts examined. No differences were observed in transcript abundance for the five candidate ISGs when endometrial explants were cultured for 6 h with or without direct contact with Day 8 blastocysts. A significant ( $P < 0.05$ ) upregulation of the ISGs tested was observed when endometrial explants were cultured for 6 h in BCM. In conclusion, exposure of endometrial explants to Day 8 blastocysts in vitro induced the expression of classic ISGs (MX1, MX2, OAS1, ISG15, RSAD2). This effect was exclusive to blastocyst stage embryos which have been shown to secrete IFNT in vitro. Direct contact between the blastocysts and the endometrial surface was not required in order to alter the abundance of these transcripts and blastocyst-conditioned medium alone was sufficient to stimulate a response. Results support the notion that limited local embryo-maternal interaction may occur as early as Day 8 of pregnancy in cattle.

**Gonadotrope-specific Loss of GATA2 Impairs FSH Production in Male Mice in Vivo.** Gauthier Schang, Emilie Brûlé, Ulrich Boehm, and Daniel J. Bernard

Mammalian reproduction is dependent on follicle-stimulating hormone (FSH) and luteinizing hormone (LH) secreted by pituitary gonadotrope cells. The dimeric hormones share a common  $\alpha$ -subunit (CGA) linked to hormone-specific  $\beta$ -subunits (LH $\beta$  and FSH $\beta$ ). Relative to LH $\beta$ , the mechanisms regulating FSH $\beta$  (Fshb) synthesis are poorly resolved. Activins are selective regulators of Fshb transcription and act via the transcription factors FOXL2, SMAD3, and SMAD4. However, these proteins are co-expressed in other tissues that do not produce FSH, indicating that they alone are insufficient to explain mechanisms of Fshb expression. Here, we tested the hypothesis that GATA2 plays a fundamental role in FSH synthesis by gonadotropes. This hypothesis derived from three previous observations. First, the mature gonadotrope-like cell line L $\beta$ T2 expresses both Gata2 and Fshb, while the immature cell line  $\alpha$ T3-1 expresses neither. Second, Gata2 is the GATA family member showing highest expression in gonadotropes, based on RNA-sequencing data. Third, conditional deletion of Gata2 in multiple mouse pituitary cell lineages led to decreases in serum FSH levels in males. Females were not previously investigated. To examine GATA2's role in gonadotropes, we crossed floxed Gata2 animals with GRIC mice, which express Cre recombinase in gonadotropes but not other pituitary cell types. Resulting conditional knockouts (cKO) were compared to littermate controls. cKO females exhibited normal puberty onset (assessed by vaginal opening), estrous cyclicity, and fertility (litter size and frequency). On the other hand, cKO males exhibited ~50% reductions in serum FSH levels compared to controls. Pituitary Fshb and Cga mRNA expression levels, and testicular weights were similarly reduced. Seminal vesicle weights were unchanged, as were pituitary Lhb expression and serum LH levels. Overall, the available data suggest that GATA2 is not required for FSH synthesis, but may contribute to sex differences in production of the hormone.

**Orexin A-Induced Changes in Melatonin Secretion and Arylalkylamine-N-Acetyl-Transferase (AA-NAT) and Tryptophan Hydroxylase (TPH1) Transcripts Expression in Ovine Pineal Gland.** Dorota A. Zieba, Katarzyna Kirsz, Malgorzata Szczesna, and Weronika Biernat

In sheep, differences in orexin A (OXA) expression level and its activity are related to changes in energy demand and seasonal reproduction. However, neither the mechanism nor the key place for the integration of the signal carried out by OXA and photoperiod, which the main biochemical agent is melatonin (MEL), are known. The aim of the study was to determine the role of OXA in MEL secretion and mRNA expression of two enzymes that are crucial for MEL biosynthesis, serotonin N-acetyltransferase (AANAT) and tryptophan hydroxylase (TPH1). The study was performed on three-year-old polish mountain ewes (n = 10) in their breeding season, during short day photoperiod (December). The animals in a good body condition score (BCS=3), were weighed  $60 \pm 3$  kg. Ewes were fed at libitum and housed in natural photoperiod (longitude: 19°57' E, latitude: 50° 04' N). Experiment started one hour before the sunset and was continued for 6 hours, in the darkness and in the presence of a dim and red light. Ringer-Locke buffer (Control group, n=5) or OXA (0.3  $\mu\text{g}$  / kg B.W., Experimental group, n=5) were administrated twice (at sunset and one hour later) directly into the cisterna magna. From the beginning of the experiment, blood samples (5 ml) and cerebrospinal fluid samples (CSF, 500  $\mu\text{l}$ ) were collected every 15 and 30 minutes, respectively, and were stored in  $-80^{\circ}\text{C}$  until ELISA for MEL. The ewes were euthanized 4 hours after the second infusion of OXA/Ringer-Locke buffer. The brains were immediately removed from the skulls, and the pineal glands were frozen in liquid nitrogen and stored at  $-80^{\circ}\text{C}$  until the determination of AANAT and TPH1 expression using real-time PCR. Total RNA (1.0  $\mu\text{g}$ ) was reverse transcribed to cDNA, then amplified using sequence detection primers and fluorescent probes. Each gene assay was run in triplicate for each cDNA sample. Expression of AANAT and TPH1 mRNA was expressed relative to  $\beta$ -actin mRNA expression as a reference gene. OXA stimulated MEL ( $P < 0.001$ ) release into plasma and CSF compared to controles. AANAT transcript level increased ( $P < 0.05$ ) after OXA treatment compared to control group. TPH1 mRNA expression was similar in both groups. The results indicate that nocturnal MEL biosynthesis and secretion in seasonally breeding sheep are directly regulated by neuropeptide, OXA. Research supported by National Science Centre, Poland (2017/01/X/NZ9/00204).

**Maestro: A Possible Conductor of the Ovulatory Symphony.** Katherine Rosewell, Patrick Hannon, James Akin, Mats Brannstrom, and Thomas Curry Jr.

Maestro (Male-specific Transcription in the developing Reproductive Organs, MRO) was initially described in the developing male testis in the mouse. Research on this gene employing targeted deletion in the mouse has shown that it is not necessary for normal sexual development of either sex. While Mro may not be essential for gonadal development in the mouse there is evidence that it is upregulated in the cumulus cells of women who have been diagnosed with polycystic ovary syndrome (PCOS). Our lab is interested in the coordination of the events that define the periovulatory period and eventually bring about ovulation of the oocyte. To explore the role of MRO in human ovulation we have employed a unique set of in vivo preovulatory granulosa cells and follicles from defined time periods; before the luteinizing hormone (LH) surge and at early (12h to  $\leq 18$ h) and late ovulatory phases ( $> 18$ h to  $\leq 34$ h) after human chorionic gonadotropin (hCG) administration in normally cycling women. MRO is significantly elevated (70 fold) during the early ovulatory phase in women and is still elevated (35 fold) in

the late ovulatory phase when compared to the preovulatory state (n=4-5 patients/group,  $p < 0.05$ ). Immunohistochemistry of whole follicles from women at the pre-, early and late ovulatory phases demonstrate no expression of MRO protein before hCG administration or during the early phase of ovulation; there was positive MRO staining in GCs during the late ovulatory phase. To further understand the regulation of MRO we employed our model of cultured granulosa-lutein cells (GLCs) from IVF patients which recapitulates key ovulatory signaling cascades. GLCs were collected on the day of oocyte retrieval (collection) and were allowed to acclimate in culture for 6 days to regain LH/hCG responsiveness. The GLCs were then treated with or without hCG (1 IU) for 0, 6, 12, and 24h. MRO gene expression is significantly increased by 6h after hCG, reaches peak levels at 12h and declines back to the 6h level after 24h (n= 4-5 patients,  $p < 0.05$ ). In order to determine which signaling pathways may regulate MRO expression we cultured GLCs with vehicle control (DMSO), RU486 (20 $\mu$ M; progesterone receptor antagonist), AG1478 (10 $\mu$ M; EGF receptor antagonist), NS398 (15 $\mu$ M, COX-2 inhibitor), hCG, hCG+RU486, hCG+AG1478 and hCG+NS398 for 0, 6, 12 and 24h. Treatment of GLCs with the AG1478 compound significantly reduced the hCG-induced increase in MRO expression at all time points post treatment (n=5-8 patients/group,  $p < 0.05$ ). Whereas RU486 only showed significant inhibition at the 24h time point; the NS398 compound had no effect on MRO expression at any time point. These data demonstrate that hCG induces MRO through the EGF and PGR signaling pathways. A functional role for MRO in the preovulatory follicle is unknown; however, MRO is reported to play a role in protein-protein interactions in other systems and may facilitate coordination of the events of the ovulatory cascade.

Supported by P01HD071875 and Lalor Foundation.

**An Environmentally Relevant Phthalate Mixture Inhibits Ovulation and Disrupts Luteinization in Mouse Antral Follicles in Vitro.** Madison E. Lane, Patrick R. Hannon, and Thomas E. Curry, Jr.

Phthalates are known reproductive toxicants commonly used as plasticizers and solvents in common personal care, building, and medical products. Humans are ubiquitously exposed to a mixture of phthalates daily, and as endocrine-disrupting chemicals, exposure can lead to defects in ovarian function. In animal studies using only single phthalate exposures, these chemicals negatively impact folliculogenesis and steroidogenesis. These processes are vital for fertility, but little is known about the effects of a phthalate mixture on the ovulatory process. This is concerning because ovulatory defects are the leading cause of infertility in women. For ovulation to occur, the surge of luteinizing hormone (LH) acts on the pre-ovulatory follicle to bring about oocyte release and formation of the corpus luteum (CL), which produces progesterone (P4). This differentiation from follicle to CL is necessary for maintenance of pregnancy and overall fertility. We hypothesized that an environmentally relevant mixture of phthalates directly decreases ovulation rates and alters the formation and/or functionality of the CL. To test this hypothesis, ovarian antral follicles (250 $\mu$ m) were isolated from CD-1 mice (post-natal day 33-35). These follicles were cultured for 96hr in supplemented media containing FSH to induce pre-ovulatory development, and treated with vehicle control (dimethylsulfoxide, DMSO) or a mixture of six different phthalates (PHTmix; 1-500 $\mu$ g/ml). This mixture was derived from urinary phthalate measurements from pregnant women. The media were then replaced with maturation media  $\pm$ human chorionic gonadotropin (hCG), an LH analogue, to induce ovulation and treated with DMSO or PHTmix for 18hr. Next, ovulation was determined, media collected for P4 measurements, and the follicle/CL collected for gene expression analysis. The genes analyzed included those involved in P4 production

(Star, Cyp11a1), P4 metabolism (Parm1), and CL functionality (Cdkn1a, Fzd4, and Wnt4). In the ovulation assay, treatment with hCG+PHTmix resulted in a dose dependent decrease in ovulation rate compared to hCG alone (n=3-9, p≤0.05), with the 500µg/ml dose nearly causing complete anovulation. Treatment with hCG increased P4 levels compared to DMSO (n=3-9, p≤0.05). Interestingly, hCG+PHT10 and 100 further increased P4 levels compared to hCG alone (n=3-9, p≤0.05). As anticipated, treatment with hCG alone increased mRNA levels of Cyp11a, Parm1, Cdkn1a, Fzd4, and Wnt4 compared to DMSO (n=5-9, p≤0.05). Treatment with hCG+PHTmix increased Star expression compared to hCG. Although hCG+PHTmix decreased Cyp11a1 expression, hCG+PHTmix decreased Parm1 levels compared to hCG, and these collective changes in steroidogenic genes could explain the increases in P4 with increasing doses of the PHTmix. Treatment with hCG+PHTmix decreased expression of Cdkn1a, Fzd4, and Wnt4 compared to hCG. Decreases in these genes suggest impaired luteinization and CL formation, which corresponds to decreasing ovulation rates with increasing PHTmix doses. These data suggest that an environmentally relevant phthalate mixture directly inhibits ovulation and disrupts normal luteinization by altering P4 production and decreasing expression of genes that regulate CL functionality. Thus, such interruptions caused by phthalate exposure could lead to impairments in fertility and have negative effects on reproductive health. Supported by P01HD071875, K99ES028748.

#### **Structure-Function Studies of the Lab Opossum Prostate Gland.** Julie Watiker and Yolanda Cruz

The mammalian prostate gland secretes fluids that, along with sperm from the testes and fluids from other glands, comprise semen. The volume and quality of semen are major aspects of male fertility in internally fertilizing animals because of their roles in conveying the sperm to the right place and the right time to effect fertilization. While the structure and function of the prostate is well known in eutherians, the anatomy of the prostate gland in metatherian mammals is poorly studied. My goal is to contribute to the knowledge regarding prostate anatomy as a way of understanding the evolution of internal fertilization as an effective reproductive strategy by exploring the homologous and analogous aspects of this organ in two different groups, metatherians versus eutherians. Through dissections of male laboratory opossums and rats (*M. domestica* and *R. norvegicus*, respectively) I collected data on their gross prostate anatomy. The rat prostate consists of three lobes, dorsal, lateral, and ventral arranged around the base of a short urethra. The opossum prostate consists of three regions, S1, S2, and S3 that wrap around a much longer urethra distinguished by color and size. Using histological analysis, I compared their microanatomy in greater detail so as to establish homologies when possible by comparing the hematoxylin and eosin staining of cross sections of each lobe of the rat prostate and each section of the opossum prostate. I investigated the nature of the secretions of the three different regions of the prostate found in opossums in comparison to that of rats. I explored whether the proteins produced in the three different lobes of the rat prostate are similarly localized in the three distinct sections of the opossum prostate. I used immunochemistry to establish the histological localizations of three prostate-specific proteins: probasin, prostatein, and dorsal protein 1 (DP1). Work by others has demonstrated that probasin is localized in the lateral lobe of the rat prostate; prostatein, in the ventral lobe, and DP1 in the dorsal lobe. Detecting the presence similarly in the distinct sections of the opossum prostate would provide insight into the functional homology of this organ as well as provide evidence that prostate genes are conserved in both species. Samples were taken from 5 individual *M. domestica* and 5 individual *R. norvegicus*. The three proteins were found localized in the 3 different lobes of the rat prostate as predicted. In the opossum, each of the three proteins was present, demonstrated a

conservation of prostate genes between the species. While the pattern of immunostaining for each of the proteins differed between S1, S2, and S3, the staining was not as localized as the lobes of the rat prostate. This suggests that the way in which the sections of the opossum prostate function differ from the lobes of the rat prostate despite the conservation of genes. Funding was provided by the Oberlin College Biology department and the Robert Rich Student Research grant.

**Exposure to an Environmentally Relevant Phthalate Mixture Inhibits Ovulatory Prostaglandin Production in Primary Human Granulosa Cells.** Patrick R. Hannon, James W. Akin, and Thomas E. Curry Jr.

Phthalates are ubiquitous environmental toxicants found in common consumer, building, and personal care products. Thus, daily exposure to a mixture of phthalates in humans is unavoidable. This is a public health concern because phthalates disrupt ovarian processes, including folliculogenesis and steroidogenesis. However, these previous studies utilized single phthalate exposures to rodents and little is known about the direct effects of phthalates on ovulation, especially in humans. This is alarming because ovulatory defects are the leading cause of female infertility. In the present study, human granulosa-lutein cells were used to test the hypothesis that an environmentally relevant phthalate mixture inhibits the periovulatory human chorionic gonadotropin (hCG)-induced increase in prostaglandins. Production of the prostaglandins PGE<sub>2</sub> and PGF<sub>2</sub>α during the ovulatory process is essential for successful oocyte release and corpus luteum formation. Specifically, blocking their synthesis or action leads to anovulation. In granulosa cells, luteinizing hormone (LH) or hCG induces prostaglandin synthases and transporters, and inhibits prostaglandin metabolic enzymes in order to increase PGE<sub>2</sub> and PGF<sub>2</sub>α levels to mediate ovulation. For these experiments, isolated human granulosa-lutein cells from follicular aspirates of IVF patients were acclimated in culture to regain LH/hCG responsiveness. Prior to hCG treatment, cells were exposed to vehicle control (dimethylsulfoxide) or a mixture of six phthalates (PHTmix; 1-500μg/ml) for 48hr. The PHTmix was derived from urinary phthalate measurements in pregnant women. Cells were treated with or without hCG and collected at 0, 6, 12, 24, or 36hr post-treatment. PGE<sub>2</sub> and PGF<sub>2</sub>α levels were measured in media. Cellular mRNA levels of prostaglandin synthases (PTGS2, PTGES, and AKR1C1), transporters (SLCO2A1 and ABCC4), and a metabolic enzyme that renders prostaglandins inactive (HPGD) were measured (n=4-9/group; p≤0.05). PHTmix exposure did not affect cell viability/metabolism at any dose. Treatment with hCG+PHTmix decreased PGE<sub>2</sub> and PGF<sub>2</sub>α levels at the 24hr (500μg/ml) and 36hr (100 and 500μg/ml) time-points when compared to hCG alone. Consistent with inhibited prostaglandin production, hCG+PHTmix decreased the mRNA levels of PTGS2 at the 6hr (100 and 500μg/ml), 12hr (500μg/ml) and 24hr (500μg/ml) time-points and decreased PTGES levels at the 6hr (500μg/ml), 12hr (500μg/ml), and 36hr (100 and 500μg/ml) time-points when compared to hCG. Interestingly, hCG+PHTmix increased AKR1C1 levels at 6-24hr (100 and 500μg/ml) when compared to hCG, suggesting an imbalanced shift towards metabolism of PGE<sub>2</sub> to PGF<sub>2</sub>α. Of the transporters measured, only SLCO2A1 was decreased by hCG+PHTmix at a dose causing inhibited prostaglandin production (12 and 24hr at 500μg/ml compared to hCG); while ABCC4 levels were decreased at only 1 and 10μg/ml compared to hCG. In further support of PHTmix decreasing prostaglandin levels, hCG+PHTmix increased HPGD levels at the 6hr (1, 100, and 500μg/ml), 12hr (500μg/ml), and 24hr (10, 100, and 500μg/ml) time-points compared to hCG. These data suggest that exposure of human granulosa cells to a relevant phthalate mixture inhibits the hCG-induced increase in ovulatory prostaglandins by decreasing

synthases/transporters and increasing metabolism of PGE2 and PGF2 $\alpha$  to an inactive state. Because prostaglandins are indispensable for the ovulatory process, exposure to phthalates may impair human ovulation and fertility. Supported by K99ES028748, Lalor Foundation, and P01HD071875.

**Molecular Characterization and Expression of Kisspeptinergic System (Kiss1) in The Hypothalamus and Corpus Luteum of Buffalo (*Bubalus Bubalis*).** G.K. Mishra, M.K. Patra, L. Kipjen Singh, V. Upmanyu, S. Chakravarti, M. Karikalan, S.K. Singh, G.K. Das, K. Narayanan, and H. Kumar

Kisspeptin (Kp), a neuropeptide is encoded from Kiss1 gene, modulates its activity through kisspeptin receptor (Kiss1r/GPR54) and form an indispensable component in control of GnRH neurons. The present study was initiated to identify the key molecules- Kiss1 gene and Kiss1r (GPR54) in buffalo and their distribution in hypothalamus and corpus luteum (CL) at transcript and protein level. Kiss1 and Kiss1r genes were amplified in fragments covering the coding region; cloned and sequenced from genomic DNA. Sequences of Kiss1 and kiss1r were annotated and submitted to NCBI GenBank with Accession numbers MF168937 and MG820539, respectively. The buffalo Kiss1 DNA sequence had two exonic segment contained complete coding sequence (CDS; 408 bp) encoding a predicted protein of 136 aa. The buffalo Kiss1 sequence shared 95.1-98.4% identity with cattle, goat and sheep at the nucleotide level. The buffalo Kiss1r DNA sequence of five segment contained complete CDS (1134 bp) encoding a predicted protein of 378 aa. Kiss1r had seven membrane spanning alpha-helix, similar to other G-protein coupled receptor as predicted by TMHMM v. 2.0 server. Three-dimensional model prediction in Swiss-model workspace revealed seven alpha helix and three beta strands linked through intervening coils. Phylogenetic analysis of Kiss1 and Kiss1r revealed that it formed a monophyletic clade with cattle, which branched from sheep and goat; while canine, swine, equine, human and mouse branched separately; while the fishes was distantly related and formed the out-group. Expression profiling and tissue distribution of Kiss1 and Kiss1r were studied at the transcript level through PCR and at protein level through immuno-reactivity in the anterior and posterior hypothalamus (AH and PH) for POA and ARC nuclei, respectively and corpus luteum (CL). Both AH and PH expressed Kp and Kiss1r in the neuronal soma, perinuclear area and some glia. In the CL, large luteal cells showed intense immuno-reactivity as compared to small luteal cells. Identification and tissue localization of these key molecules in kisspeptinergic system in buffalo will enable a better understanding of buffalo infertility and pave the way for therapeutic intervention. This research was supported by ICAR-Indian Veterinary Research Institute as part of approved project no. IXX13018.

**Epididymosomes Transfer Key Factors to Spermatozoa within the Epididymis to Enhance Fertilization in the Domestic Cat Model.** Tricia Rowlison, Mary Ann Ottinger, and Pierre Comizzoli

The sperm centrosome participates in the sperm aster formation during fertilization to enable rapid fusion of male and female pronuclei and successful completion of the first mitotic division. Research in multiple species including the domestic cat points to impaired centrosomal maturation as a source of infertility. Previously, we demonstrated that epididymosomes (small vesicles secreted by the epithelium of the epididymis) transfer key proteins to the transiting sperm cells which aid in centrosomal maturation and sperm motility. The objective of this study was to characterize the protein content and influence of epididymosomes on sperm cell ability to penetrate the oocyte and achieve rapid pronuclear

fusion. Epididymides were dissected from testes of 4 adult cats (>1 year old). Epididymosomes were isolated from each segment (caput, corpus, and cauda) and were assessed via liquid chromatography tandem mass spectrometry. Immature caput spermatozoa (n = 4 males) were exposed to epididymosomes (isolated from whole epididymides of n= 4 pools of 5 males) for 1 hour and 15 minutes at 38°C. Control treatments included caput, and cauda spermatozoa exposed to base medium. Spermatozoa were then washed free of epididymosomes prior to inseminating oocytes (n = 20 oocytes per treatment, 4 replicates total) for 16 hours at 38°C. Presumptive zygotes were then fixed in paraformaldehyde and stained with Hoeschst before evaluating the percentage of fertilization and measuring the distance between pronuclei (an indicator of the kinetic rate of pronuclear fusion). A total of 326, 197, and 210 proteins were identified in caput, corpus, and cauda-derived epididymosomes, respectively. Among those proteins, 611 proteins were present in all segments. Several proteins are related to sperm motility (hexokinase 1, adenylate kinase isoenzyme), zona binding (a disintegrin and metalloproteinase domain 7, zona binding proteins 1 and 2), or centrosome function (nuclear mitotic apparatus protein). Percentages of penetrated oocytes (range, 28-42%) were not different (P= 0.6843) after sperm exposure to epididymosomes and controls. However, pronuclei were significantly closer when oocytes were inseminated with caput spermatozoa previously exposed to epididymosomes or cauda sperm cells ( $2.4 \pm 3.7$  and  $1.2 \pm 3.5$   $\mu\text{m}$ , respectively) compared to caput spermatozoa exposed to base medium ( $16.7 \pm 3.4$   $\mu\text{m}$ ,  $P < 0.0001$ ). Results demonstrate that (1) epididymosomes contain several key proteins related to critical sperm functions, and (2) sperm exposure to epididymosomes enhances subsequent pronuclear fusion. Together, these studies will aid in our understanding of the processes involved in the development of the sperm centrosome and contribute to treatments of infertile individuals.

**Differential Expression of Kndy Transcripts in The Hypothalamus During the Estrous Cycle in the Buffalo (*Bubalus Bubalis*).** M. K. Patra, G.K. Mishra, L. Kipjen Singh, P.A. Sheikh, V. Upmanyu, S. Chakravarti, M. Karikalan, S.K. Singh, G.K. Das, K. Narayanan, and H. Kumar

The expression of KNDy neurons in the surge and pulsatile centres of GnRH in the hypothalamus is modulated by the stage of estrous cycle. Accordingly, we studied the temporospatial expression of KNDy components in the hypothalamus during the estrous cycle in the buffalo. Buffalo brains (n=24) were collected immediately after exsanguination and categorized into follicular, early luteal, mid luteal stages (FL, EL and ML) and acyclic (n=6/ group) based on the ovarian dating. The histology and serum progesterone assay were used to confirm the stage, retrospectively. Total RNA was extracted from the anterior and posterior hypothalamus (AH and PH) representing preoptic and arcuate nuclei, respectively. Real time PCR amplification of Kiss1, Kiss1r, neurokinin-B (NKB), dynorphin (Dyn), ER $\alpha$  and PR was done using GAPDH as endogenous control and acyclic hypothalamus as calibrator group. Further, immunolocalization of Kiss1 and Kiss1r was done on the hypothalamus. In the AP, significant upregulation of Kiss1, Kiss1r and NKB with a concomitant downregulation of Dyn transcripts was recorded at FL stage. However, there was downregulation of Kiss1 and Kiss1r during the EL perhaps due to the loss of estradiol as a consequence of ovulation. On the other hand, in the PH, the expression of Kiss1 revealed a significant upregulation at ML and FL and downregulation in the EL. The expression of NKB was consistently downregulated while that of Dyn was upregulated irrespective of the stage of estrous cycle suggesting that the GnRH mediated LH pulses are regulated by KNDy peptides in the caudal hypothalamus. ER $\alpha$  expression at AH during the ML and FL was upregulated, whereas it was

significantly downregulated in the EL. However, the PR upregulation was recorded in the ML and significant downregulation during the EL and FL. In the PH, the ER $\alpha$  expression was significantly upregulated in the EL, whereas, PR was abundantly expressed irrespective of the stage of estrous cycle. The immunolocalization study revealed positive signals in the AH and PH against Kp and GPR54 during the follicular and luteal stages as compared to the acyclic buffalo. The results suggest that the bubaline Kp system follows KNDy theory to regulate the GnRH neurons during the different phases of estrous cycle. This research was supported by ICAR-Indian Veterinary Research Institute as part of approved project no. IXX13018.

### **Ovulation and Colonization of the Ovary in Metastasis of Fallopian Tube-Derived Ovarian Cancer.**

Matthew Dean, Vivian Jin, Angela Russo, and Joanna E. Burdette

Recent evidence has shown that the majority of high-grade serous ovarian cancers (HGSOC) originate in the fallopian tube epithelium (FTE), raising important questions as to the role of the ovary in HGSOC. Our objectives were to 1) determine if colonization of the ovary is an important step in metastasis of FTE-derived cancer, 2) explore the role of the tearing of the ovary during ovulation, independently of hormone changes, in colonization of the ovary, and 3) identify genetic alterations and signaling pathways required for FTE cells to invade the collagen rich ovarian microenvironment. Xenografting 50,000 murine oviductal epithelial (MOE) cells stably expressing PTENshRNA + KRASG12V into the ovarian bursa resulted in formation of aggressive tumors that spread throughout the peritoneum. In contrast, when the same number of cells were xenografted into the peritoneal space, bypassing the ovary, no tumors developed (up to 150 days). We found that rupture of the ovarian surface (ovulation mimetic) resulted in increased attachment of MOE GFP and OVCAR8 RFP cells to the ovary. MOE GFP cells adhered to 3D type I collagen gels preferentially as compared to murine ovarian stroma (MOST) cells, and to stromal cells more than ovarian surface (MOSE or murine OSE) cells. In collagen-coated wells, increasing the number of MOSE resulted in a linear decrease in attachment of MOE GFP cells, collectively showing that FTE bind to the extra-cellular matrix (ECM) exposed during ovulation. RNAseq revealed that 3D collagen resulted in decreased gene expression in focal adhesion, regulation of actin cytoskeleton, and ECM-receptor interaction pathways, suggesting normal FTE cells responds poorly to a collagen rich microenvironment. In agreement, the viability of normal cells (MOE, MOSE, and IOSE80) but not HGSOC cells (OVCAR3, OVCAR4, OVCAR5, AND OVSAHO) was reduced on 3D type I collagen relative to 2D collagen. RNAseq identified that genes in the MAPK and p53 pathways were increased due to 3D collagen; however, expression of KRASG12V or mutant p53 (R273H or R248W) failed to rescue MOE cell viability. Western blot indicated that 3D collagen failed to induce AKT activation, as occurs in some other cell types. Loss of PTEN (common in HGSOC at the protein level) completely rescued MOE cell viability. MOE PTENshRNA cells also displayed increased adherence to murine ovaries, increased invasion through 3D collagen, and formed tumor spheroids in 3D collagen gels after 7 days. Experiments with MK2206 and myristoylated AKT indicated that pAKT mediated the increased invasion of MOE PTENshRNA cells, that pAKT was required by not sufficient for increased viability on 3D collagen, and pAKT did not mediate increased attachment to ovaries. Western blots showed that PTENshRNA increased phospho-JNK levels through Rac1 and independently of phosphoAKT. Inhibition of Rac1 and JNK reduced adhesion ovaries and invasion through collagen of MOE PTENshRNA. These results indicate colonization of the ovary is a key step in metastasis of HGSOC and that loss of PTEN activates RAC1 and

JNK that contribute to primary metastasis to the ovary. These pathways represent novel targets to prevent colonization of the ovary in HGSOC patients.

**Adult Mouse Ovaries are Capable of Phthalate Metabolism.** Genoa R. Warner, Zhong Li, and Jodi A. Flaws

Phthalates are synthetic chemicals commonly used as additives in consumer products with widespread human exposure. While phthalates are manufactured as diesters, they are hydrolyzed in the environment and in the body to monoesters that may be more toxic than the parent compounds. Individual phthalates have been shown to be reproductive toxicants, but few studies have examined the toxicity of mixtures of phthalates. This study tested the hypothesis that the adult ovary is able to metabolize an environmentally relevant mixture of phthalates. Ovarian follicles from adult CD-1 mice were cultured in media treated with DMSO (vehicle control) or 0.1, 1, 10, or 500 µg/mL (n = 3, 9-12 follicles per n) of a mixture composed of 35% diethyl phthalate, 21% di(2-ethylhexyl) phthalate, 15% dibutyl phthalate, 15% diisononyl phthalate, 8% diisobutyl phthalate, and 5% benzylbutyl phthalate, which is representative of exposure of pregnant women in Illinois. Follicle growth was measured daily to assess toxicity. After five days of culture, follicles were collected for mRNA extraction to measure the gene expression of the enzymes required for phthalate metabolism, isoamyl acetate-hydrolyzing esterase 1 homolog (Iah1), lipoprotein lipase (Lpl), alcohol dehydrogenase (Adh1), and aldehyde dehydrogenase family 1, subfamily 1 (Aldh1a1). Culture media were subjected to high performance liquid chromatography mass spectrometry (HPLC-MS) to measure the amounts of monoester metabolites. No effect of treatment on follicle growth was observed for 0.1, 1, or 10 µg/mL treatment groups compared to control. Follicle growth was partially inhibited for the 500 µg/mL treatment group compared to control. Expression of all metabolizing enzymes was observed for all treatment groups. Media from the 10 µg/mL treatment group contained significant concentrations of monoester metabolites compared to controls, whereas no metabolism was observed for the 500 µg/mL treatment group. This suggests that the adult ovary is able to metabolize lower doses of phthalates. As the presence of metabolites at the 10 µg/mL dose did not impact follicle growth, the metabolite mixture is likely equally or less toxic than the parent compounds alone. This research was supported by NIH T32 ES007326 and NIH R56 ES025147.

**GnRH Regulates the Expression of its Receptor Accessory Protein SET in Pituitary Gonadotropes.**

Violaine Simon, Charlotte Avet, Chantal Denoyelle, David L'Hôte, Florence Petit, Céline J Guigon, and Joëlle Cohen-Tannoudji

Reproductive function is under the control of the neurohormone GnRH, which activates a G-protein-coupled receptor (GnRHR) expressed in pituitary gonadotrope cells. GnRHR activates a complex signalling network involving notably calcium/protein kinase C (PKC) and cyclic AMP (cAMP)/ protein kinase A (PKA) pathways to regulate synthesis and secretion of the two gonadotropin hormones, luteinizing hormone and follicle-stimulating hormone, both regulating gametogenesis and steroidogenesis in gonads. Recently, in an attempt to identify the mechanisms underlying GnRHR signalling plasticity, we identified the first interacting partner of GnRHR, the proto-oncogene SET. We showed that SET binds to intracellular domains of GnRHR to enhance its coupling to cAMP pathway in

aT3-1 gonadotrope cells. Here, we demonstrate that SET protein is rapidly regulated by GnRH, which increases its phosphorylation state and decreases dose-dependently its protein expression level. Our results highlight a post-translational regulation of SET protein expression involving the proteasome pathway and a post-transcriptional regulation relying on SET mRNA targeting to RNA-induced silencing complex. We determined that SET phosphorylation upon GnRH stimulation is mediated by the kinase PKC. Phosphorylation on serine 9, a substrate of PKC, targets SET for degradation into the proteasome. Furthermore, a non-phosphorylatable SET mutant on serine 9 is resistant to GnRH-induced downregulation. Altogether, these data suggest that GnRH-induced SET phosphorylation on serine 9 mediates SET protein downregulation through the proteasome pathway. Interestingly, decrease in SET expression is associated with a marked attenuation of GnRHR coupling to the cAMP pathway, suggesting that GnRH-induced SET downregulation may contribute to desensitization of GnRHR signalling. Noteworthy, SET downregulation is also observed in more physiological contexts, i.e in response to pulsatile GnRH stimulation in LbT2 gonadotrope cells as well as in vivo in the pituitary of prepubertal female mice. Altogether, this study suggests that GnRH-induced SET downregulation contributes to the regulation of pituitary gonadotrope activity notably through the fine-tuning of GnRHR-dependent cAMP signalling. This study was supported by grants from the Université Paris Diderot, CNRS and INSERM.

**The Quantity of Bovine Immature Cocs Used for Intrafollicular Oocyte Transfer (TIFOI) Does Not Affect the Embryo Production.** José Felipe W. Sprícigo, Ligiane O. Leme, Felipe M. C. Caixeta, Andrei A. G. Fidelis, Luzia R. O. Dias, Otávio A. C. Faria, Venâncio A. O. Silva, Ivo Pivato, and Margot A. N. Dode

Recently, the immature oocyte intrafollicular transfer (TIFOI) was described as an option for in vivo production of good quality bovine embryos. However, the technique efficiency still low and one of the possible reasons could be the number of injected COCs. The aim of the present experiment was to determine if the quantity of COCs injected into the dominant follicle could affect the embryo production, after TIFOI. For the experiment, 40 heifers were submitted to a TAI protocol. First, at D-10 they received a P4 device and 2 ml of estradiol benzoate (EB). The P4 was removed at D-2, followed by the administration of 2 ml of prostaglandin. On D-1, 1 ml of EB was administered. Before injection, 52 hours after P4 removal, the animals were evaluated and only those with one dominant follicle (>10mm) were selected. The injections were performed (D0) with an ovum pick up (OPU) guide, equipped with a 7.5MHz ultrasound probe and a modified aspiration system. For the injection, 10 (TIFOI10, n=8), 25 (TIFOI25, n=11) or 50 (TIFOI50, n=12) COCs were placed in the end of a needle (27G), with 60 µL of follicular fluid. An insulin syringe at the other end of the system served to perform the injections. A single dose of semen was used for artificial insemination (AI), right after injections. For embryo recovery, uterine flushes were performed 8 days after. Before flushing, the ovaries were evaluated with a Color Doppler for the assessment of CL diameter (mm) and the luteal blood flow (BF, scale 1-5). The recovery rates were compared among groups by the ratio of the total structures (non-fertilized, degenerated oocytes and embryos) or embryos (Mo, Bi, Bl, Bx and Be) recovered (D8), over the total COCs injected (D0). The fertilization rate was calculated by the ratio of total cleaved structures (more than 2 cells), over the total injected COCs. After flushing, one structure or embryo, considered to be native from the "ovulator" was reduced from the total recovered. All the data was compared by Chi-square test (P 0.05) among TIFOI10 (3.8% and 82.8%), TIFOI25 (7.6% and 65.5%) and TIFOI50 (4.7% and 69.0%). The results demonstrated that the number of COCs injected does not influence the CL quality or the embryo

production. Thus, TIFOI is applicable for the donors with high or low number of recovered COCs. The grant for the first author was supported by FAP-DF, Brazil.

**Carbon Black Nanoparticles May Act as Novel Endocrine Disruptors of Female Ovarian and Gonadotrope Functions.** Violaine Simon, Charlotte Avet, Richard Wargnier, Chantal Denoyelle, Alice Pierre, Valérie Messent, Ghislaine Garrel, Jean-Marie Dupret, and Joelle Cohen-Tannoudji

A dramatic increase in the industrial production and use of nanoparticles (NPs) has been observed in the past decades and their potential adverse effects on human are thus of major societal concern. Carbon black nanoparticles (CB NPs) are most often produced by controlled incomplete combustion or thermal decomposition of hydrocarbons and are intensively used in industry worldwide (automobile tires, plastics, printing inks, ...). Experimental studies on animals have shown that CB NPs inhalation induce pulmonary inflammation and cardiovascular disease and CB NPs as well as their respirable aggregates/agglomerates have been classified as possibly carcinogenic to humans (group 2B). The reproductive toxicity of CB NPs has received far less attention. Recently, we demonstrated that CB NPs (13 nm) decrease aromatase expression and estradiol secretion in human granulosa cells through the recruitment of ERK1/2 signaling pathway suggesting that CB NPs could impact ovarian function. Here, we asked whether CB NPs could impact the activity of pituitary gonadotrope cells. We treated rat primary pituitary cultures and the gonadotrope cell line LbT2 with increasing concentrations of CB NPs (10 to 100 micrograms/ml). We observed by transmission electron microscopy that CB NPs are internalized in gonadotrope cells without affecting cell viability. In both primary pituitary cultures and LbT2 cells, CB NPs dose-dependently increased transcript levels of the specific beta subunit of the gonadotropin FSH (Fshb, maximal increase of  $1.4 \pm 0.1$ - and  $2.1 \pm 0.3$ -fold over control, respectively) without affecting Lhb transcript levels. Moreover, FSH secretion was increased dose-dependently by CB NPs in primary pituitary cultures (maximal increase of  $1.4 \pm 0.1$ -fold over control). We showed that CB NPs rapidly activate phosphorylation of the transcriptional factor CREB in LbT2 cells ( $1.50 \pm 0.01$ -fold over control after 10 min) and that pharmacological inhibition of the cAMP pathway with two different inhibitors, RpcAMP or H89, significantly attenuates the stimulatory effect of CB NPs on Fshb transcript levels (maximal inhibition of  $74 \pm 13$  %). Altogether, our study reveals that CB NPs may affect pituitary function through excessive stimulation of FSH production. Noteworthy, preliminary data obtained in female mice submitted to intratracheal administration of CB NPs indicated similar effects on ovarian granulosa aromatase and pituitary gonadotrope FSH expression as observed in vitro. These findings suggest that CB NP may translocate to reach ovary and pituitary wherein they act as endocrine disruptors. Altogether, our study highlights a possible detrimental effect of these common NPs on female reproductive health. This study was supported by grants from the Agence Nationale de la Sécurité Sanitaire de l'Alimentation, de l'Environnement et du Travail (ANSES, Nanovhyp project), the Université Paris Diderot, CNRS and INSERM.

**Involvement of Akt Isoforms in Ovarian Aging and Protection of the Ovarian Reserve: Preliminary Results in the PR-Cre specific AKT isoform KO.** Dadou L. Lokengo and Eric Asselin.

Alteration of the ovarian reserve, as it occurs in cases of early ovarian aging in women under 40 years of age, is accompanied by infertility. In these past decades, women postpone their first childbearing

beyond 35 years of age (20% in North America). This has the tendency to increase infertility due to depletion or alteration of the ovarian reserve. Exhaustion of ovarian reserve involves atresia and follicular growth, processes involving Akt kinase signaling. The current emphasis on therapeutic perspectives concerning the management of ovarian reserve impairment in the context of infertility involves elucidating the mechanisms of onset of this alteration. Studies establish the role of Akt in folliculogenesis but not those of its three isoforms. However, they can have different or redundant roles as described in other pathologies. From this point of view, this study seems important to us because it can open the way to specific therapies with fewer side effects for women at risk or suffering from this pathology and attempting to conceive. The objective of this study is to determine the role and involvement of each Akt isoform in alteration of the ovarian reserve, and to identify a possible synergy or redundancy between these isoforms. In this study, Utero-ovarian PR-Cre specific Knock Out mice for each Akt isoforms and their combination (45 and 100 days old) are compared to wild type by determining the number of ovarian follicles after hematoxylin eosin staining, and the expression of Akt effectors by immunohistochemistry. The preliminary results tend to show that at 45 days of age, there is no significant effect of cancellation of the Akt isoforms on the ovarian reserve but these effects are clearly observed at 100 days of age, and it appears that a double Akt isoform knockout leads to the reduction of the ovarian reserve. Some Akt effectors (Bad and FoxO3a) are specifically phosphorylated by some isoforms (Akt3 and Akt1) than by others (Akt2) in the ovary for the preservation of the ovarian reserve. Researches continue in our laboratory to consolidate these findings and to identify the specific mechanisms by which each isoform/combination might be involved in the protection of the ovarian reserve.

**Metabolically Dissecting a Paused State in Pluripotent Cells.** João Ramalho-Santos, Maria Inês Sousa, Bibiana Correia, and Ana Sofia Rodrigues

Embryo metabolism is not always the same throughout development, evolving from an oxidative metabolism during early cleavage phases towards a more glycolytic profile in blastocyst generation, pluripotency establishment/maintenance and implantation. At the late blastocyst stage the Inner Cell Mass is organized in primitive endoderm and epiblast, from where naive pluripotent stem cells (PSC)/mouse embryonic stem cells (mESC) are isolated. The ability of these cells to differentiate into distinct cell fates has tremendous potential with several Stem Cell based therapies currently under development. One exciting new avenue involves the manipulation of signalling pathways to induce a quiescent in vitro paused state. Recently, the mammalian target of rapamycin (mTOR) was found to be a central player regulating both in vivo and in vitro diapause, characterized by a decreased in DNA, RNA and protein synthesis. However, the exact mechanisms involved, and whether this strategy can be used in maintaining PSC in a controlled “stemness” status remains to be determined.

In this work, we pharmacologically inhibited mTOR in both naïve and foetal bovine serum cultured PSC, which are in a more primed state. We observed that both types of pluripotent states become less proliferative, with morphological differences within colonies and differences in cell cycle. Furthermore, pluripotency is increased in this paused state with a lower oxygen consumption rate as well as lower glycolytic flux. Consequently, their glycolytic capacity is significantly diminished. Interestingly, the metabolic adaptation to this paused state varies accordingly to the pluripotent state. These adaptations are observed not only in terms of cellular function, but also at the RNA and protein level. These results

are expected to have an impact not only in the Stem Cell Biology field envisioning the implementation of new biochemistry-based modulation methodology to maintain stem cells.

This work was financed by the European Regional Development Fund (ERDF), through the Centro 2020 Regional Operational Programme: project CENTRO-01-0145-FEDER-000012-HealthyAging2020, the COMPETE 2020 - Operational Programme for Competitiveness and Internationalisation, and the Portuguese national funds via FCT – Fundação para a Ciência e a Tecnologia, I.P.: project POCI-01-0145-FEDER-007440. CNC is funded by FCT under the strategic project UID/NEU/04539/2013. The authors also thank the grant support by FCT and FEDER/COMPETE 2020 (POCI-01-0145-FEDER-007440).

**Imatinib Treatment Diminishes Ovarian Reserve and Oocyte Development Potential.** Wael Salem, Irene Woo, Sue A Ingles, Karine Chung, Richard J Paulson, and Lynda K McGinnis

Addressing a cancer survivor's future fertility can improve their quality of life following their primary treatment. Tyrosine Kinase Inhibitors (TKI) are an emerging drug class with unknown clinical consequences on oocytes and embryo developmental potential for women undergoing cancer treatment. One of these TKIs is Imatinib, a drug which functions by specifically and competitively blocking tyrosine kinase activities of ABL, KIT, and platelet derived growth factor receptor (PDGFR). All three are expressed by the ovary and developing germ cells. Within the ovary KIT-ligand and PDGF function independently to promote primordial follicle activation, transition of primordial to primary follicle, oocyte growth, granulosa cell proliferation, and follicle survival in mice. Therefore, a biological plausibility is postulated for a potential gonadotoxic effect of Imatinib. In the present study, we developed a mouse model to analyze the effect of long-term Imatinib treatment on fertility by measurement of folliculogenesis and preimplantation embryo development.

The model included three treatments (n=10 mice/treatment): Group 1(400mg/kg intraperitoneal (IP) Imatinib daily, 4wks); Group 2 (400mg/kg IP Imatinib 6wks); Group 3 (controls, water IP daily). These doses achieved serum levels equivalent to humans undergoing treatment with Imatinib and had significant deleterious effects on placentation in our previous studies (unpublished data). CF1 females were superovulated with 5IU equine chorionic gonadotropin followed 48hr later with 5IU human chorionic gonadotropin (hCG) to trigger ovulation, then mated overnight with mature BDF1 males. 72hr post-hCG, females were euthanized, oviducts and uteri were isolated and flushed, all oocytes and embryos were collected and examined for stage of development; ovaries fixed for histology. Cleaving embryos were transferred into culture drops and cultured to 120hr post-hCG. At the end of culture, all blastocysts were fixed and nuclei stained for cell counts. Ovaries were sectioned, total follicles counted in 6 serial sections, from 6 females/treatment to give an estimate of follicle development.

Imatinib-treated ovaries had lower total follicle counts (31.4 vs 38.1 vs 50.1 ( $P < 0.004$ ) for groups 1, 2 and controls, respectively). This was primarily due to a loss of of primordial follicles in treated mice versus controls (45% vs 47% vs 66%  $p < 0.001$ , respectively). Blastocysts from treated mice had fewer cells (Group 1:  $87 \pm 37.6$ ,  $p < 0.01$ ; Group 2:  $115 \pm 29.6$ , Controls:  $137 \pm 24.2$ ) and a lower ratio of ICM to total cells (Group 1:  $13.1 \pm 6.5$ ,  $p < 0.01$ , Group 2:  $15.4 \pm 6.2$ , Controls:  $19 \pm 3.7$ ). There was no effect on ovulation rate, percentage cleaving embryos, or percentage blastocyst formation.

This study demonstrated that Imatinib treatment diminished the primordial follicle count and adversely affected blastocyst quality (lower ICM development). Since there was no significant increase in growing follicles, it's feasible that Imatinib induced apoptosis or direct gonadotoxic damage to the primordial cell line. This study highlights the potential gonadotoxicity of long-term TKI treatments on reproductive age women. Patients should have an informed discussion regarding the possible deleterious effects TKIs may have on future fertility.

**Changes in Motility Parameters of Bovine Sperm Inhibiting Different Metabolic Pathways During in Vitro Capacitation.** Edith N. Sanoguet-Crespo, Héctor Sánchez-Rodríguez, Jaime Curbelo-Rodríguez, and Enid Arcelay-Ruiz

The production of energy in sperm cells can be generated by glycolysis and cellular respiration, this to maintain the motility, which is vital for sperm function and male fertility. The metabolic pathway to generate energy in the sperm differs depending on the species and the environment in which the microgamete is located, either under aerobic or anaerobic conditions. The present study evaluated the mitochondrial function of bovine spermatozoa during in vitro capacitation by using enzymatic inhibitors [(EI); 3-chloro-1,2-propanediol (3MCPD), Sodium Oxamate (NaOx), 1-fluoro-2,4-dinitrobenzene (DNFB)] and electron transport chain uncouplers [(UC); Rotenone (Rot) and Carbonyl cyanide 3-chlorophenylhydrazone (CCCP)]. Control treatments [capacitating medium (CM) and CM+dimethylsulfoxide (CM+DMSO)] were used to compare the effect with a non-capacitating medium (NCM). Semen from four Senepol bulls was collected by electro-ejaculation, incubated for 4 h at 37° C in a 5% CO<sub>2</sub> atmosphere, and analyzed (1x/Hr) using the Computer Assisted Sperm Analysis (CASA) system to evaluate the following parameters: motility (MOT), curvilinear velocity (VCL), amplitude of lateral head displacement (ALH), beat-cross frequency (BCF), and linearity (LIN). Data were analyzed using the Proc Mixed in SAS (Statistical Analysis System). There was no interaction between treatment and time for the motility-related parameters evaluated. Although, a treatment effect for MOT, VCL, ALH, BCF and LIN (P 0.05). Although, between these and the NCM there was a difference for all the parameters (P 0.05). The sperm were negatively affected according to the hours of incubation regardless of the treatment: MOT, VCL, ALH, BCF and LIN (P 0.05). These results suggest that these enzymes are involved in motility during hyperactivation and the bovine sperm are able to produce energy and maintain their motility to achieve fertilization, depending on the conditions in which it is found.

**Reactive Oxygen Species And Human Sperm Quality: Comparisons Between Distinct Fluorescent Probes.** João Ramalho-Santos, Sara Escada-Rebelo, Artur Paiva, Teresa Almeida-Santos, and Ana Paula Sousa

In humans, 10-15% of couples have infertility issues, with male factor responsible for about 50% of the cases. Also, the average success of assisted reproductive techniques (ART) has remained at 32% for the past decades. This scenario is mainly due to the fact that sperm populations are extremely heterogeneous (containing both functional and non-functional gametes) and that current conventional tests performed both to analyze semen and suggest treatment options are unsophisticated, of limited predictive power, and have remained unchanged. This highlights the need to explore male gamete function with the goal of identifying more function-based sperm biomarkers that can be used to

improve diagnostics and select the best gametes for ART. The long-established association between mitochondrial functionality and sperm quality, enhances the use of mitochondrial parameters, namely reactive oxygen species (ROS) levels, as a useful tool to identify and segregate a more functional sperm subpopulation.

In this work following appropriate ethical clearance and informed consent human sperm samples were collected from adult males undergoing fertility treatment at the Reproductive Medicine Service (CHUC-Coimbra). A semen analysis was performed to obtain data regarding sperm parameters, such as concentration, pH, motility and morphology. Sperm cells ( $5 \times 10^6/\text{mL}$ ) were then incubated with several fluorescent probes against ROS (MitoSOX<sup>TM</sup> Red, DHE, Redox Sensor<sup>TM</sup> Red CC-1, CellROX<sup>®</sup> Orange and MitoPY1) at 37°C for defined periods of time. After incubation, the sperm cells were analyzed through Flow Cytometry (FACSCalibur - Becton Dickinson; New Jersey, USA) and the mean fluorescence intensity (MFI) values were obtained. These values were then, through statistical analysis, correlated with sperm parameters. Statistical analysis was performed using SPSS Statistics version 21.00, software for Mac (SPSS Inc., Chicago, IL, USA). Positive controls with hydrogen peroxide and Antimycin A were always carried out.

Our unpublished results show correlation between the MFI values and sperm parameters obtained from the semen analysis, proving once again the association between mitochondrial functionality and classically monitored sperm quality. This suggests a potential use of ROS as a biomarker for the selection of the best gametes (functional sperm subpopulation). Importantly, results with different probes were markedly different, clearly stressing the fact that not all ROS measurements are the same, and that preliminary studies and appropriate controls are always required. CellROX<sup>®</sup> Orange did not show any relevant correlations with sperm parameters. MitoPY1 was the probe showing less relevant correlations and only with sperm morphology. MitoSOX<sup>TM</sup> Red, DHE and Redox Sensor<sup>TM</sup> Red CC-1 showed relevant correlations with motility, and the first two (similar in terms of structure) also with concentration. Down the line, this opens the possibility of performing further studies exploring more function-based sperm biomarkers within the selected population. This work is funded by FEDER funds through the Operational Programme Competitiveness Factors - COMPETE and national funds by FCT - Foundation for Science and Technology under the strategic project UID/NEU/04539/2013 (POCI-01-0145- FEDER-007440).

**Central Blocking of Estrogen Receptors Reverses the Negative Seasonal Feedback Effect of Estradiol (E2) on LH Pulse Frequency in Ewes.** Arreguin-Arevalo JA, Maturana CF, Urias C, and Nett TM.

In ewes, the influence of daily light length on ovarian cyclicity is driven by an action of estrogens in the hypothalamus and it is reflected by a decrease in circulating concentrations of LH during anestrus seasons. We tested the hypothesis that central blocking of estrogen receptors, either at nearly the end of the breeding season or during the last third of anestrus season, will block the negative seasonal feedback effect of estradiol on the pulsatile pattern of LH, lengthening the neuroendocrine breeding season. Ovariectomized (OVX) ewes ( $n = 9$ ), carrying a subcutaneous E2 implant (to deliver 2 to 3  $\mu\text{g}$  of E2 per ml of serum), received the estrogen receptor antagonist ICI 182780 (ICI; 1.9 mg/day) or vehicle directly into the lateral ventricle of the brain, via a catheter connected to a subcutaneous osmotic pump. For experiments 1 and 2, pumps were implanted to the end of the breeding season (third week of January) or during the last third of anestrus season (third week of June), respectively. Pumps remained

in place until ewes were euthanized. Another group of OVX, E2 implanted ewes, were euthanized during breeding season as a positive control. Blood samples were collected every 15 minutes for six hours every other week starting a month before placement of pumps. For experiment 1 and 2, ewes were euthanized after a distinctive secretory profile was evident between ICI-treated ewes and vehicle-treated ewes. Hypothalamic and pituitary glands were harvested for further analyses. Administration of ICI to ewes at the end of the breeding season maintained a pulsatile pattern of LH characteristic of breeding season (artificial breeding season) during the anestrus season. Similarly, administration of ICI to ewes during anestrus season induced an earlier pulsatile pattern of LH (artificial breeding season) compared with vehicle-treated ewes. The number of kisspeptin immunoreactive cells in the arcuate (ARC) nucleus of the hypothalamus from ewes during the artificial breeding season was similar than those observed in ewes during breeding season and higher than in ewes during anestrus season. We concluded that in ewes, central blocking of estrogen receptors reverses the negative seasonal feedback effect of E2 on the secretory pattern of LH, thus extending the length of the neuroendocrine breeding season. This project was supported by Agriculture and Food Research Initiative Competitive Grant no. 11890907 from the USDA National Institute of Food and Agriculture and The College Research Council.

**Effects of Fresh Bull Semen Centrifugation with Nontoxic Colloid on Membrane Lipid Peroxidation, Mitochondrial Membrane Potential and Oxidative Stress After Sperm Cryopreservation.** Tairini Erica da Cruz, Alicio Martins Jr., Fernanda Nunes Marqui, Tatiana Issa Uherara Berton, Camila de Paula Freitas-Dell'Aqua, and José Antonio-Dell'Aqua Jr

Density gradient centrifugation through colloids has been used extensively in assisted reproductive techniques to separate viable spermatozoa from immotile spermatozoa and to reduce toxic substances as reactive oxygen species (ROS). However, centrifugation forces can lead to ROS generation and oxidative stress in sperm. The purpose of this study was to verify the effects of Percoll Plus (PP) added as a cushion solution to minimize physical sperm damages during single layer centrifugation (SLC) on lipid membrane peroxidation (LP), mitochondrial membrane potential (MMP), O<sub>2</sub><sup>-</sup> and H<sub>2</sub>O<sub>2</sub> production of fresh semen. Ejaculates (n=18) of three Nellore bulls housed at Artificial Insemination Station were collected by artificial vagina and assessed for sperm motility, concentration, and morphology. After pooling (mixture of three ejaculates of each bull), the sperm sample was split into three aliquots to form the experimental groups, as follows: group I (control), sperm immediately diluted in a freezing extender; group II, semen subjected to SLC with 70% PP; and group III, semen subjected to SLC with 70% PP, but with 1.5 ml of undiluted PP (commercially available formulation) on bottom of the centrifuge tube. In groups II and III the sperm samples were layered on top of a 9-mL column of colloid in 15-ml centrifuge tubes, just before centrifugation (13 min at 839 x g) at room temperature. After that, the supernatant was removed, the sperm pellet diluted to a final concentration of 25 millions of spermatozoa/straw, in all groups. Frozen-thawed sperm samples were assessed for O<sub>2</sub><sup>-</sup> production and MMP with the association of MitoSOX Red and MitoStatus Red probes, whereas H<sub>2</sub>O<sub>2</sub> and LP were detected with dihydrorhodamine 123 and C11-BODIPY, respectively. All evaluations were performed by flow cytometry, with sperm parameters expressed in fluorescence intensity (arbitrary unit; AU) for the total number of cells, excepted for LP (%). ANOVA and Tukey's test were used for statistical analysis (data of six replicates), with P < 0.05 taken as significant. There was no significant difference among groups for H<sub>2</sub>O<sub>2</sub> and MMP with values ranging from 15613 ± 1068 to 18015 ± 2075; 1081 ± 71.6 to 1489 ± 226, respectively. Higher production of O<sub>2</sub><sup>-</sup> was founded for II and III (1933 ± 147.7 and 1726 ± 81.6,

respectively) in comparison to I ( $1424 \pm 145.6$ ), with similar results between II and III. LP was lower in III ( $25.3 \pm 2.6$ ) in comparison to I ( $38.2 \pm 4.1$ ), however, I and III did not differ from II ( $30.3 \pm 3.6$ ). In summary, cushioned SLC was not able to consistently reduce the sperm damaged, as evidenced by the levels of ROS and mitochondrial membrane potential. However, as the results of lipid peroxidation indicated some kind of protection on phospholipids sperm membrane, further experiments need to be conducted to better understanding this finding. Acknowledgements: FAPESP (grant 2015/20986-3), Tairana Artificial Insemination Station and Botupharma, Brazil.

**Mrnip Deficiency Causes Male Infertility Due to Impaired Meiosis.** Renata Prunskaitė-Hyyryläinen, Julio Castañeda, Denise Archambeault, Zhifeng Yu, Ramiro Ramirez-Solis, and Martin M. Matzuk

Infertility affects 7-10% of all reproductive age men. Underlying genetic factors can be found in ~15% of cases. In order to identify new genetic factors of male infertility our groups undertook an in silico bioinformatic search for testis enriched genes conserved between mouse and human. Our search revealed mouse MRN complex interacting protein (Mrnip), the ortholog of human Chromosome 5 open reading frame 45 (C5orf45). RT-PCR analysis demonstrated that Mrnip is ubiquitously expressed in multiple tissues with the strongest expression in testis, kidney, and brain.

We acquired gene specific knock-out mice (3010026O09Riktm1a(EUCOMM)Wtsi) from the knock-out mouse consortium (KOMP). Fertility tests indicated that Mrnip knock-out males are infertile, whereas female fertility was not altered. Testes weights and sperm counts were reduced in Mrnip knockout mice as compared to heterozygous control mice. Histology of adult testes revealed defects appearing in the spermatocyte stage, while TUNEL staining showed more apoptotic cells were present in Mrnip seminiferous tubules as compared to heterozygous control. Also, no spermatozoa were present in the epididymis of adult Mrnip knock-out mice. Interestingly, analysis of juvenile Mrnip KO mice at P15 revealed no changes in testes morphology, suggesting that the defect in KO mice occurs in the later stages of spermatocyte development. Indeed, qRT-PCR analysis demonstrated that the expression of meiosis-specific genes was greatly reduced in Mrnip KO adult mouse testis. Antibody staining indicated that MRNIP is expressed in the pachytene stage of spermatocytes, during the stage where the defect is first observed. Our data indicate the Mrnip knock-out male infertility is likely due to an arrest during the meiotic stage.

This work was supported by Eunice Kennedy Shriver National Institute of Child Health and Human Development grant R01 HD088412 (M.M.M.), Baylor College of Medicine training grant 5T32HD007165-35 (J.C., D.A.), and the Academy of Finland and the Sigrid Juselius Foundation (R.P.-H.).

**Erasing the Methyl Mark: Mechanism of Androgen Action in the Ovary.** Sambit Roy and Aritro Sen

Androgen actions are critical for ovarian follicle growth and female fertility. While excess androgen level leads to polycystic ovary syndrome (PCOS), repressed androgen actions are often associated with abnormalities of follicular growth, low functional ovarian reserve (LFOR) and primary ovarian insufficiency (POI). Therefore, an ideal balance of androgen is needed to maintain normal ovarian function. However, how androgen regulates ovarian function or its underlying mechanism is still poorly understood. Androgen actions are mediated through 'nuclear/genomic' or 'extra-nuclear/non-genomic' actions of androgen receptor (AR). Recently we reported that androgens through both the nuclear and

extra-nuclear pathways inhibit the expression and activity of Ezh2, (a histone methyl-transferase involved in gene repression mark) to induce different genes that are imperative for ovarian function. Here, we further extend our study to elucidate other histone modifications induced by androgens and its downstream physiological effect in follicular development. The methylation status of lysine residues in histones determines the transcription of genes by modulating the chromatin architecture. We have found that in addition to regulating Ezh2 activity, androgens also regulate the expression of jumonjis (JMJD), a group of histone demethylases. Results show that androgens in mouse granulosa cells (GCs) and in KGN cells (a human GC cancer cell line), increase hypoxia-inducible factor 1 alpha (HIF1 $\alpha$ ) protein levels through the PI3K/Akt pathway, which in turn induce JMJD gene expression. We find that DHT regulates HIF1 $\alpha$  protein, but not mRNA expression through a translation-dependent mechanism. The effect of DHT on HIF1 $\alpha$  is blocked by flutamide (AR inhibitor), LY294002 (PI3K inhibitor) as well as cyclohexamide (a protein translational inhibitor). Interestingly the 5' prime end of certain JMJDs have HIF1 $\alpha$  response elements (HRE) and it is well established that several JMJDs are induced by HIF1 $\alpha$  under both normal conditions and hypoxic stress. There are different JMJD proteins that can positively or negatively influence transcription and are thought to serve as key regulators of gene expression in a broad number of contexts. Our studies show that androgen treatment specifically induces JMJD1, JMJD2, JARID1 and JMJD3 in GCs and this effect is inhibited by flutamide as well as by a HIF1 $\alpha$  inhibitor (Chetomin) or siRNA specific to HIF1 $\alpha$ . Based on these studies we propose that in GCs, androgens in a transcription independent (non-genomic) manner, through the PI3K/Akt signaling pathway, enhance HIF1 $\alpha$  protein synthesis under normoxic conditions. As a consequence, activation of HIF1 $\alpha$  drives the expression of JMJD1, JMJD2, JARID1 and JMJD3 proteins. Intriguingly, JMJD1 and JMJD3 knockout mice have severe fertility problems and JMJD2 is a co-activator of androgen receptor (AR)- mediated transcription. In summary, our studies for the first time, show a direct regulatory role of androgens on jumonji expression and/or activity in the ovary, primarily through non-genomic effects. Altogether, this study provides a mechanistic insight of androgen actions in ovarian function by modulating histone methylation enzymes.

This research was funded by NIH RO1HD086062-03 grant, Michigan State University and MSU AgBioResearch.

**Yes-associated Protein (YAP) Regulates Steroidogenesis in the Leydig Cell Line MLTC-1.** Adrien Levasseur, Nicolas Gévry, Derek Boerboom, and Alexandre Boyer

LH/cAMP/PKA signaling is essential for Leydig cell function. It stimulates the activation of signaling pathways and the expression/activation of transcription factors, which in turn regulate the expression of key steroidogenic genes required for testosterone synthesis. Yes-associated protein (YAP) is a transcriptional regulator that acts downstream of the Hippo pathway, and plays critical roles in cell proliferation, cell differentiation and homeostasis. The role of YAP in Leydig cells is unknown. In this study, using the MLTC-1 cell line, we showed that YAP was rapidly phosphorylated upon forskolin (FSK) treatment, and that the PKA inhibitor H-89 prevented his phosphorylation. Inactivation of YAP using the YAP inhibitor verteporfin (VP) resulted in a decrease in the mRNA levels of Lhcgr and Srd5a1, and an increase in the mRNA levels of Star and Nr4a1 independently of FSK treatment. Testosterone secretion by the MLTC-1 cells also increased following VP treatment. To complement the results obtained with VP, inactivation of Yap was also performed using siRNA. Knockdown of Yap also resulted in an increase in

Star and Nr4a1 expression and a decrease in Lhcgr expression in MLTC-1 cells treated or not with FSK. Unlike the results obtained with VP however, the expression of Sr5a1 was not affected. Together, these results suggest a novel role for YAP as a negative regulator of steroidogenesis in Leydig cells.

**Reproductive Performance of Sex-Sorted Semen in Lactating Dairy Cows on Pasture.** Z.Z. Xu, G. Hamil, R.J. Spelman, M. Stiaque, and R. Vishwanath

The objective of the study was to determine the reproductive performance of frozen sex-sorted semen, produced according to the SexedUltra procedures, in lactating dairy cows on pasture. The trial was a blind, split-ejaculate trial. Twenty seven ejaculates from 8 Holstein Friesian and 8 crossbred bulls (1 or 2 ejaculates per bull) were split and used to produce either frozen sexed semen at 4 million sperm per dose or frozen non-sexed semen at 15 million sperm per dose. Equal numbers of sexed and non-sexed semen straws from the same ejaculate were allocated to 72 participating herds. Semen from different ejaculates of the same bull was allocated to different herds. Herd owners were asked to use equal numbers of semen straws of the two batches from the same bull either on the same insemination day or on alternate days. Neither farmers nor AI technicians knew the treatment identity of the semen batches. The 24-day non-return rate (NRR) and conception rate (CR) based on pregnancy diagnosis with fetal aging were used to quantify reproductive performance. Results were analyzed using the generalized linear mixed model procedure of SAS with the fixed effects of region, bull, treatment, bull x treatment and random effect of herd. The NRR of sexed semen (54.6%, n = 3,333) was significantly ( $P < 0.0001$ ) lower than non-sexed semen (68.0%, n = 3,342). Similarly, CR of sexed semen (40.9%, n = 2,906) was significantly ( $P < 0.0001$ ) lower than non-sexed semen (54.2%, n = 3,031). While there was a significant bull effect on NRR ( $P < 0.001$ ) and CR ( $P < 0.05$ ), there were no significant effects of bull by treatment interactions on either NRR ( $P = 0.15$ ) or CR ( $P = 0.43$ ). It was hypothesized that the interval between semen collection and delivery to the sperm sorting laboratory ( $1.14 \pm 0.44$  h) might have an effect on semen quality prior to sorting. However, there was no significant correlation ( $r = 0.14$ ,  $P = 0.49$ ) between the interval from collection to delivery and the NRR decrease for sexed semen. Results from this trial show that reproductive performance of SexedUltra semen at 4 million sperm per dose is about 80% of that of non-sexed semen in lactating dairy cows on pasture. Either NRR or CR can be used to quantify the relative reproductive performance of different semen products.

**CRISPR-Cas9 Mediated Knockdown Of ODF2 in Porcine Testicular Somatic Cells.** Taylor Goldsmith, Dennis Webster, Dan Carlson, and Ina Dobrinski

Most of the cells in the body possess non-motile primary cilia. They can act as sensors, mediate cell-to-cell communication, and are essential in development and for differentiation of stem cells. Primary cilia were recently found to be present on somatic cells in the testes and the number of primary cilia was shown to vary at different stages of testicular development. This temporal expression strongly suggests that primary cilia are implicated in the morphogenesis of the testes.

We hypothesize that ablation of primary cilia from testicular somatic cells will inhibit testicular morphogenesis. Testicular somatic cells, mainly Sertoli cells and peritubular myoid cells, were isolated from one-week-old piglets through a two-step enzymatic digestion and separated from germ cells by differential plating. Two cilia genes were targeted with the intention of ablating cilia on somatic cells. First, two exons of *Odf2*, a critical gene for cilia formation, were targeted using the CRISPR-Cas9 system with *Odf2* guide RNA delivered using nucleofection. mRNA levels were assessed using qPCR and cilia loss was assessed by immunofluorescence for ARL13B, a ciliary GTPase. Cells transfected with a CRISPR construct lacking a targeting guide RNA sequence served as controls. To study tubular morphogenesis in vitro, cells were cultured on Matrigel for 7 days after treatment with CRISPR constructs and analyzed for tubule formation by bright field microscopy and immunofluorescence. Secondly, a siRNA against IFT88 mRNA, a protein essential for cilia elongation and formation, was delivered to the cells using lipofection. A scrambled siRNA was used as a control. mRNA levels were assessed using qPCR and cilia loss was assessed using immunofluorescence. Transfected cells were also cultured on Matrigel for 7 days.

Treatment with CRISPR-Cas9 *Odf2* guide RNAs caused a significant reduction in the number of primary cilia on testicular somatic cells ( $p < 0.0001$ ). In targeted cells,  $26.8\% \pm 5.34$  of cells had cilia, compared to  $68.74\% \pm 5.34$  unmodified cells with cilia ( $n=4$ ). Quantitative PCR showed a significant decrease ( $p < 0.01$ ) of *Odf2* expression in cells that were transfected with the CRISPR constructs ( $n=3$ ). When transfected cells were used to form tubules in vitro, cells where *Odf2* had been targeted appeared to form thinner, shorter, and less organized tubules compared to tubules formed from sham edited controls in a preliminary experiment ( $n=1$ ). Treatment with IFT88 siRNA caused a significant reduction in the number of cilia ( $p < 0.05$ ). In targeted cells,  $29.79\% \pm 7.22$  of cells had cilia, compared to  $60.52\% \pm 5.98$  in untreated cells ( $n=5$ ). qPCR results showed a significant decrease of IFT88 mRNA ( $p < 0.001$ ) in treated cells compared to scrambled controls ( $n=5$ ). Tubules formed with IFT88 siRNA treated cells, appeared disorganized without a defined structure when compared to controls.

These results indicate that primary cilia play a role in tubular morphogenesis in vitro and this approach will help provide the basis for elucidating signalling pathways involved in tubule formation.

Supported by NIH/ORIP 9 R01 OD016575-12

**Epithelial Stem/Progenitor Cells Contribute to Re-Epithelialisation Following Endometrial Shedding in a Menstruating Mouse Model.** Fiona Cousins, Dorien O., James Deane, and Caroline Gargett

Endometrial regeneration is a highly complex, tightly controlled process. Stem/progenitor cells have been implicated in the regeneration of the tissue. Using the stem cell marker telomerase reverse transcriptase (*Tert*), we have shown mouse *Tert* (*mTert*) promoter activity in epithelial, endothelial and

leukocyte populations in cycling mouse endometrium. We hypothesised that cells expressing mTert contribute to repair of the luminal epithelium following menstruation in a mouse model. mTert-GFP mice were subjected to a previously published mouse model of menses. Briefly, mice were ovariectomised, treated with steroid hormones oestradiol and progesterone, artificially decidualised and progesterone then removed to induce a menses-like event. Tissues were collected for histochemical and flow cytometry analysis at 0hrs, 8hrs, 24hrs and 48hrs after progesterone withdrawal (n=8-11/group). mTert reporter activity was identified in rare cells in the residual (non-shed) luminal epithelium during breakdown (8hrs), repair (24hrs) and remodelling (48hrs). Histological analysis of mTert reporter activity in 17,902 epithelial cells revealed that only 1.1% of epithelial cells were mTert+. A significant increase in the percentage of mTert+ luminal epithelial cells at the repair ( $p < 0.001$ ) and remodelling ( $p < 0.05$ ) time-points was observed compared with prior to tissue breakdown (0hrs). Triple immunofluorescence staining for mTert-GFP, epithelial marker EpCAM and proliferation marker Ki67 revealed extensive proliferation of residual luminal epithelial cells during repair and remodelling. mTert-GFP+ cells were typically observed as clusters, interspersed between Ki67+ proliferating cells. Proliferating epithelial cells were rarely mTert+ (0.72%). mTert+ epithelial cells did not appear to colocalise with the previously published epithelial progenitor marker CD44. These findings are the first to show putative epithelial progenitors present in repairing luminal epithelium of endometrium. The clusters of epithelial mTert-GFP+ cells suggests the endometrium prepares for cyclical re-epithelialisation by distributing stem/progenitor cells along its luminal surface. We propose that epithelial mTert activity is activated in some luminal epithelial cells to support the rapid re-epithelialisation of the endometrium, by undergoing asymmetrical division to form transit amplifying cells that rapidly divide to generate sufficient cells to repair the endometrial surface.

### **Maternal Glucose Intolerance Increases Offspring Adipose Mass and Insulin Signaling in Mice.**

Omonseigho Talton, Keenan Bates, Kylie Hohensee, and Laura Schulz

Gestational diabetes mellitus (GDM) increases the risks of obesity and diabetes in offspring. As the incidence of GDM rises globally, so does the need for studies outlining how these offspring outcomes are programmed. We previously developed a mouse model of lean GDM in which dams exhibit glucose intolerance and reduced insulin response to glucose challenge only during pregnancy, without accompanying obesity. Here, we examined how gestational glucose intolerance affects offspring risk of metabolic dysfunction. At 4, 12, 20, and 28 weeks, offspring were placed in metabolic cages that recorded metabolism over three days. One cohort of offspring was sacrificed at 19 weeks, and half of the offspring in the second cohort were placed on high-fat high-sucrose diet (HFHS) at 23 weeks, prior to sacrifice at 31 weeks. We examined body weight, body composition, glucose tolerance, adipose and liver gene expression, liver and serum triglycerides, serum insulin, leptin and adiponectin levels in offspring. Exposure to maternal glucose intolerance in utero increased weights ( $p=0.0002$ ) of HFHS-fed offspring independent of sex. On the control diet, offspring of GDM dams exhibited higher body fat percentages at 4, 12 and 20 weeks of age ( $p=0.001$ ). At 28 weeks, GDM offspring fed the HFHS but not the CD also had higher body fat percentages than offspring of CON ( $p=0.03$ ). Exposure to GDM increased the respiratory quotient (CO<sub>2</sub> produced /O<sub>2</sub> consumed) in male offspring at 20 weeks ( $p=0.01$ ) and in offspring of both sexes on either diet at 28 weeks ( $p=0.004$ ), indicating reduced fatty acid oxidation. Real-time PCR in subcutaneous adipose tissue revealed increased mRNA levels of Pparg ( $p=0.01$ ) and Adipoq ( $p=0.002$ ) in 31 week old CD-fed male offspring, and increased mRNA levels of Insr ( $p=0.001$ ) and

Lpl ( $p=0.047$ ) in 31 week old male offspring fed both CD and HFHS. In liver at 31 weeks, mRNA levels of Ppara ( $p=0.04$ ) were elevated in CD-fed male offspring of GDM dams, and male offspring of GDM dams exhibited higher mRNA levels of Insr on both diets ( $p=0.0325$ ). Together these changes suggest increased sensitivity to insulin promotion of lipid storage in adipose tissue. Serum leptin was elevated in female offspring of GDM dams fed the HFHS ( $p=0.02$ ), and serum leptin to adiponectin ratio was higher in male and female offspring of GDM dams fed the HFHS ( $p=0.01$ ). Fasting insulin, glucose tolerance and liver and serum triglyceride levels were unaffected by maternal exposure to GDM. Our findings show that GDM comprising glucose intolerance only during pregnancy programs increased adiposity in offspring, while increasing adipose tissue insulin sensitivity, preventing the development of insulin resistance and glucose intolerance. These phenotypes are partly mediated by preferential glucose versus lipid utilization in the offspring of GDM dams.

**Distinct Actions of Classical and Non-Classical Estradiol Pathways in the Pathogenesis of Granulosa Cell Tumors of the Ovary.** Victoria Cluzet, Florence Petit, Marie Devillers, Isabelle Treilleux, Isabelle Ray-Coquard, John A. Katzenellenbogen, Sung Hoon Kim, Stéphanie Chauvin, Joëlle Cohen-Tannoudji, and Celine J. Guigon

Granulosa cell tumors (hereafter named as GCT) account for ~5% of ovarian tumors. Relapses, which can occur years after initial diagnosis, remain a therapeutic challenge. Since circulating levels of the sex steroid estradiol (E2) is abnormally elevated in most patients, hormone therapy with aromatase inhibitors to decrease E2 levels is sometimes used but it displays variable efficacy. Although E2 effects have been widely studied in a large number of cancers, there is still poor information regarding GCT. We previously reported that E2 could inhibit GCT metastasis spreading through non-classical pathways involving the G protein-coupled estrogen receptor (GPER). The present study aims at deciphering the possible roles and mechanisms of action of E2 through nuclear estrogen receptors (ERs) in this pathogenesis.

We studied the expression of the nuclear estrogen receptor  $\alpha$  (ER $\alpha$ ) and  $\beta$  (ER $\beta$ ) by immunohistochemistry on tissue micro-arrays (TMA) from human adult primary ( $n=21$ ) and recurrent ( $n=10$ ) GCTs. We also conducted cell-based assays to monitor E2 effects on cell growth, apoptosis and migration, as well as molecular studies to determine the contribution of each ER and their mechanisms of action. Since ER signaling is inactive in available human GCT cell lines, we used a mouse GCT-derived cell line (AT29 cells) endogenously expressing ER $\alpha$  and ER $\beta$ .

Examination of human TMAs revealed that ERs were expressed in the majority of primary GCTs (% of GCTs with positive staining: ER $\beta$ , 48%; ER $\alpha$ , 62%; ER $\alpha/\beta$ , 81%), and that ER $\alpha$  became low in recurrent GCTs (ER $\beta$ , 50%; ER $\alpha$ , 20%; ER $\alpha/\beta$ , 50%). Noteworthy, E2 treatment significantly stimulated GCT cell growth by favoring cell survival. Preliminary profiling studies of more than 70 genes related to apoptosis/survival processes on RT-PCR arrays suggest that E2 enhanced cell survival by regulating components of the tumor necrosis factor (TNF) signaling pathway. Importantly, treatments with ER $\alpha$  and ER $\beta$  agonists (PPT and DPN, respectively) recapitulated E2 action on GCT cell survival, thus indicating that each receptor could mediate E2 effects. We conducted additional studies to gain insight into the molecular mechanisms underlying E2 actions. We observed that E2 induced a ~2-3 fold increase in the activity of an estrogen responsive element (ERE) luciferase reporter gene. Besides, we found that estradiol coupled to dendrimer conjugates (EDC), which cannot enter into the nucleus, had no effect on

GCT cell growth or survival. Thus, our results support the idea that E2 induces cell growth through nuclear pathways.

Altogether, these findings lead us to propose that E2 would promote GCT cell survival through ER $\alpha$  and ER $\beta$  nuclear regulation of a subset of genes belonging to the TNF signaling pathway. Overall, our work unveils the possible existence of dual roles for E2 in GCT pathogenesis, with GPER signaling preventing metastasis spreading and ER pathways promoting GCT growth. Systematic screening for the different forms of estrogen receptors should be a requisite prior considering hormone therapy. The use of selective drugs activating GPER and inhibiting ERs may improve the clinical outcome of patients with advanced disease.

This work was supported by Fondation ARC, GEFLUC, and the National Institutes of Health.

**Multidrug Resistance Protein 1 Deficiency Promotes Doxorubicin-Induced Ovarian Toxicity in Female Mice.** Shuo Xiao, Yingzheng Wang, Mingjun Liu, Jiyang Zhang, Yuwen Liu, Megan Kopp, and Weiwei Zheng

Multidrug resistance protein 1 (MDR1), a phase III drug transporter that exports substrates out of cells, has been discovered in both cancerous and normal tissues. The over expression of MDR1 in cancer cells contributes to multiple drug resistance, whereas the MDR1 in normal tissues protects them from chemical-induced toxicity. Currently, the role of MDR1 in the ovary has not been entirely understood. Our objective is to determine the function of MDR1 in protecting against chemotherapy-induced ovarian toxicity. Using both the in vivo transgenic mouse model and in vitro follicle culture model, we investigated the expression of MDR1 in the ovary, the effect of MDR1 deficiency on doxorubicin (DOX)-induced ovarian toxicity, and the ovarian steroid hormonal regulation of MDR1. Results showed that the MDR1 was expressed in the ovarian epithelial cells, stroma cells, theca cell layers, endothelial cells, and luteal cells. The lack of MDR1 did not affect female ovarian function and fertility, however, its deficiency significantly exacerbated the DOX-induced ovarian toxicity in both in vivo and in vitro models. The MDR1 showed significantly higher expression levels in the ovaries at estrus and metestrus stages than those at proestrus and diestrus stages. However, this dynamic expression pattern was not regulated by the ovarian steroid hormones of estrogen (E2) and progesterone (P4) but correlated to the number and status of corpus luteum (CL). In conclusion, our study demonstrates that the lack of MDR1 promotes DOX-induced ovarian toxicity, suggesting the critical role of MDR1 in protecting female ovarian functions during chemotherapy.

**A(xoneme) to Z(inc): New Paradigm of Mammalian Sperm Zinc Ion Fluctuation from Spermiogenesis to Fertilization.** Karl Kerns, Michal Zigo, Wei Xu, Erma Z. Drobniš, Lauren Hamilton, Miriam Sutovsky, Richard Oko, and Peter Sutovsky

Building on our recent discovery of the sperm zinc signature phenomenon [1], we have extensively characterized the zinc ion fluxes throughout the totality of the sperm lifespan, from spermiogenesis and epididymal sperm maturation, to ejaculation, capacitation, and fertilization. We identified four distinct types of sperm zinc ion distribution patterns (further “zinc signature”) present in boar, bull, and human spermatozoa (as reported by zinc probe FluoZin-3 AM fluorescence). Signature 1 spermatozoa have zinc

localized throughout the entire sperm head and tail; Signature 2 zinc ions map to the whole sperm head but only the sperm tail midpiece; Signature 3 has midpiece localization only (no Zn in sperm head); and Signature 4 lacks zinc ions altogether. Signature 1 was associated with a non-capacitated state, signature 2 spermatozoa displayed capacitation-induced hyperactivated motility, signature 3 spermatozoa also had capacitation-induced acrosomal changes, and the acrosomal loss and cell death occurred in the post-capacitated signature 4 spermatozoa. The zinc signature changes during in vitro capacitation (IVC) were inhibited under proteasomal proteolysis-inhibiting conditions, and the zinc-induced fluorescence was removed with a Zn-chelator TPEN. The zinc signature differed between boar collection fractions and resulted in differing capacitation rates. These differences set in sperm ejaculatory sequence likely helps establish the sequential sperm capacitation time clock. Related to boar performance in single sire artificial insemination (AI), higher fertility boars had an increased ability to achieve signature 3 after IVC, not progressing to signature 4 prematurely, likely a function of fertilization-competent state and the ability to survive post-capacitation for longer periods of time. The inclusion of ZnCl<sub>2</sub> in semen extender prevented spontaneous, pathological capacitation, by day 3 of incubation. Thus, the management of the zinc signature could allow for reducing the AI sperm dose to increase the usage of high genetic value sires. The zinc signature also differed between semen collections from the same boars. On subcellular level, the capacitation induced Zn-ion efflux could activate zinc-containing enzymes involved in sperm penetration of the zona pellucida, such as the inner acrosomal membrane metalloproteinase MMP2 that had a severely reduced activity in the presence of zinc ions. In context of the fertilization-induced oocyte zinc spark and the ensuing polyspermy-blocking zinc shield, the inhibitory effect of zinc on sperm-borne enzymes may contribute to the fast block of polyspermy. Altogether, our findings establish a new paradigm on the role of zinc ions in sperm capacitation, representing a fundamental shift in the understandings of mammalian fertilization and paving the way for the optimization of livestock AI and semen preservation/distribution, with a potential for non-hormonal contraceptive targeting. Supported by USDA-NIFA grant 2015-67015-23231 (PS), USDA-NIFA Graduate Fellowship 2017-67011-26023 (KK), NSERC (RGPIN/192093) (RO) and seed funding from the MU F21C Program (PS). [1] Kerns K, Zigo M, Sutovsky M, and Sutovsky P. (2017). Platform presentation finalist: Zinc Signature of Mammalian Sperm Capacitation (Abstract #87). 2017 Annual Meeting of the SSR, Washington D.C.

**GnRH-II and its Receptor are Critical Regulators of Testicular Steroidogenesis in Swine.** Amy T. Desaulniers, Rebecca A. Cederberg, Clay A. Lents, and Brett R. White

The second mammalian form of GnRH (GnRH-II) and its receptor (GnRHR-II) are produced in one livestock species, the pig. However, the interaction of GnRH-II with its receptor does not stimulate gonadotropin secretion. Instead, both are abundantly produced in the gonads and have been implicated in autocrine/paracrine regulation of steroidogenesis. Our data suggests that GnRH-II from seminiferous tubules interacts with GnRHR-II on porcine Leydig cells to stimulate LH-independent testosterone biosynthesis. To further study the role of GnRH-II and its receptor, our laboratory generated a knockdown (KD) swine line with 70% lower testicular GnRHR-II expression and 80% diminished basal testosterone concentrations. The objective of this study was to assess Leydig cell functionality in GnRHR-II KD (n = 4) and littermate control (n = 2) males. In the first experiment, blood was serially collected via indwelling catheters prior to and after intravenous treatment with human chorionic gonadotropin (hCG; 30 IU/kg BW); serum testosterone concentrations were measured via radioimmunoassay (RIA). A line (GnRHR-II KD versus control) x time interaction was detected (P 0.10). In both lines, testosterone levels

were reduced below basal concentrations 2 h post-treatment, staying suppressed for the remainder of sampling ( $P < 0.10$ ), suggesting adrenal origin. Concentrations of all 10 steroid hormones did not differ between genotypes after castration ( $P > 0.10$ ). These data demonstrate that knockdown of testicular GnRHR-II ablates gonadal steroidogenesis, indicating that GnRH-II and its receptor are critical regulators of steroid hormone production within porcine Leydig cells. Supported by USDA/NIFA AFRI-ELI predoctoral fellowship (2017-67011-26036; ATD) and AFRI (2017-67015-26508; BRW) funds. USDA is an equal opportunity provider and employer.

**Essential Role of TDRD5 in Pachytene PiRNA Biogenesis in Mice.** Deqiang Ding, Jiali Liu, Uros Midic, Yingjie Wu, Kunzhe Dong, Ashley Melnick, Keith E. Latham, and Chen Chen

PIWI-interacting RNAs (piRNAs) play a crucial role in silencing transposons and protecting the germline genome. piRNAs also regulate spermatogenesis-associated RNAs, and are essential for the production of functional sperm. Pachytene piRNAs comprise the largest and most diverse population of small non-coding RNAs in the testis with more than two million distinct piRNA species. These piRNAs are primarily generated from hundreds of unique genomic loci (piRNA clusters) through a primary processing pathway. The piRNA biogenesis factors involved in pachytene piRNA precursors processing are poorly understood. TDRD5 is a Tudor domain protein implicated in spermatogenesis and male fertility. However, the role of TDRD5 in piRNA biogenesis has not been established. Here we show that TDRD5 is essential for pachytene piRNA biogenesis in mice. Conditional inactivation of TDRD5 in mouse postnatal germ cells reveals that TDRD5 selectively regulates the production of pachytene piRNAs from abundant piRNA-producing precursors, with little effect on low abundant piRNAs. Unexpectedly, we provide evidence that pachytene piRNA precursor processing contains two genetically separable steps: 5' end processing and the processing of the rest of the piRNA precursors. TDRD5 is not required for the 5' end processing of the precursors, but is crucial for promoting production of piRNAs from the other regions of the transcript. Through CLIP-seq assay, we show that TDRD5 is an RNA binding protein directly associating with piRNA precursors. Together, these findings establish TDRD5 as a novel piRNA biogenesis factor and reveal two genetically separable steps at the start of pachytene piRNA processing.

**Metabolic Modeling of the Regulation of Carbohydrate Metabolism in Cultured Mink Uterine Cells.**

Jennifer Chase, Lauren Gould, Abigail Haas, Hayden Holmlund, Andrew Holston, Mario Escobar, Ayokunle Hodonu, and Jason Hunt

The nutrients used by an embryo both before and after implantation are provided by secretions from the uterine endometrium. Estrogens and progesterone coordinate storage and delivery of lipids, proteins, and carbohydrates by these endometrial cells. Dysregulation of carbohydrate metabolism in these cells, including glycogen storage, may affect fertility. However, the mechanisms by which carbohydrate metabolism is regulated have not been elucidated in uterine tissue. We have used transcriptome analysis of mink uterine tissue, as well as enzymatic and flux analysis of a mink uterine epithelial cells (GMMc) to adapt a computational model of the regulation of glycolysis to assess the distribution of flux control under basal conditions. There was substantial variation in gene expression between uterine phases in the mink (estrus, diapause, pregnancy), including hexokinase 2 and glucose-6-phosphatase. The kinetics of glycolytic enzymes extracted from GMMc were similar to other

mammalian cells, and result in a glycolytic flux at 5 mM glucose of 2.9 nmol/min/mg cells. Net glycogen degradation was observed at a rate of -0.17 nmol/min/mg cells. When the measured kinetic constants, glycogen, and glycolytic fluxes were used to modify a published COPASI model of HeLa cell glycolysis, the metabolite levels and glucose uptake rate in the cells were fairly well predicted. Metabolic control analysis using the model showed that hexokinase, as well as ATP turnover and mitochondrial pyruvate metabolism, were most controlling of glycolytic flux under the modeled conditions. The importance of hexokinase was consistent with variations in hexokinase 2 transcripts between uterine phases. While the desired rate of glycolysis for fertility is not yet known, future studies can focus more specifically on measuring the effects of estrogen and progesterone on the flux-controlling steps. The computational model can be used to generate testable hypotheses about the effect of substrates or hormones on the glycolytic flux during the uterine cycle.

This work was made possible by an Institutional Development Award (IDeA) from the National Institute of General Medical Sciences of the National Institutes of Health under Grant #P20GM103408.

**Differential Sensitivity of Interferon-stimulated Genes for Prediction of Gestation in Cattle.** Keiichiro Kizaki, Hitomi Yoshino, Kosuke Iga, Toh-ichi Hirata, Hideo Matsuda, Tadayuki Yamanouchi, Yutaka Hashiyada, Noriyuki Toji, Toshina Ishiguro-Oonuma, Toru Takahashi, and Kazuyoshi Hashizume

Practical prediction methods for gestation diagnosis have been coveted in bovine reproduction especially early gestation period. The expression of interferon-stimulated genes (ISG15 and MX2) in peripheral blood cells well predicted establishment of pregnancy within three weeks after insemination. In the present study, the ISG expression profiles in peripheral blood cells were compared in two different bovine breeds; Holsteins (H) and Japanese-Blacks (JB). Blood samples were collected with a commercial whole blood RNA preservation tube, and amount of genes expression was detected with quantitative RT-PCR using SYBR green. The cutoff values for prediction of gestation were adopted with the average values of individual ISG expression in peripheral blood cells from estrous cycle cattle. Gestation statuses were confirmed and determined by rectal palpation with at least two different experts on five to six weeks after artificial insemination (insemination day was designated as Day 0). The average values of ISG15 during estrous cycle in H and JB were detected as 0.151 +/- 0.158 (collected 135 points from 70 cows) and 0.174 +/- 0.148 (collected 42 points from 5 cows), respectively. The positive predictive values (PPV, number of true positive animals/(number of true positive animals + number of false positive animals) x 100) for gestation diagnosis by ISG15 intensity were estimated as about 70 and 80% at Day 21 of gestation in H and JB. Negative predictive values (NPV, number of true negative animals/(number of true negative animals + number of false negative animals) x 100) were over 90% in both breeds on Day 21. The significant differences were detected between the ISG15 expression average values in H and JB on Day 21 of gestation and those in estrous cycle ( $P < 0.01$ ), respectively. These analyses support the reliability of PPV and NPV. Although the average MX2 value during estrous cycle of JB was detected about 90% as NPV at Day 21 of gestation, PPV was estimated to only 60%, which was rather low compared to that in H. The lower values of PPV in JB were also detected on Days 18 to 20 of gestation. The trend of PPV and NPV by ISG15 from Day 18 to 21 of gestation were similar in H and JB. However, MX2 showed lower reliability of PPV in JB. These results suggest that the MX2 expression in peripheral blood cells may be more susceptible than ISG15 in JB, and ISG15 is rather suitable indicator for the prediction of early gestation in cattle. The Research Program on Innovative Technologies for

Animal Breeding, Reproduction, and Vaccine Development from the Ministry of Agriculture, Forestry, and Fisheries of Japan has granted for this study (REP-1003).

**Role of Wnt Signalling in Vaginal Epithelial Stem/Progenitor Cells and their Progenies.** Ayesha Ali and Pradeep S. Tanwar

The vagina is a hormone-dependent organ that undergoes regression after oestrogen withdrawal but can completely regenerate upon oestrogen supplementation. By using unbiased DNA analog based and genetic cell lineage tracing techniques, we identified a rare population of highly proliferating stem/specialized progenitor in the basal compartment of the vaginal epithelium that both self-renew and give rise to the differentiated cells. In vitro, these cells develop organoids containing all the vaginal epithelial cell lineages arranged similarly to the in vivo organisation of different epithelial cell types.

The canonical Wnt signalling pathway plays an essential role in female reproductive tract development and in adult stem cell maintenance. By using a well-established Wnt reporter mouse model and in situ hybridization-based expression analysis, we showed that Wnt signalling activity is mainly limited to the suprabasal layer of mouse vagina. This suggested that Wnt signalling might be involved in the differentiation of vaginal epithelial stem/progenitor cells. To understand the functional importance of the Wnt pathway in vaginal epithelium, we developed a mouse model and revealed that stem/progenitor cells are able to self-renew but unable to undergo differentiation in the absence of Wnt/ $\beta$ -Catenin signalling. In summary, this study identified a population of vaginal stem/progenitor cells and describes the importance of Wnt/ $\beta$ -Catenin signalling in vaginal epithelial growth and differentiation.

**The Path to Fertilization: Sperm Pairing Mechanism in *Monodelphis domestica*.** Kobi Griffith and Yolanda Cruz

New World marsupial sperm have a singular characteristic absent in their Australian counterparts: pairing. As soon as the sperm have completed development in the epididymis, they undergo a stereotypical series of maneuvers, resulting in the precise, point-by-point alignment and firm adhesion between the acrosomal aspects of two sperm heads. The sperm attach to the epithelium of the epididymis before pairing which could be important for correct positioning. Most sperm are unpaired in the caput, while approximately 50% are paired in the corpus; most sperm in the cauda are paired. Prior to fertilization the sperm unpair, possibly by anchoring to the crypts of the oviduct. A parsimonious hypothesis suggested by such sperm behavior is that pairing and unpairing are accomplished by one mechanism. I undertook this project to explore the possibility that a hyaluronidase-like glycoprotein SPAM 1 (sperm adhesion molecule 1) is the major or only protein involved in such a mechanism. Immunohistochemistry was used to localize the protein along the male and female reproductive tract (three sections of the epididymis and the oviduct) in the model organism for marsupial development *Monodelphis domestica* (lab opossum). The female reproductive tract was tested at varying days of pregnancy, pseudo pregnancy, failed pregnancy and in non-pregnant females. Immunohistochemistry was performed on 3 samples for each respective tissue. Mouse tissues were used as positive controls. Mouse and opossum sperm were fluorescently stained to determine localization along the acrosomal

head. To test if SPAM1 was involved in pairing a neutralization experiment was performed in which varying concentrations of Anti-SPAM1 and controls (TBS and naïve serum) were applied to paired sperm harvested from the caudal epididymis of three *Monodelphis domestica* and one mouse. Percentage of unpaired sperm were calculated at 0, 1 hour and 2 hours and statistical analyses were performed to determine significance. SPAM1 was localized along the lumen of the corpus and cauda of the epididymis but not the caput; the protein was also localized in all days of pregnancy including failed and pseudo pregnant females. SPAM1 was not localized in the non-pregnant oviduct of *Monodelphis domestica*. The neutralization experiment showed that as time progressed paired in the treatment groups unpaired (from approximately 75% paired to 25% paired after 2 hours). The concentration of antibody did not affect the degree of unpairing and sperm treated with the two controls did not unpair over the two hours. The localization of SPAM1 in the epithelium of the corpus and the cauda of the epididymis and in the epithelium of the pregnant oviduct suggest that SPAM1 could be involved in the adherence of sperm to the epithelium in the reproductive tracts. The unpairing of paired sperm under treatment of the antibody indicates that SPAM1 is involved in the pairing of sperm or in the stabilization of paired sperm. Taken together, these results are consistent with a role for SPAM1 in sperm pairing in New World marsupials.

#### **Comparisons Among Three Isoflavones on Perturbations in Ovarian Folliculogenesis and Atresia in Prepubertal Rats Following an In Utero and Lactational Exposure Paradigm. Monika G. Baldrige**

Consumption of dietary products rich in soy has become increasingly popular due to their reported health benefits. These soy products contain the isoflavones genistein, diadzein, and glycitein that belong to a class of non-steroidal compounds called phytoestrogens. It is documented that these naturally occurring plant estrogens provide health benefits in some tissues; however, they may act as endocrine disruptors on the development of estrogen-sensitive reproductive tissues during critical periods of development. There is a large body of research documenting exogenous phytoestrogen modulation of reproductive tissues in mature male and female subjects; however, there is a paucity of knowledge regarding reproductive effects on offspring following an in utero and lactational exposure. Herein we aimed to delineate (1) whether an in utero and lactational exposure to genistein, diadzein, or glycitein exerts adverse effects on ovarian follicle maturation, and (2) whether circulating estrogen concentrations are altered in the prepubertal Sprague-Dawley rat upon exposure. Dams were treated via subcutaneous injection on gestational days 7-21 with low (0.2-0.5 mg/kg/day) or high (5 mg/kg/day) doses of genistein (Gen), diadzein (Diad), or glycitein (Gly). Female pups were sacrificed on postnatal day 28 (chosen to follow the pups' exposure through lactation). Following sacrifice, the ovaries were excised, fixed for histology, and analyzed. The analysis included a count, measurement, and classification of preantral and antral follicles in the greatest cross-sectional area of the ovary. Blood sera collected at the time of sacrifice were analyzed to determine circulating estrogen concentrations. Radioimmunoassay results indicated no statistical significance in circulating estrogen concentrations among treatment groups ( $p > 0.05$ ). However, we observed in all treatment groups modulation of ovarian follicle maturation as evidenced by decreased numbers of preantral and antral follicles, decreased total number of healthy follicles, and increased atresia ( $p < 0.05$ ); dose-dependent effects were also noted. These data support the hypothesis that genistein, diadzein, and glycitein exert hormonal action sufficient to reduce the numbers of healthy follicles in certain size classes in rats exposed during the critical period of development, despite significant differences in binding affinity for the estrogen receptor. Atresia of

preantral and antral follicles constitutes one of the mechanisms by which these isoflavones alter ovarian folliculogenesis. Information obtained from this study further elucidates the possible female reproductive implications of exogenous estrogen exposure.

#### **Temporal Expression Pattern of HSP47 during Mouse Embryo Implantation and Decidualization.**

Yichen Wang, Ni Ma, Xin Chen, Liu Tian, Huiqi Liao, Changjun Zhang, and Honglu Diao

Embryo implantation involves the synchronized preparation of a competitive embryo and a receptive uterus; however, it remains largely unknown. Hsp47 is an endoplasmic reticulum (ER)-resident molecular chaperone that is specific for collagen. Recent studies suggested that HSP47 is essential molecular chaperone for mouse development with collagen molecular maturation in the ER. The functions of HSP47 are still unknown in the uterus during pregnancy. The aim of this project is to examine the uterine expression and regulation of HSP47 during pregnancy in mice and its regulation under pseudopregnancy, steroid hormone treatment, and artificial decidualization conditions by Realtime PCR and In Situ Hybridization. Our Pre-limited data showed that HSP47 mRNA is significantly up-regulated on implantation site in day 4.5 11:00h mouse uterus by Realtime PCR and in situ hybridization and mainly expressed the primer decidual zone and myometrium. We also get slimly results in the artificial decidualization model. Our Pre-limited data showed that HSP47 should have the important function during implantation and decidualization. Next step, we will identify molecules and proteins that can directly interact with HSP47 and downstream signaling pathways affected by HSP47 deletion in mouse in vitro induced decidualization model.

#### **Nutrient Restriction during Gestation Alters the Maternal/Fetal Endocrine Environment and Increases NPY Neuronal Projections to GnRH Neurons in the Female Bovine Fetus.**

Emma Britain Caraway, John M. Long, Meaghan M. O'Neil, Gary L. Williams, Tryon A. Wickersham, Jason E. Sawyer, M. Carey Satterfield, and Rodolfo C. Cardoso

Gestational nutrient restriction (NR) causes epigenetic and phenotypic changes in the offspring that impact several physiological processes, including neuroendocrine function, fertility, and energy metabolism. Hypothalamic neurocircuitries controlling feed intake and GnRH pulsatile release are particularly sensitive to modifications in the nutritional/metabolic status during perinatal development. Of particular interest are neuropeptide Y (NPY) neurons that comprise an important hypothalamic pathway that inhibits GnRH secretion before pubertal maturation and during periods of energy deficiency. Using the bovine model, we tested the hypothesis that moderate NR during mid to late gestation alters the maternal/fetal endocrine milieu and increases NPY neuronal projections to GnRH neurons in the female fetus. Embryos were produced in vitro utilizing sexed (X-bearing) semen from a single sire. Embryos that developed to blastocyst stage were split to generate monozygotic twins. Each identical twin was individually transferred into a virgin dam (n=72; Angus-based composite breeds). Pregnancy was confirmed on gestational day (GD) 60 and yielded 4 identical twin pairs and 18 half-sibling calves. Recipient dams were maintained on high-quality forage and beginning on GD158 were randomly assigned to receive either 100% NRC (C) or 70% NRC requirements (NR), ensuring that each monozygotic pair was assigned to either nutritional group. Maternal plasma samples were collected at GD158, 186, 214, 242, and 265. At GD265, identical twins were euthanized by barbiturate overdose and

umbilical vein plasma and fetal hypothalami were collected. Sections of the preoptic area and mediobasal hypothalamus were processed for double-label immunofluorescence. As expected, body weight was lower ( $P < 0.01$ ) in NR compared to C dams starting at GD186 and continuing until necropsy/term. NR had no effect on maternal concentrations of progesterone (C,  $n=12$ ; NR,  $n=13$ ) and an expected rise was observed during mid to late gestation. Cortisol concentrations in NR dams markedly declined after initial restriction and were lower ( $P < 0.01$ ) than in C dams starting at GD186 and continuing throughout gestation. Fetal cortisol levels did not differ between groups. Maternal leptin concentrations were analyzed in a subset of the dams (C,  $n=6$ ; NR,  $n=7$ ) and were not affected by NR. Insulin concentrations were reduced in NR compared to C fetuses ( $P = 0.04$ ). At the fetal hypothalamic level, maternal NR increased ( $P < 0.01$ ) the number of NPY projections to GnRH neurons and the percentage of GnRH neurons highly innervated ( $\geq 10$  close appositions) by NPY fibers. No changes in the number of GnRH-immunoreactive neurons were found. The reduction in maternal cortisol concentrations in response to NR suggests a compensatory response to conserve energy from maternal utilization and thus maximize potential glucose supplies for the fetus. Additionally, these results demonstrate that moderate NR during mid to late gestation results in alterations in the maternal/fetal endocrine environment that are associated with increased hypothalamic NPY tone (inhibitory). These neuroendocrine changes are likely to persist postnatally and negatively impact several reproductive processes such as pubertal maturation and estrous cyclicity in the bovine female. Supported by USDA-NIFA Hatch project-1012280 (RCC) and Texas A&M AgriLife Research-Beef Industry Competitiveness Program (MCS).

**Ganglioside GM3 Regulates EGFR/ERK Signaling Pathway in Meiotic Maturation and Cumulus Cells Expansion of Porcine Oocyte During *In Vitro* Maturation.** Hyo-Jin Park, Jae-Min Jung, Jin-Woo Kim, Seul-Gi Yang, Min-Ji Kim, Ho-Guen Jegal, In-Su Kim, and Deog-Bon Koo

Ganglioside GM3 is well known that the inhibition of cells proliferation, differentiation and tyrosine kinase site for epidermal growth factor receptor (EGFR) receptors activation. Maintenance of EGFR/ERK signaling is important role on porcine oocyte maturation. Recently, our previous study shown that addition of exogenous ganglioside GM3 reduced oocytes maturation through the decreasing of EGFR/PI3K/AKT signaling and induction of apoptotic factors in pigs. However, regulation of GM3 synthesizing enzyme ST3GAL5 by siRNA ST3GAL5 on porcine oocytes during *in vitro* maturation (IVM) has not been reported. In present study, we investigated the changes of EGFR/MAPK signaling on meiotic maturation and cumulus cells expansion according to the treatment of siRNA ST3GAL5 in porcine oocyte. Under exogenous GM3 treatment for 44 h, meiotic maturation, polar body formation and cumulus cells expansion were significantly decreased in matured cumulus oocyte complexes (COCs). Interestingly, exogenous GM3 treated COCs during IVM I (0 – 22 h) were shown the increasing of germinal vesicle breakdown (GVBD) stage, reduction of cumulus cells expansion and ST3GAL5 protein levels compared with other treatment groups. To observe the changes of EGFR/ERK signaling proteins, we performed the Western blotting of EGFR, p-EGFR, ERK and p-ERK proteins in GM3 treated COCs for IVM progression. Expression levels of EGFR and ERK proteins were significantly reduced, whereas p-ERK expression dramatically increased in GM3 treated COCs for IVM I (0 – 22 h). Thus, we selected a specific pig siRNA ST3GAL5 (#205) and performed the siRNA #205 transfection to the maturing COCs for 44 h. As results, the meiotic maturation in siRNA #205 treated COCs decreased compared with control. Expression level of p-ERK protein reduced in siRNA #205 transfected COCs. Interestingly, meiotic

maturation of porcine COCs after GM3 treatment in conjunction with siRNA #205 were recovered (GM3 1  $\mu$ M with siRNA #205;  $84.6 \pm 4.8\%$  and GM3 5  $\mu$ M with siRNA #205;  $87.2 \pm 1.9\%$ ) during IVM. These results suggest that ganglioside GM3 is involved in the regulation of EGFR/ERK signaling on oocyte maturation and cumulus cells expansion during porcine IVM. Therefore, ganglioside GM3 is required for the maintenance oocyte maturation in pigs.

Keywords: Ganglioside GM3, siRNA ST3GAL5, MAPK signaling, in vitro maturation (IVM), Pigs

#### Acknowledgements

This work was supported by IPET through Agri-Bioindustry Technology Development Program (316037-04), funded by Ministry of Agriculture, Food and Rural Affairs, Republic of Korea.

**In Vitro Derivation of Mature Sertoli-like Cells from Mouse Embryonic Stem Cells.** Dong-Won Seol, Eun-Young Shin, Jae Il Bang, Woo Sik Lee, and Dong Ryul Lee

Sertoli cells (SCs) play important roles in sex determination during embryogenesis and they support germ cells to make spermatogenesis in seminiferous tubule. Additionally, SCs are immune privileged cells, important for controlling the immune response to male germ cells as well as maintaining the tolerogenic environment in the testis. Since, ectopic SCs have been shown to survive and protect co-grafted cells when transplanted across immunological barriers. In fact, SCs are considered useful materials for therapeutic application. However, mature SCs do not mitosis, and the primary immature SCs during prolonged culture lose their unique feature. Therefore, establishing the source of these cells independent of donor testis cells is an urgent matter. Although it has been reported that Sertoli-like cells (SLCs) can be derived spontaneously from human embryonic stem cells (hESCs), their functional property and purity of the differentiated SLCs still remain to be solved. Recently another approach for the induction of SLC has been reported that direct transdifferentiated SLCs from mouse fibroblasts have shown formation of the tubular-like structures and expression of embryonic Sertoli-specific markers. However, application of this method may be considered several problems such as requiring much time, high cost and genetic modulation. Hence, the aim of this study is to differentiate from mESCs into the functional and high purity SLCs. First of all, mESCs induced mesendoderm, sequentially induced intermediate mesoderm (IM). Induced IM expressed their markers, such as Wt1, Lhx1, Pax2, and Osr1, and PAX2+LHX1+ cells were nearly 90% efficiency. Sequentially induction of 6 days resulted efficiently in ESC-SLCs. SLCs expressed their marker genes (Wt1, Sox9, Sf1, Gata4, Scf, and Fshr), but pluripotency-marker gene was decreased (Oct4). After sorting by FSHR, high purity (>90%) of SLCs was collected and it has not formed teratoma. Sorted SLCs has shown distinct properties of the SCs, such as phagocytotic activity, T cell potential activity and expressions of immune modulation-related genes. Also, when transplanted into seminiferous tubule of busulfan-treated mice, SLCs is re-located and maintained in basal of the tubule. Additionally, the prolonged culture of SLCs has shown decrease immature SC markers (Amh, Krt18, and Ncam1), and increase mature SC markers (Ar, Clusterin). These findings indicate that our robust sequential differentiation system can produce functional SLCs from mESC and may possibility of establishment of mature SLCs in vitro. Our data suggest that derivation and establishment of SLCs derived from mESCs might a useful source in infertility treatment and cell therapy. This research was supported partly by grants from the Bio & Medical Technology Development Program (2015M3A9C6028961 and 2017M3A9C8029318) of NRF and MSIP of Republic of Korea.

**Alteration of Immune Responses in Bovine Endometrial Cells Under Heat Stress Conditions.** Shunsuke Sakai, Toshimitsu Hatabu, Yuki Yamamoto, and Koji Kimura

After parturition, bacterial infections of uterus occur frequently in cows, resulting in the onset of endometritis. To eliminate these bacteria, bovine endometrial cells detect bacteria via TLR4, which constructs a complex with MD-2 and CD14, and secrete various cytokines such as tumor necrosis factor  $\alpha$  (TNF $\alpha$ ), interleukin (IL)-1 $\beta$ , and IL-6. TNF $\alpha$  and IL-1 $\beta$  promote inflammatory response, and IL-6 recruits macrophages to the site of bacterial infection. Although these immune responses cure endometritis, recovery is prolonged in summer than in any other season. Based on these findings, we hypothesized that immune responses in the uterus are suppressed by heat stress (HS), and three experiments were conducted. First, we collected endometrium tissues in summer and winter, examined using fluorescence immunohistochemistry, and measured the perpendicular distance of macrophages from the endometrial epithelial layer (n = 6). Macrophages were found to be sparsely localized throughout the endometrium in summer, whereas they were localized at the periphery of the endometrial epithelial layer in winter. Also, their distance from the endometrial epithelial layer was significantly (P < 0.05) greater in summer than in winter. Next, we cultured endometrial epithelial and stromal cells at 38.5 °C (control) and 40.5 °C (HS treatment) in the presence or absence of lipopolysaccharide (LPS). After treatment, the expression of TNF $\alpha$ , IL-1 $\beta$ , IL-6, TLR4, MD-2, and CD14 mRNA was measured in endometrial epithelial and stromal cells using quantitative RT-PCR. LPS significantly induced (P < 0.05) the expression of TNF $\alpha$ , IL-1 $\beta$ , and IL-6 mRNAs in endometrial epithelial cells (n = 6, 5, and 5, respectively), but it did not influence the expression of TLR4, MD-2, and CD14 mRNA (n = 7). Moreover, HS significantly suppressed (P < 0.05) the LPS-induced TNF $\alpha$  and IL-6 mRNA expression and induced (P < 0.05) the mRNA expression of TLR4 in endometrial epithelial cells. The expression of LPS-induced IL-1 $\beta$ , MD-2, and CD14 mRNA was not influenced by HS in endometrial epithelial cells. However, LPS significantly induced (P < 0.05) the mRNA expression of IL-1 $\beta$  and IL-6 (n = 4 and 6, respectively) in endometrial stromal cells, but did not influence the expression of TLR4, MD-2, and CD14 mRNA (n = 5). In addition, HS significantly enhanced (P < 0.05) the mRNA expression of LPS-induced IL-1 $\beta$ , IL-6, and TLR4 in endometrial stromal cells. Finally, after incubation of endometrial epithelial and stromal cells in the presence or absence of LPS under HS conditions, we collected the culture media supernatants and measured IL-6 production by EIA. IL-6 production in endometrial epithelial and stromal cells cultured at 38.5 °C was significantly increased (P < 0.05) by LPS (n = 4) but this was not detected in endometrial epithelial cells cultured at 40.5 °C (< 0.039 ng/ml). However, LPS-induced IL-6 production was significantly enhanced (P < 0.05) by HS in endometrial stromal cells. These findings suggest that HS enhanced the immune responses in endometrial stromal cells, but suppressed the immune response in endometrial epithelial cells, where bacterial infection primarily occurs. Moreover, macrophages were not recruited to the endometrial epithelial layer, and accumulated in the stromal layer under HS conditions, which may delay recovery from bovine endometritis in summer.

**Pronuclear Formation is Partially Impaired in Bovine Androgenetic Haploid Zygotes and Development Cannot be Improved by Exposure to 6-DMAP.** Luis Aguila, Joao Suzuki, Jacinthe Therrien, and Lawrence C. Smith

The generation of androgenetic haploid embryos and embryonic stem cell (ESC) lines have innumerable applications in reproductive and developmental biology. Although murine androgenetic haploid

embryos and ESC lines have been efficiently generated, in large animals, such as bovine species, haploid embryo development is low and poorly understood. Therefore, we hypothesized that this lower developmental potential is due to an inadequate pronuclear formation after activation in haploid zygotes. To test this hypothesis, bovine in vitro matured oocytes were fertilized and the oocyte's telophase-stage spindle was enucleated after 3 h to obtain haploid zygotes, which were compared with diploid counterparts. Embryo development was assessed at 48 h (cleavage), 144 h (morula), and 168 h (blastocyst) of culture, and the rate of pronuclear formation at 20 h post insemination (hpi). Our results showed that 85% of diploid zygotes cleaved, 38% developed to the morula and 32% blastocyst stages. However, only 59% of bovine androgenetic haploid embryos (bAhE) cleaved, 8% formed morula, and no blastocyst were obtained in this group, confirming that bAhE have lower in vitro developmental potential compared to diploid embryos. Then, we examined if bAhE were capable to undergoing normal rates of pronuclear (PN) formation. Although over 70% of fertilized embryos showed 2 pronuclei at 20 hpi, only 56% of bAhE formed a paternal pronucleus while over 35% contained a condensed sperm head. This data indicates that half the bAhE are unable to form PN, thereby undermining their long-term developmental competence. Previous reports have indicated that 6-dimethylaminopurine (6-DMAP), a protein serine/ threonine kinase inhibitor, can accelerate PN formation in diploid zygotes, suggesting that 6-DMAP would also improve PN formation and developmental potential of bAhE. Haploid androgenetic zygotes were treated or not (control group) with 6-DMAP (2 mM) for 4 h immediately after telophase enucleation. When exposed to 6-DMAP, bAhE PN formation rate was similar to the control group (52% vs 56%, respectively). However, the rate of partially decondensed sperm head was higher ( $p < 0.05$ ) in embryo development rates (cleavage: 67% and 59%; morula: 8% and 9%, and 0% blastocyst for 6-DMAP and control group, respectively). The present results suggest that, while 6-DMAP exposure is able to improve sperm head decondensation, it does not improve PN formation nor the development of bovine androgenetic haploid embryos.

**High Ovarian Reserve in Cystine-Glutamate Transporter Gene Deficient Mice.** Ren Watanabe, Hideyo Sato, and Naoko Kimura

Individual reproductive life of female mammals is characterized by the primordial follicles (PFs) number. We have found that cystine-glutamate transporter, which is one of the amino acid transporters, gene knockout (xCTKO) mice maintain the higher ovulation number compared with wild type (WT) at 13-15-month-old. Also, the lower mRNA level of mTOR which is promoting the transition to the primary follicle has been detected in xCTKO oocytes. mTOR is also known as an autophagy inhibitor. Autophagy is autolytic degradation mechanism of intracellular proteins and regulates homeostasis of amino acids. Recently, we have shown that the administration of autophagy inducer to neonatal mice upregulates its PFs number. Based on these findings, we hypothesized that xCTKO mice can have high PFs number due to high autophagic activity and lead to retain the ovulation number even if the aging. In this study, we clarify PFs number and autophagy related-protein dynamics in neonatal xCTKO mice were investigated and the transition of the follicle reserve with aging was examined. The ovaries from xCTKO and WT neonatal mice were collected at 36, 60 and 84 hours after birth (h). The PFs and primary follicles numbers were counted by serial sections from these ovaries (n=6 per group). ATG-related protein expressions in ovary were analyzed by immunohistological staining and western blot analysis (n=3 per group). Also, the number of follicles at each developmental stage from these mice were measured at 2- and 13~15-month-old (n=6 per group). PFs number continued to increase until 60 h after birth. Also,

primary follicles were observed after 36 h. xCTKO groups have tended to be higher PFs number than WT groups at each time (60 h; xCTKO 6,741±878.4 vs WT 5,797±1,196.2). On the other hands, xCTKO groups showed lower primary follicles number than WT groups at each time. At 60 h, the primary follicles number was significantly lower in xCTKO group (xCTKO 113±32.1vs WT 204±42.3; P < 0 .05). The ratio of LC3-II/LC3-I as an ATG marker tend to be higher in xCTKO ovaries than that in WT groups at each time. On the other hand, the expression level of p62 protein decreased in xCTKO groups compared to WT groups at 36 and 84 h. In 2-month-old, xCTKO group have significantly higher PFs number WT group (xCTKO 471.7±45.7 vs WT 378.9±26.0). And it was a similar trend at 13~15-months-old (xCTKO 131.5±23.4 vs WT 113.9±22.7). The total follicle numbers from xCTKO groups tended to be higher than that from WT groups. These results suggest that the higher ovulation number in aged xCTKO mice would be brought by the higher follicle reserve after puberty. And the high follicles number would be brought by both promoting of PF formation and suppression of progression to primary follicle at neonatal stage, via consistently high trend of autophagic activity. Additionally, inhibition of xCT may lead to abundance ovarian reserve. This work was supported by Grants-in-Aid for JSPS Research Fellow.

**The Toxic Effect of Aflatoxin B1 on Early Porcine Embryonic Development.** Kyung-Tae Shin, Jing Guo, Ying-Jie Niu, Teoan Kim, and Xiang-Shun Cui

Aflatoxin B1 (AFB1) is a type of mycotoxin produced by the fungi *Aspergillus flavus* and *Aspergillus parasiticus*. AFB1 is considered as the most toxic mycotoxin owing to its toxic effect on health. In the present study, the toxic effect of AFB1 on early porcine embryonic development and its possible mechanism were investigated. Blastocyst formation was impaired with treatment of 1 μM AFB1. Further study showed that the presence of AFB1 induced the generation of reactive oxygen species (ROS). And excessive ROS caused DNA damage. Additionally, AFB1 also disrupted the DNA damage repair through the regulation of 53BP1. TUNEL assay confirmed the generation of apoptosis, further resulting in the occurrence of autophagy. These results showed that the presence of AFB1 impaired porcine early embryonic development through oxidative stress, as well as DNA damage and repair, apoptosis, autophagy.

**Melatonin Supplementation Increased the Pluripotency of Inner Cell Mass of Bovine Blastocysts.**

Xueming Zhao, Lisha Cui, Haisheng Hao, Hao-Yu Wang, Weihua Du, Yan Liu, Yun-Wei Pang, and Hua-bin Zhu

Embryonic stem cells can self-renew infinitely and differentiate into all three germ layers, and they provide very ideal materials for gene targeting to make biomedical and gene modified livestock. Therefore, bovine embryonic stem cells are important to enhance the production of transgenic and somatic cell nuclear transfer cattle. However, the research of bovine embryonic stem cells remains difficult since that it is hard to maintain the pluripotency of inner cell mass of bovine blastocyst during the culture and propagation. Melatonin occurs naturally in the earth and is a powerful antioxidant. Meanwhile, melatonin supplementation have been proven to enhance the efficiency of mouse induced pluripotent stem cell generation by inhibiting the p53-mediated apoptotic pathway and the formation of better primary embryonic stem cell colony of buffalo blastocyst as well as in the maintenance of their pluripotency. However, little information is available about the effect of melatonin on the pluripotency

of inner cell mass of bovine blastocysts. In the present study, 10<sup>-9</sup> M melatonin was supplemented in the culture medium (CR1aa) of bovine pronuclear embryos obtained by in vitro fertilization and the culture medium (2i/LIF) of bovine inner cell mass isolated from blastocysts obtained. Then, after ten passages, the number of colony per blastocyst, alkaline phosphatase and OCT4 staining, mRNA expression and CpG methylation levels of OCT4 and NANOG of colonies obtained were examined. The results showed that the number of colony per blastocyst of 10<sup>-9</sup> M melatonin group (7.05, 620/88) was significantly higher than that of control group (3.52, 327/93). The positive staining percentage of alkaline phosphatase and OCT4 of 10<sup>-9</sup> M melatonin group (90.20%, 92/102; 93.33%, 28/30) were higher than those of control group (70.59%, 60/85; 70.97%, 22/31). The mRNA expression levels of OCT4 and NANOG of 10<sup>-9</sup> M melatonin group were significantly higher than those of control group. The CpG methylation levels of OCT4 and NANOG of 10<sup>-9</sup> M melatonin group (8.00%, 66/825; 10.48%, 22/210) were significantly lower than those of control group (20.00%, 165/825; 19.05%, 40/210). These results indicated that melatonin supplementation greatly improved the formation of bovine embryonic stem cell colony and the maintenance of pluripotency. Our findings contribute to improving the culture condition of bovine embryonic stem cells. Research supported by ASTIP-IAS06.

**RSPH6A is Essential for Sperm Flagellum Formation and Male Fertility in Mice.** Haruhiko Miyata, Ferheen Abbasi, Keisuke Shimada, Akane Morohoshi, Kaori Nozawa, Takafumi Matsumura, and Masahito Ikawa

Spermatozoa utilize a flagellum for their motility to fertilize eggs. The radial spokes found within cilia and flagella axonemes are T-shaped protein complexes that have a rod-like structure attached to individual outer microtubule doublets and project towards the central pair of microtubules. While the radial spoke proteins have been extensively studied in the unicellular flagellate *Chlamydomonas*, their function in mammals has yet to be fully elucidated. Mutant *Chlamydomonas* that lack some or all of the components of this complex have immotile flagella or display abnormal motility. Abnormal cilia motility and defective axonemal structures in humans cause several syndromic diseases termed ciliopathies, such as Primary Ciliary Dyskinesia. In several of these syndromic ciliopathies, male infertility due to immotile spermatozoa occurs. RSPH6A is a radial spoke protein located in the spokehead and is evolutionarily conserved from *Chlamydomonas* to humans. Here, we show that mouse *Rsph6a* is testis-enriched, with mRNA expression appearing at the secondary spermatocyte stage, and the protein is localized in the flagellum. We generated *Rsph6a* knockout mice using the CRISPR/Cas9 system to clarify the function of *Rsph6a*. Homozygous mutant mice were viable, but no offspring were obtained from these mice when mated to wild-type females. Further analysis showed that spermatozoa obtained from the cauda epididymis possessed short tails and were immotile. These results indicate that *Rsph6a* is essential for sperm flagellum formation and male fertility in mice.

This work was supported by Eunice Kennedy Shriver National Institutes of Child Health and Human Development grants R01HD088412 and P01HD087157.

**Variation in the Follicle Pool Of Weaned Sows: Granulosa Cell Gene Expression In Healthy Small Antral Follicles.** N. G. J. Costermans, J. Keijer, B. Kemp, N. M. Soede, and K. J. Teerds

Over the last decades, pigs have been genetically selected to produce larger litters. This resulted in decreased piglet birth weights and increased within-litter variation in piglet birth weight which are both related to higher piglet mortality.

The aim of this study was to identify the underlying mechanism of variation in the follicle pool by studying differential gene expression of granulosa cells of large and small follicles within the same antral follicle pool at the time of weaning (=onset of the follicular phase).

The right ovary of 29 multiparous sows was collected within 2 hours after weaning and immediately snap-frozen. All visible antral follicles were measured and classified as either healthy or atretic by a cleaved caspase-3 immunostaining. The variation in follicle size of the 10 largest healthy follicles was used to select a total of eight sows for further analysis; four sows with the largest variation in follicle size of the 10 largest healthy follicles and four sows with the smallest variation in follicle size. Granulosa cells of the 3 largest and 3 smallest healthy follicles of each of the 8 animals were isolated using laser-capture microdissection and differential gene expression was analyzed by individual hybridization with porcine whole-genome microarrays.

Average follicle size of the 3 largest and 3 smallest healthy follicles of the sows selected for large variation in follicle size was  $7.1 \pm 0.8$  mm vs.  $3.9 \pm 0.9$  mm and was  $6.1 \pm 0.8$  vs.  $4.9 \pm 1.1$  mm for the sows selected for small variation in follicle size. A core set of 33 genes was differentially expressed in large vs. small follicles in both the large variation follicle pools as the small variation follicle pools. The role of these core set genes will be analyzed to investigate the underlying mechanism of variation in the healthy antral follicle pool.

Surprisingly, genes involved in the final steps of the steroid synthesis pathway were already expressed in early antral follicles. Steroid profiles in serum and follicular fluid have been measured using LC-MS and data are currently analysed.

**Meiosis-Competent Human Testicular Organogenesis from Embryonic Gonads in Vitro.** Yan Yuan, Laihua Li, Qing Cheng, Qiao Zeng, Yibo Wu, Mingqian Huang, Junqing Chen, Quan Zhou, Rong Hua, Hao Zhang, Jianyu Tian, Xin Wang, Xuejiang Guo, Mingxi Liu, Zuomin Zhou, Feiyang Diao, Qi Zhou, and Jiahao Sha

Organogenesis is a complex and highly coordinated process involving cellular differentiation and the formation of new structures. The mammalian testis does not complete organogenesis until puberty when the first wave of spermatogenesis is completed. With limited availability of in vivo data, recapitulation of human testis organogenesis in vitro would be highly useful to investigate genetic, epigenetic, and environmental factors that shape germ cell development. More importantly, it may also lead to clinical approaches to overcome infertility resulting from gametogenesis defects including azoospermia. Infertility affects approximately 8-12% of couples of childbearing age.

Here, we report successful recapitulation of testis organogenesis, including the formation of mature haploid male germ cells, from human embryonic male genital ridges in vitro. Semi-submerged organ cultures of week 12-19 fetal genital ridge segments containing germ cell progenitors and immature somatic cells produced a population of self-renewing spermatogonial stem cells (SSCs), which expressed SSC-specific marker genes even after months of culture and underwent in vitro meiosis of spermatocytes followed by spermiogenesis of spermatids. Somatic cells within the cultures matured and established a functional blood-testis barrier (BTB). The nuclei of cultured germ cells recapitulated the temporal and spatial expression of key markers of chromosomal synapsis in spermatocytes, including  $\gamma$ H2AX, SYCP3 and SYCP1. We found that haploid germ cells resulting from meiosis in vitro could undergo spermiogenesis, a complex process involving dramatic morphological changes. These spermatid-like cells formed acrosome vesicles and early tail structures emanating from the centrioles. Whole-genome CNV analysis of individual spermatid-like cells collected by flow cytometry, confirmed that these contained an intact euploid genome. Furthermore, multiple human short tandem repeat (STR) sites profile analysis of spermatid-like cells demonstrated that recombination on autosomes had been achieved during spermatogenesis. The results of STR loci tests also confirmed that the haploid cells originated from cultured tissues. Bisulfite sequencing revealed that spermatid-like cells had acquired male germ cell-like methylation marks at imprinted loci. Injection of spermatid-like cells into MII oocytes derived from GV oocytes by in vitro maturation resulted in 7-cell stage embryo, indicating that spermatid-like cells can support early embryonic development.

Successful recapitulation of human testicular organogenesis and meiosis in a culture environment proves the feasibility of in vitro generation of human sperm. We demonstrate that upon exposure to morphogens and sex hormones, human germ cells recapitulate male gametogenesis in vitro, reproducing hallmarks of imprints erasure, synapsis, and recombination. In vitro studies based on human testicular organogenesis can help elucidate the complexity of spermatogenesis and the development of the testis, and will play an important role for reproductive medicine.

**In Vivo Investigations of Prostaglandin-mediated Effects in Early Canine Corpus Luteum (CL) - New Insights into Luteal Vascularization and Immunity.** Miguel Tavares Pereira, Aykut Gram, Bernd Hoffmann, Tomasz Janowski, Alois Boos, and Mariusz P. Kowalewski

In most domestic animals the absence of pregnancy results in termination of corpus luteum (CL) function due to increased production of uterine luteolysin (PGF2 $\alpha$ ). This is not the case in the domestic dog, in which no active luteolytic principle is present in non-pregnant bitches. This results in a prolonged physiologic pseudopregnancy, regularly exceeding the time span of pregnancy and terminating with a slow luteal degeneration. Since the canine placenta lacks steroidogenic activity, the CL of the dog has a central role in the maintenance of pregnancy, being the only producer of progesterone (P4). Another unique feature of canine reproduction is the presence of a transitional gonadotropic independence of the CL in the first two to four weeks after ovulation. During this time, the high expression of PTGS2/COX2, PGE2-synthase (PTGES) and cAMP-dependent PGE2 receptors (EP2, EP4) suggests an important role of PGE2 in regulation of the canine CL. Supporting this idea, the in vitro stimulation of canine luteal cells with PGE2 increases their steroidogenic output and modulates the expression of some vascular factors and of the PRL-receptor. It is noteworthy that PRL is the main luteotropic factor during the second half of canine dioestrus. Proof of the regulatory role of PGE2 in the

early canine CL, and the causality between COX2 and the luteal PGE2 synthesis by PTGES, was demonstrated in our in vivo study, in which bitches were treated for different time periods after ovulation (5, 10, 20 and 30 days) with effective doses of a COX2-specific inhibitor, firocoxib (Previcox®). This treatment suppressed luteal production of PGE2, lowered circulating P4 and negatively affected luteal development, when compared with control groups that received a placebo for the same periods after ovulation.

Considering the wide range of possible modulatory roles of PGE2 shown in different organ systems, using samples from the above described in vivo study, this follow-up project aimed to understand PG-mediated effects on vascularization, immunity and some of the regulators of the STAR protein expression and of the cell cycle in the canine CL. Expression of several factors has been assessed at the mRNA and protein levels. The inhibition of COX2 diminished the expression of angiopoietin family members ANGPT-1, -2, Tie-1 and -2 receptors that are usually linked to vascular stabilization. The expression of endothelin (ET)-1, linked in some species to PGF2alpha synthesis and luteolysis, was increased. Concerning the immune system, Previcox®-treatment led to increased expression of the pro-inflammatory cytokines, IL1 $\beta$ , IL6 and IL12, and elevated expression levels of CD4. Surprisingly, despite the previously described decrease in luteal transcriptional activity in Previcox®-treated bitches, expression of the STAR regulator cJUN and the cell cycle regulator CCNA-2 was increased. This suggests the presence of compensatory regulatory mechanisms during early luteal formation in the dog. Cumulatively, besides its involvement in regulating steroidogenesis, our results indicate a broader role of PGE2 in the canine CL, including modulation of angiogenesis, vascular stabilization and local immunomodulation. Possible cross-species translational effects are strongly implied. Supported by the Swiss National Science Foundation (SNSF); research grant number 31003A\_160251.

**Anti-CRISPR Protein AcrIIA4 Enables Off-Switches for CRISPR/Cas9 in Mouse Zygote..** Arisa Ikeda, Wataru Fujii, Koji Sugiura, and Kunihiko Naito

CRISPR/Cas9-mediated gene editing in zygotes is now widely used for production of genome-modified animals. However, the prolonged activity of zygote-stage-injected Cas9-gRNA sometimes causes mosaicism of the induced mutations, therefore the temporal control of the endonuclease activity is required. Recently CRISPR/Cas9 inhibitor proteins (anti-CRISPRs) encoded by bacteriophages have been discovered. In this study, we investigated whether anti-CRISPRs can inactivate the function of CRISPR/Cas9 in mouse zygote. At first, we assayed the inhibitory efficiencies of the anti-CRISPR proteins in mammalian cell. Human-codon optimized AcrIIA2 or AcrIIA4, which was previously reported as a candidate for anti-CRISPRs, was synthesized and introduced into HEK293 cells, together with Cas9 and hHPRT-targeting gRNA, and the mutation efficiency was evaluated by PCR-RFLP. Although AcrIIA2 showed no significant effect on the CRISPR/Cas-mediated mutation induction, co-expression of AcrIIA4 with Cas9-gRNA decreased the density of the mutation-mediated DNA band, suggesting that AcrIIA4 has an efficient inhibitory function. Next, we attempted to determine whether AcrIIA4 blocks Cas9 function in mouse zygote. Cas9 mRNA and Rosa26-targeting gRNA were injected into the C57BL/6 zygotes with or without AcrIIA4 mRNA, and the target locus was sequenced at blastocyst stages. Unexpectedly, the mutation induction was observed in almost all of the embryos regardless of the AcrIIA4 co-injection (12/12 in Cas9-gRNA injected, 15/16 in Cas9-gRNA-AcrIIA4 injected), indicating that AcrIIA4 failed to inhibit the Cas9 activity in mouse zygotes. In contrast, the addition of an SV40 nuclear localization signal

(NLS) at N-terminal of AcrIIA4 enabled the inhibition in all embryos (21/21), showing that NLS-AcrIIA4 completely inactivated the function of Cas9 also in mouse zygotes. AcrIIA4- or NLS-AcrIIA4-injection did not affect the developmental competence. In conclusion, AcrIIA4 can inhibit the CRISPR/Cas function in mouse zygote only in the presence of NLS, although it is unnecessary in HEK293 cells. A precise control of AcrIIA4 localization will accelerate the development of genome engineering using CRISPR/Cas system.

**Impaired Folliculogenesis in U12 Intron Splicing-Defective Zrsr2 Mutant Mice.** Isabel Gómez-Redondo, Raúl Fernández-González, Ricardo Laguna-Barraza, Eva Pericuesta, Keiko Horiuchi, Juan Valcárcel, and Alfonso Gutiérrez-Adán

All events controlling folliculogenesis require a tight regulation of gene expression to produce functional preovulatory follicles. Among other processes, splicing of mRNA modulates the expression of several essential genes involved in follicle maturation. *Zrsr2* is a spliceosome gene located in the X-chromosome in all mammals, involved in the recognition of 3'-splice site during the early stages of spliceosome assembly, and has a role in haematopoietic development and myelodysplastic syndromes; however, its precise role in RNA splicing and function in other tissues has remained unclear. In vitro assays suggest that ZRSR2 is required for efficient splicing of both the major (U2) and the minor (U12) introns. To study its reproductive function, mutant mice containing nonsense mutations in the RNA-recognition motif were generated using CRISPR-Cas9 technology. Three lines of homozygous mutant exhibited severe defects in growing oocytes, leading to female sterility. At 3 months of age, ovaries were smaller than control, with the presence of less advanced-stage follicles and decreased number of antral follicles and oocytes and abnormal fully-grown oocytes. To investigate the molecular basis of the ovarian defects, RNA-Seq analyses of oocytes were carried out. Oocytes were collected from 3 months-old *Zrsr2* mutant homozygous mice treated with PMSG for 48h, and cumulus cells were removed by hyaluronidase treatment. Four groups of 150 cumulus-free oocytes obtained from the *Zrsr2* mutants and three groups of wild-type mice were used to purify their RNA and perform RNA-Seq analysis. Differential expression was evaluated with two independent software (DESeq2 and edgeR), keeping solely those genes which were detected by both programs to improve the reliability of our analysis. To perform the differential splicing analysis, the levels of inclusion of each transcript were determined using vast-tools. Then, splicing events were classified as modified when the difference in their Percent Spliced In ( $\Delta$ PSI) was above 10%. Out of 412 genes identified as differentially expressed, 208 showed upregulation in *Zrsr2* mutant oocytes, and 204 showed downregulation. Gene Ontology analysis revealed that a great proportion of them are involved in processes of DNA replication, regulation of cell cycle, female gonad development, and steroid metabolic process. A total of 2026 differentially spliced events were identified and classified in five different types of splicing: Exon skipping, alternative 3' splice site, alternative 5' splice site, intron retention and microexon. Intron retention events were then checked to determine if they were U2- or U12-type intron events, as well as those U2 intron events that occur in genes that contain U12 introns. A great proportion (19.14%) of upregulated intron retention events were observed in U12 or in U2 introns in U12 harboring genes. U12-type introns represent a minimum proportion of the splicing events in the genome (~0.5%), so such enrichment confirms the crucial role of ZRSR2 in U12-type intron splicing. The splicing alterations observed in *Zrsr2* mutant mice reveal a physiological role for this factor in RNA splicing and highlight the function of U12-type introns splicing in folliculogenesis. Research supported by the Spanish Ministry of Economy and Competitiveness through the project AGL2015-66145-R and BES-2016-077794 grant.

**Role of Alternative Splicing During Sex Determination in Mice.** Benjamin Planells, Isabel Gómez-Redondo, Eva Pericuesta, Patrick Lonergan, and Alfonso Gutiérrez-Adán

Sex determination is a highly plastic process through which a bipotential gonad develops into a testis or ovary. The mechanisms of sex determination are remarkably variable among organisms. In many insects, such as *Drosophila*, sex is determined by mRNA splicing. Also, differential intron retention is implicated in sex determination in some reptile and fish species. In mice, Sry acts as a transcription factor that synergistically with Sf1/Nr5a1 up-regulates Sox9 to orchestrate testis differentiation. Moreover, splicing also plays an important role during gonad formation and sex determination in this species; WT1-KTS variant is essential for the formation of the bipotential genital ridge, and WT1+KTS variant is involved in testis determination. Gonads lacking the WT1+KTS variant fail to express male-specific genes such as Sox9 and Amh, and thereby develop through the female pathway. The aim of this study was to analyze the mRNA alternative splicing events related with sex determination in mice. RNAseq libraries were prepared from genital ridges collected from males and females (n=3 per sex) around the time of sex determination (10.5 and 11.5 days post coitus, dpc). The cDNA libraries were used for sequencing using a HiSeq2500 v4 chemistry system. Quality control of RNAseq results was assessed with FastQC. Then, the sequences were trimmed using Trimmomatic software. Alternative splicing was analyzed with vastools software, categorizing the events into 5 different groups: 3' alternative splice site, 5' alternative splice site, exon skipping, intron retention and micro-exon based on their inclusion levels. A total of 694 differentially spliced events were identified between males and females at 10.5 dpc, 433 up-regulated in females and 261 in males. At 11.5 dpc, 1058 events were differentially spliced between males and females, 644 were up-regulated in females and 414 in males. Gene Ontology analysis revealed a large proportion of these genes are involved in regulation of gene expression and regulation of mRNA processing. Alternative splicing was found in Tra2a in females on 10.5 dpc, a gene that is involved in sex determination in *Drosophila*. Differential splicing was also found in Jarid2 (in males and females on 10.5 dpc), alternative splicing in this gene is involved in sex determination in reptiles; and in Sox13 and Sox5, related with sex determination in mammals and medaka, respectively. This is the first attempt to analyze the implications of alternative splicing in sex determination in mammals. The results show a significant difference in mRNA splicing between males and females, suggesting that important steps in the mammalian sex determination process are likely to operate at the post-transcriptional level, and that splicing regulatory mechanisms constitute a common feature among sex determination in distant phyla. Supported by European Union, Horizon 2020 Marie Skłodowska-Curie Action, REPBIOTECH 675526.

**Exploring Macrophage Heterogeneity in Endometriosis: Novel Evidence Supporting a Role for Monocyte-derived Macrophages in Lesion Development.** Chloe Hogg, Andrew W. Horne, Jeffrey W. Pollard, and Erin Greaves

Endometriosis is a common chronic inflammatory disorder associated with debilitating chronic pelvic pain and infertility that affects ~176 million women worldwide. It is defined by the presence of endometrial-like tissue outside the uterus (endometriosis lesions), commonly on the pelvic peritoneum. The current management of women with endometriosis is unsatisfactory and there is an unmet clinical need for new medical treatments. Immune cells, called macrophages, play a role in the growth,

vascularization and innervation of endometriosis lesions, and offer a potential therapeutic target. We have previously shown that lesion-resident macrophages are a heterogeneous population, consisting of tissue-resident endometrial macrophages, as well as macrophages originating either from the peritoneal cavity or derived from peripheral blood monocytes. The exact contribution of peritoneal and monocyte-derived macrophages is unknown. The objective of this study was to define the role of these macrophage populations in endometriosis using our in-house mouse model. To assess infiltration of tissue-resident large peritoneal macrophages (LpM) into lesions, we used dual immunofluorescence for LpM markers F4/80 and GATA6. 4% ( $\pm$ SEM 2%) of lesion-resident macrophages co-expressed these markers suggesting they were indeed LpM (n=10). To assess the incorporation of monocyte-derived macrophages into lesions, we interrogated mouse lesions by flow cytometry (n=6). 17% ( $\pm$ SEM 6%) of total cells within lesions were F4/80hi, Ly6C+ monocyte-derived macrophages, 3% ( $\pm$ SEM 1%) were F4/80-, Ly6C+ monocytes and 8% ( $\pm$ SEM 2%) were F4/80hi, Ly6C- mature macrophages. We validated our findings using dual immunofluorescence for F4/80 and Ly6C. Since monocyte-derived macrophages represented a significant number of cells in lesions we postulated that they might play an important role in lesion development. In order to investigate this, we used C-C chemokine receptor type 2 (CCR2) -/- mice, which are deficient for the chemokine (C-C motif) ligand 2 (CCL2) receptor. CCL2 is a key chemokine responsible for the extravasation of monocytes into the peritoneal cavity, therefore these mice are deficient in monocytes and monocyte-derived macrophages in this cavity. We induced endometriosis in both wild-type (n=6) and CCR2 -/- (n=6) mice and assessed the number of lesions that developed. There was no difference in the number of lesions recovered from CCR2 -/- mice compared to WT. CCR2 -/- mice with endometriosis had an increase ( $p=0.03$ ) in monocytes in the peritoneal cavity compared to sham controls (n=8). This suggests that lesions produce a strong chemotactic signal that stimulates the extravasation of monocytes, which in this model is independent of CCR2. Our on-going work aims to characterise which chemokine is responsible for the extravasation of monocytes in our model and assess whether blocking this pathway could stop endometriosis lesions developing. In summary, we have shown that lesion-resident macrophages have different origins, and include endometrial, peritoneal and monocyte-derived macrophages. We have also demonstrated that lesions cause the extravasation of monocytes into the peritoneal cavity in a CCR2-independent manner. Thus, monocyte-derived macrophages may play an important role in endometriosis lesion development, and future therapies that target infiltration of monocytes may be of benefit in the treatment of women with endometriosis.

**Genome-wide Gene Expression Analysis in Mouse Granulosa Cells Undergoing Luteinization During Ovulation.** Yuichiro Shirafuta, Isao Tamura, Haruka Takagi, and Norihiro Sugino

Introduction: Dramatic changes of gene expressions occur in granulosa cells undergoing luteinization during ovulation after the LH surge. Here, we genome-widely investigated the time-course changes in mRNA expressions in granulosa cells undergoing luteinization during ovulation in mice. Materials and methods: 3-week-old immature mice were injected with eCG (4 IU) followed by hCG (5 IU). Granulosa cells were obtained before (0 h) and 4, 12 h after hCG injection, and total RNA was extracted. RNA sequencing was performed to investigate the genome-wide mRNA expression. Gene expression values were calculated as fragment per kilobase of exon unit per million mapped reads (FPKM). The genes whose FPKM values increased or decreased more than 2-fold by hCG injection were defined as differentially expressed genes. The roles of those genes were analyzed by Gene ontology analysis and

KEGG pathway analysis. Results: (1) 3325 genes were up-regulated after hCG injection. Among them, 2592 genes (78 %) were changed at 4 h. Gene ontology analysis showed “angiogenesis”, “cholesterol metabolic process” and “steroid biosynthetic process”, which are key functions for corpus luteum formation. Interestingly, “histone modification” was also found, suggesting that the rapid changes of gene expression at 4 h may be regulated by epigenetic mechanisms of histone modifications. KEGG pathway analysis showed “MAPK signaling pathway” and “PI3K/Akt signaling pathway”, which are well-known activated pathways for initial steps of lutenization, oocyte maturation and COC expansion. In addition, “Hippo signaling pathway” was found, and it may be involved in the enlargement of cell size from granulosa cells to luteal cells because Hippo signaling pathway is an essential pathway regulating cell morphology during differentiation. (2) The expression of 733 genes (22 %) was increased at 12 h. Gene ontology analysis showed “DNA repair”. KEGG pathway analysis showed “Sphingolipid signaling pathway” that is induced by DNA damage. These results suggest that up-regulated genes at 12 h contribute to cell survival by protecting cells from DNA damage. (3) 2778 genes were down-regulated after hCG injection. Among them, 2126 genes (77 %) were changed at 4 h. Gene ontology analysis showed “cellular response to hormone stimulus”, which is associated with the suppression of the FSH signaling. KEGG pathway analysis showed “FOXO signaling pathway”. Inactivation of this signal contributes to progesterone synthesis. (4) The expression of 652 genes (23 %) was decreased at 12 h. Gene ontology analysis showed “cell cycle”. KEGG pathway analysis showed “Ras signaling pathway”. These results suggest that the cell cycle of granulosa cells is suppressed at 12 h for differentiation to luteal cells. Conclusion: Genome-wide time-course analysis of mRNA expression revealed that a number of genes are up- or down-regulated in mouse granulosa cells undergoing luteinization during ovulation, which contributes to corpus luteum formation through the change of various physiological functions.

#### **Augmentation of Nr4a3 Expression by GnRH and its Suppressive Effect on FSH Beta Subunit (Fshb)**

**Expression.** Ryota Terashima, Masato Ikeo, Daiki Nagao, Tomotaka Saigo, Shiro Kurusu, and Mitsumori Kawaminami

Gonadotropin releasing hormone (GnRH) is a hypothalamic neuro-peptide stimulating the secretion of gonadotropin (luteinizing hormone, LH and follicle stimulating hormone, FSH) at the anterior pituitary gland. We have demonstrated that GnRH stimulates Annexin A5 (Anxa5) expression and Anxa5 promotes the secretion of LH and FSH at the pituitary gonadotrope. We also found that nuclear receptor subfamily 4, group A, member 3 (Nr4a3) gene expression is up-regulated in the pituitary gland of Anxa5 knockout mouse (Anxa5tm1Epo/Anxa5tm1Epo) and is augmented after administration of GnRH agonist. In the present study, to clarify the involvement of Nr4a3 in the physiological gonadotropin secretion, we examined Nr4a3 gene expression dynamics during the estrous cycle of rats and the relation between GnRH-Anxa5 links and Nr4a3 was further studied in vitro experiments. First, to evaluate the changes in physiological Nr4a3 expression, we determined Nr4a3 mRNA levels in the pituitary gland during the estrous cycle. Wistar-imamichi rats with a four-day estrous cycle were maintained in 14 h light/10 h dark cycle (lights on at 0500 h) and the anterior pituitaries were collected at 2-6 specific times on each day (n = 5 per group). Nr4a3 mRNA levels in the anterior pituitary gland were significantly increased from 1400 h to 1700 h on proestrus just before LH surge. While GnRH antagonist, Cetrorelix, given at 1100 h and 1400 h on proestrus did not change Nr4a3 mRNA expression at 1400 h and 1700 h, respectively, the increase of Nr4a3 mRNA expression from 1400 h to 1700 h occurred in the ovariectomized rat with the continuous administration of 17 beta-estradiol (n = 5 per group), suggesting that hypothalamic factor,

presumably GnRH, induces pituitary Nr4a3 expression. To see the effect of GnRH on Nr4a3 expression, mouse gonadotrope cell line LbetaT2 cells were incubated with  $10^{-8}$  M GnRH agonist for 0-8 h. GnRH agonist transiently stimulated Nr4a3 mRNA expression and the protein synthesis inhibitor cycloheximide (CHX) did not affect Nr4a3 mRNA expression. Immunocytochemistry clearly showed that GnRH agonist also induces intranuclear accumulation of Nr4a3. We next examined the effect of ANXA5 on Nr4a3. LbetaT2 cells were transfected with rat ANXA5 expression vector. Nr4a3 mRNA expression augmented by GnRH agonist was significantly suppressed in the cells transfected with ANXA5 expression vector. Similarly, recombinant rat ANXA5 also inhibited Nr4a3 induction stimulated by GnRH agonist. Finally, to evaluate the effect of Nr4a3 on gonadotropin subunit expression, we performed RNAi in LbetaT2 cells. Under GnRH agonist stimulation, the transfection of Nr4a3 specific siRNA significantly enhanced the expression of Fshb mRNA but not Lhb and common alpha subunit mRNA. In summary, present study clearly demonstrates that Nr4a3 is a novel regulator of FSH beta subunit synthesis under the GnRH signaling and Anxa5 inhibits Nr4a3 induction in the gonadotrope. Although precise mechanism of Nr4a3 expression in proestrous rats needs further study since the acute GnRH antagonist administration was not effective, it is suggested that the expression of Nr4a3 in the pituitary gland is facilitated by proestrous GnRH increase.

**Sheep and Pig Conceptuses Adapt to a Hypoxic Uterine Environment by Enhancing One-Carbon Metabolism.** Heewon Seo, Avery C. Kramer, Bryan A. Mclendon, Guoyao Wu, Robert C. Burghardt, Fuller W. Bazer, and Greg A. Johnson

During the peri-implantation period, sheep and pig conceptuses (embryo and placental membranes) rapidly elongate from spherical to tubular to filamentous forms. In concert with trophoblast outgrowth during ovine conceptus elongation, binucleate cells (BCs) begin to differentiate from the mononuclear trophoblast cells and migrate to the endometrial luminal epithelium (LE) to form syncytial plaques. These proliferating and migrating cells rapidly consume available O<sub>2</sub> and nutrients, resulting in metabolic stress for implanting conceptuses. Metabolism usually occurs through the tricarboxylic acid (TCA) cycle and oxidative phosphorylation. However, cells within metabolically restrictive environments, such as immune and tumor cells, switch from oxidative phosphorylation to glycolysis to provide biosynthetic intermediates that feed into other metabolic pathways that are important for cell proliferation and survival. One metabolic change that occurs in proliferating immune and tumor cells is an increase in serine biosynthesis followed by one-carbon metabolism in which glycolysis-derived 3-phosphoglycerate (3-PG) is converted to serine and then formate, a precursor for purines and thymidine that are essential for nucleotide synthesis and cell proliferation. We hypothesized that serine biosynthesis and one-carbon metabolism support proliferation and migration of conceptus trophoblast within a hypoxic, metabolically restricted uterine environment, and examined sites of conceptus implantation of sheep and pigs by H&E and immunofluorescence staining to determine: 1) if conceptuses are exposed and respond to a hypoxic environment; 2) if mechanistic target of rapamycin (mTOR) is activated in the conceptus trophoblast; 3) if enzymes that convert glucose to serine, including phosphoglycerate dehydrogenase (PHGDH), phosphoserine aminotransferase (PSAT), and phosphoserine phosphatase (PSPH) are expressed in the uterine endometrium and conceptus; and 4) if enzymes of one-carbon metabolism that convert serine to formate, including serine hydroxymethyltransferase 2 (SHMT2) and methylenetetrahydrofolate dehydrogenase 2 (MTHFD2), are expressed in the conceptus trophoblast. Our results provide insights into how the implanting

conceptuses of sheep and pigs adapt metabolically to a hypoxic environment because we observed that: 1) red blood cells accumulate within the developing vasculature of the endometrial stroma, indicating a high demand for oxygen at implantation sites of both sheep and pigs; 2) hypoxia inducible factor 1 alpha (HIF1 $\alpha$ ) is expressed by the endometrial LE and conceptus trophoctoderm of both sheep and pigs; 3) HIF1 $\alpha$  and phospho-ribosomal protein s6 (p-RPS6) expression co-localize within the conceptus trophoctoderm suggesting a metabolic link between hypoxia and activation of mTOR in the conceptus trophoctoderm of both sheep and pigs; 4) PHGDH and PSPH are expressed by the endometrial LE of both sheep and pigs; and 5) SHMT2 and MTHFD2 are expressed by the proliferating trophoctoderm of pig conceptuses and expressed by the migrating BCs of sheep conceptuses. We conclude that glucose can be converted to serine within the endometrial LE, serine can be transported into conceptus trophoctoderm, and mTOR-HIF1 $\alpha$  signaling can induce expression of SHMT2 and MTHFD2 in conceptus trophoctoderm to support trophoctoderm cell proliferation and migration within the a hypoxic, metabolically restricted environment.

**Uterine Glands Coordinate Synchrony Between the Endometrium and Embryo for Implantation and Pregnancy Success.** Andrew M. Kelleher, Jessica Milano-Foster, Susanta K. Behura, and Thomas E. Spencer

Embryo implantation and stromal cell decidualization in the uterus are central to pregnancy success, and their failure is a significant cause of pregnancy loss in women. Glands of the uterus are essential for pregnancy establishment in mice and likely humans, but their biological roles are not well delineated. Forkhead box a2 (FOXA2) is a transcription factor expressed specifically in the glands of the uterus and regulates both gland differentiation in the neonate and gland function in the adult. Foxa2 conditional knockout mice without or with glands in their uterus were generated using progesterone receptor (Pgr)-Cre and lactotransferrin (Ltf)-iCre mice, respectively. Both FOXA2-deficient models lack expression of leukemia inhibitory factor (LIF), a critical implantation factor of uterine gland origin, and are infertile due to defects in embryo nidation. By employing FOXA2-deficient mouse models coupled with LIF repletion, we reveal definitive roles of uterine glands in the coordination of on-time implantation. Absence of glands did not affect formation of specialized implantation chambers (crypts) in the uterus, and LIF repletion on GD 4 initiated HB-EGF expression in the luminal epithelium (LE), embryo attachment, and stromal cell decidualization in glandless PgrCre/+Foxa2f/f mice. Pregnancy was maintained to term in LIF-replaced gland-containing LtfiCre/+Foxa2f/f but failed by GD 10 in glandless PgrCre/+Foxa2f/f mice. Comprehensive histoarchitectural and transcriptomic studies revealed that pregnancy loss in LIF-repleted glandless PgrCre/+Foxa2f/f mice involved defects in removal of the LE and subsequent decidualization. In control and gland-containing LIF-replaced LtfiCre/+Foxa2f/f mice, removal of the LE was initiated on lateral sides of the embryo in implantation crypts on GD 5 (1800-2000 h), while the LE cells of LIF-replaced glandless PgrCre/+Foxa2f/f mice remained intact. By the morning of GD 6, implantation sites in both types of LIF-replaced FOXA2-deficient mice appeared histologically normal, although transcriptomic analysis revealed that expression of 1,332 genes were different (552 increased, 780 decreased) between glandless PgrCre/+Foxa2f/f and control mice. Of note, 53 of the differentially expressed genes are implicated in stromal cell decidualization (Bmp7, Cdh1, Cebpb, Ptgs2, Ptx3, Wnt4). Functional analysis found that these genes are enriched in biological processes related to cell adhesion, cell differentiation, cellular proliferation, immune response, and vasculature development. Compared to control and LtfiCre/+Foxa2f/f mice on GD 7, implantation sites of glandless PgrCre/+Foxa2f/f mice

exhibited decreased growth of the embryo and decidua. Indeed, Ki67-positive proliferating cells remained in the primary decidual zone (PdZ) and secondary decidual zone (Sdz) of implantation sites from LIF-replaced glandless PgrCre/+Foxa2f/f mice, whereas the number of proliferating cells declined by GD 7 in the Sdz and were absent in PdZ of control and LIF-replaced LtflCre/+Foxa2f/f mice. By GD 8, embryo resorption was particularly evident in LIF-replaced glandless PgrCre/+Foxa2f/f mice, as increased levels of apoptotic embryos and decidual cells were observed. These studies provide original evidence that uterine glands are important for synchronous embryo-endometrial interactions and coordinate on-time embryo implantation and stromal cell decidualization, thereby impacting embryo viability and pregnancy success. Accordingly, pregnancy loss, miscarriage and complications in women may have their origins in uterine gland dysfunction. Supported in part by NIH grant R21 HD087589.

**Insight into the Molecular Mechanism of HIF1alpha-mediated Regulation of Star Expression in Steroidogenic Cells.** Bettina Lanfranchi, Alois Boos, Max Gassmann, and Mariusz P. Kowalewski

Involvement of hypoxia in the regulation of steroid hormone synthesis is still not fully understood. However, some organs such as gonads are physiologically exposed to reduced oxygen (O<sub>2</sub>) tension. Consequently, important processes in ovarian follicular growth, maturation, ovulation and luteal formation, as well as testicular spermatogenesis, are inextricably linked to hypoxia. Adaptive responses to hypoxia are primarily regulated through transcriptional mechanisms mediated by O<sub>2</sub>-sensing hypoxia-inducible factors (HIFs), with HIF1alpha recognized as a key modulator in both physiological and pathological reactions to hypoxia. Its expression in the ovary is cycle stage-dependent and it is constitutively expressed in murine Leydig cells. Nevertheless, the molecular mechanisms underlying the HIF1alpha-dependent regulation of steroidogenesis, and in particular of the key steroidogenic protein STAR, remain unclear.

Recently, the effects of hypoxia and HIF1alpha have been investigated in more detail in immortalized murine KK1 granulosa cells. Evidence has been provided for HIF1alpha as a positive regulator of basal and dbcAMP-stimulated STAR expression, which under reduced (10%) O<sub>2</sub> tension (partial hypoxia) increases steroidogenesis in granulosa cells. HIF1alpha induces Star-promoter activity, mRNA and protein expression. Blocking its transcriptional activity with echinomycin or knocking down its expression reduces both basal and hypoxia-stimulated STAR. The activation of Star-promoter is predominantly regulated by the cAMP/PKA dependent pathway, which involves phosphorylation of several transcription factors. Among these, CREB and cJUN are the most prominent. Additionally, CREB binding protein (CBP/p300) is an important co-activator facilitating Star transcription. In the present study, the impact of HIF1alpha on the expression and activation, i.e., phosphorylation, of CREB and cJUN was investigated in KK1 cells under partial hypoxia in the presence or absence of echinomycin (6h time-course). The expression of CBP/p300 was also examined. Total cJUN mRNA and protein expression, as well as phosphorylation (P-cJUN), were significantly upregulated under partial hypoxia. Treatment with echinomycin resulted in the opposite outcome. In contrast, the expression of CREB was not affected by hypoxia. Surprisingly, however, P-CREB and its transcriptional activity (transactivation assay) were elevated in response to echinomycin. This was despite the decreased expression of STAR, indicating that although phosphorylated, P-CREB was not capable of inducing STAR transcription. Interestingly, the suppression of HIF1alpha activity strongly diminished CBP expression.

Furthermore, in our ongoing project, the effects of partial hypoxia and HIF1alpha on STAR expression were assessed in mLTC1 Leydig cells. Contrasting with observations made in granulosa cells, the expression of STAR was not affected by lowering O<sub>2</sub> concentrations (from 20 to 10%). However, blocking the transcriptional activity of HIF1alpha significantly reduced STAR expression under both basal and hypoxic conditions. These preliminary observations suggest that although reduced O<sub>2</sub> tension does not affect the response of STAR to dbcAMP in mLTC1 cells, similar to granulosa cells, STAR expression in Leydig cells remains under the control of HIF1alpha.

Finally, based on our results, the following hypotheses are proposed: (1) HIF1alpha regulates the expression and function of cJUN in steroidogenic cells, and (2) it is possibly involved in regulating the attraction of P-CREB to the proximal Star-promoter, either by controlling its recruitment or the availability of CBP.

**Declining Estradiol Production and Aromatase Expression are Associated with Increased Expression of the FIGLA Transcription Factor and Primordial Follicle Formation in the Bovine Fetal Ovary.** Diane Schoenherr, and Ming Yuan Yang

Despite the importance of primordial follicles (PFs) to female fertility, the regulation of PF formation is only beginning to be elucidated, especially in domestic animals and humans. In cattle, formation of PFs occurs around Day 90 of gestation (term = 271 days). Our previous studies showed that production of E<sub>2</sub> by bovine fetal ovaries is high before PF formation and then declines dramatically around the initiation of PF formation, suggesting an association between declining E<sub>2</sub> and PF formation in vivo in cattle. However, these findings on morphology and E<sub>2</sub> secretion were derived from separate experiments using different fetuses. Therefore, the first objective of the present study was to examine PF formation, E<sub>2</sub> secretion and aromatase (critical enzyme for E<sub>2</sub> synthesis) expression in developing ovaries from the same fetuses to better establish the association between a decline in E<sub>2</sub> and PF formation. Pairs of ovaries were dissected from day 60-90 (before PF formation; n = 6 pairs) and day 91-130 (after PF formation; n = 6 pairs) fetuses obtained from a local slaughterhouse. Fetal age was estimated by crown rump length. One ovary of each pair was processed to assess morphology. The remaining ovary of each pair was cut into small pieces and the pieces cultured for 24 h. After culture, medium was collected to steroid measurements while ovarian pieces were snap-frozen for aromatase mRNA analysis. No or occasional PFs were observed in ovaries from 60-90 days of gestation. In contrast, in ovaries isolated after day 90 of gestation, there was a remarkable increase (~ 100-fold) in the number of PFs. E<sub>2</sub> secreted by ovarian pieces from fetuses younger than 90 days of gestation was 20-fold higher than that by ovarian pieces from fetuses 91-130 days old (P < 0.05). Consistent with E<sub>2</sub> secretion, levels of aromatase mRNA were ~20-fold greater in ovarian pieces obtained from fetuses before Day 90 of gestation compared with fetuses after Day 90 (P < 0.05). These results extend our pilot data and support the hypothesis that a decline in E<sub>2</sub> is required for initiating PF formation. Next, we begin to explore its underlying mechanisms. Transcription factor FIGLA (factor in the germline alpha) is essential for PF formation in mice. However, the regulators of FIGLA have not yet been identified. As a first step, we investigated whether and how FIGLA is expressed in bovine fetal ovaries (n = 16 ovaries). qPCR analysis showed that in ovaries before 90 days of gestation (i.e. containing no PFs and high E<sub>2</sub>), FIGLA expression was very low. With progression of gestation, FIGLA mRNA abundance dramatically increased and peaked (~ 40-fold higher) around day 105 of gestation, the time around which E<sub>2</sub> is low

and PFs begin to actively form. In summary, declining E2 production, controlled by aromatase expression, is associated with increased expression of FIGLA and PF formation in the bovine fetal ovary, suggesting for the first time that E2 is an upstream regulator of FIGLA that likely has conserved functions in PF formation in large mammals as in mice.

**Effects of Fish Oil on LH-Induced Progesterone Secretion and Lipid Droplet Formation in Bovine Luteal Cells.** Michele R. Plewes, Jessica C. Cedillo, and Patrick D. Burns

Luteinizing hormone (LH) plays a critical role in the development and maintenance of the corpus luteum (CL). Luteinizing hormone activates protein kinase A signaling in luteal cells and increases delivery of cholesterol from lipoproteins and lipid droplet (LD) storages to mitochondria for progesterone production. After which, cholesterol is converted into progesterone via a series of enzymatic reactions within the mitochondria and endoplasmic reticulum. Studies from our laboratory have demonstrated that fish by-products alter the localization, lateral mobility, and receptor internalization of the bovine prostaglandin F2a FP receptor. However, few studies have investigated the possible adverse effects of fish oil on LH signaling in bovine luteal cells. Objectives of this study were to determine the effects of fish oil on 1) LH-induced progesterone biosynthesis, 2) cholesterol-induced progesterone biosynthesis in mixed luteal cells, 3) LH-induced steroidogenic gene and protein expression, 4) LD abundance, and 5) LH-induced mobilization of LDs in isolated small bovine luteal cells. Ovaries were obtained from a local abattoir and CL were digested using collagenase. Cells were incubated in either BSA or fish oil-supplemented media for 72 h to allow incorporation of omega-3 fatty acids into biological membranes. In experiments 1 and 2, cells were treated with 0, 1, 10 or 100 ng/mL LH, 2 ng/mL 22(R)-hydroxy cholesterol, 10  $\mu$ M forskolin, or 10 ng/mL LH + 2 ng/mL 22(R)-hydroxy cholesterol for 0 or 12 h. In experiment 3, cells were treated with LH (10 ng/mL) or forskolin (10  $\mu$ M) for 0, 6, or 12 h to determine steroidogenic gene and protein expression. In experiment 4, LDs were stained using 20  $\mu$ M BODIPY 493/503. Experiment 5 determined colocalization of LDs with  $\alpha$ -Tubulin at 0 and 120 min post-treatment with LH (10 ng/mL). In experiment 1 and 2, LH had no influence on progesterone secretion in fish oil-treated cells when compared to control BSA-treated cells ( $P < 0.05$ ). Additionally, free cholesterol induced progesterone secretion in fish oil-treated cells, but was unaffected by stimulation with LH ( $P > 0.05$ ). Surprisingly, in the presence of free cholesterol, cells supplemented with fish oil had a decrease in progesterone production when compared to control BSA-supplemented cells ( $P < 0.05$ ), yet had no influence in cells supplemented with fish oil ( $P > 0.05$ ). Taken together, fish oil appears to reduce steroidogenic capacity of luteal cells. Research supported by USDA 2013-67015-20966 to PDB.

**Uterine miRNAs Reflect the Unique Microenvironment in an Individual Murine Horn During the Window of Implantation.** Jason C. Parks, Blair R. McCallie, Nathan I. McCubbin, Darren K. Griffin, William B. Schoolcraft, and Mandy G. Katz-Jaffe

Successful implantation is dependent on the complex interchange between a viable embryo and a receptive endometrium. On the maternal side, specific adhesion molecules are required for blastocyst attachment, in addition to tight regulation of signaling molecules surrounding the implanting embryo. This study utilized a minimally invasive technique of sampling the mammalian uterine environment, immediately prior to embryo transfer, to examine microRNA expression in association with implantation

outcome. In vivo fertilized zygotes collected from super ovulated virgin female BDF-1 mice were cultured to the blastocyst stage. Two hatching, day 5 blastocysts were selected for individual embryo transfer into each uterine horn (n= 1 embryo/horn) of a pseudo pregnant BDF-1 recipient mouse (n=7). Immediately prior to the embryo transfer procedure, a gentle aspiration from the lumen of the uterine horn was performed (n=14). On Day 16 of fetal development, recipient females were sacrificed, and implantation outcome was documented. Uterine aspirates were evaluated for microRNA expression by qPCR (TaqMan®, Thermo Fisher) and analyzed for significance in association with implantation outcome, significance at  $P < 0.05$ . Six specific microRNAs were chosen based on their known roles as mediators of transcription in association with embryo implantation: miR-22, miR-145, miR-200a, miR-223, miR-3074 and miR-let7b. Analysis of the uterine aspirate revealed significant expression differences in relation to implantation for miR-22, miR-200a, miR-3074 and miR-let-7b ( $P < 0.05$ ). Specifically, miR-let-7b displayed increased expression ( $P < 0.05$ ) with successful single embryo implantation compared to a negative outcome in the opposite horn of the same female mouse. Increased expression of miR-let7b has been shown to play a regulatory role on the expression of Muc1 during the window of implantation, resulting in the establishment of viable pregnancy (Inyawilert et. al., 2015). In contrast, miR-22, miR-200a and miR-3074 displayed a significant decrease in expression with single embryo implantation ( $P < 0.05$ ) compared to a negative outcome in the opposite horn of the same female mouse. Studies have shown that dysregulation of miR-22 in conjunction with Tiam1/Rac1 signal expression inhibit embryo implantation (Ma HL et. al., 2015). In conclusion, this study has revealed that each uterine horn has a unique microenvironment containing a complex milieu of microRNAs during the window of implantation. Uterine microRNAs represent a minimally invasive means of sampling the embryo-endometrial molecular dialogue, allowing for the prediction of implantation potential which if translatable to the human, could improve IVF success for infertility patients.

### **Advanced Maternal Age Impacts Placental Epigenetics Contributing to Potential Compromised**

**Development.** BR McCallie, JC Parks, MM Denomme, NI McCubbin, DK Griffin, WB Schoolcraft, and MG Katz-Jaffe

Epigenetics is defined as heritable changes in gene expression that occur without altering the underlying DNA sequence. Imprinting is an epigenetic process that allows genes to be expressed in a parent-of-origin manner and is critical during the regulation of fetal growth and placental development. It is established by marks on the DNA, often through methylation, which can result in either gene silencing or transcription. The aim of this study was to investigate the influence of maternal aging on placental imprinting. Pregnant, female mice (young = 3 months; old = 12 months) were sacrificed on day 16 for placental tissue collection and fetal growth measurements. Placental tissue was dissected to ensure that only the fetal contribution was analyzed. RNA and DNA were isolated from each placenta using the RNA/DNA Purification Kit (Norgen Biotek) following homogenization. 10ng of DNA from individual placental dissections (n=18) underwent bisulfite mutagenesis using the EZ DNA Methylation-Direct Kit (Zymo Research) followed by amplification of four differentially methylated imprinting control regions (ICRs): Igf2r, Kcnq1ot1, Peg3, and Snrpn. Pyrosequencing was performed using the PyroMark Q24 Advanced system (Qiagen) and methylation levels were calculated as a ratio of the C to T peaks at a given CpG site. 3ug of RNA from the same placental dissections (n=18) were used for transcription analysis by real-time PCR and statistically significant genes were identified using REST 2009 software (Qiagen). On day 16 of pregnancy, results revealed both fetal length (young = 11.4mm vs. old = 9.8mm,

ns) and placental weight (young = 0.097g vs. old = 0.11g, ns) were comparable between the two maternal age groups. However, fetal weight was significantly decreased in pregnancies from the older mothers (young = 0.30g vs. old = 0.17g,  $P < 0.05$ ). DNA analysis revealed no methylation alterations for the ICRs of *Igf2r*, *Kcnq1ot1*, or *Peg3*. Conversely, significant hypermethylation was observed for the *Snrpn* ICR in placentas of older female mice (young = 38% vs. old = 42%,  $P < 0.05$ ). Real-time PCR of genes within the *Snrpn* imprinted region confirmed a disrupted epigenetic landscape with paternally expressed imprinted alleles showing significant downregulation (*Ipw* = -0.4 fold-change, *Mkrn3* = -0.6 fold-change, *Snrpn* = -0.5 fold-change,  $P < 0.05$ ) and the maternally expressed imprinted allele, *Ube3a*, displaying significant upregulation (+1.3 fold-change,  $P < 0.05$ ) in the placentas from older mothers. Other paternally expressed alleles tested in the *Snrpn* imprinted region (*Magel2*, *Ndn*, and *Peg12*) showed similar reduced transcription with no statistical significance. Downregulation of the paternally expressed (growth enhancing) genes combined with upregulation of the maternally expressed (growth repressing) genes in the *Snrpn* imprinted region leads to a disruption in the intricate balance required for placental function. This provides a mechanism for the fetal growth restriction observed in the offspring of these aged females. In conclusion, advanced maternal age has a direct impact on placental epigenetics which appears to contribute to compromised fetal development.

**Dynamic Regulation of the Mitochondrial Effector Dynamin Like 1 (DNM1L) and Steroidogenesis in the Bovine Corpus Luteum.** Michele R. Plewes, Heather Talbott, Xiaoying Hou, Pan Zhang, and John S. Davis

The corpus luteum (CL) is a transient endocrine gland that synthesizes and secretes the steroid hormone progesterone, which is essential for the establishment and maintenance of pregnancy in mammals. Luteinizing hormone (LH) activates protein kinase A (PKA) signaling in luteal cells and increases delivery of substrate to mitochondria for progesterone production. Mitochondria maintain a highly regulated equilibrium between fusion and fission, forming either individual units or interconnected mitochondrial networks within the cell. Dynamin like 1 (DNM1L previously called DRP1), a large GTPase, is a key mediator of mitochondrial fission. Phosphorylation/dephosphorylation events on two sites near the GTPase effector domain (GED) domain regulate mitochondrial fission. Phosphorylation on Ser616 activates the GTPase activity and promotes mitochondrial fission. Phosphorylation on Ser637 within the GED domain inhibits the GTPase activity, promoting mitochondrial stability and elongation. The mechanism by which DNM1L is regulated in the ovary is largely unknown. Therefore, understanding the regulation of DNM1L in luteal cells may provide novel information on the control of steroidogenesis. We hypothesize that LH via PKA will regulate the phosphorylation of DNM1L (Ser616 or Ser637) and DNM1L is required for progesterone biosynthesis in bovine luteal cells. Our objectives were to determine 1) the expression of DNM1L in bovine luteal cells, 2) the effects of LH-stimulation and PKA activation on phosphorylation of DNM1L, 3) the role of DNM1L in LH-induced progesterone secretion, and 4) the effects of prostaglandin (PG) F<sub>2</sub> $\alpha$  on phosphorylation of DNM1L in luteal cells. Bovine ovaries were obtained from a local abattoir, CL were dispersed, and luteal cells were enriched for small (SLC) and large luteal cells (LLC) via centrifugal elutriation. Transcriptome profiling revealed that the bovine CL expresses transcripts for dynamin family members, including DNM1L. Expression of DNM1L was greater in LLC when compared to SLC ( $P < 0.05$ ). Treatment with two specific inhibitors of DNM1L (Dynosore or myr-dynamin inhibitory peptide) caused concentration-dependent reductions in LH-stimulated progesterone synthesis. Furthermore, siRNA-mediated knock down of DNM1L in SLC resulted in

significant reductions ( $P < 0.05$ ) in basal and LH-induced progesterone synthesis. Western blot analysis showed that LH (10 ng/ml) and the adenylyl cyclase activator forskolin (10  $\mu$ M) rapidly increased phosphorylation of DNM1L(Ser637) (3-fold after 30 min;  $P < 0.01$ ), and inhibited phosphorylation of DNM1L(Ser 616) (60% after 30 min;  $P < 0.05$ ). Overexpression of a PKA inhibitor, blocked the effects of LH and forskolin on DNM1L phosphorylation. Additionally, treating LLC with PGF2 $\alpha$  (100 nM) or the protein kinase C activator PMA (20 nM) increased phosphorylation of DNM1L(Ser616) (10-fold after 30 min;  $P < 0.01$ ), while also increasing phospho- DNM1L(Ser637) (2-fold after 30 min;  $P < 0.01$ ). These results indicate that DNM1L is differentially regulated by LH and PGF2 $\alpha$  signaling pathways and that DNM1L is required for optimal luteal progesterone synthesis. Taken together, the findings suggest LH may stabilize luteal mitochondria and promote steroidogenesis in bovine luteal cells via modulating the phosphorylation and activity of the GTPase DNM1L; and luteolytic hormones like PGF2 $\alpha$  may stimulate mitochondrial fission by increasing the activity of DNM1L.

**Maternal age Influences Folliculogenesis and Gene Networks in the Ovaries of Beef Heifers.** Robert A. Cushman, Sarah C. Tenle, Renata Spuri Gomes, Shelby L. Rosasco, Emmalee J. Northrop, Jerica J. J. Rich, Anthony K. McNeel, Adam F. Summers, Jeremy R. Miles, Chadwick C. Chase Jr, Clay A. Lents, George A. Perry, Jennifer R. Wood, and Andrea S. Cupp

The size of the ovarian reserve is an important component of fertility and reproductive longevity in bovine females. Ultrasonographic determination of antral follicle count is the best method for estimating the size of the ovarian reserve in heifers and cows in a production setting. Antral follicle count is highly repeatable, moderately heritable, and correlates positively with the number of primordial follicles in the ovaries. Maternal age may influence the size of the ovarian reserve in daughters, because heifers born to mature cows have more antral follicles detectable by ultrasonography at a year of age than heifers born to heifers. Therefore, we hypothesized that heifers born to mature cows would have more primordial follicles than heifers born to heifers. Ovaries were collected from yearling Angus heifers born to heifers ( $n = 20$ ) or mature cows ( $n = 63$ ), all surface follicles were counted and a representative sample of each ovary was processed for histological evaluation of primordial follicle number. Ovarian cortex from four heifers born to heifers and four heifers born to mature cows was processed for RNA sequencing to identify differences in transcript abundance in the ovary based on age of dam. In agreement with previously published ultrasonographic data, antral follicle number was decreased in yearling heifers born to heifers compared to yearling heifers born to mature cows ( $P < 0.01$ ;  $37.9 \pm 8.0$  follicles and  $64.4 \pm 4.0$  follicles, respectively). Yearling heifers born to heifers also had fewer primordial follicles per histological section compared to yearling heifers born to mature cows ( $P = 0.02$ ;  $40.3 \pm 9.5$  follicles per section and  $67.4 \pm 5.0$  follicles per section, respectively). There was a tendency for primary follicle number to be decreased in ovaries of heifers born to heifers ( $P = 0.06$ ;  $7.9 \pm 1.7$  follicles per section and  $12.3 \pm 0.9$  follicles per section, respectively). The number of secondary follicles per histological section was decreased in heifers born to heifers compared to heifers born to mature cows ( $P = 0.02$ ;  $1.6 \pm 0.5$  follicles per section and  $3.0 \pm 0.3$  follicles per section, respectively). Pathway analysis clustered genes into biological processes involved in development of the circulatory system ( $P = 0.02$ ) and cellular components involved in extracellular matrix formation ( $P < 0.001$ ). Among genes that were differentially expressed after Benjamini-Hochberg correction, transcript abundance for connective tissue growth factor was decreased in the ovaries of heifers born to heifers compared to heifers born to mature cows ( $P = 0.01$ ). Conditional knockout of this gene in the murine ovary has been

associated with disrupted follicle development. These data corroborate previously published ultrasonographic data demonstrating that antral follicle numbers are greater in heifers born to mature cows and demonstrate that this difference in antral follicle number is correlated with the size of the ovarian reserve. Mechanistically, decreased vascular development and increased formation of extracellular matrix may contribute to the decreased numbers of follicles in ovaries of heifers born to heifers. USDA is an equal opportunity provider and employer.

**An Instructive Role for Vasculature in the Fetal Leydig Stem Cell Niche.** Deepti L. Kumar and Tony DeFalco

Testosterone is synthesized by Leydig cells (LCs), steroidogenic cells present in the interstitial compartment of the testis. Testosterone is important for masculinization of the fetus during development, and defects in testosterone production are linked to disorders of sexual development (DSDs), impaired spermatogenesis and male infertility. The etiology of male reproductive disorders largely remains unknown due to lack of knowledge regarding Leydig cell differentiation from their progenitors. Hence, we aim to identify the cell types important for maintenance and differentiation of Leydig cell progenitors and the fundamental mechanisms by which Leydig cell differentiation is regulated. In rodents, LC specification begins shortly after sex determination at embryonic day (E) E12.5, increasing in number throughout fetal life and peaking around birth. LCs do not divide and, therefore, rely on differentiation of interstitial progenitors or stem cells to maintain a stable pool of mature Leydig cells and to increase cell number during fetal development; premature exhaustion of the progenitor pool leads to a LC deficit and reduced androgen levels, which are deleterious to male differentiation. In addition to LC specification, development of male-specific vasculature is another important event that characterizes fetal testis morphogenesis. Testis-specific vasculature provides oxygen and nutrients to the developing gonad and serves as a conduit for export of testosterone to virilize the embryo. Whether vasculature plays an instructive role during testis differentiation is not known and represents a major knowledge gap in the field. Previous studies have described instructive roles for vasculature in organogenesis and stem cell niches in other tissues. While the role of blood vessels in gonad development is not well-defined, our previous work suggested that cells adjacent to the vasculature (i.e., perivascular cells) remain undifferentiated and represent Leydig progenitors. Hence, we hypothesize that vasculature plays an instructive role in LC differentiation and is a critical component of the fetal Leydig stem cell niche. Using genetic mouse models and ex vivo whole organ culture techniques, we sought to clearly define the Leydig progenitors and test the functional requirement of vasculature in LC differentiation. Our lineage tracing data definitively shows that perivascular cells serve as progenitors for a subset of mature fetal LCs. Additionally, disruption of vasculature in ex vivo whole gonad culture resulted in an excessive number of differentiated LCs that arise due to premature and excessive differentiation of Leydig progenitors. Finally, we show that vascular-derived Notch signaling is required to maintain Leydig progenitors in an undifferentiated state. These results indicate that, cues from the vasculature are essential for maintaining the Leydig progenitor population in the fetal testis. Understanding the mechanisms of LC differentiation is of critical importance, as it could provide valuable insights into yet unknown causes of DSDs and male infertility. This work was supported by a March of Dimes Basil O'Connor Award (TD) and CCHMC RIP and Trustee Grants (TD).

**Core Binding Factor  $\beta$  Expression in Ovarian Granulosa Cells is Essential for Female Fertility.** Somang Lee-Thacker, Yohan Choi, Ichiro Taniuchi, Takeshi Takarada, Yukio Yoneda, CheMyong Ko, and Misung Jo

Core Binding Factor beta (CBF $\beta$ ) is a non-DNA binding partner of all RUNX proteins and critical for transcription activity of CBF transcription factors (RUNXs/CBF $\beta$ ). In the ovary, the expression of Runx1 and Runx2 is highly induced by the LH surge in ovulatory follicles and corpora lutea, while Cbfb is constitutively expressed. To investigate the physiological significance of CBFs in the ovary, the present study generated two different conditional mutant mouse models in which granulosa cell expression of Cbfb and Runx2 was reduced by Cre recombinase driven by an Esr2 promoter. Cbfbgc $^{-/-}$  and Cbfbgc $^{-/-}$  \* Runx2 gc $^{+/-}$  mice exhibited severe subfertility and infertility, respectively. In the ovaries of both mutant mice, follicles develop normally, but the majority of preovulatory follicles failed to ovulate either in response to hCG administration in PMSG-primed immature animals or after the LH surge at 5 months of age. Morphological and physiological changes in the corpus luteum of these mutant mice revealed reduced size, progesterone production, and vascularization, as well as excessive lipid accumulation. In granulosa cells of periovulatory follicles and corpora lutea of these mice, the expression of Edn2, Ptgs1, Lhcgr, Sfrp4, Wnt4, Ccrl2, Lipg, Saa3, and Ptgfr was also drastically reduced. In conclusion, the present study provided in vivo evidence that CBF $\beta$  plays an essential role in female fertility by acting as a critical cofactor of CBF transcription factor complexes which regulate the expression of specific key ovulatory and luteal genes, thus coordinating the ovulatory process and luteal development/function in mice.

Supported by PO1HD71875

**An Inhibitor of N-glycan Maturation in Mouse Germ Cells.** Ayodele Akintayo, Meng Liang, Jillian Prendergast, Frank Batista, and Pamela Stanley

MGAT1, the N-acetylglucosaminyltransferase (GlcNAc-transferase) that initiates N-glycan maturation, is an ubiquitously-expressed enzyme localized in the medial-Golgi compartment, where it plays a major role in the N-glycan maturation pathway. Mgat1 global knockout (KO) is embryonic lethal but a conditional deletion (cKO) of this gene in spermatogonia induces a block in spermatogenesis at the spermatid stage which lead to infertility, revealing that MGAT1 and mature N-glycans are essential for spermatogenesis. Thus, understanding how N-glycans are regulated during spermatogenesis is important to understanding male fertility and mechanisms of male infertility. We have recently described an inhibitor of N-glycan maturation that is expressed primarily in testicular germ cells, with a stage specificity. The inhibitor is called GnT1IP for GlcNAc-I Inhibitory Protein and also GL54D or MGAT4D. The long form, GnT1IP-L, forms a complex in the Golgi with MGAT1 and specifically inhibits GlcNAc-transferase activity. We hypothesize that GnT1IP regulates MGAT1 activity during spermatogenesis. To investigate interactions between GnT1IP-L and MGAT1, we used deletion mutagenesis to identify the minimal peptide of membrane-bound GnT1IP-L that can inhibit MGAT1 activity. GnT1IP-L lost inhibitory activity when shortened from 417 to 393 amino acid, and regained activity with 397 amino acids, suggesting that the 5 internal amino acids (Pro Ser Leu Phe Arg) from position 393 to 397 are necessary for GnT1IP-L inhibitory activity. To study the in vivo role of GnT1IP-L, we generated different mouse models with global or conditional knockout of the Mgat4d gene, as well as mice with mis-expression of the transgene GnT1IP-L-Myc under the control of germ cell specific promoters: Stra8 in spermatogonia, Ldhc in spermatocytes and Prm1 in round/elongated spermatids. We found that global KO or removing Mgat4d only from spermatogonia (cKO) did not disrupt male

fertility (n=8) nor testis morphology. The same observations were made for each of the transgenic male mice (n=3-7). However, disrupting *Mgat4d* expression increased testis sensitivity to mild testicular heat stress in old (>580 day) FVB mice (n=2 heterozygotes, n=5 global KO males) and, the targeted mis-expression of GnT1IP-L in spermatogonia, spermatocytes or spermatids of 7 month C57BL6/J males induced increased resistance to heat-stress (n=5-8) compared to wild type heat-treated males (n=5). Microarray analysis is ongoing to identify gene expression differences that may shed light on functions of GnT1IP in testis. Deciphering the functions and mechanism of action of this complex N-glycosylation inhibitor in the testis will help in understanding the low resilience of spermatocyte and spermatids to stress and provide insights into how N-glycan maturation may be regulated in other contexts. Research supported by NIH NIGMS R01 GM105399 to Pamela Stanley.

**NR5A-Family Nuclear Receptor Hr39/LRH-1 Plays Conserved Roles in Follicle Maturation and Ovulation.** Elizabeth Knapp and Jianjun Sun

NR5A-family nuclear receptors consist of LRH-1 and SF-1 in mammals and Hr39 and Ftz-F1 in *Drosophila*. Both LRH-1 in mouse and Hr39 in *Drosophila* are required for ovulation; however, LRH-1 functions in mouse granulosa cells, while Hr39 functions in *Drosophila* female reproductive tract secretory cells (Duggavathi et al., 2008, *Genes Dev*; Sun and Spradling, 2013, *eLife*). Thus, it is unknown whether LRH-1 and Hr39 play conserved roles in ovulation. Recent work from our lab demonstrated that ovulation in *Drosophila*, resembling mammalian ovulation, involves the degradation of posterior follicle cells by matrix metalloproteinase 2 (*Mmp2*), the rupture of mature oocytes into the oviduct, and the formation of corpus luteum by the residual follicle cells (Deady et al., 2015, *PLoS Genet*). In addition, we found that norepinephrine-like neuron hormone octopamine (OA) activates *Oamb* receptor in follicle cells to induce  $Ca^{2+}$  influx, *Mmp2* activation, and follicle rupture in the presence of ecdysteroid signaling, parallel to progesterone signaling (Deady and Sun, 2015, *PLoS Genet*; Knapp and Sun, 2017, *PNAS*). In this study, we found that Hr39 is also required in follicle cells (equivalent to granulosa cells) to regulate follicle rupture/ovulation in parallel to LRH-1; Hr39 in follicle cells regulates components downstream of intracellular calcium rise to regulate *Mmp2* activation. In addition, we demonstrated that Hr39-regulated secretory products in the female reproductive tract are also required for OA-induced follicle rupture/ovulation. Particularly, we found that these secretory products regulate components upstream of intracellular calcium rise in follicle cells during ovulation. Furthermore, we showed that differential roles of Hr39 in follicle cells and reproductive tract secretory cells can be replaced by mouse LRH-1. Our data strongly suggest that Hr39 plays dual and non-redundant roles in the ovary and reproductive tract to regulate follicle maturation and ovulation. The conservation of Hr39 and LRH-1 suggests that LRH-1 likely functions in the mammalian reproductive tract (particularly oviduct secretory cells) to promote follicle maturation and ovulation. This work is supported by a R01 grant from NICHD (R01-HD086175).

**Alteration of Microbial Communities and Immune Populations in Patients with Endometriosis.** Nhung Le, Melissa Cregger, Nguyen Lynn, Ricardo Loret de Mola, Kathleen Groesch, Teresa Wilson, Paula Diaz-Sylvester, and Andrea Braundmeier-Fleming

Endometriosis is associated with chronic inflammation and infertility in women, it affects over 12% of reproductive aged women, and is characterized by the presence of endometrial tissue in ectopic

locations. Growth of endometriotic lesions induces peritoneal inflammation with elevated levels of several inflammatory cytokines, TNF- $\alpha$  and IL-8. Inflammation is known to alter microbial community dynamics in mucosal tissues. Therefore, there is a critical need to determine if a microbial signature is associated with endometriosis which would enable diagnosis prior to surgery and open new avenues for treatment. We hypothesized that chronic inflammation induced by endometriotic lesion growth alters the microbial dynamics of the GI and urogenital tracts resulting in a shift to microbial profiles associated with inflammation. Using a repetitive sampling model, we collected biological samples on the day of surgery (DOS) and then 2-3 weeks post-surgical intervention (PSI). To date, 32 patients have been enrolled (19 histologically confirmed endometriosis and 13 controls) at St. John's Hospital or Memorial Medical Center, Springfield IL. Biological samples collected were: peripheral venous blood, rectal/vaginal swabs and urine. Peripheral blood mononuclear cells (PBMCs) were extracted from the venous blood, and flow cytometry analyses were performed to identify immunosuppressive (regulatory T cells: Tregs) and inflammatory (Th17) T cell populations. Tregs were defined as CD4+CD25+FOXP3+ (natural Tregs; nTregs) or CD4+CD25-FOXP3+ (inducible Tregs; iTregs), and Th17 was defined as CD4+CD25+ROR $\gamma$ t. All immune profiles were analyzed using the Mann-Whitney U-test in GraphPad Prism software to calculate differences of cell populations between each study group. Briefly, vaginal, fecal and urine samples underwent DNA extraction utilizing the PowerSoil DNA isolation kit (Qiagen). To characterize the microbiome, we used Next generation sequencing (NGS) via an Illumina MiSeq system. Bacterial sequencing targeted the V4 region of the 16S rRNA gene. We used a two-step PCR approach to barcode tag templates with frame shifting nucleotide primers. Data were quality filtered and processed using a combined QIIME/USEARCH pipeline. Operational Taxonomical Units (OTUs) were clustered at 97% sequence similarity and classified using BLAST and the Greengenes-reference database for archaea/bacteria. Patients with surgically confirmed endometriosis had a 43% reduction of nTregs and 47% reduction of iTregs on DOS. At PSI, Treg populations were similar between groups, indicating that surgery could restore suppressive immune populations. Patients with endometriosis had elevated Th17 cells at each timepoint (43% DOS, 57% PSI when compared to control). The ratio of Tregs to Th17 cells was also reduced (24%) in patients with endometriosis on DOS, indicative of an inflammatory phenotype. Urogenital microbial community dynamics were also altered in disease patients, indicating a unique profile in patients with endometriosis. In summary, growth of endometriotic lesions not only creates systemic inflammation, but also alters the microbial profile within the patient. Our results may lead to an innovative diagnostic tool and novel immune-based therapies for treatment of endometriosis. This research was supported by the Endometriosis Foundation of America and the Department of Obstetrics and Gynecology, Southern Illinois University School of Medicine, IL.

**Multiple Signaling Pathways Mediate Progesterone Hormone Induction of Sperm Hypermotility in Southern Flounder Through Membrane Progesterone Receptor Alpha.** Peter Thomas, Yefei Pang, and Wenxian Tan

Development of commercial aquaculture for many marine flatfish species such as southern flounder is severely limited by poor male reproductive performance, especially reductions in sperm motility and fertility, but the underlying causes are largely unknown. A clearer understanding of the mechanisms regulating sperm motility would enable the development of more reliable and efficient methods to improve sperm quality and spawning of southern flounder and other marine flatfish species. Our previous studies have shown that acute treatment of southern flounder and Atlantic croaker sperm in

vitro with a teleost progestin hormone (20 $\beta$ -S) causes rapid induction of sperm hypermotility and increased fertility through activation of progestin membrane receptor alpha (mPR $\alpha$ ) coupled to a stimulatory G protein and increases in cAMP levels. In the present study the potential involvement of several intracellular signaling pathways in the sperm hypermotility response to 20 $\beta$ -S was investigated using specific pharmacological tools. Aliquots of freshly collected sperm, diluted in physiological saline, were preincubated with inhibitors (I) or activators (A) of Egfr (I:AG1478, A:EGF), Mapk/Erk1/2 (I: U0126), Pi3k/Akt (Pi3k I:Wortmannin, LY294002, Akt I: ML9), Acy/cAMP (I: dd-Ado, A: forskolin), Pde (I: Cilostamide), or calcium (L-type channel I:verapamil) signaling pathways for 30 min. prior to treatment with 20 $\beta$ -S or Org 02-0 (specific mPR agonist) for 1 min. and motility activation with a hyperosmotic medium. Sperm motility was observed under a microscope and recorded for 1 min with a video camera and swimming speed was calculated using motion analysis software. Calcium influx into flounder sperm was measured using Fura-2 with a fluorescence plate reader and phosphorylation of Akt and Erk 1/2 by Western blot analysis. The induction of sperm hypermotility by 20 $\beta$ -S and Org 02-0 was blocked by prior treatments with inhibitors of Egfr, Mapk, Pi3k/Akt, Pde, and Acy. On the other hand treatment with activators of Egfr (EGF) and Acy (forskolin) mimicked the effects of the progestins and induced sperm hypermotility. These results indicate that progestins induce sperm hypermotility through Egfr/Mapk/Erk1/2, Pi3k/Akt/Pde, and Acy/cAMP pathways. The progestins caused rapid calcium influx into sperm, an effect mimicked by EGF and forskolin and blocked by verapamil which also blocked progestin induced sperm hypermotility. The results suggest progestins activate multiple signaling pathways through mPR $\alpha$  in flounder sperm to induce calcium influx and hypermotility and enhance fertility. Practical methods to increase the reproductive performance of flounder broodstock could potentially be developed through pharmacological stimulation of these pathways. This research was supported in part by USDA NIFA grant 2009-65203-05757 to PT.

### **Effects of the Follicular Environment of ART Patients of Advanced Maternal Age on in Vitro**

**Maturation of Mouse Oocytes.** Paola Berrío, Ingrid Zorrilla, Ricardo Pella, Francisco Escudero, Patricia Orihuela, Ygor Pérez, Mario García, Sergio Romero

At our center 20% of patients requiring Assisted Reproductive Technologies (ART) suffer from endometriosis. Oocytes of such patients have been suggested to develop in an environment with oxidative stress. In order to alleviate such condition, patients are administered antioxidant therapy, however there is few evidence that supports the use of such therapies to improve oocyte wellbeing.

Our objective is to evaluate the effect of the follicular environment (follicular fluids, FF) of infertile patients with endometriosis on in vitro maturation (IVM) of mouse oocytes. Moreover, the antioxidant capacity of such follicular fluids was also assessed.

Ninety-Five F1 female mice (C57xBalb-c), aged 23-days, were primed for 48h with eCG in order to induce follicular growth and allow the collection of immature oocytes at the germinal vesicle stage. Follicular fluids were obtained during follicular aspiration of patients with endometriosis [3 under antioxidant therapy (+AO) and 3 without it (-AO)]. Following collection and selection of mouse cumulus oocytes complexes (COCs), COCs were randomly distributed into 5 groups: Control (without FF), G1 (20% FF), G2 (20% FF + 0.3% Bovine serum albumin, BSA), G3 (10% FF + 0.3% BSA), G4 (5% FF + 0.3% BSA). The same setup was used for both studies (+AO & -

AO). In vitro maturation was performed at 37°C, 5%CO<sub>2</sub> in air, for a period of 18h. Oocyte maturation was assessed by the presence of the first polar body.

In +AO group, the maturation rate of G1 (79.3% ± 12.5%), G2 (94% ± 8.9%), G3 (94.6% ± 8.1%) and G4 (90.2% ± 7.2%) was comparable to the control group (90.9% ± 20.3%) (p>0.05). However,

in -AO group, maturation rate of G2 (51.23% ± 25.54%) and G3 (57.0% ± 17.8%) were significantly lower than G4 (89.2% ± 4.0%) (p<0,05). Thus, these results indicate that follicular fluids of infertile patients with endometriosis without antioxidant therapy, affect maturation of mouse oocytes, in vitro. Apart from the effects on oocyte maturation, follicular fluids of infertile patients with endometriosis were analyzed for its antioxidant capacity. FF were subjected to ABTS [2,2'-azino-bis(3-ethylbenzothiazoline-6-sulphonic acid)], FRAP (Ferric reducing ability of plasma) and TBARS (Thiobarbituric acid reactive substances) assays. In the FRAP assay, follicular fluids of infertile patients of endometriosis, administered (or not) with antioxidant therapy, were significantly lower in their antioxidant capacity than the control group (FF of young donors) (p=0.0096; p=0.0442 respectively).

In conclusion, our findings suggest that the antioxidant capacity of follicular fluids in patients with endometriosis (undergoing ART treatments) administered (or not) with antioxidant therapy is lower than the donor follicular fluids; and therefore, are likely to have an effect on oocyte maturation. Since exposure to follicular fluids of such patients may have effects beyond the maturation capacity, the embryonary development of in vitro matured eggs remains to be evaluated.

**Maternal Obesity Modulates the Oocyte Methylome and Transcriptome.** A. Galvão, K.Wolodko, M. Adamowski, S. Clark, and G. Kelsey

Maternal obesity and its comorbidities lead to ovarian dysfunction and reduced fertility. Ultimately, the gamete of an obese mother develops in a hostile ovarian environment characterised by lipotoxicity, inflammation and oxidative stress. Several lines of evidence suggest the oocyte epigenome has the potential to control initial reprogramming events in the early embryo. Despite its manifest importance, little is known about the impact of maternal obesity on the oocyte epigenome. Therefore, in the present study we investigated the impact of maternal obesity on the oocyte methylome and transcriptome. Using a combined method for transcriptome and DNA methylome analysis we performed single-cell RNA-sequencing (scRNA-seq) and single-cell bisulfite sequencing (scBS-seq) in 100 MII oocytes from C57Bl/6J (B6) mice (n=5 females/group) fed chow diet (CD) or high-fat diet (HFD) for 16 weeks. The initial analysis of the transcriptome with DESeq2 identified 192 genes differently expressed between treatments (p < 0 .05). Despite no significant changes in global CpG methylation, the CD group had more homogeneous levels of methylation with a coefficient of variation (CV) of 6.75%, whereas the HFD group showed a CV of 11.98%. With regard to non-CpG methylation, HFD treated oocytes had lower CHG methylation levels (p < 0 .05) but no difference in CHH methylation. Further analysis of the scBSseq datasets revealed a gain in methylation in non-methylated regions and a decrease of methylation in hyper-methylated domains in oocytes from HFD females (p < 0 .05). Unbiased quantitation of CpG methylation across the genome followed by Chi-square test identified 536 regions differently methylated between dietary protocols (p < 0 .05). We then confirmed these differences in methylation were coupled with changes in RNAseq profile. Further analysis is being undertaken to characterise the

distribution of methylation. In conclusion, we give the first critical evidence that the oocyte transcriptome and methylome sense maternal obesity and associated ovarian metabolic changes.

AG was supported by Mari S Curie Individual Fellowship; Work funded by Polish National Science Centre programmes (2014/15/D/NZ4/01152) and (2016/23/B/NZ4/03737), UK Medical Research Council (MR/K011332/1) and Biotechnology and Biological Sciences Research Council (BBS/E/B/000C0423).

**The Hamster as a Model to Reveal Genes and Networks Associated with a Progesterone–dependent Blastocyst Implantation Process.** Bibhash C. Paria, Jennifer L. Herington, J. Courtney Reese, Katelyn Mika, and Vincent Lynch

Gene expression profiling studies are valuable for identifying genes and gene linkages associated with normal and abnormal processes. In this study, we compared the whole transcriptomes by RNA-sequencing uterine blastocyst implantation sites and inter-implantation sites from day 5 pregnant hamsters. We utilized the hamster model as this species exhibits the progesterone-dependent embryo implantation process utilized by humans. Our whole-genome analysis 4680 significantly differentially expressed genes (DEGs) at implantation sites compared to inter-implantation sites. The expression of 15 randomly selected down- and up-regulated genes were validated by examining their pattern levels using qRT-PCR. The DEGs identified by RNAseq were compared to prior results obtained by hamster cross-species hybridization microarray analysis, as well as transcriptomic studies reported by others using human endometrial receptivity samples, to identify overlapping genes. Pathway analysis of DEGs revealed up- and down-regulated pathways; notable affected pathways include cell cycle, complement and coagulation cascades, immune and inflammatory regulated pathways, metabolic pathways and thyroid hormone synthesis. Cell cycle was the most enriched pathway for upregulated genes and interferon signaling was enriched for down-regulated genes. Taken together, our results identified comprehensive uterine transcriptome changes at the hamster early implantation site and could be a resource for targeted studies on genes and pathways potentially involved in the embryo implantation process. This research was supported by NIH HD044741 to BCP and Burroughs Wellcome Fund Preterm Birth Initiative and March of Dimes Prematurity Research Center award to VL.

**SIRT7 Regulates Genome Integrity During Female Meiosis.** Berta N. Vazquez, Cecilia S. Blengini, Lourdes Serrano, and Karen Schindler

Sirtuins are NAD<sup>+</sup>-dependent protein deacylases and ADP-ribosyltransferases involved in a wide range of cellular processes including genome homeostasis and metabolism. Sirtuins are expressed in human and mouse oocytes yet their role during female gamete development are not fully understood. Here we investigate the role of a mammalian sirtuin member, SIRT7, during oocyte maturation using a mouse model of SIRT7 deficiency. In agreement with a previous report, we find that SIRT7 protein is present in prophase I-arrested oocytes and metaphase II-arrested eggs highlighting a potential role for SIRT7 in oocyte meiosis. We found that *Sirt7*<sup>-/-</sup> females produce fewer oocytes, ovulate fewer eggs, and therefore their fecundity is compromised in fertility trials. Importantly, female fertility declines rapidly with age, consistent with premature aging phenotypes that happen in the body of the *Sirt7* knockout mouse model. One function of SIRT7 in somatic cells is to deacetylate histone H3 at lysine 18 (H3K18).

Although H3K18 is deacetylated during oocyte meiotic maturation in wild-type oocytes, its deacetylation pattern is not perturbed in SIRT7 knockout oocytes suggesting that other histone deacetylases regulate this epigenetic mark. Because of the documented role of SIRT7 in DNA repair, we next investigated DNA damage load in SIRT7 knockout oocytes. Analysis of prophase I chromosome spreads revealed that Sirt7<sup>-/-</sup> oocytes are defective in repairing double-strand breaks resulting in persistent DNA damage at the dictyate stage. Taken together, our findings demonstrate a pivotal role for SIRT7 in oocyte meiosis by SIRT7-mediated repair of double-strand breaks to promote meiotic recombination completion.

This study was supported by a grant from the Human Genetics Institute of New Jersey and RO1-GM112801.

**Aging and Chromatoid Body Assembly: Are These Two Physiological Events Linked?** Rita Luiza Peruchetti, Elisa Gomes Santos, Maraisa Alves Silva, Renata Pereira Amorim, Leticia de Souza Giordano, Dayana de Sales Silva, Wilson Aparecido Orcini, and Lucas Trevisani Rasmussen

The chromatoid body (CB) is a cytoplasmic male germ cell structure that plays a role in the regulation of mRNA transcription during spermatogenesis. A proteomic analysis of this structure has identified the presence of its classic molecular markers (MVH and MIWI), as well as a significant number of transient proteins. Circadian locomotor output cycles protein kaput (CLOCK) and brain and muscle ARNT-like 1 (BMAL1), which are molecular components of the circadian clock, are likely located in the CB in a transient fashion. This study sought to determine whether aging produces morphological changes in the CBs of round spermatids similar to those previously observed in BMAL1 knockout mice. A sample of 30 male mice was divided into three groups: juvenile mice (45 days old), adult mice (120 days old), and old mice (180 days old). Aging was confirmed by viability and sperm count analyses and testosterone dosage. Squash slides prepared with fragments of seminiferous tubules were immunostained for MVH, MIWI, BMAL1, and CLOCK detection. In juvenile and adult specimens, single round CBs were observed using MVH / BMAL1 and MIWI / CLOCK immunostaining. In old specimens, many CBs displayed changes in number and morphology, as well as an increase in the interactions between MVH and BMAL1; MIWI and CLOCK. Changes in CB morphology, increased interactions between the proteins analyzed herein, and decreased amounts of these proteins in seminiferous tubules of older mice may indicate that aging influences the assembly and physiology of CBs, which may, in turn, affect fertility. This study is supported by São Paulo State Research Foundation (FAPESP). Grant numbers: 2016/04580; 2018/01554-3 -0.

**Non-overlapping Functions Of AURKB and AURKC in Regulating the Spindle Assembly Checkpoint During Oocyte Meiosis.** Cecilia S. Blengini, Alexandra L. Nguyen, and Karen Schindler

Aneuploidy, an error in chromosome number, is the leading genetic abnormality causing infertility and congenital birth defects in humans. Meiotic errors leading to aneuploidy are often a result of chromosome segregation errors during meiosis I (MI) in females. Thus, understanding the underlying causes of oocyte aneuploidy could help address a majority of clinical aneuploidies in humans. The Aurora Kinase (Aurk) gene family plays a major role in both mitotic and meiotic cell divisions. Mammalian mitotic cells require two Aurora Kinases, Aurora Kinase A (AURKA) and Aurora Kinase B (AURKB), while germline cells require a third, Aurora Kinase C (AURKC). AURKB has well-defined roles in

triggering the destabilization of improperly attached kinetochore-microtubules (KT-MT) and recruiting components of the SAC to prevent aneuploidy in mitosis. Despite this knowledge, little is known about how AURKB and its homolog AURKC regulate the SAC in meiosis where aneuploidies are a common occurrence. In mouse oocytes AURKB localizes to spindle microtubules and AURKC localizes to chromatin. Given the distinct localization of AURKB and AURKC, we hypothesized that the two kinases evolved to regulate the SAC in different pathways during female meiosis in mammals. To test this hypothesis, we used genetic and pharmacological approaches. First, we compared the SAC activity and the ability to correct improper KT-MT attachments in oocytes between AURK knockout (KO) mice: AURKC KO (C KO) and *Gdf9-Cre; Aurkbf1/fl* KO (B KO) mice in which *Aurkb* is deleted specifically in oocytes three days after birth. We observed that B KO oocytes completed MI in the presence of nocodazole and had a reduction in MAD2 recruitment to kinetochores, suggesting that the SAC is weakened in absence of AURKB. In contrast, C KO oocytes had more abnormal attachments and recruited MAD2. Then, we combined the genetic approach with a pharmacological approach to create oocytes with one active Aurora kinase, AURKB. To this end, we matured C KO oocytes in an AURKA-specific inhibitor, MLN 8237. Analyses of these oocytes confirmed that AURKB alone is sufficient to recruit and activate the SAC. Furthermore, when AURKC is absent, we observed an increase in lateral MT attachments and the dynamics of SAC satisfaction were altered. These results highlight the presence of two independent pathways that separately involve AURKB and AURKC in the activation of the SAC to ensure correct chromosome segregation during female meiosis in mouse. This research was supported by grants from NIH (R01-GM112801 and F31-HD089597).

**Loss of Adenosine Deaminase Acting on RNA (ADAR1) in Granulosa Cells Causes Infertility.** Rikki N. Nelson, Xiaoman Hong, Pavla Brachova, and Lane K. Christenson

Post-transcriptional regulation is critical to the overall expression of a gene. Acuity at this step contributes to the cell's ability to maintain or respond to its physiological environment by altering gene expression without transcriptional reprogramming at the level of the nucleus. RNA sequencing has highlighted the abundance of non-encoded polymorphisms in RNA sequences and the potential for RNA editing to contribute to post-transcriptional gene regulatory networks. Both coding and noncoding regions of mRNA can be edited resulting in altered codons, altered splice sites, changes in transcript stability, and changes in translation efficiency. Adenosine deaminases acting on RNA (ADAR) catalyze adenosine to inosine (A-to-I) editing, and comprise one family of RNA editing enzymes. There are two catalytically active adenosine deaminases, ADAR1 (*Adar*), with three distinct transcript variants, and ADAR2 (*Adarb1*), that also has three transcript variants. The third adenosine deaminase, ADAR3 (*Adarb2*), has two transcript isoforms both lacking catalytic activity. The periovulatory period provides a landscape for evaluating the role of post-transcriptional regulation as the somatic cells are undergoing differentiation and integrating signals from the maturing oocyte. Analysis of published granulosa cell RNA-seq datasets indicates that *Adar* is the highest expressed adenosine deaminase ( $10.66 \pm 0.02$  fragments per kilobase of transcript per million mapped reads) compared to *Adarb1* ( $2.11 \pm 0.17$ ) and *Adarb2* ( $0.05 \pm 0.02$ ). An organism-wide *Adar* deletion is embryonic lethal in mice, so a granulosa cell specific *Adar* depleted model was created to examine the role of ADAR1 in ovarian function. ADARFL/FL/Aromatase-Cre (n=5) and wild-type control littermate (n=6) female mice were bred to wild-type males for fertility evaluation over a 5 month period. To assess follicular development and ovulation, ADARFL/FL/Arom-Cre (n=3) and control (n=5) females were administered 5IU of PMSG, 5IU of

hCG 46 hours after PMSG, and eggs were collected from oviducts 16 hours following hCG. In the mating trial, control females had  $7 \pm 1$  pups/litter while ADARFL/FL/Arom-Cre females were infertile. Hormonal stimulation resulted in the recovery of no ovulated eggs in the ADARFL/FL/Arom-Cre females, while control mice had  $44 \pm 8$  ovulated eggs. Ovarian histology following PMSG + hCG stimulation revealed that antral follicles developed, but lacked evidence of luteinization following hCG administration. Ongoing studies are evaluating the temporal expression of the three Adar specific transcripts in granulosa cells as well as assessing the effect of Adar deletion on female cyclicity and expression of genes relating to follicular development, ovulation, and luteinization. These studies provide the foundation for identifying the mechanism by which Adar impacts ovarian function.

**The Maternal-to-Zygotic Transition in Bovine in Vitro Fertilized Embryos is Associated with Marked Class Changes in Abundance of Small Non-Coding Rnas.** Jocelyn M. Cuthbert, Stewart Russell, Kenneth L. White, and Abby D. Benninghoff

In mammals, small non-coding RNAs (sncRNAs), including microRNAs (miRNAs) and piwi-interacting RNAs (piRNAs), have been shown to be important during early embryo development. In the developing embryo, the maternal to zygotic transition (MZT) is associated with marked changes in control of gene expression that require coordination by multiple epigenetic control mechanisms, including sncRNAs. This study is the first to employ a discovery-based, small RNA sequencing approach to determine the population of sncRNAs in bovine oocytes, 8-cell embryos and blastocyst embryos. Importantly, we identified major class changes in the population of sncRNAs associated with the 8-cell embryonic development stage, coincident with the MZT in cattle. The relative abundance of miRNAs was markedly higher in 8-cell embryos compared to oocytes or blastocyst embryos, which was largely associated with up-regulation of miRNAs predicted to target genes involved in the biological processes of cell development, cell division, Wnt signaling, pluripotency and endomembrane system organization, among others. Aside from miRNA, other classes of sncRNA may also be important for the MZT, as their abundance changes over the course of parental genome silencing and embryonic genome activation. Distinct populations of piRNA-like RNAs (piRNAs) were identified in bovine oocytes and blastocyst embryos, though piRNAs were nearly absent in 8-cell embryos. PiRNA expression before the major wave of the MZT may be necessary to prevent TE activation and maintain genomic integrity as epigenetic reprogramming takes place. SnoRNAs control ribosome biogenesis by guiding the modification or processing of pre-rRNA. Also, snoRNAs are processed into smaller fragments that then may act in RNA interference. In this study, we observed that snoRNAs were highly expressed in 8-cell embryos, primarily those belonging to the C/D box subclass responsible for methylation of rRNA. Given the potential new functional role of snoRNAs in RNA interference, the observed marked increase in their abundance at the 8-cell stage points to a possible regulatory role of snoRNAs during the MZT in mammalian embryogenesis. Overall, these data reveal a strong dynamic shift in relative abundance of sncRNAs associated with the MZT in bovine oocytes and embryos, suggesting that these molecules may play important roles in the shift from maternal to zygotic control of gene expression.

**Effect of Preovulatory Estradiol on Conceptus Elongation in Beef Heifers.** M.K. McLean, T.E. Spencer, J.G.N. Moraes, M.S. Ortega, L.A. Ciernia, T.W. Geary, and M.F. Smith

At the time of fixed-time artificial insemination (FTAI), there are heifers and cows that have or have not expressed estrus. A meta-analysis of field trials involving 10,116 beef females reported a 27% increase in pregnancy rate to FTAI for animals that expressed estrus compared to those that did not express estrus. In beef heifers, expression of estrus at FTAI is associated with increased preovulatory circulating concentrations of estradiol (E2) and increased pregnancy rates on day 28 of gestation compared to heifers that were not detected in estrus. In a previous study, embryo donor cows (single-ovulation) with greater circulating concentrations of E2 after gonadotropin releasing hormone (GnRH)-induced ovulation were more likely to yield an embryo than an unfertilized oocyte, and recipient cows with greater E2 at GnRH-induced ovulation had an increased pregnancy establishment. We hypothesized that expression of estrus, via increased preovulatory E2, affects pre-implantation conceptus elongation for maternal recognition of pregnancy. The objective here was to examine the effect of preovulatory circulating concentrations of E2 on conceptus elongation at day 16 of pregnancy in beef heifers. Ovulation was synchronized in Angus heifers (n=29) as follows: GnRH and an intravaginal progesterone implant (CIDR insert) were administered on day -9; CIDR was removed and prostaglandin F2 $\alpha$  (PGF2 $\alpha$ ) administered on day -2; and GnRH was injected on day 0. Heifers were then separated into two groups, High E2 (n=6) or Low E2 (n=6), based on circulating E2 on days -2, -1, and 0 as determined by radioimmunoassay. Plasma concentrations of E2 (High E2, 9.6 $\pm$ 0.6 pg/mL vs Low E2, 4.6 $\pm$ 0.6 pg/mL) and dominant follicle diameter (High E2, 13.55 $\pm$ 0.7 mm vs Low E2, 11.35 $\pm$ 0.5 mm) on day 0 were increased (P 0.15) between High E2 (2.3 $\pm$ 0.5; 5.2 $\pm$ 1.3 cm) and Low E2 (2.5 $\pm$ 0.7; 7.1 $\pm$ 1.7 cm) heifers, respectively. These results support the idea that circulating concentrations of E2 during the preovulatory period in beef heifers do not affect pre-implantation conceptus elongation. Therefore, the likely time of embryonic loss in heifers that do not express estrus at FTAI is between days 16 and 28 during the critical implantation period of pregnancy. Supported by AFRI Grants no. 2013-67015-21076 and 2013-68004-20365 from USDA NIFA and Grant R01 HD072898 from the NIH.

**Chronic Inflammation Following Cancer Therapy in the Patient Ovary: A Potential Cause of Ovarian Tissue Damage and Follicle Loss.** Zaira Carranza, Maralee Lawson, Cecily Bishop, Fuhua Xu, Yukie Bean, Kelly Kester, Koenraad De Geest, Tanja Pejovic, and Jing Xu

Chemotherapy and radiation cause ovarian damage and follicle depletion, which could result in primary ovarian insufficiency and infertility in women. The disruption in ovarian function can last for years after the completion of cancer therapy. This implies that, besides acute events (e.g., DNA injury), additional mechanisms are involved. Cellular stress or injury by cancer therapy leads to the production of proinflammatory cytokines that recruit and activate immune cells, which in turn produce cytokines causing additional tissue damage. Here we report on the tissue conditions and inflammatory response in the ovary following cancer treatment in women. Ovarian tissues were collected from adult perimenopausal patients who underwent oophorectomy for various conditions at the Oregon Health & Science University using a protocol approved by the Institutional Review Board. The control group included 8 patients (26-43 years) who did not have a history of either chemotherapy or radiation therapy. The treatment group included 4 patients (31-47 years) who received chemotherapy and/or radiation therapy within the past 1-6 years. Ovarian cortex (~1.5 g) from each patient was fixed and

serially sectioned. Hematoxylin and eosin staining was conducted for ovarian morphology and follicle counting. Immunohistochemistry was performed to evaluate monocyte chemoattractant protein-1 (MCP1; proinflammatory cytokine) expression, as well as cells that were positive for cluster of differentiation 11b (CD11b; monocyte marker), 16 (CD16; natural killer cell marker), and 68 (CD68; macrophage marker). CD16- and CD68-positive cells were counted. Data were analyzed using nonparametric ANOVA (Wilcoxon Two-Sample Test; SAS Enterprise Guide 6.1). Patient ages were comparable between the control and treatment groups. Neovascularization was observed in the ovarian cortex from the treatment group, but not from the control group. There was minimal MCP1 and CD11b immunostaining present in the control ovarian tissue, while positive expression was evident in ovarian tissue from the treatment group. The number of CD16-positive cells negatively correlated with the number of primordial follicles present within the ovarian tissue ( $R^2 = -0.65$ ,  $p = -0.53$ ,  $p < 0.07$ ; for both CD16 and CD68). We demonstrate ongoing proinflammatory cytokine production, as well as immune cell recruitment and activation, in the ovary years post-cancer therapy. This appears to be related to the decrease in follicle numbers. The inflammatory response with chronic inflammation may be an additional potential cause of ovarian tissue damage and follicle loss associated with cancer therapy in women. Supported by NIH/NIGMS UL1GM118964 (BUILD-EXITO), NIH/NICHD R01HD082208, and NIH/OD P51OD011092.

**A Unique Lactate Dehydrogenase (LDH) Gene with Mitochondrial Signaling Peptide (MSP) Expressed in Porcine Reproductive Tissues and Early Pre-Implantation Embryos.** Stephen Tsoi and Michael Dyck

Application of the intracellular lactate shuttle theory to support the oxidation of lactate within mitochondria is currently a point of discussion in the literature. However, identification of a putative lactate dehydrogenase gene encoding the potential expression of MSP at its 5' region of the LDH gene is lacking. Here, we have used comparative and functional genomic approaches to demonstrate that there is a unique mitochondrial LDH (mLDH) gene in the pig coding signal peptide for mitochondrial membrane entrance, which is evolutionary conserved in all mammalian species responsible for lactate oxidation in mitochondria. The pig reference genome (Sscrofa11.1) was first assessed using Genome Data Viewer (<https://www.ncbi.nlm.nih.gov/genome/gdv/>) for all the LDH genes and found one unique LDH gene described as L-lactate dehydrogenase A-like 6B (Gene ID:100153697 referring to LDHAL6B) which is an intronless gene located at chromosome 1. Unlike the other cytosolic LDHs such as LDH A, LDHB and LDHC, the translated protein of LDHAL6B contains an extra long 40 amino acids at the N-terminal. Using TargetP 1.1 (<http://www.cbs.dtu.dk/services/TargetP/>) to predict the mitochondrial targeting peptide (mTP), we confirmed that the extra N-terminal amino acid sequences carried a mTP. Previously, our group had deposited the cDNA sequence of LDHAL6B (GenBank Accession ID: KM361875.1) amplified from a cDNA library constructed from preimplantation porcine in vivo generated embryo and oocytes. The details of the experimental procedure deposited at NCBI are located at SRA study: SRP005484. In order to further understanding the mLDH gene expression level at each specific developmental stages in the pig (GV, MII, 2-cell, 4-cell, 8-cell, morula and blastocyst), individual NGS data from each specific stage was downloaded from NCBI BioProject: PRJNA239206 (Cao S et al., BMC Genomics, 2014 Jan 3;15:4). Using the SeqMan NGen software program (DNASTar v.15.0, Madison, WI), FASTA-formatted files were aligned to the pig reference genome (Sscrofa11.1) for transcriptomic analysis. As normalization strategy, we used a reads per kilobase per million mapped reads (RPKM) as described by Mortazavi and associates (Nat Methods 5:621-628, 2008). For the RNA profiling of mLDH

from porcine reproductive tissues, Poly A+ RNA were obtained from testes, oocytes, oviduct, placenta tissues and D9 embryos as starting material to construct cDNAs using the SMARTer RACE 5'/3' Kit (Clontech, Mountain View, CA, USA). Finally, we used BLAST (Basic Local Alignment Search Tool) web tools from NCBI (<http://blast.ncbi.nlm.nih.gov/Blast.cgi>) (Altschul et al., 1997) to find 90 orthologous genes from other mammalian species. MegAlign Pro software (DNASTar v.15.0, Madison, WI) was used to perform multiple sequence alignment, a phylogenetic tree of mLDH was constructed. In conclusion, this is the first time to show that mLDH transcripts expressed two folds higher in oocytes and 2-cell stage than zygote and 4-cell stage of pig development. Transcripts were detected in placenta and Day 9 embryos but not in oviduct and other developmental stages. The full-length mLDH cDNA size is 1.739Kb in testes. The evolutionary tree suggests that the porcine mLDH is highly conserved among other mammals and closely related to whales & dolphins (90% sequence homology).

**Differentiation of Extracellular Vesicles from Bovine Placenta and Peripheral Blood Mononuclear Cells by Raman Spectroscopy.** Ana C. Silva, Han Zhan, Anhong Zhou, and Heloisa M. Rutigliano.

Placenta-derived extracellular vesicles (EVs) are involved in communication between the placenta and maternal immune cells possibly leading to a suppression of maternal T-cell signaling components. The ability to identify EVs in maternal blood may lead to the development of diagnostic and treatment tools for pregnancy complications. However, the detection of protein markers for bovine samples is a challenge due to the limited availability of commercial antibodies. Therefore, the objective of this project was to differentiate EVs from bovine placenta and peripheral blood mononuclear cells (PBMC) by a label-free, non-invasive technique called Raman spectroscopy. Peripheral blood mononuclear cells and trophoblast cells were isolated from late-term pregnancies (n=3/group). Both cell-types were cultured in vitro under similar conditions. Extracellular vesicles from culture supernatants were isolated by differential centrifugation. The morphology of isolated EVs was confirmed by scanning electron microscopy, and the EV size profile was assessed by dynamic light scattering. All the Raman spectra measurements were performed with a Renishaw inVia confocal Raman microscope equipped with a 785 nm near-IR laser in the spectral fingerprint range 600–1800 cm<sup>-1</sup>. Three independent replicates of the Raman spectra were obtained for the vesicles from different cell types. Approximately 35 measurements were taken in each replicate. Principal component analysis of the normalized and aligned spectra was conducted. The dynamic light scattering results show that EVs between 40 and 1000 nm were present in both samples. However, exosomes between 50 and 120 nm exhibited higher intensity which is indicative of greater abundance of these size particles in the preparation. The scanning electron microscopy images confirmed the presence and the size distribution of EVs in our preparation. Raman spectroscopy data established a fingerprint of biochemical components characteristic of EVs isolated from placental cell and PBMC-derived EVs. For instance, a cholesterol ester peak was only found in placental EVs. This may indicate differences between the EV membrane constituents, which are related to their signaling functions. Principle component analysis plots of normalized Raman spectra featured the discrimination between the cluster of placental-derived vesicles spectral group and that of PBMC-derived vesicles spectral group. The data showed that Raman spectroscopy clearly distinguished the biochemical fingerprints of the two groups without overlap. This research was supported by the Utah Agriculture Experiment Station.

**Fertility Gene MCM8 May be a Critical Signal in Stem Cells, Germ Cells, and Early Embryo Development Across Species.** Sonya M. Schuh and Nataly L. Sanchez

The highly conserved Minichromosome Maintenance 8 (MCM8) gene has been implicated in human female fertility, the number of follicles in the ovaries, age of menopause, premature ovarian failure, and mouse and fly fertility. MCM8 is also overexpressed in several types of human cancer. It may have roles in DNA double-strand break repair and homologous recombination. However, relatively little is known about whether MCM8 is expressed in human reproductive cells and tissues, and throughout human development. We aimed to investigate the expression and localization patterns of MCM8 in cultured human fibroblasts, several stem cell lines (induced pluripotent and embryonic), early germ cells, human gonads, isolated human and mouse germinal vesicle (GV) oocytes, early mouse embryos, and developing frog embryos. We used immunofluorescence, immunohistochemistry, and single-cell quantitative RT-PCR analysis to examine the expression of MCM8 throughout stem cell, germ cell, and embryo development. In vitro germ cell differentiation was performed on stem cell lines and putative germ cells were examined for MCM8 and germ cell markers including VASA. In functional studies, short oligonucleotide morpholinos targeted to MCM8 and its binding partner MCM9, were used to knockdown these genes in mouse GV oocytes and *Xenopus laevis* embryos. We discovered that MCM8, at both protein and mRNA levels, is expressed in undifferentiated human stem cells (nuclear), stem cells differentiating to the germ cell lineage (nuclear and cytoplasmic), and various stages of human and mouse germ cells and embryos, both in vitro and in vivo. Expression of MCM8 was reduced or absent in fibroblasts, cumulus cells, ovarian stromal cells, and neurons (ANOVA;  $P < 0.05$ ). Further, frog embryos lacking MCM8 had severe developmental defects and could not undergo gastrulation, or the formation of the three germ layers. Knockdown of MCM9 resulted in a developmental stall at neurulation, with an average of only 31% of MCM9 morpholino-injected embryos compared to 94% of control morpholino-injected embryos, reaching the neurula stage. Rates of cell death and embryo degeneration were high in both MCM8 and MCM9 knockdown embryos. Based on these expression and functional results, it seems likely that MCM8-mediated DNA repair pathways may be especially essential for stem cell, germ cell, and embryo function – all critical, rapidly-dividing, pluripotent cells that give rise to the next generation. The results here, along with previous genetic and loss-of-function studies, implicate this gene as a potential genetic marker for human gamete development and fertility and perhaps as a future therapeutic target (funding by NICHD F32HD061204, Faculty Research Grant, Undergraduate Student Professional Development Grant, and the SOS Summer Research Program Grant, Saint Mary's College of California).

**Ubiquitin-Proteasome System (UPS) Regulates Spermadhesin Release During Boar Sperm Capacitation.** Michal Zigo, Pavla Postlerova, Vera Jonakova, and Peter Sutovsky

The ubiquitin-proteasome system (UPS) is a complex enzymatic machinery responsible for protein degradation and turnover in all living organisms including plants. It is now well established that UPS participates in the events of mammalian sperm capacitation. To further elucidate the role of UPS in boar sperm capacitation, we studied the participation of UPS in spermadhesin release during in vitro capacitation (IVC). In vivo, the proteolytic cleavage of spermadhesins on the sperm surface is associated with the release of spermatozoa from the oviductal sperm reservoir.

At ejaculation, boar spermatozoa acquire low molecular weight (8-16 kDa) seminal plasma proteins, predominantly represented by spermadhesins, aggregated on the sperm surface. Due to their arrangement, such aggregates are relatively inaccessible to both antibody labeling and surface biotinylation. However, in IVC spermatozoa, both antibody and surface biotinylation are feasible as a result of de-aggregation and release of the outer layers of spermadhesins from the sperm surface. We took advantage of this de-aggregation to perform image-based flow cytometry studies of AQN-1, AWN, PSP-I, and PSP-II spermadhesins, which induce higher fluorescent intensity in capacitated vs. ejaculated spermatozoa. Addition of proteasomal inhibitors during IVC (20  $\mu$ M epoxomicin or 100  $\mu$ M MG132), significantly reduced fluorescence intensity of both the AQN-1 and AWN (P 0.95).

Our results demonstrate that UPS participates in the de-aggregation and shedding of spermadhesins from the sperm surface during capacitation, with a possible implication in detachment from the oviductal sperm reservoir, though other proteolytic and signaling pathways likely contribute to spermadhesin processing during capacitation.

Supported by USDA-NIFA grant 2015-67015-23231 (PS), European Regional Development Fund (ERDF) BIOCEV grant CZ.1.05/1.1.00/02.0109 (PP, VJ), the Czech Academy of Sciences (RVO:866525036) (PP, VJ) and seed funding from the MU F21C Program (PS).

**FOS is a Critical Transcription Regulator Necessary for the Ovulatory Process in Humans.** Yohan Choi, James W. Akin, and Misung Jo

FOS (a.k.a, c-fos) is a subunit of the activator protein-1 (AP-1) transcription factor and acts as heterodimeric complexes via binding with one of the Jun proteins (JUN, JUNB, JUND). Fos null mice failed to ovulate and form a corpus luteum (CL) even when given exogenous gonadotropins, indicating that ovarian Fos expression is critical for successful ovulation and CL formation. Our previous study demonstrated that the expression of FOS and Jun proteins (JUN, JUNB, JUND) increases in dominant follicles after hCG administration in normally cycling women. However, nothing is known about the regulatory mechanism involved in the expression of these transcription factors and their functions in human ovulatory follicles. In the present study, we utilized a primary human granulosa/lutein cell (hGLC) culture model that mimics key aspects of in vivo changes of periovulatory gene expression such as PGR, EGF-like factors (AREG and EREG), and PTGS2 in humans. To determine the regulatory mechanisms controlling the expression of FOS and Jun proteins, hGLC was cultured with or without hCG for various time points. qPCR and Western blot analyses showed a transient and biphasic increase in levels of mRNA and protein for FOS, which peaked at 1-3 h after hCG stimulation, declined to the time 0 h value by 6 h, and then increased again at 12 h. hCG also increased the level of JUN, JUNB, and JUND protein at all time points examined. To determine whether FOS is present as heterodimeric complexes with one of the Jun proteins, hGLC were cultured with or without hCG for 3 h and used for co-immunoprecipitation (Co-IP) analysis. Co-IP data showed that FOS interacts with all Jun proteins in hCG-treated cells, indicating that there are at least 3 different forms of FOS/AP-1 complexes in hGLC. To determine the role of FOS, hGLC was treated with or without T-5224 (a specific FOS inhibitor) in the absence or presence of hCG for various time points. T-5224 treatment inhibited hCG-induced increases in the expression of PGR, prostaglandin E synthase (PTGES), and prostaglandin transporters (SLCO2A1 and ABCG4). To determine whether FOS/AP-1 directly regulates the expression of these genes at the DNA level, CHIP assays were conducted using chromatin samples extracted from hGLC cultured with hCG. PCR

results showed that chromatin fragments containing FOS/AP-1 binding sites in the promoter region of these genes were enriched in hGLC. In summary, these data together demonstrated that hCG increases the expression of FOS/AP-1 transcription factors, which in turn regulates the expression of key ovulatory genes such as PGR, PTGES, SLCO2A1 and ABCC4 by directly binding to the promoter regions of these genes in hGLC. As the up-regulation of PGR and prostaglandins in periovulatory follicles is pivotal for successful ovulation, the present findings indicate that FOS/AP-1 transcription factors play an essential role in ovulation by regulating the expression of specific ovulatory genes in humans. Supported by PO1HD71875.

**Environmental Toxins Bisphenol A and Dibutyl-Phthalate Have Dose-Dependent Effects on Early Cleavage Divisions, Neural Development, and Embryo Survival in *Xenopus laevis*.** Sonya M. Schuh, Kyla D. Cole, Ashley L. Arancio, William C. Maloney, Chane Cilliers, and Julia Kadie

Bisphenol A (BPA) and di-n-butyl-phthalate (DBP) are widespread environmental compounds used in the production of polycarbonate plastics, resins, and epoxies. These man-made plasticizers can have endocrine disrupting properties and may negatively affect development and reproduction, as well as increase the incidence of cancers and birth defects across species. Exposure for animals, plants, and the environment is ubiquitous as BPA and DBP are in many commercial products, and consequently in our landfills, soil, and water systems. Here, we used *Xenopus laevis*, the African clawed frog, as a tractable model system for toxicological embryo studies with aims to better understand the effects of these xenoestrogenic compounds on early embryo cell division and development. Directly after in vitro fertilizations, one-cell embryos were exposed to various doses of BPA or DBP, or control Ringers baths. Embryos were counted, staged and imaged on a high resolution inverted stereomicroscope and camera for up to 48–96 hours post-exposure. We found a dose-dependent response, where BPA significantly impaired embryo development and survival, with increasing mitotic, body axis, and neural defects with increasing doses of the compound (7–10 replicates, 700 to 1,000 embryos per treatment). Most studies have focused on later stages of embryo development, and juvenile and adult animals. However, here we found that within the first 6 hours after initial exposure early cleavage divisions were already disrupted, mitoses were irregular and asymmetrical, apoptosis was apparent, and development was delayed. These effects were observed beginning at 1  $\mu\text{M}$ , and became significantly more severe with increasing doses of BPA. The percentage of abnormally developing embryos increased, and survival rates decreased, with increasing doses and lengths of exposure. The most significant embryological defects occurred at 10 and 25  $\mu\text{M}$  and during neurulation or development of the body axis and nervous system. Typical abnormalities included a curved body axis, abnormal spinal cord and brain development, and improper eye and pigment formation. DBP showed similar effects although not as severe at the respective doses, and with all embryos at the highest doses having enlargement of the gut and severely curved body axes. These findings are in alignment with endocrine disruption of the developing nervous system. The early mitotic and apoptotic effects of BPA may indicate the activation of other non-estrogen-related pathways. Future work will investigate the cellular signaling pathways of these compounds and their long term effects on the nervous and reproductive systems and fertility in surviving adults that were exposed as embryos. The adverse effects of BPA and DBP exposure could be detrimental to aquatic systems and the development of exposed humans. Great strides have been made in terms of research and attempting to limit human exposure to these compounds (banned from baby bottles and children's toys). However, we need a better understanding of what harmful levels are,

and the exact biochemical and physiological effects of these prevalent environmental toxins in animals and humans (this work was funded by the Faculty Research Grant, Undergraduate Student Professional Development Grant, and the SOS Summer Research Program Grant, Saint Mary's College of California).

**MDR-1 loss in the Ovary is Associated with Increased Vulnerability to Toxicants, Oxidative Stress, and Metabolic Dysfunction.** Lynae M. Brayboy, Laura O. Knapik, and Gary M. Wessel

The ovary is essential to the overall health maintenance of women given that its dysfunction compromises bone density, cardiovascular health, sexual function and leads to infertility. Therefore, it is necessary for the ovary to protect itself from iatrogenic gonadotoxic exposures such as chemotherapeutics and environmental toxicants in order to preserve the integrity of its fundamental endocrine and reproductive roles. Multidrug Resistance Transporters (MDRs) are a well described family of transmembrane, ATP-dependent, cell transporters with promiscuous efflux activity of over 4000 compounds including toxicants. Recent work has highlighted the importance of MDRs in a variety of reproductive processes such as gametogenesis, embryo segmentation, and maternal-fetal substrate transport. Work from our laboratory has demonstrated the indispensable role of two MDRs, Multidrug Resistance Transporter 1 (MDR-1) and Breast Cancer Resistance Protein (BCRP), in normal ovarian physiology and protection from toxicant exposure. MDR-1 (ABCB1) has 50 known polymorphisms: the C3435T polymorphism, which has 24.2% and 69.3% allele frequencies in the in the US and Ashkenazi Jewish populations respectively, is associated with increased risk of breast and lung cancer. These cancers may partially result from abnormal toxicant transport. It is therefore necessary to understand the implications of spontaneous MDR-1 mutations in ovarian physiology.

The aim of this study is to examine the physiological outcomes in *mdr1a*  $-/-$  mutant ovaries in a mouse model. Somatic cells of the *mdr1a*  $-/-$  mutant ovaries were more susceptible to cell death after exposure to cyclophosphamide, an alkylating cytotoxic agent used in cancer therapies. Increased reactive oxygen species also were elevated in mutant oocytes, even without toxic stimuli. Important to this point, the two groups had no difference in plasma isoprostane levels, which is another marker of inflammation and oxidative stress. Remarkably, metabolomic analysis of the ovary revealed an over-accumulation of mitochondrial associated metabolites in the Citric Acid Cycle, especially pyruvate, acetyl-CoA, succinate, and malate, perhaps indicative of HIF1 $\alpha$  activation and increased glycolysis. Moreover, ovarian transcriptomic analysis identified differentially expressed genes in the *mdr1a* null that were primarily associated with metabolism and the mitochondria. Ingenuity Pathway Analysis (IPA) revealed that ER $\alpha$  and ER $\beta$  interact with ABCB1 as an upstream regulator which further strengthens the assertion these transporters are critical to, and responsive of, ovarian function.

Taken together, these data indicate a link between impaired ovary function, MDR-1 expression, and mitochondrial dysfunction. Lack of MDR-1 then, may impair normal ovarian physiology and cause abnormalities even leading to carcinogenesis.

**Characterizing the Roles of Glutathione and Lipid Droplets in Mouse Oocytes.** Kelli F Malott, Laura Ortiz, Samantha Reshel, and Ulrike Luderer

Glutathione is the most abundant antioxidant in mature oocytes, with average concentrations of 10 mM per cell. It is produced intracellularly via two reactions, of which the first is rate limiting and is catalyzed by glutamate cysteine ligase. We have previously shown that female mice deficient in the modifier unit of this enzyme (Gclm) have oocyte GSH concentrations that are less than 20% than those of their wild-type counterparts. Furthermore, Gclm  $-/-$  females have smaller litter sizes, fewer uterine implantation sites, and far fewer zygotes progress to the blastocyst stage successfully when compared with Gclm  $+/+$ . Reactive oxygen species (ROS) are highly reactive compounds that are the result of sequential addition of electrons to molecular oxygen. They function as intracellular signaling molecules and in excess can be detrimental to the cell. ROS can oxidize DNA, proteins, and lipids and can ultimately damage the cell. Lipid droplets (LD) are small, monolayer organelles within a cell that act as energy and protein storage. Lipids in these organelles can react with ROS, becoming oxidized. LDs have been shown to be very important for oocyte developmental competence and preimplantation development. It has been previously shown that Gclm  $-/-$  mice do not gain weight with aging and in response to various obesogenic stimuli and have decreased overall decreased lipogenesis when compared with Gclm  $+/+$  mice. We hypothesized that Gclm  $-/-$  oocytes will have increased ROS concentration and these oocytes will display a decrease in LD concentration, as well as an increase lipid peroxidation. We measured ROS levels in oocytes using dichlorofluorescein fluorescence and the oxidation of LDs and total lipid content in oocytes from Gclm  $-/-$  and Gclm  $+/+$  littermates using BODIPY lipid stains and confocal microscopy. Lipid oxidation ratios and overall lipid fluorescence were measured using histogram analysis. We observe that Gclm  $-/-$  oocytes have higher levels of reactive oxygen species when compared with Gclm  $+/+$  (N=6). However, our preliminary data shows no difference in the ratio of oxidized/unoxidized lipids between Gclm  $-/-$  and Gclm  $+/+$  mice (N= 4). When we measured the total neutral lipid content in these oocytes, we see a decrease in cellular neutral lipid content in Gclm  $-/-$  compared to Gclm  $+/+$  (N=2). These data suggest that intracellular lipids in Gclm $-/-$  oocytes are being protected against increased ROS because of upregulation of other antioxidants. It is also possible that the overall decreased neutral lipid content in these mice means less are being oxidized and ROS molecules are oxidizing more proteins and DNA. The decreased neutral lipid content of oocytes from Gclm $-/-$  mice may be playing a role in the poor developmental competence of embryos derived from these oocytes. This research was supported by NIH R01ES020454.

**Ethinyl Estradiol Modulates Multidrug Resistance Transporter-1 (MDR-1) Expression in the Ovary.**

Laura O. Knapik, Lynae M. Brayboy, and Gary M. Wessel

The birth control pill has a multitude of benefits beyond avoiding unwanted pregnancy, including reduced risk of endometrial, ovarian, and colorectal cancers. How oral contraceptives do this is unknown. Our hypothesis is that ethinyl estradiol may modulate the MDR-1 gene, ABCB1, by increasing the transporters expression and/or functionality. Multidrug Resistance Transporters are a family of ATP-dependent, transmembrane, transporters that efflux metabolites and toxicants out of cells. Previous work from our laboratory demonstrates that MDR-1 is essential in normal ovarian physiology and protects the oocyte and entire ovary from toxicant exposure. It is known that MDR-1 has half of an estrogen response element, and work from other groups has shown that MDR-1 transcripts are reduced

in an estrogen receptor  $\beta$  knockout compared to its wildtype control. We have reported that MDR-1 mRNA expression in the ovary fluctuates with estrus cycling, and that most expression is detected after the  $17\beta$  estradiol surge. Previous work investigating the relationship between MDR-1 and estrogen has been performed on cell lines with conflicting results. It is therefore important to examine the role of estrogen in normal ovarian tissue in vivo.

The aim of this study was to test the effect of exogenous estrogen on MDR-1 expression in the ovaries of mice. FVBN mice were orally administered sesame oil and sugar alone (vehicle), or containing 1, 10 or 100 micrograms of ethinyl estradiol daily, for twenty days. Following treatment, the animals were sacrificed, and ovaries were collected for qPCR, immunoblot, and immunohistochemistry. The 1 microgram dose of ethinyl estradiol caused a significant decrease in MDR-1 steady state mRNA and protein. However, the highest dose of ethinyl estradiol corresponded to increased *mdr1* transcript from baseline, and a shift in the protein by immunoblotting. Immunohistochemical analysis revealed MDR-1 expression was enriched in follicular and luteinized granulosa cells.

MDR-1 expression is modulated by estrogen in both an upregulation and a down regulation of steady state levels, depending on concentration of hormone used. Additional work needs to be done to examine the role of estrogen in post-transcriptional and -translational modifications of MDR-1. Our future directions will be to investigate a potential synergistic effect of estrogen and progesterone together, as they are prescribed in the combined oral contraceptive pill, on both MDR-1 expression and functionality. These findings may increase our understanding on how the birth control pill reduces or prevents the occurrence of epithelial ovarian cancer.

**Effects of Dose and Route of GnRH on LH Serum Profile, Ovulation, and Conception Rate in Dairy Cows Synchronized using a modified Ovsynch Method.** Fernando Franco Polizel, Fernanda Nunes Marqui, Tairini Érica Cruz, Alicia Martins Jr., and Tereza Cristina Cardoso.

The route of administration and dose of GnRH are commonly used according to the manufacturer's instructions. However, no report was found in the literature on the use of half dose of GnRH in the vulva's submucosa (VS). Thus, this study was carried out to investigate the effects of dose and route of GnRH (buserelin acetate) administration on LH levels, as well as ovulation and conception rates in Holstein Friesian cows subjected to a modified Ovsynch program. The cows ( $n = 24$ ) were pre-synchronized ("Presynch") with two doses of  $150 \mu\text{g}$  PGF $2\alpha$ , via intramuscular, given 14 days apart. Then, 12 days later (D0) the animals received the first dose of GnRH ( $10.5 \mu\text{g}$ , i.m) followed by two doses of PGF $2\alpha$  given on D7 and D8. Then, on D9 the second dose of GnRH was administered, and the animals were examined by ultrasound to ovulation monitoring at 12 h intervals, beginning at the second GnRH moment (D9) and finishing 60 h later. Timed artificial insemination was performed on D10, with conception rate (CR) determined 28 days later by ultrasound. The cows (8/group) were divided in three experimental groups: G1 (control; saline 2.5 mL, i.m.), G2 (GnRH, 2.5 mL, i.m.) and G3 (GnRH, 1.25 mL, VS). Blood samples were collected at different times on D9 (-40, 0, 40, 80 and 120 min) in which time zero represents the moment of second dose of GnRH. Afterwards, the samples were centrifuged and storage at  $-20^\circ\text{C}$  for subsequent determination of LH concentrations by radioimmunoassay. ANOVA, Tukey and Fisher's tests were used for statistical analysis, with  $P < 0.05$  taken as significant. Higher values of LH ( $P < 0.05$ ) concentrations were obtained in G2 and G3 at 40 ( $5.3 \pm 4.0$  and  $4.5 \pm 5.1$ , respectively), 80 ( $13.2 \pm 9.6$  and  $7.5 \pm 4.9$ ) and 120 min ( $24 \pm 20.7$  and  $8.7 \pm 4.1$ ) than in G1 ( $0.75 \pm 0.14$ ,

0.85 ± 0.18, and 1.16 ± 0.30), respectively. When comparisons were made within each group, higher LH concentration ( $P < 0.05$ ) was obtained in G2 (13.2 ± 9.6 and 24 ± 20.7) and G3 (7.5 ± 4.9 and 8.7 ± 4.0) at 80 and 120 min, respectively, while lower values of LH were found in G1 at 40 min. The ovulation rate was similar between G1 (87.5%) and G2 and G3 (75%), however, there was significant difference among G1 (37.5%), G2 (87.5%) and G3 (12.5%) CR. Although lower levels of LH observed in cows receiving saline solution, ovulation rate was not negatively affected, unlike the CR. Interestingly, half dose of GnRH in the VS did not lead to satisfactory rate of conception, despite high concentrations of LH and ovulation rates obtained. However, the route of administration and dose, as recommended by the laboratory, beneficially influenced the rates of ovulation and conception. Nevertheless, it should be considered that these are preliminary results and for that reason the number of cows per experimental group is still small. Acknowledgment: Biogénesis Bagó Laboratory for the hormones, Buenos Aires, Argentina.

**Large Tumor Suppressors 1 and 2 (Lats1/2) Inhibit Initiation of High-Grade Serous Ovarian Carcinoma Derived from Mouse Surface Epithelium.** Atefeh Abedini, Omar Salah Salah, Curtis McCloskey, Manijeh Daneshmand, Mayra Tsoi, Derek Boerboom, and Barbara Vanderhyden

Epithelial Ovarian Cancers (EOC) have been reported to arise mainly from the epithelia of the ovarian surface (OSE) and distal fallopian tube. However, the molecular mechanisms underlying the initiation and progression of EOC derived from the OSE remains unclear. The Hippo signaling pathway is an important regulator of organ size and tumorigenesis through phosphorylation of Large Tumor Suppressors 1 and 2 (LATS1/2), which in turn phosphorylate and inactivate the transcriptional co-activators YAP and TAZ, leading to either their degradation or their cytoplasmic retention. It has been shown that LATS1 is expressed in human ovarian epithelium, but this expression is decreased in the transition to carcinoma, although the role of LATS1 during this process is unknown.

In this study, our objective was to explore the consequences of loss of LATS1/2 in OSE cells. OSE cell-specific deletion of Lats1/2 in the ovaries was achieved by intrabursal injection of adenovirus expressing Cre-recombinase (AdCre) into Lats1/2 (flox/flox) mice. Ovarian tumors were detected in all injected animals ( $n=10$ ) after a month. Mice subjected to injection exhibited the tumor in their ovaries and 5/10 animals had ascites with metastatic spread throughout the peritoneal cavity. Histologically, these tumors derived from the conditional deletion of Lats1/2 resembled high-grade serous carcinoma (HGSC). Tumor cells were highly proliferative as seen by Ki67 positivity. By immunohistochemistry, the tumors were found to express high levels of YAP protein, as well as ESR, PAX8, WT1 and cytokeratin, which are characteristic of the majority of HGSCs. Moreover, isolation of OSE cells from Lats1/2 (flox/flox) mice and deletion of Lats1/2 with AdCre in vitro led to the faster growth of OSE cells. Morphologically, the absence of LATS1/2 resulted in more elongated cells that formed a spindle-shaped structure. Assays to determine the capacity for substrate-independent growth showed that OSE cells lacking LATS1/2 formed colonies in soft agar while control cells did not. This increased proliferation was associated with the disruption of Hippo pathway signaling, as seen by a decrease in YAP phosphorylation and an increase in YAP-TEAD transcriptional targets, including the growth factors Ccn1, Ccn2, and Ccn5 and the apoptosis inhibitor Birc7 ( $P < 0.05$ ). To reverse this phenotype, we used verteporfin which prevents YAP-TEAD interaction. In our study, we showed that verteporfin suppresses the viability of Lats1/2 - AdCre cells and the two other HGSC mouse cell lines (ID8 and STOSE) in a dose-dependent manner and significantly downregulates the YAP-TEAD transcription targets Ccn1, Ccn2, Birc5 and Birc7 ( $P < 0.05$ ). In vivo,

verteporfin significantly decreased tumor weight of mice with conditionally deleted Lats1/2 relative to control groups ( $P < 0.05$ ) and significantly reduced proliferation as indicated by Ki67 expression. Current experiments using RNA-sequencing will further elucidate the pathway(s) by which deletion of Lats1/2 induces rapid tumorigenesis.

Collectively, the data indicate that loss of LATS1/2 is a potent stimulus for the growth of ovarian serous carcinoma and verteporfin may be a promising treatment by suppressing YAP-TEAD interaction.

### **Studying Early Onset Preeclampsia (EOPE) in a Model for Early Stage Human Placental Trophoblast.**

M. Sheridan, Y. Yang, A. Lyons, A. Jain, Y. Tian, G. Tuteja, D.J. Schust, L.C. Schulz, M. Ellersieck, T. Ezashi, and R.M. Roberts

Early onset preeclampsia (EOPE) affects about 0.4% of pregnancies, with grave consequences for both baby and mother. EOPE is characterized by impaired trophoblast (TB) invasion, resulting in a poorly perfused placenta. Our goal is to determine how early placental development differs between normal pregnancies and those affected by EOPE. Induced pluripotent stem cells (iPSC) were generated from umbilical cords of infants born to mothers who had EOPE and from controls. These iPSC were converted to TB, by exposing them to BMP4 and inhibitors of Activin A and FGF2 signaling, under 5% and 20% O<sub>2</sub>, hypothesizing that 20% O<sub>2</sub> would act as a stressor. Two embryonic stem cell lines (ESC; H1 and H9), 8 control (CTL) iPSC and 14 EOPE iPSC were tested to assess how well the differentiated TB cells invaded through a Matrigel-coated membrane. We found that 1) Under 5% O<sub>2</sub>, invasiveness of CTL-TB and EOPE-TB lines were equivalent; 2) Under 20% O<sub>2</sub>, invasiveness of EOPE-TB was lower than CTL-TB ( $p=0.024$ ); 3) invasiveness of CTL-TBs was not influenced by 20% O<sub>2</sub>; and 4) invasiveness of EOPE-TB as a group was significantly inhibited by 20% O<sub>2</sub> ( $p=0.008$ ). No significant differences in growth rate (as measured by DNA content) were observed between the CTL-TB and EOPE-TB, or between O<sub>2</sub> conditions. Both CTL-TB and EOPE-TB released more progesterone and hCG ( $p < 0.05$ ) in 20% than in 5% O<sub>2</sub>, but no difference was observed between CTL-TB and EOPE-TB. Production of placental growth factor (PGF) was increased in 20% O<sub>2</sub> in 5 of 6 CTL-TB lines tested ( $p < 0.05$ ), but in none of the EOPE-TB lines ( $n=4$ ). To identify gene expression changes that might be driving the invasion defect in EOPE-TB at 20% O<sub>2</sub>, RNA was collected from CTL-TB ( $n = 8$ ) and EOPE-TB ( $n = 14$ ) cultured in both O<sub>2</sub> conditions for sequencing. Principal component analysis revealed no difference between CTL-TB and EOPE-TB but did show separation by O<sub>2</sub> treatment. Therefore, we investigated differentially expressed pathways (between 5% and 20% O<sub>2</sub>) in each of CTL-TB and EOPE-TB, and identified genes uniquely upregulated at 20% O<sub>2</sub> in each of CTL-TB and EOPE-TB lines. A total of 365 genes were uniquely upregulated in CTL-TB and 213 in EOPE-TB, while 1308 were upregulated in both CTL-TB and EOPE-TB under 20% O<sub>2</sub> conditions. Genes uniquely upregulated in EOPE-TB at 20% O<sub>2</sub> were enriched for terms including locomotion, adhesion, angiogenesis, and preeclampsia, while no such terms were enriched in CTL-TB. WGCNA was used to compare co-expressed gene modules to the invasion assay results. Of 21 CTL-TB gene modules, four are significantly correlated with the degree of TB invasiveness, whereas none of the eight EOPE-TB gene modules are significantly related to TB invasion. Although this result was unexpected, it could imply a dysregulation of processes related to invasion by high O<sub>2</sub> in EOPE-TB, but it still remains unclear what genes are directly contributing to the reduced invasion phenotype.

Supported by NIH grants HD067759, HD077108 and HD079545

**Identification of Genomic Variants Causing Reduced Male Fertility.** Peter Sutovsky, Jeremy F. Taylor, Robert D. Schnabel, M. Sofia Ortega, and Thomas E. Spencer

A better understanding of the relationships between male genotype and sperm phenotype is crucial for the improvement of livestock reproductive performance and development of new diagnostic tools and treatments for human male and idiopathic infertility. The goal of the present Dual Purpose with Dual Benefits project of the NIH-NICHD and USDA-NIFA is to identify deleterious mutations that adversely affect sperm quality and the ability to convey high developmental potential to embryos and increased fertility to progeny genomes. Artificial insemination (AI) bulls provide a useful model system because of extensive fertility records, measured as sire conception rates (SCR). Genetic variants with moderate to large effects on fertility are being identified by sequencing the genomes of 85 fertile and subfertile/infertile sires with high ( $> +2.6$ ) or low ( $< -1.4$ ) SCR as adult AI bulls or yearling bulls that failed a breeding soundness evaluation. Variants enriched in frequency in the sequences of subfertile/infertile bulls and likely to result in the loss of protein function will be ultimately designed onto genotyping assays for validation of their effects on fertility by the widespread genotyping of bulls with SCR phenotypes. High throughput conventional and image-based flow cytometry, proteomics and cell imaging are being used to establish functional effects of variants on sperm phenotypes. Functional effects of the identified variants could manifest not only in the fertilization process but also via embryo viability. To further dissect these effects, bulls with high and low SCR values are being individually assessed in vitro. Preliminary data indicates that bulls with low SCR values produce fewer blastocysts by day 8 of development than bulls with high SCR values. In vitro fertilization (IVF) and pre-implantation development data will be integrated with field fertility data and sperm phenotypes to accelerate biomarker discovery and validation. The ultimate goal of this project is to maximize semen output from genetically superior sires and to increase the fertility of cattle, as well as to discover fertility associated genes that regulate human male fertility and pre- and peri-implantation embryo development. Supported by NIH 1R01HD084353 (PS, JT, RS), Food for The 21st Century Program of the University of Missouri (PS), and USDA-NIFA grants 2013-68004-20364, 2016-67015-24923, 2017-67015-26760 (JT, RS) and 2013-68004-20365 (TS). In-kind contributions were provided by Genex Cooperative and Select Sires Inc.

**Stable Transgenerational Inheritance of the Kinky Tail Phenotype Induced by a Repetitive Sequence Insertion into Intron 6 of Axin1.** Zhuqing Wang, Hayden McSwiggin, Yue Wang, Chong Tang, Sandy Lee, Daniel Oliver, Shuiqiao Yuan, Huili Zheng, and Wei Yan

Mice carrying Axin-fused (AxinFu) allele display a highly variable, but characteristic phenotype, a kinky tail. Although this interesting phenomenon was first reported in 1937, it was not until 2003 that Emma Whitelaw's group first demonstrated that differential DNA methylation states at a retrotransposon (IAP) within (AxinFu) correlate with the severity of the kinky tail phenotype, and specific DNA methylation patterns are associated with the kinky tail phenotype; both the DNA methylation patterns and the kinky tail phenotype can be transmitted into the next generation (PNAS 2003, 100: 2538). To test whether a transposon insertion can indeed induce DNA methylation changes in its neighboring genomic regions, leading to the specific phenotypes (i.e., kinky tails), we inserted a repetitive sequence into intron 6 of Axin1 in the mouse genome using the CRISPR-Cas9 technology. All of the mice homozygous for the insertion (L1/L1) displayed the kinky tail phenotype, whereas only ~80% of the heterozygous mice (+/L1)

showed kinky tails, and the remaining ~20% had normal tails. Heterozygous males and females with or without kinky tails (F1s) were bred with wild type females and males, respectively, and ~80% of the heterozygous offspring (F2s) displayed kinky tails. Further breeding of the F2 and F3 heterozygous males and females with wild-type controls led to F3 and F4 heterozygous offspring displaying the kinky tail phenotype with a similar penetrance (~80%). The distribution of the kinky tail phenotype of various severities appeared to be the same across all generations. We found no significant changes in DNA methylation status around the transposition site, but a larger transcript containing partial inserted repetitive sequences was identified, which appeared to result from aberrant splicing. ChIP-qPCR analyses identified H3K9ac, a marker for open chromatin, was enriched at the transposition site in the kinky tail group. We conclude that insertion of a repetitive sequence into intron 6 of Axin1 can induce the kinky tail phenotype due to aberrant splicing associated with altered histone modifications, and this epigenetic state can be stably inherited transgenerationally as long as the repetitive sequence insertion exists. Research in the Yan lab is supported by grants from the NIH (HD085506 and P30GM110767) and the Templeton Foundation.

**Identification of a DNA-Binding Sequence for ZNFO, a Novel Oocyte-Specific Zinc Finger Transcription Factor in Cattle.** Mingxiang Zhang, George W. Smith, and Jianbo Yao

ZNFO is a novel zinc finger transcription factor which is specifically expressed in bovine oocytes and early embryos. The protein contains a conserved KRAB domain at the N-terminus and nine zinc finger motifs at the C-terminus and it plays an important role during early embryonic development in cattle. Through a cyclic amplification and selection (CASTing) assay, we have identified a potential ZNFO binding element (ZBE), ATATCCTGNNNNNNNCCC. To further confirm the binding specificity of ZNFO to the identified element, an electrophoretic mobility shift assay (EMSA) was performed using IDye 700 labeled probes containing the target sequence and purified Halo-tagged ZNFO fusion protein. A competitive binding assay was also performed using 10-fold and 100-fold molar excess of unlabeled cold competitors containing the full length element and partial elements containing either ATATCCTG or CCC. The results confirmed the interaction between ZNFO and ZBE, and showed that both ATATCCTG and CCC are critical for the binding of ZNFO to ZBE. Further analysis of promoter regions of candidate bovine genes that contain ZBE may lead to the discovery of specific genes regulated by ZNFO.

**Expression of Genes Related To Steroidogenesis in the Broiler Breeder Hen Ovary.** Weaver E., Diaz F.J., Johnson A.L., and Ramachandran R.

A profound change in the productivity of the broiler chicken has been achieved through intentional genetic selection of traits deemed economically beneficial to the industry, most pertaining to rapid growth, feed conversion efficiency and breast muscle yield. The shift in focus onto these selection traits has led to poor reproductive performance in broiler breeder hens. In the breeder population, excessive feed consumption causes severe ovarian dysfunction and results in aberrant follicular recruitment, leading to suboptimal egg production and reduced fertility. In a preliminary study, we found that dietary metformin supplementation appeared to modify molecular events in ovarian follicular cells resulting in beneficial effects. To gain a better understanding on the fundamental mechanisms involved in aberrant follicular recruitment, we first examined known mechanisms and factors involved in follicular

recruitment in the normal broiler breeder ovary. We used qPCR to quantify known factors involved in folliculogenesis in Cobb 500 broiler breeders around 30 weeks of age (n=6). The birds were fed a restricted diet according to the COBB breeder management guide. Theca cells and granulosa cells collected from individual pre-hierarchical follicles were grouped by follicle diameter (3-5mm, 6-8mm and 9-12mm) and cortical follicles dissected from the ovarian cortex were grouped according to size (< 1 mm and 1-2mm). Theca cells, granulosa cells and cortical follicles from each assigned group were pooled from two individual birds to form one biological replicate, with a total of three biological replicates used for qPCR analysis (n=3). Gene transcripts analyzed included FSHR, VIPR1, STAR, CYP11A1, HSD3B1 and CYP19A1. Within the theca cell population, there was no difference in mRNA expression of each gene between the three follicle groups. Among the granulosa cell population, 9-12mm follicles expressed significantly higher levels of VIPR1, STAR, CYP11A1 and HSD3B1 mRNA (P< 0.01). The cortical follicles were not statistically analyzed due to the inability to separate granulosa cells from theca cells in these follicles, but it is interesting to note that both groups (< 1 mm and 1-2mm) expressed each of the genes mentioned above. Results were analyzed using one-way ANOVA (P<0.05) and Tukey's HSD. The results from this study form the foundation for future studies focusing on the role metformin plays in the modification of gene expression related to cell differentiation and follicular hyper-recruitment in obese broiler breeder hens.

This project was supported by Agriculture and Food Research Initiative Competitive Grant no. 2017-67015-26506 from the USDA National Institute of Food and Agriculture

**Early Anti-Müllerian Hormone Detection as a Predictor of the Ovarian Follicular Population in Water Buffalo (*Bubalus bubalis*).** Moysés Miranda, Rodrigo de Moraes, Nathália da Costa, Bruno Monteiro, Sebastião Rolim, Leanne Stalker, Allan King, Simone Santos, and Otávio Ohashi

When compared to bovines, water buffalo females are characterized as having a low ovarian follicular reserve and high individual variability in antral ovarian follicular population (AFP) limiting the widespread use of biotechnologies such as in vitro embryo production in this species. The anti-Müllerian hormone (AMH) is produced by the granulosa cells of developing follicles and plasmatic AMH level has been found to correlate with ovarian AFP and ovarian follicular reserve not only in humans but also in equines, goats, sheep and more recently bovines and water buffalo. In this study, we hypothesized that serum levels of AMH in buffalo calves could be predicative of AFP count later in life, at the beginning of their reproductive age. The plasma AMH concentration of 40 buffalo calves was measured at 8, 10, 12, 16 and 19 months (m). At the time of the last blood collection at 19m AFP was estimated by ultrasonography (follicles  $\geq 3$  mm). Results showed that AMH levels declined significantly from 8m to 10m ( $p < 0.05$ ) and then dropped again at 19m ( $p < 0.05$ ). Average AFP at 19m was  $17.5 \pm 0.9$  follicles and as predicted from previous studies, individual AFP was positively correlated to AMH levels at all ages evaluated ( $p < 0.05$ ). In order to identify animals with AFP extremes, inferior and superior percentiles were adopted to divide females into Low-AFP (n=10) and High-AFP (n=15) groups. High-AFP females had approximately twice the follicles of Low-AFP females ( $23.6 \pm 1.3$  vs.  $10.5 \pm 0.7$ ;  $p < 0.05$ ). When hormone levels of the Low- and High-AFP females were analyzed retrospectively at each age investigated, a significant difference in the AMH level between those two groups at 8, 12 and 16m was observed. ROC curve analysis showed that AMH levels detected at 8m (803.0 pg/mL), 12m (517.2pg/mL) and 16m (523.3 pg/mL) could be used to identify, with 90% sensitivity and 10% specificity, females that

would have a High-AFP later in life ( $p < 0.05$ ). In conclusion, the results obtained in this longitudinal study show for the first time the declining profile of AMH in young water buffalo females over time. We also show that from as early as 8m of age, AMH levels are positively correlated to AFP at 19m of age when females are becoming reproductively mature. Finally, we show that early serum AMH levels (as early as 8m of age) can effectively be used to detect females that will have significantly more antral follicles in their ovaries later in life. Therefore, we believe that early AMH levels may represent an important biomarker for a precocious and precise identification of reproductively superior females in water buffalo, positively contributing to the wide use of reproductive biotechnologies in this species.

**Maternal Nutrient Restriction Decreases Uterine Artery Blood Flow while Increasing Cotyledonary Blood Vessel Density in Angus and Brahman Cattle.** Caleb O. Lemley, Caitlin G. Hart, Racheal L. Lemire, Karrigan J. Bowers, Kalisha C. Yankey, E. Heath King, Richard M. Hopper, Seongbin Park, and Derris D. Burnett

Proper fetal nutrition via adequate uteroplacental blood flow is critical for maximizing offspring production potential while minimizing pregnancy wastage and calf morbidity and mortality. Our understanding of adaptations of the uteroplacenta following maternal nutrient restriction is incomplete and less is known about specific breed differences in cattle. Therefore, our objective was to examine uterine artery blood flow as well as macroscopic and microscopic placentome blood vessel density in nutrient restricted Angus and Brahman heifers. Angus ( $n = 6$ ) and Brahman ( $n = 6$ ) heifers were bred to a single sire and pregnancy confirmed at 30 days post-breeding. Heifers were randomly assigned to one of two dietary treatments consisting of 100% (adequate fed; ADQ;  $n = 6$ ) or 60% (nutrient restricted; RES;  $n = 6$ ) of net energy requirements for gestating cattle. Nutritional treatments were imposed from day 40 to 180 of gestation. Uterine artery blood flow (UBF) was collected ipsilateral and contralateral to the conceptus via Doppler ultrasonography on day 175 of gestation. Heifers underwent Cesarean sections for collection of two adjacent placentomes on day 180 of gestation. One placentome was OCT embedded and cryosectioned for microscopic immunofluorescence labeling of capillaries with anti-von Willebrand factor. The primary cotyledonary artery of the second placentome was perfused with Alexa Fluor 647 Con A conjugate to examine macroscopic cotyledonary blood vessel density via an in vivo imaging system (IVIS). Main effects of nutritional treatment and breed are reported in the absence of a significant nutritional treatment by breed interaction. Ipsilateral UBF was decreased by 48% in RES versus ADQ fed cattle, while breed did not influence ipsilateral UBF. Contralateral UBF was not different between nutritional treatments; however, contralateral UBF was decreased by 63% in Brahman versus Angus cattle. Placentome capillary number was not different between nutritional treatments or breed; however, capillary number was increased in heifers gestating male offspring ( $1,192 \pm 60$  number/mm<sup>2</sup>) versus female offspring ( $964 \pm 60$  number/mm<sup>2</sup>). Percentage of total capillary area per tissue area was increased by 42% in RES versus ADQ and 38% in Brahman versus Angus heifers. Average capillary area was increased in RES ( $113 \pm 7$  mm<sup>2</sup>) versus ADQ ( $82 \pm 7$  mm<sup>2</sup>) fed heifers. Capillary perimeter density was increased by 22% in RES versus ADQ and 23% in Brahman versus Angus heifers. Macroscopic cotyledonary blood vessel density was increased by 36% in RES vs ADQ and 82% in Brahman versus Angus heifers. In summary, these data indicate compensatory responses in macroscopic and microscopic placentome blood vessel density during maternal nutrient restriction induced reductions in uterine artery blood flow. Moreover, the greater density of cotyledonary blood vessels in Brahman heifers may protect the fetus by ensuring adequate tissue perfusion during prolonged periods of maternal nutrient

restriction. Research supported by USDA National Institute of Food and Agriculture under accession number 1011100 and USDA ARS Biophotonic Initiative number 58-6402-3-0120.

**Spleens from Bovine Fetuses Persistently infected with Flavivirus Have an Underdeveloped Adaptive Immune Response Despite an Upregulated Innate Immune Response.** Hanah M. Georges, Natalia P. Smirnova, Leticia D.P. Sinedino, Katie J. Knapek, Hana Van Campen, and Thomas R. Hansen

Bovine viral diarrhea virus (BVDV) has plagued worldwide cattle industries since it was first identified in 1946. Despite control measures, including vaccines, BVDV continues to cause substantial industry losses through the introduction of animals persistently infected with BVDV into feedlots, exposing and infecting several hundred animals in a short amount of time. Persistently infected (PI) calves are generated by infection of pregnant cows with BVDV at < 125 days of gestation, a period in which the immature fetal immune system is not capable of clearing the virus resulting in an immunotolerant state. PI animals are born and mature as immunocompromised adult animals and continuously shed the virus throughout their lifetime, possibly infecting other cattle. It is hypothesized that the innate and adaptive branches of the immune system are upregulated in fetal spleens following fetal infection with BVDV, causing immunotolerance to the virus and to a chronically heightened immune system. Naïve heifers were sham infected (controls) or infected with a noncytopathic strain of BVDV on day 75 of gestation (n = 4 each). Fetal tissues were collected on days 82 and 97; the highest viral titers in the fetal blood were detected on day 97 of gestation, 22 days post infection. RNA was isolated from fetal spleens, subjected to an affymetrix microarray analysis, and analyzed using R Software. Pathway associations were discovered in differentially expressed genes with a 2-fold or greater ( $p < 0.05$ ) difference by Qiagen Ingenuity Pathway Analysis (IPA). IPA identified the top upregulated canonical pathways in fetal spleens: IFN signaling, Th1 and Th2 activation, immune system communication, and the antigen processing and presentation pathway. Top upstream regulators included IFNG, IFNA, IRF7, and STAT1. Additional upregulated genes involved in IFN signaling included ISG15, IFIT1, and OAS1 ( $p < 0.05$ ) indicating a robust induction and upregulation of the fetal antiviral immune system. Data obtained through RT-qPCR, for validation of the microarray, further revealed a robust upregulation in DDX58, IRF7, ISG15, STAT4, LMP2, and LMP7 ( $p < 0.05$ ). The upregulation of these genes indicates a strong type I IFN response, induced through the IRF7 pathway. Additionally, an increase in STAT4 indicates a strong induction of the adaptive immune system by type I IFNs. Upregulated LMP2 and LMP7 may reflect a significant increase in antigen presentation through an increase in MHC I expression. Despite the increased type I IFN responses and antigen presentation, genes associated with T-Cell as well as B-Cell function did not change, which may contribute to immunotolerance to BVDV in day 97 PI fetuses. In the absence of T-Cell activation or response to antigen presentation, B-Cells remain unactivated by T-Cells, thereby impairing fetal production of antibodies against BVDV. This inability of the fetal adaptive immune system to rid the body of BVDV allows the virus to replicate and thrive in PI cattle. The consequences of viral infection on long-term development of PI fetuses is unknown, but is the focus of future experiments in the laboratory. Support: USDA National Needs Grant 2016-38420-25289 and USDA NIFA W3112.

### **Luteal Extracellular Vesicles Carry MicroRNA and Modulate Cytokine Secretion from Immune Cells.**

Martyna Lupicka and Joy L. Pate

Our previous study showed that cells isolated from fully functional corpora lutea induce T cell activation without the need of cell-to-cell contact. These interactions are possibly mediated by extracellular vesicles, and could play a role in the fate of the corpus luteum. Extracellular vesicles are cup-shaped membranous structures secreted by a wide variety of cells. They contain specific cargo, including microRNA, which takes part in cell-to-cell communication. Our hypothesis is that luteal steroidogenic cells communicate with luteal resident immune cells, affecting their functions, via extracellular vesicles, and that their microRNA content differs depending on the estrous cycle stage. In the present study we isolated extracellular vesicles in the size range between 50-450 nm (exosomes and microvesicles), secreted by in vitro cultured luteal cells isolated from day 10 (n=4) and regressing (n=4, 8 hr after PGF2alpha injection) bovine corpus luteum. MicroRNA were profiled in vesicles using Next Generation Sequencing. Only miR-150 was identified as differentially expressed after applying Benjamini-Hochberg false discovery rate correction, and was more prevalent in extracellular vesicles during regression of the corpus luteum compared to vesicles from day 10 of the cycle (logFC= -8.96). Targets for miR-150 were predicted by three different algorithms, and their common targets were subject to pathway analysis. Ingenuity Pathway Analysis revealed that among the top significantly enriched pathways one was associated with T cell proliferation and one with IL7 signaling. Moreover, pathway analysis of predicted targets of the most abundant 15 microRNA in luteal extracellular vesicles showed enrichment in pathways such as fatty acid synthesis and metabolism, TGFbeta receptor signaling, and immune system processes. We also performed an in vitro experiment wherein bovine T lymphocytes or monocytes isolated from peripheral blood were treated for 72 hr with isolated luteal extracellular vesicles. Concentrations of selected cytokines in post-treatment culture media were measured with ELISA. This experiment showed that TNFalpha secretion was greater in monocytes treated with either midcycle or regressing vesicles (n=3), when compared to controls. Transforming growth factor beta concentration was significantly greater in media from monocytes treated with regressing vesicles comparing with the control. Furthermore, both midcycle and regressing vesicles (n=3) induced increased secretion of TNFalpha in T lymphocytes. In summary, our current results suggest that luteal extracellular vesicles' cargo affects immune cell functions. In silico analysis of sequencing experiment results supports the hypothesis that microRNA are regulators of those functions, however further experiments are required to confirm if microRNA that are packaged into luteal vesicles can directly alter immune cell cytokine secretion. This project was supported by Agriculture and Food Research Initiative Competitive Grant no. 2016-67015-24900 from the USDA National Institute of Food and Agriculture.

### **DNA Methylation Reprogramming is Stalled in Newly Specified Primate PgcIcs.** Enrique Sosa, Ernesto J. Rojas, and Amander T. Clark

Shortly after specification of murine primordial germ cells (PGCs), early stage PGCs undergo an initial phase of global epigenetic reprogramming that results in the global loss of 5-methylcytosine (5mC) from about 50% of the genome. This global loss can be detected using immunofluorescence with antibodies that recognize 5mC. Global loss of DNA methylation is regulated by replication-coupled dilution of 5mC, and repression of the E3 ubiquitin ligase UHRF1, which recruits DNA methyltransferase 1 (Dnmt1) to replication foci. After an initial global loss of DNA methylation, locus-specific DNA demethylation occurs

in late PGCs as they colonize the genital ridge. Locus-specific DNA demethylation in late PGCs is regulated by Tet methylcytosine dioxygenases. In order to understand DNA methylation dynamics in primates, we used rhesus macaque iPSCs and the differentiation of PGC-Like cells (PGCLCs). We show that at the time of specification PGCLCs are highly methylated as expected, however with extended time in culture, the initial global loss of DNA methylation does not occur. To understand this phenomenon we first evaluated UHRF1 protein expression and discovered that it is absent in the majority of PGCLCs, suggesting that the maintenance DNA methylation machinery in PGCLCs has been disabled. Next we examined proliferation by two alternate approaches. The first involved evaluating incorporation of Edu into PGCLCs over time, as well as performing immunofluorescence for phosphor-histone H3 serine 10 (a mitotic marker) and Ki67, which marks cells in cycle. Our results indicate that most PGCLCs are Edu-negative by Day 4 of differentiation, and using antibodies that recognize phospho-Histone H3 serine 10 and Ki67, we show that the PGCLCs have also exited the cell cycle. These results indicate that the failure of PGCLCs in vitro to initiate the first global DNA demethylation event is most likely due to the PGCLCs entering quiescence rather than remaining in cycle. Therefore, coaxing PGCLCs to re-enter the cell cycle could be one critical approach for executing global DNA demethylation and therefore promoting differentiation of PGCLCs towards the generation of differentiated gametes.

**Cep215 is an Essential aMTOC-Associated Protein that Regulates Meiotic Spindle Organization in Oocytes.** Xiaotian Wang, Claudia Baumann, Luhan Yang, and Maria M. Viveiros

Acentriolar microtubule-organizing centers (aMTOCs) in mammalian oocytes play a critical role in stable meiotic spindle assembly. These unique aMTOCs are composed of essential structural and regulatory proteins, which control microtubule nucleation as well as spindle organization. Whether key mitotic centrosome-associated proteins are conserved and functional in oocyte aMTOCs is not fully understood. In somatic cells, Cep215 (Cdk5rap2) was identified as an important regulator of centrosome maturation and attachment to the spindle poles as well as spindle organization, with null mutations linked to microcephaly. Notably, Cep215 expression is conserved in mouse oocytes and we established that it localizes to aMTOCs in a pericentrin-dependent manner. Experiments in this study evaluated the regulation Cep215 expression in oocytes and directly tested its function. Western blot analysis showed higher Cep215 total protein levels in MII oocytes relative to the GV stage, suggesting a potential role during meiotic maturation. Cep215 localized specifically to aMTOCs during prophase-I arrest and throughout the progression of meiosis to MII. Notably, a brief (4h) exposure of ovulated MII oocytes to an Aurora Kinase A inhibitor (MLN8237) disrupted Cep215 distribution at aMTOCs, leading reduced Cep215 labeling at the poles of smaller spindle structures in more than 90% of total treated oocytes ( $P < 0.05$ ) compared to controls. To test function, specific siRNAs were used for transcript knockdown and effectively reduced Cep215 labeling in approximately 85% of the oocytes ( $P < 0.05$ ) compared to controls. Following a 17-h culture, the rate of maturation to MII by oocytes microinjected with Cep215 siRNAs did not differ significantly from controls. Live cell image analysis also showed similar dynamics in the progression of meiosis between the Cep215 siRNA and control oocytes. Despite maturation to MII, 42% of the Cep215 knockdown oocytes exhibited overt disruptions in spindle organization, including pronounced variations in spindle length/size as well as spindle pole focusing. These data support that Cep215 is a functional component of aMTOCs in oocytes, and plays an important role in regulating meiotic spindle organization. Funding support provided by NIH (HD 0713330 and HD086528) to MMV.

**Bisphenol Compounds Destabilize Microtubules and Disrupt Meiotic Spindle Organization in Mouse Oocytes.** Luhan Yang, Claudia Baumann, Xiaotian Wang, and Maria M. Viveiros

Accurate chromosome segregation relies on correct chromosome-microtubule interactions within a stable bipolar spindle apparatus. Hence, compounds that disrupt spindle organization can impair meiotic division and genomic stability in oocytes. The endocrine disrupting activity of Bisphenols such as Bisphenol A (BPA), widely used in plastics manufacture, is well documented. Yet, studies also point to damaging effects of Bisphenols on microtubules (MTs) that are less known. Here, we tested the effect of BPA and its common substitute Bisphenol F (BPF) on assembled meiotic spindle stability in ovulated oocytes, and assessed potential mechanism(s) of action. Surprisingly, a brief (4h) exposure to increasing concentrations (5, 25, 50 mg/ml) of either BPA or BPF was highly disruptive to meiotic spindle organization. Metaphase II (MII) oocytes exposed to BPA showed significantly ( $P < 0.05$ ) shorter spindle MTs with very broad (unfocused) spindle poles. Quantitative analysis confirmed significant alterations in spindle organization and live cell imaging revealed rapid BPA action, with initial spindle disruption observed within 1h of exposure. BPF showed similar, although less severe disruption of spindle organization. Moreover, both BPA and BPF-exposed oocytes exhibited disrupted pericentrin (Pcmt) clustering at the spindle poles. These detrimental effects were partially reversible upon compound removal. Notably, further testing revealed that MT stability (cold resistance) and MT regrowth were altered in BPA-exposed oocytes, leading to a high ( $P < 0.05$ ) incidence of aberrant multipolar spindle structures. These disruptions indicate that BPA potentially affects the regulation of MT polymerization/de-polymerization, pointing to a possible mechanism of action. While BPF promoted short spindle MT formation, MT stability was seemingly unaffected. In sum, these data demonstrate MT disrupting activity by Bisphenols that destabilize the meiotic spindle in ovulated oocytes upon brief exposure, and increase the risk for chromosomes segregation errors. Funding support provided by NIH HD086528 and a Faculty Research Grant to MMV.

**Adipokines Expression in Seminal Fluid of Normal-Weight Men.** Alice Bongrani, Yaelle Elfassy, Jean Sébastien Brun, Christelle Ramé, Namya Mellouk, Pascal Froment, Isabelle Berthaut, Soraya Fellahi, Jean Philippe Bastard, Rachel Levy, Claudine Vasseur, and Joëlle Dupont

Infertility affects 14% of childbearing-age couples and a male causal factor is involved in 20-50% of cases. Unlike women, little data is available about relation between body-mass index and spermatic parameters. It is however known that obesity is associated with impaired male fertility through a decrease of sperm quality. We hypothesized that adipokines, produced by adipose tissue, could interfere with gonadal function. Leptin's role in the interaction between energy metabolism and male reproductive system is well-known. Recently, some novel adipokines have been identified in seminal fluid and their seminal concentration is likely to be correlated with some morphologic and functional spermatic parameters. The aim of the study was to investigate expression profile of adipokines in seminal fluid of normal-weight men and compare their seminal and plasmatic concentrations. Seminal and blood samples from 70 healthy men consulting for couple infertility were collected in two Assisted Reproductive Centers (Tours, FERTIPROTECT protocol,  $n=32$ , and Paris, METASPERME protocol,  $n=38$ ) between December 2015 and October 2017. Subjects aged between 20 and 45 years and had normal BMI (20-25 kg/m<sup>2</sup>). Only men with a normal semen analysis according to 2010 World Health Organization guidelines were enrolled. Adipokines were analyzed in seminal fluid and blood plasma

using three different methods. First, human adipokine-arrays, testing simultaneously 58 adipokines, were performed on seminal and blood samples from 7 patients. The identified adipokines of interest were then quantified by enzyme-linked immunosorbent assay (ELISA) and Western-Blot analysis in the samples from Paris Centre (n=25) and Tours Centre (n=19), respectively. Preliminary adipokine-arrays showed that blood concentrations of adiponectin, leptin, chemerin and resistin, were significantly higher than seminal ones. Interestingly, others adipokines, such as visfatin, vaspin, fibrinogen, IL-8, TGF- $\beta$ 1, VEGF, CCL-2, FGF-19, HGF, calgranulin, ICAM-1 and angiotensin-1, were significantly more expressed in seminal fluid than in blood plasma. Western-Blot analysis evidenced that visfatin, FGF-19, VEGF, IL-8, HGF and CCL-2 concentrations were significantly higher in seminal fluid than in blood plasma ( $p < 0,0001$ ). Similarly, significantly higher visfatin and IL-6 concentrations in seminal fluid were confirmed by using ELISA assay ( $p < 0,0001$ ). On the other hand, adiponectin, leptin, chemerin and resistin were predominantly expressed in blood plasma ( $p < 0,0001$  for all adipokines, except for resistin,  $p=0,01$ ). In conclusion, our study shows that adipokine expression in seminal fluid is different from blood plasma. The meaning of a predominant expression of some adipokines in seminal fluid, notably including inflammatory markers, remains to be elucidated. Nevertheless, different adipokines expression in seminal and blood fluids suggests the possibility of a gonadal production or a compartment-specific regulation of adipokines in reproductive tract and peripheral blood. Immunohistochemistry characterization of adipokines, currently in progress in spermatozoa and different testicular cellular types, could allow us to better elucidate gonadal adipokines metabolism.

#### **Widespread Enhancer Activation via ER $\alpha$ Mediates Estrogen Response in Vivo During Uterine**

**Development.** Wendy N. Jefferson, H. Karimi Kinyamu, Tianyuan Wang, Adam X. Miranda, Elizabeth Padilla-Banks, Alisa A. Suen, and Carmen J. Williams

Little is known regarding how steroid hormone exposures impact the epigenetic landscape in a living organism. Here we took a global approach to understanding how exposure to the estrogenic chemical, diethylstilbestrol (DES), affects the neonatal mouse uterine epigenome. Integration of RNA- and ChIP-sequencing data demonstrated that ~80% of DES-altered genes had higher H3K4me1/H3K27ac signal in close proximity. Active enhancers, of which ~3% were super-enhancers, had a high density of estrogen receptor alpha (ER $\alpha$ ) binding sites and were correlated with alterations in nearby gene expression. Conditional uterine deletion of ER $\alpha$ , but not the pioneer transcription factors FOXA2 or FOXO1, prevented the majority of DES-mediated changes in gene expression and H3K27ac signal at target enhancers. An ER $\alpha$  dependent super-enhancer was located at the Padi gene locus and a topological connection to the Padi1 TSS was documented using 3C-PCR. Chromosome looping at this site was independent of DES exposure, indicating that it was in place prior to ligand signaling. However, enrichment of H3K27ac and transcriptional activation at this locus was both DES and ER $\alpha$ -dependent. These data suggest that DES alters uterine development and consequently adult reproductive function by modifying the enhancer landscape at ER $\alpha$  binding sites near estrogen-regulated genes.

**Decreased Esr1 Expression in Uterine Epithelium Leads to Subfertility and Dystocia.** Jessica Milano-Foster, Andrew M Kelleher, and Thomas E Spencer

Dynamic changes in ovarian estrogen and progesterone production and their actions on the uterus coordinate uterine receptivity, blastocyst attachment, stromal cell decidualization and placentation, leading to successful pregnancy. Leukemia inhibitory factor (Lif) is expressed solely by the glandular epithelium (GE) of the uterus on gestational day (GD) 4 in response to ovarian estrogen and is essential for pregnancy, as Lif null mice are infertile due to defects in embryo implantation. Likewise, female mice with global deletion of estrogen receptor alpha (ESR1) or neonatal epithelial specific deletion of ESR1 (Wnt7aCre/+Esr1f/f) are infertile, resulting from defects in oviductal transport, Lif expression and stromal cell decidualization. Here, to investigate estrogen signaling in the adult mouse uterus we conditionally deleted Esr1 in epithelium of the uterus using lactotransferrin (Ltf)-iCre mice, in which Cre recombinase is expressed under the control of the endogenous Ltf promoter and directs recombination in the uterine luminal epithelium (LE) and GE only in peripubertal and adult mice. A three-month breeding trial (n = 5 per genotype) established that LtfiCre/+Esr1f/f (Esr1 cKO) mice were subfertile, as control mice had more (P < 0.1) between the genotypes, suggesting that a threshold of ESR1 positive gland cells may be sufficient to induce Lif expression and initiate implantation. Of particular note, dystocia was observed in 50% of Esr1 cKO mice (n = 6), whereas it was absent from control females. These data support the hypothesis that epithelial Esr1 expression is required for successful pregnancy and that decreased levels of ESR1 in the uterine epithelia leads to subfertility and adverse outcomes at the end of pregnancy near parturition. Supported in part by NIH grant R21 HD087589.

**Expression of FSH Receptors in Ovine Luteal Tissues During Luteal Phase: Effect of Nutrition Plane and FSH-Treatment.** Anna T. Grazul-Bilska, Sheri T. Dorsam, Arshi Reyaz, Veselina Valkov, Casie S. Bass, Samantha L. Kaminski, and Dale A. Redmer

Corpus luteum (CL), a transient endocrine gland, critical for reproductive cyclicity and pregnancy maintenance is controlled by numerous regulatory factors. Although LH is widely recognized as the major regulator, other factors may also affect luteal functions. It has been demonstrated that FSH receptors (R) are expressed not only in ovarian follicles, but also in other tissues within the reproductive tract including the CL. To evaluate FSHR expression in FSH-treated or non-treated sheep fed a control (C), excess (O) or restricted (U) diet, CL were collected at the early, mid and/or late-luteal phases (n=4-8/group). In exp. 1, ewes from each diet were not injected, but in exp. 2, ewes were injected twice daily with FSH on days 13-15 of the first estrous cycle. CLs were dissected, and one portion was fixed in formalin and the other portion was frozen. Expression of three variants of FSHR mRNA, FSHR-1, 2 and 3, was quantified by qPCR (Sullivan et al, Reprod Biol Endocrinol 2013). Protein expression was detected by immunohistochemistry, and the percentage of positive staining out of the total tissue area was measured by image analysis (n=4 images/CL). Serum progesterone concentration was 5.5-fold greater in FSH treated than non-treated ewes. FSHR protein and mRNA were detected in the CL from all groups. In exp. 1, expression of mRNA for all FSHR variants was greater (P < 0.02-0.0003) at the late than mid or early-luteal phase, and in exp. 2, was greater (P < 0.001) at the mid than early-luteal phase. Plane of nutrition did not affect FSHR mRNA expression. Comparison of FSH-treated to non-treated ewes demonstrated that FSH increased by 7-30-fold (P < 0.001) mRNA expression for 1) FSHR-1 in all groups except U at the early-luteal phase; 2) FSHR-2 in C, O and U at the mid but not early-luteal phase; and 3)

FSHR-3 only in U at the mid-luteal phase. In exp. 1, FSH protein expression was affected ( $P < 0.02$ ) by stage of luteal development, and was less ( $P < 0.02$ ) at the mid than early and late-luteal phases. In exp. 2, interactions between diet and luteal stage demonstrated that FSH protein expression was greater ( $P < 0.03$ ) in O at early-luteal phase than any other group, except C, at the mid-luteal phase. Comparison of FSH-treated to non-treated ewes demonstrated that FSH increased FSHR protein expression by 1.5-2-fold ( $P < 0.0001$ ) in all groups, except C, at the early-luteal phase. Our data demonstrate that: 1) FSHR are expressed in ovine CL at several stages of luteal development, 2) FSHR expression depends on the stage of the estrous cycle, 3) protein, but not mRNA, expression is affected by diet, and 4) in vivo FSH-treatment enhances FSHR expression in the CL depending on diet and stage. Presence of FSHR in the CL indicates a regulatory role for FSH in luteal function in sheep. Since very little is known about the possible role of FSH and FSHR in luteal functions, further studies should be undertaken to elucidate the endocrine, molecular and cellular mechanisms of FSH effects on the CL. USDA-AFRI grant 2011-67016-30174 to ATGB and DAR.

### **Global Gene Expression in Placental Cell Types During Late Pregnancy in Sheep: Preliminary Study.**

Manuel Vásquez Hidalgo, Sheri T. Dorsam, Kishore Chittam, Kimberly A Vonnahme, and Anna T. Grazul-Bilska

The placenta is a temporary organ that allows for oxygen, nutrient and waste exchange between mother and fetus, and therefore is critical for supporting fetal growth and development. In ruminants, this nutrient exchange occurs at specialized structures called placentomes, which consist of numerous cell types, including multinuclear trophoblastic giant cells (TGC), binuclear cells (BNC), epithelial cells, endothelial cells, fibroblasts, immune cells and others. TGCs have been implicated as paracrine and endocrine regulators of placental function, including regulation of the vasculature. TGCs contribute to the overall function of the placenta, namely in allowing the placenta to be more efficient in nutrient delivery to the fetus. The objective of this study was to compare the global gene expression between TGC, BNC, and mononuclear cells (MNC) from sheep placenta. Placentomes were collected on day 90 and 130 of pregnancy ( $n=2/\text{day}$  for BNC and MNC;  $n=1$  for TGC collection). Caruncular tissue was separated, and cotyledons were cut into small pieces and enzymatically dispersed with collagenase. 65 million cells were elutriated to obtain fractions enriched with MNC (89-93%) and BNC (32-33.5%). In addition, TGCs were manually isolated using a micro-pipette from the fraction containing the largest cells. Total RNA was extracted from the three cell populations, and transcriptomes were analysed by RNA-seq. Approximately 142 million 50 bp single reads were generated from the sequencing of 10 elution libraries. Filtered reads were aligned to the *Ovis aries* genome assembly v3.1 using STAR aligner. On average, 84% of the reads aligned to the reference genome, and ~ 63% of the reads mapped uniquely. Raw read counts aligned per gene were obtained and differential gene expression analysis (DGE) was conducted in DESeq2. Principal Component Analysis showed that 67% of the variation is explained by cell type and 12% by day of pregnancy. Comparison of the days of pregnancy (90 vs. 130) and cells types (MNC, BNC and TGC) using a 5% False Discovery Rate demonstrated that on day 90, there were 28 DE genes between MNC and BNC, 2174 between MNC and TGC, and 2053 between BNC and TGC; and on day 130, 492 DE genes between MNC and BNC, 1603 between MNC and TGC, and 1758 between BNC and TGC. Venn diagram analysis demonstrated that 116 DE genes were expressed at higher levels in MNC or BNC at d90 or d130 in all comparisons, and 603 DE genes showed increased expression in TGC at d90 or d130 amongst all comparisons. Of note, one of the DE genes we identified as

being expressed at a 19.27 fold higher level in BNC vs. MNC at d130 was the estrogen-specific sulfotransferase, SULT1E1. This transcript has also been detected at a higher level in bovine BNC. This preliminary experiment demonstrates differential gene expression in placental cell types depending on the stage of pregnancy in sheep. Future studies will be undertaken to generate data from multiple sheep, and determine the specific function and level of expression of selected genes in physiological and pathological conditions. USDA-AFRI grant 2016-67016-24884 to ATGB and KAV.

**The Interaction of Protein Phosphatase I with Cell Division Cycle 25B in Mammalian Oocytes.** Eva A. Gilker, Alaa A. Eisa, Travis F. Mollick, Alexander C. Ignatious, and Douglas Kline

Mammalian oocytes are held at prophase I of meiosis until reproductive maturity is reached, when some oocytes resume meiosis to mature to an egg. The meiotic arrest and the hormonally induced release from arrest depend on the interactions of protein kinases and phosphatases that regulate the activity of key cell cycle control proteins. Dephosphorylated and activated cyclin-dependent kinase I (CDKI) triggers meiotic resumption as indicated by nuclear envelope breakdown and chromatin condensation. Cell division cycle 25B (CDC25B) is solely responsible for the activation of CDKI in oocytes. CDC25B is held in an inactive state by PKA-dependent phosphorylation and binding of the regulatory protein 14-3-3 (YWHA). The phosphoprotein phosphatase (PPP) family of serine-threonine phosphates contains members known to regulate a wide variety of cellular events. Members of the Protein Phosphatase 1 (PP1) family may regulate by three genes to produce the isoforms PPP1CA (PP1 $\alpha$ ), PPP1CB (PP1 $\beta$ ) and PPP1CC (PP1 $\gamma$ ). In addition, we have evidence that two alternatively spliced variants, PP1 $\gamma$ 1 and PP1 $\gamma$ 2, are present in oocytes. We are currently using PPP1CC knockout models and PP1 $\alpha$  protein knockdown experiments to examine the role of PP1 $\gamma$  and PP1 $\alpha$  proteins that may interact with CDC25B. A pull-down protein assay using recombinant PP1 $\gamma$ 1 protein and ovarian lysates indicates that PP1 $\gamma$ 1 binds to CDC25B. Immunoprecipitation analysis indicates that PP1 $\alpha$  also binds to CDC25B from ovarian lysates. In the PPP1CC knockout model, in the absence of PP1 $\gamma$ 1 protein, the expression of PP1 $\alpha$  is greater in ovarian tissues and in oocytes and eggs. PP1 $\gamma$ 1 and PP1 $\alpha$  proteins are found in the cytoplasm and nucleus of mouse oocytes with some greater localization for both in the nucleus. Localization of PP1 $\alpha$  protein to the nucleus is enhanced in the absence of PP1 $\gamma$ 1 protein. While PPP1CC knockout animals appear to undergo normal oocyte maturation and are fertile, the data suggests some interplay between PP1 $\gamma$  and PP1 $\alpha$  and CDC25B in the regulation of oocyte maturation.

**Effect of Microwave-Assisted Dehydration on Follicular Morphology and Survival within the Ovarian Tissue in the Domestic Cat Model.** Lee P. C., Adams D. M., Amoretti L. A., White K. K., Whitaker M. G., and Comizzoli P.

Ovarian tissue contains large pools of preantral follicles, making it an attractive target for fertility preservation in female cancer patients, livestock and wild species. Dry-preservation allows supra-zero temperature storage, making it less expensive and less constraining than cryopreservation. Controlled microwave dehydration that preserves cellular functions in a stable trehalose glass currently is applied with encouraging results to cat germinal vesicles and spermatozoa. The objective of the present study was to examine the effect of microwave-assisted dehydration (MAD) on follicular morphology and survival in feline ovarian tissue. Experiment 1 examined the effect of different trehalose concentrations

and MAD on follicular morphology and viability after rehydration and tissue culture. Ovarian cortical tissues obtained from peri-pubertal cats were dissected into 1 x 1 x 0.2 mm<sup>3</sup> pieces. One piece from each replicate was fixed immediately as fresh control. The rest was permeabilized with digitonin, exposed to trehalose (0, 0.2, 0.5 or 1.0 M) for 10 min, dehydrated with a CEM SAM 255 microwave for 30 min, and then stored in moisture-barrier bags at 4°C for at least 24 hours. Cortical pieces then were rehydrated and cultured for 0 or 3 days before assessing follicular morphology (hematoxylin-eosin staining; n = 86, in 10 replicates) and viability (live/dead assay; n = 60, in 6 replicates). Rehydrated cortical pieces dried without trehalose had lower percentages (P < 0.05) proportion of normal follicles (range, 43.1 to 52.3%) compared to the controls. However, total follicle numbers decreased (P < 0.05) the follicular viability compared to the fresh control (range, 47.5% to 90.1%). Experiment 2 investigated the effect of different microwave time on the morphology and transcriptional activity of follicles. Digitonin-permeabilized cortical pieces were exposed to 0.5 M trehalose and then dehydrated for 0, 5, 10, 15, 20, 25 or 30 min. Samples were rehydrated immediately after drying to assess follicular morphology and transcriptional activity (n = 24, in 3 replicates). Percentages of morphologically normal follicles were not different (P > 0.05) among fresh control and any treatment groups (range, 47.0 to 86.9%). However, percentages of transcriptionally active follicles sharply diminished (P < 0.05) after 10 min of drying (Fresh, 0 and 5 min: range, 75.0 to 91.9%; 10 and 15 min: range, 10.5 to 17.9%) and reached 0% after 20 min. Collectively, the results suggest that (1) trehalose treatment is beneficial to maintain follicular morphology during dry-preservation, and (2) follicle survival is partially preserved for short MAD treatment but compromised after extended period of drying. Future work will focus on optimizing MAD protocol for ovarian tissue to better preserve follicular survival and function under dried condition.

**Postpartum Uterine Infection Disrupts the Follicular Environment at the Time of Breeding.** John J. Bromfield, and Rachel L. Piersanti

Postpartum bacterial infection of the uterus results in clinical disease in approximately 40% of dairy cows. Cows that develop metritis have reduced follicle growth and plasma estradiol immediately after parturition. Interestingly, cows with metritis also have reduced pregnancy and calving rates after the resolution of disease. Cows with metritis accumulate the pathogen associated molecule lipopolysaccharide in follicular fluid of the dominant follicle. Granulosa cells exhibit an innate immune response to lipopolysaccharide and other pathogen associated molecules, altering the follicular environment and increasing local concentrations of proinflammatory cytokines. We have previously shown that exposure to lipopolysaccharide increases meiotic errors in oocytes during bovine in vitro maturation. To better understand the mechanisms of metritis associated infertility we assessed the follicular environment of cows with resolved disease at the time of breeding compared to control cows. Metritis was defined by the presence of fetid watery red-brown uterine discharge within 21 days post-partum (n = 41). Animals were classified as control (n = 50) if they were either healthy or presented non-uterine diseases, such as ketosis, laminitis and digestive problems within 21 days post-partum. Estrous cycles were synchronized and the dominant follicle was sampled by transvaginal ultrasound guided follicle aspiration on day 65 ± 1 postpartum. Plasma TNF $\alpha$ , IL-6 and progesterone were evaluated by ELISA at days 7, 21, 35 and 50 postpartum. Granulosa cell whole transcriptome was analyzed by RNAseq. Uterine cytology at the day of follicle aspiration confirmed the absence of subclinical endometritis in all cows. As previously reported, primiparity and calving intervention were positively associated with development of metritis (P = 0.0104 and P = 0.008, respectively). Evaluation of plasma progesterone

revealed that cows with metritis took longer to return to cyclicity when compared to control cows, defined by concentrations above 1 ng/ml ( $P = 0.029$ ). Plasma IL-6 was not different between groups, and TNF $\alpha$  was below the limit of assay detection. Dominant follicle diameter and follicular fluid estradiol concentration at the time of follicle aspiration were similar between groups. Granulosa cell transcriptomic analysis revealed 177 differentially expressed genes in metritis cows. Cows with metritis had 33 down regulated genes, including LHCGR, PIDD1 and STX17; while 144 genes were upregulated, including IL18, FGF14, ITLN1 and CD28. Ingenuity Pathway Analysis indicated that pathways involved in cell-to-cell signaling, cell death, growth and proliferation were impacted by metritis. Physiological systems affected in granulosa cells by metritis included immune response and embryo development. The mechanisms responsible for metritis associated infertility are not fully understood; however, it is evident that the impact of uterine infection on the follicular environment is present well after the clearance of infection. An altered follicular environment may be a potential source of reduced fertility in cows suffering metritis.

Supported by the Eunice Kennedy Shriver NICHD R01HD084316.

**The Role of MicroRNA-21 (miR-21) in Inflammation and Fibrosis in Endometriosis.** M. Ariadna Ochoa Bernal, Niraj Joshi, Yong Song, Samantha Bond, and Asgerally Fazleabas

Endometriosis is an estrogen-dependent inflammatory disease characterized by the presence of endometriotic tissue outside the uterine cavity. The mechanisms associated with the origin of the disease and processes involved such as inflammation, lesion growth and fibrosis remain unclear. Previous data from our laboratory has shown that the presence of endometriotic lesions alter microRNA expression in both the eutopic and ectopic endometrium of baboons with endometriosis. MicroRNA-21 (miR-21) was altered in endometriosis and it may play a role in inflammation and fibrosis as a consequence of elevated interleukin (IL)-6 levels. Numerous studies have shown that concentrations of IL-6 are increased in the peritoneal fluid of women with endometriosis, which could contribute to inflammation. In addition, our previous data has shown that fibrosis is progressive during lesion development in baboons with increasing collagen deposition *in vivo*. Studies have also suggested that miRNA-21 promotes transforming growth factor (TGF- $\beta$ ) signaling to increase fibrosis and promote epithelial to mesenchymal transition (EMT). TGF- $\beta$  expression is increased in endometriotic lesions and peritoneal fluid of women with endometriosis. The present *in vitro* study was designed to explore the role of miRNA-21 in the development of fibrosis and inflammation associated with the disease and the mechanisms by which IL-6 can modulate the expression of miRNA-21. Endometriotic epithelial cells (12Z) were cultured in triplicate to 70-80% confluence. The cells were transfected with a miRNA-21 mimic or non-targeting negative controls. After 48 hours, RNA and protein were collected from the cells and qRT-PCR was carried out to check the expression of inflammatory response genes and fibrosis related genes. Furthermore, to verify if IL-6 can modulate the expression of miRNA-21, 12Z cells were plated in triplicate to 70% confluence. These cells were treated with 10ng/ml of IL-6 or vehicle for 6, 12, 24 and 48 h following which RNA and protein were isolated. Each experiment was repeated three times. Quantitative RT-PCR was performed to analyze the expression of miRNA-21, the inflammatory response and expression of fibrosis related genes. Overexpression of microRNA-21 in 12Z cells resulted in an increase in the expression of collagens (COL1A1, COL1A2 and COL5A1) suggesting that miRNA-21 may contribute to progressive fibrosis by increasing collagen expression during lesion development. Western

Blot analysis also confirmed the increase in TGF- $\beta$  in the overexpressed cells. In addition, treatment of 12Z cells with IL-6 increased the expression of miRNA-21 suggesting regulation by IL-6. This study suggests that the upregulation of miRNA-21 in the endometriotic epithelial cells (12Z) is associated with the increased expression of collagen related genes, which may play a role in the development of fibrosis. These cells also showed an increase in TGF- $\beta$ , an EMT inducer, which was shown in our previous baboon studies to be correlated with the extent of fibrosis and pSMAD staining. Furthermore, the increased levels of IL-6 triggered the overexpression of miRNA-21 suggesting that IL-6 regulates the expression of miRNA-21 to upregulate TGF- $\beta$  to promote lesion development. (Supported by RO1HD083273 and T32HD087166).

**Serine, a Likely Component of One-Carbon Metabolism in Oocytes, is Transiently Transported During Meiotic Maturation.** Jenny Han Zhang, Megan Meredith, and Jay Baltz

The epigenome carries vital information for development, and disrupting the establishment of epigenetic marks can adversely affect the health of embryos. A major epigenetic mark that contributes heavily to gene regulation is DNA methylation. Global erasure and re-establishment of DNA methylation occurs once during gametogenesis, and again in the blastocyst around the time of implantation, when the initial embryonic epigenome is established. An adequate methyl pool is required to support DNA re-methylation. The folate cycle is the principal source of the methyl pool used by DNA methyltransferases. Since serine is the main one-carbon donor into the folate cycle, we were interested in profiling the transport of serine into oocytes and identifying the responsible transporter(s). Using radiolabeled [3H]serine, we measured uptake of serine as a function of time throughout meiotic maturation of mouse oocytes. We did not detect serine uptake into fully-grown oocytes before meiotic maturation. However, serine transport developed soon after oocytes were released from meiotic arrest and persisted for much of first meiotic metaphase. Serine transport was then lost and was absent in mature eggs. The serine uptake rate was highest during the 4 hours following germinal vesicle breakdown (resumption of meiosis), ranging between 0.04 and 0.07 fmol/oocyte/min. At 4 hours, where the transport rate was both high and consistent among measurements, we carried out a competition assay with the substrates of known transporters of serine to identify candidate transporters. Substrates diagnostic for amino acid transport systems B<sup>0,+</sup> and b<sup>0,+</sup> as well as classical systems A and GLYT1 did not affect uptake of [3H]serine, while excess alanine, cysteine, and leucine in media nearly eliminated [3H]serine uptake into oocytes. Serine uptake was also measured with and without sodium (Na<sup>+</sup>) in the external medium, since amino acid transport has classically been categorized based on sodium-dependent or -independent activity. Labeled serine transport was eliminated in sodium-free media. These measured transport characteristics indicated that the system ASC variant ASCT2 (SLC1A5) or several members of the System A/N (SLC38) family may be candidates for the transporter of serine in oocytes during meiotic maturation. Quantitative RT-PCR is being carried out to help determine the molecular identity of the transporter in oocytes. Further study of serine transport in oocytes may give insight into the formation of the methyl pool needed for establishing correct epigenetic marks for the healthy development of eggs and embryos. Thus far, our investigations have revealed a transient activation of serine transport as an unexpected feature of mouse oocyte maturation. Supported by Canadian Institutes of Health Research Operation Grant MOP 97972.

**Serum miRNA's as Clinical Markers of Endometriosis.** Victoria E. Turpin, Sanjay K. Agarwal, and Warren G. Foster

Because of cost, invasiveness and delay in diagnosis using laparoscopy to diagnose endometriosis, the search for a minimally invasive diagnostic marker of endometriosis remains a high clinical and research priority. Recent results suggest that measuring circulating miRNA is a promising avenue that requires further investigation. However, replication across different populations and potential differential expression across the menstrual cycle remains to be elucidated. Therefore, the objective of this study was to investigate several target serum miRNAs previously shown to be differentially expressed in women with endometriosis compared to healthy controls and examine the effect of menstrual cycle stage in women with and without endometriosis. In this case-control study, informed written consent and serum samples were collected from women (n=134) undergoing laparoscopic surgery for endometriosis and other routine gynecological procedures according to an approved institutional ethics review board protocol (12-083T). The presence or absence of endometriosis was confirmed using the combination of operative and pathology reports. Menstrual cycle stage was determined via endometrial biopsy obtained at the time of laparoscopy. miRNA was extracted from the serum of women with endometriosis (n=60), women with endometriosis receiving hormonal treatment for ovarian suppression (n=43) and controls (n=31). miR-9, -17, -20a, and reference gene expression were quantified using qPCR. Differences in target miR expression in the menses, proliferative, and secretory stages of the menstrual cycle were determined using one-way ANOVA. Differences in expression between cases and controls were determined using unpaired t-tests. A p value of 0.05 was considered significant for all statistical procedures. miR-9, -17, and -20a expression was unaffected by menstrual cycle stage in women with endometriosis ( $p = 0.611$ ,  $0.660$ , and  $0.974$ ) and the control ( $p = 0.550$ ,  $0.780$ , and  $0.798$ ) group, respectively. In women with endometriosis, circulating concentrations of miR-9 ( $p = 0.233$ ), miR-17 ( $p = 0.442$ ) and miR-20a ( $p = 0.178$ ) expression was non-significantly lower in comparison to controls. In contrast to women with endometriosis, miR-9 ( $p = 0.240$ ), miR-17 ( $p = 0.542$ ) and miR-20a ( $p = 0.399$ ) expression was non-significantly higher in the serum of women with endometriosis receiving ovarian suppression compared to the control group. IN conclusion, serum miR-9, -17, and -20a were unaffected by menstrual cycle stage. In contrast to previous findings serum miRNAs examined in our study population were not differentially expressed in women with endometriosis compared to a control population. We speculate that divergent results in miRNA studies may arise from differences in characteristics of the study population examined, methods employed, and the inherent heterogeneity of the disease arising from different disease stages and lesion types.

Funding for this study was provided by the Canadian Institutes of Health Research (MOP142230).

**Protein Profile During Placentome Maturation in Dairy Cows.** Contreras D. A., Salgado-Hernandez E. G., González-Lozano M., Valdez-Magaña G., and Guerrero-Netro H. M.

Placenta retention is a problem that affects around 20% of dairy cattle. In ruminants, the placentome is responsible for connecting the uterous with the placenta. Each placentome is formed by fetal cotyledon and a maternal caruncula. During parturition, the placentome requires changes in protein expression, such as collagenases and metalloproteinases. These changes in protein expression are known as placentome maturation and result in the expulsion of the placenta; However, the mechanisms that take

place during placentome maturation remain unknown. The objective of this study was to elucidate the mechanisms involved during placentome maturation.

The animal welfare and ethics committee of FMVZ UNAM approved all experiments. Placentomes were collected from Holstein cows that presented normal placenta expulsion (up to 12 hrs) or placenta retention. Samples were stored in RIPA buffer containing phosphatase inhibitor and protease inhibitor. Protein concentration was determined using Bradford assay, 50µg of protein was used for Mass spectrometry (Thermo Scientific Q Exactive Orbitrap Mass Spectrometer). The results were analyzed by Thermo Scientific Proteome Discoverer software 2.1 along FASTA UniProtKB/Swiss-Prot databases.

Mass spectrometry identified 5 significantly up-regulated and 5 downregulated proteins during placenta retention. The up-regulated proteins included fetuin-A, globin-1, apolipoprotein-a1, sterile  $\alpha$  motif domain cloning 7, and tyrosine 3-monooxygenase. These proteins seem to play a role during inflammatory process and apoptosis. On the other hand, the down-regulated proteins included: globin C1 and A1, Serotransferrin, alpha 1 acid glycoprotein, alpha 2-HS-glycoprotein. These down-regulated proteins are involved in the formation of hemoglobin, oxygen transport and in the cholesterol reverse transport. These results to the best of our knowledge are the first to demonstrate different pathway activation during placenta retention, further work is required to assess the signaling pathways involved during placentome maturation.

This work was supported by FMVZ-UNAM-MEXICO.

### **Bone Morphogenetic Factor-2 (BMP2) or Estradiol-17 $\beta$ (E2) Facilitates the Differentiation of Ovarian Somatic Cells into Granulosa Cells in the Hamster.** Prabuddha Chakraborty and Shyamal K. Roy

During female gametogenesis, oocyte development is supported by surrounding somatic cells (SCs). The initial stage of follicle development starts with the formation of primordial follicles (PF) at either fetal or postnatal life in mammals. It has been suggested that established primordial follicle reserve, and dynamic small antral follicle reserve are linked, and a decrease in the size of the established follicle reserve reduces the size of the small antral follicle pool, thus affecting the development of ovulatory follicle(s) and fertility. The communication between the oocytes and surrounding SCs plays an important role in ovarian folliculogenesis. Earlier we have shown that estradiol-17 $\beta$  (E2) as well as BMP2 promotes PF formation in the hamster. Formation of PF requires oogonia to oocyte transition and either concurrent or tandem differentiation of SCs into granulosa cells (GC). However, it remains unclear whether oogonia to oocyte transition was sufficient to induce SC differentiation or the action of ovarian factors, such as BMP2 or E2 is necessary for SC differentiation into granulosa phenotype. The objective of the present study was to determine if BMP2 or E2 would facilitate SC to GC differentiation well after the formation of the oocytes. Hamsters were used according to UNMC IACUC and USDA guidelines.

To address the objective, we cultured 15-day old (E15) fetal hamster ovaries from C0 through C8 where C1 corresponded to 24h culture and C8 corresponded to postnatal day 8 (P8) when PF first appear in vivo in the ovary. BMP2 (50ng/ml) or E2 (1ng/ml) was administered to culture on C6, when small percentage of low-intensity FOXL2 positive cells begin to appear. For some groups, E2 was administered from C0-C8 and BMP2 was administered on C6 or E2 plus BMP2 were added on C6. In hamsters, oogonia to oocyte transition is completed by P4 and C4. Therefore, factors affecting PF formation were expected

to facilitate SC differentiation on C6 independent of oocyte formation. Control cultures received no exogenous factor. Ovaries were retrieved on C6 (for control only), C7 or C8, and processed for immunofluorescence detection of FOXL2, as a potential marker for GCs, MVH and cleaved-caspase 3. The percentage of FOXL2 positive SCs in ovary sections was determined. There were three E15 fetuses for each group. The percentage of low-intensity FOXL2 positive cells was low on C6 and small, but noticeable increase was observed on C7 as expected. However, BMP2 or E2 alone or together significantly increased FOXL2 positive cells with robust expression. E2 effect was suppressed by ICI182,780 (0.1M) whether added from C0 or C6. These results suggest that BMP2 or E2 facilitates the differentiation of SCs into GCs to make GC available for oocyte-GC assembly. Based on these findings, it stands to reason that endogenous BMP2 or E2 facilitates SC to GC transition for PF formation.

### **Interleukin-6 (IL-6) Activates NOTCH1 Signaling Pathway Through E-Proteins in Endometriotic Lesions.**

Yong Song, Ren-Wei Su, Niraj R. Joshi, Tae Hoon Kim, Samantha Bond, Erin Vegter, Bruce A Lessey, Jae-Wook Jeong, and Asgerally T. Fazleabas

Endometriosis is an inflammatory disease. The pathophysiology of endometriosis is still unknown often due to the delay between the onset of symptoms and diagnosis of the disease. The Notch signaling pathway, via four transmembrane receptors (Notch1-4) plays an important role in diverse cellular functions such as proliferation, differentiation and survival. We have observed that NOTCH1 can actively promote endometriotic lesion development in both the baboon and in the NOTCH1 intracellular domain (N1ICD) overexpression mouse model of endometriosis. IL-6 is increased in peritoneal fluid (PF) of women with endometriosis and it has been shown to induce NOTCH1 through E-proteins including E2A and HEB in the thymus and in cancer development. Based on the previous findings, the objective of the present study is to understand the role of E-proteins in inducing NOTCH1 expression under the regulation of IL-6 in the context of pathophysiology of endometriosis. Our results showed that mRNA of E2A and HEB was up-regulated in ectopic endometrium (ECE) compared with eutopic endometrium (EUE) in both women with endometriosis and our baboon model of endometriosis; E2A and HEB were both positively correlated with NOTCH1 expression. We further found that E2A, HEB and NOTCH1 were all significantly up-regulated in glandular epithelium (GE) of ECE compared to EUE. Then, NOTCH1 expression was analyzed in human endometriotic epithelial cells (12Z) following IL-6 (10ng/ml) treatment: our data proved that treatment of 12Z cells with IL-6 can significantly induce expression of NOTCH1 for 24 hours, as well as E2A and HEB, the two potential mediators of IL-6 regulating NOTCH1. In order to further study the regulation of E2A and HEB on NOTCH1 expression, siRNA mediated inhibition of E2A or HEB was used on 12Z cells following IL-6 treatment. But only HEB knockdown in 12Z cells was able to abolish the induction of NOTCH1 by IL-6. NOTCH1 was identified as a direct downstream target gene for both E2A and HEB in 12Z cells by chromatin immunoprecipitation. In addition, following IL-6 treatment for 24h, binding efficiency of both E2A and HEB is significantly higher at positions of the predicted E2A binding sites (-2106 to -2097) and the HEB binding sites (-269 to -259) on the NOTCH1 promoter. Finally, in the *Pgrcre/+Rosa26mT/mG* mouse model of endometriosis, mice (n=3) treated with IL-6 (5µg/kg, every 3 days for 2 weeks), showed significantly more and larger ectopic lesions along with increased expression of E2A, HEB and NOTCH1 in GE of the lesions compared with control group(n=3). In conclusion, our study suggests that IL-6 promotes NOTCH1 expression through E-proteins in ectopic glandular cells and could play an important role in the early endometriotic lesion development in endometriosis. This research was supported by NIH HD042280 to ATF.

**Effects of Past Exposure to Environmental Chemicals on Future Generations of Medaka Fish.** Ramji Bhandari, Jacob Cleary, Albert Thayil, Frederick vom Saal, and Donald Tillitt

Health effects of past exposure to environmental chemicals on current and future generations is currently a topic of interest in the scientific community as the chemicals that were once in the environment do not exist anymore, but their effects are being carried by current generations in the form of adverse health conditions and may be inherited by future generations. Hence, it is important to develop the tools that can identify the nature of the past exposure and at the same time can reliably predict future consequences, particularly with regards to human and ecosystem health. Given that there is an association between epigenetic modifications and past exposure to environmental chemicals, it is possible that epigenetic biomarkers may serve as useful tools to mitigate the past exposure related health issues. Our laboratory is using comparative model (fish and mice) to identify common epigenetic biomarkers of the past exposure to chemical contaminants. We have found that bisphenol A (BPA), ethinylestradiol (EE2), and atrazine (ATZ) do not cause immediate phenotypic abnormalities at adulthood because of a brief embryonic exposure, but can still induce transgenerational reproductive impairment in the third and fourth generations. We also have found that these chemicals induce differential DNA methylation profile (epimutations) in the germ cells and these epimutations are transferred to somatic cells in the third generation. In my talk, I will discuss some of our findings that demonstrate transgenerational reproductive impairment in future generations and associated epigenetic modifications induced by past embryonic exposure to BPA, EE2, and ATZ.

**Adar1 A-to-I RNA Editing Alters Mrna Stability in Oocytes.** Pavla Brachova, Nehemiah S. Alvarez, Xiaoman Hong, Kailey A. Vincent, Keith E. Latham, and Lane K. Christenson

Fully grown mammalian oocytes and eggs are transcriptionally quiescent, and thus have a unique RNA milieu in which cellular processes depend on post-transcriptional regulation. RNA editing of adenosines into inosines (A-to-I) by adenosine deaminases acting on RNA (ADARs) is a common post-transcriptional gene regulatory mechanism, yet it has not been systematically studied in oocytes. We performed a genome-wide RNA editing analysis in pools of transcriptionally active growing oocytes from postnatal day 12 (PND12) mice (n=3), fully grown germinal vesicle (GV) oocytes (n=3), and transcriptionally quiescent metaphase II (MII) eggs (n=7). We identified an abundance of A-to-I editing of mRNA transcripts in GV oocytes ( $3,207 \pm 117$  transcripts per sample; Mean  $\pm$  SEM) and MII eggs ( $3,003 \pm 290$ ), with significantly fewer levels in PND12 immature oocytes ( $733 \pm 49$  edited transcripts/sample) ( $p < 0.05$ , one-way ANOVA). This was consistent with increased ADAR1 transcripts and protein in GV oocytes and MII eggs, compared with PND12 oocytes. Compared to somatic tissues, oocytes exhibited a distinct pattern of RNA editing, with a high proportion of RNA edits occurring in coding regions. These edits resulted in nucleotide substitutions that were enriched at the third nucleotide of the codon (wobble position) and altered codon usage. Codon usage can affect mRNA stability and translation efficiency, and RNA editing of the six most frequently edited codons was associated with unstable transcripts in GV oocytes and MII eggs. ADAR1 RNA editing may affect overall mRNA stability through editing of codons. To examine the functional role of ADAR1 in mouse oocytes, we crossed ADARFL/FL mice with ZP3-Cre mice to generate oocytes deficient in ADAR1-mediated RNA editing. After mice were administered PMSG and hCG (2.5 IU), ADARFL/FLZP3-Cre female mice ovulated at normal levels, however embryos generated after timed breeding to WT C57B/6 males had delayed entry into 2-cell and 8-cell stages.

Timed breeding resulted in the recovery of 63% of 2-cell embryos from control mice, while ADARFL/FLZP3-Cre mice produced 24% ( $p < 0.05$ , X2 test;  $n=3$ ). Embryos flushed from the oviducts of control mice ( $n=2$ ) were 97% at the 8-cells stage, while ADARFL/FLZP3-Cre mice ( $n=2$ ) had 28.5% at this stage. In summary, we provided evidence in support of a previously unreported phenomenon of selective ADAR1 editing at the codon wobble position, and mice with deficient ADAR1-RNA editing in oocytes had increased numbers of delayed and degenerate embryos. Editing of gene transcripts specifically at the wobble position has the potential to fine tune post-transcriptional gene regulation through altered codon usage, and ongoing studies will examine the importance of RNA editing for early embryo development.

**Ovarian-Dependent, Germ Cell-Independent Control of Metabolic and Immune Function and Longevity in Post-Reproductive Female Mice.** Jeffrey Mason, Tracy Habermehl, Kyleigh Tyler, McKenna Walters, and Kate Parkinson.

Major hallmarks of the menopausal transition include chronic inflammation, dyslipidemia and impaired glucose tolerance. Our preliminary and published data show that replacement of senescent ovaries in postreproductive mice with young ovaries extends longevity and health and ameliorates menopause-associated dyslipidemia, impaired glucose tolerance and chronic inflammation. However, the factors responsible for this ovary-dependent enhancement of health remain unknown. We hypothesized that this phenomenon was driven by germ cell-stimulated ovarian hormone production from the new ovaries. Our objective here was to determine if removal of germ cell influence would alter ovarian-dependent extension of life and health span. To test this hypothesis, we chemically depleted germ cells from young ovaries prior to transplantation. At 28 days of age, ovary-donor mice received daily intraperitoneal injections of 160mg/kg 4-vinylcyclohexene diepoxide for 20 days to deplete germ cell-containing follicles. At 65 days of age, germ cell-depleted ( $n=10$ ) and intact (germ cell-containing;  $n=10$ ) ovaries were collected from donor mice, and transplanted to postreproductive (13-month-old) virgin CBA/J mice. At 19 months of age (6 months post-transplantation), samples were collected and assayed. Data were analyzed with two-factor ANOVA and a Tukey-Kramer post-hoc test was used to determine difference between groups. Mice that received young, germ cell-depleted ovaries lived significantly longer than mice that received germ cell-containing ovaries, measured as days past surgery (371d vs. 287d, respectively, a 29% increase). In addition to extended life span, mice that received young, germ cell-depleted ovaries also demonstrated decreased circulating total cholesterol and triglyceride levels, improved glucose tolerance and improved immune function. Compared with age-matched controls, total cholesterol was decreased 26%, triglyceride decreased 43% and glucose tolerance improved 22%. Immune function was assessed by T-cell subsets (CD4+ central naïve-to-memory T-cell ratio increased 57%) and pathological inflammation (severity of inflammation was decreased to 8% of that seen in age-matched controls). Importantly, these improvements were no different than the metabolic and immune function improvements demonstrated by postreproductive mice that received young, germ cell-containing ovaries. The beneficial effects of dietary restriction on glucose and lipid metabolism in intact female rodents do not appear in ovariectomized rodents, supporting a central role for the ovary in female metabolic health. Naturally-menopausal women possess a health advantage over surgically menopausal women, suggesting that the ovary provides a health advantage, independent of active germ cells. In worms and flies, depletion of gonadal germ cells can significantly extend longevity and health. These effects are dependent on the retention of the somatic gonad. We propose that gonadal somatic

cells strive to facilitate germline transmission by preserving the somatic health of the organism, thereby positively influencing health and longevity. Future work will include identification of a potentially evolutionarily conserved, germ cell-independent molecular mechanism that contributes to the ovarian tissue-dependent extension of health and life span. In conclusion, germ cell depletion enhanced the longevity-extending effects of the young, transplanted ovaries and, as with germ cell-containing ovaries, decreased the severity of chronic inflammation, dyslipidemia and glucose intolerance. This research was supported by Utah State University, School of Veterinary Medicine, Department of Animal, Dairy and Veterinary Sciences.

**Lipopolysaccharide Reduces Estradiol Secretion by Bovine Granulosa Cells of Small and Medium Size Follicles.** Mackenzie J. Dickson and John J. Bromfield.

Estradiol production is integral to the success of a growing follicle. Perturbations to the follicular environment, including altered estradiol production can alter the oocyte's fate. Uterine infections are common in post-partum dairy cows and influence the ovarian environment. The pathogen-associated molecular pattern, lipopolysaccharide (LPS), accumulates in follicular fluid of cows with uterine infection and stimulates an innate immune response, altering the local environment. Granulosa cells isolated from large follicles decrease estradiol secretion and aromatase expression in response to LPS; however, the mechanism of LPS regulation of estradiol production is yet to be determined. Our objective was to elucidate the molecular pathways activated by LPS which result in reduced granulosa cell estradiol production. Bovine granulosa cells were isolated from small and medium sized follicles (0.05). Under these culture conditions, LPS effected estradiol secretion at high doses, while expression of selected estradiol regulators were unaffected in bovine granulosa cells from small or medium sized follicles. These data suggest LPS does impact steroidogenesis in the growing follicle, yet the mechanism is still ambiguous. Further work investigating other upstream regulators of estradiol production is still needed. Supported by the Eunice Kennedy Shriver NICHD R01HD084316.

**Potential Involvement of Activin a in Development of Fibrosis in Chronic Testicular Inflammation by Upregulating Fibrotic Genes in Peritubular Cells and Fibroblasts.** A. Christine Kleinert, Nour Nicolas, Sudhanshu Bhushan, Eva Wahle, Daniela Fietz, Martin Bergmann, Kate A. Loveland, Andreas Meinhardt, Mark P. Hedger, and Monika Fijak

Infertility is a significant medical problem worldwide. Studies indicate that lymphocytic infiltration and immune deposits are present in approximately 10% of idiopathic male infertility cases, with fibrosis being a common feature. Experimental autoimmune orchitis (EAO) in mice reflects this immunopathology, but the specific intratesticular cells responsible for production of extracellular matrix components (ECMC), leading to fibrosis in the EAO testis, are unknown. Resident fibroblasts or the myoid peritubular cells (PTC) are potential sources. Activins are members of the transforming growth factor- $\beta$  superfamily that regulate cell growth and differentiation, and are fundamental regulators of fibrosis and inflammation in various tissues. In the male reproductive tract they control spermatogenesis and steroidogenesis under physiological conditions, but activin A levels increase substantially during the development of EAO. However, it is not known whether activin A is directly involved in the testicular fibrosis observed in EAO.

In order to investigate the pro-fibrotic role of activin A and potential cellular origins and regulation of ECMC-producing cells in EAO, we measured fibrotic gene expression by qRT-PCR and Western blot in PTC from 21 day-old mice and NIH 3T3 mouse fibroblasts treated with human recombinant activin A (25 and 50 ng/ml), the activin-binding protein, follistatin-288 (FST288; 100 ng/ml), or a combination of both. Treatment with activin A increased the level of fibronectin mRNA, and production of collagen type I and fibronectin by both PTC and 3T3 fibroblasts. Activin A also increased alpha-smooth muscle actin mRNA and protein expression in 3T3 fibroblasts, while collagen type IV mRNA levels were significantly upregulated in PTC. FST288, a potent antagonist of activin A, significantly inhibited these effects.

Also, activin A concentration was measured in supernatants of Sertoli cells from 21 day-old mice in response to treatment with TNF (25 ng/ml and 50 ng/ml) and FST288 (100 ng/ml) by ELISA. While TNF treatment resulted in a significant increase of activin A, FST288 treatment led to reduction of activin A production. These findings reveal that Sertoli cells have a basal expression of activin A under physiological conditions. Since TNF is elevated during the course of EAO, these results also indicate an importance of the extent of activin production by Sertoli cells in response to TNF to the outcome of orchitis.

Consistent with the data from our animal model of EAO, we also found an increase of collagen and fibronectin deposition and an upregulation of activin A (*Inhba*) mRNA levels in human testicular biopsies with lymphocytic infiltrates and impaired spermatogenesis, whereby *Inhba* levels positively correlate with the increase in total collagen, fibronectin deposition and severity of fibrosis in these patients. These data indicate that both resident fibroblasts and PTC may contribute to the progression of testicular fibrosis under activin A control. Hence, we propose that exploring the use of activin antagonists as therapeutics may be beneficial in limiting fertility impairment in these patients.

**Towards a Better Understanding of Post-meiotic DNA Double-Strand Breaks Formation.** Tiphonie Cavé, Marie-Chantal Grégoire, Marc-André Brazeau, and Guylain Boissonneault

The paternal inheritance of de novo mutations have been linked to neurodevelopmental disorders. Although meiotic recombination allows for the reshuffling of alleles and independent assortment of chromosomes, the genetic consequences of the post-meiotic maturation of the haploid male gamete are yet unknown despite an important surge in DNA double-strand breaks (DSBs) observed during the process. Meiosis in the fission yeast, *Schizosaccharomyces pombe*, share similarities with that of male mammals and we have observed post-meiotic DNA DSBs during sporulation pointing to the highly conserved nature of this phenomenon and a powerful genetic model to study the underlying molecular mechanism of DSBs formation and repair. In-gel nuclease digestion assays combined with mass spectrometry allowed the identification of candidate endonucleases potentially involved in the process including Pnu1, the functional homolog of the mammalian Endonuclease G responsible for inducing DNA fragmentation during caspase-independent apoptosis and which we have shown to be expressed in elongating mouse spermatids coincident with the surge in DSBs. Generation of Pnu1 deletion mutant in the synchronizable Pat1-114 strain should yield information about its role in the post-meiotic DSBs formation as well as its contribution to meiosis and sporulation steps. Results from these experiments could provide evidences of post-meiotic DSBs contribution to mutagenesis and adaptation, and direct further analyses in mammalian spermatids. New hypotheses regarding the paternal origin of genetic

disorders can emerge from this work. Funded by the Canadian Institutes of Health Research (#MOP-136925).

**A Novel Approach of Modified Handmade Cloning in Porcine Embryos.** Eun Ji Lee, Dong Eon Kim, Kulatunga Dalawellage Chanuka, Beom Sik Kim, Kyu Hyeon Kim, Eun Young Kim, Ji Hye Lee, Ju Lan Chun, and Min Kyu Kim

Somatic cell nuclear transfer (SCNT) using micromanipulator is a traditional cloning technique and has been applied various researches during the last decades. However the micromanipulator is expensive and relatively longer training period is required to operate it efficiently. Handmade cloning (HMC) is an alternative cloning method in a simplified way compared to the traditional cloning. In this study, we suggested modified porcine handmade cloning (mHMC) as a new approach to clone porcine embryos. In previous report, a nuclear in an oocyte was removed by bisection method in HMC. Here, in mHMC, a nuclear was removed by the aspiration method by using a glass pipette, instead of bisection method. In this study, we investigated the efficiency of the enucleation method in mHMC by assessing the developmental competence of embryos in comparison with the traditional cloning method, SCNT. First, the efficiency of enucleation was evaluated based on the enucleation accuracy and oocyte survivability. In mHMC the enucleation accuracy was lower compared to those in SCNT ( $98.01 \pm 0.57$  vs  $83.83 \pm 2.47$ ), and the survival rate of oocytes was also lower in mHMC ( $96.50 \pm 0.84$  vs  $90.10 \pm 2.11$ , respectively). Next, the developmental competence was assessed. The cleavage rate of embryos showed no difference between mHMC and SCNT. However, the rate of blastocyst formation was significantly higher in mHMC group ( $13.53 \pm 2.08$  vs  $20.48 \pm 0.99$ ). In addition, the levels of apoptosis and ROS were investigated. The expressions of apoptosis-related genes and ROS showed no difference between groups. Finally, the relative expressions of mRNA of pluripotency genes (Oct4 and Sox2) and reprogramming genes (DNMT1 and DNMT3a) were evaluated. Although DNMT1 and DNMT3a were not differently expressed in two group, the expression of the pluripotent gene, Oct3 was significantly higher in mHMC. In conclusion, we showed that the efficiency of mHMC was comparable with SCNT in porcine embryos. Therefore, mHMC could be a suitable alternative technique to clone embryos in cost effective way compared to SCNT using the micromanipulator.

This work was supported by Korea Institute of Planning and Evaluation for Technology in Food, Agriculture, Forestry and Fisheries (IPET) through Technology Commercialization Support Program, funded by Ministry of Agriculture, Food and Rural Affairs(MAFRA)(816007-3)

**Effects of Exogenous Progesterone Administered to Ewes During the Pre-Implantation Period of Pregnancy on Fetal and Placental Growth in Late Gestation.** Katherine Halloran, Emily Hoskins, Kathrin Dunlap, Gregory Johnson, Michael C. Satterfield, Guoyao Wu, and Fuller W. Bazer

Sheep embryos develop into spherical blastocysts on Day 9, mature from spherical to tubular forms on Day 12-13, reach their filamentous stage by Day 14, and attach to the uterine luminal epithelium (LE) by Day 16-18. In a previous study, administration of progesterone (P4) to ewes during the first 9 to 12 days of pregnancy accelerated blastocyst development by Day 12 of pregnancy when progesterone (P4)-treated ewes had filamentous conceptuses while controls remained spherical. In that study, exogenous

P4 up-regulated expression of key genes in uterine epithelia responsible for secretion of proteins, including growth factors and expression of nutrient transporters. The molecules transported into the uterine lumen form histotroph, which is essential for conceptus survival. This study determined if exogenous P4-induced acceleration of blastocyst development during the peri-implantation period affects fetal-placental development on Day 125 of pregnancy. Suffolk ewes (n=40) were mated to fertile rams and assigned randomly to receive daily intramuscular injections of either corn oil vehicle (CO, n=20) or 25 mg progesterone in CO (P4, n=20). After breeding (Day 0), treatments began on Day 1.5 and continued through Day 8 of pregnancy. Ewes from each treatment group were hysterectomized on Day 125 of pregnancy. After separating the endometrium from the chorioallantois, sections of placentomes, caruncles, cotyledons, and endometrium were processed to assess expression of mRNAs and proteins. Plasma from maternal and fetal blood was analyzed for concentrations of P4 by RIA. Samples of allantoic and amniotic fluid were obtained for analysis of glucose, fructose, amino acids, and polyamines. Volumes of the fetal fluids were measured. Fetal parameters recorded included weight, crown-rump length, abdominal and chest circumferences, and sex. Placental measurements included weight, length, and number of placentomes. There was no difference in fetal growth nor placental growth due to treatment; however, placentae of single pregnancies were longer ( $P < 0.0001$ ) and had more placentomes ( $P < 0.0001$ ) than those in twin pregnancies. qPCR analysis showed differential expression of genes between P4 and CO treated ewes in endometrium and placentomes. Low affinity cationic amino acid transporter SLC7A2 mRNA increased ( $P = 0.0022$ ) in endometria of P4 treated ewes, while VEGFA and TUB were increased ( $P = 0.0242$ ) and decreased ( $P = 0.0089$ ), respectively, in single pregnancies. In placentomes, P4 treated ewes tended to have decreased ( $P < 0.10$ ) mRNA levels for ODC1. Expression of both ACTB and TUB mRNAs increased ( $P = 0.0019$ ) and ( $P < 0.0001$ ), respectively, in placentomes of P4 treated ewes. SDHA and GAPDH were used as control genes. There was no difference in concentrations of glucose in fetal plasma, allantoic, or amniotic fluid between treatment groups. This research was supported by Agriculture and Food Research Initiative Competitive Grant no. 2016-67015-24958 from the USDA National Institute of Food and Agriculture.

**Effects of Exogenous Progesterone During the Peri-Implantation Period of Pregnancy on Growth and Development of Ovine Conceptuses.** Emily Hoskins, Katherine Halloran, Kathrin Dunlap, Gregory A. Johnson, Michael C. Satterfield, Guoyao Wu, and Fuller W. Bazer

Treatment of early pregnant ewes with exogenous progesterone (P4) accelerates development and elongation of ovine conceptuses (embryo and associated placental membranes). This occurs by advancing down-regulation of P4 receptors to allow expression of genes by uterine epithelia that encode for secreted proteins and nutrient transporters responsible for accumulation of histotroph. Histotroph is essential for conceptus development during the peri-implantation period of pregnancy. This study was conducted to confirm that exogenous P4 administered during the pre-implantation period (Days 1.5 to 8) advances conceptus growth, development, and implantation to Day 12 of gestation. Additionally, this study determined how exogenous P4 affects enzymes involved in the classical (ornithine decarboxylase 1) and novel pathways (arginine decarboxylase and agmatinase) of conversion of arginine to polyamines. Suffolk ewes (n=40) were assigned randomly to receive daily intramuscular injections of either 25 mg P4 in 1 ml corn oil (P4, n=20) or 1 ml corn oil alone (CO, n=20) from Day 1.5 through Day 8 of pregnancy. Ewes from each treatment group were hysterectomized on Day 9 (n=10) or Day 12 (n=10) of pregnancy. Blastocysts were collected by flushing the uterus with 20 ml

of sterile phosphate buffered saline (pH=7.2). Photomicroscopy was utilized to capture images of all blastocysts and conceptuses for morphological analyses and volume measurements. Endometrial tissue from the uterine horn ipsilateral to the CL was collected and frozen for storage at -80°C for qRT-PCR analysis and adjacent tissue was fixed in OCT and frozen for immunofluorescence analyses. Tissues were also fixed in 4% paraformaldehyde for immunohistochemistry. Concentrations of P4 in plasma from ewes were determined by RIA. Concentrations of P4 were greater for D9 P4 than D9 CO ewes ( $p < 0.008$ ) and for D9 P4 than D12 P4 ewes ( $p < 0.0317$ ). There was no difference between D12 P4 and D12 CO ewes, indicating that circulating concentrations of P4 return to basal levels after approximately 36h. There was no difference in the volumes of blastocysts from D9 CO and D9 P4 ewes, but blastocyst survival (calculated by comparing number of corpora lutea to number of blastocysts obtained) was lower in D9 CO and D12 P4 than D12 CO ewes ( $p < 0.05$ ). Conceptuses from D12 P4 ewes were elongated, while all D12 CO conceptuses remained spherical at the time of necropsy. Glucose transporter SLC2A1 increased 3.5-fold in CO D12 ewes and 3.15-fold in D12 P4 ewes compared to D9 P4 ewes ( $p < 0.001$ ). Cationic amino acid transporter SLC7A1 increased 2.7-fold in CO D12 ewes and 2.15-fold in P4 D12 ewes compared to D9 P4 and D9 CO ewes ( $p < 0.002$ ). Expression of ODC1 mRNA was greater for D9 CO ewes than D9 P4, D12 CO, and D12 P4 ewes with a day x treatment interaction ( $p < 0.05$ ). ODC1 protein was more abundant for D9 CO ewes in endometrial luminal and superficial glandular epithelia and stromal cells. There was no effect of treatment on expression of mRNAs for ADC or AGMAT. This research was supported by Agriculture and Food Research Initiative Competitive Grant no. 2016-67015-24958 from the USDA National Institute of Food and Agriculture.

**Mammalian Cell-Free System for the Study of Mitochondria Inheritance.** Dalen Zuidema, Won-Hee Song, and Peter Sutovsky

Mitochondria and mitochondrial genes are exclusively inherited from mothers in most animals. This maternal mitochondrial inheritance is a conserved developmental mechanism which is not fully understood. It is known that this clonal inheritance pattern is ensured by the degradation of the paternal, sperm-borne mitochondria, shortly after fertilization. Male mitochondria are located in the midpiece mitochondrial sheath of the spermatozoa and degraded through a nuanced autophagic process known as the post-fertilization sperm mitophagy. Early research has shown that the ubiquitin proteasome system (UPS) plays a pivotal role here, but as the UPS degrades proteins one molecule at a time, it cannot be solely responsible for sperm mitophagy. Indeed, research from our lab has shown a synergistic effort between ubiquitin-binding receptors, SQSTM1 and GABARAP, and the proteasome-interacting ubiquitinated protein-dislocase VCP, during sperm mitophagy. To build upon this research, a better understanding of cofactors and substrates involved in these processes must be gained. Additionally, it is hypothesized that other branches of the autophagic pathway and their molecules may be involved in the process of sperm mitophagy. A key tool in the research arsenal that will be used to conduct this exploration is our novel mammalian cell-free system composed of demembrated boar spermatozoa and porcine oocyte extract. Our preliminary data demonstrated that the post-fertilization mitophagic events which take place in a zygote can be accurately replicated in such cell-free system. We have found that SQSTM1 from oocyte extracts binds to sperm mitochondria during sperm-oocyte extract coinubation and this binding is inhibited by the addition of anti-SQSTM1 antibodies. Species specificity of sperm mitophagy precludes the use of convenient frog egg extracts for mammalian studies. However, the porcine model is compatible with the cell-free system and the porcine oocytes are

relatively easy (compared to other mammalian models) to collect and mature in large quantities, which are need for the cell-free protocol. The main benefit that the cell-free system provides is the ability to observe thousands of spermatozoa, interacting with ooplasmic mitophagy receptors in a single trial, overcoming the limiting factor of one sperm per fertilized oocyte that can be observed using a monospermic IVF or ICSI protocol. Furthermore, we can incorporate protein tracers into the cell-free system in order to isolate, identify and investigate molecules involved in sperm mitophagy by proteomic approaches. Proteins of interest will be further studied using both IVF and ICSI protocols to fully understand the roles that they play in sperm mitophagy. We expect to find molecules which work in concert with SQSTM1 and GABARAP, as well as those involved in alternative autophagic pathways. Research supported by USDA-NIFA grants 2013-67015-20961 and 2015-67015-23231, and MU F21C Program (PS).

**Establishment of Transgenic Porcine Embryonic Stem Cell Lines for In Vitro Brain Tumor model.** Seon-Ung Hwang, Mirae Kim, Kiyong Eun, Gabsang Lee, Hyunggee Kim, and Sang-Hwan Hyun

Pigs are brain tumor models more suitable than mice. Because the pig's brain is larger than the mouse and has an anatomical structure that is more similar to humans. In this study, we are using a CreERT2 (Cre recombinase fused to a mutated ligand-binding domain of the human estrogen receptor) inducible system for the establishment of in vitro brain tumor model. First, we made a one vector constructs. It is a 2A peptide-dependent polycistronic expression construct carrying DsRed, SV40LT, and HrasV12 genes after CreERT2-associated recombination. Whether the introduction of the transgene was confirmed by PCR and fluorescence activated cell sorter. Somatic cell nuclear transfer (SCNT) was performed using the established transgenic (TG) cell line and then whole seeding was performed using SCNT blastocysts. As a result, two TG porcine embryonic stem (pES) cell lines were established. Both TG pES lines showed a primed form and showed bFGF-dependent properties. This is consistent with previously reported characteristics of pES cell lines. We confirmed the insertion of the brain tumor-inducing gene through PCR. Immunohistochemical staining showed that both cell lines express Oct4, pluripotent marker. Alkaline phosphatase (AP) stain results showed AP positive and embryonic bodies (EB) formation were also confirmed. In conclusion, we established an embryonic stem cell line of an in vitro brain tumor model through SCNT. Further studies are needed to confirm the teratoma formation.

This work was supported, in part, by a grant from the “National Research Foundation of Korea Grant funded by the Korean Government (NRF-2016R1D1A1B03933191, NRF-2017R1A2B4002546)”, “The Global Research and Development Center (GRDC) Program through the National Research Foundation of Korea (NRF) funded by the Ministry of Education, Science and Technology (2017K1A4A3014959)” and “Business for Cooperative R&D between Industry, Academy, and Research Institute funded Korea Small and Medium Business Administration in 2017 (Grants No. 2017020681010101)”, Republic of Korea.

**Functional Signaling and Gene Regulatory Networks Between the Oocyte and the Surrounding Cumulus Cells.** Fernando Biase and Katelyn Kimble

The maturation and successful acquisition of developmental competence by an oocyte, the female gamete, during folliculogenesis is highly dependent on molecular interactions with somatic cells. Most of

the cellular interactions identified, thus far, are modulated by growth factors, ions or metabolites. We hypothesized that this interaction is also modulated at the transcriptional level, which leads to the formation of gene regulatory networks between the oocyte and cumulus cells. We tested this hypothesis by analyzing transcriptome data from bovine single oocytes and the surrounding cumulus cells collected from antral follicles employing an analytical framework to determine interdependencies at the transcript level. We generated single-cell RNA-seq data for 16 bovine oocytes and RNA-seq data for the corresponding cumulus cells. We quantified the expression of 10,327, 10,471 genes in oocytes, and cumulus cells, respectively. We overlapped our transcriptome data with putative protein-protein interactions and identified 12,243 ligand-receptor pairs that can transduce paracrine signaling between an oocyte and cumulus cells. We determined that 499 ligand-encoding genes expressed in oocytes and cumulus cells are functionally associated with transcription regulation (FDR 0.85, FDR < 1 .8x10<sup>-5</sup>) patterns between oocytes and cumulus cells. Hundreds of co-expressing genes showed clustering patterns associated with biological functions (FDR < 0 .05) necessary for a coordinated function between the oocyte and cumulus cells during folliculogenesis (i.e. 'regulation of transcription', 'translation', 'apoptosis', 'cell differentiation' and 'transport'). Our analyses revealed a complex and functional gene regulatory circuit between the oocyte and surrounding cumulus cells. The regulatory profile of each cumulus-oocyte complex is likely associated with the oocytes' developmental potential to derive an embryo.

**Non-Invasive Procedures to Measure Male Spermatogenesis in Cancer Patients.** Lucy Pullan, Maria Carrillo, and Kenneth Campbell

Current methods to detect spermatogenesis in male cancer patients during or after chemo- or radiation therapy are invasive, expensive, or ill-suited to serial monitoring. This study focused on exploring possible use of urine sediment cells to provide a novel non-invasive, inexpensive alternative. Using buffer-washed, aldehyde-fixed sperm from volunteer donors, several means of staining and quantifying sperm with or without the presence of epithelial cells (similarly washed and fixed and obtained from volunteers) were evaluated. Serially diluted sperm suspensions stained with the DNA intercalating dye SYBR Green I, with fluorescein-labeled peanut agglutinin (PNA), or with a fluorescein-labeled mouse monoclonal antibody to the sperm surface protein Spag-1 all yielded graded responses with minimal cell detection levels of about 300-3000 sperm per well by fluorimetry. To decrease the limit of detection, especially in the mixed population of epithelial and sperm cells expected in urine sediments, pure and mixed populations of sperm and epithelial cells were also examined in a fluorescence activated cell sorter, FACS. In preparation for that examination, tests were run to see if mild sonication could be used to remove the tails of fixed sperm to make the cells more symmetrical and more optimal for cell separation in the FACS; ~80% of sperm lost tails but remained microscopically intact with up to 100-150 seconds of sonication. FACS runs employing fixed, unsonicated, unstained cells (using optical side scatter), or FITC PNA, or SYBR Green I stained cells showed good optical and flow cytometric separation of sperm, epithelial cells, and debris in multiple levels of cell mixture. Microscopy and early FACS runs of urine sediment samples indicate optimal FACS counting requires separation of sperm cells from epithelial cells and debris. Thus, affinity purification and enrichment of cell preparations, panning, on immobilized peanut agglutinin was also explored. PNA binds preferentially to carbohydrate sidechains containing galactosyl- $\beta$ (1-3)-N-acetylgalactosamine on cell surface proteins of spermatozoa. Immobilized PNA can therefore separate sperm cells from mature epithelial cells and debris; ~50%-80%

of sperm samples with 7,250-116,000 sperm per mL of PBS buffer can be recovered after panning in microtiter wells by incubating with 500 mM galactose. Released cells can be labeled with fluorescent PNA and the sperm cell density determined using fluorimetry or FACS. Samples tested have also included washed, fixed female epithelial cells from women who are not recently sexually active. These were evaluated in parallel with pure sperm or in admixtures. The collective results suggest that by using non-invasively collected, longitudinal, urine sediment samples prepared by preliminary purification on immobilized PNA, sperm counts can be inexpensively generated for pre- and post-treatment male cancer patients. When compared to population or pretreatment norms for similar men these counts may then be used to evaluate rate of loss or rate of recovery of spermatogenesis in male patients.

**Aberrant Corpus Luteum Development and Function in GnRH-II Receptor Knockdown Gilts.** Amy T. Desaulniers, Rebecca A. Cederberg, and Ginger A. Mills, Brett R. White

The second form of GnRH (GnRH-II; His5, Trp7, Tyr8) and its receptor (GnRHR-II) are produced in only a few mammals, including the pig. Paradoxically, however, their interaction does not mediate the production of LH or FSH. Instead, GnRH-II and its receptor have extra-pituitary reproductive functions. We demonstrated that both are abundantly produced within swine testes and their interaction mediates testosterone production in an autocrine/paracrine manner. However, the function of GnRH-II and its receptor has not been evaluated in the female pig. To further study the role of GnRH-II and its receptor in pigs, our laboratory generated a GnRHR-II knockdown (KD) swine line. The objective of this study was to compare pubertal development, ovarian characteristics and steroidogenesis in GnRHR-II KD (n = 8) and littermate control (n = 7) gilts. Prepubertal animals were monitored for age and weight at puberty. During the third estrous cycle, blood samples were collected via jugular venipuncture at the onset of estrus (follicular) and 10 d later (luteal). Animals were euthanized 7 d after onset of their fifth behavioral estrus. Ovarian weight, ovulation rate and weight of each excised corpus luteum (CL) were recorded. Serum samples were subjected to high performance liquid chromatography tandem mass spectrometry to quantify concentrations of corticosteroids (11-deoxycorticosterone, 11-deoxycortisol, corticosterone, cortisol, cortisone, aldosterone), androgens (dehydroepiandrosterone, dehydroepiandrosterone sulfate, androstenedione, androsterone, testosterone, dihydrotestosterone), estrogens (estrone, 17 $\beta$ -estradiol) and progestogens (17 $\alpha$ -hydroxyprogesterone, progesterone). Age and weight at puberty, as well as estrous cycle length, did not differ between genotypes (P > 0.10). A line (GnRHR-II KD versus control) x phase (follicular versus luteal) interaction was detected for serum progesterone concentrations (P = 0.0341). In follicular samples, serum progesterone levels were not different between GnRHR-II KD and control females (P > 0.10). As expected, progesterone concentrations increased in luteal samples of females from both lines (P > 0.10) whereas ovulation rate was reduced in GnRHR-II KD compared with control gilts (14.1  $\pm$  0.7 versus 17.0  $\pm$  0.7 CL, respectively; P = 0.0123). However, CL weight was greater in GnRHR-II KD (347  $\pm$  13.7 mg) compared with control (277  $\pm$  13.7 mg) females (P < 0.0001); therefore, total CL weight tended to be reduced in transgenic gilts (P = 0.0958). Ultimately, these data suggest that GnRH-II and its receptor may regulate ovulation rate, CL development and progesterone production in gilts. Supported by USDA/NIFA AFRI-ELI predoctoral fellowship (2017-67011-26036; ATD) and AFRI (2017-67015-26508; BRW) funds.

### **Supplement of GDF8 During Porcine in Vitro Culture Enhanced SOX2 Expression in Blastocyst Stage.**

Junchul David Yoon, Eunsong Lee, and Sang-Hwan Hyun

Growth differentiation factor8 (GDF8) is the member of the transforming growth factor- $\beta$  which has been identified as a paracrine factor. Current studies, the GDF8 is detected in oviduct fluid and uterus which led us to suggest that the GDF8 may effect on preimplantation embryonic development and act paracrine role to correlate with successful late-blastocyst implantation. We investigated the effect of GDF8 supplement during porcine in vitro culture (IVC) derived from in vitro fertilization (IVF) embryo on specific gene transcription levels, and SOX2 and CDX2 protein expression in blastocyst (BL). Data were analyzed by one way ANOVA, followed by Tukey's range test. The experimental groups were as follows; control (0), 0.2, 2, and 20 ng/mL of GDF8 supplement group, respectively. At day 7 after IVC, more than expanded grade BL were selected and sampled. Using the achieved IVF BLs, the specific gene expression patterns were evaluated. In 0.2 group, the embryo development competence marker Pdna, Pou5f1 and Sox2 (1.81, 2.85 and 2.09 times, respectively), and cell junction assembly regulator Adam10, Adam17, Tjp1, Cdh1 (1.40, 1.98, 1.79 and 1.80 times, respectively) gene mRNA transcription levels were significantly increased compared with control. Moreover, pro-apoptotic factor Cas3 gene mRNA transcript levels were significantly decreased in 0.2 group than control (0.62 times). Furthermore, in the immune-stain result, the 0.2 supplement group showed significantly increasing SOX2 expressing cell number and SOX2 per CDX2 ratio than control. In conclusion, the supplementation of 0.2 ng/ml GDF8 during IVC significantly improved embryonic developmental potential via regulating embryo developmental competence markers and cell junction assembly regulator transcriptional levels.

This work was supported, in part, by a grant from "the National Research Foundation of Korea Grant funded by the Korean Government (NRF-2017R1A2B4002546)" and "Korea Institute of Planning and Evaluation for Technology in Food, Agriculture, Forestry and Fisheries (IPET) through Advanced Production Technology Development Program, funded by Ministry of Agriculture, Food and Rural Affairs (MAFRA) (Grant number: 115103-02)", Republic of Korea.

**Hypoxic Culture of Donor Fibroblasts for Use in Somatic Cell Nuclear Transfer Improves in Vitro Development and Gestational Day 35 Survival of Cloned Pigs.** Bethany R. Mordhorst, Joshua A. Benne, Raissa F. Cecil, Kristin M. Whitworth, Melissa S. Samuel, Lee D. Spate, and Randall S. Prather.

Preimplantation embryos exhibit characteristics of a Warburg Effect (WE)-like metabolism. We hypothesized that hypoxia could drive fibroblast metabolism to become more WE-like; and thus after Somatic Cell Nuclear Transfer (SCNT) may have improved nuclear reprogramming and better subsequent in vitro embryonic development and in utero survival. Fetal fibroblasts were cultured for one week in either 5% oxygen (CON) or a decreasing oxygen gradient (HYP; 5%: 2 d, 2.5%:1 d, 1.25%: 4 d) prior to use in SCNT. Sequencing of mRNA from 4 replicates of CON and HYP fibroblasts revealed differential expression of 51 genes determined by fitting the read counts to a generalized linear model implemented in edgeR-robust. Functional annotation established that hypoxia activated upregulation of 7 genes for glycolytic pathway enzymes in addition to 12 other well-characterized hypoxia-response genes. For statistical analyses, at least three biological replicates were collected in each experiment. Data were assessed for normality via Shapiro-Wilk test then analyzed for main effect of treatment (and cell line where applicable) using a MIXED model procedure in SAS software with Tukey-adjusted P-values. Numbers shown are generated least squared means and standard errors. Scanning electron microscopy

and flow cytometric analysis demonstrated ( $P < 0.01$ ) that HYP fibroblasts had an increased number of mitochondria compared to CON (14.0 vs.  $10.7 \pm 0.3$  mitochondria per cell monolayer section;  $1097.3$  vs.  $668.8 \pm 22.9$  AU MitoTracker green fluorescence). In experiment 1 we tested in vitro development of clones derived from the cell line used in cytometric analyses. In experiment 2, two different cell lines were treated as CON or HYP, used for SCNT, and transferred to 3 pairs of surrogate gilts. Each cell line and treatment combination was represented between the uteri of the pair in a complete block-type fashion. Subsequently, d 35 fetuses were collected and genotyped to determine which treatment, HYP or CON had survived in utero. In experiment 1 we determined that blastocysts from HYP donors contained more cells than CON ( $P < 0.01$ ;  $52.7$  vs.  $35.1 \pm 2.9$  cells). In experiments 1 and 2 a higher percentage of embryos from HYP fibroblasts formed blastocysts than CON ( $P \leq 0.01$ ; 1:  $34.5$  vs.  $21.8 \pm 2.3\%$ ; 2:  $55.4$  vs.  $47.0 \pm 1.9\%$ ). Moreover in both experiments clones from HYP fibroblasts had formed blastocysts at an earlier timepoint (by day 5;  $P \leq 0.02$ ) than those from CON fibroblasts (1:  $28.2$  vs.  $17.4 \pm 2.2\%$ ; 2:  $32.6$  vs.  $24.1 \pm 2.3\%$ ). In experiment 2, an equal number of blastocysts from each treatment ( $n = 18$  to  $23$ ) were transferred to surrogates and 2 of 6 gilts became pregnant. Survival probability as calculated by number of d 35 fetuses collected from total number of blastocysts transferred to the 6 surrogates indicated that a higher percentage of HYP-derived clones survived compared with those from CON ( $P = 0.04$ ;  $8.4$  vs.  $2.6 \pm 2.0\%$ ). Currently we are awaiting results from more embryo transfers to validate our findings and further investigations are underway to determine the underlying biological basis of these results.

**Recombinant Growth Differentiation Factor 9 and Bone Morphogenetic Protein 15 Regulate Canine Oocyte Meiotic Resumption and Cumulus Expansion.** Dong Eon Kim, Kang Sun Park, Kuk Bin Ji, Eun Ji Lee, Kulatunga Dalawellage Chanuka, Gyeong Yeob Kim, Ryoung Eun Kim, Eun Young Kim, Ji Hye Lee, Tae Young Kil, Ju Lan Chun, and Min Kyu Kim

Post-ovulatory maturation, prolonged communication between oocyte and cumulus cells are unique characteristics of canine reproductive physiology which lead to the low efficiency of in vitro maturation (IVM), as main oocyte secreted factors (OSFs), growth differentiation factor 9 (GDF9) and bone morphogenetic protein 15 (BMP15) could be closely related to the unique reproductive process in canine. In this study, exogenous recombinant GDF9 and BMP15 were used during IVM of canine cumulus oocyte complexes (COCs). Results show that endogenous GDF9 and BMP15 were expressed in the COCs from luteal, anestrus and follicular phases, and the highest levels of GDF9 and BMP15 were detected in the anestrus and follicular phase, respectively. Exogenous recombinant GDF9 and BMP15 significantly improved the meiotic resumption rate and cumulus expansion index ( $P$

**Investigating the Effect of Acrylamide in the Male Reproductive Tract and the Impact on Future Generations.** Caitlin Chambers, Aimee Katen, Belinda Nixon, Simone Stanger, Brett Nixon, and Shaun Roman

Acrylamide is a toxicant that humans are chronically exposed to in carbohydrate rich foods cooked above  $120^{\circ}\text{C}$ . After exposure acrylamide is converted to glycidamide solely by the enzyme CYP2E1, a protein found within the male reproductive tract. In our previous studies we have chronically administered acrylamide via the drinking water to male mice at doses of  $0$ - $2$  mg/kg bw/day, including doses equivalent to human exposure, for periods up to 12 months. Using a modified version of the comet assay, we have established that such exposure leads to a time and dose dependent increase in

glycidamide adducts with the DNA of spermatocytes of exposed mice. Further, we investigated DNA damage in mature spermatozoa following chronic exposure to acrylamide and found increased levels of DNA damage in exposed males. We have also previously examined DNA damage in the mature spermatozoa of mice exposed to acute doses of acrylamide (25mg/kg/day for 5 days i.p.) during spermatogenesis and post-testicular transit. DNA damage was highest when sperm were exposed during epididymal transit or at the pachytene spermatocyte stage of spermatogenesis, which correlates with CYP2E1 expression, as determined by immunohistochemistry. As CYP2E1 is integral to the damaging effects caused by acrylamide exposure in the male reproductive tract, further investigations into CYP2E1 abundance is one key aspect of our current studies. It is established that the administration of CYP2E1 substrates results in increased abundance of the protein in multiple organs in the body. In our present studies, we find that acute administration of acrylamide (12.5 and 25 mg/kg/day for 5 days i.p.) or another CYP2E1 substrate, ethanol (0.5 and 1 g/kg bw/day for 5 days i.p.), leads to an increase in the abundance of CYP2E1 in the spermatocytes of exposed male mice. We found that acrylamide (25 mg/kg bw/day) induced CYP2E1 to 150% of control and ethanol increased CYP2E1 to 131% and 138% of control for 0.5 and 1 g/kg bw/day respectively, as assessed by immunohistochemistry. We have previously identified that chronic acrylamide administration in male mice, at a human relevant dose (1 µg/mL) for 6 months also results in an induction of the CYP2E1 protein within spermatocytes. Notably, this induction of CYP2E1 was inherited in the male offspring of acrylamide-exposed fathers, despite this generation having had no direct acrylamide exposure. This raises concerns for increased susceptibility of the F1 mice to acrylamide induced DNA damage. We are elucidating this with a second chronic acrylamide exposure of the male offspring of acrylamide-exposed fathers. Investigating these exposed F0 fathers we confirmed that our exposure regimen (3 months at 1 µg/mL) increased DNA damage in the sperm of acrylamide-exposed males (127% of control). To determine the effects of paternal acrylamide exposure on the susceptibility of the offspring we are conducting a comparison of our exposed and unexposed F1 generation.

**Distinct Expression of a Novel Transcript Governs the Survival of Chicken Primordial Germ Cells.** Bo Ram Lee and Jae Yong Han

The development of primordial germ cells (PGCs) and germ-line lineage is tightly controlled by the expression and functionality of germline specific-genes. To date, significant efforts have been made to elucidate the avian specific-mechanisms regulating germ cell fate for practical applications in the fields of avian biotechnology. However, only a small number of studies report on germline specific-genes expression for the purpose of describing critical functions to demonstrate the physiological status in chicken PGCs. Herein, we found a novel transcript on chicken PGCs through large scale gene expression data, in which it is composed of NLS and F-box like domain. The novel transcript was specifically upregulated in PGCs including the germ-line lineage in gonads in both male and female by both quantitative RT-PCR and in situ hybridization. The targeted RNA-interference knockdown for a novel transcript had significant effects on DNA double-strand breakage and subsequent severe apoptosis in germ cells in vitro and in vivo, indicating that primary role of it regulates the survival of chicken PGCs in response to DNA damage and safeguard apoptosis. Furthermore, we examined the proteomic analysis to gain the mechanistic insight into early events occurring after knockdown. Collectively, our results first time demonstrate that chicken PGCs display the specialized molecular mechanisms regulating survival and apoptosis in response to DNA damage and a novel transcript plays pivotal roles in the survival of

chicken primordial germ cells. Finally, knowledge of germline specific-genes in chicken PGCs will make a significant contribution to better understanding germ fate and its application to avian biotechnology as well as reproductive biology.

**Selection of the Optimal Time Point for Immature Oocytes Collection in hCG Only-Primed Mouse for in Vitro Maturation and Further Embryonic Development.** Sook Young Yoon, Min Ji Lee, Dong Hyuk Shin Jung Jae Ko, Woo Sik Lee, and Dong Ryul Lee

To overcome the risk of the ovarian hyperstimulation syndrome (OHSS) in patients have polycystic ovarian syndrome (PCOS) and to prepare emergency fertility preservation in patients undergoing anticancer treatment, several researchers have reported IVM of oocytes retrieved from ovaries exposed by only hCG priming. However, the maturation rate and the developmental potential of embryos from IVM oocytes are significantly lower than those of oocytes matured in vivo. Here, we investigated the optimal time point for immature oocyte collection at post hCG only injection for in vitro maturation, in vitro fertilization and blastocyst formation. Immature GV oocytes were collected from 25 days old B6D2F1 female mouse at 12hr, 14hr, 16hr or 24hr post hCG injection only. Oocytes were collected from antral or late secondary follicle by puncturing with 26 G needle. Collected oocytes were cultured in G2 medium with 10% FBS, FSH, estradiol, and hCG for 16 hr in vitro, and MII mature oocytes were examined in vitro fertilization with sperm from epididymis of same strain male mice or subjected intracellular zinc level measurement. Further embryonic development was investigated for 5 days from IVF. To examine ovarian follicular status, we estimated the numbers of primordial, primary, secondary follicle and antral follicle on ovaries with HE staining. There is no difference in the number of oocytes per mice. Oocytes collected at 14 hr post hCG injection were shown higher maturation rate to MII stage and blastocyst formation compare to other three groups ( $p < 0.01$ ). However, there is no difference in the maturation rate on the other three groups. Also, there are no differences in apoptotic signal with TUNEL assay or anti-PARP staining or Granulosa cell proliferation test with anti Ki-67 or anti AMH in ovaries from all experimental groups. Zinc ion has come out into view, as a key regulator in oocyte maturation and fertilization. As the time increased, intracellular zinc level in these oocytes tended to increase gradually in immature oocytes, but to decrease in mature MII oocytes ( $P < 0.05$ ). According to these results, there are no significant differences in four different time points at 12hr, 14hr, 16hr or 24hr of collection of immature oocytes in hCG primed mouse. However, oocytes from 14 hr post hCG injection showed higher percentages of maturation rate, in vitro fertilization rate, blastocyst formation. This work was supported by a grant program from Bio & Medical Technology Development Program (2015M3A9C6028961) of NRF and (NRF-2017R1D1A1B03028155) of Republic of Korea.

**Gestational Overnutrition Alters Fetal Hypothalamic Melanocortin Circuitry in a Sexually Dimorphic Manner.** B. R. C. Alves, M. M. D. CA Weller, B. C. Carvalho, G. B. Santos, M. M. Campos, F. S. Machado, P. P. Rotta, M. I. Marcondes, F. S. Machado, and M. F. Martins

The hypothalamic arcuate nucleus (ARC) is responsive to circulating metabolic-related hormones such as leptin, playing a pivotal role in nutritional control of reproduction. One key ARC neuronal population co-expresses leptin receptor (LEPR) and POMC, which encodes the anorexigenic alpha-Melanocyte-Stimulating Hormone (alpha-MSH). The melanocortin receptor MC4R intermediates the actions of alpha-MSH, which promotes stimulatory effects over GnRH release, and has been associated with nutritional programming of puberty in mammalian species, including cattle. Gestational overnutrition has been

linked with metabolic disruptions and early puberty in offspring of rodents and human, possibly due to metabolic interference on prenatal development of ARC circuitries. However, association of maternal nutrition with fetal hypothalamic function has been mostly assessed in rodent species, in which neural development is poorly completed at term. The bovine species is monotocous, precocial and has a 40 wk-long pregnancy. In this study, male and female bovine fetuses, collected at middle and late gestation, were evaluated. We aimed to determine if maternal overfeeding affects fetal expression of hypothalamic melanocortin-related genes. Non-lactating multiparous Holstein x Gyr cows were bred by one Holstein bull and, on gestational day 60, assigned to either control (CON, n=22, 100% energy requirements) or overnutrition (OVN, n=19, 190% energy requirements) groups, which were balanced according to fetal sex. The same diet was offered individually for both groups, either in controlled amounts (CON, 1.15% of body weight in dry matter) or ad libitum (OVN). Cows were humanely euthanized at gestational week (wk) 20, 28, 34 or 38. Fetal hypothalami were harvested and frozen, and later, the ARC was removed from the hypothalamic block using a 5-mm punch, and processed for RNA extraction. Quantitative real-time PCR was performed to assess expression of POMC, MC4R and LEPR. Data was analyzed using the mixed procedure of SAS. Maternal diet, fetal sex, gestational age and their interactions were considered fixed effects. Fetal weight within wk was not altered by maternal diet ( $p>0.05$ ). In male fetuses, maternal overnutrition increased ( $p 0.05$ ) by maternal nutrition. In females, whereas LEPR and MC4R were not affected by diet, a week x diet effect was observed for POMC expression: OVN was associated with decreased expression at wk 34 ( $p < 0.0001$ ) and conversely, with increased expression at wk 38 ( $p=0.05$ ). This data supports the premise that maternal overnutrition affects the fetal hypothalamic melanocortin circuitry, and importantly, that this effect is dependent of both fetal sex and gestational age. Future investigation is warranted to determine if those hypothalamic alterations are carried over during the postnatal life. Nonetheless, increased hypothalamic POMC expression appears to be a suitable mechanistic way to explain the link between maternal overnutrition and early puberty in female offspring. M. Weller and M. Martins held productivity research fellowship from the Brazilian National Council for Scientific and Technological Development (CNPq).

**The Roles of Peroxiredoxin I in Senescence of Mouse Embryonic Fibroblast.** Pil-Soo Jeong, Seon-A Choi, and Sun-Uk Kim

Senescence is now understood to be the final phenotypic state in life of cells and caused by a variety of biological processes, such as telomerase shorting, chromosome instability, oxidative stress, etc. Recently, antioxidant enzyme, superoxide dismutase 1 (SOD1), glutathione peroxidase 1 (Gpx 1), peroxiredoxin II (Prx II) were reported to be pivotal roles in the regulation of reactive oxidative species (ROS)-mediated cellular senescence. The present study was designed to elucidate the effect of Prx I, recently characterized antioxidant enzyme, cellular senescence in mouse embryonic fibroblasts (MEFs). MEFs were prepared from wild and Prx I knockout fetuses of 13.5 days post-coitum, cultured until 10 passage, and examined for cellular senescence. The typical senescence phenotypes, such as the impaired cell growth, and the increased senescence associated- $\beta$ -galactosidase (SA- $\beta$ -gal) activity and cell size, and the elevated ROS levels were observed in Prx I knockout MEFs throughout the passage analyzed. Moreover, the aged Prx I knockout mice showed an increased number of cells with SA- $\beta$ -gal activity in a variety of tissues. Increased ROS levels and SA- $\beta$ -gal activity in Prx I knockout MEFs and reduction with a chemical antioxidant further supported an essential role for Prx I peroxidase activity in cellular senescence that is mediated by oxidative stress. The up-regulation of p16INK4a expression in Prx

I knockout MEFs and suppression by overexpression of Prx I indicate that Prx I possibly modulate cellular senescence through ROS/p16INK4a pathway. This study was supported by grants from the KRIBB Research Initiative Program (KGM4251824), Rural Development Administration, Republic of Korea.

**Roles of Peroxiredoxin in Differentiation of Mouse Embryonic Stem Cells.** Pil-Soo Jeong, Mun-Hyeong Lee, Joo-Young Kim, Ju-Hyun An, Hae-Jun Yang, Jae-Jin Cha, Seon-A Choi, Seung-Bin Yoon, Seung Hwan Lee, Kyung Seob Lim, Young-Ho Park, Jong-Hee Lee, Bong-Seok Song, Bo-Woong Sim, Ji-Su Kim, Yeung Bae Jin, Sang-Rae Lee, and Sun-Uk Kim

Although physiological levels of reactive oxygen species (ROS) are required to maintain the self-renewal capacity of stem cells, elevated ROS levels can induce chromosomal aberrations, mitochondrial DNA damage, and defective stem cell differentiation. Over the past decade, several studies have shown that antioxidants can not only alleviate oxidative stress and improve stem cell survival but also affect the potency and differentiation of these cells. Although peroxiredoxin (Prx) well known maintain cellular homeostasis as ROS scavenger, we investigated the significance of Prx in the differentiation potential using Wild type, Prx I<sup>-/-</sup> and Prx II<sup>-/-</sup> mouse embryonic stem cells (mESCs). Interestingly, we found that Prx I and II exhibit distinct functional properties in regulating differentiation propensities of mESCs. Prx I<sup>-/-</sup> mESCs showed marked increase of pluripotent genes compared to WT mESCs. Genes related to ectoderm and endoderm (Tubb3 and Gata6, respectively) revealed similar patterns across all mESCs but mesodermal gene, Brachyury was highly up-regulated in Prx<sup>-/-</sup> cells. In addition, Prx I and Prx II appear to have a tight association with the mechanism underlying the protection of ESC stemness in developing teratomas. Therefore, our findings have important implications for understanding of maintenance of ESC stemness through involvement of antioxidant enzymes and may lead to development of an alternative stem cell-based therapeutic strategy for production of high-quality neurons in large quantity. This study was supported by grants from the KRIBB Research Initiative Program (KGM4251824), Rural Development Administration, Republic of Korea.

**The Initiation of Sperm Nuclear Decondensation in Fertilized Oocytes by Sperm Perinuclear Theca Resident Glutathione-S-Transferase Omega 2 (GSTO2).** Lauren E Hamilton, Joao Suzuki, Jiude Mao, Marie-Charlotte Meinsohn, Wei Xu, Peter Sutovsky, and Richard Oko

The post-acrosomal sheath (PAS) of the perinuclear theca (PT) is the first compartment of the sperm head that is released into the ooplasm upon sperm-oocyte fusion, implicating its constituents in early zygotic developmental events. This study investigates the role of Glutathione-S-Transferase Omega 2 (GSTO2), an oxidative-reductive enzyme found in the PAS and perforatorial regions of the sperm head. GSTO2 uses the conjugation of glutathione, an electron donor previously implicated in nuclear decondensation and pronuclear formation, to oxidize and reduce disulfide bonds. We hypothesize that sperm-borne GSTO2 enzymes may be implicated in the initiation of nuclear decondensation and male pronuclear formation before the recruitment of GSTO enzymes from within the ooplasm. Through preliminary inhibition studies in combination with in vitro fertilization (IVF) in swine and mouse, we have been able to show this involvement of sperm-borne GSTO2 enzymes as important constituents of the initiation of male nuclear decondensation and pronuclear formation. To specifically isolate the functionality of the PAS GSTO2 enzymes within the developing oocytes, we combined inhibition studies

with intracytoplasmic sperm injections in mouse. Enzyme activity was inhibited through sperm pre-incubation with a membrane permeable probe specific to the active site of GSTO enzymes prior to performing IVF or ICSI. These findings are also supported by additional IVF studies investigating GSTO involvement from the female perspective, functional enzymatic assays, fluorescent gel electrophoresis, and fluorescent immunocytochemistry experiments. Our findings suggest that the inactivation of sperm-borne GSTO2 enzymes from the PAS results in a developmental delay in pronuclear formation and ultimately cleavage in both swine and mouse, and implicates GSTO enzymes as important facilitators of successful nuclear decondensation and male pronuclear formation.

This work was supported by NSERC (RGPIN/192093) (RO), Agriculture and Food Research Initiative Competitive Grant no. 2015-67015-23231 from the USDA National Institute of Food and Agriculture (PS), as well as by seed funding from the Food for the 21st Century Program of the University of Missouri (PS).

**Trophoblast EMT, Necessary for Conceptus Attachment to Endometrium in the Bovine Species, is Regulated by Transcription Factor OVOL2 Down-Regulation.** B. A. I. Rulan, Kusama Kazuya, Sakurai Toshihiro, and Imakawa Kazuhiko

Embryo implantation into the uterine endometrium is required for pregnancy establishment in most mammals. We previously found that bovine trophoblasts go through the process of epithelial-mesenchymal transition (EMT) on day 22 (day 0 = day of estrus), 2-3 days after the initiation of conceptus attachment to the uterine epithelium. By using global expression analysis, we identified that the molecule expressed in bovine conceptuses were indicative of EMT when the trophoblasts adhered firmly with the endometrium, and found that a transcription factor OVOL2, a repressor for mesenchymal genes in cancer, was down-regulated.

To determine the relationship between OVOL2 and EMT in bovine trophoblasts during the peri-implantation period, bovine trophoblast CT-1 and F3 cells were subjected to knockdown and overexpression experiments using siRNA and OVOL2 expression construct, respectively. Down-regulation of OVOL2 increased EMT-associated transcription factors, ZEB1 and SNAI2, and the mesenchymal cell marker vimentin (VIM), whereas epithelial cell marker, E-cadherin (CDH1), was down-regulated. In contrast, OVOL2 overexpression in bovine trophoblast cells exhibited a decrease in ZEB1 and VIM expression and an increase in CDH1. It was further found that OVOL2 was reduced in CT-1 cells when allowed to attach to EECs.

To elucidate molecular mechanisms associated with OVOL2 and EMT related gene expression, signaling pathways regulated by attachment between trophoblast and EECs were investigated. Along with OVOL2, high NOTCH2 expression was found in day 20 bovine trophoblasts, which declined on day 22. To determine the effect of Notch signaling on OVOL2 and EMT-related factor expression during the peri-implantation period, NOTCH2 siRNA was transfected into CT-1 cells that were then cocultured with EECs. Although trophoblast CDH1 and OVOL2 down-regulation was not affected by NOTCH2 knockdown, the expression of ZEB1, CDH2, and VIM induced by cell attachment was further up-regulated in CT-1 cells. Similar to OVOL2 and NOTCH2, high expression of YAP and TEAD3 in day 20 trophoblasts was decreased on day 22. Accordingly, down-regulation of YAP and TEAD3 in vivo was also observed in trophoblast cells that were directly attached to EECs in vitro. Furthermore, the expression of OVOL2, CDH1, and NOTCH2 was up-regulated when YAP with TEAD3 was overexpressed in cultured trophoblast

cells. CHIP assay was further performed and revealed that TEAD3 could bind to the upstream region of OVOL2, allowing direct control of TEAD3 on OVOL2 transcription.

In summary, we demonstrate that high expression of OVOL2 on day 20 was decreased on day 22 via down-regulation of the TEAD/YAP signaling pathway, which enabled EMT progression in non-invasive bovine trophoblasts. These observations suggest that successful implantation in the bovine species is initiated by OVOL2 down-regulation.

### **MicroRNA-582-5p Suppresses Epithelial-Mesenchymal Transition via Down-Regulating Sorcin in Mouse Endometrium.** Kanchan Gupta, Vijay K Sirohi, Rohit Kumar, and Anila Dwivedi

Our earlier studies have shown that sorcin is present in human endometrium and is also involved in the process of embryo implantation in mice. The present study was aimed to identify miRNAs regulating sorcin expression and playing role in endometrial receptivity and embryo implantation. Using bioinformatics target prediction tool target scan, we identified miR-23a-3p, miR-425-5p and miR-582-5p as predicted to target 3'UTR of sorcin mRNA. Among three identified miRNAs, miR-425 and miR-582 showed time specific changes during period of early pregnancy. We selected miR-582 for detailed exploration as its expression pattern was contrary to the sorcin expression on days -5 and -6 of pregnancy suggesting its probable role in pregnancy establishment. Over-expression of miR-582 caused significant down-regulation of sorcin in uterus and in mouse primary endometrial epithelial cells as observed by western blotting, quantitative real time PCR and immunofluorescence. In-vivo over-expression using mimic of miR-582 significantly reduced the implantation sites indicating its inhibitory role in embryo implantation. Also, the receptivity marker integrin  $\beta 3$  expression was found to be decreased in miR-582 over-expressed uterine horn as compared to control horn. In-vitro study on endometrium–trophoblast interaction further supported these findings. Upon transfection, the attachment and expansion of BeWo spheroids on RL95-2 endometrial cells were significantly reduced when these cells were transfected with mimic miR-582. Over-expression of miR-582 led to activation of epithelial marker E-cadherin and inhibition of mesenchymal markers N-cadherin, vimentin resulting into the suppression of migratory and invasive capacities of mouse primary endometrial epithelial cells. The study suggests that miR-582 causes suppression of epithelial to mesenchymal transition via targeting sorcin and hence plays important role during embryo implantation in mice uterus. This work was supported by Council of Scientific & Industrial Research (CSIR).

### **Analysis of the Transition State for Putative Canine Induced Pluripotent Stem Cells.** Mirae Kim, Seon-Ung Hwang, Gabsang Lee, and Sang-Hwan Hyun

Canine induced Pluripotent Stem Cells (ciPSCs) have great potential for regenerative veterinary medicine. However, none have described cellular gene expression changes that occur during the reprogramming process of canine adult fibroblasts (CAFs). To generate integration-free ciPSCs, CAFs were reprogrammed using the Venezuelan equine encephalitis (VEE) RNA replicon that expresses four reprogramming factor ORFs (OKS-iG; hOct4, hKlf4, hSox2 and hGlis1). The putative ciPSC colonies first appeared between day 15-25. They were identified by immunohistochemistry of live cells using TRA-1-60 antibody and also showed alkaline phosphatase (AP) activity. By comparing gene-expression levels of

putative ciPSC colonies and CAFs, the expression levels of exogenous (VEE-hOct4, VEE-hKlf4, VEE-hSox2 and VEE-hGlis1) and endogenous (Brg1 and Rex1) genes were confirmed. RT PCR was performed to analyze the intermediate stage that occurs during the reprogramming process. Marker genes representing transition states include Brg1 and Rex1. The transcription factor Brg1 suppresses the reprogramming capacity and Rex1 is the representative pluripotent marker gene. Among the exogenous VEE-hOct4, VEE-hKlf4, VEE-hSox2 and VEE-hGlis1 transcripts, only the exogenous VEE-hOct4 gene was expressed in the putative ciPS cell lines. Furthermore, endogenous Oct4, Klf4, Sox2 and Glis1 were not expressed. Instead, Brg1 expression was clearly observed in CAFs, but not in the putative ciPS cell lines. Also, low expression of Rex1 was observed in the putative ciPSC #7 cell lines. These results have shown that the initial colonies were speculated to partially reprogrammed. Taken together, these findings suggest that these putative ciPSCs may be in a transition state, and it is necessary to further study the mechanism from the transition state to the fully pluripotent state.

#### Acknowledgements

This work was supported, in part, by a grant from the “National Research Foundation of Korea Grant funded by the Korean Government (NRF-2016R1D1A1B03933191, NRF-2017R1A2B4002546)”, “Korea Institute of Planning and Evaluation for Technology in Food, Agriculture, Forestry and Fisheries (IPET) through Advanced Production Technology Development Program, funded by Ministry of Agriculture, Food and Rural Affairs (MAFRA) (Grant number: 115103-02)”, “The Global Research and Development Center (GRDC) Program through the National Research Foundation of Korea (NRF) funded by the Ministry of Education, Science and Technology (2017K1A4A3014959)” and “Business for Cooperative R&D between Industry, Academy, and Research Institute funded Korea Small and Medium Business Administration in 2017 (Grants No. 2017020681010101)”, Republic of Korea.

#### **Development of Novel Porcine Promoter Leading to Stable and Enhancing Expression of HLA-E in**

**Porcine Primary Fibroblast Cells.** Hyeon Yang, Haesun Lee, Kyung-Woon Kim, Jeom Sun Kim, Sung June Byun, Jae-Seok Woo, Hwi-Cheul Lee, Hoonsung Choi, Sun Keun Jung, and Keon Bong Oh

Pig has been considered as an attractive model animal for biomedical researches including xenotransplantation. However, useful porcine promoters to adopt generation of transgenic pig have not been well developed. Here, we report that porcine elongation factor 1 alpha promoter (pEf1 $\alpha$ ) regulated high level expression of target gene than cytomegalovirus enhancer chicken beta-actin promoter (CAG) which has been most widely used to generate transgenic pigs. We cloned two porcine promoters, 1.5kb of pEf1 $\alpha$  promoter ranged from -710 to +750 bp and 1.7kb of porcine actin promoter (pActb) ranged from -1390 to +773 bp. pEf1 $\alpha$ , pActb and CAG promoters were inserted into pGL3 luciferase vectors. The comparative promoter activity for luciferase expression showed that the pEf1 $\alpha$  have 2.2-fold higher level ( $p < 0.001$ ) than CAG in porcine primary ear fibroblast cells (pEFs). We were not able to analyze comparative activity of pActb with CAG. We construct Human Leukocyte Antigen-E (HLA-E) expression cassette, which plays an important role in inhibitory factor to NK cell activation, under control of pEf1 $\alpha$  and CAG. The cassettes were transfected into pEFs and selected using neomycin in culture medium. We performed quantitative real-time RT-PCR. The results showed that pEf1 $\alpha$  lead to 2.42-fold higher expression ( $p < 0.001$ ) of HLA-E than that of CAG. Flow cytometry analysis showed 30.90 % of cells were positive on HLA-E by pEf1 $\alpha$ , whereas 7.69% cells were positive by CAG. In conclusion, in this study, we

verified that pEf1 $\alpha$  is one of the very potential promoters to use in generation of transgenic pig for diverse purposes.

Acknowledgements : This study was supported by the grants from the research project (No. PJ01260301), Rural Development Administration, Republic of Korea.

**Protein Glycosylation is Disrupted in the Proliferative Phase Uterine Microenvironment of Idiopathic Infertile Women.** Harriet Fitzgerald, Lois Salamonsen, and Tracey Edgell

The regenerative, proliferative phase of a woman's menstrual cycle is a critical period which lays the foundation for the subsequent, receptive secretory phase. Although endometrial glands and their secretions are essential for embryo implantation and survival, the proliferative phase, when these glands form, has been rarely examined. We have recently shown significant changes in both the cytokine profile and proteome of proliferative phase uterine fluid from infertile women, indicating a disturbance in the development of the endometrium during this time. Post-translational modifications i.e. glycosylation can greatly influence a protein's functional effects. Specific changes in protein glycoforms and their association with female infertility and disturbed proliferative phase endometrial development, have been seldom investigated. We hypothesised that alterations in the glycoproteome of uterine fluid of idiopathic infertile women would indicate a disturbance in the endometrial regeneration during the proliferative phase. Our aim was to compare the glycoproteome of proliferative phase uterine fluid of fertile and infertile women. To examine the glycoproteome of proliferative phase uterine fluid, lectin affinity capture with lectin Ricinus Communis Agglutinin I (RCA), and mass spectrometry were used. Changes in the proteins which have RCA binding sugar residues were examined in proliferative phase uterine fluid from fertile (n=6) and infertile women (n=9). WebGestalt was used to identify biological processes that were enriched for the proteins identified in this analysis. An alpha-2-macroglobulin (A2M) -Luminex assay with the lectin Lycopersicon esculentum (LEL) was developed to examine the LEL binding glycoforms in proliferative phase uterine fluid (fertile, n=7; infertile, n=7). Glycoproteomic analysis employing RCA lectin affinity capture identified three proteins significantly upregulated ( $P < 0.05$ ) in infertile women and four proteins significantly downregulated, including alpha-1-antichymotrypsin ( $P < 0.0001$ ) and A2M ( $P = 0.021$ ). Two proteins were unique to fertile women. Enrichment analysis of proteins significantly upregulated in infertile women showed these proteins were involved in biological processes of regulation of reactive oxygen species and metal ion homeostasis. Proteins significantly downregulated in infertile women were involved in the acute inflammatory and innate immune response, and regulation of the protein activation cascade. LEL binding A2M glycoform was significantly lower ( $P < 0.05$ ) in infertile women. Our findings further highlight the complexity of the human uterine microenvironment. The altered glycoproteome of proliferative phase uterine fluid from infertile women suggests a disturbance in the formation of the endometrium. This disruption in endometrial development could prevent the endometrium from differentiating and reaching a receptive state for embryo implantation, rendering a woman infertile. Further investigations into the effect of altered glycosylation on the function of these proteins may provide interesting insights into the development of the human endometrium as well as potential therapeutic targets to address idiopathic infertility in women. Research supported by Monash University FMNHS Postgraduate Research Scholarship (HCF), NHMRC fellowship 1002028 (LAS), the Victorian Government's Infrastructure Support Program, L.E.W. Carty Charitable Fund, and Monash IVF Research and Education Fund.

## **Leptin Signalling Characterisation in the Ovary of Diet-Induced Obese and Pharmacologically Hyperleptinemic Mouse.** Karolina Wołodko, Marek Adamowski, and Antonio Galvao

Obesity epidemics prevails worldwide and is associated with numerous comorbidities, such as cardiovascular disease, cancer and others. Recently, more attention has been paid to the link between obesity and infertility. It is well known that obese people have menstrual dysfunctions, anovulation and pregnancy complications. However, it is not clear what drives ovarian pathology. During obesity, increased circulating leptin level activates leptin signalling in different organs. We hypothesise that obesity is associated with the establishment of leptin resistance in the ovary. Thus, in the present work we characterised leptin signalling in the ovary of diet induced obese (DIO) mice and validated an in vivo mouse model for pharmacological hyperleptinemia (LEP), in order to further interrogate the molecular pathways responding to leptin receptor b (ObRb) hyperactivation in the ovary.

In DIO protocol, C57BL/6J mice were fed chow diet (CD) or high-fat diet (HFD) for 4 and 16 weeks (wk), while in LEP protocol, the daily dose of 100ug of leptin or NaCl were administered intraperitoneally during 9 or 16 days (d) (n=10/group in both protocols). Ovaries were collected for mRNA and protein analysis and the phenotype of LEP animals was evaluated. In order to characterise leptin signalling activation, we studied the leptin receptor isoform b (ObRb), the leptin receptor isoform b phosphorylated at tyrosine 985 (OBRB985), the signal transducer and activator of transcription 3 (Stat3) and the suppressor of cytokine signalling 3 (Socs3) mRNA and protein level in DIO and LEP protocol. The mRNA level of *Obrb* decreased in the 16wk HFD group ( $p < 0.5$ ). Protein phosphorylation of OBRB985 was significantly increased after 4wk HFD ( $p < 0.05$ ) and decreased after 16wk comparing to CD ( $p < 0.05$ ). STAT3 protein phosphorylation was increased after 4wk ( $p < 0.05$ ) and no differences were found for 16wk of HFD. Furthermore, *Socs3* mRNA was significantly increased after 16wk of HFD ( $p < 0.05$ ), whereas its protein level increased after 4 and 16 wk of HFD ( $p < 0.05$  and  $p < 0.01$  respectively). With regard to LEP protocol, the phenotype characterisation showed a decrease in body weight and fat mass after 16d leptin treatment ( $p < 0.001$ ). While phosphorylation of OBRB985 increased after 9 days ( $p < 0.05$ ), a trend was evident after 16d suggesting its inhibition ( $p=0.08$ ). Finally, *SOCS3* mRNA and protein were increased after 16d of leptin administration ( $p < 0.05$ ).

Our DIO protocol evidences a temporal response of leptin signalling components during obesity progression. After short exposition to HFD (4wk) leptin seems to signal through STAT3 in order to initiate the production of SOCS3. After long exposition to HFD (16wk), decreased phosphorylation of OBRB985 and expression of SOCS3 evidences the establishment of leptin resistance. Moreover, our LEP model evidenced a decrease in body weight and increased SOCS3 levels. In conclusion, we give the first characterisation of leptin signalling in the ovary of DIO mice and validate an in vivo model to further interrogate the effects of ObRb hyperactivation in ovarian dynamics.

Work supported by National Science Centre (2014/15/D/NZ4/01152) and KNOW Consortium: "Healthy Animal - Safe Food" (Ministry of Sciences and Higher Education; Dec: 05-1/KNOW2/2015)

**Derivation of Putative Embryonic Stem-like Cells from Porcine Embryos in Vitro Fertilization.** Ga-Hye Kim, Kyoung-Ha So, Dibyendu Biswas, Gab-Sang Lee, and Sang-Hwan Hyun

In the biotechnology, pigs draw great advantages than other domestic animals such as continuous cycling, short generation interval, large litter size and immunological and physiological similarities to human. Porcine embryonic stem cells (pESCs) have become an advantageous experimental tool in the biotechnology field for developing therapeutic applications and producing transgenic animals. However, despite plenty of putative pESC lines reports, deriving validated pESC lines from embryos produced in vitro remains difficult. The aim of the present study was to establish porcine embryonic stem-like cells (pESLCs) from in vitro-produced embryos. Porcine blastocysts derived from in vitro fertilization (IVF) that produced by  $5 \times 10^5$ /ml of sperm concentration with over 70% sperm motility and used porcine oocytes number is 366. We confirmed the embryonic development rate of 2 cell embryos were  $78.40 \pm 2.50\%$  (286 oocytes), and blastocysts were  $34.2 \pm 6.47\%$  (125 oocytes), respectively. putative porcine ESC lines were produced in vitro were chosen at day 7 or day 8 to establish pluripotent cell lines. Zona pellucida were removed by chemical treatment dissection under the microscope using 0.5% protease, and then the whole, zona-free blastocysts were seeded on mitotically inactivated mouse embryonic fibroblast (MEF) feeders. The pESLCs were cultured with low glucose DMEM/F10 (Gibco) supplemented with 1% nonessential amino acids, 1% glutamine, 0.1 mM  $\beta$ -mercaptoethanol, 1% antibioticantimycotic with 4 ng/mL of basic fibroblast growth factor (bFGF, Invitrogen) and 15% FBS. The established pESLCs line have a similar typical morphology that were revealed alkaline phosphatase (AP) activity during maintenance. pESLCs line also have shown the expression patterns of the surface markers TRA-1-60. In general, we established a pESLCs, which have shown common properties of pluripotency like other species on short-term culture maintenance that will has further study as stability on long-term culture.

**Acknowledgments:** This work was supported by a grant from the Korea Research Fellowship (KRF) Program through the National Research Foundation of Korea (NRF) funded by the Ministry of Science and ICT (NRF-2015H1D3A1066175), in part of the NRF funded by the Ministry of Science and ICT (NRF-2016R1D1A1B03933191, NRF-2017R1A2B4002546), and the Global Research and Development Center (GRDC) Program through the NRF funded by the Korea government (Ministry of Science and ICT, MIST) (NRF-2017K1A4A3014959), Republic of Korea.

**Histone-to-Protamine Transition is Impaired in Spermatids Lacking PnlDC1.** Yue Zhang, Yiqiang Cui, Xuejiang Guo, Jiahao Sha, and Mingxi Liu

Piwi-interacting RNAs (piRNAs) are a class of small non-coding RNAs with key regulatory roles in gametogenesis. Production of piRNAs encompasses a vital exonuclease activity that trims longer piRNA intermediates from their 3' ends to obtain shorter mature piRNAs. Our previous study has elucidated that mice deficient for Poly(A)-specific ribonuclease (PARN)-like domain containing 1 (PnlDC1) accumulated 3' extended piRNAs with impaired function in their testes, thus confirming the conserved role as trimmer involved in piRNA maturation for PnlDC1 in mammals. Electron microscopy revealed defected chromatin condensation of spermatids from PnlDC1 knockout mice. Histone-to-protamine transition is of great significance for proper chromatin condensation of elongating spermatids. Our recent work showed residual of histones H3 and H4 in step-14 spermatids, accompanied by retention of transition protein-2 (Tnp2) in step-16 spermatids of PnlDC1 knockout mice. Although deposition of protamin 2 (prM2) on chromatin was observed in a small number of spermatids from step 15 to step 16

in testes from Pnlcd1 knockout mice, the total amount of prn2 and prn2 precursor was under detectable level when evaluated by western blot analysis. Transition protein-1(Tnp1) and Transition protein-2(Tnp2) were also reduced in testes from Pnlcd1 knockout mice. These evidences implicated a connection between piRNA dysfunction and histone-to-protamine transition defects.

**Determination of Highly Sensitive Physical Markers for Sperm Freezability.** Do-Yeal Ryu, Sung-Jae Yoon, Won-Hee Song, Won-Ki Pang, Ki-Uk Kim, Kyu-Ho Kang, Ki-Jin Kwon, Sae-Han Kang, Md Saidur Rahman, and Myung-Geol Pang

Sperm cryopreservation is an essential process for preserving spermatozoa and playing a significant role in humans and animals. This process is known to be influenced by many factors. Among them, sperm freezability is well known as one of factor to decide the quality of spermatozoa for cryopreservation. However, the prediction of sperm freezability remains the subjects of further study. Therefore, we performed sperm analysis to identify sperm physical marker related to sperm freezability. First, we conducted the computer assisted sperm analysis (CASA) during each step of cryopreservation. The cryopreservation process involves following steps: (Step 1) dilution with the extender/cooling, (Step2) addition of cryoprotectant, and (Step 3) freezing/thawing. Spermatozoa were altered their motility and motion kinematics differently by each cryopreservation step. Therefore, we categorized them into three groups as good freezability (GF), damaged by cryoprotectant (DCP), and damaged by freezing (DF). Subsequently, we identified various characteristics of each group in the different step of cryopreservation. Our results demonstrated that DCP group was significantly decreased in motility and rapid speed in Step 2, whereas slow speed is increased in Step 3. In addition, DF group was significantly decreased in motility and rapid speed, whereas slow speed was significantly increased in Step 3. Simultaneously, motility of DF group was significantly higher than DCP group in Step 2. GF group was significantly higher than DCP and DF groups in motility, rapid/slow speed in Step 3. Secondly, we evaluated capacitation status of spermatozoa using Hoechst 33258/chlortetracycline fluorescence staining. Acrosome-reacted pattern of all groups was continuously increased following each step, and DCP and DF groups were significantly higher than GF group in Step 3. Additionally, DF group was higher than the others in all steps. Simultaneously, non-capacitated pattern of DF and DCP were significantly decreased in Step 3, whereas capacitated pattern did not show any difference between all groups. Thirdly, to analyze the mitochondrial activity of spermatozoa, Rhodamine 123 staining was performed. Even though mitochondrial activity is significantly decreased in all groups at Step 3, GF group is significantly higher than the others in Step 3. Similarly, the sperm viability of all groups is significantly decreased in Step 3. Herein, we demonstrated spermatozoa have different physical properties for freezability, and thus might be differently altered by different step of cryopreservation process. Based on our findings, various sperm physical parameters provide a strong guideline to predict the sperm freezability, which is directly associated with fertility and efficient genome resource banking. Further studies are required to elucidate the underlying mechanism which influence the sperm freezability.

This work was supported by Korea Institute of Planning and Evaluation for Technology in Food, Agriculture, Forestry, and Fisheries (IPET) through Agri-Bio Industry Technology Development Program, funded by Ministry of Agriculture, Food, and Rural Affairs (MAFRA) (116172-3).

**ZBED3, an Unknown Function Maternal Protein, is Involved in Mouse Early Embryogenesis.** Chun Zhao, Xiaodan Shi, Jiayi Wang, Ye Yang, Junqiang Zhang, and Xiufeng ling

Stored maternal factors in oocyte regulate oocyte differentiation into embryos during early embryogenesis. ZBED3 is a oocyte-specific maternal protein which is screened from the mouse oocyte protein expression profile. It is still lack of clear functional coverage in early embryogenesis. Zbed3 mRNA is highly expressed in mouse ovary and uterus, especially in zygotes and two-cell embryos. We used CRISPR/Cas9 system to construct Zbed3 knockout mice, Zbed3 null female mice exhibited sub-fertility. Realtime PCR analysis revealed that the expression of Zar1, Mater, Npm2, Stella, Filia, Gas6, which belong to maternal genes were significantly decreased in Zbed3 KO female mice. In vitro oocyte maturation (IVM) of GV oocytes obtained by superovulation showed the MII oocytes formation rate of KO group was about 16% lower than that in WT group. Subsequently, we collected zygote from WT and KO female mice, cultured in vitro to blastocyst; the results showed that zygote, two-cells, four-cells and blastocyst formation rate were not significantly different between two groups. To explore the stage of the loss of offspring, we observed E11.5d and E7.5d Embryos; There's no difference in embryo implantation spots, but the number of embryos in the KO group decreased by about 50%, that is, about 50% embryonic development stagnated. We conclude that ZBED3 affects the implantation outcomes of offspring by affecting the developmental potential of oocytes and early embryogenesis.

**SPACA1 Cleavage During Acrosome Reaction Allows for Translocation of IZUMO1 to the Equatorial Segment.** Kenji Yamatoya, Marika Kousaka, Chizuru Ito, Mitsuaki Yanagida, Yoshihiko Araki, and Kiyotaka Toshimori

SPACA1 localize to outer and inner acrosomal membrane of the equatorial segment. SPACA1 at inner acrosomal membrane anchors acrosome to the nucleus during spermatogenesis. SPACA1 knock out male mice are sterile due to globozoospermia. IZUMO1 is a type1 transmembrane protein essential for sperm egg membrane docking. IZUMO1 is localized in anterior acrosome before acrosome reaction and translocate to the whole head during acrosome reaction. This translocation is essential for sperm-egg membrane fusion and it is regulated by actin fibers. Acrosome reaction is a highly regulated multi-step phenomenon essential for physiological fertilization. To elucidate the mechanism of acrosome biochemistry, characterization of each steps and those acrosome reacted sperm must be purified.

In this study, we differentiated acrosome reaction in to 7 populations using 2 different antibodies to acrosomal membrane proteins. Using the method, we have found that SPACA1 become cleaved during acrosomal content release. The IZUMO1 then translocate to equatorial segment where SPACA1 was cleaved.

Material and methods: 1) Differentiation of acrosome reaction in to 7 steps. Acrosome reacted sperm were fixed with 4% paraformaldehyde for 10 min and washed 3 times with PBS. The sperm were immune labeled using 2 epitope defined antibodies to acrosomal membrane proteins. One antibody recognizes the epitope in the acrosomal lumen. Another antibody recognizes the epitope between plasma membrane and outer acrosomal membrane. The immune labeled sperm were subjected to flow cytometry and the each differentiated populations were purified for further analyses.

2) Purification of SPACA1 cleaving complex. Sperm lysate were fractionated using protease inhibitor conjugated column. The Fraction containing SPACA1 cleaving enzyme was further purified using ion exchange column. The purified SPACA1 cleaving complex were identified by LC-MS/MS analysis. Results and Discussion: The flow cytometry showed that acrosome reacted sperm could be differentiated in to 7 populations.

The time dependent analyses using acrosin-GFP sperm determined the transition order and the timing of the release of acrosomal content. Immunoblotting of purified population showed that SPACA1 was cleaved after transition to population 5. In population 5 and 6, IZUMO1 did not translocate to where SPACA1 signal remained. The Mass analyses of purified SPACA1 cleaving enzyme complex showed that SPACA1 and IZUMO1 formed a complex. Ion exchange column fractionation showed that the complex containing cleaved SPACA1 interacted with IZUMO1.

Conclusion: SPACA1 become cleaved after rupture of outer acrosomal membrane and IZUMO1 forms a complex with the cleaved SPACA1.

**Effect of the Dietary Addition of Vitamin E, Zinc, Selenium, Folic Acid and N-3 Polyunsaturated Fatty Acids on Semen Quality in Dogs.** Salvatore Alongea, Monica Melandria, Raffaella Leocib, Giovanni M. Lacalandrab, Michele Cairab, and Giulio Aiudibi

Sub- and infertility represent common challenges in small animal reproduction and practitioners look forward to specific treatments to solve them. A major constraining factor of breeding programs is the poor sperm concentration and/or function, thus several authors investigated different protocols to improve semen quality both in human and veterinary medicine supplementing a certain daily intake of micronutrients, but few information are available for dogs. The present study aimed to investigate if a daily dietary supplementation of vitamin E, Zinc, Selenium, Folic Acid complex with a 6.6 06:03 ratio can improve semen quality in dogs. Serial semen analysis, from seven normospermic healthy dogs (26-34 kg, 2-3 years), fed with the same commercial diet before being enrolled in the study, were performed on day 0 (T0) and repeated on days 30 (T1), 60 (T2) and 90 (T3) to assess: total sperm count (spz x 10<sup>6</sup>) and Hamilton Thorn analyzer (Sperm CASA) indexes, mortality (eosine-nigrosine staining) and functional membrane integrity (hypoosmotic swelling test, HOS),. The commercial diet was supplemented with a mix of vitamin E (5mg/kg), Zinc (3mg/kg), Selenium (7µg/kg), Folic Acid (0.625 mg/kg) complex with a 6.6 06:03 ratio. One-way ANOVA assessed the effect of time on semen quality (p < 0 .05). Statistically significant results are reported (mean±st.dev).

The given supplementation significantly improved total sperm count (1030.24±562.69 and 1010.25±223.81 vs 365.50±147.85) at T2 and T3 vs T0. A similar trend was obtained for progressive motility (77.29±12.70 and 83.14±7.9 vs 51.43±22.64) with an increase in rapid (88.86±6.34 and 90±7.14 vs 72.71±15.01) and medium (8.43±4.65 and 7.43±4.96 vs 5.57±6.65) motile sperms and a decrease in slow movement ones (2.00±1.83 and 1.71±1.80 vs 10.29±6.47), and a significant decrease in static sperms percentage since T1 (0.71±0.76 and 0.86±0.90 vs 12.57±5.88, and already 3.14±1.95 at T1). Moreover, this result was confirmed by a significant decrease in sperm mortality (1.37±1.32 and 1.60±1.00 vs 8.65±5.90) and an increase in sperms with functional membrane integrity since T2 (HOS curled-sperms: 97.57±1.74 and 95.43±2.15 vs 91.00±4.12).

Present results demonstrate that the supplementation of a healthy diet with a vitamin E, Zinc, Selenium, Folic Acid complex with a 6.6:0.3 ratio can improve the count, function and motility in the patients' ejaculate. Sperm motility represents a central index of fertility strongly influenced by environmental factors, with diet being one of the most important modifying agents. A balanced supplementation of trace elements, playing an important role in the male reproductive process, and of antioxidants, exerting a positive effect on the motility of the fresh and liquid-stored sperm by the prevention of oxidative stress damage, is mandatory. A healthy diet with a 2-month supplementation may be an inexpensive and safe way to improve semen quality and fertility. Present results prompt to consider the curative effects of diet supplementation in the treatment of canine infertility and its effects on sperm parameters, especially when the decrease in sperm concentration, motility and function may result from an inadequate intake, reduced absorption, increased losses, or increased demand or to attenuate the impact of age.

**Appropriate Regulation of Noggin Expression in Follicles is Critical for Female Fertility in Mice.** Koji Sugiura, Chihiro Emori, Tomoaki Kogo, Takuya Kanke, Haruka Ito, Wataru Fujii, and Kunihiko Naito

Oocyte-derived paracrine factors (ODPFs) and estrogens cooperatively play critical roles in regulating development of ovarian follicles in mammals. We have previously reported that the expression of a bone morphogenetic protein (BMP) antagonist, noggin (NOG) is promoted by ODPFs, whereas suppressed by estrogen, in cumulus granulosa cells, and that recombinant NOG is capable in suppressing oocyte-derived BMP signals in vitro. Therefore, the reciprocal regulation of the NOG expression between ODPFs and estrogens in follicles may mediate, at least in part, the cooperation of ODPFs and estrogens. The present study investigated the effects of disrupting the NOG-mediated cooperation of ODPFs and estrogens in vivo using a transgenic mouse model. Mice conditionally expressing NOG in granulosa cells (GC-Nog mice) were obtained by mating *Amhr2-cre* mice (expressing Cre recombinase under the control of a granulosa cell-specific *Amhr2* promoter) and *STOP-Nog* mice (possessing a transgene in which *Nog* expression is prevented by a floxed "STOP" sequence). In this GC-Nog mice, deletion of the "STOP" sequence results in conditional expression of transgenic *Nog* in granulosa cells. Fertility of GC-Nog or control (either *Amhr2-cre* or *STOP-Nog* mice) female mice mated with age-matched wild-type males was assessed by counting litter size for 3 months. The developmental competence of oocytes was assessed by in vitro fertilization (IVF) using oocytes obtained by superovulation treatment. In addition, dynamics of follicular development was assessed by observing ovarian histology. Although vaginal plugs were frequently observed, no litters were observed in GC-Nog mice during the 3 month of fertility test period, indicating that GC-Nog female mice are infertile. GC-Nog mice ovulated significantly fewer oocytes compared to the control mice responding to superovulation treatments (14.1 +/- 7.0 and 34.0 +/- 5.0 oocytes, respectively), but the developmental competence of the ovulated oocytes assessed by IVF was not significantly different between them. Histological assessment revealed that ovaries of GC-Nog mice contained all of the follicular developmental stages with significantly increased number of atretic follicles. Moreover, layers of mural granulosa cells in antral follicles tended to be thinner in GC-Nog mice. In addition, some of the oocytes were trapped in developing corpus luteum after the superovulation treatment in GC-Nog mice. These results suggest that suppression of *Nog* expression in vivo, probably by estrogen, is critical for both the development and survival of follicles and for normal ovulation. Therefore, the NOG-mediated cooperation of ODPFs and estrogens during follicular

development is likely to be a critical mechanism for normal female fertility. Research supported in part by a grant from the Japan Society for the Promotion of Science (No. 17H03900 to KS).

**A Model for Studying Transdifferentiation of Granulosa Cells Into Sertoli-like Cells in Mice.** Haruka Ito, Kasane Kishi, Chihiro Emori, Wataru Fujii, Yoshiakira Kanai, Kunihiko Naito, and Koji Sugiura

The maintenance of the gonadal ‘femaleness’ requires active mechanism in which forkhead box L2 (FOXL2) transcription factor plays a fundamental role. Inducible deletion of *Foxl2* in vivo resulted in the transdifferentiation of granulosa cells into Sertoli-like cells in adult mice; however, the precise mechanism of this “sex transdifferentiation” is poorly understood due to the lack of culture system replicating this process. We had previously reported that maintaining of FOXL2 expression in granulosa cells in vitro requires stimulation by both oocyte-derived paracrine factors and estrogen, and that the granulosa cells start to express testis-specific transcription factors such as *Sox9* and *Sox8* in a specific culture condition containing ovarian follicular fluid. Moreover, these cultured cells form a web-like structure similar to Sertoli cells cultured in vitro. Therefore, it is likely that these cultured granulosa cells have transdifferentiated into Sertoli-like cells, at least, to some extent; however, their characteristics as Sertoli cells have not fully investigated in detail. The objective of the present study is to test whether these cells are able to survive and support spermatogenesis in Sertoli-cell-depleted testis. Granulosa cells were isolated from 3-week-old transgenic (Tg) mice that ubiquitously express enhanced green fluorescent protein (EGFP), and were cultured in medium supplemented with either fetal bovine serum (FBS) or porcine follicular fluid (pFF). Due to the small size of mouse ovaries, pFF was used in this study. After the culture, the cells were evaluated for their expression of the testis- and ovary-specific transcripts and proteins by real-time PCR and western blot analysis, respectively. Then, the cultured granulosa cells or isolated testicular cells (positive control) from EGFP Tg mice were transplanted into the testes of 3-week-old recipients (*Amh-Treck* Tg male mice) pre-treated with diphtheria toxin to deplete Sertoli cells. After 10 days of transplantation, recipient testes were dissected and evaluated for the presence of EGFP positive cells by immunohistochemical staining. The increase of SOX9 protein and *Sox8* transcript was detected in granulosa cells cultured with pFF, but not with FBS. On the other hand, other testis-specific transcripts, such as *Dmrt1*, were undetectable in both cells cultured with pFF and FBS. Web-like structure was observed in cultured Sertoli cells and the granulosa cells cultured with pFF, but not with FBS. The EGFP positive cells were observed in the testis transplanted with the testicular cells, indicating the survival of transplanted cells in the recipient testis. However, the EGFP signals were not observed in the granulosa cell-transplanted testes, regardless of the culture conditions. These results suggest that the transdifferentiation of granulosa cells into Sertoli cells observed in our model is incomplete and that these SOX9-positive granulosa cells seems to be an intermediate state between granulosa cells and Sertoli cells. These cells may provide a valuable model for studying the precise mechanism of the sex differentiation. Research supported in part by grants from the Japan Society for the Promotion of Science (No. 17H03900) and the Ministry of Education, Culture, Sports, Science, and Technology of Japan (No. 25132704).

**Polypyrimidine Tract Binding Protein (Ptbp1) Expression by Sertoli Cells is Essential for Sperm Production.** Manabu Ozawa, Masahito Ikawa, and Nobuaki Yoshida

Alternative splicing (AS), by which multiple forms of protein from a single gene are translated, is an important mechanism for regulating proper development or homeostasis of specific type of cells in mammals. Testis shows more AS than any other tissue except brain. Although AS regulation in testicular germ cells during spermatogenesis is becoming to be uncovered, its role in Sertoli cells, testicular somatic cells and play an essential role to support spermatogenesis through the life period, is almost unknown. In the present study, we showed that expression of polypyrimidine tract binding protein (PTBP1), known as one of key factors to regulate AS, in Sertoli cells is essential for spermatogenesis. We show that PTBP1 is abundantly expressed by Sertoli cells and spermatogonia in the testis, and less evident or none in spermatocyte or spermatid. Eighty-three percent (five out of six) of Sertoli cell specific *Ptbp1* KO male (*Ptbp1* cKO) were infertile, and sperm counts from epididymis at 8 to 9-week-old was almost 50-fold lower compared to the Control ( $0.5 \times 10^6$  vs  $24.2 \times 10^6$ ,  $P < 0.01$ ). Immunohistochemical analysis revealed that *Ptbp1* cKO shows an increase of apoptosis of germ cells but not of Sertoli cells, and the presence of giant multinucleated cells in the lumen of seminiferous tubules. Furthermore, aberrant expression of Connexin43, a key protein of gap junction contributing blood-testis-barrier, and abnormal detachment of Sertoli cells from basal membrane were frequently observed in the *Ptbp1* cKO. The data suggests that *Ptbp1* plays an important role to regulate germ cell differentiation into spermatid. NGS analysis for determining transcriptome and splicome of *Ptbp1* cKO Sertoli cells are currently ongoing.

**Oocyte Stage-Specific Effects of MTOR Determine Granulosa Cell Fate and Egg Quality in Mice.** You-Qiang Su, Jing Guo, Teng Zhang, Tao Sun, and Lanying Shi.

Complex pathways and signaling networks control the development and function of oocyte and granulosa cells, distortion of which compromises ovarian function and female fertility. Mechanistic target of rapamycin (MTOR), a widely recognized integrator of signals and pathways key for cellular metabolism, proliferation, and differentiation, is implicated in the control of ovarian functions. However, the specific role of MTOR in the control of the coordinated development and function of oocytes and granulosa cells remains unclear. Here by specific deletion of *Mtor* in non-growing oocytes of developmentally quiescent primordial follicles and in growing oocytes of primary follicles, respectively, we show that oocyte-expressed MTOR elicits oocyte development stage-specific effects during follicular development, which differentially controls granulosa cell fate and egg quality in mice. Conditional knock out (cKO) of *Mtor* in non-growing oocytes causes defective follicular development, progressive degeneration of the oocytes, and transdifferentiation of granulosa cell to Sertoli-like cells, which subsequently cause primary ovarian insufficiency and infertility. In contrast, *Mtor* cKO in growing oocytes compromises egg quality and fertility without overtly affecting folliculogenesis. These phenotypes correlate with oocyte accumulation of DNA damage and alteration of expression of genes critical for oocyte maturation and granulosa development. Therefore, there are oocyte developmental stage-specific effects of the MTOR-dependent pathways taking place within the oocyte that control granulosa cell fate and oocyte meiotic and developmental competence. Though affecting different downstream processes, MTOR-dependent pathways in both stages of oocyte development are crucial for fertility.

[Research supported by grants from National Basic Research (973) Program of China (2014CB943200, 2013CB945500), National Natural Science Foundation of China (31471351, 31271538), and NSF of Jiangsu Province (BK20140061) to Y.-Q.S.]

**Bovine Endogenous Retroviral Genes Necessary for the Trophoblast Fusion are Up-Regulated by PPARG and Camp After Conceptus Implantation.** Kazuya Kusama, Rulan Bai, Masako Suzuki, John Greally, and Kazuhiko Imakawa

Placental formation requires trophoblast cell fusion in many mammalian species. In the bovine species, two genes with fusogenic activity, endogenous retroviruses (ERVs) proteins, syncytin-Rum1 and BERV-K1, are expressed in trophoblastic binucleate cells (BNCs), and then fuse with neighboring cells, mononuclear cells or endometrial epithelial cells, resulting in the formation of trinucleate cells. It was reported that syncytin-Rum1 was inserted into the genomes of ruminants, including cattle, sheep, and goats, while BERV-K1 was integrated only to the genome of bovine species. Syncytin-Rum1 and/or BERV-K1 are thought to induce cell-cell fusion in these species, but molecular mechanisms by which these ERVs are transcribed have not been well characterized. To investigate whether conceptus implantation induces the expression of syncytin-Rum1 and/or BERV-K1, we examined their expressions in days 17 (day 0 = day of estrus, pre-attachment), 20 (right after attachment to endometrium), and 22 conceptuses, and 35 and 45 trophoblast membranes. Both syncytin-Rum1 and BERV-K1 were up-regulated in days 35 and 45 trophoblasts compared with days 17, 20, and 22 conceptuses. We next studied the localization of syncytin-Rum1 and BERV-K1 in these conceptuses. Notably, BNCs started to appear in day 20 trophoblast cell layers, concurrent with the expression of syncytin-Rum1 and BERV-K1 in BNCs. In addition, we demonstrated that PPARG and cAMP activators up-regulated both syncytin-Rum1 and BERV-K1 expression in a time and dose dependent manner. To further investigate molecular mechanisms of PPARG and cAMP signal transduction in bovine trophoblasts, we performed RNA-sequencing (RNA-seq) analysis of bovine trophoblast F3 cells that were treated with PPARG or cAMP activator, showing that PPARG and cAMP regulated several transcription factors, among which GATA4, FOXO4 and TCF7L2 were extracted with enrichment analyses of RNA-seq data and confirmed with gene knockdown experimentations. Moreover, using an immunoblotting with pharmacological inhibitors, we demonstrated that PPARG and cAMP stimulated P38MAPK and AKT signaling pathways, which regulated GATA4, FOXO4 and TCF7L2 expression. To further examine whether PPARG and cAMP regulated epigenetic modification of syncytin-Rum1 and BERV-K1 long terminal repeat (LTR), a promoter region of ERV gene, we performed chromatin immunoprecipitation (ChIP) assay following the treatment with PPARG or cAMP activator, resulting in up-regulation of histone H3K9 and H3K27 acetylation. We further confirmed that treatment of F3 cells with tricostatin A, a histone deacetylase inhibitor, up-regulated syncytin-Rum1 and BERV-K1 expression. These findings indicated that ERVs, syncytin-Rum1 and BERV-K1, in bovine trophoblasts including BNCs appeared just after conceptus implantation, and suggested that PPARG and cAMP regulated P38MAPK and AKT signaling pathways, which up-regulated transcription factors, GATA4, FOXO4 and TCF7L2, resulting in these ERVs expression in BNCs required for placental formation.

**The Role of CDKN2A SNPs in Ovarian Cancer in the Laying Hen.** Lucia Borlle, Elizabeth Ann Staiger, Heather J. Huson, Leif Andersson, and Patricia Johnson

CDKN2A (cyclin dependent kinase inhibitor 2A) is an important tumor suppressor gene that encodes proteins involved in stabilizing p53. Expression of p53 has a well-known tumor suppression function and is widely regarded as the guardian of the genome. Deregulation of p53 has been found to be the most common mutation in ovarian cancer. Recent studies suggest that mutations in the CDKN2A gene are associated with plumage patterns in chickens. Four single-nucleotide polymorphisms (SNPs 1, 2, 3, and 4) within the CDKN2A gene were shown to be responsible for various feather pigmentation patterns and also implicated in regulation of proteins modulating p53 activity. Our work is focused on the use of the laying hen as a model for ovarian cancer in the women. Hen ovarian cancer has common features with the human counterpart: it is an age-related disease, has high spontaneous incidence (up to 35% in 3.5 year old hens), and presents with similar clinical signs and histological classification. Additionally, p53 mutations have been identified in hen ovarian cancers. Given the remarkably high incidence of ovarian cancer in domesticated chickens, we aimed to determine whether the identified SNPs in CDKN2A could be associated with the development of ovarian cancer in the hen. Genomic DNA was obtained from the liver of age-matched hens with ovarian cancer (n=16) and from control hens (n=13). Primers for the region encompassing SNPs 1, 3, and 4 of chicken CDKN2A were designed, amplified by PCR, and amplification verified by gel electrophoresis. Sanger sequencing was performed at the Cornell University Core Laboratories Center. Sequencher 5.4 software and Omega Clustal were used to align the sequences and call SNP genotypes. SNP and haplotype association analyses were performed using PLINK v1.07 software. There was no significant difference in the occurrence of these SNPs nor the haplotypes resulting from their combinations between samples from hens with ovarian cancer compared to controls. Our data indicate that these germline SNPs (1, 3, and 4) within the CDKN2A gene are unlikely to explain the high susceptibility of hens to the development of ovarian cancer.

**Phosphoproteomic Profiling Revealed Complex Protein Tyrosine Phosphorylations in Mouse Testis.**

Xiaofei Liu, Yiwei Cheng, Haojie Li, Junqing Chen, Jun Zhang, Yaling Qi, Zuomin Zhou, Jiahao Sha, and Xuejiang Guo

Phosphorylation of protein is a reversible post-translational modification and it is modified on tyrosine, serine, and threonine in eukaryotes, of which tyrosine phosphorylation is most difficult for identification because of its extremely low abundances. Phosphotyrosine modification has been known to play important functions in spermatogenesis by single gene studies. Systemic profiling protein tyrosine phosphorylation in mouse testis will help the elucidation of regulation of spermatogenesis.

To identify the phosphotyrosine-modified proteins in mouse testis, 6-week mouse testis protein were subjected to trypsin digestion, immunoaffinity purification enrichment by Src superbinder, and Ti4+-IMAC enrichment. The enriched peptides were analyzed using a LTQ Orbitrap Velos mass spectrometer (ThermoFinnigan, San Jose, CA) coupled directly to a Proxeon Easy-nLC 1000. After MaxQuant calculation, 1297 phosphotyrosine sites in 927 phosphoproteins were identified. DAVID Bioinformatics Resources 6.8 analysis revealed that these tyrosine-phosphorylated proteins are mainly localized in cytoplasm (607 proteins), nucleus (379 proteins), plasma membrane (259 proteins), extracellular region (223 proteins), Golgi apparatus (84 proteins), endoplasmic reticulum (75 proteins) and centrosome (39 proteins), indicating diverse roles of tyrosine-phosphorylated proteins in testis. Function annotation

indicated that tyrosine-phosphorylated proteins in Alternative splicing (294 proteins), Acetylation (279 proteins), Ubl conjugation (120 proteins), Cytoskeleton (117 proteins) as well as Methylation (92 proteins) were enriched. KEGG pathway analysis revealed enrichment in ErbB signaling pathway (22 proteins), Fc epsilon RI signaling pathway (18 proteins), Insulin signaling pathway (25 proteins), Neurotrophin signaling pathway (23 proteins) and Tight junction (23 proteins). The enrichment of these pathways showed important functions of tyrosine-phosphorylation in these processes.

Although tyrosine phosphorylation is of low abundance, it has wide regulatory functions in spermatogenesis. Our study provides a resource for the further functional analysis of the tyrosine phosphorylation in testicular development and spermatogenesis, which remains a challenge to surmount.

**The Early Conceptus and Circulating Progesterone Concentrations in Caribbean Jennies.** B.N. Roberts, R.O. Gilbert, D.R. Bergfelt, E.W. Peterson, J.C. Samper, and H.M. French

Donkeys are essential in many parts of the world. Few studies have explored the early pregnancy in jennies. The aim of this study was to define the development of the early conceptus in jennies; such as the day of first detection of the embryonic vesicle (EV), day of fixation, morphological changes, detection of the embryo proper, heart beat and allantoic sac. Additionally, this study compares circulating progesterone during non-pregnant and pregnant cycles in relation to corpus luteum (CL) volume and EV diameter.

Eight Caribbean jennies were monitored through four non pregnant estrous cycles via daily transrectal ultrasonography and every other day blood collection for determination of serum progesterone concentration. At estrus, the same jennies were bred to a jack of proven fertility daily until ovulation. Thereafter, daily ultrasound exams and blood collection continued to determine the volume of the CL and progesterone concentrations. In all jennies, pregnancy was confirmed by day 10. The diameter of the EV was measured to evaluate growth rate. Day of fixation was defined as the day the embryo ceased movement. Subsequent to fixation, daily ultrasonography was used to monitor morphological shape changes and detection of embryo proper, fetal heartbeat and emergence of allantoic sac. Monitoring of the conceptus, CL volume and progesterone concentration ceased on day 30 of pregnancy.

Six of the EV were identified on day 9 and the remaining two on day 10, with the mean diameter 2.4 mm ( $\pm 0.77$  SEM). During the mobility phase, growth rate of the embryo showed linear progression at 3.75 mm/d ( $\pm 0.19$  SE). From day 18 to 28, growth rate plateaued and the slope was not significantly different from zero. Linear growth resumed on day 28. Fixation occurred between day 13 and 16 with the mean diameter of the vesicle 23.9 ( $\pm 0.47$  SE). In 7/8 jennies, the vesicle size one day prior to fixation was less than 22 mm. Once the EV became greater than 22 mm in size, fixation occurred. This suggests that size of the vesicle is more important to fixation than day of pregnancy. Morphological changes, day of first detection of the embryo proper, embryonic heart beat and emergence of the allantoic sac was consistent with past studies in mares and jennies.

For the first 10 days post ovulation, progesterone concentrations were significantly higher in pregnant donkeys compared to their non-pregnant cycles ( $P < 0.001$ ). From day 10 to day 16, the diameter of the

EV was significantly positively correlated to cumulative progesterone exposure ( $P < 0.0001$ ). Cumulative progesterone exposure up to Day 9 was higher for those jennies in which the conceptus was detected on Day 9 than in those for whom first detection was on Day 10. These results suggest that the effects of early pregnancy on luteal function occur sooner than previously thought. Additionally, larger EV are correlated to higher amounts of circulating progesterone, suggesting a greater chance of survival. This is the first report of different progesterone profiles during the early pregnancy of equids and the first correlation between progesterone and embryo growth.

**The Pubertal Transition Impacts Egg Quality Parameters in the Mouse.** Atsuko Kusuvara, Luhan T. Zhou, Allison R. Grover, Sarah R. Wagner, Teresa K Woodruff, and Francesca E. Duncan

Egg quality dictates fertility outcomes, and there is a well-documented decline that occurs with advanced reproductive age that contributes to infertility, miscarriages, and birth defects. How egg quality changes at the other age extreme of the pubertal transition is less understood. Anthropologic and epidemiologic studies suggest that egg quality may be suboptimal during this period as well. For example, adolescence is associated with a period of sterility following menarche, and the incidence of embryo aneuploidy is lowest in females between 26-30 years old. Here we established a mouse model of the pubertal transition that spans postnatal day (PND) 11 to PND40. In this model, animal weight and the incidence of vaginal opening increased across the age spectrum, and serum levels of inhibin B, a marker of gonadal maturation, increased after PND11-15. Together these results validate the pubertal transition model, which we then used to systematically evaluate egg quality parameters. Both oocyte yield and diameter increased across puberty, and there was an age-associated acquisition of meiotic competence, or the ability of oocytes to resume meiosis and reach metaphase of meiosis II (MII) following in vitro maturation (IVM). Oocytes from mice younger than PND15 lacked meiotic competence, but there was a progressive increase in the percentage of oocytes that reached MII between PND 16 and PND18, which plateaued thereafter. The meiotic spindle was analyzed in mature eggs following IVM. The spindle-to-cytoplasmic volume ratio decreased across the pubertal transition, and eggs from the youngest age cohort (PND16-20) had a higher incidence of chromosome configuration abnormalities relative to the other ages. Specifically, a larger proportion of these cells had a telophase I configuration, indicating a cell cycle delay and suggesting that eggs obtained immediately following the acquisition of meiotic competence require further maturation. Analysis of ovarian tissue histologic sections across the pubertal transition revealed that oocytes from the youngest cohort of mice were derived from the smallest antral follicles with the least number of cumulus layers per oocyte. Thus given their small size and fewer number of associated somatic cells, oocytes from the youngest age cohort likely lack cytoplasmic competence, and this is consistent with the observation that these oocytes also have thinner zonae pellucidae. Understanding egg quality during this developmental period has important clinical implications because mature eggs from prepubertal and adolescent girls obtained through ex vivo IVM are cryopreserved in the fertility preservation setting.

This work was supported by the MS-RSM Program and the Center for Reproductive Health After Disease (P50 HD076188) from the National Centers for Translational Research in Reproduction and Infertility (NCTRI)

**Zika Virus Reduces Embryo Attachment and Growth in a Rhesus Macaque in Vitro Peri-Implantation Model.** Jenna Kropp Schmidt, Lindsey N. Block, Matthew T. Aliota, Thomas C. Friedrich, Michele L. Schotzko, Gregory J. Wiepz, and Thaddeus G. Golos

Zika virus (ZIKV) infection in human pregnancy has been associated with severe fetal malformations including microcephaly, as well as adverse pregnancy outcomes such as miscarriage and fetal growth restriction. Human case reports have established that ZIKV is sexually transmitted and that viral RNA persists in semen for an extended duration beyond clearance of blood viremia. Infectious virus in semen thus presents a concern for the use of assisted reproductive technologies as it is not known whether the presence of the virus in semen poses a risk to embryonic and placental development. It has been proposed that the first trimester conceptus may be the most vulnerable to infection, however, the impact of ZIKV on early embryonic development of the primate placental lineage has been unexplored. Nonhuman primates are excellent models for studying human placentation, thus our objective was to define the impact of ZIKV on early embryonic development and early placental development in a rhesus macaque model. We hypothesize that ZIKV can infect the preimplantation embryo, negatively impact embryonic development, and disrupt trophoctodermal differentiation and subsequent placental development. Previously, we established a nonhuman primate in vitro peri-implantation model where in vitro fertilized (IVF) rhesus macaque embryos demonstrated embryo attachment, trophoblast outgrowth, and hormone secretion. Rhesus IVF embryos were inoculated with ZIKV virus/H.sapiens-tc/PUR/2015/PRVABC59\_v3c2 (PRVABC59) at fertilization, after blastocyst hatching, six days post-plating on Matrigel, or were cultured as non-infected controls. Gametes were co-incubated with  $1.82 \times 10^5$  PFU ZIKV overnight during IVF, whereas embryos plated in the peri-implantation model were incubated with ZIKV at a dose of  $1.82 \times 10^5$ ,  $1.82 \times 10^4$ , or  $1.82 \times 10^3$  PFU ZIKV for five hours. Physiologically relevant doses were estimated based on existing literature regarding sexual transmission of ZIKV. Embryos infected at fertilization were not significantly different from control embryos in terms of cleavage (72% infected vs 76% control) or blastocyst (30% infected vs 29% control) rates. Inoculation of hatched blastocysts with ZIKV resulted in a dose-dependent effect on embryo attachment by day 2 of culture with 0% ( $10^5$  PFU), 33% ( $10^4$  PFU), and 50% ( $10^3$  PFU) of inoculated embryos attached, compared to 56% of control embryos. No hatched embryos inoculated with high dose ZIKV survived to day 10 of culture, whereas 100% of low dose and control embryos survived. However, embryonic outgrowth diameter of low dose inoculated embryos was reduced compared to control embryos at day 10. Progesterone secretion into culture medium from day 6 to day 10 was significantly lower in culture medium from embryos inoculated with  $10^4$  PFU compared to control embryos ( $86.72 \pm 36.63$  ng/mL vs  $645.17 \pm 237.23$  ng/mL;  $P < 0.01$ , unpaired t-test). Overall, these results suggest that the zona-enclosed embryo is not affected by ZIKV, but embryos that have formed the trophoctoderm, the placental progenitor lineage, are severely impacted by ZIKV exposure. Thus early stages of pregnancy may be profoundly sensitive to infection and fetal loss.

**SPAR1 is a Novel Transmembrane Protein Required for Acrosome Formation in Mice.** Julio M. Castañeda, Yuhkoh Satouh, Darius J. Devlin, Martin M. Matzuk, and Masahito Ikawa

The sperm acrosome is a cytoplasmic organelle adjacent to the nucleus that is required for fertility in many species. This organelle contains receptors that are required for binding to the egg surface to initiate sperm-egg fusion. Failure to form the acrosome leads to globozoospermia (round-headed

sperm) and male infertility. Using an in silico approach, we have identified a novel mouse gene required for sperm acrosome formation, Spar1. Sperm Acrosome Required 1 (Spar1), is a mammalian specific, transmembrane-encoding gene conserved from platypus to humans. To study Spar1 function, we generated Spar1 mutant alleles in mice using CRISPR/Cas9. Males homozygous for a +1-frameshift mutation have sperm that can initiate acrosome formation; however, step 7 round spermatids begin to display acrosome vesicle detachment from the nuclear envelope with loss of the vesicle in later steps of spermiogenesis. Spermatids absent the acrosome also display defects in their nuclear shape, reminiscent of globozoospermia. Using a FLAG tagged allele of endogenous Spar1, we have localized SPAR1 to the inner membrane of the acrosome vesicle adjacent to the nuclear envelope. SPAR1 localization suggests that SPAR1 functions to anchor the acrosome vesicle to the acroplaxome, a protein complex containing structural proteins located between the acrosome vesicle and nucleus. Interestingly, SPAR1 protein is not expressed in elongated spermatids and not present in epididymal spermatozoa, indicating that the role of SPAR1 in anchoring the acrosome is restricted to the initial stages of spermiogenesis. We have also generated a hypomorphic allele of Spar1 missing only one amino acid (F43). Males homozygous for the hypomorphic allele are also infertile; however, these males display spermiogenesis comparable to wildtype controls. Current work is focused on determining the SPAR1 interactome to help explain the molecular function of SPAR1. The studies on both the null and hypomorphic allele will be presented.

This work was supported by Eunice Kennedy Shriver National Institutes of Child Health and Human Development grants R01HD088412 and P01HD087157.

**Prostaglandins Elicit Different Intracellular Calcium Signalling Patterns in Vitro in a Cell-Specific Manner That May Have Consequences for Human Uterine Function.** Jessica Edge, Katarina Tencheva Miteva, Lynn McKeown, and Niamh Forde

During the menstrual cycle in humans, changes in the steroid hormone concentrations in circulation throughout the cycle drive transcriptomic and phenotypic alterations to the different cells of the uterine endometrium. One of the main processes that occurs is to establish uterine receptivity (UR) to implantation. If successful implantation does not occur, the endometrium is shed during menses to allow a new menstrual cycle to begin. Two members of the group of lipid molecules known as prostaglandins (PGs), play a major role in this process. Prostaglandin E2 (PGE2) can modify gene expression in the endometrium to help establish UR, while Prostaglandin F2 alpha (PGF2 $\alpha$ ) plays a role in menstruation in the non-pregnant state. The functional role that PGE2 and PGF2 $\alpha$  play in modifying the endometrium may occur in part, by differential activation of calcium signalling in the different cells of the endometrium. This project tested the hypothesis that these two PGs elicit different intracellular calcium signalling cascades, in a cell-specific manner in different in vitro cell models of human endometrium. To test this hypothesis, two in vitro cell lines were used: 1) human umbilical vein endothelial cells (HUVECs) and 2) Ishikawa cell line (endometrial epithelium). These cell lines (early passages) were cultured with DMEM/F12 to 70% confluence under 37°C and 5% CO<sub>2</sub>. Both HUVECs (50,000 live cells/well) and Ishikawa cells (70,000 live cells/well) were treated with PGE2 and PGF2 $\alpha$  in a dose dependent manner (n=3 biological replicates, n=6 technical replicates) for 1 hour. Following pre-treatment with PGs cells were either 1) left untreated (control), treated with 2) vehicle, (70% EtOH) 3) ATP (10 $\mu$ M) or 4) thrombin (2.5U/mL). Both ATP and thrombin are activators of calcium signalling.

Mobilisation of intracellular calcium was determined by measuring changes in fluorescence in cells preloaded with Fura-2 using the Flex station. In HUVECs, PGE<sub>2</sub> significantly reduces thrombin activated calcium signalling (P 0.05). Neither PGs had an effect on ATP induced calcium signalling in HUVECs or Ishikawa cells (P>0.05). Preliminary analysis showed pre-treatment of Ishikawa cells with PGE<sub>2</sub> enhanced and PGF<sub>2</sub>α inhibited thrombin activation of intracellular calcium signalling. Future work will focus on how PGs alter intracellular calcium signalling in endometrial endothelial and or stromal cells and how these may alter endometrial function. These data could have implications for enhancing UR to implantation or identifying new targets to regulate menstruation.

**O-GlcNAcylation is a Highly Conserved Modification with Distinct Subcellular Targets During Meiosis in Bovine and Human Gametes.** Luhan Tracy Zhou, Chad E. Slawson, Mary Ellen Pavone, John Zhang, Raquel A. Romar, and Francesca E. Duncan

The mammalian oocyte has high metabolic demands as it undergoes oogenesis and meiotic maturation in preparation for successful fertilization and preimplantation embryo development. Thus, the oocyte is likely highly susceptible to changes in nutrient availability. O-GlcNAcylation – the addition of a single sugar residue (O-linked β-N-acetylglucosamine) on proteins - is a unique post-translational modification that acts as a cellular nutrient sensor. O-GlcNAc metabolism is part of the hexosamine biosynthetic pathways (HBP) and is sensitive to carbohydrate, amino acid, fatty acid, and ATP fluxes. O-GlcNAcylation of proteins is mediated by the opposing actions of two enzymes: O-GlcNAc transferase (OGT) which adds O-GlcNAc onto proteins and O-GlcNAcase (OGA) which removes it. Thousands of proteins are O-GlcNAcylated, and perturbation of O-GlcNAc cycling is a hallmark of diabetes, cancer, aging, cardiovascular disease, and neurodegenerative conditions. Given the broad effects of O-GlcNAc cycling on cellular function, our goal was to investigate O-GlcNAcylation dynamics in bovine and human oocytes during meiosis and determine the consequence of O-GlcNAc perturbation on oocyte meiosis in the bovine. We examined the expression and localization of OGA, OGT, and O-GlcNAcylated substrates in oocytes at different stages of meiosis following in vitro maturation (IVM) of bovine cumulus oocyte complexes (COCs). Using western blot analysis, we observed immune-reactive bands corresponding to O-GlcNAcylated proteins (>250, 250, 200, 150, 110, and 70 kDa), OGA (140 kDa), and OGT (120 kDa). Based on immunocytochemistry and confocal microscopy, we found that O-GlcNAcylated substrates, OGA, OGT localized throughout the gamete cytoplasm but were also enriched at specific subcellular localizations. For example, O-GlcNAcylated proteins were concentrated at the nuclear envelope at prophase I, OGA at the cortex throughout meiosis, and OGT at the meiotic spindles. We have further extended these studies to human eggs obtained from the Northwestern University Reproductive Tissue Library under Institutional Review Board-approved protocols. The localization of these proteins was similar across species demonstrating high conservation of this modification. To examine the function of O-GlcNAcylation, we disrupted O-GlcNAc cycling in bovine gametes using Thiamet-G (TMG), a highly selective, water-soluble inhibitor of OGA. Treatment of COCs with 50 μM TMG during IVM resulted in a dramatic increase in O-GlcNAcylated substrates and a compensatory increase in OGA expression in both cumulus cells and the oocyte. Despite the increase in O-GlcNAcylated proteins, there was no effect on cumulus expansion nor on meiotic progression, as equal numbers of treated and untreated gametes reached metaphase of meiosis II. In vitro fertilization (IVF) studies are ongoing to determine the ability of TMG-treated gametes to undergo fertilization and preimplantation embryo development. Our

research has important implications for metabolic conditions such as maternal diabetes, where intracellular O-GlcNAc levels are elevated in mouse blastocysts and development is compromised.

**Evaluation of Lipid Membrane Peroxidation, Mitochondrial Membrane Potential and Oxidative Stress of Bull Sperm Cryopreserved in Iodixanol-Containing Extender.** Tairini Erica Cruz, Fernanda Nunes Marqui, Alicio Martins Jr., Tatiana Issa Uherara Berton, Camila de Paula Freita-Dell'Aqua, José Antônio Dell'Aqua Júnior, and Eunice Oba.

The process of freezing causes cryoinjuries to the mitochondrial-rich sperm midpiece associated with the uncoupling of oxidative metabolism, increasing reactive oxygen species (ROS) production and changing phospholipids membrane configuration. Few researches have suggested that iodixanol acts as an antioxidant agent on spermatozoa membrane, preserving their motility and preventing the oxidative stress during cryopreservation. This study was designed to investigate the effects of different concentrations of iodixanol added to the freezing extender on lipid membrane peroxidation (LP), mitochondrial membrane potential (MMP), O<sub>2</sub>- and H<sub>2</sub>O<sub>2</sub> production after sperm thawing. A total of 18 ejaculates from 3 Nelore bulls (6 replicates, once per week) were obtained at Artificial Insemination Station during the months of May and June. The sperm samples were assessed through routine laboratory work, consisting of motility, vigor, concentration and sperm abnormality. A commercially available bovine freezing extender consisted of egg yolk-glycerol supplemented with iodixanol at concentrations of 0, 2.5, 5, and 10%, was used to form the control, IOX-2.5, IOX-5, and IOX-10 groups, respectively. Following dilution, 3 pooled sperm samples were cooled (4°C for 5 h) and loaded into 0.50 ml French straw to contain a final concentration of 30 x 10<sup>6</sup> sperm/insemination dose, just before freezing. Afterwards, the semen samples were thawed in a water bath at 37°C/30s and stained with the combination of MitoSOX Red and MitoStatus Red probes to measure the production of O<sub>2</sub>- and changes in MMP. Assessment of H<sub>2</sub>O<sub>2</sub> and LP was performed using dihydrorhodamine 123 and C11-BODIPY, respectively. Sperm samples were analyzed by flow cytometer with results expressed as fluorescence intensity (arbitrary units; AU), considering the total number of cells or percentage of damaged cells for LP. Analysis of variance and Tukey's test were used for statistical analysis with P < 0.05 taken as significant. There was no significant difference among groups for LP, MMP, and O<sub>2</sub>-. Higher fluorescence was observed in IOX-10 (153.6 ± 5.2) for H<sub>2</sub>O<sub>2</sub> in comparison to control (129.8 ± 4.6), but similar results for H<sub>2</sub>O<sub>2</sub> were found among IOX-10, IOX-5, and IOX-2.5, as well as for control group, IOX-5, and IOX- 2.5. These are the first report, to our knowlegment, on the use of fluorescent probes to assess oxidative stress, LP and MMP status in bovine semen frozen with iodixanol. In addition, it can be concluded that added iodixanol had no beneficial effect on sperm membrane phospholipids, membrane mitochondrial function, H<sub>2</sub>O<sub>2</sub>, and O<sub>2</sub>-. Acknowledgements: CAPES, Tairana Artificial Insemination Station and Botupharma, Brazil.

**Myo10 is Required to Regulate Mtocs Clustering and Sorting in Mouse Oocytes.** Ahmed Z. Balboula, Magdalena Zernicka-Goetz, and David M. Glover

A critical step in oocyte maturation is the formation of a bipolar spindle that provides the machinery for accurate chromosome segregation. In contrast to mitotic cells, oocytes lack centrosomes and, therefore, bipolar spindle assembly in meiosis depends on self-organization of numerous microtubule organizing

centers (MTOCs) into two poles. The molecular mechanism regulating this self-organization in oocytes is not fully understood. Using high-resolution time-lapse confocal microscopy to trace fluorescently labeled DNA and MTOCs, we revealed that MTOCs undergo two critical processes, MTOCs clustering and sorting to assemble bipolar spindle. However, how these two processes are regulated in mammalian oocytes has remained largely unknown.

Myosin 10 (Myo10) is an actin-based motor that belongs to unconventional myosin family. We found that inhibition of Myo10 using siRNA-mediated knockdown resulted in Metaphase I (Met I) arrest with a significant increase in the proportions of multipolar spindle. To understand the mechanism in more detail, we examined Myo10-depleted oocytes using both time-lapse confocal microscopy and immunocytochemistry. Our results revealed that Myo10 is an essential regulator of MTOC clustering. Myo10-depleted oocytes showed a significant increase in MTOC number and a decrease in their size. Moreover, MTOC sorting was also perturbed in Myo10-depleted oocytes, where MTOCs were distributed along the longitudinal axis of the spindle and failed to be allocated into two spindle poles. However, the question remains open of how Myo10 regulates these functions.

Interestingly, in contrast to mitosis, actin filaments (F-actin) localize to the meiotic MT spindle and forms a structure called the actin-spindle. How F-actin localizes to the spindle and the significance of such localization for bipolar spindle assembly are still unknown. We found that depolymerizing F-actin using Cytochalasin D or Latrunculin B phenocopied MTOC clustering and sorting defects in Myo10-depleted oocytes, and consequently resulted in increased percentages of multipolar spindle at Met I.

Interestingly, Myo10 has a MyTH4 domain at its C-terminal region which enables it to bind MTs directly, suggesting that Myo10 might act as a linker between F-actin and MTs in mammalian oocytes. Accordingly, we asked whether Myo10 functions to recruit F-actin to the meiotic spindle of mouse oocytes. We found that Myo10 localizes to the meiotic spindle, and such localization is perturbed after depolymerizing MTs but not after depolymerizing F-actin, suggesting that Myo10 spindle localization is a MT-dependent. Importantly, F-actin was unable to localize to the spindle in Myo10-depleted oocytes, suggesting that Myo10 is required for F-actin localization to the meiotic spindle to form an actin-spindle and to regulate spindle bipolarity. These results are consistent with the finding that artificial enrichment of actin to the spindle using MAP4-UtrCH results in sharply focused spindle poles.

Our results suggest a model of a positive feedback mechanism where Myo10 is required to recruit F-actin to MTs which, in turn, form the platform for the Myo10 motor to cluster and sort MTOCs. Moreover, these findings reveal an unexpected function of actin in bipolar spindle assembly in mammalian meiosis, a process that is notoriously prone to mistakes. This research supported by Marie Curie Individual fellowship (Horizon2020,706170) to DMG and AZB.

**Concurrent Mutations in Kristen Rat Sarcoma and AT-Rich Interactive Domain 1A are Sufficient to Cause the Development of Endometriosis and Ovarian Cancer in Mice.** Jillian R. Hufgard, Xiyin Wang, Diana Monsivais, Robert Emerson, and Shannon M. Hawkins

Endometriosis is a debilitating gynecologic disease that affects 5-10% of US women. Women with endometriosis are at increased risk of ovarian cancer, specifically, endometrioid and clearcell ovarian adenocarcinomas. Recent work showed that loss-of-function mutations of AT-rich interactive domain 1A (ARID1A) were common in these endometriosis-associated ovarian cancers. However, work from us and

others showed that deletion of *Arid1a* in mouse models was not sufficient to induce cancer. Because 29% of endometriosis-associated ovarian cancers from women have oncogenic mutations in *KRAS*, we added oncogenic *Kras* to our *Arid1a* conditional knockout mouse model. To study the interactions between loss of *Arid1a* and gain of oncogenic *Kras*, we created and characterized the *Arid1aflox/Arid1aflox;Kras lox-stop-lox-G12D (mut)/Kraslox-stop-lox-G12D (+);Amhr2Cre/Amhr2+* (*Arid1aflox/flox;Krasmut/+;Amhr2cre/+*) mouse. When bred to wild-type males *Arid1aflox/flox;Krasmut/+;Amhr2cre/+* female mice demonstrated a decreased number of pups per litter compared to controls (11 versus 1.4,  $p \leq 0.001$ ,  $n=4-5$  per group). Long-term survival studies demonstrated that *Arid1aflox/flox;Krasmut/+;Amhr2cre/+* female mice had decreased survival with 70% of mice dying by 335 days ( $n=20-21$  per group,  $p \leq 0.01$ ) compared to control mice. Uterine to body weight ratios in *Arid1aflox/flox;Krasmut/+;Amhr2cre/+* mice were decreased from 6 to 12 weeks, while ovarian weight to body weight ratios were increased starting as early as 3 weeks. Gross ovarian endometriosis-like lesions were observed as early as 4 weeks in *Arid1aflox/flox;Krasmut/+;Amhr2cre/+* mice with over 59% (13/22) penetrance by 12 months. Detailed pathological evaluation of all *Arid1aflox/flox;Krasmut/+;Amhr2cre/+* ovaries confirmed the presence of endometriosis with endometrial glands, stroma, and hemosiderin-laden macrophages. 55% (6/11) of *Arid1aflox/flox;Krasmut/+;Amhr2cre/+* mice had pathology confirmed endometriosis by 9 months of age. This penetrance increased to 68% (15/22) at 12 months. Interestingly, 27% (3/11) of *Arid1aflox/flox;Krasmut/+;Amhr2cre/+* female mice at 9 months developed benign hemangiomas. 18% (4/22) of *Arid1aflox/flox;Krasmut/+;Amhr2cre/+* female mice at 12 months developed malignant ovarian spindle cell sarcomas. The *Arid1aflox/flox;Krasmut/+;Amhr2cre/+* female mice represent a new developmental model of endometriosis. This work was supported by NCIR03CA19127.

### **A Highly Efficient Method for Generating Knock-In Mouse with CRISPR/Cas9 System and Ssodn.**

Yiqiang Cui, Guanglei Li, Xuejiang Guo, and Jiahao Sha

It has emerged that the RNA-guided DNA endonuclease Cas9 is a useful tool for genome engineering. It has ushered in the new vane of gene editing history. CRISPR/Cas9 system has its advantages of convenient construction, high knock-out efficiency and various usages in cells and organisms system, and it has been widely used in genetic research. In studying diseases caused by genetic deficiency, there are many single nucleotide polymorphisms (SNPS) locus associating with many diseases according to big data screening, in addition to genetic deficiency which directly affects gene expression. We applied the CRISPR/Cas9 system, firstly using T7en1 enzyme to test sgRNA efficiency in 3T3 cell line and efficient sgRNA was gained, then combining Cas9 mRNA with single oligonucleotide donor (ssODN) for embryo injections, successfully constructed directional point mutant mice. In order to optimize this gene editing tool, we constructed a 293T cell line with a single copy of the BFP gene by lentiviral vector. Since there is only one amino acid difference between BFP and GFP gene, we used different lengths of ssODN as a repair template comparison, flow cytometry analysis was used to found that the use of the antisense strand mutation efficiency was higher than the use of sense chain. Next, we compared the HR efficiency of different ratio of the distance between DSB point and mutation point. We summarized all designed sites and their ssODN in order to obtain more efficient design for point mutation by high-throughput analysis: 1. When multiple sgRNAs are located near the mutation site, the sgRNA with the highest cleavage efficiency was selected. 2. The sgRNA cleavage site is as close as possible to the mutation site. 3. Donor ssODN mutation sites locate at DSB 5' or 3' side. The mutation efficiency of the 3' side is higher

than 5' side. Our findings can enable rational design of sgRNA and donor ssODN for efficient point mutation genome editing on gene therapy.

**Effects of CoQ10 on in Vitro Semen Quality of Chickso (Korean Brindled Bull) Semen Stored in Triladyl Diluent.** Sung Woo Kim, In-Sul Hwang, Chan-Lan Kim, Namtae Kim, and Ik Soo Jeon

This report focuses on the effects of CoQ 10 and storage temperature on in vitro characteristics of chickso (Korean brindled bull) semen stored in Triladyl egg yolk diluent. The semen was diluted 1:9 at room temperature and stored at 5 °C of BOD incubator for 6 days with treatment of 1, 10, 50 µg/ml of CoQ 10 at a concentration of 40~60x10<sup>6</sup> sperm/ml. After low temperature preservation, the motility of sperm was assessed by using Sperm Motility Analysis System (Medical Supply, Wonju, Korea). CoQ10 treatment yielded better motility rate at 4 to 6 day (Control vs 50 µg/ml CoQ10; 74.6% vs 82.3% at day 4, 54.2% vs 68.6% at day 6, P < 0 .05). The sperm membrane integrity was assessed by using the Live/Dead sperm viability test kit. The CoQ10 treatments protected the membrane integrity rate than control (42.6% vs 59.6% at day 6, P < 0 .05). In conclusion, our findings showed the possibility of long term preservation of chickso fresh semen with CoQ10 treatment with incresement of longevity of spermatozoa and integrity of sperm membranes; further results on in vitro fertilization and embryo development are ongoing.

**Integrated Analysis of Differentially Expressed Circrnas, Mirnas and Mrnas Provide Novel Insights Into BPA Induced Reproductive Toxicity.** Honggang Li, Huimin Li, and Xiaotong Wang

Our study aimed to investigate the epigenetic regulation of non-coding RNAs in BPA induced reproductive toxicity. High-throughput sequencing was carried out to reveal the circRNA/miRNA/mRNA expression profiles of 120µM BPA treated GC-2 spd cells and normally grow cells. A total of 4706 and 6486 circRNAs candidates were identified in normally grow GC-2 cells and 120µM BPA treated cells for 48h, respectively. And miRNAs and circRNAs sequencing also showed more miRNAs and miRNAs were up-regulated than down-regulated after BPA treatment, suggesting the activated RNA regulation in BPA toxicity. GO and KEGG analysis revealed that most of these dysregulated RNAs were enriched in processes like DNA damage, DNA repair, cell cycle, etc. Comprehensive ceRNA network and translation potency analysis showed a number of hotspot circRNAs that may play roles by sponging miRNAs or translate proteins. The 25 most differentially expressed circRNAs were validated by RT-PCR. And among them 8 most abundant circRNAs were overexpressed and these circRNAs showed significant effects in alleviating or aggravating the process of BPA induced apoptosis. Junction target siRNAs were designed for four of these eight circRNAs, and apposing effects were observed compared to the gain of function study. Downstream molecular mechanism analysis suggested that these circRNAs may take active apart in BPA induced apoptosis by sponging multiple miRNAs. All these results revealed that active non-coding RNA regulation takes part in BPA induced spermatocyte apoptosis. A number of circRNAs may serve as new targets in blocking the reproductive toxic effects of BPA.

**Conserved Genetic Pathways for Follicle Maturation and Ovulation.** Jianjun Sun, Lylah Deady, Wei Li, and Elizabeth Knapp

In the past several years, we investigated the cellular and molecular mechanisms of follicle maturation and ovulation in *Drosophila*, which proved to be highly conserved as in mammals. *Drosophila* oocytes

are surrounded by a layer of follicle cells, equivalent to granulosa cells in mammals. Ovulation in *Drosophila* involves a proteolytic degradation of posterior follicle cells, follicle rupture, and formation of a corpus luteum-like structure with residual follicle cells. In order for ovulation to occur, follicle cells need to differentiate properly to express matrix metalloproteinase 2 (Mmp2) at the posterior end and an adrenergic receptor (Oamb) in the entire follicle cell layer (Deady et al., 2015, PLoS Genet). We found that norepinephrine-like neuronal hormone octopamine (OA) activates Oamb receptor in follicle cells, which induces Ca<sup>2+</sup> influx, Mmp2 activation, and follicle rupture (Deady and Sun, 2015, PLoS Genet). Parallel to progesterone in mammalian ovulation, we also found that ecdysteroid signaling is activated in mature follicle cells and essential for Mmp2 activation and ovulation (Knapp and Sun, 2017, PNAS). With powerful genetic tools available, we performed RNAi-based screens and identified multiple novel follicular factors involved in ovulation. In this presentation, I will present two novel factors (a zinc-finger transcription factor Hindsight and a NADPH oxidase). We discovered that Hindsight, homologous to Ras-response element binding protein 1 (RREB-1), is upregulated in mature follicle cells which sequentially activates Mmp2 expression in posterior follicle cells and Oamb expression in all follicle cells. This role can be replaced by human RREB-1, indicating the possible role of RREB-1 in mammalian ovulation (Deady et al., 2017, eLife). In addition, we also discovered that the NADPH oxidase (Nox) is highly enriched in mature follicle cells. Nox enzymatic activity is controlled by OA/Oamb-Ca<sup>2+</sup> signaling. Nox knockdown in mature follicle cells leads to reduction of superoxide and defective ovulation. Furthermore, extracellular superoxide dismutase 3 (Sod3) is required to convert superoxide to hydrogen peroxide, which acts as a key signaling molecule for ovulation, independent of Mmp2 activation. Since ROS is essential for mammalian ovulation and Nox homologs are also expressed in mammalian follicles, our results strongly suggest that Nox-dependent hydrogen peroxide plays a conserved role in regulating ovulation. Thus our work is establishing a complex signaling network in follicle cells that mediate follicle maturation and ovulation, which is likely conserved in mammals. This work is supported by a R01 grant from NICHD (R01-HD086175).

**Effect of Preovulatory Estradiol or Postovulatory Progesterone on Pregnancy Rate in Postpartum Beef Cows.** L. A. Ciernia, M. F. Smith, G. A. Perry, J. J. Rich, E. J. Northrop, S. D. Perkins, R. E. Geisert, J. A. Green, A. L. Zezeski, and T. W. Geary

Preovulatory secretion of estradiol and postovulatory secretion of progesterone are essential for preparing the uterine environment for pregnancy in cattle. In a previous study, preovulatory estradiol at gonadotrophin releasing hormone (GnRH)-induced ovulation (d 0) and postovulatory progesterone on d 7 were the two most important factors affecting establishment of pregnancy. Therefore, two experiments were conducted to further examine the effect of circulating concentration of estradiol at GnRH-induced ovulation (d 0) as well as the change in estradiol from prostaglandin F<sub>2α</sub> (PGF)-induced luteolysis (d -2) to GnRH-induced ovulation (d 0; Exp 1) and the effect of supplementing progesterone (d 4 to d 11; Exp 2) on pregnancy rate in postpartum beef cows. In Exp 1, ovulation was synchronized in cows (n=719) as follows: on d -9 GnRH and an intravaginal progesterone implant (CIDR) was administered, on d -2 the CIDR was removed and PGF was injected, and on d 0 GnRH was administered. Estrus detection patches (Estroject) were placed on cows on d -2, and any cow with an activated patch on d 0 was considered to have exhibited estrus and removed from the study (n=302). Blood samples were collected on d -2 and 0, and plasma measured for estradiol by RIA. Recipient cows were sorted based on their d 0 (mean ± SEM) concentration of estradiol as follows: low (2.43±0.68a pg/ml; n=155),

middle ( $3.95 \pm 0.46$  pg/ml;  $n=117$ ), or high ( $5.82 \pm 1.03$  pg/ml;  $n=145$ ) estradiol groups ( $abcP < 0.0001$ ). Each cow received an in vivo produced embryo on d 7 and pregnancy diagnosis occurred between d 30 and 34, and d 81 and 118 of gestation. Pregnancy rate on d 30 to 34, and d 81 to 118 for the low, middle, and high estradiol groups were 28%<sup>a</sup>, 47%<sup>b</sup>, and 55%<sup>b</sup> ( $abP = 0.0017$ ) and 26%<sup>a</sup>, 42%<sup>b</sup>, and 50%<sup>b</sup> ( $abP = 0.007$ ), respectively. Change in estradiol (between d -2 and d 0), but not estradiol on d -2, had a positive effect ( $P = 0.0002$ ) on pregnancy rate. In Exp 2, ovulation was synchronized as described for Exp 1; however, cows ( $n=174$ ) were artificially inseminated to a single bull at 66 h following PGF-induced luteolysis and CIDR removal. Cows were allotted to a control ( $n=88$ ) or treatment ( $n=86$ ) group by breed, age, body condition, and days postpartum. Treatment included insertion of a CIDR on d 4 and removal on d 11. Pregnancy rate on d 43 or 49 for the control and CIDR groups were 68% and 71%, respectively ( $P = 0.70$ ). In summary, elevated preovulatory estradiol on d 0 and an increasing estradiol concentration from d-2 to 0, increased pregnancy rate after embryo transfer; however, supplemental progesterone supplied by a CIDR from d 4 to 11 had no effect on pregnancy rate of beef cows receiving TAI. Supported by AFRI Grant no. 2013-67015-21076 from the USDA NIFA.

**Luteal Metabolomics Suggests a Role for Lipid Mediators as Regulators of Cell Death, Cell Migration, and Immune Function.** Camilla K. Hughes, Lindy M. Wetzel, Remy Bosviel, John Newman, and Joy L. Pate

The corpus luteum (CL) is a transient endocrine gland that produces progesterone and maintains pregnancy. Although the CL contains high concentrations of lipid in the form of steroid hormone precursors and is also a site of prostaglandin production, little is known about the abundance or function of other luteal lipid mediators. To address this knowledge gap, luteal lipid mediator profiling was performed on bovine CL. In the first experiment, CL from day 4, 11, and 18 were compared. In the second experiment, day 11 CL were compared to CL that had been collected at 1, 4, 8, 12, and 24 hours after induction of luteal regression with PGF<sub>2A</sub>. In the third experiment, CL of day 18 of the estrous cycle and pregnancy were compared. Seventy-nine lipids were measured using ultra-performance liquid chromatography-tandem mass spectrometry. Lipid concentrations were Box-Cox transformed, center-scaled, and analyzed by either an ANOVA with a Tukey posthoc test or a T-test. Partial least squares analysis demonstrated clustering of lipids from individual treatment groups. Twenty-four lipids were differentially abundant as the estrous cycle progressed and all were greater on day 11 than on day 4, with nine remaining high on day 18, indicating a general upregulation of lipid mediator synthesis. Luteal regression altered the abundance of 35 lipids. Cluster analysis was used to group lipids with similar patterns of expression during luteal regression. The two clusters with the most differentially abundant lipids showed similar bimodal patterns of abundance, with an early increase (1 or 4 hours), a decrease around 8 hours, and another peak and nadir at 12 and 24 hours, respectively. Only one lipid, 15-KETE, was lesser during early pregnancy, with a tendency ( $p$  <http://www.metaboanalyst.ca/>) indicated modulation of arachidonic acid metabolism and alpha linolenic and linoleic acid metabolism as the estrous cycle progressed and alteration of PGD<sub>2</sub> signaling and arachidonic acid metabolism during luteal regression. Lipids that were differentially abundant during early pregnancy were integrated with a dataset of differentially abundant transcripts from early pregnancy. The top gene-lipid networks containing both differentially abundant genes and lipids indicated that lipids may be regulators of MAPK and MYC signaling, and may regulate cell movement and migration, cell interaction, and immune cell differentiation. These data suggest a role for lipid mediators during luteal development, regression, and

early pregnancy, as regulators of immune cells, intracellular signaling, and cell death. Funding provided by the C. Lee Rumberger and Family Endowment to JLP and USDA NIFA predoctoral fellowship no. 2017-67011-26062 to CKH.

**SMAD1 and SMAD5 are essential for female fertility and hormonal response.** Diana Monsivais, Ph.D., Keisuke Shimada, D.V.M, Ph.D., Maya L. Kriseman, M.D., Clark Hamor, Renata Prunskaitė-Hyyryläinen, Ph.D., Stephanie A. Pangas, Ph.D., Masahito Ikawa, Ph.D, Martin M. Matzuk, M.D., Ph.D.

The establishment and outcome of a successful pregnancy is dictated by effective communication between the implanting embryo and its mother. At the cellular level this communication consists of physical interactions between various ligand/receptor complexes and by subsequent intracellular responses initiated by cytokines, growth factors and hormones. It was previously determined that maternal signals mediated by the bone morphogenetic proteins (BMPs) and their cognate cell surface receptors are critical for early and mid-gestation embryo development. Despite the crucial roles of the BMP ligands and receptors during pregnancy, little is known about the global genomic networks that are activated or repressed downstream of BMPs by the SMAD1/5 transcription factors. Global inactivation of SMAD1 and SMAD5 results in embryonic lethality precluding its study in reproductive function, therefore, we generated mice with conditional inactivation of SMAD1 and SMAD5 using progesterone receptor cre (*Smad1flox/flox;Smad5flox/flox;Pgr-cre+/-*, or “*Smad1/5 cKO*”). Histological and molecular analyses determined that sterility was the result of impaired uterine receptivity. At 4.5 days post-coitum (dpc) implantation sites were not visualized by Chicago blue vascular dye injection, yet fertilized unattached blastocysts were recovered from the lumen of *Smad1/5 cKO* mice, indicating failed embryo attachment to the luminal epithelium. During the window of implantation, uteri of *Smad1/5 cKO* mice responded abnormally to estradiol and to progesterone and showed elevated expression of estradiol-regulated genes and decreased expression of progesterone-responsive genes. Further analyses determined that the blunted uterine progesterone response was the result of decreased levels of progesterone receptor gene expression in the *Smad1/5 cKO* mice. Uteri of *Smad1/5 cKO* mice did not respond to an artificial decidual stimulus and the stroma failed to differentiate. At 12 weeks of age *Smad1/5 cKO* mice presented enlarged cystic uterine glands that developed into hemorrhagic lesions as the mice aged. 3-dimensional analysis of the uterus by optical projection tomography also demonstrated abnormalities in uterine glandular orientation and coiling of the *Smad1/5 cKO* mice during early pregnancy. Decidualization defects in the absence of SMAD1 and SMAD5 were also observed in human endometrial stromal cells. Cumulatively, these results demonstrate that the SMAD1/5 transcription factors have crucial roles in uterine homeostasis, are crucial for female fertility, and control the uterine response to hormones by modulating the expression of the progesterone receptor.

Support: NICHD R01-HD32067 (to MMM), IRACDA K12-GM084897 (DM), Postdoctoral Enrichment Award from the Burroughs Wellcome Fund (DM).

**Na<sup>+</sup>/H<sup>+</sup> Regulatory Factor-1 in Spermatozoa is Correlated with Boar Fertility.** Ki-Uk Kim, Won-Ki Pang, Sae-Han Kang, Ki-jin Kwon, Kyu-Ho Kang, Do-Yeal Ryu, Won-Hee Song, Md Saidur Rahman, Woo-Sung Kwon, and Myung-Geol Pang

Na<sup>+</sup>/H<sup>+</sup> regulatory factor-1 (SLC9A3R1) is closely associated with various physiological aspects in spermatozoa. It has been reported that SLC9A3R1-null mice die 30–35 days postpartum. In addition, localization of SLC9A3R1 has been confirmed in midpiece of mouse spermatozoa and interacts with other proteins in spermatozoa to facilitate sperm anion exchange during capacitation. Since capacitation is the penultimate steps in fertilization, the role of SLC9A3R1 in fertilization need to be elucidated. Here, we evaluated the expression levels of SLC9A3R1 in boar spermatozoa (n = 20) of different fertility by qRT-PCR. To obtain prospective fertility of boars (litter size), we conducted artificial insemination (AI) field trial (semen was inseminated to 615 sows for ≥ 19 times). The litter size cut-off value (average litter size = 12.1; high fertility=12.8; low fertility=11.4) was established by receiver operating characteristic (ROCs) curve. In addition, motility parameters and capacitation status of spermatozoa were measured by computer-assisted sperm analysis and Hoechst 33258/chlortetracycline fluorescence staining, respectively. A significantly positive correlation was found between the expressions of SLC9A3R1 and boar fertility (r=0.543; P=0.013). The overall accuracy of SLC9A3R1 for predicting litter size was 75%. Unexpectedly, we did not find any correlation between the levels of SLC9A3R1 with motility, motion kinematics, and capacitation status of spermatozoa. Based on the current findings, we summarized that SLC9A3R1 might consider as a biomarker to systemically examine boar fertility even it did not correlate with other physical markers of fertilization such as motility, motion kinematics, and capacitation ability. Thus, the marker may provide new developmental tools for the prognosis and diagnosis of male fertility as well as male contraceptive targeting. However, further studies are required to validate our initial findings.

This work was supported by Korea Institute of Planning and Evaluation for Technology in Food, Agriculture, Forestry, and Fisheries (IPET) through Agri-Bio Industry Technology Development Program, funded by Ministry of Agriculture, Food, and Rural Affairs (MAFRA) (116172-3).

**Effect of Cisplatin and Doxorubicin on Prepubertal Testicular Germ Cells.** Norah Spears, Prathima Tholeti, Richard A. Anderson, Satish K. Adiga, Rod T. Mitchell, and Federica Lopes

Chemotherapy drugs in childhood cancer treatment raise concerns regarding their long-term effects on fertility. Cisplatin and doxorubicin are two highly effective drugs used to treat childhood cancer patients. Whilst the drugs can cause severe damage to the adult gonads, their effects on the immature testis are less well understood. We have recently shown that cisplatin and doxorubicin both induce rapid germ cell loss in the prepubertal testis. In this work, we aimed to investigate the dose dependent response of the drugs, using an in vitro system that can support long term testis development, including the establishment of full spermatogenesis, in culture, here using the system to allow development of germ cells through to spermatocytes. Testes were obtained from CD1 mice at P5 (post-natal day 5) and cultured on polycarbonate membranes floating on culture medium containing  $\alpha$ -MEM, 10% KSR, 1% antibiotic -anti-mycotic, at 34°C/5% CO<sub>2</sub>. On Day 2, tissue was treated with cisplatin or doxorubicin for 24hrs at concentrations of 0.25mg/ml (low; n=9), 0.5mg/ml (medium; n=8) and 0.75mg/ml (high; n=10) or 0.01mg/ml (low; n=9), 0.03mg/ml (medium; n=12) and 0.05mg/ml (high; n=8), respectively. BrdU was added 24hrs prior to termination of culture for subsequent identification of proliferating cells and on Day 8, tissues were fixed in NBF or Bouin's fixative for immunofluorescence or histological studies respectively. Germ cells were identified through expression of MVH for total germ cell population, PLZF for spermatogonial stem cells (SSCs) and SCP3 for spermatocytes. Compared with P13 age-matched

tissue, germ cell density did not differ between cultured and non-cultured tissue, showing similar developmental pattern between in vitro cultured tissue and in vivo testis. The density of SSCs and of all germ cells was reduced in a dose dependent manner after exposure to either cisplatin (cell density as percentage of control: SSCs - low 29%; medium 18%; high 13% and total germ cell population - low 24%; medium 13%; high 6%) or doxorubicin (cell density as percentage of control: SSCs - medium 46%; high 19% and total germ cell population - low 60%; medium 43%; high 24%) ( $p < 0.001$  for all). The remaining SSCs after drug exposure showed no change in proliferation rate. The density of spermatocytes showed a significant dose dependent reduction after cisplatin treatment group (cell density as percentage of control - low 14%; medium 10%; high 5%;  $p < 0.001$ ), while doxorubicin treatment resulted only in a much smaller reduction in spermatocytes and only after exposure to the high doxorubicin concentration (cell density as percentage of control - 55%;  $p < 0.05$ ). In summary, exposure to cisplatin or doxorubicin led to a dose-dependent reduction in the germ cell and specifically in the SSC population of the prepubertal testis. No effect was seen on the proliferative ability of remaining SSCs. The main difference between the two drugs was their effect on spermatocytes, with cisplatin but not doxorubicin leading to a marked reduction.

#### **Elevated Cytokeratin Expression in Spontaneously Occurring Epithelial Ovarian Tumors.** Gopalan Lalitha and Ramachandran Ramesh

Ovarian cancer is a highly metastatic disease that leads to high mortality and has poor 5-year survival rates in women who were diagnosed with advanced stages of the disease. Animal models that spontaneously develop ovarian cancer can be very useful in understanding the pathogenesis of ovarian cancer and to develop early diagnostic tools. Leghorn chickens ovulate 400-times or more within 2 years of age and develop ovarian cancer spontaneously at very high incidence rate (>25%). Previous studies have shown that ovarian cancer metastasizes in the chicken model as it does in women. Considering the extensive metastasis, it is important to distinguish primary ovarian cancer from cancers arising from other organs but metastasized to the ovaries. Cytokeratin is a cytoskeletal intermediate filament which is specifically related to the stem cell and progenitor cell activity in endocrine and glandular epithelium. As specific keratin expression is associated with the cell types, keratins can be used as markers for the epithelial cancers. Furthermore, keratins also play a role in tumorigenesis by rendering tissues permeable to cancer cell invasion. The hypothesis for the present study was that expression of cytokeratin is higher in epithelial ovarian tumors compared to normal ovaries. Leghorn hens in the age group of 3-4 years were monitored for signs of an advanced stage of ovarian cancer (anovulation, paleness of comb, ascites, inanition, dyspnea, gait abnormalities) and were euthanized for collection of the ovary for histology and RNA extraction. Total RNA was extracted from the ovary and reverse transcribed using MMLV-reverse transcriptase and random primers. Cytokeratin mRNA and 18S ribosomal protein mRNA abundance in a cancerous ovary and normal ovary ( $n=8$ ) was quantified using Perfecta SYBR green fast mix in 7500 Fast Real-time PCR systems (Applied Biosystems). Relative abundance of cytokeratin 8 mRNA was assessed and compared between normal and cancerous ovaries. Cytokeratin 8 mRNA levels were found to be 28-fold higher in cancerous ovaries compared to normal ovaries ( $P < 0.01$ ; Student t-test). Paraffin-embedded ovarian tissue sections of normal and cancerous ovaries were subjected to immunohistochemical staining for cytokeratin using monoclonal anti-human cytokeratin AE1/AE3 antibody (Millipore). Distribution of cytokeratin was analyzed using a semi-quantitative method by grading (0- no staining to 4+ extensive staining). The ovarian tumor tissues

section had a staining intensity grade of 3+ to 4 + as compared to the normal ovarian tissues which had a grade of 0-2+. Cytokeratin staining in ovarian tumor sections was diffuse throughout the stroma with intense staining on the surface epithelium, while the staining was restricted to the surface epithelium in the normal ovary. These results suggest that cytokeratin expression is elevated in the ovarian tumors and possibly served as the source of cancerous cells for invasion in other visceral organs.

Research reported in this publication was supported by National Cancer Institute of the National Institutes of Health under award number R03CA208573

### **Attainment and Maintenance of Pubertal Cyclicity May Predict High A4 cows with Reduced Fertility.**

Sarah Nafziger, Mohamed A. Abedal-Majed, Sarah Tenley, Adam Summers, Mariah Hart, Jeff Bergman, Scott Kurz, Jennifer Wood, Robert Cushman, and Andrea S. Cupp

The UNL physiology herd has a population of cows that secrete excess androstenedione (A4) in follicular fluid. These High A4 cows are less fertile, have irregular cycles and are often anovulatory. Ovarian cortex cultures of High A4 cows also secrete 43 fold more A4 than controls. Interestingly, these High A4 cows (n=46) reached puberty 45 days earlier than control cows (n=59), but this difference did not reach statistical significance ( $P = 0.17$ ). To further examine age at puberty in these heifers and potentially identify females that may be predisposed to become High A4 cows, blood plasma samples were collected from weaning to breeding (October-May) each year from 2012-2016 (total n=497). There were approximately 13 blood samples collected in 2012- and 2013-born heifers, and frequency of sample collection was increased to weekly for the 2015-2016 sample collections. Progesterone (P4) for each sample was detected by RIA with 1ng/ml, the current industry standard, used to define puberty date and monitor cyclicity. A custom SAS analysis was developed to detect four distinct puberty groups using puberty date as time of first  $P4 \geq 1$  ng/ml and whether cyclicity continued over the sampling period, with first sampling date removed due to stress at weaning: 1) Early Puberty-  $315.0 \pm 4.2$  days of age with continued cyclicity (n=106); 2) Typical Puberty-  $380.3 \pm 2.4$  days of age with continued cyclicity (n=230); 3) Start-Stop Puberty-  $263.7 \pm 4.1$  days of age with discontinued cyclicity (n=85); and 4) Non-Cycling- no  $P4 \geq 1$  ng/ml during the sampling period (n=76). At breeding, heifers were given 2 injections of prostaglandin  $F2\alpha$  14 days apart, and all heifers that showed estrus in response to prostaglandin were artificially inseminated. Typical (78.9%) and Early (79.5%) puberty heifers displayed the greatest percentage estrus in response to prostaglandin ( $p < 0.001$ ). Interestingly, a greater percentage of Start-Stop heifers (50.3%) displayed estrus and were artificially inseminated compared to Non-Cycling heifers (12.6%) ( $p < 0.001$ ). Start-Stop heifers have similar progesterone profiles to Non-Cycling heifers except for small progesterone peaks early in the sampling period but do not continue cycling. To determine if Start-Stop and Non-Cycling heifers had other characteristics of High A4 cows, ovarian cortex was cultured, and both Start-Stop (3.0 ng/ml) and Non-Cycling (4.2 ng/ml) heifers had ovarian cortex that secreted increased A4 in culture media compared to cortex from Typical (0.062 ng/ml) or Early (0.091 ng/ml) puberty heifers. The greater concentrations of A4 produced by ovarian cortex of Start-Stop and Non-Cycling heifers along with irregular or no cyclicity indicates that these females could be predisposed to become High A4 cows with decreased fertility. USDA is an equal opportunity provider and employer. This research was funded through USDA grant 2013-67015-20965.

**Comparison of Endothelial Growth Medium and MEM-Based Medium for Culture of Isolated Cat Ovarian Follicles.** J. B. Nagashima, H. Kenar, R. El Assal, U. Demirci, D. E. Wildt, and N. Songsasen

Antral cavity development during folliculogenesis depends on vascularization of the growing follicle. Recapitulation of this process in vitro for producing a developmentally competent oocyte will require maintaining endothelial (EC) and follicular cells during culture. Endothelial growth medium (EGM2) developed to support ECs has not yet been tested for in vitro follicle culture. Our laboratory previously observed a detrimental influence of fetal bovine serum (FBS, 10%) on incubated domestic cat ovarian tissue-enclosed follicles. However, 2 to 5% FBS is typically used to promote EC growth in vitro in other mammalian species. Here, we assessed the influences of EGM2 and FBS on growth and survival of isolated cat follicles. The hypothesis was that EGM2 promotes development of early antral and antral stage follicles compared to MEM, but that a high FBS concentration (7%) is detrimental to follicle survival. Mechanically isolated cat follicles were embedded in a 0.35% alginate hydrogel, then cultured in MEM or EGM2 with 2 or 7% FBS. Preantral (223  $\mu\text{m}$ , n = 97) follicles were cultured for 10 d at 38°C and 5% CO<sub>2</sub>. At the end of culture, diameter (as indicator of growth) and morphology (survival) were determined for each follicle and oocyte as well as antral cavity expansion. Medium had no effect (P > 0.05) on preantral or early antral follicle growth, whereas antral follicles grew larger (P < 0.05) of medium or FBS on follicle survival. Antral cavity expansion occurred in 7.7% and 10.6% of follicles in MEM and EGM2, respectively (P > 0.05), and exclusively for only early antral and antral stage follicles. In summary, we demonstrated a stage-specific influence of medium, but not FBS concentration, on cat follicle growth in vitro. Results indicate that (1) an MEM-based medium, supplemented with critical growth factors as necessary, is preferred for antral follicle-EC co-culture in the domestic cat model, and (2) a moderate FBS concentration (needed for EC maintenance) is not detrimental to follicle growth or survival. This work represents an important first step in the development of a culture system for large mammalian follicles supportive of stromal cells, for application to genome rescue and fertility preservation. (Supported by NIH F32HD090854).

**Non-Nuclear Core Somatic Histones are Novel Constituents of the Rat PT and Appear to be De Novo Synthesized During Spermiogenesis.** Morgan Lion, Genevieve Acteau, Lauren Hamilton, Nicole Protopapas, Wei Xu, Peter Sutovsky, and Richard Oko

The perinuclear theca (PT) is a cytoskeletal structure that houses various proteins involved in important cellular processes during spermiogenesis and fertilization. In a previous publication, we provided unprecedented evidence for the localization of non-nuclear core somatic histones within the bovine PT. Our current goal was to explore the extractability, localization, and developmental origin of non-nuclear core somatic histones in the sperm head of rat. SDS-PAGE analysis of SDS- or HCl-extracted rat sperm revealed bands at 14kDa, 17kDa, 18kDa and 19kDa which, by immunoblotting with anti-core somatic histone antibodies, corresponded respectively to calf thymus core histones (H3, H2B, H2A and H4) run in adjacent lanes. Immunofluorescent and immunogold labeling demonstrated the localization of these histones to the PT, specifically to the post-acrosomal sheath (PAS) and the perforatorium (PERF). Developmentally, the core somatic histones were associated with the microtubules of the manchette within the cytoplasmic lobe of elongated spermatids and in the wake of the manchette's nuclear descent, appeared to be deposited into the PAS and PERF regions of the PT. Since the PAS and PERF are formed at the end of the elongation phase of spermiogenesis, well after the nuclear somatic histones

have been discarded, we hypothesized that PT-derived somatic histones are de novo synthesized in round spermatids. To test this hypothesis, we performed QRT-PCR analysis on mRNA from STAPUT isolated testicular cells and demonstrated that the expression of H2B was 2.6X higher in haploid cells than in tetraploid cells (when normalized to DNA content of respective cells). In summary, the core somatic histones not only reside in the PAS of murid as they do in bull sperm, but also in an additional compartment of the PT, called the perforatorium. Our findings also suggest that non-nuclear core somatic histones in the PT of mammalian sperm are synthesized de novo during spermiogenesis, rather than recycled from the nucleus.

This work was supported by NSERC (RGPIN/192093) (RO), Agriculture and Food Research Initiative Competitive Grant no. 2015-67015-23231 from the USDA National Institute of Food and Agriculture (PS), as well as by seed funding from the Food for the 21st Century Program of the University of Missouri (PS).

### **Differential Co-expression Analysis of Transcriptome Data from Beef Heifers of High and Low Fertility.**

Sarah E. Dickinson, Brock A. Griffin, Michelle F. Elmore, Joshua B. Elmore, Paul W. Dyce, Soren P. Rodning, and Fernando H. Biase

The identification and selection of heifers with high fertility potential remains a central limitation in cattle production systems because of the highly polygenic nature and low heritability of reproductive traits. Here, we leverage molecular genetic biotechnology to further our understanding of the genetic architecture of fertility in beef heifers. The objective of this study was to determine if differences in heifer fertility potential could be associated with differential co-expression of genes expressed in peripheral white blood cells (PWBC) collected at the beginning of a heifer's first breeding season. We generated mRNA sequencing from PWBC collected at the time of insemination from phenotypically similar, pubertal beef heifers that became pregnant at first service to fixed-time artificial insemination (high fertility (HF) potential; n=6) or failed to become pregnant after artificial insemination followed by a 42-day breeding season in the presence of a fertile bull (low fertility (LF) potential; n=6). We identified 10,832 genes in our dataset and quantified Pearson's correlation (r) values for all pairs of genes. Over 58.6 million correlations were quantified, of which 5670 genes formed 24,790 pairs that displayed high correlation values in both groups of heifers. Across the datasets (HF and LF), high positive correlation ( $r > 0.99$ ) was observed in 17,616 pairs formed by 3,496 genes, and high negative correlation ( $r < -0.99$  in LF heifers; loss of correlation:  $|r| > 0.99$  in HF and  $r \sim 0$  in LF heifers; or inverted correlation:  $r > 0.99$  in HF and  $r < -0.99$  in LF heifers or vice-versa). Co-expression was gained in 2,139 pairs formed by 2,280 individual genes. Furthermore, co-expression was lost in 449 pairs formed by 662 genes. While no gene ontology biological process was enriched among genes that developed co-expression, 76 of the 662 genes whose correlation were lost ( $r \sim 0$ ) in LF heifers were enriched in the gene ontology biological process 'regulation of transcription, DNA-templated' (FDR < 0.08). Furthermore, we identified inversions in correlations of 16 pairs formed by 23 individual genes (FDR < 0.0001). Notably, gene ontology analysis of these 23 genes revealed significant enrichment of the gene ontology biological processes 'steroid metabolic process' (LDLR, SRD5A1; FDR < 0.01) and 'regulation of transcription' (ZNF350, ZSCAN29, FOXO1, ENSBTAG00000046664; FDR < 0.08). In conclusion, differential co-expression of genes expressed in PWBC may reveal fine-tuned integration of immune cells with the well described hormonal interaction in the hypothalamus-ovary axis. Funding: This work was partially funded by the Alabama Agricultural

Experiment Station, and the Hatch program of the National Institute of Food and Agriculture, U.S. Department of Agriculture.

**Mapping Extracellular Matrix Protein Composition Across Ovarian Compartments and Remodeling during Folliculogenesis.** Nathaniel F. C. Henning, Kelly A. Even, Brian J. FitzSimmons, Monica M. Laronda

Premature ovarian insufficiency (POI) can occur in childhood cancer survivors as a result of their disease treatments or diagnosis. The only option for fertility preservation in children or women, who cannot undergo egg harvesting, is to remove a piece of ovarian tissue and preserve it for later use. In many cases, the children at increased risk of POI have diagnoses that render the preserved tissue unsafe to transplant. Therefore, our ultimate goal is to understand the ovarian niche and its role in maintaining the follicle pool and supporting folliculogenesis. The extracellular matrix (ECM) is a complex network of carbohydrates and proteins that forms the organ 'skeleton' and provides both structural and biochemical support. Additionally, the ECM also provide signals that modify cell proliferation, differentiation, and migration. In this project we describe our method for mapping the distribution of the ECM and associated proteins in the porcine ovary. The cortex is the first 0.5 mm of the ovary and contains the majority of the primordial follicles while the medulla (>0.5 mm) contains the majority of activated follicles (primary, secondary, and antral). We are correlating this data with changes in ECM composition as folliculogenesis occurs in situ. Towards this end, we have deconstructed porcine ovaries into 0.5 mm slices, removed the cellular components while isolating ECM and associated proteins through decellularization, and performed an unbiased proteomics analysis. By processing ovaries both cranially and sagittally we constructed an ECM protein map throughout the entire ovary and across both the cortical and medullary compartments. We found that decellularized cortex slices are 1.1 times denser (0.39 g/cm<sup>3</sup>) than medulla (0.35 g/cm<sup>3</sup>) slices. We identified over 1000 proteins of which the expression of 317 were significantly different (FDR < 0.01) across depths of the ovary. We then examined the relationship between maturation of the ovarian follicle and the dynamics of the ECM using in situ culture methods. Previously our lab has cultured ovarian biopsies taken from humans, cows, and pigs. We have examined robust reorganization into a spheroid that re-established the ovarian surface epithelium (OSE) and contained growing antral follicles within the center. We cultured biopsy punches and examined ECM dynamics using semi-quantitative protein and mRNA expression assays targeting ECM proteins found via our proteomics analysis, to elucidate how the ECM remodels during the stages of folliculogenesis. Using qPCR we identified increases in expression of two ECM remodeling genes as the ovarian spheroids form in culture (ADAMTS16 and MMP14). Additionally, we observed changes in expression for markers of folliculogenesis such as cannabinoid receptor 1 (CNR1) and potassium two pore domain channel subfamily K member 9 (KCNK9). We predict that this foundational work will further define how the ovarian niche supports or is remodeled by folliculogenesis and inform the design of an effective engineered scaffold with appropriate mechanotransductive cues for a bioprosthetic ovary transplant.

### **Hyper-O-GlcNAcylation Impairs the Therapeutic Effect of Progesterone in Endometrial Cancer Cells.**

Nicole Morin Jaskiewicz and David H. Townson

While the incidence of most types of cancer has declined in the U.S. in recent years, the number of cases of endometrial cancer continues to rise. Mean age of onset of endometrial cancer in U.S. women is 60 years, but in 14% of the cases diagnosed the women are of reproductive age, and are often obese, and/or suffer from metabolic disorders like insulin resistance and hyperglycemia. Fertility-sparing progestin treatment rather than surgical intervention is often the therapy of choice in these women, but the efficacy of this approach in the midst of metabolic disorders is unknown. Such disorders often lead to adverse alteration of cellular proteins, including hyper-O-GlcNAcylation, which is associated with many cancers including endometrial cancer. The objective of the current study was to initially evaluate the effects of hyper-O-GlcNAcylation in endometrial cancer cells in vitro, including the efficacy of progestin therapy. Endometrial cancer cells (Ishikawa) were pre-exposed to the O-GlcNAcase inhibitor, Thiamet-G (ThmG), to induce hyper-O-GlcNAcylation. Subsequently, cultures of the cells were treated without/with 100nM progesterone (P4) to assess cellular proliferation, invasion, and expression of cyclin-dependent kinase inhibitors (p21 and p27) that influence cell cycle control. As expected, P4 alone inhibited cellular proliferation ( $p < 0.05$ ). Treatment with P4 similarly impaired cellular invasion ( $p < 0.05$ ,  $n=2$  independent experiments), as measured by Matrigel invasion assays, but the effect was negated by hyper-O-GlcNAcylation and resulted in higher rates of cellular invasion ( $p < 0.05$ ) in both P4-treated and non-treated cultures. Mechanistically, the therapeutic effect of progestin is hypothesized to be mediated in part by an upregulation of p21 and p27 proteins. In the current study, however, immunodetectable p21 and p27 was observed only in cultures exposed to the combination of ThmG and P4 ( $n=5$  independent experiments). The results suggest hyper-O-GlcNAcylation, which is common in obese and diabetic patients, hinders the therapeutic efficacy of P4 in endometrial cancer cells. Thus, O-GlcNAcylation status might provide insight about the likelihood of progestin therapy success in endometrial cancer patients. This material is based upon work supported by the National Science Foundation Graduate Research Fellowship under Grant No. (DGE 1450271).

### **Identification and Characterization of piRNAs in Male Dogs.** Leanne Stalker, Stewart Russell, Fernanda Dos Santos, and Jonathan LaMarre

PIWI interacting RNAs (piRNAs) are a sub-class of small non-coding RNAs, 26-32 nucleotides in length, with a 5' uridine bias and 3' methylation. These RNAs associate specifically with protein members of the Argonaute family of RNA binding proteins, known as PIWIs (P-element-Induced-WImpy-testis) to form piRISC silencing complexes. The canonical function of piRISCs is to suppress transposable elements during gamete and embryo development. Recent studies have suggested that piRNAs may perform additional regulatory functions through targeting complementary mRNA sequences, leading to downstream changes in gene expression. Most mammalian research on the PIWI system has been performed in rodents however we recently investigated PIWIL1 biology in the dog and found that PIWIL1 expression in testis increases with sexual maturity. Here, we examined the small RNA population present in both mature and immature canine testes ( $n=3$  per stage) using Next Generation Sequencing. After data processing and filtering, collapsed reads were annotated against non-coding RNA databases using Uunitas (<http://www.smallrnagroup.uni-mainz.de/software.html>). Unannotated sequences between 24-32nt were then mapped against the unmasked dog reference genome (CanFam3.1). A large

percentage of mapped sequences showed piRNA-like (pilRNA) features, including a distinct 1U bias and the presence of a 5'-5' overlap indicative of a ping-pong signature. Reads were further analyzed for genomic clustering as well as retrotransposon mapping. PilRNAs were compared against human, mouse and rat piRNA sequences present in public piRNA databases revealing substantial conservation of piRNAs to syntenic genomic loci. Differential expression analysis was then conducted between pre- and post-pubertal groups. The pilRNAs were classified in 3 groups according to the expression tendency over maturity: down regulated, if  $\log(\text{RPKM})^2$  and neutral if no significant differences were observed. Differential expression was verified on selected pilRNAs using qRT-PCR. To investigate potential mRNA targets the pilRNAs were aligned with the canine mRNA transcript database, using blastn optimized for short sequence queries. Putative pilRISC targets expressed in testes were subjected to GO and KEGG analysis with results suggesting involvement in sexual maturation. This work describes the first characterization of piRNAs in the dog, and demonstrates that piRNA populations, although frequently conserved through mammalian evolution, can be altered over sexual maturity and may target mRNAs in addition to retrotransposons. This work was funded through the Found Animals Foundation, Michelson Prize and Grants.

**Conceptus-Derived Proteins with Conserved Sequences in Different Mammalian Species, Alter Expression of Candidate Mrnas in the Endometrium in Vitro, in a Species-Specific Manner.** Haidee Tinning, Lauren Mayo, Alisha Taylor, Matthew M. Lucy, Georgious Oikonomu, Miguel A. Velazquez, Achim Treumann, Mary J O'Connell, and Niamh Forde

In most mammalian species, bilateral communication between the conceptus (embryo and extra-embryonic membranes) and the maternal uterine environment is essential for successful early pregnancy. In cattle, maternal recognition of pregnancy (MRP) must occur by day 16 following fertilization, to maintain the corpus luteum and enhance uterine receptivity to implantation. The process of MRP is mediated by production of sufficient quantities of Interferon Tau (IFNT) by the conceptus however we have previously shown that the conceptus produces proteins (including CAPG and PSAT1) other than the IFNT that may facilitate the MRP or uterine receptivity to implantation. We tested the hypothesis that some conceptus-derived proteins other than IFNT alter the transcriptome of the endometrium to enhance the pregnancy recognition process and that these changes may be conserved amongst different mammalian species. To test this hypothesis, we tested the conservation of these proteins across different mammalian species. FASTA format sequences were downloaded from ENSEMBL and aligned using multiple sequence alignment. Permutation Tail Probability testing and likelihood mapping were performed to test for phylogenetic signal for these proteins. Recombinant forms of these proteins were produced by using an E. coli expression vector system for CAPG (bovine), PSAT1 (bovine and human) and IFNT (bovine). These proteins were added in a dose dependent manner (10, 100, 1000ng/ml) to either abattoir-derived bovine endometrial explants from mid-late luteal phase uteri (2 hr and 24 hr: n=3 biological replicates) or immortalized human Ishikawa endometrial epithelial cells (24 hr: n=3 biological replicates) alone or in combination. Quantitative real-time polymerase chain reaction (qRT-PCR) was carried for candidate mRNAs associated with MRP. Both CAPG and PSAT1 had 83% and 93% sequence conservation between human and bovine forms of these proteins. ANOVA analysis of qRT-PCR data demonstrated exposure of bovine endometrial explants to CAPG in combination with IFNT significantly altered expression of interferon stimulated genes ISG15, RSAD2, MX1 and MX2 (P 0.05). Collectively these data indicate that although these proteins may be conserved across different

species it is possible they elicit a different response in the endometrium of different species. Future work will focus on analyses of other candidate mRNAs associated with MRP as well as effect of PSAT1 in these in vitro model systems. We would like to acknowledge the funding from N8 Agrifood which contributed to this work, and are also grateful to the University of Leeds Protein Production Facility, funded by the University of Leeds and the Royal Society Wolfson Laboratory Refurbishment Grant.

**Follicular and Luteal Dynamics of the Estrous Cycle Under Tropical Conditions in Caribbean-Based Donkeys.** Rachael L. Ambrosia, Robert O. Gilbert, Don R. Bergfelt, Juan C. Samper, Eric W. Peterson, and Hilari M. French

Eight non-pregnant, regularly cycling Nevisian Jennies were examined via transrectal ultrasound to define the ovarian dynamics under tropical conditions. Daily palpation of each donkey took place over four consecutive ovulatory cycles to map and measure each follicle and subsequent corpus luteum. Jugular venipuncture was performed every other day and aliquots of serum stored for progesterone hormone assays to confirm estrous cyclicity and define luteal function with volume. Previously published literature gave conflicting data on the number of follicular waves prior to a dominant ovulatory follicle emerging, and luteal functional volume in donkeys has not previously been studied. The mean ( $\pm$ SEM) inter-ovulatory interval across all donkeys and cycles was found to be 22.93d ( $\pm$ 1.99d), and was repeatable within each donkey. This value was substantially shorter (by 2 and 3 days) than previously published data, which could be attributable to breed or global location. Follicles were retrospectively characterized into groups defined as small, medium, and large defined as average diameters  $\leq$ 10mm, 11 to 19mm, and  $\geq$ 20mm, respectively. Once a follicle grew to  $>$ 30mm, the donkey was monitored via transrectal ultrasonography every 6 hours to more accurately determine pre-ovulatory size. Mean maximum follicular diameter was 34.63mm ( $\pm$ 2.91mm), which was significantly different on paired t-test ( $P=0.029$ ) from the immediate pre-ovulatory follicular diameter average of 34.11mm ( $\pm$ 3.31mm). Both of these values were significantly correlated ( $P=0.0008$  and  $0.0023$ , respectively) to the inter-ovulatory interval for each donkey, indicating longer intervals were associated with larger sized follicle and pre-ovulatory follicles. When the largest follicle was isolated from each day, a two-wave pattern became evident with the first wave reaching maximum diameter (around 23-25mm) around day 7 or 8 post-ovulation, and the second wave of follicles  $\geq$ 10mm emerged around day 14. The first wave was usually a minor wave (largest follicle  $<$  2.5mm) consistently in 6 out of the 8 donkeys. When looking specifically at follicular dynamics, it became evident that the total follicular numbers were consistent within each jenny, but not between them. There is also a correlation between the total number of follicles present throughout a cycle, and serum progesterone levels. Jennies that had more total follicles had lower serum progesterone concentrations; while those that had fewer total numbers of follicles, had higher serum progesterone concentrations. Serum progesterone and luteal volume were also closely related. Five days after ovulation, luteal tissue reached maximal volume before falling gradually after day 15; while progesterone slowly climbed to its maximum serum concentration by days 9 to 10, but then declined precipitously around day 14 or 15. This suggests that steroidogenesis of a corpus luteum decreases much more rapidly than volume at the end of the luteal phase. This study helped clarify and define normal estrous cycle characteristics, which in turn can be utilized in population-control efforts that are ongoing throughout the Caribbean Islands. Future research into other reproductive characteristics will better define specific differences between breeds of donkeys or areas of the globe for use with either population management or improving reproductive techniques.

**In Vivo Antral Follicle Wall Biopsy: A New Research Technique to Study Folliculogenesis at the Cellular and Molecular Levels.** Ghassan M. A. Ishak, Shah T. Bashir, Gabriel A. Dutra, Gustavo D. A. Gastal, Melba O. Gastal, Clay A. Cavinder, Jean M. N. Feugang, and Eduardo L. Gastal

In vivo studies involving molecular markers of the follicle wall associated with follicular fluid milieu are crucial for a better understanding of folliculogenesis. Several ultrasound-guided techniques have contributed to understand mammalian folliculogenesis; however, there is a need to develop an in vivo follicle wall biopsy (FWB) technique to harvest samples during different stages of antral follicle development, without jeopardizing ovarian function. The aims of this study in mares were to: (i) develop ex vivo a minimally invasive technique for harvesting of FWB samples (Experiment 1); (ii) validate in vivo the FWB technique for simultaneous collection of FWB and follicular fluid (FF) samples (Experiment 2); and (iii) characterize the in vivo expression of luteinizing hormone receptor (LHR) and estradiol receptor (ER $\alpha$ ) in follicle wall layers, and intrafollicular estradiol concentration from follicles during different developmental stages (Experiment 2). In Experiment 1, samples (n=47) of six slaughtered mares were collected from 8-10-, 11-19-, and 21-29-mm follicle groups. All follicles were sampled twice using two techniques: biopsy forceps and scalpel blade (control). FWB samples were collected using an endoscopic biopsy forceps (5FR gauge, 60 cm, Karl Storz) located inside a 12 G needle. In Experiment 2, 18 mares were repeatedly used for simultaneous harvesting of FWB and collecting of FF samples (n=72 follicles). The FWB system used in Experiment 1 was mounted on a transvaginal ultrasound-guided transducer for collecting samples from 10-, 20-, and 30-mm follicle groups. Immediately after FWB harvesting, a FF sample was obtained. Histology, immunohistochemistry, and Elisa techniques were used to process the FWB and FF samples. In Experiment 1, the FWB sample recovery rate was 100%, and the thickness of granulosa, theca interna, and theca externa layers was not influenced ( $P>0.05$ ) by the harvesting techniques. In Experiment 2, the overall recovery rates of fragments and FF were 97% and 100%, respectively; however, samples containing all layers of the follicle wall and clear FF samples varied, such as: 10-mm group, 59% FWB and 71% FF; 20-mm, 80% FWB and 90% FF; and 30-mm, 79% FWB and 100% FF. The FWB samples measured  $3.5\pm 0.3$  mm (area),  $7.9\pm 0.4$  mm (perimeter), and  $2.6\pm 0.3$  mg (weight). Follicle diameter did not influence ( $P>0.05$ ) the area, perimeter, or weight of the FWB samples. Expression of LHR was mostly confined in the theca interna layer, with ER $\alpha$  in the granulosa and theca interna layers. The 30-mm follicle group had greater ( $P < 0.05$ ) LHR expression in the theca interna and ER $\alpha$  in the granulosa layer compared to the other groups. The overall expression of LHR and ER $\alpha$ , and the intrafollicular estradiol were higher ( $P < 0.05$ - $P < 0.0001$ ) in the 30-mm follicle group. In conclusion, the FWB technique developed for mares can be used repeatedly and simultaneously to harvest in vivo FWB and FF samples with a satisfactory recovery rate without jeopardizing ovarian function. This technique may bring a new era for in vivo folliculogenesis studies, since it provides sufficient materials for various cellular and molecular techniques associated with FF milieu, and has the potential to be translated to other species, including humans.

**A Role for Epigenetic Regulation of ADAMTS Genes in Abnormal Placentation and Preterm Birth.**

Sneha Mani, Jayashri Ghosh, Yemin Lan, Suneeta Senapati, Teri Ord, Carmen Sapienza, Christos Coutifaris, and Monica Mainigi

Preterm birth (PTB) is the leading cause of infant morbidity and mortality worldwide. However, little is known about its etiology, possibly due to the multifactorial nature of the disease. Assisted reproductive

technologies (ART) such as in vitro fertilization (IVF) increase the risk of PTB and cause genome-wide epigenetic change. The objective of this study was to utilize patients undergoing IVF as a unique population to identify genes responsible for PTB. We hypothesize that common early perturbations due to IVF lead to epigenetic changes in genes responsible for at least a subset of PTB. Using Illumina's Infinium array technology, we interrogated 850,000 methylation sites genome-wide in placentas from 24 term IVF, 11 preterm IVF, 24 term Control and 12 preterm Control pregnancies. We found 7321 CpGs within 1980 genes that were differentially methylated in term vs. preterm IVF placentas and 4379 CpGs within 1316 genes disrupted in Control samples. 618 genes overlapped between both gene sets. Genes disrupted in both IVF and Control groups were predominantly hypomethylated and displayed high correlation between the datasets. Analysis was limited to CpGs with methylation differences of at least 5%, and genes with at least 2 differentially methylated CpGs. To identify candidate genes playing a role in PTB, we carried out Ingenuity Pathway Analysis, which revealed epigenetic dysregulation in canonical pathways, diseases, and regulators associated with cell migration and invasion. Specifically, we found multiple members of the ADAMTS gene family represented in both IVF and Control datasets. These genes function in extracellular matrix regulation and tumor cell invasion, processes similar to those carried out by invasive trophoblasts (EVTs) during early placentation. We validated DNA methylation changes in multiple ADAMTS genes, including ADAMTS12 and ADAMTS16, using bisulfite pyrosequencing. No significant differences in placental gene expression were seen between term and preterm IVF placentas using real-time qPCR. However, we examined control samples during the first and second trimesters and found that both ADAMTS12 and ADAMTS 16 demonstrate a peak of expression at the end of the first trimester, suggesting that epigenetic changes might alter their function during early pregnancy. Localization by immunofluorescence on formalin-fixed paraffin sections demonstrates that both genes are present in all trophoblast cells but are highly enriched in invasive EVT. To understand the functional role of ADAMTS12 and ADAMTS16 during early placentation, we carried out siRNA knockdowns in an EVT cell line. Matrigel invasion assays indicate that knockdown of either gene results in poor EVT invasion through a Matrigel layer. In support of this, gelatin zymography indicates that both genes are important for normal matrix metalloproteinase activity, a marker of EVT invasion. In conclusion, we have identified a potential role for ADAMTS methylation in the development of PTB using a unique population with increased risk for PTB. Functional examination further suggests that at least a subset of PTB may be due to epigenetic abnormalities of genes critical to early placentation. This work identifies novel gene candidates responsible for the development of PTB, which may aid in the development of treatment strategies for women at risk.

**Effect of Fresh vs Frozen Embryo Transfer Technology on the Placental Epigenome.** Jayashri Ghosh, Carmen Sapienza, Monica A. Mainigi, Christos Coutifaris, Kurt T. Barnhart, and Suneeta Senapati

In vitro fertilization involves the transfer of fresh embryos into a superovulated in-utero hormonal environment or the transfer of frozen embryos into a physiologic in-utero hormonal environment. We hypothesized that the type of embryo transfer might influence the maintenance of epigenetic marks after preimplantation epigenetic reprogramming, thereby causing methylation differences at birth. Our group and others have shown that fresh embryo transfers result in placental global hypomethylation of LINE1 elements; yet the differential impact of the in-utero hormonal milieu on gene-specific methylation remains unknown. In the present study, we used the Illumina Infinium MethylationEPIC BeadChip which features > 850,000 CpGs, to identify genes and potential pathways involved in the observed epigenetic

differences in pregnancies conceived after fresh and frozen embryo transfers in a discovery cohort and validated our findings in separate cohort. In the discovery cohort, we assayed 68 placental samples obtained at delivery (20 fresh, 24 frozen and 24 controls) to identify differentially methylated CpGs between fresh and frozen embryo transfers. In the validation cohort, we assayed 96 samples (52 fresh and 44 frozen). CpG sites with two-tailed t-test p-values  $\leq 5\%$  were considered to be significantly different ( $n=16,412$  CpGs). We further identified significant genes as those with at least 2 differentially methylated CpG sites, which resulted in 6501 CpGs. We used similar filtration strategies in the validation cohort and were able to validate methylation differences in 381 CpGs. More than 96 % (367 CpGs) were differentially methylated in the same direction (hypermethylated or hypomethylated) in both the cohorts. Among these, 365 CpGs were hypomethylated in the fresh embryo transfer group compared to the frozen transfer group. Pathway analysis identified multiple genes in the thyrotropin releasing hormone receptor signaling pathway (PLCB4, CACNA1E, PLCB1, TRHR, CACNA1A, CACNB2) to be hypomethylated in pregnancies resulting after fresh embryo transfers. Finally, we evaluated the methylation differences of these two embryo transfer groups compared to controls (natural conceptions) in the discovery cohort. We observed that fresh embryo transfers resulted in more than three times the number of methylation differences (93 differentially methylated CpGs) than frozen embryo transfers (27 differentially methylated CpGs) compared with controls. Furthermore, all of the significant CpGs were hypomethylated in fresh transfers and hypermethylated in frozen embryo transfers compared to controls. Hence, our study indicates that hypomethylation of genes in fresh embryo transfers may result in a dysregulated thyrotropin releasing hormone receptor signaling pathway. This research was supported by Society of Reproductive Endocrinology and Infertility (SS), March of Dimes (CC, MM) and National Institute of Health (P50-HD-068157 (CC, CS); 5K12HD001265 (SS)).

**Crocetin Impacts the Metabolism, Quality and Development of in Vitro-Produced Embryos.** Erika Cristina dos Santos, Riccardo Varchetta, Camila Bruna de Lima, Jessica Ispada, Herculano da Silva Martinho, Patricia Kubo Fontes, Marcelo Fabio Gouveia Nogueira, Bianca Gasparrini, and Marcella Pecora Milazzotto

The earliest stages of embryo development are deeply influenced by reactive oxygen species (ROS), which are byproduct of the mitochondrial oxygen metabolism playing a key role as a messenger in normal cell signal transduction and cell cycling. Although this positive effect, the imbalance due to excess of ROS over an efficient antioxidant control can lead to oxidative stress, with negative consequences to the cell such as DNA damage, metabolic changes, mitochondrial stress and cell death. In this work, crocetin, a natural antioxidant, was added to the culture media of bovine embryos to evaluate the efficiency of its antioxidant capability during the embryo culture. Oocytes were in vitro matured and fertilized according to standard procedure. Embryos were cultured at 38.5°C under humidified air with 5% CO<sub>2</sub>, 7% O<sub>2</sub>, and 90% N<sub>2</sub> in Synthetic Oviduct Fluid (SOF) medium supplemented with amino acids and 5% of FBS (SOFaa) – CTRL; or additional supplementation with 1µM crocetin - CROC. At D5, embryos were transferred to individual drops of culture media. At D7, embryos were assessed by means of blastocyst rates, morphophysiological analyzes (total cell number, ROS and mitochondrial activity levels), transcript quantitation of 91 genes from metabolism and metabolomic evaluation of the culture media by Raman spectroscopy. Embryos from CROC developed more to blastocyst stage and presented increased total cell number and decreased intracellular levels of ROS.

These embryos also had upregulation of genes related to transcriptional control, cell proliferation, antioxidant response and homeostasis (ACACA, ATF4, CCND2, DNMT1, DNMT3B, FOXO3, IMPDH1, IMPDH2, SOD2, SOX2, SREBF1 and SREBF2). Raman spectroscopy revealed a more active lipid and amino acid metabolism. The absence of crocetin in the culture media resulted in higher ROS level as well as up regulation of genes related to DNA damage, energy metabolism and electron transport chain (MORF4L2, PFKP, PGK1, PPARGC1A and PTGS2). Raman spectroscopy also revealed a more active energy metabolism in the CTRL group. In conclusion, crocetin supplementation impact ROS level, leading to an increase in both blastocyst yield and quality as well as changes in metabolic profile of in vitro produced embryos.

**WISP1: A Potential Regulator of Ovarian Tumorigenesis Induced by Constitutively Active Transforming Growth Factor Beta Receptor 1 in Mice.** Nan Ni, Xin Fang, and Qinglei Li

Ovarian granulosa cell tumors (GCTs) belong to sex cord-stromal tumors, accounting for ~5% of ovarian tumors. Although considered to be of low malignant potential, GCTs are generally associated with long disease history and frequent recurrence, and can be a significant cause of death. The molecular pathogenesis of GCTs is poorly understood, preventing the development of new therapies. Transforming growth factor beta (TGFB) signaling regulates ovarian development and function and is involved in gonadal sex cord-stromal tumor development. Our recent studies showed that constitutive activation of TGFB receptor 1 (TGFB $\beta$ R1) in the mouse ovary using anti-Mullerian Hormone receptor type 2 (Amhr2) Cre recombinase promotes GCT formation (termed TGFB $\beta$ R1-CA). However, the molecular basis underlying tumor initiation and progression remains to be defined. Therefore, the objective of this study is to explore the signaling mechanism that contributes to the oncogenesis of GCTs. Our initial next generation sequencing analysis using ovarian tissues from control and TGFB $\beta$ R1-CA mice revealed potential activation of WNT signaling pathway in GCT pathogenesis. Using immunohistochemistry, we examined the expression and localization of beta-catenin (CTNNB1), the effector of the WNT signaling, in the ovary of TGFB $\beta$ R1-CA and control mice. The results showed that the expression of CTNNB1 was mainly detected in early stage follicles within control ovaries. However, strong staining of CTNNB1 was observed in tumor tissues from TGFB $\beta$ R1-CA mice, with variable degree of nuclear staining. Moreover, immunohistochemistry and quantitative real-time PCR revealed the involvement of WNT1 inducible signaling pathway protein 1 (WISP1), a critical regulator of WNT signaling, in GCT development. In addition, real-time PCR demonstrated that the transcript levels of biglycan (Bgn) and decorin (Dcn), two binding factors of WISP1, were increased in TGFB $\beta$ R1-CA ovaries versus controls (n = 4; P < 0.05). Consistently, Creb5, which is essential for transcriptional activity of WISP1, was also upregulated in the ovary of TGFB $\beta$ R1-CA mice. In summary, our results suggest that TGFB signaling interacts with WNT pathway in the pathogenesis of ovarian GCTs. Further studies are needed to identify the functional role of WISP1 and its associated molecules in granulosa tumor cells.

**Interleukin-6 Has Embryotrophic Effects Before and After Embryonic Genome Activation in Bovine Preimplantation Embryos.** Lydia K. Wooldridge and Alan D. Ealy

Previous work from this group determined that interleukin-6 (IL6) supplementation to in vitro produced (IVP) bovine embryos from day 5 post-fertilization to day 8 increases the percentage of blastocysts at

day 8 and increases inner cell mass (ICM) blastomere numbers. Here we sought to determine if supplementation of IL6 from day 1 to day 8 post-fertilization is also beneficial to bovine IVP embryos. In the first study, embryos in group culture were supplemented with either carrier only (NC), 100 ng/ml IL6 provided beginning from either day 1 (D1) or day 5 (D5), 100 ng/ml IL6 administered at day 1 and again at day 5 (D1D5), or 200 ng/ml IL6 provided at day 1 (200D1). Day 8 blastocysts from each treatment (n=16-20 blastocysts total from 4 replicates) were processed for cell counting. All IL6 treatments increased ICM numbers ( $44.2 \pm 4.6$ ,  $81.3 \pm 6.2$ ,  $80.1 \pm 7.9$ ,  $117.4 \pm 11.1$  and  $79.8 \pm 7.9$  for NC, D1, D5, D1D5 and 200D1 treatments, respectively). ICM blastomere numbers also were greater ( $P < 0.05$ ) in the D1D5 treatment than any of the other IL6 treatment groups. In a subsequent study, we cultured embryos individually to determine if IL6 can support embryonic development in the absence of media conditioning from group culture. Embryos were cultured individually from day 1 in the presence of 0 (0IC), 100 (100IC) or 200 (200IC) ng/ml IL6 (n=25 embryos/treatment/replicate; 4 replicates). Embryos in 100IC received additional IL6 via the addition of 1  $\mu$ l of treatment-concentrated culture media at day 4 (total 200 ng/ml IL6/drop), while the other treatments received carrier only. The development of the embryos in each individual treatment at days 4, 7 and 8 post-fertilization was compared with a group control (GC; 25 embryos/50  $\mu$ l SOF-BE1; 1-2 drops/replicate; 4 replicates). The percentage of cleaved embryos was decreased ( $P=0.01$ ) in 0IC versus other treatments (65, 79, 73 and 78.9% for 0IC, 100IC, 200IC and GC, respectively). The percentage of 8+ cell embryos at day 4 was decreased ( $P < 0.05$ ) in all individual culture treatments, but the addition of IL6 to the individual cultures partially ameliorated this effect ( $P < 0.05$ ) (4.6, 15.2, 15.1 and 32.6% for 0IC, 100IC, 200IC and GC, respectively). At day 7, no blastocysts were detected in any of the individual culture groups, but the addition of IL6 to individual culture increased ( $P < 0.05$ ) the proportion of cleaved embryos that developed to morulae in comparison to the 0IC treatment (0, 16.5 and 13.7% for 0IC, 100IC and 200IC, respectively). At day 8, IL6 supplementation increased blastocyst formation ( $P < 0.05$ ), albeit not to the same level as GC (0, 8.9, 9.6, and 21% for 0IC, 100IC, 200IC and GC, respectively). To summarize, IL6 supplementation from day 1 post-fertilization increases ICM development in group-cultured embryos and promotes blastocyst development in embryos cultured individually. These results support the notion that IL6 acts as an embryokine and suggest that IL6 has embryotrophic actions before the embryonic genome becomes active.

**Early Indications of Placental Inefficiency During the Peri-Implantation Period in Obese Sheep.** Sarah R. McCoski, Connor Owens, Rebecca R. Cockrum, and Alan D. Ealy

Exposure to maternal obesity in utero is associated with marked developmental effects in offspring. The placenta is likely a primary mediator of adverse fetal outcomes resulting from a poor maternal environment. It is responsible for regulating embryonic and fetal growth throughout pregnancy. Furthermore, maternal obesity affects placental nutrient transfer, vasculature, and blood flow. The goal of this work was to determine how maternal obesity alters the expression of genes involved in placentation in peri-implantationovine conceptus and endometrial tissue. Dorset ewes were randomly assigned to obese or lean groups. An obese state (BCS  $\geq 4.5$ ; 5-point scale) was established by ad libitum exposure to high quality pasture and feeding 1 kg corn/day. Lean ewes (BCS = 3) were kept on a maintenance diet composed of previously grazed pasture and low-quality hay. Upon reaching the desired BCS, lean and obese ewes were bred to genetically-related Dorset rams. At day 14 post-breeding, ewes were sacrificed, the uterus was excised, conceptuses were flushed, and endometrial

tissue was collected. RNA was isolated from endometrial and conceptus tissues, and a subset of samples was selected for RNA-sequencing (n=6 endometrial samples/treatment, and n=4 conceptus samples/sex/treatment). Samples were sequenced by Cofactor Genomics using an Illumina-based sequencing platform with single end 75 base reads. Sequences were mapped to the *Ovis aries* (NCBI; Oar\_4.0) genome. Differential gene expression was determined using the Differential Expression analysis within CLC Genomics Workbench. Results were filtered (FDR  $\leq$  0.05 and  $\geq$  2-fold change,  $\geq$  0.2 RPKM), and a list of differentially expressed genes (DEGs) was generated. A GO term for placenta does not currently exist, so a literature search was conducted to filter placenta-associated DEGs. Analysis of endometrial tissue identified 669 DEGs between obese and lean females, with 125 DEGs also associated with the trophoblast lineage and the placenta. Panther Pathway Analysis revealed these placenta-associated DEGs were involved in WNT signaling, angiogenesis, and integrin signaling. Additionally, several genes were uniquely expressed in one group and absent from the other. Lean samples contained 5 and obese samples contained 17 unique genes, including 3 pregnancy-associated proteins (PAGs). This was surprising, as PAGs are trophoblast-specific, yet they were detected in the preimplantation endometrium. Effects of maternal obesity were detected in preimplantation conceptuses as well. Sample analysis identified 21 DEGs between obese- and lean-derived samples. Of these DEGs, 4 had a known role in placenta development and function. An additional 137 DEGs were identified between male and female conceptuses, regardless of obesity exposure, with 33 reported to have a role in placentation. Conceptus gene expression was also affected in a sex\*treatment manner, with 330 total DEGs identified, 86 of which were involved in placental development. Collectively, these data indicate that the preimplantation endometrium and conceptus are susceptible to the effects of obesity. Moreover, it appears pregnancies of obese females are programmed for placental inefficiencies in a sex and treatment\*sex manner. This work may represent some of the earliest indications of placentation alterations caused by maternal obesity.

**Apoptosis Markers in Cryopreserved Equine Ovarian Tissue by Slow-Freezing or Vitrification Methods After *in Vitro* Culture.** Gustavo Gastal, Francisco Aguiar, Ghassan Ishak, Clay Cavinder, Scott Willard, Peter Ryan, Jean Feugang, and Eduardo Gastal

Recently, ovarian tissue cryopreservation (OTC) and *in vitro* culture (IVC) systems have been described in horses (Gastal et al. 2017; *Theriogenology* 97:139-147). However, information about the potential of cryopreserved-thawed equine ovarian tissue to adapt and survive after IVC is still scarce. This study aimed to evaluate the effect of two cryopreservation methods (slow-freezing, SF, and vitrification, VIT) on the equine ovarian tissue after 1, 3, and 7 days of IVC by assessing: (i) preantral follicle morphology and distribution of follicle classes; (ii) protein expression of Bax and Bcl-2; and (iii) DNA fragmentation. Equine ovarian fragments (n=480; 3x3x0.5mm) were processed within  $\alpha$ -MEM medium containing 0.4% BSA, 93.3 U/ml penicillin-G, 36.8 U/ml streptomycin sulphate, 0.047 mmol/l pyruvate, and 2.5 mM Hepes. Fragments were randomly distributed among 12 treatment groups [fresh: day 0 (control), IVC day 1 (IVC1), day 3 (IVC3), day 7 (IVC7); SF: day 0 (SF-control), SF-IVC1, SF-IVC3, SF-IVC7; and VIT: day 0 (VIT-control), VIT-IVC1, VIT-IVC3, and VIT-IVC7]. All fragments were fixed in paraformaldehyde for morphological analysis, immunohistochemistry assay (Bax and Bcl-2 protein expression), and DNA fragmentation (TUNEL). Statistical differences among groups were analyzed by Kruskal–Wallis test and Mann–Whitney U test. Percentage of morphologically normal preantral follicles was impaired (P 0.05) Bcl-2 expression and lower (P 0.05) Bax expression, but SF-IVC3 had lower (P 0.05) to SF-IVC7 group;

however, Bcl-2 expression did not differ ( $P>0.05$ ) among groups. In summary, VIT-IVC7 has shown a greater percentage of morphologically normal preantral follicles compared to SF-IVC7, but higher expression of Bax and DNA fragmentation after 7 days of culture. Our results lead to the two following assumptions: (i) greater percentage of normal follicles in VIT-IVC7 demands higher cell metabolism, causing higher Bax protein expression and DNA fragmentation; and (ii) although there is a greater percentage of normal follicles at day 7 of culture, cell metabolism is overburdened and apoptosis pathways are activated, leading to tissue death. These findings demonstrate the equine ovarian tissue functionality and capacity for adaptation after OTC by slow-freezing and vitrification methods during IVC. Therefore, the IVC system for cryopreserved equine ovarian tissue seems to be promising and warrants further investigation to advance fertility preservation programs.

**Effect of Grape Seed Extracts and Procyanidin B2 on Human Granulosa Cells: Cell Proliferation and Apoptosis, Steroidogenesis, Oxidative Stress and Cell Signaling.** Alix Barbe, Romain Bazilie, Namya Mellouk, Jérémy Grandhaye, Christelle Ramé, and Pascal Froment Joëlle Dupont

The polyphenol-rich plants are widely used in medicine and in preparation of foods and drinks, but their effect on reproduction and more particularly in human ovarian functions has not been largely studied yet. Polyphenols have been found to be beneficial in protecting against the generation of oxidative stress in various peripheral tissues. It is well known that the oxidative stress induces changes in cell proliferation, apoptosis or steroidogenesis. The balance between reactive oxygen species (ROS) and antioxidants is involved in fertility and precisely, in the oocyte maturation, follicular development, fertilization. In our study we investigated the effect of grape seed extracts (GSE) and procyanidin B2 (GSPB2), one of the main polyphenols of GSE with potent antioxidant activity on cell proliferation, viability, steroidogenesis, oxidative stress and signalling pathways in both human tumour granulosa cells, KGN cells and human primary granulosa cells (hGC). Cells were stimulated for different times with various concentrations of GSPB2 and GSE (0, 1, 10, 20, 50, 100  $\mu\text{g}/\text{mL}$ ) in DMEM medium with 10% fetal bovine serum. We showed that cell proliferation as determined by thymidine incorporation and apoptosis as measured by trypan blue exclusion was significantly decreased and increased, respectively after 24h of stimulation with 50 and 100  $\mu\text{g}/\text{mL}$  of GSE and GSPB2 in both KGN and hGC cells. These data were confirmed by a reduction in the amount of PCNA, Cyclin D2 and an increase in p27 cyclin dependent kinase protein and caspase 3 level as determined by immunoblot. They were also associated to a strong reduction in Akt and FOXO phosphorylation after short and longer incubation of GSE and GSPB2. In response to GSE and GSPB2 (50 and 100  $\mu\text{g}/\text{mL}$ , 24h), we observed large autophagic vacuoles and oxidative stress as determined by using the cellrox assay was significantly increased. At lower doses (10 ng/ml until 10 mg/ml), no significant effect was observed on these physiological parameters. Interestingly, by using ELISA assays, we showed that GSE and GSPB2 increased in dose dependently (10ng/ml to 10 mg/ml) progesterone and oestradiol secretion by human granulosa cells. These data were associated to an increase in CREB phosphorylation. Taken together, GSE and GSPB2 at 10 ng/ml until 10 mg/ml exert beneficial effect on human granulosa cell steroidogenesis whereas at higher doses (50 -100 mg/ml) they reduce cell proliferation, increase oxidative stress and induce apoptosis.

**Stage Specific Depletion of SF-1 in the Mouse Ovary Results in Varied Impairment of Steroidogenesis and Fertility.** Olivia Eilers Smith, Marie-Charlotte Meinsohn, Micka C. Bertucci, Rodrigo Gonzalez-Lopez, and Bruce D. Murphy

Steroidogenic factor 1 (SF-1; Nr5a1) is an orphan nuclear receptor primarily found in steroidogenic tissues and is involved in the transcription of various enzymes that regulate hormone biosynthesis. Since its discovery in the early 1990's, many studies have demonstrated the essential role of SF-1 as a transcription factor in embryo development and sex determination in mammals, and in the adrenal cortex and gonads of adult. While it has been shown that granulosa cell-specific depletion of SF-1 in mice results in hypoplastic ovaries (Pelusi et al. Biol. Reprod. 79:1074, 2008), impaired ovulation and infertility, its specific action in ovarian development remains to be determined. Due to its presence in ovarian cell types and its role in hormone biosynthesis, we hypothesized that SF-1 is essential for granulosa and theca cell function as well as in corpus luteum (CL) formation.

We developed three novel conditional KO (cKO) mouse models with SF-1: (1) a theca-specific depletion linked to the transcription of Cytochrome P450 17 $\alpha$ -hydroxylase (Cyp17Cre/SF-1 cKO), (2) an antral follicle granulosa-specific depletion linked to aromatase transcription (Cyp19Cre/SF-1 cKO), and (3) a luteal cell-specific depletion using the progesterone receptor (PR; PrCre/SF-1 cKO) in ovarian cells. Fertility trials showed that both Cyp17Cre/SF-1 and Cyp19Cre/SF-1 cKO are fertile, suggesting that SF-1 may not play an essential role in the preovulatory follicle. Alternatively, the expression of LRH-1 (Nr5a2), a transcription factor closely related to SF-1 with highly similar DNA binding domains, increased significantly in granulosa cells as did Amh, showing that compensation may be occurring. Homozygote PrCre/SF-1 cKO females are infertile and heterozygous females (PrCre/SF-1 Het) have reduced litter size. Moreover, the ovarian weight in PrCre/SF-1 cKO mice is significantly reduced, and histological analysis of ovaries collected at 11h and 24h post hCG injection show the near absence of ovulation and impaired CL formation. Ovarian mRNA analysis of all three models showed that SF-1 depletion causes the deregulation of genes necessary for steroidogenic gene expression, including Cyp11a1, Cyp17 and Scarb1. These results indicate that SF-1 plays an essential role in female fertility and suggest it may directly regulate the luteinisation of granulosa cells. The absence of pregnancies in the PrCre/SF-1 cKO females indicates that SF-1 plays a key role in progesterone biosynthesis, a hormone required for gestation progression in mammals. Finally, this investigation has provided new insights into the mechanisms of action of this nuclear receptor in female fertility.

Supported by Project Grant 125936 from the Canadian Institutes of Health Research to BDM.

**Ovarian-Specific Regulation of Inflammasome in Obese Mice.** Marek Adamowski, Karolina Wolodko, and Antonio Galvão

Obesity and its comorbidities represent a main burden in our health systems. Expanding adipose tissue promotes chronic low-grade inflammation, through different mechanisms. Indeed, recent studies evidenced the ovaries from obese female mice exhibit mitochondrial dysfunction, endoplasmic reticulum stress, and lipid accumulation. These factors may promote local inflammation through inflammasome activation. The vertebrate innate immune system presents germline-encoded receptors

that protect against internal threats. Among various mediators, the NLRP3 inflammasome is best characterised. These cytosolic multiprotein complexes recruits and activates caspase-1, which in turn promotes maturation and secretion of the inflammatory cytokines, IL-1 beta and IL-18.

In the present work, we characterised the inflammasome activation in both ovaries and liver from diet induced obese (DIO) mice. C57BL/6J female mice (n=8/group) were fed chow diet (C) versus high fat diet (HFD) during four (4w) or sixteen weeks (16w). Livers and whole ovaries were collected to perform comparative studies on mRNA and protein expression of NLRP3, CASP1 and IL-18. Ovarian Nlrp3 mRNA was significantly increased in 16w-HFD group comparing to C ( $p < 0.05$ ). Regarding protein expression in the ovary, CASP1 and IL-18 were increased in the ovary ( $p < 0.01$ ;  $p < 0.05$  respectively) after 4w of HFD. However, all inflammasome markers were decreased in the ovary of 16w-HFD group ( $p < 0.05$ ). The liver presented opposite signatures, with protein levels of NLRP3 and IL-18 being significantly increased in the same animals after 16w-HFD group ( $p < 0.05$ ).

In the present work, we evidenced for the first time the activation of NLRP3 inflammasome in the ovary of DIO mice. Our time-course study highlighted the upregulation of inflammasome in the ovary after 4w HFD treatment; however, a chronic exposition to HFD (16w) was associated with a downregulation of inflammasome members in the same organ. Furthermore, a different response was found in the liver of the same animals, in which inflammasome components were highly expressed after 16w HFD. This denotes an ovarian specific regulation of the inflammasome during obesity. Further studies are needed to better understand the regulation of the inflammasome in the ovary of obese female mice, instigating putative interactions with steroids and other ovarian mediators.

Work supported by National Science Centre (2014/15/D/NZ4/01152) and KNOW Consortium: “Healthy Animal - Safe Food” (Ministry of Sciences and Higher Education; Dec: 05-1/KNOW2/2015).

**Adipokine Expression Profiles During Early Broiler Embryo Development: Regulation by Maternal Feeding Restriction and Fish Oil Supplementation.** Namya Mellouk, Christelle Ramé, Joel Delaveau, Christophe Rat, Maxime Marchand, Frédéric Mercierand, Pascal Froment, and Joelle Dupont

In broiler chickens, the intense genetic selection for rapid growth has resulted in an increase in growth rate and fat deposition that induce reproductive dysfunction over generations. The maternal transfer of egg yolk factors may set the stage for improving physiological phenotypes and fertility impairment. In human, maternal intake of fish oil (FO) is associated with reduced adiposity in children that could attenuate reproductive damages. Thus, in our study, we aimed to investigate the effect of intergenerational transmission of FO on chicken embryo development with an emphasis on adipokine (adiponectin, visfatin and chemerin) levels in plasma and metabolic tissues (adipose tissue, muscles, liver) and activation of specific signaling pathways (AMPK, Akt, MAPKs ERK1/2 and P38). Our study included four groups of eighty broiler hens fed with four different diets: restricted with (RtFO) or without FO (Rt) and ad libitum with (AdFO) or without FO (Ad). Hens were artificially inseminated and fertile eggs were incubated. All eggs and hatched chicks were weighed. We retrieved eggs (or chicks) at different times: 15 (E15), 20 (E20) days of incubation, hatching and 10 days after hatching (D10). All chicks were fed with the same traditional overfeeding diet until D10. We collected blood samples (n=10/stage), subcutaneous adipose tissue, muscles and liver (n=8) at these different periods of development. The restricted diet induced thinner eggs with a small yolk vesicle and consequently

thinner embryo at hatching. Moreover, at hatching, we have also found that FO reduced the weight of chicks from AdFO hens ( $P < 0.05$ ). Even if the chicks were all fed with an overfeeding diet after hatching, chicks from Rt hens were still thinner after D10 and even more when hens received FO ( $P < 0.05$ ). At the plasma level, visfatin and adiponectin decreased from E15 to hatching and slightly increased from hatching to D10 and chemerin decreased from E15 to D5 and remained stable. From E15 to D10, FO decreased circulating visfatin levels of embryos/chicks from AdFO hens as compared to those from Ad hens. At E15 and E20, FO increased circulating adiponectin levels of embryo from AdFO hens as compared to embryo from Ad hens while it had no effect on circulating chemerin levels. At D10, the weight of the chicks was negatively correlated with plasma visfatin levels and positively correlated with those of adiponectin. By western blot, we have shown at hatching that FO increased the expression of visfatin and adiponectin in adipose tissue while it decreased their expression in muscle of RtFO. However, at D10 only visfatin expression was increased in muscles of chicks from RtFO hens. In addition, FO induced higher ERK phosphorylation and lower Akt phosphorylation in adipose tissue and no effect of signaling pathways in muscles in 10 days old chicks from RtFO hens than those from Rt hens and higher ERK phosphorylation in 10 days old chicks from AdFO hens than those from Ad. In conclusion, the development of chicken embryos and chicks depends on the maternal nutrition especially, FO content through the regulation of circulating and local adipokine levels.

**The Post-Acrosomal Sheath and Perforatorial Regions of the Perinuclear Theca of Rat Spermatozoa Share Common Developmental Origins and Protein Constituents.** Nicole Protopapas, Lauren Hamilton, Wei Xu, Peter Sutovsky, and Richard Oko

The perinuclear theca (PT) is a dense cytosolic protein layer that surrounds most of the nucleus of the mammalian sperm head. It can be divided into two structurally continuous, but functionally and compositionally different regions: the subacrosomal layer (SAL) and the post-acrosomal sheath (PAS). In falciform-shaped spermatozoa, as seen in murids, a third separate region of the PT emerges that surrounds and extends beyond the apical aspect of the nucleus called the perforatorium. The formation of the SAL and PAS vary, with the former assembling early in spermiogenesis concomitant with acrosome formation, and the latter dependent on the manchette during spermatid elongation, providing a means of transport for cytosolic protein to be deposited in the PAS. Perforatorial proteins are also proposed to make use of the manchette for the passage and accumulation of polypeptides into the perforatorium prior to its condensation in the final steps of spermiogenesis. The similar means of assembly between the PAS and perforatorium suggest they share common protein constituents. The goal of the present study was to investigate the compositional similarities and differences between the PAS and perforatorium using a combination of cell fractionation, immunoblotting and immunolocalization. Compositional analysis of the perforatorium revealed its major protein constituent is a 15-kDa polypeptide called PERF15, shown to be exclusive to the perforatorium and ventral spur of the PT. Further proteomic analysis of the PT has identified and localized several PAS-resident proteins including GSTO2, PAWP, WBP2 and the core somatic histones, which span the area of the PAS and perforatorium. These findings are in support of the developmental homogeneity between the PAS and perforatorium, indicating a similar means of assembly between these two separate regions of the PT. Taken together, the PT of falciform-shaped spermatozoa can be compositionally organized into three major regions, including the SAL, PAS, and perforatorium, with the latter two sharing similar protein constituents and developmental characterization.

**Global Protein Analysis Reveals Potential Involvement of Insulin-Like Neuropeptide Relaxin 3 in Granulosa Cell Differentiation in the Laying Hen.** Kahina Ghanem and Alan L. Johnson

Similar to the hierarchical organization of laying hen preovulatory follicles, pre-recruitment follicles are also organized into a size hierarchy. Although in vivo dye tracing indicates that pre-recruitment follicles are recruited sequentially according to size, the molecular differences among these follicles that determine their sequential recruitment has not been investigated. Accordingly, the objective of this study was to characterize and compare global protein expression in the granulosa cells of the most recently recruited follicle and the four largest pre-recruitment follicles; plus the theca layer of the most recently recruited follicle and the largest pre-recruitment follicle. Contrary to the theca layer, granulosa cells during recruitment, undergo a significant differentiation process to accommodate the rapidly growing oocyte. Therefore, it was hypothesized that differences, if any, in protein expression reside within granulosa cells (GC) and not the theca tissue. Ovaries of 34 week old laying hens (N=4) were harvested 8 h after ovulation. GC from the most recently recruited follicle (9-12 mm) and the four largest pre-recruitment follicles (6-8 mm), and theca tissue from the most recently recruited and the largest pre-recruitment follicles were collected, washed free of yolk, and total protein was extracted and quantified. Samples were labelled with isobaric tags for relative and absolute quantitation (iTRAQ), and LC/MS/MS was performed to quantify and compare the relative protein expression. Real-time qPCR was used to verify expression patterns. Results indicate among the 2000+ detected proteins, no proteins were significantly differentially expressed between the theca of the most recently recruited and largest pre-recruitment follicles. By comparison, in GCs, 9 proteins were differentially expressed (Kruskal-Wallis Test;  $p = 0.05$ ; Benjamini-Hochberg  $p < 0.05$ ). Pathway analysis confirmed that TGFB1, protein transport, and endocytosis pathways were increased in the most recently recruited follicle, whereas the cell death pathway was suppressed. Given the well-known role of relaxins 1 and 2 in the mammalian ovary, and that this is the first time relaxin 3 (RLN3) has been reported in the chicken ovary, RLN3 was chosen for further investigation. First the localization of RLN3 was confirmed to be in GCs but not theca. Additionally, high levels of RLN3 mRNA were detected in the pituitary and cerebellum, but not in the kidneys, liver, adipose, or muscle. In the ovary, RLN3 mRNA was highest in 9-12 GC and lowest in GCs from 3-5mm follicles and cortex ( $p=0.05$ ). Results from this study confirm that during follicle recruitment the major changes occur in the GC. Additionally we report, for the first time, that relaxin 3 protein and mRNA are expressed in chicken ovarian follicle GCs and are highest in the most recently recruited follicle. Studies are underway to investigate RLN3 and its involvement in follicle recruitment and GC differentiation.

**The Immune Response is a Key Component for Angiogenesis in Pregnancy.** Kenneth Beaman, Alice Gilman-Sachs, and Svetlana Dambaeva

Cells thought to be part of the immune system occupy much of the placenta, particularly the transitional zones between maternally derived and fetally derived tissues. The common opinion is that the immune system is being inhibited by a fetal factor or factors from the “angry” maternal immune system. Even though much of the data does not support this hypothesis, it persists as a dogma. We present data that suggest that the immune response at the maternal fetal interface is active and aids in fetal and placental growth and in no way inhibits the pregnancy under normal conditions. In knockout mice, we examined the murine implantation site by flow cytometry, histochemistry, RNA sequencing and Western blots. In

particular we focused our examination on metrial gland cells, also known as ILC-3 and NK cells. In addition we examined other innate cells of the neutrophil and macrophage lineage. Finally, we analyzed 2 distinct immune modulators, the Notch modifying, a2V-ATPase that appears early in gestation, and IL-22, which is measurable upon inflammatory challenge. The cytokines studied are unique because of their expression and effector activities. While a2V-ATPase is abundantly expressed in the placenta, it is highly expressed in the non-pregnant endometrium and early in gestation. The expression of IL-22 was observed only upon LPS challenge late in pregnancy, although the expression of IL-22RA1 was highly upregulated in postpartum endometrium, indicating the important role of IL-22 in epithelium regeneration after labor. In Knockout mice the absence of a2V-ATPase did not affect pregnancy in the female but in the male the absence was associated with complete sterilization. Conversely the elimination of IL-22 had no effect on the initial fecundity of the female but the female's fecundity decreased drastically with each subsequent pregnancy. Finally, our data show that IL-22 produced by various cells including DBA positive uNK cells reacts with placental cells, luminal epithelium and endometrial stromal cells adjacent to uterine lumen. A2V-ATPase produces a protein that reacts both proximally on self and distally on immune cells such as macrophage and neutrophils. When this a2V-ATPase protein and IL-22 are expressed their activity increases angiogenesis and does not lead to cell destruction and cell death. In both cases the activity of the immune response causes pro-embryogenic, not destructive actions.

**Exploration of Chemerin System in Human Granulosa Cells: A New Insight for Polycystic Ovarian Syndrome.** Namya Mellouk, Alice Bongrani, Christelle Ramé, Fabrice Guérif, and Joëlle Dupont

Studies on fertility disorders related to metabolic abnormalities have highlighted the importance of the role of hormones produced by adipose tissue (adipokines) on the appearance of pathologies such as polycystic ovary syndrome (PCOS). Chemerin is a new adipokine able to bind three G protein-coupled receptors: CMKLR1 (chemokine-like receptor 1), GPR1 (G protein-coupled receptor 1), and CCRL2 (Chemokine (CC motif) receptor like 2). Recently, a role for the chemerin/CMKLR1 pathway in ovarian follicle function and steroidogenesis has been reported in mammals. In both human primary granulosa (hCGs) and human ovarian granulosa-like tumour cell line (KGN), chemerin inhibited IGF-1-induced steroids production. Thus, we aimed to investigate chemerin system in human granulosa cells from PCOS patients and cell line and modulation of its signaling activities using a CMKLR1 nanobody (C4910). Our study included six groups of 10 patients aged from 22 to 41 years old: control (undergoing in vitro fertilization for men infertility), obese (BMI >30), PCOS (presenting two of the three Rotterdam criteria), ECHO (presenting only enlarged polycystic ovaries by ultrasound), PCOS-O (PCOS and obese) and ECHO-O (ECHO and obese). Patient's clinical and biological parameters as well as granulosa cells were obtained in collaboration with the CHRU Bretonneau (Tours, France). In parallel, cultured KGN cells were stimulated (5, 10, 30 and 60 minutes) or not with human recombinant chemerin (200 ng/ml, n=3) and/or with C4910 (10<sup>-8</sup> and 10<sup>-9</sup> M, n=1). The mRNA expression of chemerin and its receptors in patient's granulosa cells was analysed by RT-qPCR and after stimulation, proteins from KGN cells were extracted and co-immunoprecipitation experiments (homodimerization / heterodimerization of the CMKLR1) and western blot (signaling pathway) were carried out. Chemerin mRNA was highly expressed in granulosa cells of obese (3.56 ± 0.51), PCOS-O (5.14 ± 1.02) and ECHO-O (2.47 ± 0.29) patients as compared to control (0.16 ± 0.02), PCOS (0.18 ± 0.02) and ECHO (0.28 ± 0.05) patients and we observed opposite profile for CMKLR1. The mRNA expression of CCRL2 was lower in PCOS (0.013 ± 0.001), obese (0.011 ±

0.001) and ECHO-O ( $0.013 \pm 0.002$ ) patients as compared to control ( $0.017 \pm 0.002$ ), ECHO ( $0.014 \pm 0.002$ ) and PCOS-O ( $0.014 \pm 0.001$ ). In parallel, we found that in KGN cells CMKLR1 and CCRL2 receptors formed a heterodimer after 5 minutes of stimulation with chemerin and gradually increased until 60 minutes. We also showed that chemerin rapidly activates (5 minutes) MAPK ERK 1/2, P38 and Akt phosphorylation and more slowly (30 minutes) AMPK and  $\beta$ -arrestin phosphorylation in KGN cells. Preliminary in vitro experiments of KGN cell co-incubated with chemerin and the CMKLR1 nanobody (C4910) showed a lower phosphorylation of P38 after 5 minutes than in cells only incubated with chemerin. According to the literature, our results indicated that chemerin system was expressed in granulosa cells and a deficit of CMKLR1 seems protect against follicular development disruptions in PCOS patients. We also described the chemerin signaling involved in inflammation and steroidogenesis that was partially blocked by a potential therapeutic nanobody targeting CMKLR1.

**Acute Exposure to High Fat, High Sugar Diet Results in Insulin Resistance During Pregnancy in Mice: A Novel Model of Gestational Diabetes.** Kathleen A. Pennington and Pradip K. Saha

Gestational diabetes mellitus (GDM), is defined as diabetes that begins during pregnancy and affects up to 18% of all pregnancies depending on diagnostic criteria. Although obesity is a risk factor for GDM, it occurs in women who are not overweight. GDM has both immediate and long term impacts on metabolic and cardiovascular health of the mother and fetus. Despite its high prevalence, there is no widely accepted animal model. To address this we recently developed a non-obese mouse model of GDM that also exhibits diabetic complications later in life. Dams exposed to an acute high fat, high sugar (45% fat, 18% sugar HFHS) diet one week before and throughout pregnancy develop multiple GDM-like symptoms. Notably these animals are glucose intolerant during pregnancy and have reduced serum insulin levels; however it is unknown if these dams are also insulin resistant as observed in women with GDM. We hypothesized that dams exposed to HFHS one week prior to and during pregnancy would exhibit insulin resistance compared to control dams. To test this hypothesis we performed Euglycemic Hyperinsulinemic Clamps in conscious pregnant d13.5 mice as follows. At 8 weeks of age C57BL/6J female mice were randomly assigned to either the control or GDM group and with their respective control (CD; n=7) or HFHS diet (n=7). Following one week on these diets mice were mated and maintained on their respective diets for the study. At day 8.5 of pregnancy surgery was performed to insert catheters for Euglycemic Hyperinsulinemic Clamp experiments and mice were allowed to recover. On day 13.5 of pregnancy Euglycemic Hyperinsulinemic Clamps were performed in conscious mice. Euglycemic Hyperinsulinemic Clamps were also performed in non pregnant mice fed either CD or HFHS for 21 days (equivalent diet exposure time to d13.5 mice). Basal glucose production was not different between control ( $15.56 \pm 0.90$  mg/kg/min) and GDM ( $17.63 \pm 0.53$  mg/kg/min) at day 13.5 of pregnancy. Glucose infusion rate was significantly decreased ( $p < 0.01$ ) in GDM ( $9.07 \pm 1.04$  mg/kg/min) compared to control ( $20.92 \pm 2.89$  mg/kg/min) dams. Hepatic glucose production was significantly increased ( $p < 0.05$ ) in GDM ( $9.38 \pm 1.02$  mg/kg/min) compared to control ( $6.54 \pm 0.80$  mg/kg/min) dams. Placental glucose uptake was significantly increased ( $p < 0.01$ ) in GDM ( $25.62 \pm 0.49$  mg/kg/min) compared to control ( $19.93 \pm 1.5$  mg/kg/min) dams. Non pregnant animals did not show signs of insulin resistance either on CD or HFHS. Acute exposure to a HFHS diet one week before and during pregnancy results in insulin resistance in our mouse model. These data further validate this animal model as a good and relevant model for GDM. Future work is planned to assess complications in insulin secretion in this model and work to use this animal to identify the underlying mechanisms resulting in GDM.

## **The Involvement of Protein Kinase C (PKC) Isozymes in the Regulation of Cysteine Rich 61-Connective Tissue Growth Factor-Nephroblastoma Overexpressed 1 (CCN1) in Human Tumor Granulosa Cells.**

Joseph Miseirvitch, Christine Coticchia, John Davis, Marsha Moses, and Paul Tsang

Angiogenesis is required for optimal ovarian follicular and luteal function. Previously, we reported that an angiogenic inducer, Cysteine-rich 61 Connective Tissue Growth Factor Nephroblastoma Overexpressed 1 (CCN1), was highly expressed in the young bovine corpus luteum (CL) (day 4; day 0 = estrus). Subsequently, we also determined that cow and human tumor (KGN) granulosa cells also expressed CCN1. In KGN cells, we observed that prostaglandin F2 alpha (PGF) and phorbol 12-myristate 13-acetate (PMA) stimulated expression of CCN1 mRNA, suggesting the involvement of the PKC pathway. However, the contributions of specific isozymes within the PKC family, conventional, novel and atypical, are unclear. Using Calphostin-C, an inhibitor of conventional and novel PKCs, we found no effect on CCN1 mRNA expression in KGN granulosa cells. However, treatment with Pseudo Substrate Inhibitor (PSI), an inhibitor of atypical PKCs, resulted in the suppression of CCN1 mRNA expression in KGNs ( $p \leq 0.0001$ ). Since the differential regulation of CCN1 by PKC isozymes may be mediated at the level of transcription factors, the objective of the present study was to determine the expression of the nuclear factor kappa light-chain of activated B cells (NF- $\kappa$ B) in KGN cells. In addition, we also sought to determine the possible involvement of the protein kinase B (Akt) pathway in the regulation of CCN1 expression in KGN cells. Cells were grown to confluency before they were serum-starved for 2 hours. They were then treated for 15 minutes with PMA (10 nM), PMA and Calphostin-C (10 nM and 50 nM, respectively), and PMA and PSI (10 nM and 0.05  $\mu$ M; respectively). Cell lysates were analyzed by InstantOne ELISA kits to determine total NF- $\kappa$ B and Akt, and phosphorylated NF- $\kappa$ B (Phospho-p65, Ser536) and Akt (Akt 1/2/3, Ser473). In the presence of PMA, approximately 50% of NF- $\kappa$ B, relative to total, was phosphorylated. Phosphorylated NF- $\kappa$ B remained high following treatment with Calphostin-C, while it dropped (relative to PMA) by approximately 20% in the presence of PSI. This decrease in phosphorylated NF- $\kappa$ B is coincident with the observed decrease in CCN1 expression following PSI. In contrast, 23% of Akt, relative to total, was phosphorylated in the presence of PMA, and phosphorylated Akt was further increased when KGNs were treated with Calphostin-C and PSI. Thus far, these results suggest that CCN1 expression in KGN cells may involve atypical PKC isozymes acting through NF- $\kappa$ B with the role of Akt requiring further investigation.

[The authors acknowledge the support of the New Hampshire Agricultural Experiment Station (PCWT) and the Breast Cancer Research Foundation (MAM).]

## **Temporal Regulation of Bovine Interferon-tau Gene by the Transcription Factor EOMES in the Peri-Implantation.** Min-Su Kim, Kwan-Sik Min, Kazuhiko Imakawa, Ik Soo Jeon, and Sung Woo Kim

Interferon tau (IFNT) regulation, an anti-luteolytic factor produced by conceptuses of the ruminant ungulates, is essential for the maintenance of early pregnancy, but a definitive mechanism for its temporal transcription has not been elucidated. We and others have observed, the T-box protein eomesodermin (EOMES) exhibited high mRNA expression in the embryonic trophectoderm; thus, CDX2, ETS2 and JUN coexist during the early stages of conceptus development. Objective of this study was to examine the effect of EOMES on IFNT gene transcription when evaluated with CDX2, ETS2 and JUN transcription factors implicated in the control of cell differentiation in the trophectoderm. In this study, reverse-transcriptase-PCR analysis between ovine trophoblast cells was initially performed, finding that transcription factors Eomes and several transcription factor mRNAs were specific to trophectoderm

cells. These mRNAs were also found in days 15, 17, and 21 ovine conceptuses. Furthermore, human choriocarcinoma JEG3 cells were co-transfected with an ovine IFNT (-654bp)-luciferase reporter (-654-oIFNT-Luc) construct and several transcription factor expression plasmids. Transfection of alone CDX2, and/or ETS2, AP1(JUN) were had very effective in the up-regulation of the IFNT construct transfected into JEG3 cells. However, down-regulated by EOMES transcription factor, when cells were initially transfected with EOMES followed by transfection with CDX2, and/or ETS2, AP1(JUN) the expression of -654-oIFNT-Luc was reduced to levels. Also, EOMES factor inhibited the stimulatory activity of CDX2 alone. These results suggest that as conceptuses attach to the uterine epithelium, IFNT gene transcription is down-regulated by an increase of EOMES factor expression in the attached trophoblast cells.

**Dietary Supplementation Of 0.4% L-Arginine Between Days 14 and 30 Of Gestation Stimulates Placental Transport of Water in Gilts.** Cassandra M. Herring, Shengdi Hu, Fuller W. Bazer, Gregory A. Johnson, Heewon Seo, Avery Kramer, Bryan McLendon, Mohammed Elmetwally, and Guoyao Wu

Most embryonic loss in pigs occurs before Day 30 of gestation. Arginine is a “conditionally essential” amino acid in the diet that is important for embryonic survival and development by affecting placental growth and angiogenesis. This study was conducted to test the hypothesis that dietary arginine supplementation between Days 14 and 30 of gestation increases placental transport of water and nutrients in gilts. Each gilt was fed 1 kg of a corn- and soybean-meal based diet containing 12% crude protein twice-daily beginning on Day 0 of gestation (the day of breeding). Either 0.4% L-arginine (as L-arginine-HCl, n=7) or an isonitrogenous amount of L-alanine (n=6) was supplemented to the basal diet between Days 14 and 30 of gestation. On Day 30 of gestation, gilts were fed either L-arginine-HCl or L-alanine 30 min before they were hysterectomized. Uterine tissue, embryos, fetal membranes and fetal fluids were collected. Placental transport of  $^3\text{H}_2\text{O}$  was measured with the use of Ussing chambers containing 5 ml of oxygenated Krebs buffer with physiological concentrations of amino acids and glucose.  $0.2 \mu\text{Ci } ^3\text{H}_2\text{O}$  was added to the “mucosal” side of each chamber, and an aliquot of  $20 \mu\text{L}$  solution was obtained from the “serosal” side of the chamber at 5, 10, and 15 min for the measurement of  $^3\text{H}_2\text{O}$  using a liquid scintillation counter. Extraction of RNA and RT-qPCR were performed to determine expression of aquaporins in the placenta. Data were analyzed by the unpaired t-test. Compared to the control group, arginine supplementation increased ( $P < 0.05$ ) allantoic fluid volume by 25% and amniotic fluid volume by 48%. Aquaporins 1, 2, 3, 4, 5, 8, 9, and 11 were expressed in the placentae of gilts on Day 30 of gestation. Arginine supplementation enhanced ( $P < 0.05$ ) the expression of placental aquaporin 1 by 40%. The rates of net water transfer by the placentae in the Ussing chambers were  $0.370 \pm 0.025$  and  $0.498 \pm 0.036 \mu\text{l/mg wet tissue/min}$  ( $P < 0.05$ ) from control and arginine-supplemented gilts, respectively. Arginine supplementation also increased ( $P < 0.05$ ) placental transport of glycine and glutamine by 35-50%. We conclude that dietary arginine supplementation to pigs between Days 14 and 30 of gestation improves survival and development of the conceptuses through stimulating placental water and amino acid transport, as well as angiogenesis. This research was supported by Agriculture and Food Research Initiative Competitive Grant no. 2015-67015-23276 from the USDA National Institute of Food and Agriculture.

**Determining the Lowest Dose of Prostaglandin Needed for Luteolysis of a Mature Corpus Luteum in Cycling Donkeys in the Caribbean.** McKinsey Landers, Ava Kent, Erik Peterson, Robert Gilbert, and Hilari French

Although considered a nuisance on many Caribbean islands, some donkey breeds are facing extinction. By gaining a better understanding of the jenny's reproductive characteristics efforts can be made to improve breeding management for population control, or in the case of endangered species, better reproductive efficiency. Although donkeys are often treated similar to horses there is evidence that they metabolize agents very differently. Dinoprost tromethamine (Lutalyse®) is labeled as a luteolytic agent in cycling mares to control time of estrus. In mares, some adverse effects such as sweating, increased respiratory rate and abdominal pain have been noted fifteen minutes after injection. In order to reduce side effects in mares, experimental results have shown that 1/8th of the labeled dose is effective and does not cause unwanted side effects. The aim of this study was to determine the lowest effective dose of dinoprost tromethamine (Lutalyse®) in cycling jennies in the Caribbean. The study also characterized adverse side effects at each tested dose of dinoprost tromethamine. Seven reproductively sound, non-pregnant Caribbean jennies between the ages of 3 and 12 were monitored via transrectal ultrasonography daily to detect follicular and corpus luteum (CL) formation. Seven days after the formation of a CL one of four dinoprost tromethamine treatment doses (Full, Half, Quarter, Lowest) was administered. Donkeys were monitored for 30 minutes following treatment and pulse, respiration and behavior recorded every 5 minutes. Following treatment, the measurement of the two largest follicles as well as the CL were recorded daily until a new ovulation occurred, thus creating a new CL. Seven days later, donkeys received a different assigned treatment. Donkeys continued in this cycle until all four treatments were concluded. Estrous cycle lengths were extracted from this information and compared by treatments. Cycle length was analyzed by mixed effects multiple linear regression using Jenny as a random variable and treatment dose as fixed effects. Overall clinical signs decreased or stayed unchanged as the treatment dose of dinoprost tromethamine decreased. Respiration rate and heart rate were similar throughout all treatment groups but behavior was notably different. Jennies that received the full dose all showed characteristic cramping behavior while those in lower treatment groups had varied responses. It should be noted that the lowest dose had no cramping behavior observed. All treatment doses of dinoprost tromethamine were effective at reducing the estrous length compared to the jennies normal cycle. The lowest dose showed the most variable response ( $P=0.001$ ) while all other treatments were significantly reduced ( $P < 0.0001$ ). The results of these experiments correlate to those found in mares and prove that lower doses of dinoprost tromethamine are effective at luteolysis in the Jenny. Future research will test the efficacy of a different synthetic prostaglandin, cloprostenol (Estrumate®) and lower dose treatments.

**Heat-Induced Hyperthermia Impacts the Follicular Fluid Proteome of the Periovarian Follicle in Lactating Dairy Cows.** Louisa A. Rispoli, Ky G. Pohler, Chelsea R. Abbott, Stephen Russell, Rick Jordan, Richard I. Somiari, Rebecca R. Payton, F. Neal Schrick, Arnold M. Saxton, and J. Lannett Edwards

Elevated temperatures during the first half of in vitro maturation heightens cumulus-derived progesterone production, suppresses matrix metalloproteinase 9 secretion, and alters the transcriptome. Culture of follicle cells (mural granulosa and theca combined) at elevated temperatures increases gonadotropin-stimulated progesterone synthesis. Thus, we hypothesized that hyperthermia-induced

perturbations in the cumulus cells enveloping the maturing oocyte may extend to the mural granulosa of the periovulatory follicle in the heat-stressed cow, collectively altering the proteome of the follicular fluid. Lactating Holsteins with a corpus luteum were administered PGF2 $\alpha$ ; CIDR was inserted and GnRH given 11 days later. Seven days thereafter, PGF2 $\alpha$  was given and CIDR was removed. Cows with a dominant follicle ( $16.9 \pm 2.3$  mm) were transported to a climate-controlled facility 35 h later; GnRH was given 40 h after final PGF2 $\alpha$  to induce an LH surge. Thermoneutral cows ( $n = 5$ ) were maintained at  $66.5 \pm 0.6$ . To induce hyperthermia ( $n = 5$  cows), THI was increased 2.7 units per h for  $\sim 12$  h (final THI  $82.5 \pm 0.9$ ). The rectal temperature (RT,  $39.8 \pm 0.5^\circ\text{C}$ ; max  $40.5 \pm 0.2^\circ\text{C}$ ) and respiration rate (RR,  $11.5 \pm 1.3$  breaths/min [bpm]) of hyperthermic cows were increased ( $P < 0.0001$ ) compared to thermoneutral cows ( $38.6 \pm 0.3^\circ\text{C}$  and  $57.3 \pm 15.5$  bpm). After  $\sim 12$  h, hyperthermic cows were returned to thermoneutral conditions; RT and RR decreased by  $1.12 \pm 0.48^\circ\text{C}$  and  $47.05 \pm 8.78$  bpm per 15 min. At 45 min, hyperthermic and thermoneutral cows were similar,  $38.9^\circ\text{C}$  and 65.0 bpm versus  $38.5^\circ\text{C}$  and 48.0 bpm, respectively. Fluid of the dominant follicle was aspirated at  $\sim 16$  h post GnRH (1.5 average E2:P4 ratio). Protein changes in individual follicle fluid aspirates were evaluated by quantitative tandem mass spectrometry (nano LC-MS/MS) using Tandem Mass Tags. We identified 706 high confidence proteins (false discovery rate  $< 0.01$ ) and performed Gene Ontology (GO) classification of the proteins using Protein Discoverer 2.2. In follicular fluid derived from hyperthermic versus thermoneutral cows, 34 proteins were identified as differentially-expressed using a threshold  $P < 0.1$ . Of the proteins that were GO annotated, greater than 40% were associated with metabolic process or regulation of biological process and 65% were related to either catalytic activity, enzyme regulation activity or receptor binding (molecular function). Analysis of the differentially-abundant proteins revealed three KEGG pathways (DAVID 6.8): complement and coagulation cascades, ECM-receptor interaction and focal adhesion. A query of the Reactome database yielded proteins of interest associated with keratinization plus the regulation of IGF transport and uptake by IGF binding proteins. Whether hyperthermia-induced changes in the follicle fluid milieu reflect changes in cumulus and mural granulosa secretions and/or transudative changes from circulation remains to be determined. Regardless of origin, changes in the follicular fluid milieu may explain in part some of the negative consequences of hyperthermia on the developmental competence of the maturing oocyte housed within the periovulatory follicle. This project was supported by Agriculture and Food Research Initiative Competitive Grant no.2016-67015-24899 from the USDA National Institute of Food and Agriculture.

**Increased Expression of Insulin-Like Growth Factor Receptor in Granulosa cells From Older Mares May Reduce Overall Insulin Sensitivity.** Nadya Ashwish, Elaine Carnevale, Gerrit Bouma, George Barisas, and Deborah Roess

Changes in gene expression in granulosa cells from mares may result from the animals' aging or development of metabolic disease. We used qPCR to quantify expression of equine insulin receptor (IR), insulin-like growth factor receptor (IGF-1R), glucose transporter type 4 (GLUT4) and adenosine monophosphate-activated protein kinase (AMPK) subunit genes in granulosa cells from young (4-9 years;  $n=6$ ), middle-aged (10-16 years;  $n=4$ ) and older ( $>16$  years;  $n=8$ ) mares. Granulosa cells were isolated following follicular aspiration and were incubated in the presence (+FBS/glucose) or absence (-FBS/glucose) of 10% fetal bovine serum (FBS) and 30mM glucose for 24 hrs. In some experiments cells were then treated for 1 hr with insulin (100nM), IGF-1 (10nM) or epidermal growth factor (EGF; 1 $\mu\text{M}$ ). RNA samples were analyzed in duplicate and housekeeping genes were used as internal controls. SAS

Mixed Procedure for Repeated Measures analysis was performed for these data.  $\Delta$ Ct values for IGF-1R or IR expression did not differ significantly for any age group. However, there were statistically significant differences in the ratio of  $\Delta$ Ct for IR relative to  $\Delta$ Ct for IGF-1R for young, middle and old animals. Young animals expressed increased IGF-1R relative to IR in the both +/- FBS/glucose media and in cells treated with insulin or IGF-1. Conversely, middle-aged animals expressed increased IR relative to IGF-1R under both control conditions and following treatment with insulin or IGF-1. Finally, older animals expressed approximately equal amounts of IR relative to IGF-1R (-FBS/glucose) or increased IR relative to IGF-1R (+FBS/glucose) and treatment with insulin or IGF-1 increased IGF-1R relative to IR. Changes in the relative numbers of IR and IGF-1R monomers expressed from IR and IGF1R genes may affect the particular receptor dimers assembled from these monomers: a weakly-expressed monomer together with a strongly expressed monomer will most likely appear in hybrid receptors which are less responsive to insulin. The strongly expressed monomer will, in addition, form receptor homodimers which differ in insulin responsiveness (IR >IGF-1R). In evaluating fold change  $2^{-\Delta\Delta$ Ct in gene expression, we observed significant increases in IGF-1R expression (+FBS/+glucose;  $p < 0.03$ ), GLUT4 expression (+FBS/+glucose;  $p < 0.05$ ) and AMPK  $\alpha 2$  expression (-FBS/-glucose;  $p < 0.03$ ) in older mares relative to young animals. Together, these results indicate that young animals differ from older animals in several ways. Young animals maintain stable ratios of  $\Delta$ CT for IGF-1R to  $\Delta$ CT for IR and these ratios are not affected by 1 hr exposure to insulin or IGF-1. Thus, it is likely that young animals maintain higher levels of IGF-1R homodimers and hybrid receptors and that receptor numbers, including insulin receptors, remain stable, particularly when circulating glucose and insulin levels are high. Older animals, on the other hand, are more labile with respect to  $\Delta$ CT for IGF-1R relative to  $\Delta$ CT for IR. Exposure of granulosa cells to high levels of glucose, insulin, IGF-1 or EGF increased IGF-1R expression. This potentially decreased numbers of more highly insulin-responsive insulin homodimers and increased hybrid receptors and IGF-1R homodimers, both less sensitive to insulin, thus decreasing insulin responsiveness and insulin effects on metabolism.

**Dose-Dependent Effects of Chronic Glyphosate Exposure on the Estrous Cycle, Ovarian Proteome and Steroid Hormone Levels in Mice.** S. Ganesan, K. L. Clark, B. C. McGuire, A. F. and Keating

Representing 50% of U.S. herbicide usage, environmental glyphosate (GLY) abundance is extensive, and exposures are via oral and dermal ingestion. Based upon findings in cell culture models, we hypothesized that GLY would impact ovarian steroidogenesis and folliculogenesis pathways at environmentally relevant chronic exposure levels. Female C57BL6 mice were orally administered vehicle control (saline (C)) or GLY at 0.25 (G0.25), 0.5 (G0.5), 1.0 (G1.0), 1.5 (G1.5), or 2 (G2.0) mg/kg five days a week for 20 weeks. Body weight and feed disappearance were recorded weekly and vaginal cytological assessments of the estrous cycle stage was performed for the final 21 days of exposure. At the end of the treatment period, mice were euthanized in the proestrus phase of their estrous cycle. The ovary, uterus, liver, kidney, and heart weights were recorded and blood collected for hormone assays. Ovaries were flash frozen in liquid nitrogen for protein isolation. Compared to controls, G2.0 and G1.5 had increased ( $P < 0.05$ ) feed intake and G1.0 mice had increased ( $P < 0.05$ ) body weight from week 6 of treatment onwards. When normalized to body weight, increased weights of the ovaries in G2.0 ( $P = 0.06$ ), heart in G1.0 ( $P = 0.07$ ), spleen in G2.0 ( $P = 0.1$ ), kidney in G1.0 ( $P = 0.05$ ) but decreased hepatic weight in G1.0 ( $P = 0.07$ ) were observed. Estrous cycle effects ( $P < 0.05$ ) included decreased estrous cycle length in G0.5 mice, increased diestrus phase length in G1.0 and decreased proestrus phase length

in G0.25 mice. Circulating  $17\beta$ -estradiol tended towards being increased ( $P = 0.06$ ) in G1.5 relative to control mice but no impacts of GLY on progesterone were observed. GLY did not affect the abundance of AKT, pAKT, STAR, HSD3 $\beta$ , CYP11A1, CYP19A1, or ER $\alpha$  protein but decreased ER $\beta$  ( $P < 0.05$ ) was observed in G0.5 mice. Global proteome changes were determined by LC-MS and approximately 793 proteins per sample were detected. Compared to control, 4, 5, 61, 157 and 180 proteins were decreased ( $P < 0.05$ ) by G0.25, G0.5, G1.0, G1.5, and G2.0, respectively. In terms of proteins in greater abundance, 20, 27, 5, 3 and 5 proteins were increased ( $P < 0.05$ ) by G0.25, G0.5, G1.0, G1.5, and G2.0, respectively. KEGG pathway analysis of proteome changes identified alterations to glutathione metabolism (GPX1, GSTa4, GSTk1), PI3K-AKT signaling (YWHAH, PCK2, EIF4B, PRKAR2B, EEF2, HSPA8, APOA2, ACAA1A and PRMT1), steroidogenesis (CYP11A1, HSPA8) and cell death (CTSB, TUBA1B, CTSZ, BUB3, HMGB1) by GLY exposure. These data support that chronic GLY exposure may affect appetite and negatively impact ovarian function in a dose-dependent manner. Supported by R21ES026282 from the NIEHS to AFK.

**Investigating the Role of Wnk1 in Mouse Uterine Morphology and Pregnancy.** Ru-pin Alicia Chi, Nyssa Adams, San-pin Wu, Chou-Long Huang, John Lydon, and Francesco DeMayo

Decidualization is an essential process in pregnancy during which the endometrium stromal cells undergo differentiation to form the 'decidua'. This is the maternal tissue which will go on to form a part of the placenta, the maternal-embryo interface serving crucial functions for the developing foetus. WNK lysine deficient protein kinase 1 (Wnk1) was previously shown to play important roles in decidualization in vitro, as siRNA-mediated knock-down impaired differentiation, proliferation and migration in cultured HESC cells. In this study, we examined the in vivo role of Wnk1 in uterine homeostasis and pregnancy using a uterine Wnk1 deletion mouse model. Wnk1 was conditionally ablated in the whole uterus by crossing the floxed Wnk1 allele carrying mice (Wnk1f/f) to mice carrying progesterone receptor driven recombinase Cre. The impact of uterine deletion of Wnk1 (Wnk1d/d) was evaluated with respect to the ability of the uterus to support pregnancy and uterine morphology. A 6-month breeding trial revealed that Wnk1d/d mice were severely subfertile with decreased rate of pregnancy, fewer number of litters, smaller litter size, and increased neonatal lethality when compared to the Wnk1f/f control mice. Using high-frequency ultrasound, we demonstrated abnormality in both the maternal pregnancy parameters and embryonic development, including increased decidua thickness and decreased gestational sac size and crown-rump length. In addition, embryo resorption was frequently observed in Wnk1d/d mice. In non-pregnant mice, we observed adenomyotic-like uterine morphology associated with Wnk1 deletion whereby the glandular epithelium is adjacent to or present in the myometrial layer. Moesin, a biomarker for adenomyosis, gland marker FOXA2, smooth muscle marker CALD1 and extracellular matrix fibronectin all showed increased mRNA levels in the Wnk1d/d mice, proposing that these altered protein levels may contribute to the abnormal gland-muscle morphology. These results demonstrate a crucial role of Wnk1 in the uterus, where a disruption in this pathway impairs both the uterine glands and smooth muscle, failing the maintenance of normal uterine homeostasis, and eventually resulting in adverse pregnancy outcomes.

**Anti-Angiogenic and Pro-Apoptotic Effects of Flaxseed in Ovarian Cancers of the Hen: Role of 2-Methoxyestradiol (2-ME) and Docosaheptaenoic Acid (DHA).** Purab Pal, Jim Petrik, Karen Hales, Dale Buck Hales

Flaxseed diets reduce the occurrence and severity of ovarian cancer in laying hen – the only spontaneous animal model for ovarian cancer. Flaxseed diets cause increases in 2-ME via induction of CYP1A1. 2-ME is known to destabilize microtubules, induce apoptosis and inhibit angiogenesis. The objective was to determine if the anticancer actions of flaxseed are mediated by increased production of 2-ME, and to determine the mechanism of 2-ME action.

TUNEL and immunohistochemical staining for angiogenesis markers (CD-31,  $\alpha$ -smooth muscle actin, VEGF and VEGFR2) were performed on normal and cancerous ovarian tissue from control and flax-fed hens. Human ovarian cancer cells BG1, HeyC2 and TOV112d; were treated with docosahexaenoic acid (DHA), 2ME, with or without SB203580, a p38-MAPK inhibitor. p38 and phospho-p38 (pp38), caspase 3 (cleaved and total) phospho-histone H3 (pHH3) and gH2Ax expression were examined by western blot. Angiogenesis was examined by chorioallantoic membrane (CAM) assay; cell cycle dynamics were analyzed by flow cytometry; mRNA expression was quantified by qPCR.

Increased apoptosis and decreased angiogenesis markers were observed only in ovarian tumors from flax-fed hens. 2ME treatment caused an increase in pp38, and apoptosis in ovarian cancer cells which was blocked by SB203580, consistent with p38-mediated action of 2-ME. 2-ME caused increased expression of gH2Ax and pHH3 suggesting increased DNA damage response and pro-apoptotic histone modification. FACS analysis showed G1 accumulation and an increase in sub-G1 cells. Both 2-ME and DHA exhibited a dose-dependent anti-angiogenic activity on CAM but DHA did not cause apoptosis. SB203580 reversed the anti-angiogenic effects of 2-ME on CAM, but the p38 inhibitor did not reverse the anti-angiogenic actions of DHA.

Flax diet promotes production of 2ME and DHA which work together to attack ovarian cancer in hens: 2ME promotes apoptosis and inhibits angiogenesis via activation of p38-MAPK, causes DNA damage and G1 phase accumulation in cancer cells. DHA has potent anti-angiogenic and anti-inflammatory actions but does not work via activation of p38 MAPK {NIH RO1AT005295}

### **Genome Editing and Developmental Rates of Bovine Zygotes Following CRISPR Delivery at Different Microinjection Times.** Ismael Lamas-Toranzo and Pablo Bermejo-Álvarez

CRISPR technology enables direct gene ablation (knock-out, KO) in zygotes, allowing the generation of KO embryos to unequivocally assess the role of a particular gene in a specific developmental process. CRISPR-mediated gene ablation is based on the generation of insertion-deletions (indels) in the coding region of a gene. However, the randomly generated indels must disrupt the open reading frame of the gene (i.e., they should not be multiple of three) to result in gene ablation. In this sense, mosaicism (i.e. the presence of more than two indels on the same embryos) should be avoided, because it greatly reduces the chances of generating KO embryos, as all indels of a single KO embryo must be frame-disrupting. CRISPR microinjection following conventional IVF protocols in bovine result in virtually 100 % mosaicism, as the zygote has already replicated its DNA (4c) by the time of CRISPR delivery (~20 h post-insemination –hpi-). In this study, we have compared the developmental and genome edition rates obtained after conventional IVF (microinjected at 20 hpi) or following two IVF protocols pursuing an earlier CRISPR delivery: short gametes co-incubation time (10 h, microinjected at 10 hpi) or fertilization

without cumulus cells (microinjected before fertilization, 0 hpi). CRISPR components were delivered by ooplasm injection of ~3 pl of 300 ng/ $\mu$ l Cas9 mRNA and 100 ng/ $\mu$ l of a sgRNA designed against an intronic region of DNMT3A. Non-injected zygotes obtained after gametes co-incubation for 20 or 10 h displayed similar cleavage rates (92.5 $\pm$ 1.2 vs 85.4 $\pm$ 2.7 %, respectively), but fertilization of cumulus-free oocytes resulted in a significant reduction compared to the other non-injected groups (71.6 $\pm$ 0.7 %, ANOVA  $p < 0.05$ ). However, blastocyst rate did not display significant differences between non-injected groups (32.5 $\pm$ 3.7 vs 29.2 $\pm$ 3 vs 25.8 $\pm$ 2.1 %, for 20, 10 or 0 hpi groups, respectively). Microinjection resulted in a significant reduction of both cleavage and blastocyst rates compared to non-microinjected controls, but no significant differences were noted between microinjected groups (Cleavage: 68.6 $\pm$ 2.7 vs 70.4 $\pm$ 6.5 vs 57 $\pm$ 3.8 %; Blastocysts: 20 $\pm$ 1.7 vs 18.3 $\pm$ 4.3 vs 17.6 $\pm$ 3.3, for 20, 10 or 0 hpi groups, respectively). Genome edition of blastocyst derived from microinjected zygotes was also similar in all microinjected groups (85.7 % -6/7- for 20 hpi vs 84.6 % -11/13- for 10 hpi vs 88.9 % 16/18 for 0 hpi). In conclusion, CRISPR delivery before fertilization or following short gamete co-incubation times result in similar developmental and genome edition rates than those obtained following conventional co-incubation times.

**Germline Expression of the Histone Variant H3.3 is Required for Completion of Spermatogenesis in the Mouse.** Gill M. E., Gaspa Toneu L., Rohmer A., Royo H., and Peters A. H. F. M.

Post-replicative cells incorporate increasing levels of the DNA synthesis-independent H3 variant H3.3 over time. The male germline represents a differentiation process in which a substantial portion of development occurs after a final replication step. Here we report that mutation of one copy of an H3.3-encoding locus, H3f3b, specifically in male germ cells results in infertility. Testes from mutant animals exhibit a primary block in spermatogenesis during post-meiotic differentiation, when most histone proteins are being evicted from chromatin. Transcriptional and chromatin characterization of spermatids from mutant animals reveals a moderate number of mRNAs showing up-regulation, without a large-scale alteration of chromatin structure. Mutations of additional H3.3-encoding loci reveal increasing levels of disruption of spermatogenesis during both pre-meiotic and meiotic differentiation, suggesting additive functions for these loci in the regulation of this process. We propose that H3.3 is required at specific points during male germ cell differentiation, and plays a role in the proper repression of specific transcripts in post-meiotic cells.

**Fertilizing Ability of Cryopreserved Canine Spermatozoa with Brief Equilibration in Skim Milk-Based Extender.** Yasuyuki Abe, Tomoyoshi Asano, Ichiko Wakasa, Aiko Kume, Sakimi Yokozawa, Rika Umemiya-Shirafuji, and Hiroshi Suzuki

Cryopreservation of canine spermatozoa provides potential exchange of genetic materials, and may lead to improvement in the breeding management programs used to produce working dogs such as guide dogs for the blind. We previously reported that skim milk is an effective cryoprotectant for cryopreservation of canine spermatozoa instead of conventional cryoprotectant “egg yolk” that disturbs the transportation of frozen semen when avian influenza is prevalent. In addition, long term equilibration after dilution with egg yolk extender is required before freezing of spermatozoa. For the establishment of a simple method for cryopreservation of canine spermatozoa, we examined the effect

of brief equilibration at low temperature on sperm motility, acrosomal integrity and fertilizing ability after cryopreservation with skim milk-based extender. Collected ejaculates were diluted with the first extender composed of skim milk and raffinose (SR extender) at 4C or room temperature (RT), and then they were cooled to 4C (first equilibration). After the first equilibration for 0 to 180 min, the equivalent volume of the second extender, which was SR extender supplemented with 14% (v/v) of glycerol at 4C, was added to the semen aliquots. The semen samples were left at 4C for 15 min (second equilibration), loaded into a 0.25-ml straw, and then were immersed into liquid nitrogen. The post-thaw semen samples were examined the proportion of total motile spermatozoa (TMS) by computer-assisted sperm analysis and the acrosomal integrity by staining with FITC-conjugated peanut agglutinin. TMS of the samples without the first equilibration after extending with SR extender at RT ( $26.7 \pm 12.9\%$ ) was lower than those of equilibrated samples (30min,  $32.5 \pm 3.7\%$ ; 60 min,  $32.2 \pm 10.5\%$ ; 180 min,  $28.5 \pm 17.2\%$ ). However, when ejaculates were diluted with cooled extender (4C) without the first equilibration, TMS improved to  $38.3 \pm 11.8\%$ . The acrosomal integrities without the first equilibration regardless of the temperature of SR extender (RT, 71.9%; 4C, 78.6%) were lower than those of equilibrated samples (30min, 73.6%; 60 min, 88.6%; 180 min, 92.7%). To examine the fertilizing ability, frozen spermatozoa after extending at RT or 4C with or without 60 min first equilibration were transcervically inseminated into 5 recipient bitches, respectively. The delivery rate and litter size were low when semen was extended at RT without the first equilibration (20% and 2.0, respectively). The cooled extender group showed higher delivery rate (80%) even without the first equilibration, although there was no different in the litter size (2.5). On the other hand, the prolonging the first equilibration term to 60 min after extending at RT resulted in a higher delivery rate (80%) and litter size (5.5), and the rate was similar with standard manner that equilibrated in SR extender for 180 min (80% and 6.0, respectively). These results suggested that it is necessary to lower the temperature of the semen aliquots before adding the second extender and to ensure a certain equilibration term. In the conclusion, the first equilibration for 60 min with skim milk-based extender is useful and time-efficient for cryopreservation of canine spermatozoa.

#### **Decreased WISP2 Gene Expression in Testis Correlates with Increased Sertoli Cell Proliferation in Letrozole-Treated Juvenile Boars.** Simin Tang and Trish Berger

Previous experiments showed that weekly treatment of neonatal boars with letrozole, an aromatase inhibitor, reduced estradiol and increased Sertoli cell proliferation during the first 6.5 weeks of age. Preliminary gene expression data indicated that Wnt1 Inducible Signaling Protein 2 (WISP2) mRNA in testis was significantly reduced at 5 weeks of age following weekly letrozole treatment; immunohistochemistry and ELISA both confirmed the presence of WISP2 protein in the testis. The mechanisms leading to increased proliferation of Sertoli cells is yet to be elucidated. In this experiment, the potential relationship between WISP2 expression and Sertoli cell proliferation was evaluated. WISP2 gene expression in testis was measured by qPCR with RARS as the reference gene. Reduced WISP2 expression following weekly letrozole treatment at 5 weeks of age is consistent with the reduced mRNA level in the preliminary experiment. In a group of six littermate pairs, WISP2 expression is significantly lower in 5-week-old boars following letrozole treatment compared with vehicle-treated littermates. However, in a group of seven littermate pairs at 6.5 weeks of age, WISP2 expression in letrozole-treated boars was not different from the vehicle-treated littermates. Hence, WISP2 gene expression decreased with letrozole treatment at 5 weeks of age, a time point immediately the preceding significant increase in Sertoli cell numbers observed following letrozole treatment. The time difference between decreased

WISP2 expression and proliferation response is consistent with a role in mediating the response to reduced estradiol. This research was supported by Jastro Shields graduate research scholarship and W3171.

**Uterine Double Conditional Knockout of SMAD2 and SMAD3 Results in Uterine Cancer Due to an Aberration in Estrogen Feedback.** Maya Kriseman, Diana Monsivais, Julio Agno, Ramya Masand, Chad Creighton, William Gibbons, and Martin Matzuk

The transforming growth factor  $\beta$  (TGF $\beta$ ) superfamily proteins are key regulators in many reproductive processes. SMAD2 and SMAD3 are downstream proteins in the TGF $\beta$ , GDF9, and activin signaling cascade that are important in translocating signals to the nucleus, binding DNA, and regulating the expression of target genes. While previous studies have shown the role of TGF $\beta$  family receptors upstream of SMAD2/3 in the uterus, as well the role of SMAD2/3 in the ovary, we do not fully understand the roles of SMAD2/3 in the uterus and their implications in the reproductive system. Because complete loss of SMAD2 results in embryonic lethality and to avoid deleterious effects of SMAD3 deletion, a conditional knockout (cKO) mouse model was generated. Given previous data showing the redundant function of SMAD2 and SMAD3, a double conditional knockout was constructed using progesterone receptor-cre mice. The SMAD2/3 cKO mice were noted to be infertile due to endometrial hyperproliferation observed as early as 6 weeks of postnatal life. Endometrial hyperproliferation worsened with age, and all cKO mice went on to develop bulky endometrioid-type uterine tumors with a 100% mortality rate by 8 months of age. The phenotype was estrogen-dependent and could be prevented with ovary removal at 6 weeks of age with hyperplasia returning with reintroduction of estrogen; however, uterine tumor formation was not avoided if ovary removal was delayed until 12 weeks. Uterine tumor epithelium was associated with a decreased expression of genes involved in the steroid biosynthesis pathway and increased expression in inflammatory response genes, as well as abnormal expression of cell cycle checkpoints. Our results indicate the crucial role of SMAD2/3 in maintaining normal endometrial function and confirm the estrogen-dependent nature of SMAD2/3 in the uterus. The hyperproliferation of the endometrium affected both implantation of pregnancy as well as sustaining a pregnancy. Our findings not only generate a mouse model to study the role of SMAD2/3 in the uterus but also serve to provide insight into the mechanism by which the endometrium can escape the plethora of growth regulatory proteins.

This research was supported by Eunice Kennedy Shriver National Institute of Child Health and Human Development grant R01-HD033438 (to M.M.) and by a Postdoctoral Enrichment Program Award from the Burroughs Wellcome Fund (to D.M).

**The Effects of Oocyte Retrieval Methods on Bovine Oocyte Competence and Global Gene Expression Dynamics.** Brittany A. Foster, Emilio J. Gutierrez, Zongliang Jiang, and Kenneth R. Bondioli

Optimization of in vitro embryo production rates relies on maximizing initial oocyte quality through ideal retrieval and handling methods. The aim of this study was to determine the effect of oocyte retrieval methods on oocyte global gene expression and embryo development. Oocytes were recovered via transvaginal ultrasound guided oocyte pick up (OPU) from cross-bred beef cows either at random time

intervals or following a super-stimulation protocol where cows were given 200 mg follicle stimulating hormone. A third group of oocytes were harvested from post-mortem collected ovaries. Oocytes from all three retrieval methods were randomly assigned to one of three treatment groups; snap frozen at the germinal vesicle (GV) stage, snap frozen at metaphase two (MII), or matured in vitro and fertilized for embryo culture. A total of 232, 238 and 375 oocytes were recovered from OPU, stimulated OPU and post-mortem ovaries, respectively, for embryo production and RNA sequencing analysis. For gene expression analysis, four oocytes from each group were pooled and Smart-seq protocol was followed to make sequencing libraries. Fewer oocytes from unstimulated OPU developed to the morula stage, compared to other collection methods ( $P= 0.078$ ) (14%, 27% and 6% of oocytes for post-mortem, stimulated OPU and OPU derived oocytes, respectively). This pattern held and gained significance for blastocyst development from cleaved zygotes, ( $P= 0.0066$ ) with 49%, 55% and 20% of cleaved embryos developing to blastocysts for post-mortem, stimulated OPU and OPU, respectively. RNA Sequencing showed that a total of ~6000 genes changed their expression as a result of maturation, with the majority of genes being up-regulated as maturation proceeded, regardless of oocyte retrieval method. Retrieval method significantly impacted gene expression with oocytes recovered from post-mortem ovaries having the most unique gene expression profiles; 34 genes were up-regulated and 356 down-regulated when compared to OPU oocytes, and 49 up-regulated and 856 down-regulated compared to stimulated OPU oocytes, at MII. OPU oocytes had significantly different expression of genes controlling meiotic progression, while those oocytes recovered from post-mortem ovaries had multiple irregularities in genes controlling mitochondrial function. FSH stimulation prior to OPU resulted in oocytes with up-regulation of genes involved in sperm-oocyte binding, and oocyte activation compared to oocytes from other retrieval methods. Results indicated that while post-mortem recovered oocytes have higher blastocyst developmental rate, they have a very different gene expression profile than those of oocytes collected from live cows. The irregularities in genes controlling mitochondrial function may lead to metabolic irregularities later in development. When combined, results indicated that FSH-stimulation prior to OPU is an optimal method of oocyte retrieval in cattle.

**Analysis of the Uterine Luminal Secretome in Heifers with Superior Uterine Capacity.** Joao G.N. Moraes, Susanta K. Behura, Thomas W. Geary, and Thomas E. Spencer

The uterus clearly impacts conceptus (embryo and associated extraembryonic membranes) survival and programs its development, thus affecting pregnancy success in ruminants. Serial transfer of in vitro produced (IVP) embryos was used to classify heifers as high fertile (HF=100%), subfertile (SF=25-33%), or infertile (IF=0%) based on day 28 pregnancy rates [Geary et al., Biol Reprod 2016]. On day 17 (10 days post-transfer), pregnancy rate was higher in HF (71%) and SF (90%) than IF (20%) heifers [Moraes et al, Proc Natl Acad Sci 2018]. The conceptus was longer in HF (mean 10.6 cm; range 1.2-32.2 cm) than SF (mean 4.7 cm; range 1.5-13.5 cm) heifers, and the endometrial and conceptus transcriptome was dysregulated in SF heifers. Here, we investigated the uterine lumen secretome of day 17 nonpregnant (NP) HF, SF and IF heifers, and pregnant (P) HF and SF heifers. At slaughter on day 17, the uterine lumen was gently flushed with 20 ml of sterile PBS. The conceptus was removed if present, and the uterine lumen flush (ULF) clarified by centrifugation. Mass spectrometry was used to evaluate proteins, metabolites, fatty acids and prostaglandins (PG) in the ULF, and glucose was determined using a fluorometric assay. Glucose and PG data was analyzed in SAS by analysis of variance (ANOVA). Proteomics data was analyzed using Scaffold by Fisher's exact test. Analysis of fatty acids and

metabolites were performed by either t-test or ANOVA using the web server MetaboAnalyst3.0. Significant metabolic pathways associated with differently expressed metabolites were determined using MetaboAnalyst3.0. Glucose was greater ( $P=0.32$ ) in ULF of NP HF, SF and IF heifers. Total fatty acid in ULF was not different ( $P>0.17$ ) by pregnancy status, but 16 fatty acids were different ( $P<0.04$ ) in the ULF of P HF and SF heifers, and 2 fatty acids differ ( $P<0.04$ ) in ULF of NP HF and SF heifers. Many proteins were differentially abundant in the ULF of P and NP heifers (447), between P HF and SF heifers (222), and among NP HF, SF, and IF heifers (48). Comprehensive metabolomics analysis found 531 metabolites different in ULF of P and NP heifers, 293 different between P HF and SF heifers, and 81 different in ULF among NP HF, SF and IF heifers. Metabolic pathways associated with the differential metabolites included the urea cycle, phenylalanine and tyrosine metabolism, and amino sugar metabolism. The observed differences in the uterine secretome are hypothesized to influence uterine capacity for pregnancy establishment and conceptus survival and development. Supported by NIH grant 1 R01 HD072898.

### **Notch Signaling Regulates Proliferation and Differentiation of Mouse Ovarian Granulosa Cells.** Rexxi Prasasya and Kelly Mayo

The balance between proliferation and differentiation in preovulatory granulosa cells is a complex process that requires proper integration of endocrine and local ovarian signals. The highly conserved Notch signaling pathway is widely used throughout development to direct cell-fate determination during tissue patterning and has been shown to be important in ovarian follicle formation and development. We found that Notch activity and expression of Notch ligands and receptors are positively regulated following activation of the LH-receptor in the prepubertal mouse ovary. The localization of JAG1, the most abundantly expressed Notch ligand in the mouse ovary, revealed a striking shift from oocytes to somatic cells following hormone stimulation. Activation of Notch signaling in primary granulosa cells co-cultured with immobilized JAG1 or JAG2 ligands indicates that expression of Jag1 in ovarian somatic cells occurs downstream of canonical Notch receptor activation. Consistent with patterning of other multi-layered tissues, Notch signaling appears to be propagated across the granulosa cells of multi-layered follicles through lateral induction of ligand expression. Based on the localization of JAG1 in the ovary following hCG treatment, we hypothesized that it might function to promote the steroidogenic phenotype. Using primary cultures of differentiating granulosa cells, we investigated the functions of JAG1 using siRNA knockdown. The loss of JAG1 led to a suppression of granulosa cell differentiation, as assessed by reduced progesterone and estrogen secretion. This is a consequence of decreased expression of key genes involved in steroid hormone biosynthesis. Intracellular signaling analysis revealed suppressed activation of YB-1, a known regulator of granulosa cell differentiation genes, following JAG1 knockdown. Accompanying this disrupted differentiation, JAG1 depleted cells retained an enhanced rate of proliferation that is associated with continued activation of the mitogenic PI3K/AKT and MAPK/ERK signaling pathways. Depletion of the obligate Notch transcription factor RBPJ using siRNA knockdown replicated these phenotypes, although in a less robust manner, consistent with the altered proliferation and differentiation being a consequence of suppressed canonical Notch signaling. We are currently investigating the specific Notch receptor(s) through which JAG1 signals to promote the differentiated steroidogenic phenotype, as well as the mechanisms through which Notch activity couples to intracellular proliferation and differentiation pathways. Overall, this study demonstrates a role for Notch signaling in regulating the proliferation and differentiation of ovarian granulosa cells,

adding to the diversity of pathways known to promote the periovulatory phenotype. Supported by the Eunice Kennedy Shriver NICHD Program Project Grant (NIH P01 HD021921) and NIGMS Cellular and Molecular Basis of Disease Training Grant (NIH T32 GM08061).

**Influence of Dimethyl Sulfoxide Concentrations and in Vitro Culture on Equine Endometrial Tissue Explants.** Riley Thompson, Aime Johnson, Tulio Prado, Christopher Premanandan, Megan E Brown, Brian Whitlock, and Budhan Pukazhenth

Availability of viable frozen-thawed endometrial tissues could facilitate detailed studies into physiologic and disease processes influencing the endometrium. This study was designed to better understand cryopreservation of equine endometrial tissue. Previous studies in the human and horse have focused on cryopreservation of dissociated endometrial cells. To our knowledge, there are no studies on cryopreservation of endometrial explants. Our objective was to determine the influence of differing concentrations of the permeating cryoprotectant dimethyl sulfoxide (DMSO) on viability and structural integrity (histology) of cryopreserved endometrial tissues over a 5-day culture interval. Endometrial tissue (1-2 biopsies from 4 mares) were cryopreserved using a slow cooling method in Minimum Essential Medium (MEM) containing 20% fetal bovine serum and 0%, 10%, or 20% (v/v) of DMSO. Histology (score 1-6; 1 = non-intact stroma with absent glandular structure; 6 = presence of intact stroma and glandular structures with no signs of necrosis) and cell viability (SYBR-14 and propidium iodide staining) were evaluated before and after cryopreservation. Fresh and cryopreserved endometrial tissues also were subjected to a short-term culture (37°C; 5% CO<sub>2</sub>) on agarose blocks in two different media (Dulbecco's Modified Eagle Medium [DMEM] and MEM) to determine tissue viability and function. Data were analyzed using ANOVA and a Tukey Post-hoc test to compare effects of DMSO treatment and culture conditions. Viability ( $46.6 \pm 6.2\%$ , mean  $\pm$  SEM) and histology score ( $5.4 \pm 0.5$ ) were high in all fresh tissue controls prior to culture. After in vitro culture of fresh tissue, the histology score (DMEM,  $4.4 \pm 0.4$ ; MEM,  $4.5 \pm 0.3$ ) was not different ( $P > 0.05$ ) from the fresh control. However, viability was markedly reduced ( $P < 0.05$ ). No difference was found between 10 and 20% DMSO concentration or culture medium in the short-term culture on histology score or cell viability. Results demonstrate the sensitivity of equine endometrial tissue to low temperature storage and the capacity to protect the structural integrity but not cell viability with DMSO. In conclusion, although equine endometrial tissue can be cryopreserved in DMSO, further studies are warranted to minimize loss of cell viability. (Riley Thompson was supported by the University of Tennessee – Knoxville, and funds from Mr. Mike Baudhuin and Ms. Gay Barclay)

**Long Term Exposure to Supraphysiological Temperature (Heat Stress) Impairs Growth of Bovine Preantral Follicles in Vitro.** Luís H. de Aguiar, Kendall A. Hyde, and Anna C. Denicol

Detrimental effects of heat stress on development of pre-ovulatory oocytes and preimplantation embryos are associated with reduced fertility in cattle and other species; however, the effects of heat stress on developmental competence of preantral follicles remain poorly understood. In this study we used a novel approach to simulate the changes in temperature likely experienced by preantral follicles in vivo to evaluate responses regarding growth, viability and gene expression. Preantral follicles (diameter  $81.2 \pm 16.5 \mu\text{m}$ ) were extracted from slaughterhouse-derived bovine ovaries, selected under a

stereomicroscope and stained with 0.02% trypan blue to assess viability. Viable primary, early-secondary and secondary follicles were randomly and uniformly allocated into one of two experimental groups, placed individually in 96-well plates, imaged and measured. Control (CON) follicles were cultured for 7 days at 38.5°C, and heat-stressed follicles (HS), for 16h at 38.5°C and 8h at 41.0°C daily during 7 days. At the end of culture, follicles were stained again to assess viability, imaged and measured; viable and non-viable (n=3 of each/treatment/ replicate) individual follicles were used for gene expression of BAX, HSP70 and SOD genes by qPCR using BETA-ACTIN as endogenous control. A total of 261 follicles in 8 replicates were analyzed by ANOVA using proc GLM of SAS (version 9.4). CON follicles had a higher growth rate ( $12.5 \pm 2.3 \mu\text{m}$ ;  $p=0.02$ ) and a greater percentage of growth relative to initial size ( $16.2 \pm 2.7\%$ ;  $p=0.02$ ) compared to HS ( $5.0 \pm 2.5 \mu\text{m}$  and  $7.4 \pm 3.0\%$ , respectively). Although there was a greater proportion of growing follicles after 7 days among CON compared to HS follicles ( $71.6 \pm 3.5$  vs.  $57.1 \pm 3.5\%$ ,  $p=0.02$ ), a high proportion of follicles remained viable in both groups (75% and 66% for CON and HS;  $p=0.19$ ). Interestingly, follicles that remained viable after 7 days under HS had similar growth rates to CON ( $17.0 \pm 2.9 \mu\text{m}$  and  $21.4 \pm 2.3 \mu\text{m}$ , respectively;  $p=0.21$ ) and similar proportion of growth relative to initial size (26% and 20.5% for CON and HS;  $p=0.19$ ). Expression of BAX and HSP70 increased 8.7- and 8.4-fold in unviable compared to viable follicles in the CON group ( $p < 0.05$ ), and increased 9.8- and 10.4-fold in HS unviable compared to viable follicles ( $p < 0.01$ ). Expression of SOD increased 6.4-fold in unviable compared to viable HS ( $p < 0.01$ ), as opposed to no change in CON unviable and viable follicles. There was no change in expression of BAX and HSP70 when only viable follicles were compared between CON and HS; SOD expression tended to be higher in viable HS follicles (3.78-fold;  $p=0.058$ ). Results indicate that after 7 days of daily heat stress, a similar proportion of follicles maintained viability compared to non-stressed follicles, but perhaps at a higher energy expense since growth rate was lower in viable heat-stressed follicles. Expression of BAX and HSP70 was elevated in non-viable follicles in both groups. Interestingly, only heat-stressed follicles that became unviable had over 6-fold increase in SOD expression compared to viable counterparts. Finally, HS follicles that remained viable after 7 days behaved similarly to CON in terms of growth rate and gene expression, suggesting that these follicles might carry intrinsic mechanisms that confer increased heat resistance.

**Transcriptomic Analysis of Conceptus and Endometrium During Pregnancy Failure at the Preimplantation Stage in Holstein Cows.** Leticia D.P. Sinedino, Bethany E. Liebig, Jeanette V. Bishop, Kevin D. McSweeney, Ann M. Hess, Hana Van Campen, Milton G. Thomas, and Thomas R. Hansen

Embryonic mortality in dairy cows is substantial and mostly occurs before the period of maternal recognition of pregnancy through unknown biological mechanisms. It was hypothesized that interferon (IFN) signaling, and consequently, action on the endometrium was disrupted in normal (N) vs. embryo mortality (EM) conceptuses at the preimplantation period. Estrous cycles (estrus = Day 0) were synchronized in 19 lactating Holstein cows. Pregnant cows were artificially inseminated; whereas nonpregnant cows representing the estrous cycle (EC; n = 7) were not exposed to semen. On Day 16, uteri were flushed and endometrial biopsies performed. Recovered conceptuses were classified as N (n = 7) or EM (n = 5) based on morphology and length. Conceptuses were classified as EM if they were pink or red, opaque, or failed to elongate. Total RNA from conceptuses (n = 12) and endometrium (n = 19) were subjected to RNA-Seq analysis. The uterine fluid was evaluated for IFN tau (IFNT) and the endometrium for ISG15 protein concentrations by Western blot. RNA-Seq data were analyzed using the DESeq2 package in R controlling for false discovery rate (FDR) using the Benjamini-Hochberg procedure.

Biological relevance was interpreted by pathway analysis of the differentially expressed genes ( $FDR \leq 0.05$ , fold change  $> 1.5$ ) using Ingenuity Pathway Analysis<sup>®</sup>. Continuous variables were analyzed by ANOVA in R. EM conceptuses were smaller than N ( $50.4 \pm 11.3$  vs.  $111.8 \pm 10.1$  mm;  $P < 0.05$ ) from EC cows. In total, 2,267 transcripts were up- and 365 were downregulated in EM relative to N conceptuses. The top canonical pathways in EM conceptuses were T helper (Th) 1 and Th2 activation pathways, dendritic cell maturation, and production of nitric oxide and reactive oxygen species in macrophages, all of which were upregulated. Top upstream regulators in EM compared with N conceptuses included TNF, IFNG, IL1B, and IFNA, all predicted to be upregulated. Endometrial transcriptome also changed between EM and N (65 up- and 440 downregulated genes), and between N and EC (374 up- and 74 downregulated). Top canonical pathways in EM compared to N endometrium included IFN signaling, iCOS-iCOSL signaling in Th cells, and Th1 pathway, all of which were downregulated. Top endometrial upstream regulators included IFNA, IRF7, IFNG, IFNA2, and IFNAR, all predicted to be downregulated. Collectively, pregnancy failure involved remarkable changes in the conceptus and endometrial transcriptomes. The downregulation of type I IFN responses in the endometrium of EM cows is consistent with a lack of maternal recognition of pregnancy; whereas the upregulation of inflammatory, cell death, and immune cell responses in EM conceptuses was unexpected and presents novel insights on pregnancy loss in dairy cows. Supported by USDA AFRI W3112.

**Prostaglandin Release Following Oxytocin Challenge in Pregnant Non-Lactating Cows.** Sydney T. Reese, Gessica A. Franco, Andrea S. Lear, Felipe G. Dantas, Tatiane S. Maia, Taylor B. Ault, Savannah L. Speckhart, F. Neal Schrick, Michael F. Smith, and Ky G. Pohler

Prostaglandin  $F_{2\alpha}$  ( $PGF_{2\alpha}$ ) is the luteolytic factor responsible for regression of the corpus luteum. However, circulating  $PGF_{2\alpha}$  remains present during early pregnancy without negative consequences and pulses may be induced around the time of active placentation, approximately day 30 of gestation in the cow. Due to the dependence of  $PGF_{2\alpha}$  release from the endometrium on presence of oxytocin (OT) receptors in the uterus, the objective of this study was to evaluate uterine release of prostaglandin in response to an OT challenge in pregnant non-lactating cows. Our hypothesis was that cows at day 30 of gestation would respond to an OT challenge resulting in an increased prostaglandin  $F_{2\alpha}$  ( $PGF_{2\alpha}$ ) release which would decrease progesterone (P4) concentrations following a peak in  $PGF_{2\alpha}$ . Non-lactating cows ( $n = 25$ ) were artificially inseminated on day 0 following an industry standard synchronization protocol and diagnosed as pregnant ( $n = 8$ ) 30 days after AI based on the presence of an embryonic heartbeat via ultrasound. Pregnant cows were then fitted with a jugular catheter and blood samples were collected every 15 minutes beginning 45 minutes before OT injection to establish a baseline measurement and 4 hours following OT injection. At time 0 (day 30 of gestation), 100 I.U. of oxytocin was administered intramuscularly to treatment animals ( $n = 5$ ) and control animals ( $n = 3$ ) received a saline injection of the same volume. Prostaglandin  $F_{2\alpha}$  metabolite (PGFM), progesterone (P4) and pregnancy associated glycoprotein (PAG) concentrations were determined via validated ELISA and RIA approaches from collected plasma. Data were analyzed by repeated measures in SAS. Following the OT challenge, the mean concentration of PGFM peaked 2 hours after OT injection in treatment animals ( $739.15 \pm 150.11$  pg/mL) and no peak was observed in control animals (range 340.10 - 379.56 pg/mL;  $P < 0.05$ ). Furthermore, there was no difference in P4 concentration between treatment and control animals ( $P > 0.05$ ) even though there was a release of  $PGF_{2\alpha}$ . Circulating PAG concentrations increased above the baseline ( $2.95 \pm 0.27$  ng/mL) concentration beginning 1 hour after injection ( $P < 0.05$ ). In addition, all

cows in both the treatment and control groups, successfully maintained pregnancy until day 65 of gestation. Based on the increased PGFM in response to OT injection, the uterus seems to clearly have OT receptors, but the release of PGF $2\alpha$  did not result in luteal regression or embryonic mortality. This project was supported by Agriculture and Food Research Initiative Competitive Grant no. 2017-67015-26457 from the USDA National Institute of Food and Agriculture.

**Loss of Estrogen Signaling in the Testis Alters Spermatogonia Proliferation.** Samantha B Schon, Caleb Sultan, Adrienne N Shami, and Sue Hammoud

Spermatogenesis is a highly organized and cyclical process allowing for reproduction throughout the male lifespan. This unique process begins with mitotic replication and differentiation of spermatogonial stem cells, followed by meiotic division to primary spermatocytes, and ultimately nuclear compaction via spermiogenesis. The maintenance of a spermatogonia progenitor pool is critical for continuous sperm production throughout an individual's lifespan. In the testes, these stem cells are supported and functionally modulated by several somatic cell types that are under the control of reproductive hormones such as estrogen and testosterone. While testosterone was traditionally considered the dominant hormone dictating reproductive function in males, accumulating data over the past several decades has suggested a critical role of estrogen in both normal reproductive development and continued reproductive function. Estrogen exerts its effect via both direct and indirect mechanisms. Specifically, estrogen may bind to nuclear receptors ESR1 and ESR2 which mediate their effects through direct transcriptional activation or instead estrogen may act through nongenomic intracellular mechanisms or in a ligand-independent manner. Previous whole-body knockout models of ESR1 resulted in total sterility with abnormal sperm count and function, and impaired efferent ductule epithelial cell differentiation which resulted in fluid reabsorption defects, luminal dilation, rete testes dilation, and atrophy of the seminiferous tubules. While atrophy of the seminiferous tubules has largely been attributed to alterations in fluid resorption, we hypothesize that ESR signaling may have a more direct role on spermatogenesis. To test this hypothesis, we utilize a germ cell- and Leydig-specific knockout model of ESR1 (Stra8-Cre or Cyp17-cre). The loss of estrogen in germ cells results in a decrease in the proliferative ability of Plzf+ germ cells as indicated by BRDU, while exogenous administration of estrogen results in increased proliferation in wild-type animals, but not in the ESR knockout. Furthermore, we find increased germ cell death likely at the pachytene checkpoint. The increase in germ cell death was not attributed to change in Sertoli cell number. RNAseq analysis of germ cell ESR null vs. WT Kit+ spermatogonia shows an elevation in DNA damage and repair signaling pathways. Overall, we believe loss of ESR signaling may induce premature differentiation of damaged germ cells which are subsequently cleared at the pachytene checkpoint.

This work was supported by 5K12HD065257-07 (SBS) and 1DP2HD091949-01 (SSH)

**Culture of Mouse Embryos in Palmitic Acid causes Activation of the ER Stress Pathway which is not blocked by AMPK Activation or JNK Inhibition.** Michele Calder, Maisoon Yousif, Jin Tong Du, Dean Betts, and Andrew Watson

There is a human obesity epidemic due to high calorie, high fat diets and sedentary lifestyle. Obese females have elevated serum free fatty acids, and poorer fertility due to anovulation, increased time to conception, pregnancy complications and birth defects. Obese females are a significant proportion of the ART population and have poorer embryo quality and decreased pregnancy rates. Cultured embryos can be affected by Endoplasmic Reticulum (ER) stress, which consists of activation of three pathways, PERK, IRE1 $\alpha$  and ATF6. These lead to activation of transcription factors such as ATF3, CHOP (Ddit3) and splicing of XBP1 to make active XBP1. Initially these factors attempt to alleviate stress by inhibition of protein translation, protein degradation and enhanced expression of ER chaperones to increase protein folding. However prolonged ER stress can lead to apoptosis. High fatty acids in diet or in culture, especially unsaturated palmitic acid (PA), can cause lipotoxicity and activation of ER stress pathways. We hypothesize that PA treatment would activate the ER stress pathway and decrease in vitro development of early mouse embryos. Two cell mouse embryos were cultured for 48h in increasing doses of PA under a 5%O<sub>2</sub>/5%CO<sub>2</sub>/90%N<sub>2</sub> atmosphere. There was a dose-dependent decrease in blastocyst development with a significant decrease in development between control (74.0 $\pm$ 7.1%) and 100 $\mu$ M PA (18.2 $\pm$ 3.1%),  $P < 0.001$ . 100 $\mu$ M PA treatment induced a significant increase in Atf3 ( $P < 0.002$ ) and Ddit3 ( $P < 0.003$ ) mRNA expression as well as increased Xbp1 splicing. In female mice, as well as humans, obesity can lead to decreased AMPK activity. AMPK activators such as metformin or AICAR can be used to improve AMPK activity. We next tested the hypothesis that AICAR-treatment would alleviate PA-induced ER stress. We treated control or PA-treated embryos with increasing doses of AICAR (0, 250 or 500 $\mu$ M). Blastocyst development was lower in groups treated with PA and AICAR did not rescue this decrease. As well, Atf3 and Ddit3 mRNAs remained elevated ( $P < 0.02$  and  $P < 0.005$ , respectively) and Xbp1s was spliced in PA-treated groups. The JNK MAPK pathway can be activated in lipotoxicity and ER stress. We hypothesized that JNK inhibition would block the negative effects of PA treatment. SP600125 is an inhibitor of JNK and was used at 10 $\mu$ M. Two cell embryos were treated with PA, SP or a combined treatment where SP was used as a pretreatment for two hours before PA exposure. In a two way ANOVA, only PA had an effect ( $P < 0.001$ ) and SP or combined treatment did not affect blastocyst development rates; controls (82.6 $\pm$ 3.1%), SP (87.4 $\pm$ 3.5%) versus PA (1.4 $\pm$ 1.0%) and PA+SP (5.6 $\pm$ 4.3%),  $P < 0.001$ . Only PA treated affected Atf3 and Ddit3 mRNA expression ( $P < 0.01$  and  $P < 0.001$ , respectively), and Xbp1 remained spliced and not reduced by SP600125. We conclude that exposure of early cleavage stage embryos to PA is detrimental to development in culture. Furthermore, neither activation of AMPK nor inhibition of JNK MAPK blocks the adverse effects of PA. As obesity rates increase, there must be more awareness and treatment options to combat the negative effects high serum fatty acids on early embryos. Funded by CIHR.

**BHC80 is a Co-Repressor of NOTCH/RBPJ Signaling in Sertoli Cells.** Parag Parekh, Pooja Gandhi, Brian Danysh, Gunapal Shetty, Marvin Meistrich, and Marie-Claude Hofmann

In the seminiferous tubules of the testes, Sertoli cells are a critical component of the spermatogonial stem cell (SSC) niche. We have previously demonstrated that NOTCH signaling in Sertoli cells actively downregulates the production of Gdnf and Cyp26b1, two factors that maintain the stem cell state.

NOTCH signaling therefore indirectly mediates spermatogonial differentiation. The NOTCH pathway is itself triggered by the ligand JAG1, which is expressed by spermatogonia. This interplay between germ cells and Sertoli cells is crucial for sperm production, as dysregulation leads to sterility. RBPJ is a nuclear mediator of NOTCH signaling that can function as a repressor or activator of NOTCH targets, depending on associated co-factors. Using the yeast-2-hybrid assay, we have discovered a novel RBPJ-interacting protein, called BHC80. BHC80 is encoded by the gene Phf21a and is highly expressed in mammalian brain and testis. The objective of this study was to test the role of BHC80 within the RBPJ repressor/activator complex in Sertoli cells.

We used Tg(AMH-cre)1Flor RFP/RFP mice bred with NOTCH GFP-reporter (TNR-GFP) to isolate NOTCH active and inactive Sertoli cells by a 2-step enzymatic digestion followed by fluorescence activated cell sorting (FACS). We also stimulated NOTCH signaling in cultured primary Sertoli cells with JAG1 ligand immobilized in Matrigel for 24 or 48 hours. To inhibit NOTCH signaling in culture, we used DAPT. Following NOTCH activation or inhibition, co-IPs were performed to dissect the composition of the RBPJ complex. Additional co-IPs were performed after down-regulation of BHC80/Phf21a expression.

We found that BHC80 associates with the RBPJ repressor complex, which also contains HDAC1/2 and KDM1A, a H3K4 demethylase. The repressor complex downregulated expression of the NOTCH targets Hes1 and Hey1. Because HES1 and HEY1 are transcriptional repressors, expression of Gdnf and Cyp26b1 was upregulated. Conversely, JAG1 stimulation or inhibition of BHC80/Phf21a expression via RNAi converted the RBPJ complex into an activator complex that downregulated Gdnf and Cyp26b1 expression.

Our data indicate that BHC80 is a co-repressor of RBPJ. Its functional role could be to downregulate NOTCH signaling in Sertoli cells and modulate spatiotemporal differentiation of SSCs within their niche.

Supported by NIH R01-HD081244 to MCH.

**Pig Conceptuses Secrete Interferon Gamma (IFNG) to Recruit Activated T-Cells to the Uterine Endometrium During the Peri-Implantation Period.** Bryan A. McLendon, Heewon Seo, Avery C. Kramer, Cassandra M. Herring, Guoyao Wu, Robert C. Burghardt, Fuller W. Bazer, and Greg A. Johnson

Our current understanding of the immunology of pregnancy is that it is a host-graft model in which an immune suppressive state protects the semi-allogeneic conceptus (embryo/fetus and associated placental membranes) from the maternal immune system. This host-graft model of pregnancy may be outdated because evidence is accumulating to indicate that immune responses at the endometrial-placental interface are highly dynamic, and that trophoblast cells of the placenta direct how endometrial immune cells respond to the implanting conceptus. Early pregnancy in pigs may conform to this new paradigm because trophoblast cells of elongating, implanting pig conceptuses secrete large amounts of the pro-inflammatory cytokine IFNG, suggesting a role to elicit T helper 1-driven inflammatory responses within the endometrium that is remodeling to support the initial stages of placental development. Therefore, we examined implantation sites of pig conceptuses to determine if: 1) the endometrium exhibits characteristics of an inflamed state; 2) activated T cells are present within the endometrium; and 3) IFNG increases the expression of chemokines that potentially recruit activated T cells to the endometrium. We collected endometria from gilts on Days 10, 12, 15, 18, 24 and 30 of

pregnancy and analysed those tissues by real-time PCR, H&E, immunofluorescence, and TUNEL staining. Further, on Day 13 of estrogen-induced pseudopregnancy, we fitted gilts with indwelling Alzet 2ML1 Osmotic Pumps containing either 50 µg control serum proteins or 50 µg recombinant porcine IFNG, collected the endometrium on Day 18, and analysed the tissues using real-time PCR. Our results provide new insights into the immunology of implantation sites in pigs by revealing: 1) molecular and histological hallmarks of hypoxia, increased vascular development, accumulation of immune cells, and apoptosis of stromal cells within the endometrium at sites of implantation during the period of IFNG secretion by conceptuses; 2) accumulation of proliferating cell nuclear antigen (PCNA)-positive T cells within the endometrium of implantation sites; 3) significantly increased abundances of T cell co-signaling receptors including programmed cell death protein 1 (PDCD1), CD28, cytotoxic T-lymphocyte associated protein 4 (CTLA4), and inducible T cell co-stimulator precursor (ICOS), as well as the chemokines CXCL9, 10, and 11 in implantation sites; and 4) significant increases in T-cell co-signaling receptors, PDCD1 and ICOS, and chemokine CXCL9 in the uterine endometrium of gilts infused with IFNG. We conclude that trophoblast cells of pig conceptuses secrete IFNG to recruit activated T cells to the endometrium to contribute to an inflammatory environment that supports the active breakdown and restructuring of the endometrium in response to implantation of the conceptus. These results support the new paradigm that implantation sites during pregnancy are not immunologically suppressed, but rather, highly inflammatory to favor stromal remodeling, tissue injury and subsequent repair, and extensive vascularization required for successful pregnancy in pigs. Research supported by Agriculture and Food Research Initiative Competitive Grant no. 2015-06857 from the USDA National Institute of Food and Agriculture.

**Implantation Induces Robust Expression of Secreted Phosphoprotein 1 [SPP1, also known as Osteopontin (OPN)] in the Mouse Endometrium.** Avery C. Kramer, David W. Erikson, Heewon Seo, Bryan A. McLendon, Fuller W. Bazer, Robert C. Burghardt, and Greg A. Johnson

SPP1 is an extracellular matrix protein that binds integrins involved in cell-cell and cell-ECM communication to promote cell adhesion, migration, and survival. In vivo evidence from sheep and pigs, and in vitro evidence from sheep, pigs, humans and mice suggest that SPP1 binds integrins to attach the apical surfaces of conceptus (embryo and placental membranes) trophoblast and endometrial luminal epithelium (LE) during the adhesion phase of implantation. We previously reported that estradiol administration in ovariectomized mice induced modest levels of Spp1 mRNA in the endometrial LE. The objective of this study was to determine the temporal-spatial distribution of Spp1 mRNA during pregnancy in mice. Ten-week old outbred CD-1 female mice were mated to an intact male (copulatory plug = Day 1 of gestation), and uteri were collected on Days 4, 4.5, 5, 9, 10, 11, 12 and 16 of pregnancy. In situ hybridization analysis revealed that on Day 4 of pregnancy, Spp1 mRNA was present in cells of the inner cell mass of the blastocyst, in scattered unidentified cells within the uterine stroma and in focal extents of the LE monolayer of cells directly contacting the trophoblast cells of the blastocyst within the implantation chamber. Spp1 mRNA was absent from endometrial LE within the implantation chamber by Day 5; however, a robust hybridization signal for Spp1 mRNA was maintained in all LE cells between sequential implantation chambers (i.e., in all LE cells of inter-implantation sites) and mRNA remained in these cells for the duration of gestation. In addition, robust levels of Spp1 mRNA were observed in the uterine natural killer (uNK) cells of the decidua. These were confirmed to be uNK cells as Spp1 mRNA was not detected in the decidua of interleukin-15 null mice that lack uNK cells.

Further, by Day 12, Spp1 mRNA was detected in trophoblast giant cells, and by Day 16, Spp1 mRNA was present in regions of fetal bone and cartilage. We hypothesized that the robust induction of Spp1 mRNA in the endometrium of pregnant mice is a direct result of implantation. Therefore, we utilized a delayed implantation model to determine the effect of nidatory estrogen and implantation on the localization of Spp1 mRNA. Ten-week old virgin CD-1 female mice were ovariectomized on gestational Day 4 and administered 2 mg progesterone on Days 5, 6, and 7, and 25 ng estradiol on Day 7. Uteri were collected 24 hours following estradiol injection. Implantation induced a similar pattern of Spp1 mRNA localization to that of pregnancy. High levels of Spp1 mRNA were present in both the LE and uNK cells. Therefore, we propose that implantation directly induces Spp1 expression in mouse endometrium that: 1) may be involved in adhesion during initial blastocyst attachment to the LE, but subsequently is down-regulated at sites of attachment to allow for embryo invasion; 2) is maintained in the LE of inter-placentation sites as an adhesive molecule to contribute to closing the uterine lumen between implantation chambers; and 3) is secreted from uNK cells to support vascular development within the decidua.

**Role of Gremlin-2 in a Murine Model of Primary Ovarian Insufficiency.** Rydze R. T., Torralba H. S., Gibbons W. E., Rajkovic A., and Pangas S. A.

Premature ovarian insufficiency (POI), affects 1-2% of women. Mouse models have been key in identifying candidate genes for this disease. The bone morphogenetic proteins (BMPs) play an essential role in primordial germ cell (PGC) specification and ovarian folliculogenesis. BMP are powerful developmental morphogens, and their signaling is held in check by a number of extracellular antagonists that include Gremlin-1 and Gremlin-2. We previously published that Grem1 expression is controlled by BMPs and GDF9, and that GREM1 expression in cumulus cells can be used as a surrogate marker of oocyte quality. The function of GREM2 in the developing or adult ovary in the mouse or human is not understood. To test this, we generated mice null for Grem2 using CRISPR/Cas9 engineering. Grem2<sup>-/-</sup> mice were viable and reproduce in Mendelian ratios, unlike the perinatal lethality seen in Grem1<sup>-/-</sup> mice. We verified full deletion of Grem2 by quantitative PCR in multiple tissues, including the ovary and the lung, where it is normally highly expressed. We tested fertility in 8-month continuous mating trials (n=3 females per genotype). We found that while Grem2<sup>-/-</sup> females had normal litter sizes, they showed a statistically significant reduction in the numbers of litters per month compared to the controls (0.65 litters month for the mutant versus 1.0 for the control, \*P < 0.05). Initial histologic analysis of newborn Grem2<sup>-/-</sup> ovaries showed they are grossly normal. Our fertility data suggest that Grem2<sup>-/-</sup> mice have irregular estrous cycles, particular after 5 months of age, consistent with early reproductive senescence. While the disruption of the estrous cycle is indicative of dysfunction in the hypothalamic-pituitary-gonadal axis, we did not find that Grem2 is expressed in the pituitary. Therefore, our working hypothesis is that the phenotype stems from ovarian dysfunction. We have also identified a novel nonsynonymous mutation in GREM2 located within the GREM2-BMP interface in POI patient samples that is predicted to be disruptive. In total, our data indicate that GREM2 has a key role in adult ovarian function and fertility and is a new candidate gene for POI. These studies were supported by NIH/NICHD R01 HD085994 (to S.A.P.).

**Herbicide Propanil Acutely Alters Reproductive Hormones and Immune Cell Populations in Heat-Killed *Streptococcus Pneumonia* Exposed Female Mice.** Malia Berg, Jennifer Franko, Ida Holásková, Rosana Schafer, and Robert Dailey

Propanil is a post-emergent herbicide used on rice and wheat fields. It has previously been demonstrated that propanil exposure (200mg/kg) increases the number of antibody-secreting cells in the spleen after heat-killed *Streptococcus pneumoniae* (HKSP,  $2 \times 10^8$  CFU) immunization. The hypothalamo-pituitary-gonadal axis has been demonstrated to be required for this response in female, but not male mice. As a result, it was hypothesized that propanil will alter progesterone, prolactin and estradiol levels, as well as modify immune cell populations. To test this hypothesis, 24 C57Bl/6 female mice were challenged with HKSP and assigned to four treatment groups (6 mice each) in a 2x2 factorial arrangement. Factor one represented propanil treatment (propanil, control). The second factor represented two collection time points (24h, 72h). Serum progesterone, prolactin, and estradiol concentrations were measured using hormone-specific ELISA assays. Splenic T cells (CD4+ and CD8+), B-cells and CD11b+ populations were analyzed by flow cytometry. Twenty-four hours post-propanil exposure and HKSP immunization, progesterone ( $p=0.0311$ ) and prolactin ( $p=0.0167$ ) levels were significantly increased in comparison to HKSP immunized controls. Estradiol levels were not affected. Propanil decreased the total number of splenocytes ( $p < 0.0001$ ), CD8+ T cells ( $p=0.0012$ ), CD11b+ cells ( $p=0.0022$ ) and B cells ( $p=0.0003$ ). The percentage of CD8+ T cells ( $p=0.0001$ ) and CD11b+ cells ( $p=0.0022$ ) were increased, while the percentage of B cells ( $p=0.0003$ ) decreased. No significant effects were noted 72 hrs post-propanil exposure. The results supported the hypothesis that propanil has an effect on reproductive hormones and immune cells. Future studies will investigate the mechanism by which propanil alters hormone levels and immune cell populations.

**Participation of Adrenomedullin 2 Receptors on Bovine Oocyte Maturation Process.** Oscar Omar Morales Morales, María Eduvigis Burrola Barraza, and Blanca Sánchez Ramírez

Intermedin/Adrenomedullin 2 (IMD/ADM2) is an oocyte-secreted factor (OSF) identified in rat, which has antiapoptotic action suppressing the expression of both 3 and 7 caspases. On a reproductive level, IMD/ADM2 function is related to oocyte maturation, invasion, and migration of the trophoblast. This OSF is recognized by the cumulus cells through the complex calcitonin receptor-like receptor with any one of the receptor activity-modifying protein 1, 2 and 3 (CLR:RAMP1, CLR:RAMP2 and CLR:RAMP3), maintaining a tridimensional structure of the cumulus-oocyte complex (COC). Also, this peptide promotes the expression of connexin 43 in cumulus cells, which is essential for the bidirectional communication between the cumulus cells and the oocyte. The presence and functionality of IMD/ADM2 and its receptors have not been fully reported in bovine. The objective of the study was to demonstrate the localization of the CLR:RAMPs complexes in bovine COCs, and its participation in the maturation process. For this purpose, COCs were obtained from the local slaughterhouse and cultured for oocyte maturation. Total RNA was isolated from the different maturation stages of COCs, as well as from the cells that compose it. RT-qPCR was performed to determine CLR, RAMP1, 2 and 3 relative expressions. Western blots were carried out to confirm the protein presence, the localization of this receptors was evaluated by immunolocalization using FITC-polyclonal antibodies. Finally, their participation in the maturation process was evaluated by the addition of polyclonal antibodies of each receptor in the culture media. The result demonstrated that COCs and the cells that integrate them had

diferent levels of mRNA expression of the receptor proteins, being the highest expression for ramp1 in oocyte and cumulus cells. However, the oocyte that reaches the metaphase II the mRNA expression of all the receptors was suppressed; otherwise the relative mRNA expression of all receptors in cumulus cells remained. The western blot analyses showed different complexes of the receptors in immature COCs, CLR:RAMP2 and CLR:RAMP3 moreover the ratio of the complexes was not always 1:1 due that CLR:RAMP complexes were found in 2:1 ratio; furthermore, the homodimer RAMP3:RAMP3 was found. The immunolocalization assays demonstrate that the receptors are located in the membrane alike in oocytes and cumulus cells. However, the immature oocytes showed a higher signal of RAMP1 in comparison with the cumulus cells. While the cumulus cells exhibited the highest signal on RAMP2. Finally, when antibodies for each one of the different receptors were added separately to the culture media, a decrease in oocyte maturation percentage was detected, an inhibition according to order; RAMP1>RAMP2>RAMP3. Furthermore, the addition of CLR antibodies in combination with each one of RAMP antibodies decreased maturation followed the same order. These results suggest that CLR:RAMP1 complex has a central role in the maturation process in the cell that composes the COC. Additionally, the presence of different CLR:RAMPs complexes suggest different pathways of signaling could participate in other cellular processes. Research supported by a grant from CONACYT-BÁSICA, Project number: 168991.

**The Small Non-coding RNA Transcriptome of the Juvenile Monkey (*Macaca mulatta*) Testis and Altered Expression Associated with Gonadotropin-induced Spermatogonial Differentiation.** William H. Walker, Paula Aliberti, Suresh Ramaswamy, Rahil Sethi, Alicia Belgorosky, Uma R. Chandran, and Tony M. Plant

The molecular mechanisms responsible for initiation of spermatogenesis including the decision of spermatogonial stem cells to differentiate at the onset of puberty remain poorly characterized, especially in higher primates. Using RNA seq, 537 mature miRNAs, 322 small nucleolar RNAs (snoRNAs) and 49 small nuclear RNAs (snRNAs) were identified in the testis of vehicle-treated juvenile rhesus monkeys (n=3). These transcripts are considered to make up the small non-coding RNA transcriptome of the juvenile monkey testis. Pathway analysis of the 20 most highly expressed miRNAs including seven members of the Lethal-7 (Let-7) and MIR-10 families suggest that these miRNAs contribute to limiting the proliferation of undifferentiated spermatogonia and/or somatic cells in the juvenile monkey testis. Pulsatile infusion of LH and FSH into juvenile monkeys (n=3) for 48 h, which initiated differentiation of a population of Type A spermatogonia into B spermatogonia (Human Reproduction 2017, 32:2088-2100), was associated with differential expression of 12 snoRNAs, 4 snRNA and 35 miRNA transcripts. Eight of the 12 differentially expressed snoRNAs were members of the C/D box class of snoRNAs called SNORDs and were localized to an imprinted region located on chromosome 7 that is associated with Prader-Willi syndrome and neural development. The population of differentially expressed miRNAs did not include any of the most highly expressed transcripts. Five of the differentially expressed miRNAs were expressed from the X chromosome. These X-linked miRNAs are known to regulate cell proliferation and may contribute to the cell fate decisions of spermatogonial stem cells. Another 10 differentially expressed miRNAs were derived from the imprinted DLK1-DIO3 locus of macaque chromosome 7 that is linked to maintenance of pluripotency. The differentially expressed miRNAs derived from the DLK1-DIO3 locus are predicted by pathway analysis to regulate the polycomb repressive complex 2 (PRC2) and the PI3K-mTOR signaling pathways that contribute to the maintenance of stem cells. Together, these studies

provide the first small non-coding RNA transcriptome for the monkey testis and identify the changes in small RNA expression that occur coincident with initiation of spermatogonial differentiation in a representative higher primate.

**Developmental Programming of Muscle Stem Cell Fate by Intrauterine Growth Restriction (IUGR).**

Yennifer Cortes, Karin Amilon, Claire Stenhouse, Cheryl Ashworth, Cristina L. Esteves, and F. Xavier Donadeu

Selection for high-prolificacy in pigs has brought a significant increase in the frequency of naturally occurring IUGR, with negative consequences for the pork industry. IUGR piglets are significantly smaller than their littermates and show reduced neonatal survival. A key feature of IUGR littermates is reduced muscle mass associated with smaller numbers of fibers formed prenatally, and a tendency to accumulate fat in different body stores during post-natal growth. This results in poor growth and reduced carcass quality, with lower percentages of lean tissue. Our aim is to investigate the developmental mechanisms of altered lean tissue development in IUGR pigs by elucidating the effects on fetal muscle progenitor cell populations. The lightest (L) and heaviest (H) male fetuses were collected from Landrace X Large White litters at gestational day 90 (n=5 litters). In each litter, the L fetus was defined as IUGR based on body weight below 2 standard deviations below the mean litter weight. Mononuclear progenitor cell fractions were obtained by enzymatic digestion of semitendinosus muscle samples and were expanded in DMEM media supplemented with FBS and bFGF. Cells were differentiated under myogenic (serum-free) or adipogenic (media supplemented with rabbit serum, Dexamethason, 3-isobutyl-1-methylxanthine and Insulin) conditions, followed by analyses of lineage markers using immunocytochemistry and PCR. In addition, paired muscle samples from H and L fetuses from all 5 litters were submitted for mRNA-sequencing, and differentially expressed transcripts were identified (FDR

Financial support for this study was provided by Comisión Nacional de Investigación Científica y Tecnológica (CONICYT), Chile, and the Biological and Biotechnology Research Council (BBSRC), UK.

**Western Blot Evaluation of Fecal Transthyretin (TTR) for Use as a Pregnancy Test in Polar Bears *Ursus maritimus* in Search of the Golden Compass of Population Management Tools.**

Victoria C. Kennedy, Terri L. Roth, Elizabeth M. Donelan, and Erin Curry

A non-invasive test for pregnancy in polar bears would be invaluable to research and management of this vulnerable species. Distinguishing whether reproductive failures coincide with conception, diapause, or pregnancy maintenance remains a challenge. Previously, potential pregnancy biomarkers were identified in fecal samples collected from zoo bears. Transthyretin (TTR), a thyroid hormone binding protein synthesized by the placenta during pregnancy, was one of those proteins and the experimental focus in this study. The objective was to quantify TTR subunits (30kDa and 17kDa) present in fecal samples of polar bears from differing reproductive states. A Western blot method employing multiplex fluorescent staining and stain-free gels was developed to assess TTR concentrations in pregnant (P), pseudopregnant (PP) and nonpregnant (NP) bears. For the pregnant group, samples were chosen on or around -120, -90, -50, -45, -40 -35, -30, and -20 days from parturition (day 0). For the pseudo-pregnant

group, day 0 was the end of pseudo-pregnancy, based on fecal progesterone concentrations. Day 0 for the non-pregnant group was the mean cubbing date for North American zoo polar bears. Total protein per sample was quantified by viewing total UV fluorescence of stain-free gel bands. Two antibodies and their respective secondary antibodies were selected for multiplex fluorescent imaging of sample TTR, with native-human TTR as a positive control (CON). Multiplex fluorescence image analysis was performed to assess signal intensity of two TTR protein bands, 30 and 17kDa TTR, . Signal intensity was compared against CON TTR signal and stain-free total protein. Longitudinal profiles were created for both comparison methods; comparison of TTR in samples vs. CON was selected for further analysis. Mean baseline concentrations of total, 30 and 17kDa TTR vs. CON were determined, with +1.5 standard deviations from the mean considered elevated. After log transformation and removal of outliers, statistical analysis was performed using SAS proc mixed procedures comparing pregnancy status (P vs. NP vs. PP; PregStatus) and pregnancy stage (diapause vs. placental pregnancy; PregStage over time. Baseline analysis revealed only a few scattered values were elevated. There was no significant difference between PregStage ( $P = 0.73$ ), PregStatus ( $P = 0.46$ ), nor an interaction of PregStatus and time ( $P = 0.10$ ) for total TTR. For 17kDa TTR, there was a tendency for an interaction between PregStatus and time ( $P = 0.07$ ). No differences were seen between PregStage ( $P = 0.55$ ). For 30kDa TTR, no differences were seen by PregStage ( $P = 0.62$ ), PregStatus ( $P = 0.24$ ), nor an interaction of PregStatus and time ( $P = 0.13$ ). It should be noted that this detection method is reliant on intact antibody-binding sites on TTR molecules and the challenge of measuring a protein that may have been denatured in a fecal sample remains an inherent obstacle. Whereas, our results indicate fecal TTR may not be a suitable marker for pregnancy in polar bears, this methodology provides a template for future analyses of other previously identified potential protein biomarkers, which may have vital prospective applications in wildlife diagnostic techniques.

**Growing Evidence: Protein Hormone Translation Products are Nested Information Systems.** Kenneth L. Campbell, Nurit Haspel, Brian Hall, Mohamed Anwar, James Hoang, Yang Cheng, Naomi Stuffers, Cassandra Gath, Noelle Palmstrom, Indira Nouduri, and Seraphina Yang

Protein hormones usually act via cell surface receptors linked to intracellular transduction pathways. However, these macromolecules seem too complex and energetically expensive to synthesize and regulate to be economical as single-message molecules. Earlier studies show proteolytic fragments of some protein hormones have additional functions. In addition, examination of protein hormone translation products shows many contain multiple secreted products including poorly characterized proteins. Some even include pairs of hormones with counterpoised actions. If telescoped secondary functions are released during proteolytic processing at the synthetic cell, in circulation, or at the target cells, organisms might gain the efficiencies necessary to justify using proteins instead of smaller molecules as common chemical signals. We are using bioinformatics to explore the structures and potential functions of the ~1000 known soluble human protein hormone translation products. All translation products have now been processed through the proteolysis prediction program PROSPER to find any residual peptides left after exposure to 24 known proteases. So far, ~40% of the protein translation products have proteolytically resistant peptides of > 10-15 residues, many of which are lysine or glutamic acid rich. The residual peptides are being compared to other proteins in the human database using BLASTp to see if the hormone fragments match surface motifs of other proteins; such matches could allow the proteolytic peptides to modulate protein-protein interactions as non-canonical

signals. NCBI BLASTp sequence alignments with other proteins show ~60% of the fragment matches are non-parent/family proteins. When matched peptide containing proteins were seeded as central nodes in the network neighborhood program STRING, ~30% of the network neighbors had a PDB structure that allows mapping of the matched peptide to the protein surface, including known protein-protein interaction surfaces. A good example of this approach is the PDB for a co-crystal of BMP7 and Noggin that shows a surface sequence in BMP7, that is a match for a proteolytic peptide from TGF $\beta$ 1, is directly involved in Noggin contact. BMP7 and Noggin can now be bench tested for their sensitivity to the matching peptide from TGF $\beta$ 1. Multiple sequence alignments using MAFFT and MUSCLE when overlaid by the PROSPER cleavage predictions demonstrate the conservation of primary sequences in the protein hormones that allow clipping of the proteins at the ends of segments of secondary structure. Further examination shows that similar alignments of proteolytic sites also occur at the exonal boundaries in the translation products of these proteins. It appears that not only multiple signals may be released during processing of protein hormone translation products and the protein hormones themselves, but also structural and additional functional information intrinsic to the individual exons from which the protein hormones are assembled. The telescoping of all this information into the final protein translation products is profound. A clearer understanding will provide a next generation of biological tools and biomedicines.

**Vitrification and in Vitro Culture Support Follicle Viability in Bovine Ovarian Cortical Tissue.** Hayley Benham, Rolando Pasquariello, Rebecca Krisher, and Jennifer P. Barfield

Currently, it is not possible to utilize cryopreserved ovarian tissue for sourcing viable oocytes for further use in ART procedures in cattle. Maintaining tissue and oocyte viability throughout the cryopreservation and in vitro culture process is critical for developing this technology. Vitrification is an effective cryopreservation method for ovarian cortical tissue in other species including mice and humans. The objective of this experiment was to investigate the effects of vitrification and in vitro culture of vitrified/warmed bovine ovarian tissue on cell viability. Ovaries from three mature cows were collected at a local abattoir, and ovarian cortical tissue was dissected into 1 mm thick strips. Cortical strips were immersed in 1ml equilibration medium containing 7.5% ethylene glycol and 7.5% DMSO for 25 minutes. Tissues were then transferred to 1ml vitrification medium with 15% ethylene glycol, 15% DMSO, and 0.6M trehalose for 15 minutes. Strips were then placed onto a Cryo Device<sup>®</sup> (Kitazato) and plunged into liquid nitrogen. Strips were warmed by immediately submerging vitrified tissue into 1ml of 1M trehalose thawing solution for 1 minute, followed by 3 minutes in a 0.5M trehalose dilution solution, and two sequential 5 minute washes in 0M trehalose wash solution. Vitrified and warmed strips from each of the 3 cows were either immediately snap frozen for qPCR analysis, or further cut into 1mm<sup>3</sup> cubes. Eight cortical cubes from each strip were placed on Millipore inserts and cultured above 350  $\mu$ l modified DMEM culture media containing 10% Serum Substitute Supplement<sup>™</sup> (Irvine Scientific) for 48 h at 38.5°C in 5% CO<sub>2</sub>, and then snap frozen for qPCR analysis. Representative cortical pieces post vitrification/warming, both cultured and not cultured, as well as a fresh cortical tissue positive control were fixed in 4% paraformaldehyde and embedded in paraffin for histological analysis. Stromal and follicular morphology was assessed using both Hematoxylin and Eosin (H&E) and DAPI staining. Cortical pieces post vitrification/warming, both cultured and not cultured, were analyzed and compared to non-vitrified cortical tissue controls using qPCR to determine expression levels of the following genes associated with cellular proliferation and folliculogenesis: MKI67, AHR, GDF9, BMP15. Statistical analysis

of all data was performed using one-way ANOVA with Tukey's range test; differences were considered significant at  $p < 0.05$ . Histological analysis showed morphologically normal follicles in tissues from all groups. There were no differences between tissue type in the expression of MK167 and AHR, indicating maintenance of cellular proliferation and viability in vitrified/warmed cortical tissue, both cultured and not cultured, compared to fresh controls. Tissue cubes cultured post vitrification/warming had increased expression of GDF9 and BMP15 compared to both vitrified/warmed uncultured tissue and fresh controls, indicating active folliculogenesis in cultured cortical cubes. Our data suggests that vitrification/warming and subsequent in vitro culture can effectively preserve bovine ovarian tissue viability and support ongoing folliculogenesis. Future work will use vitrified/warmed/in vitro cultured cortical tissue to determine the efficacy of in vitro activation of dormant ovarian follicles to produce viable oocytes for use in in vitro cattle embryo production.

**Heat-Induced Hyperthermia Impacts the Transcriptome of Cumulus and Mural Granulosa Cells in the Periovarian Follicle in Lactating Dairy Cows.** Jessica L. Klabnik-Bradford, Rebecca R. Payton, Louisa A. Rispoli, Ky G. Pohler, Chelsea R. Abbott, Clark Bloomer, Lane K. Christenson, Matthew Huff, Margaret E. Staton, Arnold Saxton, Kelly A. Campen, F. Neal Schrick, and J. Lannett Edwards

Hyperthermia during early meiotic maturation reduces developmental competence of the oocyte. To better understand mechanisms mediating negative effects of hyperthermia, the transcriptomes of the cumulus and mural granulosa cells from the periovarian follicle of thermoneutral versus hyperthermic cows were evaluated after a pharmacologically-induced LH surge. Lactating dairy cows with a corpus luteum were given PGF2 $\alpha$ ; 11 days later a CIDR was inserted and GnRH administered. Seven days thereafter, CIDRs were removed and PGF2 $\alpha$  given. Cows with a dominant follicle ( $14.9 \pm 1.5$  mm) were moved to a climate-controlled facility 35 h later. Forty hours after final PGF2 $\alpha$ , GnRH was given to induce an LH surge. Thermoneutral ( $n = 3$ ) cows were maintained at a temperature-humidity index (THI) of  $64.7 \pm 0.9$ . Hyperthermia ( $n = 3$  cows) was induced by increasing THI by 2.7 units/h for  $\sim 12$  h (final THI  $80.7 \pm 1.42$ ). Elevating THI increased rectal temperatures (RT,  $40.1 \pm 0.04^\circ\text{C}$ ; max  $40.6 \pm 0.1^\circ\text{C}$ ;  $P < 0.0001$ ) and respiration rates (RR,  $112.4 \pm 1.3$  breaths/minute, bpm;  $P < 0.001$ ) in hyperthermic compared to thermoneutral cows ( $38.0 \pm 0.44^\circ\text{C}$  and  $47.78 \pm 10.02$  bpm). Cows were returned to thermoneutral conditions after  $\sim 12$  h; RT and RR decreased by  $1.38 \pm 0.48^\circ\text{C}$  and  $52.99 \pm 11.32$  bpm per 15 min. Transvaginal aspiration of dominant follicle contents was performed  $\sim 16$  h after GnRH. Total RNA (13.5 – 50 ng) from cumulus cells mechanically removed from the oocyte and from the mural granulosa cells recovered from the ovulatory follicle was subjected to stranded mRNA library preparation (Universal Plus mRNA-seq; Nugen). Sequencing was completed on the Illumina HiSeq 2500 and then aligned against the Ensemble Bos taurus genome (UMD 3.1). Differential gene expression was determined using DeSeq2 package (Bioconductor) with a false discovery rate of 0.1 and analyzed for functional annotation clustering (DAVID 6.8). Cumulus cells from hyperthermic cows differentially expressed 258 transcripts (88 up and 170 down regulated) compared to those obtained from thermoneutral cows. In mural granulosa cells, 31 transcripts were differentially expressed in hyperthermic cows (17 up & 14 down regulated). Clustering analysis of differentially expressed cumulus transcripts in hyperthermic cows revealed gene clusters related to immune responses to viruses, DNA repair/metabolism, RNA processing or protein-to-protein interactions while those contained within mural granulosa clustered into a single group related to post-translation modification and/or protein folding in the endoplasmic reticulum. Heat-induced differences in expression of 14 transcripts were

shared between cumulus and mural granulosa cells (RAB38, TRPM3, NEFH, SCN7A, MOXD1, CCDC80, ATMIN, HPRT1, PRDX2, ACER3, TRA2B, RBM3, SANP, PALMD). Acute heat stress exposure sufficient to induce hyperthermia, after the LH surge, can impact cumulus and mural granulosa cell transcriptomes that may have negative and/or protective effects on the developmental competence of the maturing oocyte. This project was supported by Agriculture and Food Research Initiative Competitive Grant no. 2016-67015-24899 from the USDA National Institute of Food and Agriculture.

**Establishment and Applications of Hormone-Responsive Uterine Epithelial Organoids From Human and Mouse Endometrium.** Pramod Dhakal, Linda M. Rowland, Danny J. Schust, Andrew M. Kelleher, and Thomas E. Spencer

The human and mouse endometrium are comprised of several different cell types, including two types of epithelium (luminal and glandular) and stroma. Recent studies in mice found that uterine glands are essential for pregnancy establishment with biological roles in uterine receptivity, blastocyst implantation, stromal cell decidualization, and embryo growth and survival. With the exception of leukemia inhibitory factor (Lif), the factors that mediate the biological functions of glands remain undefined. A method to derive hormone-responsive human and mouse uterine epithelial cell organoids (UECO) was recently reported in which UECO rapidly developed that possessed long-term expansion capacity. (Turco MY et al., *Nature Cell Biology* 2017; Boretto M et al., *Development* 2017). Using a slight modification of those protocols, epithelial cells were isolated from adult mouse uteri or biopsies of human endometrium using enzymatic dissociation, suspended at a density of 10,000 cells in 30 microliters of 70% Matrigel, placed in a 48-well dish, and then continuously cultured under a defined WNT-activating stem cell media. Round epithelial organoids were established within 3 to 4 days and after 10 days were differentiated with steroid hormones. Mouse UECO were differentiated with estradiol-17 $\beta$  (E2; 1nM) for 2 days and progesterone (P4; 50 ng/mL) for 2 days and Human UECO with estradiol-17 $\beta$  (E2; 10nM) for 2 days and medroxyprogesterone acetate (MPA; 1  $\mu$ M) for 4 days. Both human and mouse UECO immunostained positive for FOXA2, ESR1, and CDH1, but not PGR, which are signatures of differentiated glands of both mouse and human endometrium. The UECO phenocopied physiological responses of uterine glands to hormones, including increased cell proliferation under E2 and differentiation under P4. Treatment with E2 alone increased PGR, and P4 decreased PGR to undetectable levels. Mouse UECO faithfully responded to E2 with up-regulation of Cxcl15 and P4 with up-regulation of Ihh, Prss28, and Prss29 and down-regulation of Cxcl15. Similarly, human UECO up-regulated Olfm4, Paep (glycodelin), and Spp1 in response to MPA. To investigate the impact of UECO on stromal cell decidualization, mouse UECO were grown for 8 days and then isolated and purified stromal cells added to the cultures. As a control, some wells did not contain UECO or contained UECO only. Cells were then treated with either vehicle or P4 (50 ng/mL) for 4 days (n=6 per treatment per group). Quantitative PCR found that expression of Prl8a2, a decidual marker gene, was 8-fold higher (P < 0.02) in stromal cells only and 130-fold higher (P < 0.01) in stromal cells cultured with UECO as compared to UECO only. Collectively, the results strongly support the hypothesis that uterine glands produce secretions that impact stromal cell decidualization. These novel in vitro models will be useful to study key paracrine secreted factors from the uterine glands and their impact on uterine physiology, providing a powerful tool for studying mechanisms underlying the establishment of pregnancy and uterine pathologies. Supported in part by NIH Grant R21 HD087589.

**Deletion of the Mouse X-Linked Prame Gene Causes Germ Cell Reduction During the First Wave of Spermatogenesis.** Wan-Sheng Liu, Chen Lu, Randall M. Rossi, Aihua Wang, Mingyao Yang, and Francisco Diaz

PRAME is a cancer/testis antigen (CTA), and is expressed at high levels in testis and a wide variety of malignant tumors, and has been used as a prognostic marker for patients with various cancers. PRAME has been extensively studied in cancer cells, and is involved in varying signaling pathways with a general function to inhibit cell apoptosis and to promote cell proliferation. In testis and germline, members in the PRAME gene family are highly expressed in all types of germ cells, including the inner cell mass (ICM) of blastocysts, primordial germ cells (PGCs), embryonic stem cells (ESCs), spermatogonial stem cells (SSCs), spermatogenic cells and mature spermatozoa. However, the functional role of PRAME in gametogenesis is largely unknown. The multicopy nature of the mouse Prame gene family raises significant challenges in generation of a Prame-related gene knockout model for the functional analysis. Here, we report the generation of a conditional deletion of one gene in the family and generated a Prame (X-linked) knockout (cKO) mouse model by mating the floxed homozygous females (Prame<sup>fl/fl</sup>) with Stra8-Cre male mice. We found that the Prame cKO mice (Stra8-Cre; Prame<sup>-/Y</sup>) had a normal fertility. The only visible phenotypic difference between the Prame cKO and the floxed and wild type (WT) groups was that the testicle size was significantly reduced (by 12%) in the Prame cKO mice at the age of 4 months ( $P < 0.01$ ). Consistent with a modest decrease in testicle size, cauda epididymal sperm count was reduced about 13% ( $32.50 \times 10^6$  in the Prame cKO mice, compared to  $37.38 \times 10^6$  in the floxed males) ( $P < 0.05$ ). Histological analysis of testis cross sections collected from postnatal day 7 (P7), P14, P21, and P35 indicated that approximately 4-5% of the seminiferous tubules were clearly degenerated at P21 and P35, while there was no difference observed between the Prame cKO and floxed (or WT) testes at P7. Germ cells in these degenerated seminiferous tubules were lost during the first wave of spermatogenesis, and by P35, all germ cells were depleted and a Sertoli-cell-only syndrome (SCOS) pattern was observed for these affected tubules. Apoptotic cells were observed by TUNEL assay at P7 and reached the peak level at P14, and then decreased at P21. Number of germ cells under apoptosis was significantly higher in the Prame cKO testes than that in the floxed testes at P7, P14 and P21 ( $P < 0.05$ ), but not at P35. The results suggest that the mouse X-linked Prame is involved in spermatogenesis, and different paralogs in the Prame gene family may be functionally and partially redundant. We proposed that the loss of germ cells in the affected seminiferous tubules is triggered in a subset of SSCs that lack PRAME and are not rescued by Prame paralogs in the Prame cKO testis.

**Mycotoxin Zearalenone(ZEA) Induces Toxicity and Alters MicroRNA Expression in C57Bl/6 Mouse Placenta.** Christian Lee Andersen, Rong Li, Lianmei Hu, Ahmed E. El Zowalaty, Zidao Wang, and Xiaoqin Ye

Zearalenone (ZEA) is a major mycotoxin derived from *Fusarium* fungi and is a common food contaminant in ppb~ppm range. With its estrogenicity and potential chronic exposure, ZEA poses a great risk to the general health of both animals and humans, especially female reproduction. ZEA in feed causes reproductive disorders in domestic animals such as swine. Previously we demonstrated in mice that ZEA diets (20-40 ppm) impaired female fertility. Since the placenta plays an essential role in female fertility and ZEA can be metabolically activated by placental enzymes, ZEA may have adverse effects on placental development leading to impaired female fertility. To determine the effects of ZEA on placental

development, young virgin female mice were mated with stud males and checked for a vaginal plug the next morning. The day of vaginal plug detection was designated as gestation day 0.5 (D0.5). On D5.5 (post-implantation), the plugged females were randomly assigned into five groups and fed with 0, 0.8, 4, 10, and 40 ppm ZEA diets. Body weight was recorded daily. The mice were dissected on D13.5. There was an increased rate of implantation site resorption in 40 ppm group, placental hemorrhage in 10 and 40 ppm groups, reduced weight of live fetus in 40 ppm group, and reduced weight of placentas with live fetus in 40 ppm group. Placental histology indicates dose-dependent changes in the labyrinth layer, most dramatically in the 40 ppm group, such as dilated fetal capillaries filled with nucleated fetal blood cells, dilated maternal blood spaces filled with enucleated maternal blood cells, or areas with reduced sinusoids. These data indicate disorganized placental labyrinth upon ZEA treatment resulting in insufficient fetal-maternal interface for efficient nutrient and gas exchange, which may count for the reduced fetus weight in the 40 ppm ZEA-treated group. ZEA treatments (0.8, 4, 10, and 40 ppm) also led to lipid accumulation in the labyrinth layer of D13.5 placentas. Placental cells have unique epigenetic profiles to regulate gene expression thus placental functions. Disrupted epigenetic profiles may lead to defective placental development. Our microRNA (miRNA) array analysis on the above D13.5 placentas in the 0, 4, and 40 ppm groups (N=4/group) reveals a unique placental miRNA profile and a set of differentially expressed placental miRNAs upon ZEA treatment. Interestingly, several of these differentially expressed miRNAs were also dysregulated in the placentas from patients with preeclampsia. Confirmation of the differential expression of miRNAs and identification of their target genes in the mouse placenta are underway.

**Small Extracellular Vesicles Isolated From Bovine Follicular Fluid During the Late Luteal Phase are Enriched of Precursor Mirnas.** Juliano C. Da Silveira, Ana Clara F.C.M de Ávila, Gabriella M. Andrade, Felipe Perecin, and Flávio Vieira Meirelles

Ovarian follicle comprises an unit important for oocyte growing and maturation. Follicular cells secrete extracellular vesicles (EVs) in follicular fluid (FF) that are involved in intercellular communication. Extracellular vesicles have bioactive material like microRNAs (miRNAs) that can be found in precursor and mature forms. Precursor miRNAs are processed by nucleases in mature miRNAs, which can modulate translation of target-mRNAs through the silencing complex (RISC). Thus, the aim of this study was to evaluate the levels of precursor and mature miRNAs in small EVs from bovine FF of growing follicles during late luteal phase. For this, slaughterhouse ovaries were collected in pairs and classified in late luteal phase based on corpus luteum appearance (orange, 1.6-2 cm and visible vasculature) as well as progesterone concentration in FF ( $158.8 \pm 17.47$  ng/mL). Follicles between 3-6 mm were aspirated to obtain FF. Follicular fluid (n=5) was centrifuged at 300 xg for 10 min, 2000 xg for 10 min and 16500 xg for 30 min to pellet live cells, cellular debris and large EVs, respectively. Follicular fluid was filtrated (0.22 $\mu$ m) and centrifuged at 119700 xg for 70 min twice in order to pellet small EVs. The small EVs pellet was used to characterize particles size and concentration by Nanoparticle Tracking Analysis as well as miRNAs contents by real time-PCR. Reverse transcription for precursor and mature (precursor/mature) miRNAs were obtained using miScript HiFlex buffer while only mature miRNAs were obtained using miScript HiSpec buffer. Relative levels of 384 miRNAs were determined using miR-99b as normalizer. Differences in relative levels of precursor/mature and mature miRNAs were determined by student's t-test, considering significant p-value of  $\leq 0.05$ . Small EVs obtained from FF had on average  $123.62 \pm 3.40$  nm of size and  $6.52 \times 10^{11} \pm 1.28 \times 10^{11}$  particles/mL of concentration, thus corresponding to small EVs.

A total of 191 mature miRNAs and 320 precursor/mature miRNAs forms were identified in small EVs from FF in the late luteal phase. A total of 145 altered miRNAs were identified when we compared the levels of mature and precursor/mature. Of these 139 precursor/mature forms were upregulated in comparison with mature forms. Bioinformatics analysis of upregulated precursor/mature miRNAs forms are related to PI3K-AKT, MAPK signaling pathway, RNA transport and oocyte meiosis. In conclusion, we demonstrated increase abundance of precursor miRNAs in EVs isolated from bovine FF during the late luteal phase. These results suggest that EVs are important mediators of cell communication within FF, and the presence of increased levels of precursor miRNAs suggest that miRNAs present in EVs are functional. Therefore, is important to investigate the miRNA processing machinery in recipient cells in order to gain a better understand of the communication mediated by EVs within follicle environment. This research is supported by FAPESP (grant 2014/22887-0; 2015/21829-9; 2017/02037-0).

**Expression and Phenotypic Effects of the G Protein-Coupled Receptor 56 GPR56 Knockout in Male and Female Reproductive Tissue with Focus on the Cauda Epididymal Epithelium.** Tara H.

Balasubramanian, Steven M. Neal, Madeleine G. Purcell, Maria E. Teves, and James A. Foster

GPR56 is a member of the adhesion family of G protein-coupled receptors and has been shown in mammals to be important in several important developmental processes (e.g. cerebral cortex development) and in several pathologies (e.g. malignant melanoma, bifrontoparietal polymicrogyria). A knockout mouse model has shown that GPR56 is necessary for normal testis development and male fertility (Chen et al, Dev Dyn. 2010) and our further analysis has found phenotypic effects on sperm morphology and motility as well as epididymal structure and function. Western analysis showed that GPR56 is expressed at similar levels in caput, corpus, and cauda epididymides. To evaluate the phenotypic effects of the Gpr56 knockout on the epididymis, samples of caput and cauda epididymides from wild-type (Gpr56+/+), Gpr56+/-, and Gpr56-/- males were prepared for light and electron microscopy. No effects were detected in the caput epididymis of Gpr56-/- mice but the cauda epididymis appeared somewhat distended and less firm than the wild-type. The epithelium of the cauda epididymis was significantly thinner and the lumen wider than the wildtype. Also, there were few sperm and many residual bodies in the cauda epididymal lumen of Gpr56-/- mice. The low numbers of sperm in the cauda epididymis are likely due to developmental abnormalities in the testis (Chen et al. 2010 and us) and the appearance of excess residual bodies suggest a role for GPR56 in Sertoli cell-spermatogenic cell interactions involved in residual body uptake. Since GPR56 appears to be expressed at similar levels throughout the epididymis it is unclear why effects were only seen in the cauda; we hypothesize that this may be related to the absence of sperm cells in the lumen. In addition, areas of wavy, slightly disorganized basement membrane were seen in Gpr56-/- epididymides; disorganization of basement membranes has been seen in other tissues of GPR56-null mice. Since some Gpr56-/- males have normal testis size and are fertile, we used RT-PCR to evaluate mRNA expression and found that these mice have "leaky" expression of Gpr56; thus, in future experiments it will be necessary to carefully monitor Gpr56 expression in all Gpr56-/- mice. Finally, during breeding some Gpr56-/- females had difficulty with parturition and had dystocia and still-born pups. Western analysis showed that GPR56 was expressed in the uterus and ovaries of wild-type females. Analysis of uterine histology in Gpr56-/- females showed no real difference in phenotype between knockout and wild type samples; however, since the Gpr56-/- females in the histological analysis were not evaluated for leaky expression, further analysis of Gpr56-/- females will need to be performed to make a conclusion about potential phenotypic effects of the

absence of GPR56 on the uterus. Overall, we found that GPR56 is expressed in the caput, corpus, and cauda epididymis, uterus, and ovary, and the data suggests a role for GPR56 in the cauda epididymal epithelium and perhaps in the uterus. Support: Randolph-Macon College Schapiro Undergraduate Research Fellowship, the William E Betts, Jr. Undergraduate Science Research Fellowship from the Virginia Federation of Independent Colleges, and the Jeffress Memorial Trust.

**Ovarian Dynamics and Concentrations of Fatty Acids in Follicular Fluid and Blood Serum of Beef Cows Supplemented with Calcium Salts of Soybean Oil.** C. L. Timlin, D. Powers, N. W. Dias, F. V. Santili, A. Maucieri, A.J. Lengi, B.A. Corl, and V. R.G. Mercadante

We investigated the effects of supplementing *Bos taurus* beef cows with calcium salts of soybean oil (CSSO) high in omega-6 fatty acids on fatty acid composition of follicular fluid (FF) and blood serum (BS), as well as ovarian dynamics including follicular diameter, corpus luteum (CL) volume, and progesterone concentrations. A total of 25 cows were stratified by body weight and body condition score and randomly assigned to one of two treatments: 1) 0.7 kg/head/d corn gluten feed with 0.1 kg/head/d of prilled saturated fatty acids (Energy Booster, Milk Specialties, Eden Prairie, MN; CON; n = 12); or 2) 0.7 kg/head/d corn gluten feed with 0.1 kg/head/d of CSSO (Essentiom, Church and Dwight Co., Inc., Princeton, NJ; CSSO; n = 13). All cows were maintained in a common pasture with ad libitum access to forage and water. Cows were sorted every day and penned individually for supplementation. Cows were adapted to diets for 21 d prior to d 0. On d -7, a superovulation protocol was initiated following follicle ablations and CIDR insertion. On d -5, twice daily injections of FSH in decreasing concentrations were administered until d -2. On d 0, follicle aspirates were collected. Immediately thereafter, a 7-day CO-Sync+CIDR estrus synchronization protocol was initiated. Blood samples were taken on d 0, 7, every day from 10-18, 25, and 28 for progesterone measurement. Transrectal ultrasonography was performed on d7 and d 14 to measure dominant follicle diameter and CL volume, respectively. Fatty acids were extracted and methylated from FF collected d0 and BS collected d0 and d25 for gas chromatography analysis. In BS, the ratio of linoleic acid (LA) to alpha-linolenic acid (ALA) was increased in the CSSO group at d25 ( $6.33 \pm 0.18$ ) compared to d0 ( $4.89 \pm 0.19$ ) and was increased relative to CON at d0 and d25 ( $2.17 \pm 0.19$  and  $2.44 \pm 0.19$ , respectively;  $P < 0.001$ ). Concentration of LA in BS increased over time in CSSO cows compared to CON and was greatest at d25 ( $0.85 \pm 0.04$  and  $0.52 \pm 0.04$  mg/mL, respectively;  $P < 0.001$ ). Total ALA content in BS differed between treatments but did not differ by day ( $0.20 \pm 0.01$  mg/mL CON and  $0.13 \pm 0.01$  mg/mL CSSO;  $P < 0.001$ ). In FF, the LA:ALA ratio in CSSO cows was greater than CON cows ( $4.29 \pm 0.056$  vs.  $2.16 \pm 0.26$ ;  $P < 0.001$ ). FF concentration of ALA tended to be greater in CON vs. CSSO cows ( $0.04 \pm 0.01$  and  $0.03 \pm 0.004$  mg/mL, respectively;  $P = 0.067$ ). In addition, total amount of identified omega-3 fatty acids in FF tended to be greater in CON cows than CSSO cows ( $P = 0.07$ ). However, diameter of the dominant follicle at d7 did not differ between treatments ( $P = 0.7861$ ), nor did CL volume at d14 ( $P = 0.8699$ ). Progesterone concentrations increased over time ( $P < 0.001$ ), but did not differ between treatments ( $P = 0.277$ ). We conclude that supplementation of CSSO to beef cows changed fatty acid profile of BS and FF, however it did not alter diameter of the ovulatory follicle, CL volume, or progesterone concentration following ovulation.

**Transformation of Uterine and Vaginal Bacteriome Throughout Synchronization Protocol Between Pregnant and Non-Pregnant Postpartum Cows.** T.B. Ault, B.A. Clemmons, F.G. Dantas, G.A. Franco, S.T. Reese, P.R. Myer, and K.G. Pohler

Up to \$1.4 billion and \$600 million are lost annually in the beef and dairy industries due to infertility. Human research has shown the diversity and abundance of bacterial communities in the reproductive tract can influence fertility, however, little research has been conducted in bovine to evaluate the relationship of fertility to the bacteriome of their reproductive tract. Our group recently characterized the bacteriome of non-pregnant postpartum beef cows two days prior to fixed timed artificial insemination (FTAI) and evaluated the differences between the uterus and vagina. Results indicated there was significantly greater diversity in the vagina than the uterus. The present study examines the bacteriome of the postpartum beef cow uterus and vagina over the duration of a FTAI protocol to determine bacterial community differences and their change over time in those who become pregnant and those who fail to conceive. We hypothesize the bacteriome will differ between resulting pregnant and non-pregnant cows. For the study, 30 purebred Angus beef cows, an average of 82 days postpartum, were synchronized using the 7 Day Co-Synch protocol ending with FTAI on Day 0 (D 0). Uterine and vaginal flushes with pH measurement and blood sampling occurred on each day of the protocol (D -21, D -9, and D -2). Transrectal ultrasound was performed at D 30 following FTAI to determine pregnancy status. Following, pregnancy diagnosis, 10 pregnant and 10 non-pregnant cows were selected for sequencing. Bacterial DNA was extracted from all flush samples to sequence the V1-V3 hypervariable region of the 16S rRNA gene. Operational taxonomic unit (OTU) picking was completed utilizing the cleaned sequences binned with the pairwise identity threshold of 97% similarity. Results indicated a significant decrease in the diversity of the bacteriome over the duration of the protocol in the uterus of pregnant ( $P = 0.001$ ) and non-pregnant ( $P = 0.0002$ ) cows. The only significant difference in the diversity between pregnant and non-pregnant cows occurred in the vagina at D -21 ( $P = 0.04$ ). Principal coordinate analyses using unweighted UniFrac distances depicted strong clustering by day in uterine and vaginal samples ( $P < 0.0001$ ). Significant differences in the relative abundance of phyla were observed between pregnant and non-pregnant cows. Many differences occurred in the uterus at D -2 with phyla Actinobacteria ( $P = 0.005$ ), Fibrobacteres ( $P = 0.02$ ), and Unassigned ( $P = 0.009$ ). Numerous significant phyla differences were observed in the uterus and vagina of pregnant and non-pregnant cows between each time point in the protocol ( $P < 0.05$ ). Overall, evaluating the bacteriome of postpartum cows through a synchronization protocol indicates a shift in bacterial communities in the uterus to decrease the diversity that may be important for pregnancy development. Further research may lead to identifying the causes for the variability in bacterial communities and development of a probiotic to help improve reproductive efficiency. The present study was supported by the Angus Foundation.

**Biochemical Mechanisms of Epididymal Sperm Maturation Involve PP1g2, GSK3 and Calcineurin.**

Suranjana Goswami, Rahul Bhattacharjee, Sumit Bhutada, Souvik Dey, Douglas Kline, and Srinivasan Vijayaraghavan.

Mammalian sperm exiting the seminiferous tubules undergo maturation in the epididymis acquiring motility and the ability to fertilize eggs. Despite the proposed roles for calcium, pH, and cAMP the biochemical basis for epididymal sperm maturation remains unknown. We proposed that high catalytic activity of the sperm specific serine/threonine phosphatase (PP1) isoform, holds motility in check in

immature spermatozoa. The PP1g2 isoform is present in all mammalian spermatozoa studied - mouse, rat, hamster, bovine, non-human primate, and human. The serine/threonine protein phosphatase 1 (PP1) inhibitors, PPP1R2, PPP1R7 and PPP1R11, are highly conserved and evolutionarily ancient proteins in a variety of organisms from yeast to mammals. Surprisingly, these three ubiquitous PP1 inhibitors were identified as regulators of sperm-specific PP1g2.

The purpose of this study was to investigate how changes in the activity of PP1g2 occur in epididymal sperm. We hypothesized that changes in sperm PP1g2 activity effected by binding to its regulatory proteins are critical for the development and regulation of sperm function. We show that the association of PPP1R2, PPP1R7, and PPP1R11 to PP1g2, changes during epididymal sperm maturation. In immotile caput sperm, PPP1R2 and PPP1R7 are not bound to PP1g2. In motile caudal sperm PPP1R2, PPP1R7 and PPP1R11 are bound to PP1g2 as hetero-dimers or -trimers. Binding of PPP1R11 remains unchanged in caput and caudal sperm. The spatiotemporal expression of PPP1R2, PPP1R11 and PPP1R7 matches with PP1y2 expression during spermatogenesis. The inhibitors and PP1y2 are co-localized within mature spermatozoa.

Changes in association of these inhibitors are likely due to changes in their phosphorylation status and the interrelated roles of GSK3, PKA, calcineurin, and PP1g2. In mature caudal sperm from mice lacking GSK3, PPP1R7 is not bound to PP1g2, resembling immature caput sperm. Moreover ATP and net adenine nucleotides levels also resemble immature caput sperm. Altered binding of PPP1R7 is also found in sperm lacking cAMP due to the absence of soluble adenylyl cyclase. Sperm lacking calcineurin which impairs epididymal maturation have altered GSK3 activity. All the three regulators of PP1g2 contain consensus sites for GSK3 and PKA phosphorylation. Our studies show that GSK3, PKA, calcineurin, and PP1g2 are mechanistically interrelated in regulating the development of motility and fertilizing ability of sperm during their passage through the epididymis.

This work was supported by NIH grant R15HD068971 and R21HD086839.

### **The Membrane Androgen Receptor ZIP9 Mediates Pro- and Antiapoptotic Responses in Atlantic Croaker Ovarian Follicle Cells.** Aubrey Converse and Peter Thomas

Until recently the identity of a receptor that mediates rapid, nonclassical androgen actions was elusive. The novel membrane androgen receptor ZIP9 was recently cloned from Atlantic croaker ovaries, which has allowed for the examination of the receptor's role in ovarian follicles. Testosterone activation of ZIP9 mediates a stimulatory G protein (Gs)-induced apoptotic pathway in croaker ovarian granulosa cells collected from fish at the peak of their reproductive season. Interestingly, testosterone has an antiapoptotic effect on granulosa cells isolated from croaker with smaller ovaries, but it is unknown what androgen receptor mediates this response. The preliminary finding that mibolerone, a nuclear androgen receptor agonist, has no effect on survival of granulosa cells that respond to testosterone in a pro- or antiapoptotic manner led us to hypothesize that ZIP9 mediates both responses, possibly through differing signaling mechanisms. To help address this, we developed a method of isolating primary granulosa cells from distinct populations of follicle size classes. Testosterone treatment of granulosa cells derived from follicles >400  $\mu\text{m}$  causes apoptosis while treatment of granulosa cells from follicles 400  $\mu\text{m}$  this increase in bound [35S]-GTP $\gamma$ S can be immunoprecipitated with an antibody specific to Gs, while in granulosa cells from follicles < 300  $\mu\text{m}$  the increase in [35S]-GTP $\gamma$ S binding is

immunoprecipitated with an antibody towards Gi. This suggests that testosterone activates different G proteins depending on the follicle size class from which the granulosa cells are derived, and that ZIP9 coupling to different G proteins may be the mechanism behind these different responses. This is the first study to report that ZIP9 can couple to different G proteins to elicit opposite responses. ZIP9 has also been shown to mediate androgen-induced apoptosis in a number of human cancer cell lines. Thus, it is of interest to determine the means by which ZIP9 can switch its apoptotic response in croaker granulosa cells in order to better understand the potential mechanisms by which the receptor may operate in other cell models. This research was funded by private foundation support to PT.

**Vaspin is a New Adipokine Expressed in Adipose Tissue but Also In Ovarian Follicles: A Study in Two Pig Breeds with Different Fattening (Polish Large White and Meishan).** Patrycja Kurowska, Alix Barbe, Justyna Chmielińska, Namy Mellouk, Christophe Staub, Eric Venturi, Christelle Rame, Joelle Dupont, and Agnieszka Rak

Vaspin (Visceral adipose tissue-derived serpin) is an adipokine involved in the development of obesity, insulin resistance or pathogenesis of inflammatory reactions of the body. A role of vaspin in female reproduction has never been described. The aim of the present study was to investigate mRNA and protein expression of vaspin in the ovary in two porcine breeds : Large White (LW) and Meishan (MS) that have different fattening but also prolificacy. Indeed, the MS breed can produce up to 30-40% live piglets per litter than LW breed. Reproductive parameters including age of puberty, number of cycles, number of piglets and levels of steroid hormones (P4 – progesterone and E2 – estradiol) were investigated in both breeds. Ovarian follicles (4-6 mm) and adipose tissue were collected from mature sows at 10-12 days of the estrous cycle. Vaspin expression mRNA and protein levels were determined by real time PCR and Western Blot, respectively. Vaspin concentration in plasma and follicular fluid was determined by ELISA assay. Statistical analyses were performed using Graph Pad Prism 5 software, and the data were analyzed using a one-or two-way ANOVA test, by Tukey's honest significant difference test. We observed that the number of cycles, number of piglets and levels of steroid hormones were significantly higher in MS than LW (n=15 for each breed,  $p < 0.001$ ). mRNA expression of vaspin was higher in the ovarian follicles (small, medium and large) collected from MS, however on protein expression we observed higher level in LW (n=3,  $p < 0.05$ ). Both mRNA and protein levels of vaspin in adipose tissue was higher in MS than in LW (n=3,  $p < 0.05$ ). Preliminary data concerning vaspin concentration in serum and follicular fluid suggest no difference between the two breeds (n=15); however this study should be repeated. In conclusion, our results show for the first time an ovarian expression of vaspin in pigs. We showed higher protein levels of this adipokine in adipose tissue of MS, while no difference in vaspin protein in ovarian tissue was observed. Taken together, vaspin could be a new adipokine involved in the metabolism and reproduction interactions. More experiments are investigating concerning the role of vaspin in in vitro ovarian cell proliferation and steroidogenesis.

**Mate Order, but Not Ejaculate Quantity, Determines Male Reproductive Success in American Black Bears (*Ursus americanus*).** Alexia Gee, Mark Teshera, Henry Kwon, Brendan Himelright, Ramona Gonzales, Penny Dye, and Thomas Spady

Prior studies documented that 91% of American black bear (*Ursus americanus*) cubs are sired by dominant rank males of large body size (>135 kg) and prime (7-10 yr) or older age. The goal of our study was to begin to elucidate which sexual selection mechanism is most responsible for this skew in reproductive success towards large dominant prime males. Although sperm competition has long been assumed to play a key role in the reproductive success of black bears, it has yet to be empirically studied in this species. We hypothesized that if sperm competition were the principal sexual selection mechanism, then these superior quality males (large, dominant, prime-age) should, on average, ejaculate greater volumes of semen into the females' reproductive tracts than their lesser quality competitors. Alternatively, if mate choice was the major mechanism, then superior quality males should be first to mate estrous females so that their sperm were first to reach the ovulated eggs. As a proxy for ejaculate volume during natural breeding, we measured the average ejaculate volume produced by 10 electro-ejaculation stimulations of 3 adult males and multiplied this value by the number of quivering (ejaculation) behavior bouts observed for each male by quality category (body size, age, rank). Mate order was documented by behavioral observation and paternity assigned using PCR amplification of polymorphic microsatellites. Contrary to our hypothesis, large males ejaculated the same average volume of semen as medium and small males ( $n = 29$ ,  $p > 0.70$ ; randomization test, 5000 iterations). Similarly, neither age nor social dominance rank had significant effect on average ejaculate volume ( $n = 29$ ,  $p > 0.70$ ). Moreover, the average ejaculate volume of sires was not different from that of non-sires ( $n = 10$ ,  $p = 0.80$ ). These results suggest that the volume of ejaculated sperm is not responsible for the inter-male differences in black bear reproductive success. Among females that were mounted by more than one male during an estrus, the order in which the males mounted did not differ based on their body size ( $H = 0.71$ ,  $df = 2$ ,  $p = 0.70$ ; Kruskal-Wallis), age ( $H = 0.85$ ,  $df = 2$ ,  $p = 0.65$ ) or social rank ( $W = 297.5$ ,  $n = 17$ ,  $p = 1.00$ ; Mann-Whitney U). Interestingly, all offspring (9/9) were sired by the males that mated the estrous dam first. Moreover, males that mated first in order did not have greater ejaculate volume than those that mated subsequently ( $n = 17$ ,  $p = 0.84$ ). Taken together, these data suggest that female mate choice (as reflected by mate order) likely plays a more significant role in black bear male reproductive success than sperm competition. Moreover, the lack of female preference for 'high quality' males in our study hints at the possibility of post-copulatory sexual selection mechanisms such as cryptic female choice.

**Live-cell Imaging of Neonatal Porcine Gonocytes in Prolonged Culture Reveals Unique Migratory and Colony Formation Patterns.** Awang Hazmi Awang-Junaidi, Eiko Kawamura, LaRhonda Sobchisin, and Ali Honaramooz

Gonocytes in the neonatal testis are the precursors of all future types of germ cells; thereby, testis cell culture may provide a potential means for in vitro proliferation and manipulation of these male germline stem cells. We have recently developed an optimized system for short-term culture of neonatal porcine gonocytes. In the present study, we used this optimized culture system to study the organization and ultrastructure of neonatal porcine gonocytes in prolonged culture. Neonatal porcine testes (< 1 wk old,  $n = 40$ ) were used to isolate parenchymal testis cells using a three-step enzymatic digestion, designed to

yield ~40% gonocytes. The cells were cultured for 4 weeks in Dulbecco's modified Eagle Medium supplemented with 10% fetal bovine serum in 6 well-plates at a seeding density of  $3.0 \times 10^5$  cells/well and incubated at 37°C in a humidified atmosphere with 5% CO<sub>2</sub>. The real-time interactions of cultured testis cells were frequently assessed using live-cell imaging. This included collecting differential interference contrast images from ten randomly selected fields using a 20× objective every 1 hr for 24 hr from day 0 to day 3, every 2 hr for 24 hr from day 4 to day 7, and every 1 hr for 24 hr at days 14, 21, and 28. Live-cell imaging of shorter interval (every 2.5 sec) was also performed using a 100× objective from three randomly selected fields for 5 min after completion of each imaging session (i.e., every day from day 1 to day 7 and after a full day imaging at days 14, 21, and 28). For the live-cell imaging, the microscope was fitted with a humidified stage-top incubator to maintain cells at 37°C and 5% CO<sub>2</sub>. Samples of cultured cells were also taken at days 7, 14, 21, and 28 and subjected to scanning electron microscopy, transmission electron microscopy, immunocytochemistry (using DBA as a gonocyte marker; OCT-4 as a pluripotency marker; and F-actin as a cytoskeletal marker), as well as morphometric evaluations. We documented an amoeboid-like movement of gonocytes in culture throughout the study, assisted by their formation of extensive cytoplasmic projections, which under scanning electron microscopy appeared as membrane ruffles, lamellipodia, filopodia, and blebs. Within the first week of culture, gonocytes formed loose attachments on top of the somatic cell monolayer and in week 2 formed colonies of multiple gonocytes (grape-like clusters), which over time grew in cell number. Starting at week 3 of culture, some of these grape-like clusters transformed into multinucleated three-dimensional embryonic body-like colonies; likely as a result of the fusion of gonocytes. The number and size of individual gonocytes and the number and size of the embryonic body-like colonies increased over time ( $p < 0.05$ ). The density and number of organelles in gonocytes, as observed through transmission electron microscopy, also increased over time. In conclusion, cultured porcine gonocytes displayed extensive migratory behavior facilitated through their various cytoplasmic projections, propagated, and transformed into colonies that increased in size and complexity over time.

Supported by a discovery grant from the Natural Sciences and Engineering Research Council (NSERC) of Canada.

### **The Pathway of Stimulation of Endogenous Cells by Mesenchymal Stem Cells Transplanted Into**

**Porcine Cervix.** Zdzislaw Gajewski, Anna Burdzinska, Jaroslaw Olszewski, Bartosz Pawlinski, Maria Sady, Magdalena Gajewska, and Malgorzata Domino

Mesenchymal stem cell (MSC) were discovered as a plastic adherent, colony-forming cell populations derived from bone marrow. Afterwards MSC were shown to demonstrate trilineage differentiation potential and became useful in regenerative medicine. In recent study we revealed that MSC survived after transplantation into the muscle layer of porcine uterine cervix and demonstrated significantly higher proliferative potential than smooth muscle cells. We suggested MSC acts as stimulator of the endogenous cells of muscle layer of cervix. Hypothesing a paracrine signaling pathway and putting under consideration expression of hepatocyte growth factor protein as a potential regulatory protein. We examined the HGF expression after transplantation of MSC into the muscle layer of uterine cervix in sow to find a correlation with Ki67 expression and MSC survival. Polish Landrace sows (n=9) were subjected to three surgeries in GIA in order to collect bone marrow, transplant the MSC (after three weeks) and collect the cervix (after next four weeks). According to this protocol, the 40ml of red bone marrow

gathered from the head of the humerus was used to isolate and cultivate the MSC during in vitro growing. Afterwards MSC was successfully labeled with PKH26 and DID during 3 weeks in vitro cultivation. The supernatant with PKH26 and DID positive MSC were transplanted into muscle layer of uterine cervix and took under examination. The cervixes were cut into 10- $\mu$ m thick slices and labeled with primary (anti-Ki67 and anti-HGF) and fluorescent secondary antibodies, and the nuclei were stained with Hoechst or NuclearGreen. Then MSC, Ki67 and HGF were imaged qualitatively and quantitatively using confocal microscope LeicaTCSSP8 and scanning cytometer TissueFacsPLUS. Both cell populations, positive and negative (endogenous cells) for PKH26 and DID, showed Ki67 and HGF expression in cytoplasm which was estimated as a mean% of positive and double positive cells $\pm$ SEM. The high expression of Ki67 in PKH26 (22.28% $\pm$ 3.13 double Ki67 and PKH26 positive cells) and DID (28.87% $\pm$ 9.19 double Ki67 and DID positive cells) were strong positive correlated with HGF expression. Since the Ki67 and HGF expression were non-normally distributed, correlation was assessed using Spearman's rank correlation coefficient and it valued  $r=0.81$  for  $p=0.032$ . The HGF expression was higher ( $p=0.014$ ) in places of transplantation and the colocation with MSC was estimated at the level of 3.07% $\pm$ 1.72 for PKH26 and 2.35% $\pm$ 2.28 for DID positive cells compared to no transplantation places (0.42% $\pm$ 0.34). The expression of HGF in transplantation places close to MSC was also higher ( $p < 0.001$ ) than in control group (3.07% $\pm$ 1.72) and demonstrated medium positive correlation ( $r=0.68$ ;  $p=0.040$ ) with Ki67 expression. HGF plays a role as a regulator of cell growth, mitogenesis, motogenesis and morphogenesis. HGF is secreted by both MSC and endogenous cells and may be a part of paracrine signaling pathway in tissue regeneration process. HGF plays an important role in normal development of tissue and its regeneration. The hypothesis that MSC underwent a progressive loss of proliferative potential leading to the senescent state may be rejected. The HGF secretion and endogenous cell proliferation may be stimulated by MSC transplanted into muscle layer of porcine cervix.

**Ultrasound Biomicroscopic Evaluation of Developmental Changes in Testis Cell Implants and Testis Tissue Grafts from Donor Piglets in an Immunodeficient Mouse Model.** Mohammad Amin Fayaz, Awang Hazmi Awang-Junaidi, Jaswant Singh, and Ali Honaramooz

Subcutaneous grafting of neonatal testis tissue fragments and implantation of testis cell aggregates from diverse donor species can lead to maturation of the testis cells/tissue and complete spermatogenesis in recipient mice. As such, this system can be used as an in vivo model to study testis development, spermatogenesis, and steroidogenesis of various target species in a laboratory model. The objectives of the present study were 1) to validate the use of ultrasound biomicroscopy (UBM) for non-invasive monitoring of the implants/grafts over time, and 2) to correlate the findings from UBM with the physical attributes of retrieved implants/grafts. Donor testis fragments and isolated cell aggregates were prepared from the testes of 1-week-old donor piglets ( $n=30$ ). Cell aggregates were obtained using a three-step enzymatic digestion, designed to yield  $\sim$ 40% gonocytes. Recipient mice (hairless severe combined immunodeficient, SHO,  $n=8$ ) were grafted subcutaneously on the right side of the dorsal midline with donor testis fragments (one  $\sim$ 5 mm<sup>3</sup> piece in each of four sites) and were injected on the left side with testis cell aggregates ( $\sim$ 100 $\times$ 10<sup>6</sup> cells, each) in four analogous sites (i.e.,  $n=8$  total sites per mouse). Three-dimensional transcutaneous Doppler UBM of all implants/grafts was performed (VisualSonics Vevo3100, 32-55 MHz MX550D transducer) and a randomly selected cell implant and corresponding tissue graft were removed at 2, 4, 6, and 8 weeks ( $n=3$  randomly selected mice per retrieval). UBM data recorded immediately prior to retrieval were compared with physical attributes of

removed implants/grafts. The weight and physical volume (measured using water displacement) of the harvested testis cell implants and testis tissue grafts did not differ ( $p=0.75$  and  $p=0.96$ , respectively); however, the weight and volume of the harvested implants/grafts increased from 2 to 8 weeks (mean $\pm$ SEM;  $26.0\pm 9.0$  to  $74.0\pm 9.0$  mg,  $p=0.008$ ), and  $20.0\pm 9.2$  to  $56.7\pm 9.2$  mm<sup>3</sup>,  $p=0.01$ ). Based on the UBM images, the maximum width (lateromedial dimension) of implants/grafts did not change over time but the maximum length (craniocaudal dimension) increased from week 2 to 8 ( $6.1\pm 0.3$  to  $7.2\pm 0.3$  mm,  $p=0.03$ ). The volumes of implants/grafts calculated from the UBM data did not change over time ( $p=0.47$ ); however, they were correlated with the physical measurements of retrieved implants/grafts (for volume:  $r = 0.75$ ,  $p=0.001$ ; for weight:  $r = 0.71$ ,  $p=0.001$ ). UBM also allowed observation of developmental changes in the implants/grafts including the gradual encapsulation, neovascularization, and formation of new testicular tissue. In conclusion, UBM findings correlated with the physical attributes of the implants/grafts, validating its use as a non-invasive, accurate and informative tool to quantify the developmental changes in ectopic testis cell implants and testis tissue grafts.

This study was supported by a discovery grant from the Natural Sciences and Engineering Research Council (NSERC) of Canada.

**Genetic Containment in Livestock via CRISPR-Mediated Gene Knock-In.** Joseph R. Owen, Amy E. Young, Luis H. De Aguiar, Pablo J. Ross, and Alison L. Van Eenennaam

Animals engineered for improved health, nutrition, or production traits have the potential to positively impact the global food supply. However, current methods for inserting a gene into a targeted location in the genome need to be improved in order to efficiently generate such animals. Additionally, management practices to minimize associated physical and biological risks to the environment need to be developed. Some methods for environmental containment have been proposed, but recent advances in the field of gene editing, such as the discovery of the CRISPR/Cas9 system, may facilitate the development of animals that would present few or no new environmental risks. One such method would be to create a construct that renders animals carrying the transgene infertile, thereby containing the transgene to a single generation. In addition to containment issues, there is growing concern regarding our nation's role in fighting hunger and ensuring global food security. As worldwide demand for animal-source protein continues to rise, efficient and sustainable production of livestock is of growing importance. Increasing the proportion of male offspring that result from a terminal sire (i.e. a sire used to produce offspring specifically for slaughter) mating would result in improved efficiency of beef production since males finish at heavier weights, gain weight more quickly and efficiently than females, and are easier to manage due to lack of estrus behavior. We hypothesize that a CRISPR/Cas9-mediated gene knock-in of SRY onto the X chromosome in cattle will produce fertile XSRYY cisgenic bulls. When mated with XX females, these bulls will produce phenotypically all male offspring, half of which will be fertile XY males, and the other half of which will be infertile cisgenic XXSRY phenotypic males. This would provide an approach for containment of transgenes that could be transferred alongside the XSRYY gene knock-in. To test this hypothesis, we have generated a male bovine fibroblast line containing the SRY promoter and coding sequence inserted downstream of the ZFX locus in the X chromosome. Expression plasmids for the guide-RNA and Cas9 protein were electroporated using the Amaxa Nucleofector kit with a transfection efficiency of 76.4% and resulting in a mutation rate at the target site of 74.1% after puromycin selection. The donor vector, containing the SRY promoter and coding

sequence along with a UV40 promoter upstream of the puromycin coding sequence, was electroporated alongside these expression plasmids. Puromycin selection was used to isolate knocked-in cells and individual cells were selected and clonally expanded for somatic cell nuclear transfer cloning. This work could aid in the development of methods to efficiently create gene-edited animals using gene knock-in through the CRISPR/Cas9 system, which could ultimately address food supply and food security concerns by improving the efficiency of beef production. It may also provide a method for containment of transgenes by inserting the SRY gene into a region that does not undergo recombination, thereby limiting transmission of the transgene to sterile males.

**The Regulation of Apoptosis and Proliferation Process in Endometrium Affected with the Equine Endometrosis.** Malgorzata Domino, Dominika Domańska, Lukasz Zdrojkowski, Malgorzata Masko, Magdalena Gajewska, Maria Sady, and Zdzislaw Gajewski

Equine endometrosis is a multifactorial disease considered as a one of the most important causes of equine infertility. It's diagnosed with biopsy. Samples were classified according to Kenney & Doig (1986) to categories: I, II A, II B and III. Those structural changes may cause problems with maternal recognition of embryo, implantation and defects in embryo development in the beginning of pregnancy. In breeding herds such disorders may lead to culling of mare. It is thought that balance disturbance between apoptosis and proliferation in mucous membrane in uterus is the main cause of CDE. However, still many questions remain unanswered. Hepatocyte Growth Factor (HGF), Insulin-like Growth Factor 1 (IGF1), basic Fibroblast Growing Factor (bFGF) and Vascular Endothelial Growth Factor (VEGF) are known as important proteins involved in regulation of diffusing stromal and perivascular fibrosis. The aim of the study was to assess expression of regulatory proteins: HGF, IGF1, bFGF, VEGF in respect to proliferation (Ki67) and apoptosis (Cas3) markers to evaluate potential regulatory pathway of degeneration during endometrosis. The study group was Warmblood mares (n=12) with age varying from 12 to 20 years which were removed from the herd due to infertility. The biopsy samples from uterus were fixed in formalin, embedded in paraffin, stained with hematoxylin eosin (HE) and labeled with specific anti-HGF, anti-IGF1, anti-bFGF, anti-VEGF, anti-Ki67 and anti-Cas3 antibodies. The expression of proliferation-apoptosis balance markers was evaluated with confocal microscope (Leica SP8) and quantified with scanning cytometry (TissueFAXS Plus). Samples stained with HE were classified according to Kenny and Doig (1986) into groups: I, IIa, IIb and III, while each group contained two independent samples taken from three mares at 3 weeks intervals. Both control expressions (Ki67 and Cas3) decreased significantly from category I (Ki67: 3.94%±0.29; Cas3: 14.27%±0.14%) to category II A (Ki67: 2.24%±1.15%; Cas3: 7.69%±1.77), II B (Ki67: 1.88%±0.96; Cas3: 4.43%±0.29) and III (Ki67: 0.88%±0.51; Cas3: 4.42%±2.50%). We found no significant differences in expression of HGF in category I (1.80%±0.30), IIA (2.22%±0.14) and IIB (2.16%±1.36) in opposite to decrease in category III (0.46%±0.01). We observed no significant differences in expression of IGF1 in all examined categories I (2.27%±0.49), IIA (1.10%±0.66), IIB (0.84%±0.94) and III (1.20%±0.07). We noted significantly higher expression of bFGF in category I (10.89%±0.72) than in all other categories IIA (3.61%±0.67), IIB (3.13%±0.87) and III (2.02%±0.68). The expression of VEGF wasn't correlated with degree of CDE. We observed significantly higher expression of VEGF in category I (7.11%±1.76) and IIB (7.69%±4.92) in contrast to category IIA (2.83%±0.57) and III (2.85%±0.25). The changes in bFGF expression indicate reduction of neovascularisation. On the other hand, in CDE the interaction between IGF1s and IGF1 receptors probably doesn't trigger signaling cascade leading to cellular proliferation and inhibition of apoptosis. Another pathway of apoptosis

inhibition could be examined in CDE. Similarly, the VEGF probably isn't activated during CDE due to fibrosis and lack of tissue progression. Basing on the preliminary results, we believe that bFGF and HGF are interesting and probably useful markers of pathological changes in CDE.

**Role of Hippo Signaling Pathway During Bovine Oocyte Maturation.** Diana Carvajal, Laura A. Favetta, and Pavneesh Madan.

Oocyte maturation is largely regulated by endocrine and paracrine factors, as well as by several ovarian signaling pathways. One of these pathways is the Hippo signaling pathway, known for its role in cellular growth and cell fate determination. It is controlled by upstream regulators, downstream effectors, and core cascade factors, involved in cell adhesion, shape and polarity. In mammalian ovaries, the Hippo signaling pathway can prevent follicular growth during both preantral and antral stages of follicular development. Additionally, recent studies conducted on the fragmentation of ovaries performed in mice, murine, and humans, have also shown that the disruption of the ovarian Hippo signaling pathway through the polymerization of actin, can stimulate follicular development and oocyte maturation. However, no information exists about the role of Hippo signaling pathway during bovine oocyte maturation. Therefore, the purpose of this study is to test the hypothesis that Hippo signaling pathway is an important regulator of bovine oocyte maturation. This hypothesis was tested using qPCR analysis to characterize the expression of the upstream and downstream core cascade components of the Hippo signaling pathway including Mammalian Sterile Twenty Like 1 and 2 (Mst1/2), Yes Associated Protein 1 (Yap1), and Transcriptional Co-Activator with PDZ Binding Domain (Taz), in four different oocyte groups (n = 40 oocytes per group). The groups consist of 1) immature oocytes with cumulus cells, 2) mature oocytes with cumulus cells, 3) immature oocytes with no cumulus cells, and 4) mature oocytes with no cumulus cells. Gene expression analysis comprised three biological and three technical replicates using relative quantification versus two housekeeping genes (PPIA and YWHAZ). Results showed that mRNA transcripts of the Hippo pathway core components are present in both immature and mature bovine oocytes, and their expression changes with oocyte maturation. During bovine oocyte maturation, the expression of the upstream component Mst1 decreased, and the expression of Mst2 increased. The expression of the downstream component Yap1 also increased with oocyte maturation, whereas the expression of Taz decreased. Additionally, it was shown that cumulus cells may play a suppressing role on the expression of Hippo pathway components in oocytes, since the expression of Mst1, Mst2, Yap1 and Taz was lower in immature and mature oocytes with cumulus cells compared to the expression in immature and mature oocytes without cumulus cells. These results provide new knowledge about the role of the Hippo signaling pathway during oocyte maturation in the bovine species, suggesting that the pathway is active throughout oocyte maturation, and that the activity of the components may depend on specific stages of oocyte development. Further studies will involve protein localization of Hippo pathway constituents on the same four experimental groups of oocytes using immunofluorescence in order to determine how the location of these pathway proteins changes with oocyte maturation. Collectively, these results will provide insight about the role of cumulus cells in modulating Hippo pathway components during oocyte maturation and highlight the importance of this pathway on the developmental capacity of oocytes. This research was supported by NSERC.

**Pulsatile flow of viscoelastic fluid promotes large-scale collective upstream swimming of sperm.** Jelani Lyles, Chih-Kuan Tung, Soon Hon Cheong, and Susan S. Suarez

In humans and cattle, natural coitus places semen in the vagina at the entrance to the cervix. Sperm must then migrate into and through the cervix, uterus, and lower oviduct to reach the site of fertilization. In all of these organs, sperm encounter thick, elastic mucous secretions that generally flow from the upper to lower tract, i.e., toward the vagina. In recent years, we have used microfluidic models to show that a steady fluid flow directs bovine sperm to swim with an upstream bias. Furthermore, fluid viscoelasticity induces sperm to swim collectively, in clusters. Previously, we showed that sperm cluster sizes increase as the viscoelasticity of the fluid increases, as well as when sperm concentrations increase. Elasticity is the primary inducer of collective swimming, because increasing fluid viscosity without increasing elasticity does not increase cluster sizes. Here, we report that adding a transient flow to viscoelastic fluid is an efficient way to generate a large cluster (> 200 cells). We examined the behavior of washed fresh bull sperm swimming in a microfluidic device in a 0.7% solution of long-chain polyacrylamide (PAM, 5-6 MDa) and 1% polyvinylpyrrolidone (PVP, 360 kDa) in sperm Tyrode's albumin lactate pyruvate (TALP) medium, which was used to mimic the viscoelasticity of estrous bovine cervical mucus. In the absence of fluid flow, 700 million sperm/mL were seeded at an entrance port of the microfluidic device and allowed to swim into a chamber filled with the viscoelastic fluid. Once in the chamber, sperm formed clusters of  $21 \pm 4$  cells (mean  $\pm$  SD). When a syringe pump was turned on to produce flow in the chamber ( $80 \pm 10$   $\mu\text{m/s}$  or  $1.0$   $\mu\text{L/min}$ ) sperm aligned upstream; however, a significant portion of sperm were swept downstream ( $21 \pm 4\%$  lost over 1 min). If we only applied the flow for a short period of time by ramping up the pump for 1 min and then immediately ramping down the pump for 1 min, we were able to generate large clusters of aligned sperm (as many as 253 sperm in a cluster) without sweeping sperm downstream (only  $3 \pm 4\%$  of sperm were swept downstream over the 1 min ramp up). Sperm in the large clusters maintained the upstream swimming bias for 11 min after the pulse of flow dissipated. During this time, sperm could have travelled in the range of centimeters. In the female tract, pulses of smooth muscle contractions have been reported to occur in the uterus (including the uterine cervix) and oviduct after coitus. These contractions could generate pulsatile flows of mucus secretions, which could increase collective swimming and enhance sperm transport. The effects of mucus and fluid flows might be most important for assisting sperm penetration into the cervical canal. Bull sperm are inseminated into the vagina near the entrance to the cervical canal at very high concentrations (300-2500 million/mL) and encounter highly viscoelastic cervical mucus flowing out of the canal. The pulse secretion of viscoelastic mucus from the cervix may facilitate sperm cluster formation. National Science Foundation (NSF) HRD Grant 1665004 to CKT.

**Following Mouse Vaginal Cycles with DNA Quantity and Integrity.** Emily J. Millen and Kenneth L. Campbell

A basic marker of physiological status in mammals from apes to zebras is the stage of the ovarian cycle. The biomarker commonly used to follow this is the cytology in vaginal lavages. Lavages show tissue responses to estrogen with initial epithelial division followed by the apoptosis-like process of cornification which includes organellar loss, inter-nucleosomal DNA cleavage, and keratinization. In the 1920s Papanicolaou found that cell cytology in urine sediments provided an alternative, serially accessible, non-invasive method to track these same cycles. Our lab has radiolabeled extracted DNA

from serial, human volunteer, urine sediments and shown a cyclical apoptotic pattern of DNA laddering that matches rises in urinary estrogen levels. We have also demonstrated that the fluorescence intensity (FI) of DNA stained with intercalating dyes, e.g., SYBR Green I, is a function of both DNA mass and average DNA molecular size. Serially diluted DNA samples from commercial DNA preparations that vary in average molecular size can be used to simultaneously estimate both the mass and average size of unknown sample DNA extracts by first matching the slope of the FI versus concentration curve of the unknown to those of the standards, then using the slope of the best-matched standard to compute the mass of DNA in the unknown. This approach is a single plate evaluation of both apoptotic DNA status and DNA mass applicable to DNA samples of  $< 100$  ng. To translate these earlier observations into a viable diagnostic test for humans we have begun to track vaginal cycles in mice as an animal model using vaginal lavages and DNA extracts of the lavages. Samples from six normal, six-week old CD-1 female mice (Charles River) were collected over the course of thirty-three days. Counts of early and late epithelial cells and polymorphonuclear lymphocytes (PMNs) varied by estrous stage as anticipated and indicated typical 4-5 day cycles. Plots of percent of maximum PMNs and epithelial cells established cycle patterns. DNA extracts were made for all study samples using proteinase K, SDS digestion followed by phenol/phenol-chloroform extraction, and cold sodium acetate/ethanol nucleic acid precipitation. Absorbance readings at 260 nm (A260) and 280 nm were used to evaluate DNA purity and to gauge the volume of extract needed in the dye binding assays. FI of SYBR Green I binding estimated average DNA size (as a proxy for apoptotic state) and DNA mass. A260 and FI were compared to original cell counts. DNA mass fluctuated with overall cell numbers and approximate DNA size declined during cytological estrous. The study suggests the feasibility of using this approach to track small DNA samples such as those from human urine sediments or vaginal lavages from other small animals. Correlation of DNA status in female urine sediments with parameters such as: hormonal status, presence of Y-chromosomal DNA, and status of urogenital microbial fauna will provide powerful new tools for monitoring female reproductive status and health.

**Lean Maternal Gestational Diabetes Mellitus Impacts the Ovarian Proteome Basally and in Response to a Stressor in Later Life.** Kendra L. Clark, Omonseigho Talton, Shanthi Ganesan, Laura C. Schulz, and Aileen F. Keating

Gestational diabetes mellitus (GDM) is an obstetric disorder affecting approximately 10% of pregnancies. GDM is normally resolved at delivery, but may associate with lasting health effects for mother and progeny, with both having a higher risk of acquiring diabetes later in life. The 4HFHS (High Fat High Sucrose) mouse model emulates GDM in lean women, who comprise ~50% of GDM cases, which is characterized by insulin resistance in the first trimester, and glucose intolerance in the second-third trimester. Dams are fed a HFHS diet one week prior to mating and throughout gestation, which inhibits beta cell expansion, leading to inadequate insulin response to glucose in mid-late pregnancy. We have discovered that the ovarian response to DNA damage and environmental chemical insult is altered by metabolic changes that occur during obesity. Since the offspring of HFHS dams have increased adiposity, we hypothesized that maternal metabolic alterations during lean GDM would compromise ovarian function in offspring both basally and in response to a dietary stress later in life. Pups received either a control or HFHS diet from 23-31 weeks of age. Briefly, DLPC were lean dams and control diet pups; DLPH were lean dams and HFHS pups; DHPC were HFHS dams and control diet pups and DPH were HFHS dams and HFHS pups. Ovarian protein was isolated, LC-MS performed and bioinformatic

analysis completed. Proteins were considered to differ between treatments if the fold-change was above 1 and the P-value was  $< 0.1$ . A HFHS challenge in the absence of maternal GDM (DLPC vs. DLPH) increased 3 and decreased 30 ovarian proteins. Maternal GDM in the absence of a dietary stress (DLPC vs. DHPC) increased abundance of 4 proteins and decreased abundance of 85 proteins in the offspring ovary. Finally, 4 proteins increased and 87 proteins decreased in offspring ovaries due to dietary challenge and exposure to maternal GDM in utero (DLPC vs. DHPH). Interestingly, canopy FGF signaling regulator 2 (CNPY2), DAZ associated protein 1 (DAZAP1), and septin 7 (SEPT7) were altered across multiple groups. Relative to offspring who did not experience GDM in utero or a dietary stress in later life (DLPC), CNPY2 decreased ( $P \leq 0.05$ ) by 2.18-fold in offspring exposed to both GDM and HFHS diet (DHPH) and in offspring either from GDM pregnancies (DHPC; 1.72-fold) or fed a HFHS diet (DLPH; 1.65-fold). DAZAP1 also decreased ( $P < 0.05$ ) by 5.13-fold in the DLPC vs. DHPH offspring and by 2.43-fold in the DLPC vs. DHPC. Similar patterns were also observed for SEPT7, with a 1.07-fold decrease ( $P < 0.05$ ) in the DLPC vs. DHPH and decreases of 1.43-fold and 1.04-fold in DLPC vs. DHPC and DLPC vs. DLPH, respectively. Altered abundance of ovarian proteins in offspring who experienced maternal GDM underscore the potential long-term effects of metabolic changes on ovarian function. Together, these findings suggest a possible impact on fertility and oocyte quality in relation to GDM exposure in utero as well as in response to a western diet in later life.

### **C-type Natriuretic Peptide (CNP) Signaling in Human Periovarian Follicles: A Gatekeeper of Final Oocyte Maturation?**

Maíra Casalechi, Júlia A. Dias, Luiza C. Lima, Verônica Lobach, Maria T. Pereira, Ines K. Cavallo, Adelina M. Reis, Cynthia Dela Cruz, and Fernando M. Reis

C-type natriuretic peptide (CNP) is a member of the natriuretic peptide family that signals through the second messenger cGMP once bound to its membrane receptor (NPR2). Studies in animals have shown that CNP stimulates preantral and antral follicles to growth, and inhibits the early meiotic resumption of the oocytes. However, the relationship of ovarian CNP signaling with oocyte maturation in humans is unknown. The aim of the study was to evaluate whether CNP signaling varies in human periovarian follicles according to the stage of oocyte maturation. Follicular fluid (FF) and luteinized granulosa cells were collected from 43 individual follicles of 13 patients submitted to controlled ovarian stimulation (COS) for intracytoplasmic sperm injection (ICSI). All the patients enrolled in the project signed a consent form, which was approved by our Institutional Review Board. CNP levels were measured in the follicular fluid by enzyme immunoassay (EIA). The mRNAs encoding for the CNP precursor, NPPC, and its receptor, NPR2, were quantified in granulosa cells by reverse-transcription real-time PCR, while cGMP was measured in isolated cumulus cells and immature oocytes by direct EIA. CNP was detected in all samples of follicular fluid (range in 0.13 to 1.0 ng/ml). CNP levels were similar in the FF of follicles containing metaphase II oocytes (0.49 +/- 0.22 ng/ml, n=21), metaphase I oocytes (0.53 +/- 0.23 ng/ml, n=8), prophase I / germinal vesicle stage oocytes (0.56 +/- 0.29 ng/ml, n=6) and in follicles where no oocyte was retrieved (0.53 +/- 0.30 ng/ml, n=8,  $P=0.212$ ). However, the gene expression of CNP precursor was 1.45 fold higher in the granulosa cells from follicles containing immature oocytes than in granulosa cells from follicles harboring mature (metaphase II) oocytes ( $p=0.037$ ). NPR2 gene expression did not vary as a function of oocyte maturation. In immature cumulus-oocyte complexes, cGMP levels were barely detectable in cumulus cells (0.03 +/- 0.05 fMol/cell) and much higher in the oocytes themselves (175 +/- 2 fMol/cell). In conclusion, the full pathway CNP-NPR2-cGMP is expressed in human periovarian follicles, and CNP mRNA in granulosa cells (but not peptide secretion into the FF) appears to be more

abundant in follicles containing immature oocytes. These preliminary findings suggest that paracrine CNP signaling may contribute to delay oocyte maturation in humans. However, to develop this hypothesis, further studies should test directly the effects of CNP on in vitro models of human folliculogenesis and oocyte maturation. Funding: Conselho Nacional de Desenvolvimento Científico e Tecnológico (grant # 311154/2015-8).

**The Ratio of GDF9:BMP15 Plays a Role in Determining Litter Size in Mammals.** Janet L. Pitman, Efthimia R. Christoforou, Abdulaziz A. Alhussini, Gene W. Swinerd, and Zaramasina L. Clark

Ovulation quota and subsequent litter size between different mammalian species varies widely. The identification of two oocyte-secreted factors (OSF), namely growth differentiation factor 9 (GDF9) and bone morphogenetic protein 15 (BMP15) two decades ago has provided some insight. In this study, we have advanced this knowledge through investigations in a range of mammalian species that differed in litter size. Specifically, in this study we compared results from rats, sheep, red deer and pigs that have approximate litter sizes of 5-16, 1-3, 14-18 and 1, respectively. Our objectives were to: 1) examine the molecular forms of oocyte lysate and secreted GDF9 and BMP15; 2) compare the responses of granulosa cells (GC), in regards to proliferation rate, gene expression levels of key receptors and phosphorylation of downstream signaling proteins, following same- and cross-species co-incubations with oocytes; and 3) test differing GDF9:BMP15 ratios on blastocyst rate of sheep oocytes following in vitro maturation (IVM) and in vitro fertilisation (IVF). Examination of the molecular forms revealed that there was a higher ratio of promature:mature protein forms in oocyte lysate than in conditioned media (secreted form) for both GDF9 and BMP15 of sheep, red deer and pig. Whilst the GDF9 promature:mature protein ratio did not differ in oocyte lysates or conditioned media of sheep, red deer and pig, there was a higher ( $P < 0.05$ ) BMP15 promature:mature protein ratio in oocyte lysates of sheep and red deer, compared to the pig. Moreover, N-linked glycosylation sites were more common in GDF9 than BMP15. N-linked glycosylation was observed on pig promature and mature GDF9, as well as on sheep mature GDF9. N-linked glycosylation of BMP15 was only observed on the pig promature form. Neither cervine form of GDF9 or BMP15 exhibited N-linked glycosylation. Careful collections of GC from cleanly extracted pig follicles revealed that pig GC expressed GDF9 mRNA, thus rectifying low GDF9 expression in pig oocytes and re-establishing the high GDF9:BMP15 ratio hypothesised for poly-ovulators. Examination of GC responsiveness to OSF supports the solitary role of GDF9 in regulating GC function in rats, whilst both GDF9 and BMP15 regulate GC function in sheep and pigs. Red deer GC were mainly regulated by BMP15 but a role for GDF9 was revealed. Additionally our results showed that in general, oocytes that secreted GDF9 and BMP15 or predominantly BMP15 activated SMAD2/3 or SMAD1/5/8 pathways, respectively. Finally, supplementation of IVM media with a high (6:1) compared to a low (1:6) ratio of recombinant pig GDF9:BMP15 improved blastocyst by ~20% ( $P < 0.05$ ). In summary, these results provide evidence that species differences exist in both intra-follicular GDF9:BMP15 ratios and GC responsiveness. Our investigations leads to the hypothesis that the ratio of secreted GDF9:BMP15 within the ovarian follicle is positively correlated with litter size.

This work was supported by the Royal Society of New Zealand Marsden fund.

**Species Differences in Tgf $\beta$  Proteins: Implications for Reproduction.** Kelly L. Walton, William Stocker, Sara Zangana, Degang Wang, Gerogia Goodchild, Monica Goney, and Craig A Harrison

Many members of the large family of transforming growth factor- $\beta$  (TGF- $\beta$ ) proteins have fundamental roles in reproduction. For example, activins and inhibins regulate follicle stimulating hormone (FSH) production by the anterior pituitary, GDF-9 and BMP-15, secreted by the oocyte, control follicle maturation and ovulation rate, and AMH is a negative regulator of primordial follicle activation. In addition, BMP8B in males is critical for the maintenance of spermatogenesis. Interestingly, unlike most family members, these “reproductive” TGF- $\beta$  ligands display significant sequence variation across species, raising the possibility that the physiological roles of these proteins may also differ between mice and (wo)men. Over several years, we have used in vitro methods to assess differences in expression and activity of mouse and human forms of these reproductive TGF- $\beta$  ligands. We now understand why mBMP15 and hBMP8B are expressed very poorly and why hGDF9 is secreted in a latent form. Additionally, we have found that synthesis of mouse inhibins and activins appears to diverge from that of humans. Our insights provide the means to determine whether species differences in TGF- $\beta$  ligands underlie the variation in mammalian reproductive capacity. Many members of the large family of transforming growth factor- $\beta$  (TGF- $\beta$ ) proteins have fundamental roles in reproduction. For example, activins and inhibins regulate follicle stimulating hormone (FSH) production by the anterior pituitary, GDF-9 and BMP-15, secreted by the oocyte, control follicle maturation and ovulation rate, and AMH is a negative regulator of primordial follicle activation. In addition, BMP8B in males is critical for the maintenance of spermatogenesis. Interestingly, unlike most family members, these “reproductive” TGF- $\beta$  ligands display significant sequence variation across species, raising the possibility that the physiological roles of these proteins may also differ between mice and (wo)men. Over several years, we have used in vitro methods to assess differences in expression and activity of mouse and human forms of these reproductive TGF- $\beta$  ligands. We now understand why mBMP15 and hBMP8B are expressed very poorly and why hGDF9 is secreted in a latent form. Additionally, we have found that synthesis of mouse inhibins and activins appears to diverge from that of humans. Our insights provide the means to determine whether species differences in TGF- $\beta$  ligands underlie the variation in mammalian reproductive capacity.

**Sperm Cryopreservation Prior To Gonadotoxic Therapies: A Large Academic Center's Experience.**

Pouya Joolharzadeh, Stephanie S. Rothenberg, Marie N. Menke, Joseph S. Sanfillipo, Kyle E. Orwig, and Hanna Valli-Pulaski

The utilization and outcomes of sperm cryopreservation in patients undergoing potentially gonadotoxic therapies has not been well studied. A cohort of 278 post-pubertal male patients with a medical diagnosis (malignant or non-malignant) requiring gonadotoxic therapies who contacted the Fertility Preservation Program (FPP) in Pittsburgh between 2010 and 2017 for fertility preservation counseling were included. Patient demographics, time from diagnosis to fertility preservation counseling, time from fertility preservation counseling to semen collection, semen analysis results, and whether cryopreserved sperm was later utilized for fertility treatment during the study period were collected and analyzed. The average age of participants was 25.89 $\pm$ 8.82 years, with 17.63% less than 18 years old. Diagnoses included testicular cancer (26.26%), Hodgkin's lymphoma (21.22%), non-Hodgkin's lymphoma (5.76%), leukemia (14.39%), musculoskeletal cancers (14.39%), non-malignant diseases requiring bone marrow

transplant (2.88%), and other neoplastic diseases (20.14%). Seventy-four percent of patients who contacted the FPP proceeded with cryopreservation. Various time points during the treatment process were collected: initial diagnosis to first contact with FPP for all patients ( $30.76 \pm 53.93$  days), first contact with FPP to semen collection for patients who desired to proceed with fertility preservation ( $5.032 \pm 8.673$  days), and initial diagnosis to semen collection ( $32.98 \pm 54.40$  days). Patients 18 and older had a higher number of collections ( $1.75 \pm 0.072$ ) compared to patients under 18 ( $1.42 \pm 0.107$ ). Of the samples collected, 7.91% of samples were discarded, 1.44% of samples were transferred to a different facility, and 1.39% were utilized for intrauterine insemination or in vitro fertilization. Approximately 10% of patients have died. These results demonstrate that a high proportion of male patients counseled for fertility preservation at our center proceeded with sperm cryopreservation. When compared with previous literature, time from initial diagnosis to semen collection was relatively short. Timely appointments may contribute to the high proportion of patients who elected to participate in sperm cryopreservation at our center. This work was supported from 2011 to present by the Scaife Foundation, the Richard King Mellon Foundation, the Magee-Womens Research Institute and Foundation, the Volunteer Service Board of Magee-Womens Hospital, gift funds from Sylvia Bernassoli and the Department of Ob/Gyn and Reproductive Sciences and Urology of the University of Pittsburgh.

**Growth of Dominant Anovulatory and Ovulatory Follicles and Associated Endocrine Profiles During Spontaneous Cycles in Women.** Shah Tauseef Bashir, Angela R. Baerwald, Melba O. Gastal, Roger A. Pierson, and Eduardo L. Gastal

The human menstrual cycle is characterized by two-three waves of antral follicle development. The growth and endocrine dynamics in ovulatory versus anovulatory follicular waves in women are not fully understood. The objective of this study was to compare dominant anovulatory and ovulatory follicles during spontaneous cycles in different types of follicular waves. Follicular profiles of 55 women (mean age = 28.3 years) were mapped using transvaginal ultrasonography. A total of 63 dominant follicles were classified into wave 1 (W1ADF;  $n = 8$ ) and wave 2 (W2ADF;  $n = 6$ ) anovulatory dominant follicles, and wave 2 (W2OvF;  $n = 33$ ) and wave 3 (W3OvF;  $n = 16$ ) ovulatory follicles. Comparisons were made between W1ADF and W2ADF, and W2OvF and W3OvF. W1ADF emerged closer to the preceding ovulation, and W2ADF emerged in the late luteal or early follicular phase. The interval from emergence to maximum diameter was shorter ( $P$  vs  $7.6 \pm 0.6$  days) and tended ( $P$  vs  $10.5 \pm 0.2$  days). Selection of W3OvF occurred at a smaller ( $P$  vs  $0.8 \pm 0.1$  mm/day). Also, W1ADF were associated with lower ( $P$  vs  $5.6 \pm 0.6$  mIU/mL), and higher ( $P$  vs  $35.2 \pm 5.2$  pg/mL) and progesterone ( $8.3 \pm 1.4$  vs  $0.7 \pm 0.1$  ng/mL). In contrast, W3OvF were associated with higher ( $P$  vs  $4.6 \pm 0.2$  mIU/mL) and higher ( $P$  vs  $6.2 \pm 0.6$  mIU/mL) compared to W2OvF. However, W2OvF were associated with higher ( $P < 0.05$ ) mean progesterone ( $1.1 \pm 0.1$  ng/mL) than W3OvF ( $0.8 \pm 0.1$  ng/mL). Differences were observed in the growth and endocrine profiles associated with dominant anovulatory and ovulatory follicles that emerged at different stages of the menstrual cycle. This knowledge is expected to assist in optimizing ovarian stimulation regimens in women undergoing assisted reproductive therapies.

**Ovarian Stimulation Affects Mouse Oocyte Mitochondrial DNA Copy Number.** Rolando Pasquariello, Deirdre Logsdon, Jennifer P. Barfield, William B. Schoolcraft, and Rebecca L. Krisher

Ovarian stimulation using exogenous gonadotropins results in retrieval of high numbers of oocytes, but ART success may be compromised due to a detrimental impact on oocyte quality. Mitochondria are important organelles related to acquisition of oocyte competence. However, it is unknown whether ovarian stimulation affects the mechanisms controlling mitochondria number and function in oocytes and embryos. Our objective was to determine whether ovarian stimulation influences mitochondrial function and mitochondrial DNA (mtDNA) copy number in germinal vesicle (GV) and metaphase II in vivo matured (IVO MII) oocytes and blastocysts from unstimulated and stimulated CF1 outbred females. In unstimulated females, GV oocytes were collected by puncturing ovarian follicles. IVO MII oocytes were obtained from the oviduct the morning after mating with vasectomized males. Blastocysts were collected by flushing uterine horns 3.5 days after mating with intact males. For stimulated females, GV were obtained after ovarian stimulation using 5 I.U. PMSG 48 h before collection. IVO MII oocytes were collected after PMSG followed in 48h by 5 I.U. hCG, 15 h before collection. Some IVO MII oocytes were in vitro fertilized and cultured to produce blastocysts. Mitochondrial DNA copy number was determined in single oocytes and blastocysts using a qPCR based assay for absolute quantification by comparison to a standard curve obtained by cloning MT-RNR1. Blastocyst mtDNA copy number was also determined relative to nuclear DNA (GAPDH). Mature oocytes were further analyzed for mitochondrial membrane potential (MMP) using JC-1 live staining. The ratio of red:green pixel intensity was measured in four cortical, intermediate and perinuclear regions of each oocyte. MMP was averaged per oocyte and region and expressed in arbitrary units. Overall, GV and MII oocytes and blastocysts from unstimulated females had higher ( $P < 0.05$ ) mtDNA copy number than those from stimulated females: GV,  $232,159 \pm 5,002$  vs  $174,921 \pm 8,820$ ; MII,  $246,236 \pm 6,143$  vs  $143,061 \pm 12,843$ ; blastocysts,  $184,050 \pm 7,308$  vs  $107,749 \pm 13,717$ , respectively. Similarly, mtDNA copies per cell were higher in blastocysts from unstimulated females than stimulated females:  $4406 \pm 562$  vs  $2760 \pm 249$ . Interestingly, GV and MII oocytes from stimulated animals differed in mtDNA copy number, with mtDNA copy number decreasing during maturation from GV to MII, while GV and MII oocytes from unstimulated females did not differ in mtDNA copy number. MMP was not different between MII oocytes from stimulated and unstimulated females in the cortical and intermediate regions of the ooplasm. The perinuclear region of MII oocytes from unstimulated females had higher ( $P < 0.05$ ) MMP than that of stimulated females ( $1.65 \pm 0.11$  vs  $1.19 \pm 0.08$ , respectively). Active mitochondria were predominantly distributed within the cortical region for both stimulated and unstimulated females. These results demonstrate that ovarian stimulation affects oocyte mitochondrial reserve but does not significantly alter mitochondrial function. The alteration in mtDNA persists until the blastocyst stage, and could potentially affect embryo viability post transfer. This study suggests that women undergoing clinical ART may be susceptible to anomalies in mtDNA copy number that could potentially affect treatment success.

**Uhrf1 is Essential for Spermatogenesis and Participates in Silencing Retrotransposon in Male Germ Cells.** Yanqing Wu, Juan Dong, Congcong Cao, Yujiao Wen, Xiaoli Wang, and Shuiqiao Yuan

Transposable elements are predominant biological factors that can cause genome mutations. Inactivation of transposable elements is critical to protect genome integrity. DNA methylation and repressive histone marks are essential for controlling transposon silencing in mammalian germ-line.

Uhrf1 has been demonstrated to play important roles in DNA methylation and histone modifications. However, the role of Uhrf1 in male germ cell development is still elusive. Here, we report that Uhrf1 is essential for spermatogenesis and silencing retrotransposons in mouse male germ cells. Conditional deletion of Uhrf1 in mouse male germ cells causes male sterility and exhibits meiotic arrest at pachytene stage with massive germ cell apoptosis. To gain a molecular understanding of the meiotic failure, we observed an up-regulation of Line1 and IAP transposons as well as DNA damage activation in Uhrf1 mutant testes, accompanied by an increase in 5-hydroxymethylcytosine. Methylation analysis revealed that the global DNA hypomethylation as well as attenuate methylation of Line1 and IAP DNA in Uhrf1 mutant testes. Furthermore, Uhrf1 mutant testes have severely reduced levels of prepachytente piRNAs populations at P14. In addition, down-regulation of H3K9me3 and up-regulation of H3K4me3 histone modifications were found in Uhrf1 mutant germ cells, which directly implying the critical role of Uhrf1 in transposons silencing by changing the histone modification. Collectively, our results demonstrate that Uhrf1 plays a novel role in germ cell development by inactivating retrotransposons through DNA methylation and histone modification during spermatogenesis.

**Cryopreservation Induces Mitochondrial Permeability Transition in the Bovine Sperm Model.** Favian Treulen, María Elena Arias, Luis Aguila, Pamela Uribe, and Ricardo Felmer

When the mitochondria of somatic cells are exposed to pathological calcium overload, these trigger the mitochondrial permeability transition (MPT) leading to mitochondrial dysfunction and cell death. On the other hand, cryopreservation procedures expose mammalian spermatozoa to physical and chemical stressors, which affect plasma membrane integrity and induce a pathological calcium overload that gradually promote loss of sperm quality and eventually function. Although several studies highlight the role of calcium in many physiological and pathological processes, the MPT induced by an intracellular calcium increase and its effect on cell quality of mammalian spermatozoa are unknown. The aim of this study was to evaluate the effects of cryopreservation on MPT and its relationship with the deterioration of sperm quality in the bovine model. To do this, frozen bovine spermatozoa were thawed and adjusted to  $2 \times 10^6$  mL<sup>-1</sup> and incubated for 4 h at 38°C. By using flow cytometry we evaluated MPT by the calcein-AM and cobalt chloride method, intracellular Ca<sup>2+</sup> level using FLUO3-AM, plasma membrane integrity by exclusion of propidium iodide, mitochondrial membrane potential (DYm) with tetramethylrhodamine methyl ester perchlorate and intracellular ROS production with dihydroethidium. ATP levels were assessed by a quimioluminescent method. The results showed that thawed spermatozoa trigger MPT associated to an intracellular calcium increase and this was accompanied by DYm dissipation, decrease of ATP levels and ROS production, and deterioration of the plasma membrane integrity. In conclusion, the cryopreservation induces MPT and this is associated with loss of sperm quality.

**Expression of Growth Factors IGF-I, FGF10 and EGF and their Relationship with Adhesion Molecules Like Integrin Avβ3, Fibronectin and Selectin in the Binomial Embryo-Uterus Around Implantation.**

Valdez-Magaña G., Morales M. M. V., Villegas C. A. Q., Contreras D. A., Gutierrez P.O., and Trujillo O. M. E.

Implantation is the biological process by which the blastocyst attaches to the uterus. When happens correctly it allows the embryo to develop a functional placenta that supports pregnancy. This mechanism, implies the formation of cell to cell union between the blastocyst trophoblast cells with the tunic coat from the uterus, and is mediated by a complex cascade of molecular signals with the objective of establishing the embryo maternal communication. In fact, failure in implantation cause 75% of all pregnancies lost in human, and in animal production, gestational loss generate great interest from an economic perspective, for example this mechanism in the sow accounts for 30% of embryo losses.

For implantation to be successful, maternal epithelial cells must be previously sensitized by sexual steroids, so that the endometrium can experience morphological changes. Molecules such as cytokines, hormones, growth factors, adhesion molecules, lipids, are among those that influence secretion during a period denominated "window of receptivity".

However, attachment mechanisms that take place during implantation process are not well clarified. Therefore, the aim of this study was to identify the localization of the expression of growth factors IGF-I, FGF10 and EGF and their relationship with the regulation of adhesion molecules such as Integrin  $\alpha\beta 3$ , fibronectin and selectin in the binomial embryo-uterus during early developmental stages where the implantation window occurs, all this using the pig as a model.

All experiments were approved by the animal welfare and ethics committee, National Autonomous University of México-FMVZ. Sows were synchronized, artificially inseminated and slaughtered between days 12 to 22 of exact known gestation. Uterine horns were dissected, and implantation sites were collected from different gestational stages. Paraffin sections were used for immunohistochemical localization of IGF-I, FGF10, EGF, EP2, Integrin  $\alpha\beta 3$ , fibronectin and laminin proteins.

Localization of expression of growth factors IGF-I, FGF10 and EGF in the uterus implantation sites showed co-localization with expression of Integrin  $\alpha\beta 3$ , fibronectin and selectin, specifically in the endometrium close to the uterine light. Interestingly, IGF-I localization seems to be expressed not only in glandular epithelium but also in the myometrium when compared with non-pregnant uterus. Therefore, it could be suggested that both, adhesion molecules and growth factors, are playing a role in the regulation of trophoblast adhesion. Although more research is needed to further understand the growth factors-mediated physiological events required for embryo attachment during the peri-implantation period.

Acknowledgments to UNAM-DGAPA-PAPIIT-IA208516

**The Use of SP-10 Protein as an Acrosome Marker in Stallion Seminiferous Tubules.** Anamaria Cruz, Derek Sullivan, Karen Doty, Rex Hess, Igor F. Canisso, and Prabhakara P. Reddi.

Testicular dysfunction is a major cause of poor reproductive performance in stallions, leading to losses to the horse industry. Diagnosis of declining testicular function requires employment of proper methods to evaluate the progression of spermatogenesis. Previous studies in mice and men have shown the intra-acrosomal antigen SP-10 as a useful marker for round spermatids and spermatozoa. The goal of this study was to evaluate the usefulness of the SP-10 antibody in the staging of the stallion seminiferous epithelium using immunohistochemistry. Adult stallion (n=4) testis cross sections were treated with an in-house guinea pig polyclonal antibody raised against the mouse SP-10 antigen. The Zeiss Axiovert

200M Widefield microscope, the Axiocam 506 Color camera, and ZenPro software were used to capture images. Two hundred tubule cross sections were observed per horse. We have found the SP-10 antibody labeling to be highly specific for the acrosome and were able to follow the progression of acrosome development. Based on the acrosome staining pattern we were able to identify 16 separate steps of spermatids in the horse. High degree of demarcation in acrosome morphology in turn helped us to identify the distinct sets of male germs found in association with spermatids at various developmental time points within testis cross sections. Thus, we were able to identify 12 stages of the cycle of seminiferous epithelium in the stallion. Prior to our study, staging of the horse seminiferous epithelium has relied on the morphology of the acrosome as shown by the H&E or PAS staining. These studies found only 8 stages in the horse, likely owing to the poor resolution of acrosome morphology offered by the H&E and PAS staining. Because the SP-10 antibody clearly outlined the acrosome in spermatids, we were able to discern 16 steps of spermatid development and 12 stages in the horse seminiferous epithelium. Unlike the rodent which typically shows one stage per tubule cross section, we observed multiple stages represented per tubule cross section (60% of the time). In this regard, the stallion exhibited similarities to the human seminiferous epithelium wherein multiple stages are found in a given cross section. Overall, we have found that the SP-10 antibody is an extremely useful reagent for staging of the horse seminiferous epithelium. Future studies will explore its utility in understanding declining fertility in stallions.

**Xenografting Prepubertal Human and Non-Human Primate Testicular Tissue Into Mice Indicates Differences in Niche Factors Essential for Promoting Graft Maturation.** Sherin David, Meena Sukhwani, Hanna Valli, and Kyle Orwig

Testicular tissue xenografting has been extensively studied as a tool to elucidate spermatogenesis and for the generation of mature gametes from prepubertal tissue. Successful application of this method to human testicular tissue could serve as an approach for fertility preservation in prepubertal males at a risk for iatrogenic infertility. Previous studies have demonstrated that testicular tissue obtained from prepubertal primates can undergo complete spermatogenesis when grafted into recipient mice. It has also been shown that human chorionic gonadotropin (hCG) enhances maturation of monkey grafts. In the current study, we hypothesized that treatment of recipient mice with hCG along with vascular endothelial growth factor (VEGF) would promote maturation of human prepubertal testicular grafts. To test this hypothesis, we grafted prepubertal human testis tissue into castrated immunodeficient mice. Recipient mice received hCG and /or VEGF treatments and were compared with untreated mice. To compare the efficacy of these treatments in promoting maturation of human testicular grafts with that observed in monkey tissue, we also grafted prepubertal monkey testicular tissue into mice under the same treatment groups. At 7 months post grafting recipients that received hCG had significantly larger grafts for both donor species. Monkey grafts obtained from hCG and hCG+VEGF treated mice showed tubular expansion with lumen formation. Germ cells expressing meiotic and post-meiotic markers, Piwi-like protein 1 (PIWIL1) and Transition protein 1 (TP1) were also observed. Monkey grafts from hCG and hCG+VEGF treated mice were also digested to isolate spermatozoa. These results demonstrate that treatment of recipients with monkey testicular grafts promoted maturation of prepubertal donor tissue. Mice with monkey grafts that received hCG and/or VEGF had significantly larger seminal vesicles compared to castrated mice that did not receive grafts. In contrast, in mice with human grafts only the ones that received hCG+VEGF had a significant increase in seminal vesicle size compared to castrated

controls. In addition, human grafts retrieved from all treatment groups showed Sertoli cell only phenotype at 7 months post grafting. These results indicate that factors that promote prepubertal monkey graft maturation and spermatogenesis are not sufficient for inducing spermatogenesis in prepubertal human testicular grafts in mouse hosts.

The monkey work was supported by grants from Eunice Kennedy Shriver National Institute for Child Health and Human Development grants HD076412 and HD075795. The human work was supported by HD092084; the US-Israel Binational Science Foundation and internal funds from Magee-Womens Research Institute.

**Maternal Low Protein Diet During Gestation Programs Offspring Glucose Intolerance in Adulthood Regardless of Postnatal Plane of Nutrition in Female Mice.** Kathleen A. Pennington, Ryan Fleischmann, Celia Pena Heredia, Chandra Yallampalli, and Marta L. Fiorotto

The ‘developmental origins of health and disease’ (DOHaD) hypothesis states that a poor nutritional environment during gestation and/or neonatal life increases the risk for obesity and diabetes in adulthood. These long-term effects may be exacerbated when a mismatch occurs in the plane of nutrition of the offspring in the transition between developmental stages. Our objective was to distinguish the contributions to the increased risk of adult onset diabetes of increased adult adiposity vs direct programming of the pancreas and insulin sensitivity. We hypothesized that mismatched nutrition would increase adiposity resulting in glucose intolerance. To test this, mice were exposed to one of two nutritional planes during gestation (G) by being born to FVB dams fed a control diet (CON; 20% protein, 7.5% fat) or a low protein diet (LP; 8% protein, 7.5% fat) and then cross-fostered at birth to one of three nutritional planes: dam fed a control diet and 7 pups/dam (CON), dam fed a control diet and 4 pups/dam (over nourished, OV), or dam fed LP with 8 pups/dam for a total of 6 groups: CON-CON, CON-LP, CON-OV, GLP-CON, GLP-LP, GLP-OV. At weaning all offspring were weaned to CON. At 1 year of age body composition was measured by quantitative magnetic resonance and intraperitoneal glucose and insulin tolerance tests (ipGTT and ipITT) were performed on female offspring. CON-LP and GLP-LP were similar in weight and body composition, but weighed less ( $p < 0.05$ ), with lower fat and lean mass compared to all other groups; percent body fat was not different among groups. At 30 minutes, blood glucose was increased ( $p < 0.01$ ) in GLP-CON and GLP-LP compared to all other groups as was their total area under the curve ( $p < 0.05$ ), indicating that these offspring were glucose intolerant compared CON-fed dam offspring regardless of postnatal nutrition. GLP-OV had slightly improved glucose tolerance compared to GLP-CON and GLP-LP as evidenced by reduced blood glucose at 30 minutes of the ipGTT. Among all offspring, adiposity affected glucose tolerance independently of the early life dietary experience ( $p=0.01$ ). GLP-LP had improved ( $p < 0.05$ ) insulin tolerance compared to CON-OV and CON-CON indicated by reduced blood glucose levels 90 minutes post insulin injection; no other differences in ipITT were observed among groups. In summary, a maternal LP diet during gestation programmed glucose intolerance in adulthood even when postnatal and adult nutrition was optimal. This response was exacerbated by increased adiposity regardless of plane of nutrition either in utero or postnatally. The ipITT indicated that offspring exposed to the LP diet both in utero and postnatally had increased insulin sensitivity. The ipGTT data are consistent with reduced pancreatic function as a consequence of exposure to low protein diet during gestation. However, when followed by persistent exposure to a low plane of nutrition throughout development, a “thrifty” phenotype is manifested as an increase in insulin

sensitivity that may serve to combat glucose intolerance. A mismatch between pre- and post-natal nutrition does not exacerbate glucose tolerance, but there is no benefit gained from increased insulin sensitivity. Funded by USDA/ARS/CSREES 6250-51000-051(MLF) NIH AR46308 (MLF).

**Evaluation of Amino Acid Metabolic Pathway Interactions in Bovine Mammary Epithelial Cells Using Label-Free Quantitative Proteomics.** Tatiana Ruiz-Cortés, Camilo Calle, Laura López, Peter Yoder, and Mark D. Hanigan

Studying the regulation and interactions of different pathways of amino acid (AA) metabolism in mammalian cells is important to understand the molecular and cellular mechanisms by which AA exert control on the synthesis and turnover of mRNA and milk proteins. Primary bovine mammary epithelial cells were cultured for 6 days after reaching confluence in lactogenic DMEM containing insulin, prolactin, progesterone, transferin, hydrocortisone, and epidermal growth factor. Following lysis of cells, cellular total protein concentration was measured by BCA (Pierce®). Extracts of total protein were subjected to label-free, quantitative proteomics using liquid chromatography separation and mass spectrometry analysis after proteins were labelled by treatment with differing isotopic labels (ISOQuant®). To study metabolic pathway mapping and annotation, a multi-fasta file was created with all protein sequences and submitted to BlastKOALA in KEGG (Kyoto Encyclopedia of Genes and Genomes) resulting in the annotated data. KEGG pathways (n=10) and KEGG brite functions (n=20) of interest were included in the analysis. For data processing, a matrix with 17 dichotomous (presence, absence) variables corresponding to 17 AA pathways and 14 variables of Environmental Information Processing-EIP (signaling pathways) were created and analyzed with R-project software. Subsequently, multiple correspondence analysis was used to detect complementarity or antagonism between the different metabolic pathways. Results from 1163 total proteins were studied. Protein sequences and the multi-fasta file from KEGG indicated that 89.5% of those total proteins were analyzed for a total of 1041 annotated entries. EIP and AA metabolism were the focus of interest of the research. In the AA pathways, 70 significant proteins were found. Amino acid metabolic pathways, the first component, and environmental processing including signalling pathways (the second component), explained 21,18% and 17,15% of the variation of general AA metabolism, respectively. Those low percentages suggest that different, possibly adjacent, metabolic pathway interactions are regulating amino acid pathways requiring further analyses. Among the total proteins, 8 epithelial keratins were detected validating the epithelial origin of the cells; another 60 proteins were associated with mammary gland development and function including milk protein production; 9 of those proteins appeared in the signaling network associated to AA metabolism. The KEGG brite results of pathways interaction/functions of pathways analyzed with multiple correspondence with AA metabolism pathways indicated that there is a strong direct association between phenylalanine, tyrosine and tryptophan biosynthesis and phenylalanine metabolism and the different amino acid pathways. Also, a moderate direct association was detected between the synthesis and metabolism of alanine, aspartate and glutamate and tyrosine and other amino acid pathways. Additionally, a moderate direct association was shown between cysteine and methionine metabolism and the biosynthesis of arginine with the global amino acid metabolic pathways. As for inverse associations, histidine metabolism was moderately related with general AA metabolism and the metabolism of beta-alanine and the degradation of valine, leucine, isoleucine, lysine and tryptophan were slightly associated with global AA metabolic pathways. We conclude that besides the

specific character of epithelial cells it is a useful tool for studying the AA metabolism and milk proteins production of mammary epithelial cells.

**Effects of Uterine Seminal Plasma Infusion on Endometrial Inflammation in Cattle.** Jason A. Rizo, Pedro L. P. Fontes, G. Cliff Lamb, and John J. Bromfield

Seminal plasma is the non-cellular, fluid fraction of semen derived from the male accessory glands. Following insemination in mice, swine and humans, seminal plasma interacts with epithelial cells of the female reproductive tract to elicit the production of pro-inflammatory cytokines. Post-insemination endometrial inflammation is absent following mating with seminal vesicle deficient mice, or condom-protected intercourse in humans, establishing a causal link between seminal plasma and cellular inflammation of the female reproductive tract. The expression of embryotrophic factors in the oviduct is also increased in response to seminal plasma to support the developing embryo. In cattle, swine and humans supplementation with seminal plasma at the time of insemination or embryo transfer increases pregnancy rates, suggesting that seminal plasma induced changes contribute to pregnancy success. Seminal plasma exposure at insemination has also been associated with alterations in ovarian function of swine and mice. It is unknown if seminal plasma influences the endometrial environment of cattle in a similar manner to other species. During semen processing for artificial insemination in cattle, seminal plasma is significantly diluted, potentially reducing seminal plasma mediated sire to dam communication. We hypothesize that uterine exposure to seminal plasma at the time of artificial insemination drives acute endometrial inflammation and alters ovarian function in cows. Uterine infusion with 1 ml of either saline, seminal plasma alone (pooled from 33 bulls and filtered), commercial AI semen of one bull, or seminal plasma + semen was performed in 54 randomly assigned beef cattle. Endometrial biopsies were collected 24 hours after treatment infusion from uterine horns, ipsilateral and contralateral to the ovulatory follicle. Expression of genes involved in inflammation, embryo development and ovarian function were evaluated by qPCR, and plasma progesterone was measured by ELISA. Expression of endometrial IL1 $\beta$  was significantly increased by infusion of seminal plasma alone compared to the saline alone control group (3.17-fold;  $P < 0.05$ ), while expression of CD45 was significantly reduced in the seminal plasma + semen group when compared to saline control (2.37-fold;  $P < 0.05$ ). Exposure to AI semen alone increased endometrial expression of IFNG by 1.79-fold compared to saline controls ( $P < 0.05$ ). Endometrial expression of CSF2, IL6, IL8, PTGS2, IL1A and TNFA were not affected by treatment. Interestingly, expression of CSF2 was increased in the ipsilateral horn by 2.88-fold of saline control cows compared to the contralateral horn ( $P < 0.05$ ). Plasma progesterone concentration was measured 7 days post-insemination. Treatment had no effect on day 7 plasma progesterone; however, cows infused with seminal plasma alone had a positive correlation between dominant follicle size prior to ovulation and plasma progesterone ( $P = 0.07$ ), while no other treatment showed a significant correlation. Seminal plasma is a complex fluid that may modulate the maternal reproductive tract during early pregnancy in the cow. Further investigation is required to determine the extent of seminal plasmas influence on the female reproductive tract of cattle and subsequent impact on pregnancy.

This research was supported by Select Sires and the Southeast Milk checkoff.

**Sexual Dimorphism of the Liver in a Circadian Mutant Mouse.** Erica L. Schoeller, McKenna R. Sinkovich, Rujing Shi, and Pamela L. Mellon

Pheromones play a critical role in reproductive behaviors in mice, including copulation and aggression. We have previously found that male circadian mutant mice (Bmal1 KO) are deficient in both copulatory and aggressive behaviors. Both behaviors in mice are regulated in part by a class of pheromones called the major urinary proteins (MUPs), which are high molecular weight proteins transcribed in the liver and excreted in the urine. MUP expression is sex-specific, with males secreting higher levels, and dependent on testosterone and growth hormone (GH). We found that Bmal1 KO males had reduced levels of MUPs. While WT mice exhibited a circadian expression pattern, circadian regulation of MUPs was absent in the KO mice, possibly responsible for the abnormal MUP-regulated behaviors in Bmal1 KO males.

MUP pheromone expression is a marker of sexual dimorphism of the liver. In male mice, high levels of testosterone and pulsatile secretion of GH drive high MUP transcription in the liver, while low testosterone and continuous patterns of GH secretion drive low MUP expression in females. In addition to MUPs, many genes in the liver are regulated in a sexually dimorphic manner, including the Cytochrome p450 genes (Cyps) that regulate steroid and xenobiotic metabolism. Because MUPs were decreased in Bmal1 KO males, we also examined the transcription of other sexually dimorphic liver genes. We found expression of many sexually dimorphic liver genes, including Cyp2a4, Cyp2b13, Elovl3, and Fmo3, was abnormally expressed in Bmal1 KO males' livers.

We sought to determine the cause for reduced MUP pheromone expression in Bmal1 KO males. Since testosterone is necessary for both MUP production and reproductive behaviors, we gonadectomized WT and KO mice and provided testosterone pellets (gdxT) to normalize testosterone levels between mice. GdxT did not restore MUP levels or reproductive behaviors, suggesting that replacement of testosterone was not sufficient to restore MUP expression and MUP-regulated behaviors. Since the pulsatile release of GH from the pituitary is critical for establishing masculine liver gene expression, we next sought to determine whether pulsatile GH secretion was disrupted in circadian mutant mice. By conducting serial blood sampling of mice every 10 minutes over 6 hours, we found that Bmal1 KO males had a more continuous, female-like, GH secretion pattern, while WT males had a highly pulsatile secretion pattern. In summary, we determined that pulsatile release of GH is disrupted in Bmal1 KO male mice, and that this correlates with abnormal expression of liver genes regulated by GH, including MUPs and Cyps.

**Wrestling With Meiosis: Determining the Role of Sumoylation in the Metaphase-to-Anaphase Transition of Meiosis I in Mouse Oocytes.** Shawn M. Briley, Amanda Rodriguez, Maud Demarque, Anne Dejean, and Stephanie A. Pangas

Defects in chromosome segregation during meiosis that result in aneuploidy pose a serious threat to women's fertility and the health of their children. Ovulation and fertilization of an egg that cannot properly complete meiosis can result in spontaneous abortion or stillbirth, and is estimated to be the cause of 4% and >35% of each, respectively. It can also cause developmental diseases, such as Down syndrome as a result of trisomy 21, and Turner syndrome as a result of a missing X chromosome in females. Aneuploidy has a strong maternal bias, an estimated 20-30% of fertilized eggs are aneuploid, compared to only 4-5% of spermatozoa. The frequency of aneuploidy is strongly associated with maternal age, and is thought to be caused by premature loss of cohesin and errors in the spindle

assembly checkpoint (SAC). The SAC is an essential mechanism in the regulation of chromosome segregation that functions to delay the onset of anaphase and correct erroneous kinetochore-microtubule attachments. Compared to mitosis, the SAC in oocyte meiosis has a high rate of error. The chromosomal passenger complex (CPC) destabilizes irregular kinetochore-microtubule attachments and maintains an active SAC, allowing proper attachments to be made. Several CPC and SAC associated proteins have been shown to be regulated by SUMOylation in mitosis. SUMOylation, a highly dynamic post-translational modification (PTM), has been shown to be essential for proper formation of the meiotic spindle and proper chromosome segregation in mouse oocytes in vitro, and inhibition of SUMOylation in oocytes leads to meiotic arrest or aneuploidy. In yeast, this PTM is required for efficient proteolysis mediated by the anaphase promoting complex/cyclosome, and, in its absence, cyclin B and securin accumulate. Despite the known importance of SUMOylation in many cell functions, there is very little research on its role in meiotic maturation of mouse oocytes. Our lab has developed an oocyte-specific knockout of Ubc9, the sole E2 SUMO ligase, at the primordial follicle stage. Ubc9<sup>flox/flox</sup>Gdf9<sup>icre</sup> females are sterile. Using live cell imaging, we observed that Ubc9 null oocytes undergo germinal vesicle breakdown, but do not complete meiosis I, and subsequently undergo degeneration. We also examined the MI spindle by immunofluorescence to examine spindle formation and chromosome alignment. Confocal analysis showed that the majority of eggs from Ubc9 knockout mice had normal appearing spindles and chromosomes properly aligned at the metaphase plate. Therefore, we suspect that there is a defective metaphase-to-anaphase transition in meiosis I that may be regulated by SUMOylation of key proteins of the SAC and APC/C. This work will provide insight into a process that, when not executed properly, can cause aneuploidy in women and may contribute to the increased frequency of aneuploidy in aging women. These studies were supported by NIH/NICHD RO1 HD085994 (to S.A.P.).

**Effects of Uterine Luminal Secretions on Conceptus Growth in Sheep.** Eleanore V. O'Neil, Gregory W. Burns, Kelsey E. Brooks, and Thomas E. Spencer

In sheep, the day 8 hatched blastocyst develops into an ovoid or tubular conceptus by day 12 and then elongates and forms a filamentous type conceptus by day 14. Coincident with conceptus elongation, the trophoctoderm produces interferon tau (IFNT) that signals pregnancy recognition and modulates uterine receptivity. In vitro studies with embryos and in vivo studies with the uterine gland knockout (UGKO) ewe model support the idea that gland-derived secretions are essential for blastocyst/conceptus survival and elongation. Study One determined effects of uterine luminal fluid (ULF) on blastocyst growth. The uterine lumen of wildtype (WT) day 14 cyclic (C) and pregnant (P) ewes was gently flushed with 4 ml of sterile PBS. The conceptus was removed if necessary, and ULF clarified by centrifugation and stored at -80°C. Alzet 2ML1 osmotic pumps were secured to the mesosalpinx of each uterine horn of day 8 bred WT ewes, and the attached catheter inserted into the uterine lumen. Osmotic pumps contained one of the following treatments: (1) 2 ml C ULF; (2) 2 ml P ULF; or (3) 101 µg recombinant ovine IFNT (IFNT) (n=5 ewes per treatment). Ewes were collected on day 12. Conceptuses from uteri infused with P ULF were longer ( $P < 0.05$ ) than those infused with C ULF (3.5 vs 1.5±0.5 mm) or IFNT (3.5 vs 1.9±0.5 mm). Study Two determined if C ULF repletion could rescue conceptus survival and growth in UGKO ewes. UGKO ewes were generated by treating ewe lambs from birth to 9 weeks with medroxyprogesterone acetate (MPA; 9.5 mg/day). ULF was obtained from day 14 C WT ewes as in Study One, but using only 2 ml of sterile PBS. Adult UGKO ewes were bred at estrus and an osmotic pump was

implanted into the uterine horn ipsilateral to the corpus luteum on day 10 that contained either PBS (n=3) or C ULF (n=5). All ewes were collected on day 14, including a group of bred WT ewes (n=5). A conceptus was recovered from two PBS-infused UGKO ewes (1 and 21 cm in length) and three C ULF-infused UGKO ewes (1.3, 3.1, and 4.1 cm). Notably, all of the UGKO conceptuses were much thinner than those from WT ewes (mean 14.4 cm, range 6.2-25.0 cm). Western blot analysis determined that total IFNT in the ULF correlated with conceptus length and was substantially greater ( $P < 0.01$ ) in the ULF of WT compared to UGKO ewes. Collectively, these results support the ideas that: (1) adoptive transfer of ULF is not detrimental to conceptus survival and growth; (2) factors other than IFNT in the ULF of day 14 P ewes stimulate blastocyst growth; and (3) infusion of ULF from WT ewes into UGKO ewes does not affect conceptus growth. This project was supported by competitive grants 2015-67015-23678 and 2016-67015-24741 from the USDA National Institute of Food and Agriculture.

### **Genetic Regulatory Mechanisms Critical for Mammalian Germline Stem Cell Identity and**

**Differentiation.** Kathryn J. Grive, Jennifer K. Grenier, Eileen Shu, Andrew Grimson, and Paula E. Cohen

Spermatogonial stem cells (SSCs) are germline stem cells which serve as the progenitors for mature male gametes (spermatozoa) throughout life-long steady-state spermatogenesis. These cells, derived from primordial germ cells, represent an extremely rare but essential cell type within the mammalian testis. Unlike other stem cell populations, SSCs are pluripotent, with their haploid progeny, the sperm, essential for the generation of every cell type in the embryo. In addition to being absolutely critical for sexual reproduction, SSCs can also be utilized for unique translational applications, including fertility preservation and, conversely, for male contraceptive development. Offsetting these benefits, however, is the fact that we know relatively little about SSCs compared to other stem cell populations. SSC propagation is poorly understood, and even less is known about SSC genetic signatures which may determine their viability and differentiation capacity.

To this end, we have performed initial transcriptome-profiling experiments by collecting mouse testes at 1 week of age, at the onset of SSC specification and the first wave of spermatogenesis, and magnetically sorting cells for surface markers Thy1 (marking SSCs), or cKit (marking differentiated spermatogonia). From these enriched populations, RNA was isolated and mRNA and small RNA sequencing libraries generated. As expected based on published data, we observed enrichment of transcripts from known SSC markers including *Plzf*, *Gfra1*, *Id4* and *Sall4* in Thy1+ populations, as well as negative enrichment of differentiation marker cKit, indicating that our enrichment and sequencing protocols are robust. Data from these pilot experiments have revealed over 6000 differentially-expressed mRNA transcripts as well as over 100 differentially-expressed miRNAs between Thy1+ and cKit+ murine cell populations, some of which likely represent novel SSC markers and transcriptional regulators.

To further expand our studies and define gene expression transitions over developmental time, we have begun utilizing 10X Genomics approaches to analyze murine SSC transcriptional dynamics on a single-cell basis. Our preliminary data span six timepoints from post-natal day 6 through adulthood, encompassing the first waves of spermatogenesis as well as steady-state spermatogenesis. These data provide us for the first time with an in-depth single-cell analysis of SSC specification as well as differentiation through the early waves of spermatogenesis which are known to exhibit many unique features compared to steady-state spermatogenesis. In addition to revealing previously unknown gene expression dynamics

during this developmental time, these data also potentially reveal novel genetic markers of the SSC population.

These studies will not only provide us with incredibly fine temporal and developmental resolution of the transcriptomic changes during SSC differentiation, but it will also help us better understand differential gene expression during first-wave spermatogenesis versus steady-state spermatogenesis. As we intend to expand these studies to cat, dog, and human (species from which we are also currently enriching SSCs), such studies will also define the common features of gene expression in SSCs and their progeny cells across species, giving insight into conserved and divergent mechanisms of SSC maintenance in mammals.

**Validation of Gene Expression "Barcodes" That Mark Distinct Cell Types in the Mouse and Human Spermatogenic Lineages.** Lorena Roa de la Cruz, John R. McCarrey, Sherman J. Silber, and Brian P. Hermann

Spermatogenesis is the developmental process by which sperm are produced in the testis. Differential gene expression patterns underlie the unique biological processes required to sustain the spermatogenic lineage (e.g., spermatogonial stem cell fate regulation, male meiosis, spermiogenesis). Previous studies of these gene expression patterns have relied largely upon analyses of bulk RNA from aggregates of multiple spermatogenic cell types or from enriched populations of specific cell types. While informative, these bulk analyses are incapable of revealing the extent of heterogeneity in gene expression patterns among the aggregated cells, and unable to resolve gene expression patterns in less prevalent cell types. To address this deficiency, we recently completed extensive single-cell profiling of the entire spermatogenic lineage in both mice and men, and defined genes which are differentially expressed among 11 different spermatogenic cell types or subtypes in mouse or human testes. In addition to providing comprehensive transcriptomes of spermatogenic cell types, these data yielded gene expression identifiers ("barcodes") unique to each cell type/subtype. To validate the specificity and utility of these gene expression barcodes, we performed high-throughput qRT-PCR to detect transcripts from these genes in cDNA samples generated from a daily series of mouse testes isolated from animals at postnatal days 6 (P6) through P30, in which each spermatogenic cell type emerged sequentially. We found that expression of these genes also emerged successively and that as few as 3 genes/barcode were sufficient to selectively identify each specific cell type or subtype. Additionally, similar 3-gene expression barcodes were derived from single-cell transcriptome analyses of whole human testis tissue samples from 29 adult men, as well as enriched populations of human spermatogonia, spermatocytes, and spermatids, and qRT-PCR experiments confirmed the specificity of these barcodes to distinct spermatogenic cell-types in the human testis. Overall, our results demonstrate the potential for these gene expression barcodes to serve as convenient and accurate tools with which to rapidly and easily detect and/or distinguish the presence or absence of specific spermatogenic cell types or subtypes in testis tissue from either humans or mice.

Supported by NIH grants HD062687 (BPH), HD078679 (JRM), HD090007 (BPH), MD007591 (UTSA), NSF grant DBI-1337513 (BPH), the Max and Minnie Tomerlin Voelcker Fund (BPH), the Helen Freeborn Kerr Charitable Foundation (BPH), and the Robert J. Kleberg, Jr. and Helen C. Kleberg Foundation (JRM).

### **Melatonin Protects Bovine Oocytes Against Thermal And Oxidative Stress During in Vitro Maturation.**

Fernanda Cavallari de Castro, Cláudia Lima Verde Leal, Zvi Roth, and Peter J Hansen

Melatonin possesses antioxidant activity and has been reported to improve fertility in heat-stressed cows. The aim was to evaluate whether melatonin protects oocytes during in vitro maturation from deleterious effects of elevated temperature (i.e., heat shock) and oxidative stress caused by the oxidizing agent menadione. Bovine cumulus-oocyte complexes (COC) were obtained from slaughterhouse ovaries and transferred to 6 well plates (25-30 COC/well) in 300µl maturation medium ± 1 µM melatonin and exposed to the following treatments: 38.5°C, 41°C, and 38.5°C + 5 µM menadione. In experiment 1 (four replicates), COCs were matured in vitro for 3 h with 5 µM CellROX®, denuded of cumulus cells and analyzed by epifluorescence microscopy to quantify production of reactive oxygen species (ROS) using ImageJ analysis of pixel intensity. Intensity of ROS was higher ( $P=0.0577$ ) for oocytes treated with 41°C or menadione than for oocytes at 38.5°C; melatonin reduced ( $P=0.0002$ ) intensity. Least-squares means ± SEM for groups with and without melatonin were 560±294 and 711±294 for 38.5°C, 610±293 and 874±296 for 41.5°C, and 629±290 and 966±291 units for menadione. Experiment 2 involved the same treatments as experiment 1. COC were matured for 22 h, fertilized and the embryos cultured for 7.5 days at 38.5°C, 5% CO<sub>2</sub> and 5% O<sub>2</sub>. Oocyte cleavage and blastocyst formation (12 replicates) were recorded on Day 3 and 7.5 after fertilization, respectively. Cleavage rate was reduced ( $P=0.0001$ ) for 41°C and menadione as compared to 38.5°C and increased ( $P=0.0041$ ) by melatonin. Least-squares means ± SEM for groups with or without melatonin were 68±3 and 66±3 for 38.5°C, 60±3 and 52±3 for 41.5°C, and 59±3 and 50±3% for menadione. There was no effect of treatment on percent of cleaved embryos that developed to the blastocyst stage, but this endpoint was increased by melatonin ( $P=0.0634$ ; 28±3 vs 24±3%). The percent oocytes becoming blastocysts was reduced ( $P=0.0031$ ) by 41°C and menadione vs 38.5°C and increased ( $P=0.0086$ ) by melatonin. Least-squares means ± SEM for groups with and without melatonin were 20±3 and 18±3 for 38.5°C, 17±2 and 11±2 for 41°C, and 15±2 and 12±2% for menadione. In conclusion, melatonin reduced ROS production of maturing oocytes and protected oocytes from deleterious effects of 41°C and menadione. The fact that effects of heat shock on the oocyte was reduced by an antioxidant suggests that ROS are an important mechanism involved in heat-shock induced damage of the oocyte during maturation (Support: BARD US-4719-14; FAPESP 2015/20379-0 & 2017/04376-6).

### **Comprehensive Mapping of Human Testis Cell Types by Single-Cell RNA Sequencing.**

Adrienne N. Shami, Sarah Munyoki, Qianyi Ma, Chris Green, Jun Li, Kyle Orwig, and Sue Hammoud

Spermatogenesis is a well-organized and tightly regulated biological process composed of three distinct biological activities: 1) Continuous stem cell self-renewal and the expansion of progenitor cells (mitosis), 2) the production of haploid cells from diploid progenitor cells (meiosis), and 3) the terminal differentiation of haploid cells into spermatozoa (spermiogenesis). The transition between these developmental stages is precisely timed, and is dependent upon germ cell intrinsic and extrinsic factors secreted by supporting cells (e.g. Sertoli, Leydig, myoid and immune cells). The distribution and organization of these cells across the seminiferous tubule has been determined histologically, and their contribution to spermatogenesis in distinct model organisms has been revealed through the purification of predefined subpopulations, followed by bulk gene expression profiling (microarray/RNA-seq). However, similar analysis has not been conducted in the human testis due to limitations in isolating pure

cell populations. To overcome the pre-selection limitations, we implemented single cell RNA-sequencing (scRNA-seq) using the Drop-Seq platform to distinguish functionally distinct cell populations within and among various cell types based on differential gene expression. Clustering analyses of scRNA-seq data from ~13,000 human cells from three individuals, ages ranging 20-30 years old, has begun to unveil distinct and rare key developmental transitions. Specifically, our analysis revealed the developmental trajectory of germ cells from spermatogonia to elongating spermatids, and we identify transcriptional regulators and markers at several critical transition points during differentiation. Taken together, our data will serve as a community resource essential for understanding the structural and functional diversity of human germ cell development, answering new mechanistic questions regarding spermatogonial stem cell (SSC) regulation and signaling processes, and defining underlying causes of male infertility.

### **Dnmt2 Mediates Intergenerational Transmission of Paternally Acquired Metabolic Disorders Through Sperm Small Non-Coding Rnas.** Qi Chen

The discovery of RNAs (e.g. mRNAs, non-coding RNAs) in sperm has opened the possibility that sperm may function in delivering additional paternal information aside from solely providing the DNA. Increasing evidence now suggests that sperm small non-coding RNAs (sncRNAs) can mediate intergenerational transmission of paternally acquired phenotypes, including mental stress and metabolic disorders. How sperm sncRNAs encode paternal information remains unclear, but the mechanism may involve RNA modifications. Here we show that deletion of a mouse tRNA methyltransferase, DNMT2, abolished sperm sncRNA-mediated transmission of high-fat diet (HFD)-induced metabolic disorders to offspring. Dnmt2 deletion prevented the elevation of RNA modifications (m5C, m2G) in sperm 30-40nt RNA fractions that are induced by HFD. Also, Dnmt2 deletion altered the sperm small RNA expression profile, including levels of tRNA-derived small RNAs (tsRNAs) and rRNA-derived small RNAs (rsRNA-28S), which might be essential in composing a sperm RNA 'coding signature' that is needed for paternal epigenetic memory. Finally, we show that Dnmt2-mediated m5C contributes to the secondary structure and biological properties of sncRNAs, implicating sperm RNA modifications as a novel layer of paternal hereditary information.

### **Uterine Epithelial Immune Response Upon the Initial Embryo-Maternal Physical Interactions During Implantation Initiation.** Xiaoqin Ye, Zidao Wang, Christian Lee Andersen, and Yuehuan Li

Embryo implantation is a mandatory initial step for successful pregnancy in mammals. How a uterus transiently transforms into a receptive state (uterine receptivity) for embryo implantation is the least well understood step during pregnancy. Uterine epithelium is the first maternal contact for an implanting embryo and their initial physical interactions are crucial for successful implantation. Implantation initiation involves embryo apposition and adhesion to the uterine luminal epithelium (LE). To understand the molecular changes in the LE during implantation initiation, we use mouse as a model, which has implantation initiation ~gestation day 4.0 (D4.0), to profile gene expression in D3.5 (preimplantation) and D4.5 (post-implantation initiation) LE. Microarray reveals an overall downregulation of chemokine mRNA levels in the 4.5 LE compared to D3.5 LE, although mRNA levels of different chemokines vary greatly in the peri-implantation LE. Of the 36 CXCL and CCL chemokines in the

microarray, 21 (58.3%) show significant downregulation and none shows significant upregulation in D4.5 LE. Among the 19 chemokine receptors in the microarray, 12 (63.2%) are significantly downregulated and none is upregulated in D4.5 LE. Co-immunostaining of E-cadherin (epithelial marker) and vimentin (mesenchymal marker) in D0.5~D4.5 uteri indicates peak presence of vimentin-positive cells in the D1.5 LE, which also has massive apoptosis detected by in situ end-labeling plus (ISEL+), but not in D3.5, D4.0, or D4.5 LE, which rarely has apoptotic cells detected by ISEL+; vimentin-positive cells line up the LE subepithelial area in D4.0 and D4.5 uteri but not D0.5~D3.5 uteri. Although the identity of these migrating vimentin-positive cells have not been determined, they are most likely leukocytes. Vimentin-positive cells do not infiltrate into the LE but line up the LE subepithelial area when embryo implantation initiates ~D4.0, and there is an overall downregulation of mRNA levels for chemokines and chemokine receptors in D4.5 LE compared to D3.5 LE, suggesting that the immune response in the LE is checked to facilitate the attachment of an embryo, which is either a semiallograft or an allograft (for a surrogate uterus). Meanwhile, we have identified a novel phenomenon that uterine epithelium becomes more acidic during implantation initiation revealed by LysoSensor Green DND-189 dye (pKa ~5.2), indicative of lysosomal acidification. Lysosome acidity regulates lysosome functions. Chemokines bind to their G protein-linked transmembrane chemokine receptors to exert their biological effects, especially in regulating immune responses. Lysosomes play important roles in endocytic chemokine receptor trafficking that regulates chemokine signaling. We are investigating the functions of uterine epithelial lysosomes in regulating uterine epithelial immune response upon the initial embryo-maternal physical interactions during implantation initiation. (Supported by NIH R15HD066301, and NIH R01HD065939 (co-funded by ORWH & NICHD))

**Maternal Obesity Due to Diet or Loss of Satiety Differentially Impacts Fetal Growth and Placental Efficiency Which May be Due to Differences in Excess Circulating Lipids.** Andrea R. McCain, Alana L. Rister, Miranda E. Wordekemper, Eric D. Dodds, and Jennifer R. Wood

Obesity affects 33% of reproductive age women and 17% of children in the US. It is well documented that maternal obesity negatively impacts fetal development and thereby increases childhood risk for obesity and metabolic syndrome. Multiple genetic and diet-induced mouse models of obesity are currently used to study obesity effects on fertility and developmental programming. We use the lethal yellow mouse, which develops progressive obesity due to a deletion mutation on the C57BL/6 (B6) genetic background that inhibits satiety (LY model). Alternatively, obese phenotypes are induced in B6 mice using Western diet with 42% of kilocalories from fat and 34% sucrose by weight (DIO model). We hypothesized that LY and DIO female mice are metabolically different resulting in distinct effects on fetal and placental growth. To test this hypothesis, age-matched LY (n=7), DIO (n=5), and lean control (B6, n=6) females were mated with lean B6 males, pregnancy was confirmed, and dams were euthanized on day E12.5 of gestation. Maternal blood serum was collected, extracted using methanol-chloroform, and purified into polar and non-polar fractions with 50% methanol/water and 100% methanol. Maternal visceral adipose tissue was weighed and liver was cryopreserved and lipid droplets detected in transverse sections with BODIPY. Individual fetuses and placentas were weighed, tail somites counted, and fetal/placental weight ratios calculated. Fetuses were genotyped to determine gender and phenotyped to distinguish between LY and B6 fetuses. When the fractionated serum was subjected to mass spectrometry, there were several significant (P 0.2). Thus, intrauterine growth restriction is a phenotype of LY but not DIO fetuses. Based on these collective data, the model for attaining obesity

differentially impacts the metabolic profile of the dam, growth of the fetus, and efficiency of the placenta. Thus, the mechanism of obesity development should be considered a key factor when studying its impact on placental function and programming of the offspring. Supported by UN Foundation funds.

**A Method to Estimate Relative Telomere Length for Breeding and Reintroduction Management in 27 Taxonomically Diverse Avian Species.** Haleigh Wood, Patricia Byrne, and Thomas Jensen

Telomere length shortens with chronological age due in part to the accumulated damage from cell division. Studies on wild avian species have shown that other factors such as stress, diet, and health can increase or decrease the rate of telomere shortening and therefore have a significant effect on life expectancy. The possibility of estimating life expectancy, the effects of long-term stress, and other environmental factors could help determine the best individual candidates for breeding or reintroduction. We describe a universal method that can be easily adapted to a broad range of species, providing a unique new tool for the management of captive bird breeding populations.

Individuals of known age representing 27 species in 13 orders (Galliformes, Anseriformes, Phoenicopteriformes, Eurypygiformes, Columbiformes, Cuculiformes, Gruiformes, Cathartiformes, Accipitriformes, Bucerotiformes, Coraciiformes, Psittaciformes, Passeriformes) were sampled to develop control (18S) and to verify the previously described telomere (tel1b/tel2b) qPCR primers. gDNA was isolated from frozen blood samples and qPCR amplified to determine the relative telomere length (RTL). We designed and tested five different 18S primer sets to identify the pair with the highest multi-species efficiency. The efficiency of the telomere primers has been verified in previous studies. The relationship between RTL vs. chronological age was established using the coefficient of determination ( $R^2$ ) for four species with six to 50 individual samples covering multiple ages.

The average qPCR efficiency for the 18S primers for all species was  $94.7\% \pm 1.2$  and ranged from 85.2% to 107.6% across the species. The  $R^2$  values for chronological age vs. relative telomere length were 0.074 for nene (*Branta sandvicensis*), 0.003 for alala (*Corvus hawaiiensis*), 0.407 for blue and gold macaw (*Ara ararauna*), and 0.256 for blue-bellied rollers (*Coracias cyanogaster*).

We successfully developed a technique to detect and measure relative telomere length in a taxonomically broad range of avian species. Our data (low  $R^2$  values) suggest that relative telomere length may not be as useful for chronological age estimation in captive populations as it has been reported to be in wild populations. This discrepancy could be due to variability in different individuals' response to physiological challenges, such as long-term stress from captivity, proximity to conspecifics, other species, or visitors. Furthermore, because dam age influence offspring telomere length and captive females continue to breed at ages older than wild females, there could be more variability in captive chicks. It may be that monitoring the rate of telomere shortening, rather than relative telomere length at any given time, is a better measure of physiological stress and or life expectancy. We anticipate that this technique can be used in captive avian management for long-term stress monitoring, life expectancy estimation, and determining the individuals best suited for breeding and reintroduction.

**Chorioallantoic Membrane Culture Increases the Percent of Live Cells in Cryopreserved Transgenic Quail (*Coturnix Coturnix*) Testicular Tissue.** Jonathan Molina, Patricia Byrne, Haleigh Woods, and Thomas Jensen

A population's genetic diversity can be at risk when genetically valuable animals die before reproducing. Gonads from genetically valuable non-reproductive animals, collected during necropsy, could potentially be used in future assisted reproductive technologies (ART) as they contain germline stem cells (GSCs). GSCs represent future gametes that, if successfully matured, can effectively extend the deceased's reproductive lifespan, by contributing to the future gene pool. Cryopreservation increases the utility of post-mortem collected gonads, as the tissue can be stored and revitalized at a time convenient for ART, such as transfer of GSCs to host embryos. However, cryopreservation is harmful to cells and tissues, making an effective post-thaw recovery protocol necessary. We devised a technique utilizing the chorioallantoic membrane (CAM) of developing quail embryos as an in-ovo culture system for post-thaw recovery of cryopreserved transgenic quail testicular tissue. The CAM is a well-vascularized extra-embryonic membrane previously shown to be very receptive to foreign tissue transplantation.

Testes tissue pieces from quail (*Coturnix coturnix*) expressing the transgene *dendra2* (fluorescent protein) were cryopreserved in 10% DMSO, thawed at 41°C using a step-wise cryo-protectant dilution protocol (7.5%, to 5% and 0% DMSO), and cultured 24hrs in plating medium overnight (41°C, 5% CO<sub>2</sub>). Tissues were transplanted onto the CAM of HH stage 30-31 quail embryos and incubated for seven days. Transplanted tissues were recovered, dissociated into single cell suspension and stained with propidium iodide to determine percent live cells. In addition, FL1 median fluorescence intensity (MFI) was measured by flow cytometry to confirm *dendra2* protein expression. Testes from two *dendra2* transgenic quail were used for the CAM transplants (n=42).

Fresh tissue survival was 91.3%±0.7, post-thaw 54.3%±0.6, 24-hour culture 36.7%±0.6, and post CAM transplant tissue survival was 86.5%±1.1. The average MFI for fresh transgenic testes was 6,244±1,724, thawed transgenic tissue 800.5±50.5, 24-hour culture 2,840±179, and after CAM transplant 8,454±117.

Transgenic quail testes pieces exhibited a significant decrease in survival post-thaw, which continued to decline through 24 hours of post-thaw culture (ANOVA, Tukey post hoc analysis df=7, F=1104.25, p < 0.001). This is likely due to apoptotic cell death which takes time to manifest. Subsequent CAM transplantation increased the percent live cells to levels similar to, but significantly lower (p=0.04), than fresh levels. This is most likely due to clearing of dead cells rather than cell proliferation. At thaw the MFI decreased significantly (df=7, F=15.49, p < 0.04), indicating that the fluorescent protein had degraded during cryo-preservation. Following 24hr culture and CAM transplantation the MFI increased to fresh tissue levels (p=0.39), demonstrating that *dendra2* protein was being synthesized. The increase in percent live cells and the increase in MFI indicates that the tissue is healthy. In conclusion, in ovo CAM culture is a useful technique for recovery of cryopreserved testicular tissue.

**Xenotransplantation of Gonadal Tissue onto the Chicken CAM: A Model for Avian Germplasm Preservation.** Patricia Byrne, Kathryn Storey, and Thomas Jensen

A challenge facing efforts to conserve endangered species is the death of a genetically valuable individual before it reproduces and contributes to the gene pool. A promising solution to this potential

loss of biodiversity is the xenotransfer of genetically valuable germline stem cells to host embryos. However, keeping donor tissue alive until xenotransfer is critical. Here we describe the development of a method for xenotransplantation of donor testes onto the chorioallantoic membrane (CAM) of chicken embryo hosts to maintain tissue viability. Previous studies have used xenotransplantation onto chicken CAMs as a model to investigate tumor angiogenesis during cancer. Our approach is novel in the use of CAM transplantation as a method for conservation of gonadal tissue of avian species.

Pieces of testes from adult quail were xenotransplanted onto HH stage 31-32 host chicken embryo CAMs, followed by recovery at stage 40. We tested different fenestration methods (air cell or side of the egg), angiogenesis promoting methods (agitation of blood vessels or addition of VEGF [Vascular endothelial growth factor]), VEGF application methods (injection into transplant, on tissue surface, or onto filter paper placed beneath the transplant), and inner shell membrane over transplant removed or not. Techniques were evaluated by gross morphological examination of transplants for blood vessel formation and host embryo survival.

The overall survival rate of the host embryos was 63.8% (249/390) across all treatments. Of the embryos that survived, 31.7% had vascularized transplanted tissue. There was no difference in survival (2-tailed chi-square test  $p=1.00$ ) of the host embryo between fenestration through the side (66.7%,  $n=60$  embryos) or the air cell (65.9%,  $n=167$  embryos) with agitation of the CAM blood vessels and replacement of inner shell membrane following transplantation. There was no difference in percent of vascularized tissue ( $p=0.5971$ ) for side fenestration (32.5%) or air cell fenestration (40.9%). We therefore used air cell fenestration (ease of method), CAM agitation and inner shell membrane replacement following transplantation for statistical comparison between a variety of VEGF and agitation treatments outlined below.

Removal of the inner shell membrane and agitation of CAM ( $n=40$  embryos) resulted in a 75% survival ( $p=0.6831$ ) and 26.7% vascularization ( $p=0.4183$ ). Placement of transplant onto VEGF (1ng) soaked Whatman paper (to keep transplant from moving during incubation;  $n=66$  embryos) resulted in a 71.2% survival ( $p=0.7342$ ) and 8.5% vascularization ( $p=0.0021$ ). Injection of VEGF into transplant (1ng;  $n=45$  embryos) resulted in a 37.8% survival ( $p=0.0819$ ) and 52.9% vascularization ( $p=0.6440$ ). Application of VEGF topically to transplant and placed onto Whatman paper ( $n=9$  embryos) resulted in a 33.3% survival ( $p=0.3776$ ) and 0% vascularization ( $p=0.2819$ ). The air cell fenestration with CAM agitation and inner shell membrane replacement method was further evaluated yielding  $24.9\% \pm 4.6$  (mean  $\pm$  SEM) live cells by propidium iodide (PI) staining and flow cytometry.

In conclusion the most successful and practical method was air cell fenestration with CAM agitation and inner shell membrane replacement following transplantation. This method resulted in high donor tissue survival rates, making xenotransplantation of testes a viable method for future use in assisted reproductive technologies.

**Cold Storage Prior to in Vitro Culture is Beneficial to Cat Ovarian Tissue.** Dragos Scarlet, Gustavo Desire Antunes Gastal, Claudia Höchsmann, Ingrid Walter, and Christine Aurich

In vitro culture (IVC) of ovarian tissue is a promising approach to recover fertility of humans, domestic animals, and endangered species. The domestic cat (*Felis catus*) is an excellent model to study fertility

preservation of endangered felids and ovarian specimens can easily be collected during routine spaying. However, transportation of ovarian specimens to specialized centers might be required to perform IVC of ovarian tissue. Moreover, the adaptation process of the ovarian tissue from in vivo to in vitro environment may disturb cell metabolism. The aim of this study was to investigate the effects of storing fresh cat ovarian tissue at 4°C for 24h prior to IVC on the morphology and functionality of feline preantral follicles. Ovarian cortical tissue from domestic cats (n=90 fragments, 5 replicates) was dissected using scalpels and a Thomas Stadie-Riggs Tissue Slicer to produce thin slices (1 x 1 x 0.5 mm). Fragments were randomly distributed among the treatment groups: fresh control (0h), fresh IVC 1 day (fresh-IVC1), fresh-IVC7, stored (4°C for 24h) control, stored-IVC1, and stored-IVC7. Fragments were stored and cultured (38.5°C and 5% CO<sub>2</sub>) within MEM medium containing 2 mM L-glutamine, 50 µM ascorbic acid, 10 µg/ml insulin, 5.5 µg/ml transferrin, 5 ng/ml selenium, 0.3% polyvinyl alcohol, 10 µg/ml FSH, 10 ng/ml EGF, 100 µg/ml penicillin, 100 µg/ml streptomycin, and 25 mM HEPES. Culture medium was replaced every other day. All fragments were fixed in 4% formaldehyde for morphological analysis and immunohistochemistry assay (EGFR and Bcl-2 protein expression). Statistical differences among groups were analyzed by Kruskal–Wallis test and Mann–Whitney U test. Overall, 3542 preantral follicles were recorded. The percentage of total normal follicles did not differ ( $P > 0.05$ ) between fresh control ( $65.3 \pm 9.3$ ) and stored control ( $68.6 \pm 11.5$ ), and between fresh-IVC1 ( $28.6 \pm 4.1$ ) and stored-IVC1 ( $34.7 \pm 5.0$ ) groups. However, stored-IVC7 group had higher ( $P < 0.05$ ) percentage of total normal follicles compared to fresh-IVC7 group ( $40.3 \pm 19.6$  and  $7.0 \pm 8.4$ , respectively). Moreover, stored-IVC7 had greater ( $P < 0.05$ ) percentage of normal developing follicles compared to fresh-IVC7 ( $49.9 \pm 12.2$  and  $6.9 \pm 3.4$ , respectively). EGFR was expressed in stroma and granulosa cells of all preantral follicle classes in both fresh and stored cat ovarian tissue treatment groups. However, stored-IVC7 had stronger EGFR expression compared to fresh-IVC7 group. Bcl-2 expression was similar among all treatment groups and limited to stroma cells. In conclusion, our results demonstrate that cold storage of cat ovarian tissue prior to in vitro culture may be beneficial for adaptation to the medium, as demonstrated by higher EGFR expression, better follicular development and morphology. Nevertheless, the effects of transportation and/or storage on fresh cat ovarian tissue and its capability to resume folliculogenesis after in vitro culture and/or cryopreservation warrant further investigation.

**Dietary Supplementation with L-Arginine to Gilts Between Days 14 and 25 of Gestation Enhances Placental Expression of Angiogenic Proteins.** Mohammed A. Elmetwally, Xilong Li, Gregory A. Johnson, Robert C. Burghardt, Cassandra Herring, Fuller W. Bazer, and Guoyao Wu

Dietary supplementation of gilts with 0.4 or 0.8% L-arginine (Arg) between Days 14 and 25 of gestation enhances placental angiogenesis and embryonic survival. However, the underlying mechanisms are largely unknown. This study tested the hypothesis that Arg supplementation stimulated placental expression of proteins related to angiogenesis: endothelial nitric oxide synthase (eNOS), vascular endothelial growth factor (VEGF), placental growth factor (PGF), GTP cyclohydrolase-I (GTP-CH), and ornithine decarboxylase (ODC). Gilts were checked daily for estrus with boars and bred at onset of their second estrus and 12 h later (the time of breeding = day 0 of gestation). Between Days 14 and 25 of gestation, 10 gilts/treatment were housed individually and fed twice daily 1 kg of a corn-soybean meal-based diet supplemented with 0.0, 0.4, or 0.8 % Arg. All diets were made isonitrogenous by addition of L-alanine. On Day 25 of gestation, gilts were hysterectomized to obtain conceptuses for histochemical and biochemical analyses. eNOS and VEGF receptor-1 proteins were localized in the wall of blood vessels

at the maternal placental interface. Compared with the control, dietary supplementation with 0.4 or 0.8% Arg increased ( $P < 0.05$ ) the amounts of NOx (nitrite plus nitrate) and polyamines (putrescine plus spermidine plus spermine) in allantoic and amniotic fluids; placental concentrations of PGF, NOx, polyamines and BH4; placental syntheses of NO and polyamines; and placental activities of GTP-CH and ODC1. Collectively, these results indicate that dietary Arg supplementation to gilts between Days 14 and 25 of pregnancy increase placental angiogenesis by increasing the expression of genes for angiogenic proteins.

**TP53BP1 Regulates Chromosome Alignment and Spindle Bipolarity by Controlling MTOCs During Meiosis in Oocytes.** Zhe-Long Jin, Suk Namgoong, and Nam-Hyung Kim

Meiotic oocytes lack classic centrosomes; therefore, bipolar-spindle assembly depends on the clustering of acentriolar microtubule-organizing centers (MTOCs) into two poles. Tumor suppressor P53-binding protein 1 (TP53BP1) is a known mediator in DNA damage response. Recent studies have revealed a new role of TP53BP1 in maintaining centrosome integrity in mitosis. However, the role of TP53BP1 in oocyte meiosis is unclear. Our results show that TP53BP1 involved in the establishment of chromosome alignment and spindle bipolarity by controlling the clustering of MTOCs during oocyte maturation. TP53BP1 was localized in the cytoplasm and concentrated around the spindle/chromosome region. TP53BP1 was also required for the clustering of MTOCs into two spindle poles during pro-meiosis I. Deletion of TP53BP1 induced perturbation in MTOC-localized Aurora Kinase A (AURKA). The knockdown of TP53BP1 induced microtubules to dis-attach from the kinetochores and increased the rate of aneuploidy. Taken together, our data show that TP53BP1 plays crucial roles in chromosome stability and spindle bipolarity during meiotic maturation by regulating the clustering of MTOCs.

**Influence of Retinoic Acid on Cryopreserved Lamb Testicular Explants After in Vitro Culture.** M. M. Molloy, M. E. Brown, E. Escobar, A. A. Aguirre, B. S. and Pukazhenth

The majority of wild ungulate species are threatened or endangered by extinction. Populations managed in zoos and breeding centers serve as 'insurance' for species sustainability and future reintroductions. However, 10-15% of animals born in ex situ collections die before reaching puberty and, thus, fail to contribute to conservation breeding. Understanding the in vitro culture requirements for producing gametes from gonadal tissues could facilitate the rescue of germplasm from genetically valuable individuals. Most studies to date have focused on the laboratory mouse, and there is limited information on larger animal models. Retinoic acid (RA) is the biologically active form of vitamin A and is involved in the early steps of spermatogenesis by promoting meiosis in progenitor cells and proliferation and/or differentiation of gonocytes (G) and Sertoli cells (SC) in various species. We hypothesized that RA would promote G and SC proliferation in testicular explants that were cryopreserved and thawed before culture. Testicular pieces (1-2 mm<sup>3</sup>) from 6-7 week-old lambs ( $n = 4$ ) were cryopreserved in Minimum Essential Medium (MEM) supplemented with dimethyl sulfoxide and fetal bovine serum (FBS) at 3:1:1 (v/v) ratio. Tissues were thawed at room temperature (1 minute), then in water (25°C; 1 minute), followed by three washes (5 minutes each) in MEM containing 20% FBS, 25 mM HEPES, and antibiotics. Thawed explants (5 pieces/treatment/week/lamb) were cultured for 5 weeks in the absence (0 mM, control) or presence (1 mM, 2 mM, or 5 mM) of RA. Specifically, tissues were cultured on agarose blocks in MEM supplemented with 10% (v/v) FBS, sphingosine-1-phosphate (2 mM; for the first 2 weeks), insulin (2 mg/ml), transferrin (1.1 mg/ml), selenium (1 mg/ml), pyruvate (0.1 mM), glutamine (2 mM)

and antibiotics. Tissues were harvested weekly and assessed histologically. Twenty tubules of uniform size per piece were evaluated for the number of Gs and SCs. Analyses were by ANOVA followed by a Dunnett's post-hoc comparison. There was no influence ( $P > 0.05$ ) of RA on G proliferation, but G numbers per tubule increased ( $P = 0.03$ ) with time in culture for weeks 1 through 3 compared to week 0. Both RA and culture duration had an impact on SC number per tubule ( $P = 0.02$ ,  $P = 0.003$ , respectively). Lower RA concentrations (1 mM and 2 mM) had no effect on SC number per tubule ( $12.9 \pm 0.6$ ,  $12.9 \pm 0.7$ , mean  $\pm$  SEM, respectively) and 5 mM RA was detrimental ( $12.4 \pm 0.7$ ;  $P = 0.04$ ). Compared to control week 0 ( $14.2 \pm 1.1$ ), weeks 1 through 3 had higher ( $P < 0.05$ ) in SC number in week 4 and 5. Results demonstrate that 1) in vitro culture of cryopreserved lamb testicular explants in serum-free medium promotes SC proliferation for 3 weeks, and 2) RA failed to promote G or SC proliferation and/or differentiation in lamb testes.

**Mice with Patched1 Deletion in Pituitary Folliculo-Stellate Cells Exhibit Adult Onset Hypogonadotropic Hypogonadism.** Yi Athena Ren, Teresa Monkkonen, Daniel J. Bernard, Helen Christian, Mike T. Lewis, Carolina Jorgez, Joshua Moore, Swarnima Singh, Ik Sun Kim, Xiang Zhang, and JoAnne S. Richards

One of eight couples in the United States suffers from infertility, and more than a third of the cases are idiopathic (with unknown causes). Recently, we discovered that in addition to their traditional roles in host defense, immune cells may play a previously underappreciated role in regulating fertility and pituitary endocrine function. Herein we report adult onset hypogonadotropic hypogonadism in a genetically engineered mouse line with conditional deletion of the hedgehog signaling receptor Patched1 (Ptch1) using S100a4 promoter-driven Cre recombinase expression. Mice carrying combinations of S100a4Cre and Rosa26mTmG (R26mTmG) with or without Ptch1fl/fl alleles were generated to provide control (S100a4Cre;R26mTmG) and mutant mice (S100a4Cre;R26mTmG;Ptch1fl/fl; hereafter: Ptch1-cKO). R26mTmG drives expression of a membrane-associated red fluorescent protein mT that is switched to membrane-associated green fluorescent protein (GFP) mG upon Cre-mediated gene recombination, allowing all cells in which this recombination has occurred (GFP+ cells) to be tracked. Using flow cytometry analysis we found that more than 90% of GFP+ cells in the pituitary are CD45+, confirming their identity as immune cells. Transmission electron microscopy of immunogold labeling for GFP further confirmed that Cre expression in the pituitary is restricted to pituitary-specific immune cells, namely folliculo-stellate (FS) cells. Both adult male and female Ptch1-cKO mutant mice exhibit severely reduced circulating gonadotropin levels; reduced expression of mRNA encoding the glycoprotein hormone alpha subunit (Cga), and follicle stimulating hormone and luteinizing hormone beta subunits; as well as significantly reduced pituitary sizes when compared with controls. The reproductive tracts and ovaries in the female mutants are hypotrophic, and the ovaries lack large antral follicles or corpora lutea. When transplanted into the ovarian bursa of control littermates, the ovaries from mutant females displayed large antral follicles and well-formed corpora lutea, indicating ovarian phenotypes in the mutants likely derived from extra-ovarian factors. In the mutant males, sperm counts and epididymis weights were significantly reduced compared to controls, suggesting impaired testis function and testosterone production. Potential effects of Ptch1 deletion in the brain also need to be assessed. Intriguingly, no pituitary or gonadal phenotypes were observed in either sex at 4 weeks of age. The first endocrine abnormality detected in the Ptch1-cKO mutant mice was reduced pituitary Cga expression at 5 weeks of age. This observation suggests that PTCH1 in FS cells may play an important role in pituitary function during pubertal-to-adult transition period. Together, our results provide in vivo

evidence for the importance of FS cell in regulating fertility and pituitary endocrine function. Our studies have the potential to shed light on previously unappreciated causes of infertility conditions such as hypogonadotropic hypogonadism. NIH-HD-076980, T32 HD007165, NSF-1263742, NIH-CA-127857.

### **Reprogramming of Primary Somatic Cells Source From Brain Cancer Patients Using Mrna Tool.**

Kyoung-Ha So, Young Seok Park, Gab-Sang Lee, and Sang-Hwan Hyun

The ability to generate patient's induced pluripotent stem cells (iPSCs) could provide tremendous promises for regenerative medicine. It has reported that choice of reprogramming tools is important for the safety and the increasing efficiency of reprogramming process and transduction. Non-integrating techniques as like mRNA based reprogramming protocols are useful for the production of genetically stable iPSCs while avoiding the risks of genomic integration. In this study, we generate human iPSCs derived from brain cancer patient's fibroblast by mRNA's reprogramming tool. We obtained patient's somatic tissues at brain tumor surgery that informed consent obtained according to institutionally-approved protocols. Patient's primary somatic cells were isolated, and then used as the cell source for iPSCs generation under xeno-free conditions. Reprogramming produced by non-integration methods utilized the combination of reprogramming mRNAs as like Yamanaka's factors (OSKMNL) with evasion mRNAs (EKB) (Stemgent) during four days. Reprogrammed cells were formed the colonies like iPSCs after six days of transduction, and the colonies were expanded until pick-up at day 14. These colonies were stained for pluripotency-associated genes using TRA-1-60 and TRA-1-81 by immunocytochemistry. Established colonies were also expanded without feeder condition and stained with Alkaline Phosphatase. In the further study, generated patient's iPSCs will be required to investigate their availability of the clinical application under xeno-free conditions which could provide a path to good manufacturing practice applicability that should facilitate the clinical implementation of patient- or disease-specific iPSCs therapies.

### **Tracking Human Embryonic Stem Cell with Superparamagnetic Iron Oxide Nanoparticles in Huntington's Disease Rat Model.** Bao Tram Tran, Hyeong Cheol Moon, Sang-Hwan Hyun, Kyoung-Ha So, and Young Seok Park

Stem cell therapy is a potential therapeutic strategy in Huntington's disease. Previous studies suggested that human embryonic stem cells transplantation can lead to a behavioral recovery in quinolinic acid-induced Huntington's disease rodent models. Other group showed that mesenchymal stem cell transplanted into the striatum of quinolinic acid rat model could be observed by 1.5 Tesla MRI by labeling with superparamagnetic iron oxide nanoparticles (SPIONs) in the long-term period up to 60 days. The objectives of this study were to track human embryonic stem cell labeled by SPIONs and to determine whether human embryonic stem cell transplantation can improve motor dysfunction in AAV2 Htt171-82Q transfected Huntington rat model. The infected rats (n=10) were injected AAV--2- Htt171-82Q, and the sham rats (n=10) were injected PBS into the right striatum. After six weeks, all the rats were transplanted human embryonic stem cells into randomly left or right striatum (n=5 per group). We performed cylinder test and stepping test every two weeks after AAV<sub>2</sub> Htt171-82Q injection and stem cells transplantation. Stem cell tracking was performed once per two weeks using T2 and T2\*-weighted image at 9.4 Tesla MRI. We also performed immunohistochemistry and immunofluorescence staining to

detect the presence of human embryonic stem cell markers, huntingtin protein aggregations and iron in the rat striata. The results showed that the injection of AAV<sub>2</sub> Htt171-82Q induced motor dysfunction in transfected rats. After embryonic stem cells injection, the transfected Huntington rats exhibited a significant behavioral improvement in stepping test compared to the sham rats. We observed human embryonic stem cell labeled by SPIONs using 9.4 Tesla MRI and the presence of iron using Prussian Blue staining at the injected site in all groups and non-injected site in contralateral Huntington group but not in ipsilateral Huntington group and sham groups. We also observed huntingtin protein aggregations using EM48 immunostaining at injected site. In summary, the present study showed that human embryonic stem cell labeled by SPIONs could be tracking by 9.4T MRI and transplantation of the stem cell also can lead to a behavioral improvement in stepping test in AAV--2 Htt171-82Q transfected Huntington rat model. Further studies will be required to investigate more about the effect of human embryonic stem cell in Huntington animal models and the ability of stem cell tracking by MRI at other magnets strengths and using other nanoparticles.

Acknowledgments: This work was supported by the National Research Foundation of Korea (NRF) funded by the Korea government (Ministry of Science and ICT, MIST) (NRF-2016H1D5A1908909, NRF-2014K1A3A1A21001372, NRF-2015H1D3A1066175, and NRF-2016R1D1A1B03933191), Republic of Korea.

#### **Ovarian Cortex from High A4 Cows Secrete Excess Steroid Hormones Contributing to Arrested Follicle Development, Increased Oxidative Stress and Fibrosis Which can be Rescued by Angiogenic**

**VEGFA165.** S. A. Springman, M. A. Abedal-Majed, M. L. Hart, V. Largen, M. P. S. Magamage, S. G. Kurz, K. M. Sargent, J. Bergman, R. M. McFee, R. A. Cushman, J. S. Davis, J. R. Wood, and A. S. Cupp

We identified a population of cows within the UNL physiology herd characterized by excess androstenedione (A4; High A4) in follicular fluid, anovulation, 17% reduction in calving rate and 43-fold higher A4 secretion from ovarian cortex cultures. We also demonstrated that genetically un-related heifers at the U. S. Meat Animal Research Center (14 out of 17 tested) secreted 18-fold greater A4 into media from ovarian cortex cultures; suggesting, that the High A4 phenotype may be present in other herds. We hypothesized that ovarian folliculogenesis is disrupted in High A4 cows due to excess A4 synthesis by the ovarian microenvironment; and vascular endothelial growth factor A (VEGFA) isoform treatment would rescue folliculogenesis by decreasing A4 production. Ovarian cortical pieces were collected from High A4 (n = 5) and Control (n = 5) cows at ovariectomy and treated with PBS or VEGFA165 (50 ng/ml) for 7 days. Media was collected daily for steroid analysis. Ovarian cortex from High A4 cows treated with PBS secreted greater (P = 0.004) concentrations of A4 and other steroids and steroid metabolites including 11-deoxycorticosterone, 11-deoxycortisol, 17-OHP, androsterone, DHEA-S, DHT, E2, P4, and testosterone compared to controls. Concentrations of A4 and other steroids and metabolites in blood plasma were not different in High A4 cows compared to controls. Treatment with VEGFA165 dramatically (P = 0.004) reduced the concentration of A4 and other steroid hormones secreted by the ovarian cortex of High A4 cows. Numbers of primordial follicles were greater (P = 0.004); however, there were fewer primary (P = 0.01), secondary (P = 0.0001) and antral follicles (P = 0.008) in uncultured High A4 cow ovarian cortex when compared to Control cows. Treatment with VEGFA165 for 7 days stimulated greater follicular progression to the secondary (P = 0.0005) and antral (P = 0.02) stages in ovarian cortex from Control cows than High A4 cows. Further, ovarian cortex treated with PBS from

High A4 cows had increased staining for markers of oxidative stress and fibrosis. Treatment with VEGFA165 reduced staining for oxidative stress and tended ( $P = 0.056$ ) to reduce staining for fibrosis in High A4 ovarian cortex compared to controls. Taken together, these results indicate that the ovarian cortex from High A4 cows secrete greater concentrations of steroid hormones which may contribute to increased oxidative stress and fibrosis, leading to follicular arrest. VEGFA165 isoform treatment can rescue follicle development and reduce ovarian cortex steroid secretion. Thus, VEGFA165 may be a potential therapeutic to restore the ovarian microenvironment and enhance follicular maturation. This research was funded through USDA grant 2013-67015-20965. USDA is an equal opportunity provider and employer.

### **Prefoldin-5 is a Novel, Mirna Regulated Cell Survival Factor in the Pathogenesis of Endometriosis.**

Warren B. Nothnick, Tommaso Falcone, and Amanda Graham

**INTRODUCTION:** Endometriosis is a common disease in women of reproductive age in which endometrial tissue establishes and survives in ectopic locations, yet its pathogenesis is poorly understood. Utilizing differential proteome screening, we identified prefoldin-5 (PFDN5) as a novel factor associated with endometriotic epithelial cell survival. As the role of PFDN5 in the pathophysiology of endometriosis is essentially unknown, the objective of the current study was to define PFDN5 expression as well as explore its regulation and function in human endometriotic tissue and cells.

**METHODS:** mRNA/miRNA expression and protein localization were assessed in paired peritoneal endometriotic lesion/ovarian endometrioma tissue and matched eutopic endometrium from women with endometriosis ( $N = 48$  subjects which provided a total of 55 red peritoneal lesions and 10 ovarian endometriomas, with multiple lesions from 10 of the 48 subjects). miRNA regulation of PFDN5 and functional impact of PFDN5 on cell survival were assessed in vitro using the endometriotic epithelial cell line, 12Z, while whole tissue correlation between PFDN5 and markers of proliferation were also evaluated. Initial analysis of data controlling for stage of menstrual cycle and stage/severity of endometriosis revealed no influence of either on outcomes. As such, data were analyzed as ectopic peritoneal lesions versus matched eutopic and ovarian endometrioma versus matched eutopic.

**RESULTS:** PFDN5 was expressed in both eutopic and ectopic lesion tissue. Peritoneal lesion PFDN5 expression was significantly greater (2.4-fold change;  $P < 0.001$ ) compared to matched eutopic tissue, while ovarian endometrioma expression of PFDN5 was not significantly different compared to matched eutopic endometrium (1.21-fold increase;  $P = 0.29$ ). PFDN5 protein localized predominantly to epithelial cells in both eutopic and ectopic tissue. Peritoneal red lesion, but not ovarian endometrioma tissue PFDN5 expression positively correlated with that of cell proliferation/survival markers c-Myc, ( $R=0.5811$ ;  $P < 0.001$ ) and RPLP1 ( $R=0.7112$ ;  $P < 0.001$ ). Knockdown of PFDN5 by transient transfection of 12Z cells was associated with a reduction in cell survival (47% compared to controls;  $N=3$ ;  $P < 0.05$ ). As our preliminary assessment suggested that PFDN5 translation appeared to be regulated by miRNAs, we evaluated its regulation in 12Z cells by miR-182-5p, a proposed modulator of PFDN5, which is expressed in human endometriotic lesion tissue. Transfection of 12Z cells with miR-182-5p mimics resulted in a significant up-regulation of miR-182-5p which was associated with a significant ( $P < 0.05$ ), 45% reduction in PFDN5 expression in vitro. In endometriotic peritoneal lesion tissue, but not ovarian

endometriomas, an inverse relationship between miR-182-5p and PFDN5 expression was detected supporting our in vitro findings.

**CONCLUSIONS:** The average level of PFDN5 expression is significantly elevated in endometriotic peritoneal lesion tissue, but not in ovarian endometriomas. Peritoneal lesion PFDN5 expression positively correlates with expression of cell survival markers and may contribute to lesion survival. PFDN5 is regulated by miR-182-5p and an inverse relationship between the two was detected in human peritoneal lesion, but not ovarian endometrioma tissue. Our observations support a role for PFDN5 and its regulation by miR-182-5p, in the pathophysiology of endometriosis, which may be more relevant in peritoneal lesions compared to ovarian endometriomas.

#### **Identification of Adult Stem Cells in Mouse Endometrium.** Shiyong Jin

The uterus is a highly regenerative organ, its endometrium, which is composed of epithelia and stroma, continually cycles through phases of cell proliferation, differentiation, and degeneration in response to steroid hormones secreted from the ovary throughout a female's reproductive life. Adult stem cells that may support this cyclical regeneration have been proposed years ago, but the existence, identity and roles of these proposed stem cells remain unknown. To directly address this question, I have established a CreERT2-LoxP based single-cell lineage tracing system in mouse endometrium, by which, single epithelial cell was genetically labeled, and its fate could be traced over cycles. Some cells with a highly proliferative potential in the mouse endometrial epithelium have been identified, which capable of surviving uterine degeneration and continually produce epithelial lineages over multiple estrous cycles. These characteristics make this cell population be a potential candidate of the proposed epithelial stem cells in mouse uterus. Further work will be conducted to address the identity and function of this cell population in uterine homeostasis and regeneration. This work provides the first in vivo direct evidence for the existence of potential adult stem cells in the mouse uterus.

#### **Environmental Toxicant Exposure Promotes an Exaggerated Inflammatory Response to Infection Mimic in Organ-on-a-Chip Model of Human Fetal Membranes.** Tianbing Ding, Juan S. Gnecco, Ava M. Wilson, David M. Aronoff, Kaylon Bruner-Tran, and Kevin G. Osteen

In spite of decades of animal and human research, preterm birth (PTB) remains a leading cause of child mortality and morbidity. Although infection-related inflammation frequently contributes to the risk of PTB, the presence of an infection alone is not sufficient to predict its occurrence. However, certain women are more susceptible to bacterial-induced PTB, often in association with premature rupture of the fetal membrane (PPROM). Recent human population studies have shown that women living near point sources of combustion-associated environmental toxicants have an increased risk of PTB in the absence of other known risk factors. At this juncture, human population studies have not addressed whether an environmental toxicant exposure history might also impact infection-related risk for a poor pregnancy outcomes. Our previous murine studies have demonstrated that nearly 40% of adult female mice with a history of developmental TCDD exposure exhibit spontaneous PTB. However, when additionally exposed to a low level viral or bacterial infection, 100% of TCDD exposed mice will deliver preterm. In contrast, control mice were resistant to the same low dose infections and all pregnancies

progressed to term delivery. To potentially translate our murine-based PTB findings to women; herein, we utilized an ex vivo culture of human fetal membrane (FM) tissues and a novel instrumented organ-on-a-chip model of the fetal membrane (IFMOC). First, using FM punch biopsies prepared from non-laboring, term placentae maintained in culture for 48 hrs, we found that TCDD pretreatment led to elevated pro-inflammatory cytokine release (IL-1 $\beta$ , TNF- $\alpha$ , IL-6, IL-8) following a secondary lipopolysaccharide (LPS) treatment compared to LPS in the absence of TCDD. While LPS treatments stimulated both pro-inflammatory and anti-inflammatory cytokine release in FM tissues, the balance between pro-and anti-inflammatory cytokine expression significantly favored pro-inflammatory cytokines. Specifically, levels of IL-1 $\beta$ , TNF- $\alpha$ , IL-6, IL-8 were 5-10 fold higher than levels of IL-10, a protein secretion pattern confirmed by FM tissue mRNA analysis. The combination of TCDD and LPS exposures also decreased E-cadherin expression in amniotic epithelial cells, suggesting a potential loss of cellular integrity as observed in PPROM. We next utilized a recently established two-chamber microfluidic culture system, the IFMOC, which allows long-term studies of the in vivo-like paracrine signaling relationships among resident cell types. Using the IFMOC, we confirmed and extended our FM findings, demonstrating that TCDD treatments, followed by LPS exposure, increased the secretion of inflammatory cytokines as well as matrix metalloproteinases (MMPs) and physically disrupted the integrity of adjacent amniotic epithelial cells as measured by increased barrier permeability. Taken together, our FM and IFMOC models demonstrated environmental toxicant exposure leads to an enhanced fetal membrane response to an infection, synergistically promoting a PPROM-like phenotype. (Supported by VA BX0025853 and EPA G13L10292).

**Sexual Dimorphism of Preeclampsia-Dysregulated Transcriptomic Profiles and Endothelial Function in Fetal Endothelial Cells.** Chi Zhou, Yan Qin, Qing-Yun Zou, Chanel Tyler, Xin-Qi Zhong, Ronald R. Magness, Ian M. Bird, and Jing Zheng

**INTRODUCTION:** Preeclampsia (PE) is a leading cause of fetal and maternal morbidity and mortality during human pregnancy worldwide. Although PE is considered as a maternal endothelial disorder, evidence indicates that PE also adversely impacts fetal endothelial function. Importantly, PE-offspring are at increased risk of cardiovascular diseases in adulthood, implicating that PE adversely programs fetal vasculature in utero. Fetal sex has been reported to be associated with the risk of preeclampsia. To date, there is limited information on PE-dysregulated genes/pathways in fetal endothelial cells. We hypothesize that preeclampsia alters fetal endothelial transcriptome and disturbs cytokine and growth factor-induced endothelial function in a fetal sex-specific manner.

**METHODS:** Highly purified, unpassaged human umbilical vein endothelial cells (P0-HUVECs) were isolated immediately after delivery from normal term (NT; 39.2 $\pm$ 0.5weeks) and PE (37.5 $\pm$ 0.5weeks) pregnancies with male (M; n=6 for NT & PE) & female (F; n=5~7 for NT & PE) fetuses. Transcriptomic differences between NT and PE P0-HUVECs were identified using RNAseq with an Illumina HiSeq2000 sequencer and further confirmed with RT-qPCR. Bioinformatics and statistical analysis were performed using skewer, STAR, RSEM, and EdgeR software. Functional genomics analysis was performed with ingenuity pathway analysis software to identify pathways that are dysregulated in PE. Multiple testing correction was performed using false discovery rate (FDR) adjustment in all data analyses when

applicable. Cell proliferation, migration, and monolayer integrity assays were performed with passage 1 (~5 days of culture) female and male HUVECs from NT and PE pregnancies (n=5 each fetal sex/group).

**RESULTS:** Compared with NT groups, PE dysregulated 721 and 100 genes in female and male P0-HUVECs, respectively. PE dysregulated eNOS and atherosclerosis signaling pathways-associated genes in a fetal sex-specific manner in P0-HUVECs. TNF-, TGF $\beta$ 1-, TGFBR1-, FGF2, and ESR1-regulated genes are differentially dysregulated in male and female PE HUVECs. Compared with NT HUVECs, the TNF $\alpha$ -/FGF2-induced cell proliferation was attenuated in male, but not female PE cells. TNF $\alpha$  significantly induced cell migration in female and male NT HUVECs; This TNF $\alpha$ -induced cell migration was inhibited in female but was enhanced in male PE HUVECs. TNF $\alpha$  and TGF $\beta$  significantly decreased the endothelial monolayer integrity in both female and male NT HUVECs. PE further reduced the TNF $\alpha$ /TGF $\beta$ -weakened monolayer integrity in female, but not in male HUVECs. Additionally, PE inhibited the FGF2-strengthened monolayer integrity in female, but not in male HUVECs.

**CONCLUSIONS:** PE differentially dysregulates cardiovascular diseases- and endothelial function-associated genes/pathways in female and male fetal endothelial cells. PE also dysregulates fetal endothelial responses to cytokines (TNF $\alpha$  and TGF $\beta$ 1) and growth factor (FGF2) depending on fetal sex. These fetal sex-specific PE-dysregulated genes/pathways in fetal endothelial cells could serve as potential sex specific therapeutic targets and biomarkers for fetal endothelial dysfunctions and increased risk of adult-onset cardiovascular diseases in PE offspring. [AHA 17POST33670283, NIH HD38843, HD038843-14S1, & HL117341]

**Embryonic Outcomes and Sex-Specific Epigenetic Impacts of Low and High Dose Maternal Folic Acid Supplementation in Assisted Reproduction.** Sophia Rahimi, Josée Martel, Gurbet Karahan, Camille Angle, Donovan Chan, and Jacquetta Trasler

Assisted reproductive technologies (ART) are responsible for the conception of up to 6% of children worldwide; however, the use of these techniques has been linked to a greater incidence of adverse outcomes in the offspring, including growth and genomic imprinting disorders. DNA methylation profiles established during germ cell and early embryo development have been shown to be sensitive to these procedures. Importantly, folate from the diet contributes methyl groups essential for the proper establishment of these epigenetic patterns. The goal of this study was to determine whether clinically relevant doses of folic acid supplementation can prevent adverse developmental and epigenetic outcomes associated with ART. Female mice were fed control (2 mg/kg; CD), low (8 mg/kg; 4FASD) or high (20 mg/kg; 10FASD) dose folic acid-supplemented diets for six weeks prior to ART and throughout gestation. Mouse ART involved superovulation, in vitro fertilization, embryo culture and embryo transfer. Upon collection of midgestation embryos and placentas (n = 74-99 embryos/group), we assessed for developmental delay and morphological abnormalities. ART led to an increased proportion of developmentally delayed embryos (12.1% to 24.5%, p=0.02). This proportion was significantly decreased following folic acid supplementation with the 4FASD (11.0%, p=0.03) yet was unaffected by the 10FASD (26.1%). Interestingly, a trend towards an increased proportion of abnormal embryos was observed in the 10FASD group (31.3%) relative to the 4FASD group (18.5%, p=0.09) and craniofacial malformations were more prevalent in the 10FASD group (p=0.08). To better understand the differential effects on embryonic outcomes embryos and placentas were examined at the epigenetic level. We assessed methylation at imprinting control regions (ICRs) of four imprinted genes (Snrpn, Kcnq1ot1,

Peg1, and H19) in matched midgestation embryos and placentas (n = 31-32/group). In both tissues, ART was associated with increased methylation variance and decreased mean methylation at some or all ICRs. Exposure to the 4FASD decreased methylation variance whereas the 10FASD was associated with a significant increase in methylation variance at certain ICRs in embryos and placentas. Furthermore, ART induced female-biased methylation defects at three ICRs (Snrpn, Kcnq1ot1, and H19), which were resolved with low and/or high dose folic acid supplementation. Next we examined genome-wide DNA methylation patterns in midgestation placentas from normal embryos (n = 6 per sex/group) using reduced representation bisulfite sequencing. ART resulted in 12206 and 10102 differentially methylated tiles (DMTs) in male and female placentas, respectively. The majority of DMTs (>90%) exhibited DNA hypomethylation after ART, with females showing larger magnitude methylation changes than males. Folic acid supplementation corrected up to 14.5% of the ART-induced methylation defects in placentas, with more effective correction in males than in females. However, folic acid supplementation was also associated with additional methylation perturbations, which were more pronounced in males than females especially after exposure to the 10FASD. Taken together, our results suggest that low dose folic acid supplementation may be beneficial while high dose supplementation may be deleterious to ART pregnancies. In addition, we report sex-specific epigenetic responses to ART and folic acid supplementation. (Supported by Canadian Institutes of Health Research)

#### **The Role of Tyramine in the Mouse Ovary.** Shelbi Peck, S. M. Bukola Obayomi, and D. Page Baluch

Complications with ovulation are associated with nearly 40% of infertility cases in women each year yet little is known about the causes of ovarian dysfunction. Understanding the signaling pathways that control maturation and release of oocytes from the ovary might provide insight into how signal regulation could be corrected, especially for women experiencing infertility due to ovarian dysfunction. Ovarian follicles possess numerous cell types that share common morphological features with smooth muscle such as the tunica albuginea, chordae, and theca externa. These smooth muscle like cells play a role in the cycling of oocytes within the ovary, and ultimately their expulsion from the follicle. Smooth muscle contraction is modulated by many sources such as neurotransmitters (i.e. norepinephrine), hormones (i.e. epinephrine) and chemicals (i.e. nitrous oxide). This study is focused on an alternative modulator of smooth muscle activity called tyramine which is a monoamine produced in the catecholamine biosynthesis pathway. During catecholamine biosynthesis, dopamine, tyramine, octopamine, and norepinephrine are all derived from the tyrosine precursor. Tyramine is known to be associated with peripheral vasoconstriction, increased cardiac output, and increased respiration which are all affected by smooth muscle activity. Previous studies have shown that the uterus, which is composed of innervated smooth muscle, can be induced to contract by the biogenic monoamine tyramine at levels similar to estrogen. Because tyramine can modulate uterine contractions, this project investigated what affect tyramine may have on the ovary. Ovaries taken from estrus and non-estrus mice were analyzed by HPLC (high-pressure liquid chromatography) and were found to contain higher levels of tyramine prior to ovulation. Additionally, receptors specific to tyramine were found to localize predominantly near tertiary follicles. In order to visualize the effect of tyramine on the ovary in non-estrus mice, ovaries were isolated and briefly treated with physiological concentrations of tyramine, which resulted in induced ovulation and follicle rearrangement. The results of this study confirm the presence of tyramine within the mouse ovary and provide preliminary data suggesting a possible role in

ovulation. Further research into the actions of this monoamine may provide additional insight into understanding the signaling mechanisms involved in ovary function.

**Differential Expression of Proteins in the Wild Type and Dcaf17 Mutant Mice Testis: A Proteomic Analysis.** Abdullah Assiri, Raed Abu Dawud, Maha Alanazi, Mohamed Rajab, Ayodele Alaiya, Fowzan Alkuraya, and Bhavesh Mistry

The DDB1– and CUL4–associated factor 17 (Dcaf17) gene encodes a putative substrate receptor protein for ubiquitin E3 ligase complex, which plays critical roles in many cellular processes. Previously, we showed that loss of function of DCAF17 in mice caused male infertility due to defective spermatogenesis. In this study, we have used the proteomic approach to identify differentially expressed proteins in the wild type (WT) and mutant testes with the objective of analyzing their roles in normal testicular function and male fertility. By using tandem mass-spectrometry (LC-MS/MS), we found that a large proportion of proteins showed significantly variable expression in Dcaf17 knockout mouse testis as compared to that of the wild type mouse testis. Indeed, subsequent bioinformatics analysis highlighted that many of these differentially expressed proteins play a possibly role in spermatogenesis, chromatin modification, nucleosome assembly, ubiquitination, protein stabilization, transport protein, heat shock proteins, movement of cilia and apoptosis, which is in agreement with the observed phenotype of defective spermatogenesis. Also, some metabolism associated proteins like enzymes were detected as differentially expressed. Cumulatively, these data provide a rich resource for further elucidating the cellular/molecular mechanisms of DCAF17 that may contribute to the onset of male infertility.

**The Effects of Heat Stress or Lipopolysaccharide Exposure on Ovarian Heat Shock Protein Expression in Pigs.** Jacob T. Seibert, Malavika K. Adur, Porsha Q. Thomas, Aileen F. Keating, Lance H. Baumgard, and Jason W. Ross

Heat stress (HS) undermines efficiency for a variety of economically important variables in animal agriculture, including reproduction, and it also poses a major concern for human health. Heat stress impairs the intestinal barrier function, allowing for translocation of the resident microflora and endotoxins, such as lipopolysaccharide (LPS), out of the gastrointestinal environment. While much is known about the cellular function of heat shock proteins (HSPs), the *in vivo* ovarian HSP response to stressful stimuli, such as HS or LPS exposure, remains ill-defined. The purpose of this study was to investigate the effects of HS or LPS exposure on ovarian HSP expression in pigs. Our hypothesis was that the ovarian heat shock response (HSR) occurs during HS or LPS challenges in pigs. This study consisted of three independent live-phase experiments. In all experiments, altrenogest (15 mg/d) was administered *per os* for estrus synchronization (14 d) prior to treatment. In the first experiment, gilts were exposed to cyclical HS ( $31.1^{\circ} \pm 1.4^{\circ} \text{C}$ ;  $n = 6$ ) or thermoneutral (TN;  $20.3 \pm 0.5^{\circ} \text{C}$ ;  $n = 6$ ) conditions immediately following altrenogest withdrawal for 5 d during follicular development. Similarly, in experiment two, gilts were subjected to saline (CON;  $n = 3$ ) or LPS ( $0.1 \mu\text{g}/\text{kg BW}$ ;  $n = 6$ ) I.V. infusion immediately following altrenogest withdrawal for 5 d. In the third experiment, gilts were subjected to TN ( $20 \pm 1^{\circ} \text{C}$ ;  $n = 7$ ) or cyclical HS ( $31$  to  $35^{\circ} \text{C}$ ;  $n = 7$ ) conditions 2 d post estrus (dpe) until 12 dpe during the luteal phase. All animals were sacrificed at the end of each experiment and ovarian samples were

appropriately preserved for analysis. Heat stress during the follicular phase (Exp. 1) increased whole ovarian protein abundance of heat shock factor 1 (HSF1; 53%;  $P = 0.05$ ), heat shock protein family A (HSP70) member 1A (HSPA1A; 101%;  $P = 0.01$ ), heat shock protein family D (HSP60) member 1 (HSPD1; 95%;  $P < 0.01$ ), and heat shock protein family B (Small) member 1 (HSPB1; 101%;  $P = 0.01$ ) compared to TN controls. Exposure to LPS during the follicular phase in experiment 2 increased ovarian HSPA1A (86%;  $P = 0.01$ ) and tended to increase HSF1 ( $P = 0.08$ ) and HSPB1 ( $P = 0.09$ ) compared to CON gilts while HSPD1 was not influenced by LPS ( $P = 0.89$ ). In experiment three, HS increased abundance of HSPB1 (175%;  $P = 0.03$ ) in corpora lutea while HS only numerically increased HSF1 ( $P = 0.17$ ) and HSPD1 ( $P = 0.17$ ); HSPA1A in corpora lutea was not influenced by HS ( $P = 0.51$ ). Thus, these data support that HS and LPS exposure regulate expression of specific ovarian HSPs. The similarities of LPS infusion and HS on ovarian protein changes suggest intraovarian signaling following HS may be at least partially the result of compromised intestinal integrity and subsequent increased circulating LPS. This project was supported by the Iowa Pork Producers Association and the National Pork Board.

**Placenta as a Sensitive Indicator of Genome-Wide DNA Methylation Perturbations Associated with Assisted Reproductive Technologies.** Sophia Rahimi, Josée Martel, Gurbet Karahan, Donovan Chan, Camille Angle, and Jacquetta Trasler

Assisted reproductive technologies (ARTs), now commonly used worldwide, have been linked with adverse perinatal outcomes and an increased incidence of genomic imprinting disorders, often associated with defective DNA methylation. The objective of this study was to examine the changes induced by ARTs on genome-wide DNA methylation profiles in normal female embryos, placentas and delayed female embryos in a mouse model. CF1 females underwent natural mating (NAT group) while the females of the ART group were subjected to superovulation, in vitro fertilization, embryo culture and non-surgical blastocyst transfer. Embryos and placentas were collected at mid-gestation (embryonic day 11.5). DNA methylation patterns were examined on a genome-wide basis using Reduced Representation Bisulfite Sequencing (RRBS) on representative female embryos and/or placentas ( $n=6$  for normal embryos and placentas;  $n=3$  for delayed embryos). Analysis of the RRBS data demonstrated many differentially methylated tiles (DMTs), being either hypo- or hypermethylated, when the ART group was compared to the NAT group. Results from normal embryos showed that ART induced mainly hypomethylation (1225 hypomethylated and 292 hypermethylated DMTs). A more pronounced ART effect was observed in the delayed embryos with 6705 hypomethylated and 3815 hypermethylated tiles, exhibiting a higher magnitude of change in methylation as well. Interestingly, the normal placentas also exhibited a higher susceptibility to ART, with 9600 hypomethylated tiles and 502 hypermethylated tiles. Furthermore, gene ontology analysis revealed that the genic hypomethylated regions in normal placentas and in delayed embryos exhibited a very similar enrichment in genes involved in cellular and nervous system differentiation, that are key for embryo development. Eight of their top 10 pathways were identical: neuron differentiation, neurogenesis, generation of neurons, cell projection organization, neuron development, neuron projection development, cell morphogenesis and cellular component morphogenesis. Our results suggest that the placenta may reflect what is happening in more affected embryos. A similar analysis is currently being performed on RRBS data comparing natural mating to a group of females that underwent ART procedures limited to only superovulation and embryo transfer. Taken together, these results suggest that the placenta of normal embryos may be

used as a sensitive indicator of the genome-wide DNA methylation perturbations generated by ART. (Supported by the Canadian Institutes of Health Research).

**The Interplay Between Two Mesenchymal Factors, AR And COUP-TFII, in Controlling Epithelial Fate Decisions of the Male Reproductive Tract.** Verda E. Agan, Fei Zhao, Paula R. Brown, Karina F. Rodriguez, and Humphrey H.C. Yao

During sexual differentiation, androgens promote the growth and survival of the male reproductive tract epithelium. Androgen action on the male tract epithelium is mediated by the androgen receptor (AR) in the surrounding mesenchyme. Mesenchymal factors are known to determine the fate and differentiation of ductal epithelium. COUP-TFII (chicken ovalbumin upstream promoter transcription factor II) is an orphan nuclear receptor that is specifically expressed in the male tract mesenchyme. In contrast to the role of androgen in promoting male tract survival, COUP-TFII in the mesenchyme acts to inhibit the growth of the male tract. In the male embryo, therefore, AR action must antagonize COUP-TFII action to allow the survival of the male tract. Given that AR and COUP-TFII are co-localized in the mesonephric mesenchyme, it is possible that AR antagonizes COUP-TFII through suppressing Coup-tfII/COUP-TFII expression. However, real-time PCR data showed that Coup-tfII expression was not altered by the presence or absence of androgen receptor action. We thus hypothesize that the functional antagonism between AR and COUP-TFII may be through a physical interaction between the two mesenchymal factors. To test the potential protein-protein interaction between AR and COUP-TFII in the male tract mesenchyme, we first used Western blotting to detect AR and COUP-TFII at embryonic day 14.5 (E14.5) in the mouse when reproductive tract differentiation begins. We have successfully detected AR and COUP-TFII from E14.5 male tract tissue homogenate with expected molecular weight approximately 110 and 50 kDa, respectively. Next, we performed pull-down experiments with AR or COUP-TFII primary antibodies attached to glutathione-agarose beads in order to immunoprecipitate target proteins. Assays with IgG and female tract tissue homogenate were used as negative controls. Protein complexes recovered from the beads were resolved by SDS-PAGE and analyzed by Western blotting. We detected both AR and COUP-TFII proteins in AR and COUP-TFII pull-down complexes from male tract tissue, suggesting a protein-protein interaction between AR and COUP-TFII under in-vivo conditions. This physical interaction between AR and COUP-TFII could attenuate each other's action in regulating their target gene expression. We plan to carry out real-time PCR to investigate whether expression of COUP-TFII regulated genes is altered by AR action; and whether expression of AR regulated genes is altered by COUP-TFII action. Results from these experiments not only demonstrate the mechanism underlying the functional antagonism between COUP-TFII and AR in determining epithelial cell fate, but also provide a streamlined platform to identify protein partners in sexual differentiation. This research was supported by NIEHS Intramural Research Funds and NIEHS DIRA award.

**BRCA1 Regulates Cell Death and Differentiation in Human Placental Cells.** Rachel West, Natascha Heise, Gerrit Bouma, and Quinton Winger

Early human placental development strongly resembles carcinogenesis in otherwise healthy tissues. There is rapid cell proliferation within the cytotrophoblast. These cells then begin to differentiate, some

towards the highly invasive and migratory extravillous trophoblast which mimics tumor metastasis. One key difference between cancer progression and placental development is the tight regulation of these oncogenic processes and the oncogenes that drive them. Often, tumor suppressors and oncogenes work synergistically to regulate cell proliferation and differentiation in a restrained manner compared to the uncontrollable growth in cancer. One example of this partnership is the regulation of the oncofetal protein HMGA2 by BRCA1. BRCA1 forms a repressor complex with ZNF350 and CtIP to bind to the promoter region of HMGA2 to prevent transcription. We have determined by chromatin immunoprecipitation that BRCA1 forms this repressor complex in the human trophoblast cell lines, ACH-3P and Swan71, suggesting a role in the placenta. Interestingly, using immunofluorescence to localize BRCA1 and HMGA2 in the first trimester placenta, we found that HMGA2 localizes primarily to the undifferentiated cytotrophoblast whereas BRCA1 is found primarily in the differentiated syncytiotrophoblast. This suggests that HMGA2 is important during early placental cell proliferation, losing expression as cells differentiate. In contrast, BRCA1 is not upregulated until cells have begun to differentiate. Immunofluorescence of human term placenta show BRCA1 in all cell types, suggesting that BRCA1 is important in differentiated cells throughout pregnancy. Additionally, BRCA1 is an important tumor suppressor involved in DNA repair and apoptosis pathways in healthy tissues. BRCA1 is an essential protein during early placental development as BRCA1<sup>-/-</sup> mice are embryonic lethal at approximately E7.5 due to poor organization of the trophoblast. As BRCA1 is a very important protein involved in many cellular processes involved in placentation we hypothesized that BRCA1 is essential for normal trophoblast cell proliferation. To test this hypothesis, we used CRISPR-Cas9 gene editing to knockout BRCA1 in the Swan71 cell line as the Swan71 cells had significantly higher BRCA1 levels compared to ACH-3P cells. HMGA2 mRNA and protein was significantly increased in the BRCA1 KO cells compared to control cells. Chromatin was immunoprecipitated using an antibody for ZNF350 and PCR was for the promoter region for HMGA2. BRCA1 repressor complex binding to HMGA2 was significantly reduced in the knockout cells compared to our control cells, leading us to conclude that increased HMGA2 was due to decreased binding of the BRCA1 repressor complex. Additionally, we tested levels of apoptosis in our cells. After serum starving cells for 16 hours, we found that Caspase 3 and 7 levels were significantly higher in our BRCA1 KO cells compared to controls. This data suggests that BRCA1 is an important factor in the regulation of the oncofetal protein HMGA2 and promotes cell survival in human placental cells.

This research was supported by USDA-NIFA grant 1012350, the USDA regional project #W3171, and the Colorado State University CVMBS College Research Council.

**Modification of Development of Bovine Embryos by Choline..** Eliab Estrada-Cortes, Charles R. Staples, and Peter J. Hansen.

Choline is a precursor of membrane phospholipids and betaine, a methyl donor for DNA methylation. In dairy cows, supplementation with rumen-protected choline (RPC) improved postpartum reproductive performance. The objective was to determine whether addition of choline to culture medium improves development of in vitro-produced embryos and alters blastocyst gene expression. In Experiment 1 (n=5 replicates), putative zygotes (PZ) produced in vitro were incubated in BBH7 culture medium with 0.0, 1.3, 1.8 or 6.37 mM choline chloride (ChCl). All treatments were isotonic. Concentrations of ChCl approximated total choline in plasma of cows at weeks 1 (1.30 non-RPC and 1.80 RPC cows) and 10

postpartum (6.37 non-RPC cows). Pools of 10 embryos (n=5 replicates) were used to analyze expression of 91 genes by qPCR. Percent oocytes that cleaved was  $73.3 \pm 3.7$ ,  $75.1 \pm 3.6$ ,  $77.3 \pm 3.4$  and  $68.5 \pm 4.0\%$  ( $P=0.03$ ), percent oocytes becoming blastocysts was  $34.6 \pm 3.3$ ,  $33.7 \pm 3.4$ ,  $35.3 \pm 3.4$  and  $27.1 \pm 3.0\%$  ( $P=0.03$ ) and percent cleaved embryos becoming blastocysts was  $47.5 \pm 3.2$ ,  $45.1 \pm 3.3$ ,  $45.9 \pm 3.2$  and  $39.6 \pm 3.2\%$  ( $P>0.1$ ) for 0.0, 1.3, 1.8 and 6.37 mM ChCl, respectively. Transcripts for 5 genes (ASGR1, CCR2, FGF4, MST1 and NANOG) were increased by 1.3 mM ChCl and two genes (GNAT2 and TCF23) by 6.37 mM ChCl ( $P < 0.05$ ). For Experiment 2 (n=7), PZ were incubated in one of two media (SOF-BE2 or BBH7) with 0.0 or 1.3 mM ChCl. Effect of treatment and the interaction were not significant. For Experiment 3 (n=8), PZ were treated with vehicle, 1.3 mM phosphatidylcholine (PC) or 4.0  $\mu$ M ChCl (concentration in blood of early postpartum cows). Percent oocytes that cleaved was  $70.4 \pm 2.3$ ,  $68.7 \pm 2.3$ , and  $74.5 \pm 2.2$  ( $P=0.079$ ), percent oocytes becoming blastocysts was  $27.6 \pm 3.3$ ,  $19.2 \pm 2.7$  and  $30.2 \pm 3.5\%$  ( $P=0.0005$ ) and percent cleaved embryos becoming blastocysts was  $39.3 \pm 4.1$ ,  $28.2 \pm 3.5$  and  $40.7 \pm 4.1\%$  ( $P=0.014$ ) for vehicle, PC and ChCl, respectively. In summary, addition of ChCl at 6.37 mM reduced cleavage and addition of PC at 1.3 mM reduced cleavage and subsequent embryonic development. ChCl altered expression of specific genes. (Support: Larson Endowment).

**Brain Plasmalogen Controls Gonadotropin Secretion From the Bovine Anterior Pituitary.** Hiroya Kadokawa, and Onalenna Kereilwe

We recently discovered that the orphan G-protein-coupled receptor (GPR) 61 colocalized with GnRH receptors (GnRHRs) on the surface of most of bovine gonadotrophs. A recent study suggested that ethanolamine plasmalogen (PI) is a ligand for GPR61 in mouse neuroblastoma. Therefore, this study evaluated the hypothesis that PI controls LH and FSH secretions from the bovine anterior pituitary. We prepared bovine anterior pituitary cells from post-pubertal heifers (26 months old), and cultured the cells for 3.5 days. We treated the cells with increasing concentrations (0, 5, 50, 500, 5,000, 50,000, or 500,000 pg/mL) of phosphoethanolamine PI (PEPI) extracted from bovine brain, or L- $\alpha$ -lysophosphatidylethanolamine PI (LEPI) extracted from bovine brain, for 5 minutes before either no treatment or GnRH stimulation. The medium samples were harvested 2 hours after culture for LH and FSH assays. Phosphoethanolamine PI (50–500 pg/mL) stimulated ( $P < 0.05$ ) the basal secretion of FSH, but not LH. PEPI at 50 pg/mL also enhanced ( $P < 0.05$ ) GnRH-induced FSH secretion. However, a higher (500–500,000 pg/mL) PEPI suppressed GnRH-induced FSH secretion. Moreover, 50–500,000 pg/mL PEPI suppressed GnRH-induced LH secretion. None of the tested concentrations of LEPI showed any effect on the basal or GnRH-induced LH or FSH secretion. Pretreatment with SMAD pathway inhibitors suppressed the FSH secretion induced by PEPI, whereas the extracellular signal-regulated kinase pathway inhibitor suppressed the PEPI suppression of GnRH-induced LH secretion. Therefore, PEPI, but not LEPI, extracted from bovine brain, controls FSH and LH secretion from the anterior pituitary.

**Effect of Increased Ambient Temperature on Porcine Endometrial Heat Stress Response During the Peri-implantation Phase.** Malavika K. Adur, Matthew R. Romoser, Katie L. Bidne, Jacob T. Seibert, Elizabeth A. Hines, Aileen F. Keating, Lance H. Baumgard, and Jason W. Ross

Seasonal infertility occurs annually in commercial swine production during hot summer months and heat stress (HS) is among the putative contributors to deficits in reproductive ability. Environmental

hyperthermia induces a HS response (HSR) typically characterized by increased expression of heat shock proteins (HSPs), which facilitate in part, a cellular stress response. How the disruptive effects of HS manifest in porcine endometrium during the window of implantation is not well understood, although gilts exposed to hyperthermic conditions for the first 10-15 days post-breeding have reduced embryo survival rates. Our working hypothesis is that environmental HS alters HSP expression in the maternal endometrium, which negatively affects the uterine microenvironment compromising conceptus survival. Experimental objectives were to evaluate the transcriptional response to HS during the implantation window in pigs and assess the influence of exogenous oral progestin (altrenogest) on the HSP response. Forty-two postpubertal gilts were estrus synchronized using altrenogest (ALT; 15 mg/d), of which 28 were artificially inseminated during behavioral estrus (bred) and 14 were not bred (cyclic), and then randomly assigned to diurnal HS (31 to 35°C; n = 14 bred and 7 cyclic) or thermoneutral (TN; 21 ± 1°C; n = 14 bred and 7 cyclic) conditions from day 3 to 12 post estrus. Seven of the bred animals from each thermal treatment group were given ALT, a progesterone receptor agonist (15 mg/d), from day 3 to 12 post estrus. All animals were euthanized 12 days post estrus onset and reproductive tracts were removed, followed by uterine flushing, evaluation of conceptus morphology, and collection of endometrial tissue. Heat stress did not affect the stage of conceptus elongation on day 12 in bred gilts based on the percentage that had begun rapid trophoblastic elongation (71.4%, HS vs 69.2%, TN; P = 0.66). Interestingly, for gilts administered ALT, 12 of 13 (92.5%) yielded conceptuses that had begun rapid elongation and were filamentous in morphology, increased (P < 0.01) compared to gilts not supplemented ALT, where only 6 of 14 (42.9%) yielded filamentous conceptuses. The expression patterns of endometrial HSP transcript levels for heat shock protein family A (Hsp70) member 6 (HSPA6), heat shock protein 90 alpha family class A member 1 (HSP90AA1) and heat shock protein 90 family B member 1 (HSP90B1) were evaluated. Pregnancy status, thermal treatment, nor ALT supplementation affected HSP90AA1 or HSP90B1 transcript abundance. HSPA6 transcript abundance was not influenced by interactions between environment and pregnancy status (P = 0.42) or environment and ALT supplementation (P = 0.56). However, HS increased (1.9 fold; P < 0.01) transcript abundance of HSPA6 in endometrium compared to thermoneutral gilts and was not affected due to ALT supplementation (P = 0.76). Interestingly, pregnant gilts had greater (1.8 fold; P = 0.01) HSPA6 endometrial abundance compared to cyclic counterparts. As a chaperone of the estrogen and progesterone receptors, HS-induced HSPA6 increased abundance in porcine endometrium may indicate a role in steroid mediated endometrial signaling during the window of implantation. This project was supported by the Iowa Pork Producers Association.

**PIWIL3 Function in Mammalian Female Germ Cells.** Hidetoshi Hasuwa, Kyoko Ishino, and Haruhiko Siomi

The PIWI-piRNA pathway is one of the key pathways that silence transposable elements (TEs) in animals. In mice, three PIWI proteins (PIWIL1, PIWIL2 and PIWIL4) are almost exclusively expressed in testes and little in ovaries. Therefore, Piwi knockout mice exhibit defects in spermatogenesis with an activation of TEs including LINE1, leading to male infertility. However, Piwi knockout female mice show no discernible phenotype.

Piwil3 was found as an ovary specific Piwi in most mammals except for mouse and rat. To understand possible roles of PIWIL3 in female germ cells, we have used the golden hamster (*Mesocricetus auratus*)

in which Piwi3 is expressed in the ovary. With the CRISPR/Cas9 system, we succeeded to produce Piwil3 mutant hamster lines. Piwil3 mutant females showed the subfertile phenotype as a result of abnormal pre-implantation embryo development.

Our result revealed that PIWIs have important roles even in female germ cells.

**Short-Term Heat Stress Induces Mitochondrial Degradation and Biogenesis and Enhances Mitochondrial Quality in Porcine Oocytes.** Nobuhiko Itami, Koumei Shirasuna, Takehito Kuwayama, and Hisataka Iwata

Mitochondria in oocytes play important roles in many processes, including early embryo development. Promotion of mitochondrial degradation and biogenesis through Sirtuin 1 (SIRT1) activation enhances mitochondrial function and oocyte quality. Previous studies that used somatic cells have shown that short-term heat stress (SHS) induces SIRT1-induced mitochondrial biogenesis. In the present study, we examined whether SHS can induce mitochondrial degradation and biogenesis in porcine oocytes. We collected cumulus cell-oocyte complexes (COCs) from prepubertal gilt ovaries acquired from a slaughterhouse. COCs were treated at 41.5°C (vehicle: 38.5°C) for the first one hour of in vitro maturation, and the mitochondrial kinetics, oocyte function, and developmental competence of oocytes were examined. SHS increased the expression level of heat shock protein 72, which induced the high expression of SIRT1 and the phosphorylation of AMP-activated protein kinase. SHS did not alter the mitochondrial DNA copy number in oocytes, but increased expression levels of mitochondrial biogenesis factor, PGC1 $\alpha$  and TFAM, and proteasome-associated mitochondrial degradation factor, PINK1. From the experiment using proteasomal inhibitor, MG132, we confirmed that SHS activated both mitochondrial degradation and biogenesis. Furthermore, SHS enhanced the mitochondrial membrane potential and ATP content in oocytes, and improved the ability of the oocytes to develop into blastocysts. In conclusion, it is suggested that SHS-induced mitochondrial replacement improves developmental competence of oocyte.

**KDM1A Regulates Sex Steroid Receptor Levels in Trophoblast Cells and is Possibly Involved in Placental Development.** Gerrit J. Bouma, Asghar Ali, Erin S. McWhorter, Amelia R. Tanner, Rachel C. West, and Quinton A. Winger

In addition to supporting embryo/fetal development, and as such postnatal health, abnormal placental formation and function leads to a variety of serious disorders in animals. In agricultural animals, placental dysfunction can lead to low birth weights and decreased lean muscle tissue in postnatal life. In humans, compromised placentation is associated with pregnancy disorders including intrauterine growth restriction (IUGR) and gestational diabetes mellitus (GDM) that ultimately can lead to adult onset diseases such as hypertension, diabetes, and coronary heart disease. Although the placenta itself is recognized as an endocrine organ, most notably by its secretion of progesterone, androgens and estrogens, the role or regulation of sex steroid signaling in placental development is less clear. Furthermore, the placenta is a target for steroid hormones. Our previous work has demonstrated that human and sheep trophoblast cells contain androgen receptors (AR), and in a prenatal androgenization sheep model for polycystic ovarian syndrome, AR and its gene target VEGFA exhibit abnormal placental

expression. Furthermore, the histone lysine demethylase KDM1A co-localizes and binds to AR in trophoblast cells and targets the same promoter region of VEGFA. In the current study we use both in vitro and in vivo approaches to determine the function of KDM1A in the placenta. We hypothesize that KDM1A regulates trophoblast differentiation through its interaction with AR, and also is necessary for placental angiogenesis. CRISPR-Cas9 lentiviral gene targeting constructs were generated to target both human and sheep KDM1A sequence. Both AR and ESR1 bind KDM1A in ACH-3P (human trophoblast) cells and knockout of KDM1A in results in significant ( $P < 0.05$ ) lower amounts of AR and ESR1. Furthermore, KDM1A KO ACH-3P cells have significant reduces levels of VEGFA, suggesting KDM1A possibly is involved with regulating placental angiogenesis. Finally, a pilot experiment was conducted this past winter to demonstrate a role for KDM1A in placental development in vivo, using the sheep as a model. Briefly, day 9 embryos were flushed ( $n=4$ ) and infected with a Lenti-CRISPRv2 KDM1A target construct to knockout KDM1A specifically in the trophectoderm. Infected embryos were transferred to recipient ewes and embryos were collected a week later at gestational day 16. Preliminary results indicate that KDM1A is necessary for embryo elongation. Collectively these data so far suggest that KDM1A plays a role in AR and ESR1 signaling in trophoblast cells, and is necessary for early placental development. Ultimately these studies will provide a necessary, critical advancement in our understanding on the role of KDM1A and sex steroid hormone signaling in placental development and differentiation, which is vital to our ability to better understand placental disorders that lead to compromised pregnancies in humans and domestic livestock.

Research supported by Colorado State University CVMBS College Research Council, NIH Institutional National Research Service Award Training Grant (T32 NRSA) "Biomedical Research Training for Veterinarians", and USDA National Need Fellowship.

**Integrated Epigenetic and Transcriptomic Analysis of Uterine Fibroid Genetic Sub-Types.** Jitu W. George, Huihui Fan, Benjamin K. Johnson, Amanda L. Patterson, Megan J Bowman, Anindita Chatterjee, Hui Shen, and Jose M. Teixeira

Uterine leiomyomas (or fibroids), benign smooth muscle tumors of unknown etiology, are the most common indication for hysterectomy in the USA. In order to characterize contribution of epigenetic and transcriptomics, an integrated study of DNA methylation (EPIC) array, and RNA-sequencing was performed on normal myometrium and most common fibroid genetic subtypes; fibroids with MED12 mutations (MED12mt), and those characterized with overexpression of HMGA2 (HMGA2hi) and HMGA1 (HMGA1hi). Normal myometrium and fibroid samples were obtained from African American and Caucasian women. Ethnicity of patient samples was confirmed from the EPIC array using Single Nucleotide Polymorphisms and showed a high concordance between self-reported and predicted ethnicity. To address heterogeneity and allow uniform epigenetic and transcriptional comparison between normal myometrium and fibroid samples, tissue composition was inferred by DNA methylation for different cell types. Computational analysis identified smooth muscle cell composition to be greater than 85% in both normal myometrium and fibroids. To further analyze and confirm cellular purity, flow cytometry analysis of human myometrial and fibroid tissue was conducted and, identified approximately 70% and 90%  $\alpha$ SMA-positive smooth muscle cells, ensuring a relatively homogeneous population of cells. Unsupervised clustering of CpG DNA methylation array data revealed normal myometrium and fibroid sub-types clustered separately, suggesting a similar molecular profile among the fibroids as

defined by the high degree of conservation within each compared to normal myometrium. We did not observe significant clustering by race, indicating a possible lack of racial influence on differentially methylated patterns between normal myometrium and fibroid tissues. HMGA2 over expression has been traditionally attributed to chromosomal rearrangement, however, Fluorescence in situ hybridization (FISH) analyses of HMGA2hi expressing fibroids showed lack of translocation. Instead, we identified hypomethylation of the HMGA2 gene body, indicating that DNA methylation maybe another mode of HMGA2 regulation. At transcriptome level, we observed segregation of normal myometrium and MED12mt, HMGA2hi and HMGA1hi fibroid subtypes. Consistently, the most significant dysregulated genes were involved in extracellular matrix organization, collagen formation and regulation of chromatin organization. Transcriptional analysis of HOX genes, identified overexpression of HOXA13 mRNA and the associated long-non-coding RNA, HOXA transcript at the distal end (HOTTIP). RNA transcriptional analysis and qRT-PCR confirmed upregulation of HOXA13, HOTTIP and downstream target genes, suggesting that HOXA13 could influence fibroid pathobiology. These results indicate that fibroid tumorigenesis may be attributed to accumulation of epigenetic and transcriptional changes and identify chromatin architectural and transcription factors that could mediate fibroid tumorigenesis or growth.

**Disruption to O-GlcNAc Cycling Promotes Epithelial-Mesenchymal Transition in Endometrial Cancer Cells in Vitro.** Nicole Morin Jaskiewicz and David H. Townson

Diabetic women have a 2-3 fold increased risk of developing endometrial cancer, however, the molecular aspects of this risk are not fully understood. This study investigated the alteration of cellular O-GlcNAcylation of proteins as the potential mechanistic connection between these two conditions. Aberrant O-GlcNAcylation is a potential cause of insulin resistance and is a hallmark of many cancers. For instance, O-GlcNAc cycling enzyme mRNA (OGT, MGEA5) is upregulated at the myometrial edge of endometrial tumors, suggesting a role in cancer metastasis. In the current study, in vitro analysis of the endometrial cancer cell line (Ishikawa) indicated an increase in epithelial mesenchymal transition (EMT), especially under Hyper-O-GlcNAc conditions (1 $\mu$ M Thiamet-G). Hyper-O-GlcNAcylation resulted in an upregulation of EMT associated genes (WNT5B and FOXC2), a decrease in epithelial protein (ZO-1), and an increase in mesenchymal proteins (Snail and Claudin-1). Reorganization of actin filaments into thick stress filaments, consistent with EMT, was also noted in Thiamet-G-treated cells. Interestingly, Hypo-O-GlcNAcylation (via inhibition of the OGT enzyme; 50  $\mu$ M OSMI-1) also upregulated WNT5B and FOXC2, inferring that any disruption to O-GlcNAc cycling impacts EMT. However, Hypo-O-GlcNAcylation also reduced cellular proliferation/migration. In summary, disruption of O-GlcNAc cycling (via OGT or OGA inhibition) promoted EMT at both the mRNA and protein levels. Additionally, Hypo-O-GlcNAcylation specifically had a negative impact on cellular proliferation/migration, and cytoskeletal organization. This material is based upon work supported by the National Science Foundation Graduate Research Fellowship under Grant No. (DGE 1450271).

**Acute and Subacute Effects of a Synthetic Kisspeptin Analog On Serum Concentrations of Luteinizing Hormone, Follicle Stimulating Hormone, and Testosterone in Prepubertal Bull Calves.** P. A Parker, E. A. Coffman, K. G. Pohler, J. A. Daniel, M. Beltramo, and B. K. Whitlock

Kisspeptin (KP) is a neuropeptide integral in regulating puberty and gonadotropin releasing hormone. Compound-6 (C6), a KP analog, may be more potent, have a greater half-life, and have greater clinical applications than KP. To determine the acute and subacute effects of KP and C6 on serum concentrations of luteinizing hormone (LH), follicle stimulating hormones (FSH), and testosterone (T), prepubertal bull calves ( $12.1 \pm 1.1$  weeks of age;  $91.2 \pm 10.8$  kg BW) were assigned to one of three treatment groups [Saline (n = 4), KP (n = 4; 20 nmoles), or C6 (n = 4; 20 nmoles). Treatments were administered intramuscularly daily for four consecutive days. Blood samples were collected every 15 minutes for six hours immediately following treatment administration on Day 1 (acute) and Day 4 (subacute). Serum concentrations of LH, FSH, and T were determined by radioimmunoassay. For each period, effects of treatment, time, and interactions on LH and FSH concentrations and pulse parameters were analyzed using procedures for repeated measures with JMP Software (SAS Inst. Inc., Cary, NC). During the acute period, LH concentrations were greatest following administration of C6 ( $P < 0.0001$ ). During the subacute period LH concentrations tended to be greatest following administration of C6 ( $P = 0.051$ ). Number of LH pulses were least following administration of C6 ( $P = 0.02$ ). The LH nadirs were greatest following administration of C6 ( $P = 0.04$ ). Mean FSH concentrations were greatest during the acute period ( $P < 0.0001$ ). During the subacute period FSH concentrations ( $P = 0.02$ ) and number of FSH pulses ( $P = 0.017$ ) were least following administration of C6. There was no effect of treatment ( $P = 0.33$ ), time ( $P = 0.19$ ) or treatment x time interaction ( $P = 0.44$ ) on T concentrations. In conclusion, acute and subacute C6 increased LH concentrations and pulse parameters and subacute C6 decreased FSH concentrations and pulse parameters. Despite suppression of gonadotropins with subacute C6, KP analogs may have application to affect the onset of puberty in livestock.

**Altered Blood Plasma and Follicular Fluid Lipid Profiles Predict Alterations in Cell Signaling, Metabolism, and Immune Function in Cows with Androgen Excess.** Megan A. Neilson, Renata Spuri Gomes, Sarah M. Romereim, Adam F. Summers, Mohamed A. Abedal-Majed, Sarah C. Tenley, Scott G. Kurz, Jeff W. Bergman, Robert A. Cushman, John S. Davis, Jennifer R. Wood, and Andrea S. Cupp

We have previously described cows in the UNL physiology herd with excess androstenedione (A4; High A4 > 40 ng/ml; control < 20 ng/ml) in follicular fluid of dominant follicles, reduced circulating Sex Hormone Binding Globulin, alterations in liver hormone metabolism, and arrested follicular development leading to anovulation and reduced fertility. Our objective was to determine potential differences in blood plasma and follicular fluid lipid profiles in High A4 cows and controls. Our hypothesis was that altered lipid profiles in plasma and follicular fluid in High A4 cows compared to controls would identify metabolic, signal transduction or biological process contributing to altered follicular development resulting in anovulation. Blood plasma samples were collected at day 7 and 15 of a non-stimulated cycle where cows were synchronized to initiate a new follicular wave. Blood plasma and follicular fluid was also collected at ovariectomy after FSH stimulation (20ng/ml every 12 hours ending with a Prostaglandin F2alpha (PG) injection at last FSH injection; ovariectomy 36-42 hours after last PG). A total of 863 lipid compounds were identified in the follicular fluid and plasma samples via HPLC mass spectrometry but only 115 of the lipid compounds were annotated, so some lipids are

designated by compound number. The top 4 lipid compounds per sample were chosen in High A4 compared to control cows using the Random Forest Algorithm for each sample. At day 7 of the non-stimulated cycle lysophosphatidylethanolamine 22:4 (LysoPE(22:4)), which induces the MAPK signal transduction pathway, mediating cell growth and differentiation and C760, was significantly reduced in blood plasma from High A4 cows ( $P < 0.05$ ). On day 15 of the non-stimulated cycle, blood plasma had greater concentrations of C272, lysophosphatidylcholine (LPC) 22:4 (LPC (22:4)) and lysophosphatidylcholine 22:5 (LPC(22:5)) in the High A4 cows ( $P < 0.05$ ). The LPCs interact with G protein-coupled receptors, which distinguish them as novel ligands of orphan receptors, and are involved in carbohydrate and lipid metabolism suggestive of increased metabolic rate in High A4 cows. The follicular fluid collected at ovariectomy in the FSH-stimulated cycle was different across all 4 lipids, with C825, C600 and 1-(1Z-octadecenyl)-2-oleoyl-sn-glycero-3-phosphocholine (Plg-SOPC) being increased and Sphingomyelin (SM(d18:0/16:1(9Z))) decreased in High A4 cows compared to controls ( $P < 0.05$ ). Not much is known about Plg-SOPC; however, it is produced in response to oxidative stress. Sphingomyelin helps form lipid rafts regulating signal transduction thus a reduction may inhibit these processes. Taken together, these data indicate that altered lipids in the blood plasma of High A4 cows may increase MAPK and G-protein receptor signaling to increase metabolic rate while lipids in the follicular fluid decrease oxidative stress and inhibit G-protein receptor signaling compared to controls. Thus, variations in lipid profiles of High A4 and control cows suggest potential differences in metabolic, immune and cell signaling of the High A4 cows which may contribute to their follicular arrest, anovulation and infertility. This research was funded through USDA grant 2013-67015-20965. USDA is an equal opportunity employer.

**Optical Tissue Clearing and Light Sheet Microscopy Allows for the Complete Visualization of Kisspeptin Neuron Populations in the Ovine Hypothalamus.** Danielle T. Porter, Aleisha M. Moore, Robert L. Goodman, Lique M. Coolen, and Michael N. Lehman

Traditionally, studies examining the morphology and connectivity of neuronal populations have been carried out using conventional histological and immunohistochemical methods. This often results in disruption of three-dimensional (3D) architecture and morphology due to sectioning of the tissue. However, with the development of optical tissue clearing techniques and light sheet microscopy it is now possible to visualize neuronal populations in intact tissues without disrupting 3D structure or morphology. One such technique is a protocol called iDISCO that allows for the clearing and immunolabeling of whole brain samples. In our lab, we have modified the iDISCO technique for use with multiple-label immunocytochemistry and have successfully applied this technique to detect kisspeptin neurons in the ovine hypothalamus, cells that are essential for the neuroendocrine control of fertility. Here, we report preliminary data for immunolabelling of the complete kisspeptin neuron population in the arcuate nucleus of the ewe. Hypothalami were collected from adult Suffolk ewes ( $n=4$ ) perfused with 4% paraformaldehyde. Whole mount immunolabelling was performed using iDISCO protocol (Renier et al 2014) using 7 day incubations in rabbit anti-kisspeptin primary antibody and Alexa Fluor goat anti-rabbit 647 secondary antibody. Dehydration of the tissue using tetrahydrofuran was optimized (Moore et al. 2018) from the original iDISCO protocol and brains were rendered transparent by incubation in dichloromethane and dibenzyl ether. Cleared brains were imaged using a bidirectional light-sheet microscope (LaVision) and stacks of images were collected at  $4\mu\text{m}$  optical intervals. Mosaic stacks of images were stitched together using ImageJ and projected with IMARIS software to provide 3D

visualization of kisspeptin cell bodies throughout the hypothalamus. Using this technique, we observed kisspeptin cells in 3D as a continuum throughout the entire rostro-caudal extent of the arcuate nucleus. Following establishment of this technique, our future studies will use iDISCO and 3D imaging to map subpopulations of activated kisspeptin cells during both pulsatile and surge modes of luteinizing hormone (LH) secretion in the ewe. Previous work has shown that the majority of kisspeptin neurons in both the ARC and POA are activated during the preovulatory LH surge, whereas only ARC (KNDy) kisspeptin cells were activated during pulsatile secretion. The results from our current study suggest that optical tissue clearing is a viable approach for analyzing the distribution of neuronal populations in intact, brains from large animal models, such as the sheep, as well as in rodents.

Funding: NIH R01 HD039916 to M.N.L.

**Proteomic Analysis of Follicular Fluid in Carriers and Non-carriers of the Trio Allele for High Ovulation Rate in Cattle.** Brian W. Kirkpatrick, Mamat H. Kamalludin, Alvaro Garcia-Guerra, and Milo C. Wiltbank

Follicular fluid provides a microenvironment for oocyte development and serves as a signaling medium for systemic and intrafollicular communication between cells. In previous work a major gene for high ovulation rate in cattle was confirmed and mapped to chromosome 10; subsequent gene expression analysis strongly implicated SMAD6, an inhibitor of the transforming growth factor-beta/bone morphogenetic protein (TGF-beta/BMP) signaling pathway, as the responsible gene. To increase understanding of the gene's role in affecting ovulation rate, proteomic analysis was performed to characterize differences in proteins in follicular fluid between the carriers and non-carriers of the allele. We hypothesized that proteins may be differentially expressed between the genotypic groups. A total of four non-carrier and five carrier females were used in an initial study with four and six additional non-carrier and carrier females, respectively, used in a validation study. Emergence of the follicular wave was synchronized and the ovaries containing the dominant follicle(s) were extracted by ovariectomy for follicular fluid collection. A hexapeptide ligand library was used to overcome the masking effect of high abundance proteins and to increase the detection of low abundance proteins in tandem mass spectrometry (LC-MS/MS). A total of 763 proteins were identified in the initial study; after correcting for multiple comparisons, only two proteins, Glia-derived nexin precursor (SERPINE2) and Inhibin beta B chain precursor (INHBB), were significantly differentially expressed (false-discovery rate < 0.05). In a replicate study of analogous design differential expression of these two proteins was confirmed ( $p < 0.05$ ). A total of 752 proteins were observed in the validation study, 472 of which were observed in the initial study and the remainder unique to the validation study. Joint analysis of results from the two studies was performed by combining p-values for proteins with consistent differential expression across studies using the weighted-Z method. Three additional proteins were consistently differentially expressed between genotypes at a false discovery rate < 0.05 (Phospholipase A1 member A precursor (PLA1A), Serine protease 23 precursor (PRSS23), and Procollagen-lysine,2-oxoglutarate 5-dioxygenase 1 precursor (PLOD1)). Previous studies have indicated that expression of SERPINE2, INHBB and PLOD1 is increased by TGF-beta/BMP signaling; their reduction in follicular fluid from carrier animals is consistent with the ~9-fold overexpression of SMAD6 which is inhibitory to this pathway.

**Function of TRPML1 in Mouse Corpus Luteum.** Zidao Wang, Ahmed E. El Zowalaty, Yuehuan Li, Christian Lee Andersen, and Xiaoqin Ye

Transient receptor potential cation channel, mucolipin subfamily, member 1 (TRPML1) is a six transmembrane protein encoded by mucolipin 1 (MCOLN1). It is predominantly localized on the membranes of late endosomes and lysosomes and serves as a primary lysosomal counter ion channel. Counter ion channels dissipate the transmembrane voltage built up by V-ATPase to maintain lysosomal acidity that is critical for lysosomal functions. Mutations in MCOLN1 can cause mucopolipidosis type IV (MLIV), an autosomal recessive lysosomal storage disease. Mcoln1<sup>-/-</sup> mice recapitulate phenotypes associated with MLIV, such as neurodegeneration and retinal degeneration. TRPML1 has strong expression in the mouse female reproductive system: our microarray data show that Mcoln1 is the most highly expressed counter ion channel in the periimplantation uterine luminal epithelium; our preliminary immunohistochemistry data indicate high expression levels of TRPML1 in gestation day 3.5 (D3.5) wild type (WT) corpus luteum, mainly luteal cells, and oviduct, mainly epithelial cells. The functions of TRPML1 in female reproduction have not been systemically investigated. Our preliminary data indicate comparable mating activities and comparable numbers of embryos in D1.5 oviducts between WT and Mcoln1<sup>-/-</sup> mice, but progesterone deficiency in D3.5 Mcoln1<sup>-/-</sup> mice. These observations suggest a functional hypothalamic–pituitary–gonadal axis, normal ovulation and fertilization, but luteal insufficiency in the Mcoln1<sup>-/-</sup> mice. Corpus luteum is the main site for progesterone production during early pregnancy. Ovary histology reveals a range of abnormal morphology in D3.5 Mcoln1<sup>-/-</sup> corpora lutea: some appear to have normal corpus luteal cord formation in most of the corpus luteum but not near the center cavity, others lack clear corpus luteal cords and have extensive cell debris, suggesting that corpora lutea can be formed in the Mcoln1<sup>-/-</sup> ovary but cells in the corpus luteum are being degenerated. The corpus luteum is a transient organ that will go through regression via luteal cell apoptosis. Lysosomes have been implicated in the regression of corpus luteum. Our preliminary data may suggest premature regression of Mcoln1<sup>-/-</sup> corpus luteum. (Supported by NIH R01HD065939 (co-funded by ORWH & NICHD))

**Exposure to Excess Androgen in the Ovarian Microenvironment Results in Altered Granulosa Cell Function with Altered Steroidogenesis, Signal Transduction, Cyclicity and Response to Male Exposure.** Alexandria P. Snider, Sarah M. Romereim, Adam F. Summers, Bill E. Pohlmeier, Renee M. McFee, Scott G. Kurz, John S. Davis, Jennifer R. Wood, and Andrea S. Cupp

A population of cows that secrete excess androstenedione (A4; High A4) in follicular fluid of dominant follicles were identified in the UNL herd. They exhibit irregular estrous cycles, are less fertile and secrete 43-fold greater A4 from ovarian cortex cultures compared to controls. Microarray analysis of Control and High A4 granulosa cells demonstrated 210 downregulated and 60 upregulated genes. The major upregulated gene classifications were microRNA and cell signaling which resulted in cell cycle arrest and reduced proliferation phenotype in High A4 granulosa cells. Androgen treatment of granulosa cells from slaughterhouse ovaries recapitulated reductions in cell cycle arrest and proliferation. Thus, our hypothesis is that exposure to excess androgens produced by the ovarian microenvironment altered granulosa cell differentiation resulting in abnormal cell function and identity. A screen of High A4 and control granulosa cell genes and comparison of theca genes demonstrated that three theca-enriched genes were upregulated in High A4 granulosa cells- CYP17A1 (6-fold, promotes conversion of

progesterone to A4), COL4A1, (2-fold; inhibits VEGFA signal transduction), and AS3MT, (2-fold, aids in arsenic metabolism and oxidative stress). Since microRNA that negatively target gene expression were a major category of transcripts upregulated in High A4 granulosa cells, we sought to elucidate potential relationships. MiRNA2634 was upregulated and its target BRCA1, DNA repair gene, was down regulated supporting our microarray validity. Previous studies have shown BRCA1 granulosa cell-specific KO mice became acyclic when isolated from males and had increased granulosa cell expression of olfactory receptors. These olfactory receptors are members of a family of G-protein coupled receptors that activate adenylyl cyclase-3 and have down-stream effects on other GPCRs involved with FSH and LH actions. An increase in expression of olfactory receptors (2-18 fold) was observed in granulosa cells from High A4 cows compared to Controls. Further, FSH stimulation of High A4 cows stimulated similar numbers and sizes of follicles but a 50% reduction in granulosa cell numbers compared to Controls. The upregulation of these olfactory receptors in granulosa cells of High A4 cows may affect response to FSH and LH stimulation altering follicular maturation and resulting in anovulation. Furthermore, in BRCA1 granulosa cell specific KO mice the olfactory receptor upregulation affected responses to male stimulation inducing cyclicity. In our herd, heifers that are non-cycling during the pubertal period have been predicted to become our High A4 population due to their excess A4 secretion in ovarian cortex. These non-cycling females do not achieve pubertal cyclicity or respond well to estrous synchronization and artificial insemination; however, exposure to bulls induces cyclicity that results in a pregnancy rate of 66%. Taken together these data indicate that exposure of granulosa cells to high androgen concentrations within the ovarian microenvironment results in loss of granulosa cellular function and identity which may result in anovulation and altered response to male exposure. This research was funded through USDA grant 2013-67015-20965.

#### **Microarray Analysis Predicts Differentially Expressed Genes in Theca Cells From Cows with High Intrafollicular Androstenedione are Regulated by ESR1 and VEGFA Signaling and Increased Mrna Stability.**

Kerri A. Bochantin, Adam F. Summers, William E. Pohlmeier, Kevin M. Sargent, Scott G. Kurz, Sarah M. Romereim, Oluremi Daudu, Renee M. McFee, Robert A. Cushman, John S. Davis, Andrea S. Cupp, and Jennifer R. Wood

We identified a population of cows in the UNL physiology herd with high androstenedione (High A4; >40 ng/ml) concentrations in the follicular fluid of the dominant follicle. These High A4 cows displayed irregular estrous cycles and tended to have reduced calving rates indicating that this phenotype impairs fertility. The molecular phenotype of theca cells from High A4 cows includes increased expression of steroidogenic enzymes (CYP11A1, CYP17A1) and LHCGR. In the current study we hypothesized that theca cells from High A4 cows have a unique gene expression profile, which contributes to altered function including increased androgen synthesis by these cells. To test this hypothesis, the estrous cycles of High A4 and Control cows were synchronized with an injection of GnRH and a controlled internal drug release device (CIDR). After 7 days, the CIDR was removed, an injection of prostaglandin F2 alpha was given, and ovariectomies performed 36 hours later. Theca cells were microdissected from the dominant estrogen-active follicle and RNA extracted. High quality RNA from High A4 (n = 5) and control (n = 4) cows were labeled and hybridized to Affymetrix Bovine GeneChip Gene 1.0 ST Arrays at the University of Nebraska Microarray Core facility. Following hybridization, normalized data was generated using Robust Multi-Array Averaging Whole transcriptome analysis. Normalized data were subsequently analyzed using the NIA Array Analysis tool. Hierarchical clustering showed that samples from individual

cows clustered based on A4 classification. Analysis of Variance (ANOVA, P 2) included the mitotic roles of Polo-Like Kinases, the role of BRCA1 in DNA damage response, and Rho Family GTPase signaling. Conversely, p53 signaling was inhibited (Z-score). Interestingly, several predicted regulators play an important role in mRNA stability. Specifically, ELAVL1, an RNA binding protein that stabilizes mRNAs, was activated whereas ZFP36, an RNA binding protein that destabilizes mRNAs was inhibited. In addition, microRNA families with predicted inhibition included mir-21, let-7, miR 291a-3p, and miR-483-3p. The altered expression of these important signaling and stability factors may contribute to the altered steroidogenesis and delayed follicular development phenotype expressed by High A4 cows.

### **Health Outcomes From a Dietary Intervention for Preventing Ovarian Cancer in White Leghorn Laying Hens.** Chris Weston, Karen Hales, and Dale B. Hales

Epidemiological studies indicate that a consistent incorporation of omega-3 polyunsaturated fatty acid (PUFA) and phytoestrogen lignan in the daily diet reduces the risk of inflammation-associated morbidity and mortality. The objective of our lab's research is to elucidate how dietary flaxseed and omega-3 PUFAs prevent or reduce the severity of ovarian cancer. We accomplish this task by using the White Leghorn laying hen model of ovarian cancer, given the unique ability of laying hens to spontaneously develop ovarian cancer similar to the human pathology. This current study investigates the health outcomes of more than 1,000 hens assigned to 46-week dietary regimens exposing hens to distinct compositions of PUFA and phytoestrogen lignan. Hens (3 years age; approx. n=170 per diet group) were assigned to one of five experimental, isocaloric diets in which the main corn composition was supplemented with one of the following (15% whole flaxseed, 15% defatted flaxseed, 5% flaxseed oil, 5% corn oil, and 5% fish oil) and then compared to a control diet made predominantly of corn. Hen mortality during the study responded significantly to diet, with lowest mortality in the defatted flax diet (27%) and the highest mortality in the corn oil diet (37%). Corn oil fed hens also exhibited exaggerated mortality during the molting phase of the study (2.5-fold higher than other diets). Cancer (of all types) as well as ovarian cancer were significantly more prevalent in the control diet. Logistic regression analysis indicates a reduced likelihood of ovarian cancer or other peritoneal cancer in whole flax, defatted flax, and corn oil fed hens, in reference to control diet fed hens. Two-way ANOVA shows a significant effect of diet and pathology on hen body weight, such that whole flax, defatted flax, and pathology-stricken hens weighed the least. Daily egg laying productivity was highest in whole flax, defatted flax, and fish oil fed hens, indicating a benefit of omega-3 PUFA and phytoestrogen lignan on ovarian and oviductal reproductive health. Whole flax fed hens were also least likely to experience a regressed ovary during the study, prompting greater reproductive capacity in these hens. Single cell electrophoresis (COMET) analysis revealed increased DNA damage in corn oil fed hens and reduced DNA damage in whole flax and flax oil fed hens. In summary, this research on laying hens provides evidence that daily consumption of omega-3 PUFA and phytoestrogen lignan reduces ovarian cancer morbidity, enhances overall longevity, provides leaner body mass, improves reproductive health, and enhances genomic stability. This study also suggests that the excessive consumption of omega-6 PUFAs (e.g. corn foods) is physiologically insulting in the majority of the parameters observed here. Funding: NIH RO1-AT005295

### **Cancer-Therapy Induced Ovarian Toxicity: Molecular Mechanisms and Potential Therapeutics.** Chihiro Emori, Ryan Kurtz, and Ewelina Bolcun-Filas

Women cancer survivors can suffer from early ovarian failure or infertility because their ovarian reserve is significantly depleted or lost due to cancer treatments. Many chemotherapy drugs and radiation kill cancer cells by inducing DNA damage. Quiescent oocytes in primordial follicles are very sensitive to DNA damage; therefore those treatments can also be detrimental and lethal to exposed oocytes. Severe oocyte depletion causes infertility but most importantly it also results in early menopause and health problems associated with hormonal deficiencies. In order to prevent oocyte loss caused by cancer treatments we need to understand the mechanisms of DNA damage response in immature oocytes and ovarian tissue. A previous study in our group had reported that Checkpoint kinase 2 (CHK2) is responsible for oocyte death caused by radiation-induced DNA damage. Chk2 deficient (Chk2<sup>-/-</sup>) females exposed to sterilizing doses of radiation maintain healthy ovarian reserve and fertility suggesting that CHK2 inhibition could be used as a fertoprotective treatment against radiation induced sterility. Similar protection was achieved by pharmacological inhibition of CHK2. In response to DNA damage, CHK2 phosphorylates p53 and TAp63, both of which trigger apoptosis in somatic cells and oocytes, respectively. However the underlying mechanisms of DNA damage sensitivity in meiotically arrested immature oocytes are not well understood. Therefore we aim to identify molecules and signaling networks involved in the DNA damage response in oocytes. Wild type oocytes damaged by radiation undergo apoptosis within 24 hrs after treatment. We used Chk2<sup>-/-</sup> mice as a model to study DNA damage response and repair in oocytes that survive. We previously reported the analysis of gene expression differences between wild type and Chk2<sup>-/-</sup> mouse ovaries treated with radiation by RNA-seq. We found that 70% of genes differentially expressed in the wild type after radiation were regulated by CHK2-dependent signaling. In the present study, we examined expression levels of CHK2-dependent radiation-responsive candidates that have not been studied in the context of oocyte and ovarian function but have been implicated in DNA damage response in other cell types. Wild type and Chk2<sup>-/-</sup> juvenile ovaries were exposed to radiation (0.5 Gy) and expression of three selected proteins was analyzed 6 hours after exposure. GIT2 (G protein-coupled receptor kinase-interactor 2; known substrate of ATM) is expressed in both somatic cells and oocytes which suggests a global role in DNA damage response throughout the ovary. AGO3 (Argonaute RISC catalytic subunit 3; involved in piRNA synthesis) and EDARADD (EDAR Associated Death Domain) are predominantly expressed in oocytes in primordial follicles which are exquisitely sensitive to DNA damage thus AGO3 and EDARADD may play a role in oocyte's death. We will report the effects of cancer drugs commonly used in cancer treatments on the primordial follicle reserve in Chk2<sup>-/-</sup> ovaries and analyze expression levels of radiation-responsive genes in chemotherapy treated ovaries. Collectively, our findings will contribute to a better understanding of ovario-toxicity caused by cancer therapies and to development of fertoprotective treatments for cancer patients.

**Zika Virus Infection Induces Endoplasmic Reticulum Stress in Placental Trophoblast cells.** Philma Glora Muthuraj, Ezhumalai Muthukrishnan, Aryamav Pattanik, Prakash Kumar Sahoo, and Sathish Kumar Natarajan

Zika Virus (ZIKV) infection in pregnant women is highly associated with Congenital Zika Syndrome and the development of microcephaly, intra uterine growth retardation and ocular damage in the fetus. Recent advances suggest that ZIKV can be vertically transmitted to the fetal organs including the fetal brain via the placenta. Placental infection during the first and second trimester plays a crucial role in ZIKV transmission from maternal circulation to the fetus resulting in Congenital Zika Syndrome. Further,

ZIKV infection induces placental trophoblast cell apoptosis. However, the mechanism of trophoblast apoptosis caused due to the ZIKV infection is unclear. Here we hypothesize that endoplasmic reticulum (ER) stress is the mechanism behind ZIKV-induced placental trophoblast apoptosis. Methods: HTR-8, a human normal immortalized trophoblast cells and human malignant-derived trophoblast (JEG-3 and JAR) cell lines were infected with 0.1-1.0 MOI ZIKV. X-box binding protein 1 (XBP1) splicing assay and relative C/EBP homologous protein (CHOP) mRNA expression was quantified using qRT-PCR as markers of ER stress after 3- 24 h of ZIKV infection. Apoptosis was assessed by characteristic nuclear morphology staining with DAPI and caspase 3/7 activity assay. Results: We observed a significant increase in the mRNA levels of CHOP after 12-16 h of ZIKV infection in placental trophoblast cells. We also observed a dramatic increase in the spliced form of XBP1 in placental trophoblast cells infected with ZIKV after 16 h indicating ER stress. As prolonged ER stress can cause apoptosis, we observed a dramatic increase in placental trophoblast apoptosis after 48 h of ZIKV infection as evidenced by biochemical characteristic nuclear morphology and caspase 3/7 activation. In conclusion, ER stress could be the potential molecular mechanism underlying ZIKV-induced placental trophoblast apoptosis. The critical role of ER stress activation in placental trophoblast cells with ZIKV infection is now under investigation

**Production of Knock-In Embryo By CRISPR/Cas9-Mediated Homologous Recombination to Produce Bovine Lactoferrin on Bovine B-Casein Gene Locus.** Da Som Park, Se Eun Kim, Deog-Bon Koo, and Man-Jong Kang

The production of pharmaceutical proteins by transgenic animals is one of the major successes of biotechnology. Knock-in system is a more powerful method to produce mammary gland bioreactor. To date, zinc-finger nuclease(ZFNs), transcription activator-like effector nuclease(TALENs), and clustered regularly interspaced short palindromic repeats(CRISPR)/Cas9 systems have been developed for gene targeting. The objective of this study was to develop a knock-in embryo for expression of bovine lactoferrin in the bovine  $\beta$ -casein gene locus by microinjection of knock-in vector with CRISPR/Cas9 into bovine zygote. The three replacement knock-in vectors containing a different length of homologous arm were constructed. These targeting vectors were used enhanced green fluorescent protein(eGFP) as a positive selection marker. These knock-in vectors with CRISPR/Cas9 were microinjected into the pronuclear bovine embryo. And the embryos were cultured to blastocyst in the culture medium. These blastocysts were analyzed by PCR to confirm gene targeting by homologous recombination. As a result, when bLF\_1kbHR and 40HR\_GFP knock-in vector with CRISPR/Cas9 was microinjected into cytoplasm of bovine zygotes, the efficiency of gene targeting was 22.2-26.7% but gene targeting by homologous recombination was not detected when bLF\_100HR\_GFP knock-in vector was microinjected into cytoplasm of bovine zygotes. The precise bovine lactoferrin gene integration of knock-in embryos was confirmed by DNA sequencing analysis. Our knock-in system may help to create transgenic dairy cattle expressing enhanced bovine lactoferrin protein in the mammary gland via the endogenous expression system of the bovine  $\beta$ -casein gene.

**Sensing Sperm by Bovine Uterine Epithelial Cells via TLR2 and TLR4 Signaling Pathway in Vitro.** Akio Miyamoto, Mohamed A. Ezz, Ahmed E. Elweza, Mohamed A. Marey, Tomoko Kawai, Maike Heppelmann, Christiane Pfarrer, Kazuhiko Imakawa, Samy M. Zaabel, and Masayuki Shimada

Sperm is allogenic to the female genital tract. We recently reported that sperm attachment to bovine uterine epithelial cells (BUECs) triggers uterine local innate immunity with induction of a pro-inflammatory response in vitro, but the detail mechanism remains unknown. Toll-like receptors (TLRs) are the most important innate immune cell receptors involved in the stimulation of inflammatory responses to infectious and non-infectious agents. The present study was aimed to investigate whether TLRs, in particular TLR2/4, signaling pathway plays a role in mediating sperm-BUECs interaction for initiation of the pro-inflammatory response in vitro. First, uterine tissue samples from follicular and luteal phases were subjected to immunohistochemistry to investigate the protein expression for TLR2/4 in the bovine endometrium. Immunostaining for both TLR2 and TLR4 was observed in the luminal and glandular epithelia of bovine endometrium in the follicular and luteal phase. Second, sub-confluent BUECs monolayers were co-cultured with 10<sup>6</sup> sperm/ml at 0, 1, 3, and 6 h, then, mRNA expressions of TNF $\alpha$ , IL1 $\beta$ , IL8, and PGES in BUECs were quantified by a real-time PCR. In BUECs, inflammatory responses to sperm began at 1 h, peaked at 3 h and subsided toward 6 h. To test our hypothesis, BUECs monolayers were pre-incubated with TLR2 antagonist or TLR4 antibody, then stimulated with sperm, and gene expressions were evaluated. Addition of TLR2 antagonist or TLR4 antibody to sperm/BUECs co-culture abrogated the stimulatory effect of sperm on TNF $\alpha$ , IL1 $\beta$ , IL8, and PGES mRNA expression in BUECs. The phosphorylation levels of downstream components of TLR2/4 signaling pathway, p38 MAPK, JNK, ERK1/2, NF $\kappa$ B, and IRF3 proteins were semi-quantitatively analyzed in BUECs by Western blotting after co-culture with sperm. The results showed that the levels of phospho-p38 MAPK IgG and phospho-JNK IgG increased in BUECs by the co-culture with sperm. A pre-incubation of BUECs with TLR4 antibody blocked the phosphorylation of p38 MAPK, while either TLR2 antagonist or TLR4 antibody blocked the phosphorylation level of JNK. Collectively, our data strongly suggest that sperm use TLR2/4 signaling in a MyD88-dependent pathway to activate downstream components (p38MAPK and JNK) which in turn stimulate nuclear translocation of the inflammatory transcription factor (AP-1) with subsequent transcription of pro-inflammatory cytokines (TNFA and IL-1B), chemokines (IL-8) as well as PGES in BUECs in vitro. In conclusion, bovine uterine epithelial cells sense and react to sperm via TLR2/4 signal transduction.

**Technique Development for Future in Vivo Drug Delivery Into Ovarian Follicles and Cell Imaging.** Jean M. Feugang, Ishak M. A. Ghassan, Matthew Eggert, Gabriel A. Dutra, Seong B. Park, Christy S. Steadman, Robert R. Arnold, Scott T. Willard, Peter L. Ryan, and Eduardo L. Gastal

Folliculogenesis and oogenesis processes dictate the fertility of females through the ovulation of high quality oocytes. Despite the current technological advances, the success of assisted reproduction is still limited due to the poor quality of utilized oocytes, often obtained from developing or unknown physiological status follicles. The use of a novel minimally invasive technique for follicle wall biopsy (FWB) and follicular fluid (FF) sampling, recently developed in our laboratory (Ishak et al., SSR 2018; abstract 322), preceded by an intrafollicular injection of a fluorescent dye, may facilitate the characterization of follicle status and FF milieu, and assist in the selection of high quality oocytes in live females for fertility improvement. Here, we injected fluorescent nanoparticles into ovarian follicles of live mares for imaging of FWB, granulosa cells (GC), and FF samples, and assessed drug delivery efficiency in cultured pig follicles. In Experiment 1, ovarian follicles of nine Quarter horse breed mares (8-14 years) weighing 400-600 kg (Southern Illinois University farms) were tracked daily, using a duplex color-Doppler ultrasound machine. Follicles showing continuous growth for a minimum of three

consecutive days were classified as small (SF: 15-23 mm; n=12) or large (LF: 24-30 mm; n=10). Each follicle (2-3/mare) was transvaginally ultrasound-guided injected with synthesized fluorescent liposome nanoparticles using a double-channel injection system, and non-injected follicles (SF and LF) served as controls. Twenty-four hours later, a combination of in vivo FWB harvesting and FF collection (Ishak et al., SSR 2018; abstract 322), and follicle flushing technique to obtain GC was used. Biopsy fragments, and centrifuged FF and GC samples were kept at 4°C for subsequent imaging. In Experiment 2, pig ovaries were harvested post-mortem and antral follicles dissected. After 24 h culture (5% CO<sub>2</sub>, 100% humidity), follicles were microinjected with 5 µl (94 mM) of plain fluorescent liposomes (for plasma membrane labeling) or non-fluorescent liposomes loaded with doxorubicin (for nucleus labeling) and cultured for another 24 h. Samples collected in Experiments 1 and 2 were imaged fresh and/or fixed (histology sections) for fluorescence detection (radiance efficiency) of liposomes or doxorubicin. Data were analyzed with ANOVA-1 (SPSS) and P 0.05. In Experiment 2, successful intrafollicular microinjections were confirmed with follicle cells exhibiting plasma membrane (liposome;  $1.4 \times 10^9 \pm 0.5 \times 10^9$ ) or nucleus (doxorubicin;  $1.8 \times 10^9 \pm 0.8 \times 10^9$ ) fluorescence intensities above background ( $0.4 \times 10^9 \pm 0.2 \times 10^9$ ). In conclusion, this study validates an in vivo technique for future intrafollicular drug delivery using fluorescent nanoparticles associated with FWB, FF, and granulosa cell collection in living animals for scientific and diagnosis purposes. Supported by Southern Illinois University; Mississippi State University, Office of Research and Economic Development (SEC travel grant), and USDA-ARS Biophotonics Initiative (8-6402-3-018).

**Seasonal Variation in Equine Follicular Fluid Proteome.** Gabriel A. Dutra, Ghassan M. Ishak, Seong B. Park, Christy S. Steadman, Olga Pechanova, Tibor Pechan, Daniel G. Peterson, Julio C.F. Jacob, Scott T. Willard, Peter L. Ryan, Eduardo L. Gastal, and Jean M. Feugang

Ovarian follicular fluid (FF) is composed of blood plasma exudates and follicle cell secretions. This biofluid is a microenvironment containing various proteins involved in several reproductive processes. Although FF proteome studies do exist in several species, including the horse, the seasonality influence on FF proteome has not been explored and remains unknown in livestock. Therefore, the application of large-scale shotgun proteomic analyses of FF in the horse, a seasonal breeder, has potential to identify key proteins of physiological processes controlling follicular and oocyte growth that are affected by seasonal variations. Here, we investigated the proteome profiles of equine FF obtained during breeding and non-breeding seasons. A total of seventeen mares were maintained under natural light in pasture, with ad libitum access to water and trace-mineralized salt at Southern Illinois University farms. During the non-breeding season (spring transitional anovulatory, SA), ovarian follicles greater than 6 mm in diameter were ablated to induce a new follicular wave, followed by a regular scanning (B-mode ultrasonography) of ovaries until a dominant follicle reached 30-35 mm. During the breeding season [spring ovulatory (SO), summer (SU), and fall ovulatory (FO)] mares were allowed to cycle normally without the use of any drug. Twelve days after ovulation, follicles were ablated and ovaries were scanned until a dominant follicle reached 30-35 mm, as aforementioned. The FF samples were collected during each season from dominant growing follicles (SA, n=6; SO, n=6; SU, n=6; FO, n=12) by ultrasound-guided transvaginal aspiration. Samples were centrifuged and supernatants were stored at -80°C until analyses. All frozen-thawed FF samples were digested with trypsin and subjected to nano-liquid chromatography – tandem mass spectrometry (n-LC MSMS) proteomic analyses. A total of 90 proteins were identified with high confidence (FDR < 1%), regardless of the season. All identified proteins were

annotated with NCBI (87%) or ENSEMBL (13%). The proteomes of SA, SO, SU, and FO corresponded to 63, 72, 69, and 78 proteins, respectively, with 52 proteins being shared across all seasons. Thirteen proteins were unique to SA (1), SO (3), SU (3), and FO (6), and 25 proteins were shared among 2-4 seasons. Interestingly, the quantitative proteomic analysis revealed lower ( $P < 0.05$ ; ANOVA) levels of proteins associated with various biological functions such as blood coagulation (prothrombin), thyroid hormone transport (transthyretin), and cysteine-type endopeptidase inhibitor activity (fetuin-B) in SU-FF, compared to other seasons. In conclusion, the study offers unique proteome profiles of equine FF related to seasonality, while revealing a number of proteins that may serve as candidate biomarkers for seasonal changes in mares' fertility. Supported by CAPES scholarship (PPGMV-UFRRJ#88881.133485/2016-01), Brazil; Southern Illinois University; IGBB-Mississippi State University, and USDA-ARS Biophotonics Initiative (Grant#8-6402-3-018).

**Beta-Carotene Potently Inhibits the Testicular Injuries Caused by Exogenous Scrotal Hyperthermia in Mice.** Sang-Yoon Nam, Jung-Min Yon, Jae Seung Kim, Chunmei Lin, Seul Gi Park, Jong-Geol Lee, and In-Jeoung Baek

Modern lifestyles and various environmental toxins can induce scrotal hyperthermia, resulting in male infertility. In this study, we investigated whether  $\beta$ -carotene ( $\beta$ -CA) or ellagic acid (EA) originated from various fruits and vegetables has a preventive effect on male infertility induced by exogenous scrotal hyperthermia. ICR adult mice were intraperitoneally treated with 10 mg/kg of  $\beta$ -CA or EA daily for 13 days consecutively. During this time, they were subjected to transient scrotal heat stress in a water bath at 43°C for 20 min on day 7, and their testes and bloods were collected on day 14 for histopathologic and biochemical analyses. Heat stress induced significant testicular weight reduction, germ cell loss and degeneration, as well as abnormal localizations of phospholipid hydroperoxide glutathione peroxidase (PHGPx) and manganese superoxide dismutase (MnSOD) in spermatogenic and Leydig cells. Heat stress also altered the levels of oxidative stress (lipid peroxidation, SOD activity, and PHGPx, MnSOD, and hypoxia inducible factor-1 $\alpha$  mRNAs), apoptosis (B-cell lymphoma-extra large, BCL2-associated X protein, caspase 3, nuclear factor kappa-light-chain-enhancer of activated B cells B, and transforming growth factor-beta 1 mRNAs), and androgen biosynthesis (serological testosterone concentration and 3 $\beta$ -hydroxysteroid dehydrogenase mRNA) in testes. However, these all changes were improved significantly by  $\beta$ -CA treatment, but slightly by EA treatment. These findings indicate that  $\beta$ -CA is a potent preventive agent against testicular injuries induced by scrotal hyperthermia through modulations of oxidative stress, apoptosis, and androgen biosynthesis, which may offer a preventive and therapeutic choice in the treatment of male infertility due to environmental toxicants.

**TRP Channels, Sensors for Temperature, are Localized on Bovine Endometrium and Involved in Increase of Prostaglandin Production of Bovine Endometrial Stromal Cells Under Heat Stress.** Ai Yamada, Keito Takami, Shunsuke Sakai, Yuki Yamamoto, and Koji Kimura

Recent reports indicate that the pregnancy rate of cattle dramatically decreases during the summer season owing to global warming. In ruminant species, pregnancy depends on attenuation of endometrial secretion of PGF2 $\alpha$  for maintenance of the corpus luteum (CL). In a previous study by our group, we found that heat stress (HS) enhances the secretion of both PGF2 $\alpha$  and PGE2 (PGs) in cultured bovine

endometrial cells (unpublished data), although the mechanism underlying this effect remains unknown. Several signaling pathways and cascades enable cells to sense and react to various environmental stimuli such as osmolality, temperature, and mechanical stimuli. Transient receptor potential (TRP) channels are ion channels located on plasma membranes, some of which are involved in temperature sensing. The present study investigated the role of TRP channel-mediated temperature sensing on the enhancement of bovine PG endometrial secretion under HS conditions.

The first experiment investigated the endometrial location of temperature-sensing TRP channels (TRPV3, V4, and M2), which sense bovine body temperature, by immunohistochemistry. Slaughterhouse derived uteri classified at the late luteal stage (day 14–17) were used for the experiment. Uterine horns ipsilateral to CL were fixed and sliced, and each section was immunostained with antibodies against TRPV3, TRPV4, or TRPM2. While TRPV3 was not clearly observed in the bovine endometrium, TRPV4 was slightly detected in luminal epithelial cells. TRPM2 was observed in each region of the uterine tissues, especially in luminal and glandular epithelial cells, which presented stronger signals than stromal cells, myometrium, and endothelial cells. The second experiment investigated the effect of TRP channels inhibition on PGs secretion by HS endometrial stromal cells. In our previous study, HS did not influence PGs secretion by epithelial cells (unpublished data); therefore, only stromal cells were used in the present experiment. Bovine endometrial stromal cells were collected and cultured in the presence of each of the antagonists for TRPV3, V4, and M2 ( $n = 5, 5, \text{ and } 9$ , respectively) for 34 hours, at either 38.5°C (control) or 40.5°C (HS). After incubation, the PGs concentrations in the culture media were measured by EIA. When stromal cells were cultured in the presence of TRPV3 or TRPV4 antagonists, HS significantly increased the secretion of PGs ( $p < 0.05$ ) compared to the controls, suggesting that inhibition of TRPV3 and TRPV4 does not reduce the effect of HS on PG secretion by bovine stromal cells. On the contrary, when the TRPM2 antagonist was added to the culture medium, PGs secretion significantly decreased ( $p < 0.05$ ) under HS condition. No significant difference was observed in the PGs secretion of HS and control at higher antagonist concentrations. Moreover, this effect was not detected in controls.

Taken together, these results suggest that temperature-sensing TRP channels are located on the bovine uterine endometrium and their inhibition reduces the effect of HS on PGs secretion by endometrial stromal cells.

### **Role For Systemic IGF1 in Female Reproductive Function Revealed by Disruption of Estrogen**

**Dependent Uterine IGF1 Synthesis.** Sylvia C. Hewitt, Sydney L. Lierz, Marleny Garcia, Artiom Gruzdev, Sara A. Grimm, and Kenneth S. Korach

Insulin-like growth factor 1 (IGF1) is primarily synthesized and secreted from the liver, however estrogen (E2) increases uterine, but not liver, IGF1 mRNA. IGF1 is secreted by uterine stromal cells and understood to stimulate uterine epithelial cell growth via a paracrine mechanism. Uterine estrogen receptor  $\alpha$  (ER $\alpha$ ) ChIP-seq profiles reveal a potential enhancer region distal (40-70 KB) from the IGF1 TSS with five E2-dependent peaks of ER $\alpha$  interaction (enhancers 1-5) and E2 dependent enhancer-associated characteristics, including induction of enhancer RNA (eRNA) transcription. We created two mouse models that prevent E2 mediated induction of uterine IGF1. The first model was made by deleting 430 bp encompassing enhancer 4, thereby disrupting ER $\alpha$  binding to enhancer 4, as well as E2 dependent eRNA transcription from enhancers 3, 4 and 5, and p300 binding to enhancer 3, 4 and 5 and the IGF1

transcription start site. As a result, uterine E2 induction of Igf1 mRNA was completely eliminated while liver expression of Igf1 mRNA remains unaffected. However, loss of the enhancer and consequent estrogen regulation of uterine transcribed Igf1 mRNA did not affect fertility or uterine growth responses. The second mouse model was made by deleting uterine Igf1 using PgrCreIgf1f/f, and as in the enhancer deletion model, estrogen-induced uterine growth response was not impacted. However, females are sub fertile, as indicated by the production of an average of 11.8 pups/dam by Igf1f/f females during a 3-month long continuous breeding trial, but only 6.25 pups/dam by PgrCre;Igf1f/f females during the same interval. Since pregnancies do occur, and both Igf1 and PgrCre are localized in ovarian granulosa cells, the decreased fertility may be due to an ovarian defect. E2-dependent activation of uterine IGF1 signaling was not impaired by disrupting the distal enhancer or by deleting the uterine coding transcript, as indicated by activating phosphorylation of the uterine IGF1 receptor and increased IGF1 in the uterine tissue. Our findings are consistent with systemic IGF1 entering uterine tissue during the period of increased vascular permeability known to occur in response to E2. Therefore, E2 facilitates uterine uptake of systemic IGF1, calling into question the importance of the E2-induced stroma cell-secreted IGF1 on neighboring epithelial cells. Overall, our work highlights the central role of a distal enhancer in assembly of the factors necessary for E2 and ER $\alpha$  mediated induction of Igf1 transcription in the uterus in a whole animal (mouse) model, as well as a role for systemic IGF1 in female fertility.

**The Effect of Galectin-1 on Forkhead Box P3 Protein in Bovine Caruncular Endometrium.** Daniel J. Mathew, John A. Browne, Lindsay F. Grose, Heather L. Baldwin, and Patrick Lonergan

In cattle, early embryonic mortality accounts for approximately 70% of failed pregnancies. Inappropriate maternal immune responses to the conceptus may contribute to reproductive failure. Galectins, glycan-binding proteins, have immune-modulatory activities. In rodent endometrium, galectin-1 (LGALS1) increases the number of tolerogenic dendritic cells (DC) and regulatory T-lymphocytes (Treg) that express CD11c and forkhead box P3 (FOXP3), respectively. The DC and Tregs promote maternal immune suppression during embryo implantation. Galectin-1 is expressed by the bovine conceptus and may have similar functions during early pregnancy in cattle. In a previous study, LGALS1 increased FOXP3 mRNA in bovine endometrial caruncles suggesting the presence of Treg. In this study, the effect of LGALS1 on FOXP3 protein and relative abundance of CD11c mRNA within the caruncle was explored. FOXP3 is expressed in epithelial cells; therefore, the effect of LGALS1 on FOXP3 mRNA in cultured bovine endometrial epithelial cells was tested. Caruncles and cells were collected from uteri (n=4) during the mid or late luteal phase of the estrous cycle. In Experiment 1, one to two caruncle explants from each uterus were cultured in RPMI (control) or RPMI containing 10, 100 or 1000 ng/mL of LGALS1 for 6 or 24 h. Caruncles were snap-frozen or fixed. RNA was extracted and abundance of CD11c mRNA determined using RT-qPCR. FOXP3 protein was localized within fixed caruncles from three uteri using immunohistochemistry. In Experiment 2, endometrial epithelial cells, in transwell inserts over fibroblasts, were treated with 300  $\mu$ L of RPMI (control) or RPMI containing 1, 10 or 100 ng/mL of LGALS1 for 6 h. Cell mRNA was extracted and FOXP3 mRNA measured using RT-qPCR. A MIXED procedure in SAS was used to statistically analyze the data. Residuals were tested for normality and CD11c data were corrected by transformation. A Tukey-Kramer adjustment and contrast statement, comparing control vs. all LGALS1 treatments, were included. A  $p \leq 0.05$  was considered significant. Data are presented as non-transformed least squares means  $\pm$  standard error (LSM  $\pm$  SEM). There tended to be an effect of treatment on CD11c mRNA ( $P = 0.06$ ). Compared to controls ( $0.75 \pm 0.15$ ), caruncles treated with 10 ( $P <$

0.05) but not 100 or 1000 ng/mL of LGALS1 had greater expression of CD11c (1.18, 0.98 and  $0.91 \pm 0.15$ , respectively; contrast,  $P < 0.05$ ). Dark staining of FOXP3 protein was localized within individual cells distributed throughout the stroma. There tended to be an effect of treatment, after 24 h, on the number of FOXP3 positive cells ( $P = 0.07$ ). Compared to controls ( $13 \pm 10$ ), the number of FOXP3 positive cells tended to increase with concentration of LGALS1 (10, 100 and 1000ng/mL; 16, 23 and  $22 \pm 10$ , respectively; contrast,  $P < 0.05$ ). Light staining for FOXP3 was observed within the uterine epithelium. Treating epithelial and fibroblast cells with LGALS1 had no effect on cell FOXP3 mRNA. Conceptus LGALS1 may promote expansion of DC and Treg within the bovine endometrial caruncle, contributing to immune suppression at the fetal-maternal interface in cattle. This project was funded by Science Foundation Ireland 13/IA/1983.

**Genetically Diverse Mice as a Novel Model System to Investigate Genetic Etiology of Female Infertility.**  
Ewelina Bolcun-Filas, Chihiro Emori, and Ryan Kurtz

It is estimated that nearly 50% of infertility cases are due to genetic factors, yet the causal mutations are rarely identified in patients. Hundreds of genes are involved in mammalian reproduction, and infertility likely arises from deleterious combinations of multiple alleles rather than single gene defects. Additionally, environmental factors such as diet or exposure to chemicals or drugs play an important role making the identification of infertility-causing mutations/polymorphisms that much more challenging in large-scale human genetic studies. The etiology of female infertility is complex; inability to produce offspring can be caused by disorders of the ovary, fallopian tubes, uterus or hormonal signaling. Breaking down the individual disorders into more specific reproductive phenotypes would facilitate the discovery of genetic causes underlying fertility problems. The number and quality of eggs in the ovarian reserve are two important ovarian determinants of female fertility. Deficiencies in egg quantity and quality can lead to infertility, increased incidence of miscarriages, birth defects and premature ovarian failure. The majority of mouse models of human infertility are loss-of-function mutations in a single gene in one or two inbred strains. We are using the Collaborative Cross (CC) and Diversity Outbred (DO) mice as a novel model to study genetic causes of female reproductive problems inherent to diverse population. The CC lines have been bred using a combinatorial funnel that produces a large number of multiparental recombinant lines from eight inbred founder strains. Each CC line is genetically different and represents unique mosaic of eight parental genomes; all mice within a given line are genetically identical. In contrast, each DO mouse is genetically unique (similar to a human individual) with a high level of allelic heterozygosity. The DO mouse population was seeded via random breeding of incipient CC lines. The DO population is kept as heterogeneous stock, which, through a random breeding system, provides an unlimited source of novel allelic combinations, thus offering the best available mammalian model for genetic complexity of human population. Importantly, CC lines, DO mating pairs and founder inbred strains show considerable variation in reproductive performance, which we show is due in part to female factors determining the quality and quantity of oocytes. Some DO mating pairs are non-productive or have only one or two pups per litter compared to the average of eight or maximum of 16-17 pups. Some CC lines are robust breeders while others have small and/or infrequent litters. There are also CC lines with male or female bias in offspring, which makes them difficult to maintain. These multiparent genetic resources offer the opportunity to correlate these features, similar to human instances of infertility, to genomic sequence and thereby analyze specific reproductive phenotypes and their genetic regulation. The CC is optimal for longitudinal studies of oocyte development in the context of various

allelic combinations; while the DO is ideal for high precision mapping of genetic variants regulating specific reproductive traits. We will present our analyses of selected reproductive traits in founder strains, CC lines and DO females, and their link to reproductive performance.

**Supplementation of Growth Factors Improves Mouse Oocyte Developmental Potential via Increased Glucose Metabolism During in Vitro Maturation.** John C. Becker, Rolando Pasquariello, William B. Schoolcraft, Rebecca L. Krisher, and Ye Yuan

Our previous work demonstrated that a combination of human growth factors (GFs; fibroblast growth factor-2 (FGF2, 40 ng/ml), leukemia inhibiting factor (LIF, 20 ng/ml), insulin growth factor-1 (IGF1, 20 ng/ml)) during in vitro maturation (IVM) resulted in improved developmental potential in porcine and mouse oocytes. The means by which GFs achieve this goal, however, remains relatively unclear. The objective of this study was to identify potential signaling and metabolic pathways that contribute to improved oocyte quality achieved by these GFs. Cumulus-oocyte complexes (COCs) were obtained from outbred CF1 mice (4-8 weeks old) 46-48 h after being injected with 5 IU PMSG, and then matured in defined IVM medium (0.5 mM glucose, 0.5 mM pyruvate, 4.0 mM lactate, 0.5 mM Ala-Gln, 1x MEM-NEAA, 0.25X MEM-EAA, 0.1 mM citrate, 10 ng/mL rmEGF, 1.5 mg/mL fetuin, and 2.5 mg/mL rHSA) for 18 h in 6.5% O<sub>2</sub>/7.5% CO<sub>2</sub> at 37.0°C; either in the presence (GF) or absence (CON) of the three GF combination described above. Percentage data were arcsin transformed and analyzed by one-way ANOVA to detect differences (significance,  $P < 0.05$ ). In the first experiment (four replicates,  $n=207$ ) matured COCs were fertilized and presumptive zygotes cultured in sequential culture medium to examine oocyte developmental potential. Blastocyst development per oocyte at 96 h (GF 55.79±3.61%, CON 42.86±3.25%) and blastocyst hatching at 112 h after fertilization (GF 52.63±2.95%, CON 37.50±2.92%) were both significantly improved when oocytes were matured in the presence of GFs. In the second experiment (three replicates,  $n=269$ ), COCs were matured for 18 h in both GF and CON groups, then oocytes were denuded, fixed and stained with DAPI and FITC conjugated beta-tubulin antibody. Confocal images were obtained to assess chromosome morphology and spindle alignment. More oocytes matured with GFs had correct spindle alignment than those matured without GFs (GF 91.59 ± 3.46%, CON 75.00 ± 3.71%). In the same experiment, medium was collected after maturation and glucose concentrations assessed by a fluorometric assay. The glucose concentration of control medium collected from wells without any COCs was set as 100%. COCs matured with GFs consumed significantly more glucose than those without GFs (GF 26.18 ± 1.24%, CON 38.22 ± 1.14% remained), suggesting a more active glucose metabolism in COCs matured with GFs. In summary, these results suggest that the prescribed GFs enhance glucose metabolism in COCs during IVM. Improved glucose utilization may better alleviate oxidative stress during IVM and result in less oocyte spindle damage, thereby improving oocyte quality.

**KIT Signaling Regulates Perinatal Oocyte Development in the Mouse Ovary.** Joshua Burton and Melissa Pepling

In mammalian females, fecundity is determined at the time of birth. Establishment and maintenance of the ovarian reserve must therefore be without defect to prevent the loss of fertility. The KIT signaling pathway is well known for promoting cell survival, proliferation, and differentiation in a variety of processes including gametogenesis, melanogenesis, and hematopoiesis. During fetal gonadogenesis, KIT mediates the proliferation of primordial germ cells (PGCs) that migrate to, and colonize the gonadal

primordium. As PGCs proliferate, they produce clusters of cells known as germ cell cysts. As oogenesis progresses, cysts undergo programmed breakdown during which oocytes become separated from each other and are packaged into the primordial follicles that comprise the ovarian reserve. During the process of cyst breakdown and follicle formation approximately two thirds of the oocytes are lost. However, the mechanisms regulating cyst breakdown, oocyte numbers and follicle assembly are still not well understood. We have previously shown via an organ culture system that KIT signaling promotes cyst breakdown and primordial follicle formation in the mouse ovary. Ovaries dissected at 17.5 days post coitum (dpc) and cultured for five days in media supplemented with KIT ligand (KITL) showed significant increases in cyst breakdown and the progression of follicle development, relative to untreated control ovaries. In contrast, ovaries treated with ACK2 (a KIT function blocking antibody) showed a significant reduction in cyst breakdown and follicle development relative to controls. We also showed by western blotting that ovaries cultured in media supplemented with KITL have increased MAPK activation. Based on these findings, we hypothesized that KIT activates the MAPK pathway to initiate cyst breakdown and follicle formation. Immunostaining for phosphorylated MAPK in the neonatal mouse ovary indicates activation both in the nuclei and cytoplasm of oocytes and granulosa cells. To determine whether MAPK signaling is consequential for oocyte development, ovaries were dissected at 17.5 dpc and cultured for five days with a daily dose of media containing 10 $\mu$ M of U0126 (a MEK inhibitor), or in media with 0.05% DMSO as a vehicle control ( $n \geq 5$  ovaries per group). After the culture period, ovaries were stained with a germ cell marker for confocal imaging and histological assessment. We did not observe an effect on cyst breakdown and early follicle development due to MAPK inhibition, but have demonstrated that U0126 inhibits MAPK activation in cultured ovaries. We deduce that KIT may be working through other signaling cascades such as the JAK/STAT or PI3K pathways. It may also be possible that MAPK is activated both upstream and downstream of KIT. We observed reduced phosphorylation of MAPK in ovaries treated with ACK2, and increased phosphorylation in ovaries treated with KITL. Interestingly, we also observed a decrease in phosphorylated KIT in ovaries treated with U0126, but increased KIT activation in ovaries treated both with U0126 and KITL. These observations are important as they point to the potential molecular mechanisms that regulate oocyte development, and may serve to better elucidate the etiology of reproductive disorders like primary ovarian insufficiency. Research supported by NIH R15 075257.

**Environmentally-Relevant Exposure to Dibutyl Phthalate (DBP) Results in Decreased Expression of Brca1 in the Adult Mouse Ovary.** Franchesca M. Nuñez, Xiaosong Liu, and Zeliann R. Craig

The gene Brca1 encodes a protein involved in the response to DNA damage by DNA double-strand breaks (DSBs). In women, abnormal expression of Brca1 has been implicated in infertility and in breast and ovarian cancer development. We have previously shown that environmentally-relevant oral exposure to the endocrine-disrupting chemical dibutyl phthalate (DBP) causes significant alterations in the expression of DSB sensing and repair genes, including Brca1, in the juvenile mouse ovary. However, the effects of phthalate exposure on Brca1 expression and how that consequently affects adult ovarian function is understudied. Therefore, this study was designed to investigate the effects of DBP exposure on the expression of Brca1 and the potential mechanisms mediating such effects in the adult mouse ovary. Female CD-1 mice (60 day old;  $n=8$  per treatment) received daily doses of vehicle or DBP at 10, 100, and 1000  $\mu$ g/kg/day for 30 days. At the end of dosing, ovaries were collected and processed for qPCR and western blotting analyses. Results showed that ovaries from phthalate-treated mice expressed

significantly lower Brca1 mRNA and protein levels ( $n=4-7$  mice/treatment,  $p\leq 0.05$ ) than vehicle-treated controls. Since Brca1 mRNA and protein levels were decreased with exposure to DBP, the possibility of phthalate-induced changes in epigenetic regulation of ovarian Brca1 was explored. To do so, the expression of Dnmt1 mRNA, a DNA methyltransferase responsible for maintenance of methylation patterns after DNA replication, was compared between DBP- and vehicle-treated ovarian samples. Interestingly, DBP-exposure at 100 and 1000  $\mu\text{g}/\text{kg}/\text{day}$  resulted in decreased ovarian Dnmt1 expression when compared to that present in control ovaries. To determine whether differential expression of Dnmt1 impacted the methylation profile of Brca1, DNA samples were subjected to EPITYPER assays using a region of the Brca1 promoter. Analysis produced 28 cleavage products with 11 of them flagged as possible methylation sites. Interestingly, none of the 11 sites showed differential methylation patterns between controls and phthalate-treated ovaries. However, the product CpG#6 showed a non-significant trend for increased methylation after DBP exposure. Our results provide evidence for detrimental effects of DBP exposure on the expression of ovarian Brca1 mRNA and protein. Although there was no significant change in methylation of the promoter sites, a decrease in the expression of Dnmt1 was observed. Future studies will be aimed at further understanding the consequences of decreased expression of these critical genes in the ovary. Supported by NIEHS R00ES021467 (ZRC) and R01026998-01A1 (ZRC).

**Genome-Wide Establishment of Meiotic Super-Enhancers Drives Expression of Spermatogenesis-Specific Genes.** So Maezawa, Masashi Yukawa, Akihiko Sakashita, Kris G. Alavattam, Artem Barski, and Satoshi H. Namekawa

Due to the specific expression of germline genes that facilitate the production of functional gametes, the testis has the most diverse and complex transcriptome among all organs. During spermatogenesis, germ cells go through the global suppression of a somatic gene expression program after the mitosis-to-meiosis transition; at the same time, germ cells undergo activation of thousands of spermatogenesis-specific genes. Here we demonstrate that genome-wide reorganization of super-enhancers drives expression of spermatogenesis-specific genes after the mitosis-to-meiosis transition. Using purified germ cells from four stages of spermatogenesis (undifferentiated spermatogonia, differentiating spermatogonia, pachytene spermatocytes and round spermatids), we performed ChIP-seq analysis of H3K27 acetylation, a marker of active enhancers. At the mitosis-to-meiosis transition, the mitotic type of super-enhancers is closed, while the meiotic type of super-enhancers is newly established. Therefore, super-enhancers are reorganized concomitant with the global gene expression change at the mitosis-to-meiosis transition. The meiotic type of super-enhancers persists into post-meiotic spermatids, and the number of super-enhancers is further increased in round spermatids. SCML2, a suppressor of somatic/progenitor genes in late spermatogenesis, plays a critical role in the reorganization of super-enhancers. Our comparative analysis identifies gene regulatory elements that are established uniquely after the mitosis-to-meiosis transition, revealing a molecular logic to ensure gene expression in late spermatogenesis. Our study highlights the distinct features between the mitotic type of enhancers and the meiotic type of enhancers.

**Maternal Influenza A Virus Infection Restricts Fetal Weight and Alters Placental and Fetal Thymic Gene Expression.** Thomas R. Hansen, Hana Van Campen, Jeanette V. Bishop, Gerrit J. Bouma, Quinton A. Winger, Leticia D.P. Sinedino, Christie E. Mayo, and Richard A. Bowen.

Maternal influenza A viral infections have been associated with low birth weight, increased risk of pre-term birth, stillbirth and congenital defects linked to neurological/behavioral and cardiovascular disease as adults. However, the impact of maternal influenza infection on the child's immune system has not been explored. A pregnant mouse influenza A virus infection model was used to test the hypothesis that maternal infection alters placental gene expression resulting in fetal growth restriction, and impacts the developing fetal thymus. Pregnant C57BL6 mice were inoculated intranasally with influenza A virus A/CA/07/2009 pandemic H1N1 (influenza) or PBS (control) at time points representing pre-implantation (E3.5), peri-implantation (E7.5) or complete placentation (E12.5) (n= 5 per group). Maternal infection was confirmed by serology (HI titer). Control females were seronegative. Fetuses and placentae were collected at E18.5. Influenza-inoculated female mice did not exhibit clinical signs of disease, and the number of fetuses per litter was not significantly different from controls. Influenza RNA was not detected on E18.5 in pooled fetal lung samples, or in the RNA from placentae and pooled fetal thymuses submitted for RNA-Seq. Fetal weight was reduced in mice inoculated on E7.5 (p 0.1) group. Fetal sex was not associated with E7.5 or E12.5 fetal weights. Maternal influenza infection at E3.5 resulted in decreased placenta weights (p < 0.001); however, placental weights in E7.5 and E12.5 influenza litters were not different from controls. Total RNA from individual placenta from influenza (n=3) and control (n=3) litters was subjected to RNA-Seq as were RNA samples from fetal thymuses pooled within a litter from E7.5 influenza (n=3) and controls (n=3). Differentially expressed genes (Bioconductor software in R) were detected using the DESeq2 package. The Benjamini-Hochberg procedure was used to control the false discovery rate. Differences in gene expression were 1.5 fold-change with an adjusted p ≤ 0.05. Transcripts for Pppp, Krt13, Krt15 and Tmem150a were increased in placental samples from E7.5 influenza litters versus controls. These genes contribute to integrity of epithelial cells, immune responses, cell development, catabolism and motility. In thymus, 957 genes were inhibited and 28 genes were stimulated in influenza compared to control fetuses, indicating a massive impact on developing thymus. These genes function in calcium signaling, tight junction, vasodilation, fibrosis and respiratory failure. Influenza virus infection results in decreased fetal weight, most prominently when maternal inoculation occurred at peri-placental implantation; conversely, placental weights were not significantly reduced at the same inoculation times. The upregulated placental genes in E7.5 influenza inoculated litters may reflect injury contributing to fetal growth restriction, with residual effects still evident at term. The massive inhibition of fetal thymic genes by maternal infection with influenza supports further examination of infection on the immune system and consequent susceptibility of offspring to a host of immunologic and infectious diseases. Supported by NIH/NCATS Colorado CCTSI Grant UL1 TR001082 and CVMBS CRC Interdisciplinary Award.

**Investigating the Impact of FAM170A and FAM170B Loss on Male Fertility in the Mouse.** Darius J. Devlin, Kaori Nozawa, Masahito Ikawa, and Martin M. Matzuk

A better understanding of the molecular pathways that control spermatogenesis and sperm function will improve the diagnosis and treatment of male infertility, as well as identify new targets for non-hormonal male contraception. Family with sequence similarity 170 members A and B (FAM170A and FAM170B)

are two testis-specific proteins conserved throughout mammals. FAM170B was reported in the literature to play a role in the acrosome reaction and fertilization in mice, based on in vitro assays. FAM170A, the paralog of FAM170B identified through bioinformatic analysis, was discovered in the COS7 cell line as a transcriptional activator of AP-1; however, its role in the testis is unknown. To discover the subcellular localization of FAM170A, WT adult B6;129 mouse testis and epididymis tissues were subjected to immunofluorescent staining with a commercial rabbit polyclonal antibody, and peanut agglutinin (PNA-FITC) was used as an acrosome marker. FAM170A localized specifically to the acrosome, like FAM170B; however, FAM170A localizes only to elongating spermatids and mature sperm. Using CRISPR/Cas9 zygote electroporation, we generated mice bearing targeted alleles for Fam170a (Chr 18) and Fam170b (Chr 14). Single guide RNAs (sgRNAs) targeting the start codon of either Fam170a or Fam170b were validated in vitro and electroporated with Cas9 protein into B6D2F1 two-pronuclear stage zygotes. Heterozygous offspring from the founder mice were genotyped by PCR and Sanger sequencing before being used to expand colonies for both genotypes. Heterozygous mice bearing a -2 bp deletion in the 5'-end of the Fam170a ORF (Fam170atm1Osb) were generated. The -2 bp deletion causes a frameshift that is predicted to truncate the FAM170A protein. Two unique alleles in the Fam170b ORF were generated: a -1236 bp deletion that causes loss of 34 aa near the N-terminus of the protein (Fam170btm1Osb) and a -35 bp frameshift deletion that is predicted to truncate the FAM170B protein (Fam170btm2Osb). These new genetically engineered mice will enable assessment of the impact of FAM170A and FAM170B loss on mating success, spermatogenesis, mature sperm morphology, and sperm function. Additionally, the possibility of functional redundancy for these genes can be determined by investigating mice carrying Fam170a/Fam170b double knockout genotypes. Uncovering whether the FAM170 proteins are essential for fertility may help expand the profiles of proteins in the acrosome interactome and of genes controlling spermatogenesis and gamete interaction.

This work was supported by Eunice Kennedy Shriver National Institutes of Child Health and Human Development grant HD088412 (M.M.M.) and the National Institute of General Medical Sciences training grant T32GM088129 (TBMM).

### **Biomarker Analysis of Cell-Cycle Regulatory Kinases as Targets for Male Contraceptive Drug**

**Development.** Lesya Holets-Bondar, Hannah Horky, Gunda Georg, Jon Hawkinson, Ernst Schonbrunn, and Joseph Tash

Cyclin-dependent kinases (CDKs) control the eukaryotic cell cycle by phosphorylating serine and threonine residues in key regulatory proteins. The distribution pattern of CDKs and cyclins is dependent on the stages of the spermatogenic cell cycle during testis development and maturation. Murine CDK2 knockout mice are viable, but both male and female CDK2<sup>-/-</sup> mice are sterile due to a block at meiotic prophase I. Thus, CDK2 which is essential for meiosis but not for mitosis, is a promising target for the development of novel non-hormonal male contraceptive agents. The biomarkers of CDK2 inhibition such as, phospho-RB and p53, are present in testis, play critical roles in testis development, and regulation of transition through the spermatogenic cell cycle. The goal of our study is to develop novel CDK2 inhibitors as leads to improve CDK2 specificity, in vivo anti-spermatogenic efficacy, and minimize side-effects. We used dinaciclib (Merck, SCH727965) as a potent CDK2 inhibitor control, and several recently synthesized novel CDK2 inhibitors to evaluate the changes of CDK2 activity in testes. In this assay 30-40 mg pieces of adult rat testes were obtained by using 12G biopsy needles and cultured for 6

h in 1 ml of culture medium with 0, 10 pM, 100pM, 1nM and 10nM dinaciclib or novel CDK2 inhibitors. Quantitative analysis of pRB and p53 levels indicates that ex vivo testis is highly sensitive to dinaciclib, (attenuating pRB levels with an IC50 value of 270 pM, stimulation of p53 with an IC50 value of 43 pM), novel CDK2 inhibitor A (reducing pRB levels with an IC50 value of 41 pM, and activation of p53 with an IC50 value of 108 pM), inhibitor B (shown ex vivo activity in dose 100 pM), and four other sub-nanomolar CDK2 inhibitor compounds were active in doses proximate 10 nM. Since the testis explants retain testis epithelial organization, this ex vivo method can be used to screen new inhibitors and determine IC50 values to rank compounds for in vivo testing. In vivo proof-of concept for CDK biomarker and anti-spermatogenic activity was also obtained with dinaciclib and FDA-approved CDK4/6 inhibitor palbociclib. Balb/c mice were treated with 4 single daily IP doses of dinaciclib or 7 single daily IP dose of palbociclib at 10%, 25%, 50%, 80% of the maximum tolerated dose (MTD). We found reduced pRB levels and increasing p53 levels at 10% and 25% MTD of dinaciclib. Palbociclib (CDK4/6) is much less potent in producing pRB response in testes. Administration of dinaciclib for 30 and 60 days at 10% and 25% of MTD caused significant reductions in testis size, testis mass (62-70% reduction,  $P < 0.001$  for both dosing regimens), and dramatic changes in testicular morphology and loss of spermatogenic cells in treated adult male mice similar to CDK2 null mice. Our data is the first demonstration that pharmacologic inhibition of CDK2 in adult males is a potential strategy to develop non-hormonal male contraceptives.

Supported by NIH HD080431 to JST

**Dazl-Dependent Translation of Maternal Mrna During Mouse Oocyte Maturation.** Cai-Rong Yang, Gabriel Rajkovic, and Marco Conti

Translation of maternal messenger RNAs (mRNAs) stored during oocyte development requires complex and coordinated regulations. Using a genome-wide analysis of transcripts regulated during mouse oocyte maturation, we had defined the RNA-binding Protein (RBP) deleted in azoospermia-like (Dazl) as a potential regulator of translation at the oocyte-to-zygote transition. Here, we have further investigated the role of Dazl in the translation of maternal mRNA during the GV to metaphase progression. Motif analysis of the 3' UTR of regulated maternal mRNAs identified a substantial group of mRNAs potentially interacting with Dazl in the oocyte. This interaction was confirmed experimentally with more than 800 mRNAs specifically recovered in the IP pellet after Dazl AB IP. To verify the functional role of Dazl in oocyte translation, we have compared translation of oocyte mRNAs in the presence or absence of Dazl using RiboTag IP, a strategy that monitors ribosome loading onto endogenous mRNA by RNA-Seq or qPCR. To this aim, oocytes were injected with a control or a Dazl morpholino oligonucleotides (MO), and RiboTag IP was performed at 6hrs after reentry into meiosis. Pilot experiments using RiboTag IP/qPCR verified that Dazl MO injection blocks ribosome loading onto Dazl mRNA itself and the Dazl- target Tex19.1. Analysis of the RiboTag IP/RNAseq data indicates that the control MO does not disrupt the pattern of ribosome loading onto maternal mRNA during maturation. Conversely and upon Dazl depletion of the oocyte, ribosome loading of up to 1000 transcripts is defective when compared to control. In many instances, Dazl depletion caused a decrease in ribosome loading on a transcript, consistent with a role as a translational activator. This property was confirmed by RiboTag IP/qPCR of selected candidates. Thus, Dazl itself, Tex19.1, Txnip, Rad51C, Btg4, Oosp1, Obox5, Ireb2, and Tcl1 are bona-fide Dazl targets on the basis of RiboTag IP/RNAseq, RiboTag IP/qPCR

and because they are specifically recovered in the IP after Dazl immunoprecipitation. However, we also found that ribosome loading of a group of transcripts increased after Dazl depletion, opening the possibility that Dazl may also function as a repressor of translation in oocytes. The presence of this group repressed targets is consistent with the Dazl IP/Rip-Chip data showing Dazl interaction with a subset of transcript whose translation decreases during meiosis. We confirmed this Dazl property by RiboTag IP/qPCR of selected candidates. Our results indicate that Akap10, Cenpe, Nsf, Ywhaz, Nin, YTHDF3 are direct or indirect Dazl targets on the basis of RiboTag IP/RNA-Seq, RiboTagIP/qPCR. Akap10, YTHDF3, and Nsf are specifically recovered in the IP after Dazl immunoprecipitation, but other targets, Cenpe, Ywhaz and Nin may not directly interact with Dazl. In conclusion, this genome-wide analysis indicates that Dazl plays a major role in the program of maternal mRNA translation, functioning both as a translational activator and repressor of maternal mRNAs during mouse oocyte maturation. Supported by NIH R01 GM116926 and P50 HD055764.

**Inhibition of Sirtuin-1 Aggravates Crvi-Induced Germ Cell Death During Fetal Ovarian Development Mediated Through P53 Acetylation.** Sakhila K. Banu, Kirthiram K. Sivakumar, Jone A. Stanley, Jonathan C. Behlen, and Joe A. Arosh.

CrVI has been used in various industries such as leather and textiles, metallurgical, chemical and automobile. Due to increased use and improper disposal of CrVI, its levels in the water, soil and air continue to increase. Women working in dichromate manufacturing industries and tanneries, and living around Cr contaminated areas have high levels of Cr in blood and urine and encounter gynecological illnesses, abortion, postnatal hemorrhage and birth complications. Significant contamination with CrVI has been found in the drinking water sources of several cities in the U.S. exposing Americans to various adverse health effects such as cancer and infertility. Occupational exposure to CrVI is found among approximately one-half million industrial workers in the U.S. and several millions worldwide. Our previous findings showed that gestational exposure to CrVI increased germ cell apoptosis in F1 offspring, resulting in premature ovarian failure (POF) targeting p53 pathway, and disrupting POF marker gene Xpnpep-2. One of the key mechanisms identified in CrVI-induced germ cell death is through the increased expression of p53-pathway. Sirtuin 1 (SIRT1), an NAD<sup>+</sup>-dependent deacetylase, is one of the seven mammalian sirtuins and is known to play an important role in maintaining metabolic homeostasis in multiple tissues. SIRT1 has been proposed as an anti-aging protein. SIRT1 was reported to improve the follicle reserve and prolong the ovarian lifespan of diet-induced obesity in female mice. SIRT1 deacetylates p53 and destabilizes it. Therefore, we hypothesize that CrVI increases germ cell death through increased acetylation of p53 by downregulating SIRT1. The objective of the current study is to test the hypothesis in the fetal ovaries that were exposed to CrVI prenatally. Pregnant rats were exposed to CrVI in drinking water from gestational day (GD) 9.5-14.5, and treated with Sirt inhibitor (Sirt-I, EX-527) 1, 5 and 50 mg/kg body weight, subcutaneous injections. Ovaries were collected from the fetuses on postnatal day (PND)-1 and analyzed. Data indicated that CrVI increased germ cell death. Sirt-I accelerated CrVI-induced germ cell death dose-dependently. Sirt-I also increased CrVI-induced p53 acetylation. Sirt-I increased caspase-3, Bax and AIF; upregulated p53 and its downstream candidates NOXA and PUMA; and down regulated Bcl-2 and Bcl-XL. In addition, CrVI upregulated miRNA34a. Treatment with Sirt-I further increased CrVI-induced upregulation of miRNA34a. Thus, our data indicate that CrVI induces germ cell death through p53-miRNA34a-Sirtuin-1 network. Activation of Sirt-1 may mitigate CrVI-induced germ cell death.

**A Hormonal Contraceptive That is Associated with Diversity of the Vaginal Microbiota and an Altered Vaginal Microenvironment, That May Enhance Susceptibility to HIV.**

J. M. Wessels, J. Lajoie, M. I. J. Hay Cooper, K. Omollo, A. M. Felker, D. Vitali, H. A. Dupont, P. V. Nguyen, K. Mueller, F. Vahedi, J. Kimani, J. Oyugi, J. Cheruiyot, J. N. Mungai, A. Deshiere, M. J. Tremblay, T. Mazzulli, J. C. Stearns, A. A. Ashkar, K. R. Fowke, M. G. Surette, and C. Kaushic

Women are at increased risk of sexually transmitted infections (STIs) compared to men. One reason may be the female sex hormones and use of hormonal contraceptives, and another might be dysregulation of the vaginal microbiome. In fact meta-analyses demonstrate that Depot Medroxyprogesterone Acetate (DMPA), a hormonal contraceptive commonly used in Sub-Saharan Africa, is associated with a 1.4X increased risk of acquiring Human Immunodeficiency Virus (HIV), however the mechanisms by which DMPA enhances susceptibility to HIV remain elusive. Additionally, a recent study found a significant association between diversity of the vaginal microbiota and increased risk of HIV acquisition. Unlike the highly diverse gut microbiome, a low diversity vaginal microbiota dominated by *Lactobacillus* species is associated with protection from STIs. As such, our objective was to examine the effect of DMPA on diversity of the vaginal microbiota, which has been shown to modulate genital inflammation, and thus HIV target cells. In a prospective cohort of women negative for STIs, who had Nugent Scores < 7, we found the vaginal microbiota of women on DMPA had greater bacterial diversity than women not on hormonal contraceptives ( $1.77 \pm 0.23$  vs.  $1.10 \pm 0.25$ ; Shannon Index;  $P=0.015$ ;  $N=24, 21$  respectively). In order to examine the mechanism linking DMPA with bacterial diversity, we quantified two factors associated with colonization by lactobacilli, the bacteria thought to be protective against STIs. In our cohort, DMPA was associated with suppression of vaginal glycogen ( $2.02 \pm 0.51$  vs.  $7.64 \pm 1.79$  mg/mL;  $P=0.053$ ) and  $\alpha$ -amylase ( $2.43 \pm 1.02$  vs.  $6.81 \pm 1.35$  mU/mL;  $P=0.030$ ), suggesting that the diverse array of vaginal bacteria in the women on DMPA may be a result of the suppression of key nutrients necessary for protective bacterial species. Interestingly, the results of our clinical study were recapitulated in humanized NRG mice (mice with human immune cells, and are susceptible to HIV) where DMPA significantly increased diversity of the vaginal microbiota compared to estradiol (E2) pellets ( $3.73 \pm 0.37$  vs.  $1.28 \pm 0.74$ ; Shannon Diversity Index;  $P=0.016$ ;  $N=5, 4$  respectively), significantly suppressed vaginal glycogen ( $1.5 \times 10^{-3} \pm 9.0 \times 10^{-4}$  vs.  $1.1 \times 10^{-2} \pm 3.0 \times 10^{-3}$  mg/mL;  $N=10, 8$ ;  $P=0.017$ ) as compared to control untreated mice, and significantly enhanced susceptibility to HIV-1 infection following intravaginal challenge (77% infected DMPA vs. 35% infected untreated control;  $N=22, 20$  respectively;  $P=0.014$ ). Results suggest DMPA may increase HIV susceptibility by suppressing metabolic pathways necessary for protective bacteria, and allow for colonization by other species. This might in turn recruit additional HIV target cells to the vaginal tract, and thus enhance susceptibility to HIV. Understanding DMPA-mediated mechanisms of HIV susceptibility in women is an important global health issue as the vaginal tract represents a major site of HIV acquisition, and DMPA has consistently been associated with enhanced susceptibility to HIV.

**Impact of Instructor-Assisted and Non-Assisted Case Study Completion on Student Understanding and Knowledge Retention in an Advanced Physiology Course.**

Katie L. Bidne and Renee M. McFee

Case studies have been utilized as an active-learning strategy to supplement lecture-based courses and their use has been shown to increase knowledge retention compared to use of lecture alone. However, in-class facilitation of small group case study exercises can require a relatively large amount of instructor

time. In addition, large enrollment courses may not have an adequate student-instructor ratio to allow for in-class facilitation. Therefore, we sought to determine if case studies retained the same educational benefits if students completed assignments without instructor assistance but the instructor reviewed challenging concepts from the case studies with the entire class during the following class period. We hypothesize that academic performance and knowledge retention will not be different between the 2 different case study formats: completion of assignments with instructor facilitation versus independent student completion of assignments followed by an instructor-led review. Furthermore, we hypothesize that student perceptions regarding the benefits of the case study assignments will not differ between the 2 formats. In a professional/graduate level systems physiology course, students ( $n = 27$ ) completed weekly case study assignments during class time. For the facilitated format, students were randomly assigned to groups of 3 and assistance was available from 1 faculty instructor and 2 teaching assistants during assignment completion. For the unassisted format, students were allowed to self-select groups during assignment completion and the faculty instructor led a whole-class review during the following class session. Student surveys administered after each assignment revealed that when students were allowed to self-select groups, the majority (97%) chose to work with fellow classmates rather than work independently, with the most common group size being 3 students. Most students believed discussions with their classmates improved their understanding of physiologic concepts and there was no difference ( $P > 0.05$ ) in this perceived effect between instructor-assisted (86%) and unassisted (90%) case study completion. When available, 90% of students reported asking for assistance from an instructor on assignments and 80% indicated that discussions with a teaching assistant or the faculty instructor helped improve their understanding of physiologic concepts. When students completed assignments without assistance, 70% of students reported that the subsequent in-class, instructor-led review helped with their understanding. In addition, there was no difference ( $P > 0.05$ ) in responses in agreement when students were asked if completion of assignments helped them understand physiologic concepts following instructor-assisted (81%) and unassisted (72%) case studies. These data suggest that students did not perceive learning differences between the 2 different case study formats. In regards to student performance, there was no difference ( $P > 0.05$ ) in average quiz scores when students were tested over the associated material after completion of the instructor-assisted (87%) and unassisted (81%) assignments. Throughout the semester, performance on unit exams will also be assessed as a measure of academic performance and an end-of-semester post-test will be administered to evaluate knowledge retention. Ultimately, these data could demonstrate the benefits and feasibility of different methods of case study implementation as a supplement to lecture-based physiology courses in both small and large-enrollment courses.

**The Effect of Artemis on CRISPR/Cas9 Induced DNA Repair During in Vitro Fetal Fibroblast Transfection and Embryo Microinjection.** Yunsheng Li, Malavika Adur, Blythe Schultz, Wei Wang, Christopher K. Tuggle, and Jason W. Ross

CRISPR/Cas9 is a powerful tool used to generate genetic modifications by causing DNA double-strand breaks (DSBs). Artemis (ART; also known as DCLRE1C), is an endonuclease and is essential for DSB end joining in DNA repair via the canonical non-homologous end joining (c-NHEJ) pathway. It is unknown whether ART affects CRISPR/Cas9 induced DSBs and DNA repair in somatic cells or embryos. In this study, different gene editing methods were used in porcine fetal fibroblasts (pFF) with ART mutations and embryos to test the role of ART in DNA repair following CRISPR/Cas9 induced DSB. Guide RNA

(gRNA) targeting exon 2 of Interleukin 2 receptor subunit gamma (IL2RG) was designed to evaluate CRISPR/Cas9 induced gene editing efficiency. Male and female pFF with ART  $-/-$  and ART $+/-$  genotypes were obtained by inseminating ART $+/-$  sows with semen from a bone marrow transfer rescued ART $-/-$  boar. In the first study, we used male and female ART $-/-$  and ART $+/-$  cells to discern differences in CRISPR/Cas9 induced modification rate by transfecting cells with a humanized Cas9 plasmid also expressing IL2RG gRNA. Following cell transfection and culture, a total of 766 individual clonal colonies were screened using PCR and Sanger sequencing. The PCR products from colonies showing potential desired modifications were then subcloned, and PCR products amplified from 10 independent bacterial colonies were sequenced to determine monoallelic and biallelic modification frequency. Female ART $+/-$  cells had a 10.1% (19/189) modification rate which was greater ( $P < 0.05$ ) than the efficiency detected for ART $+/-$  male cells (1.9%; 4/207) and ART $-/-$  male (2.5%; 5/202) or female (4.2%; 7/168) cell lines. Furthermore, the ability of ART deficiency to negatively affect gene editing efficiency in embryos derived from somatic cell nuclear transfer (SCNT) using ART $-/-$  pFF was evaluated. Following reconstruction, one cell stage embryos were microinjected with 20 pL containing 150 ng/ $\mu$ L of Cas9 mRNA and 20 ng/ $\mu$ L of single guide RNA (sgRNA) and then cultured to the blastocyst stage of development. Gene modification efficiency was 66.7% (8/12) in ART $-/-$  SCNT derived embryos. By comparison, ART intact embryos produced via parthenogenetic activation and injected with Cas9 mRNA and sgRNA had a 75% (15/20) modification rate in ensuing blastocysts, suggesting that ART $-/-$  pFF did not compromise gene editing efficiency in SCNT derived embryos compared to those with an intact IL2RG locus. Transfection of Cas9 and sgRNA expressing plasmid into pFF suggested ART $-/-$  female cells have reduced gene editing efficiency (in the form of insertion/deletion events) compared to ART intact female cells suggesting a potential reduction in NHEJ DNA repair. However, IL2RG mutagenesis rates were similar for SCNT derived embryos using ART $-/-$  pFF suggestive that existing ART of oocyte origin may facilitate modification following SCNT or that other repair mechanisms could be employed. This project was supported by the National Institutes of Health (5R24OD019813-03).

**Exposure to Di-n-butyl Phthalate Alters IGF1 Expression and Causes Ovarian Toxicity in the Adult Mouse.** Estela J. Jauregui, Xiaosong Liu, Jazmin Beltran-Gastelum, and Zeliann R. Craig

Exposure to endocrine disruptors is postulated to cause ovarian toxicity and associated female reproductive disorders. Di-n-butyl phthalate (DBP) is an endocrine disruptor commonly used worldwide as a plasticizer or solvent in many consumer products such as infant care, personal, and cosmetic products. We have previously reported that environmentally-relevant exposure to DBP disrupts folliculogenesis in mice. During folliculogenesis, survival and successful transition into mature follicular stages depends on the positive actions of follicle-stimulating hormone (FSH), insulin-like growth factor 1 (IGF1), and 17-beta-estradiol (E2). Therefore, the objective of this study was to determine whether DBP alters folliculogenesis by disrupting the FSH-IGF1-E2 system in the mouse ovary. To accomplish this, we orally treated 35-day-old female CD-1 mice ( $n=8$  per treatment) with tocopherol-stripped corn oil (vehicle), or one of three doses of DBP comparable to those estimated in the general population (10 mg/kg/day), occupationally-exposed individuals (100 mg/kg/day), or in classical high dose studies (1000 mg/kg/day) for 20 or 30 days. At the end of dosing, whole ovaries were collected from experimental and control animals for qPCR analysis and immunohistochemistry. Interestingly, qPCR measurements showed decreased levels of IGF1 mRNA in the whole ovaries of mice treated for 20 days with 10 mg/kg/day of DBP, or 30 days with 10 or 100 mg/kg/day of DBP. Additionally, immunohistochemistry

localizing IGF1 within the ovaries of the phthalate-treated and control mice showed decreased expression of this protein in the theca and granulosa cells within the antral follicles of the experimental animals treated with 10 and 100 mg/kg/day for 20 and 30 days in comparison to controls. Our results suggest that DBP disrupts the FSH-IGF1-E2 system in the female mouse by altering the expression of Igf1 in the ovary. Future studies will be aimed at investigating the effects of phthalate exposure on the expression and function of additional components of the FSH-IGF1-E2 system. This work was supported by NIEHS grants R00021467 (ZRC) and R01026998-01A1 (ZRC).

**The NMD factor UPF2 is Necessary for Primitive Endoderm Maintenance and Peri-Implantation Embryo Viability.** Jennifer N. Dumdie, Heidi Cook-Andersen, and Miles F. Wilkinson

During the earliest stages of embryonic development, the totipotent zygote proliferates and differentiates, generating diverse populations of cells that will ultimately form the organs and tissues of a mature organism. These early events dictate the course and success of the developing organism; however, the pathways regulating these early developmental transitions remain poorly understood, especially in mammals. In addition, most developmental studies have concentrated on the role of transcriptional regulation, which fails to account for the fact that gene expression is dictated as much by the rate of mRNA decay as the rate of RNA synthesis. Thus, what is “turned off” could be as important as what is “turned on” during developmental transitions. Nonsense-mediated RNA decay (NMD) is a highly conserved and selective RNA turnover pathway. Loss or knockdown of NMD factors leads to developmental defects in species spanning the phylogenetic scale, including humans. One of the most striking findings is that loss of all but one of the examined NMD factors leads to peri-implantation embryonic lethality in mice, as well as other higher eukaryotes. To date, there have been no studies examining the underlying mechanism.

To elucidate the role of NMD in peri-implantation mammalian development, we generated global Upf2-null mice. UPF2 is a central factor in the NMD pathway, so ablating it has been shown to impede NMD function. No Upf2-null embryos survived beyond embryonic day (E) 5.5, indicating a pre- or peri-implantation defect. However, Upf2-null E3.5 blastocysts were present at the correct Mendelian ratio, and had no obvious morphological defects, pointing to a defect between E3.5-5.5, precisely the time of embryo implantation. Defects in implantation are often associated with the trophectoderm, which establishes the connection between the embryo and the uterine endometrium. However, Upf2-null blastocysts had normal, functional trophectoderm, based on attachment and outgrowth assays, as well as expression of the trophectoderm-specific marker, CDX2. During blastocyst outgrowth, while Upf2-null trophectoderm appeared to be functional, the inner cell mass of Upf2-null blastocysts quickly regressed after only 72 hours of culture, indicating a defect specific to the inner cell mass. The inner cell mass gives rise to both the embryo proper through the epiblast, as well as the extra-embryonic yolk sac via the primitive endoderm. The differentiation of these two cell types occurs in the mid-blastocyst, and can be visualized by the expression of cell-type-specific markers. While late (E4.0) Upf2-null blastocysts expressed the epiblast-specific marker, NANOG, in this cell type, these embryos failed to express the primitive endoderm-specific marker, GATA4, and exhibited altered expression of another primitive endoderm marker, SOX17. Thus, Upf2-null embryos are defective in the generation and/or maintenance of the primitive endoderm lineage. RNA sequencing and RNA half-life studies to identify the mRNAs directly regulated by UPF2 at this central developmental transition are in progress. This study reveals

that UPF2 is critical for maintaining the primitive endoderm in mammalian embryos and that RNA decay via the NMD pathway is necessary for embryonic viability during implantation.

**Bisphenol A and Bisphenol AF Potentiate Endometriosis Differently Based on Hormonal Status in Female Mice.** Katherine A. Burns, Stephanie A. Lang, Rebecca L. Jones, Jessica A. Kendzierski, and Alexis D. Greene

Endometriosis is a gynecological disease affecting 1 in 10 women of reproductive age. Endometriosis incidence has risen; however, whether this is due to disease awareness or environmental contamination is not well known. Our objective was to determine if Bisphenol A (BPA) or Bisphenol AF (BPAF) potentiate the development of endometriosis and if hormonal status changes how toxicant exposure affects disease. A mouse model of endometriosis, where minced uterine tissue is injected into the peritoneal cavity of a host mouse, was used to examine the effects of BPA or BPAF on endometriosis in ovariectomized and hormonally intact mice. BPA or BPAF were delivered through diet to include no-observed-adverse-effect-level (NOAEL) and the low-observed-adverse-effect-level (LOAEL) exposure levels. After six weeks, lesion weight, lesion volume, lesion and uterine proliferation, lesion and uterine apoptosis, and lesion gene expression analysis were collected to assess the effects of BPA and BPAF on endometriosis. In BPA and BPAF treatment groups, depending on dose and hormonal status, BPA and BPAF increase endometriosis lesion growth, and lesion and uterine proliferation. Gene expression changes in endometriosis lesions after BPA and BPAF treatment are dependent on hormonal status. BPAF, more so than BPA, increases endometriosis lesion growth. BPA and BPAF have the potential to potentiate endometriosis in intact mice, specifically increasing distal lesion volume. While BPAF is being used as a substitute in place of BPA, BPAF appears to be similar if not more estrogenic than BPA, and may be impacting the environmental contribution of the increased incidence of endometriosis.

**Exotic Tubulins in the Manchette, the Key to Precise Regulation of Spermiogenesis by KATNAL2.**

Jessica Dunleavy, Hidenobu Okuda, D. Jo Merriner, Anne O'Connor, and Moira O'Bryan

A key aspect of spermiogenesis is the formation of a streamlined, compacted sperm head that will allow for efficient motility. The manchette, a transient microtubule sheath, is widely acknowledged to drive remodelling of the distal half of the spermatid nucleus. Despite this, the mechanisms that govern manchette formation and dissolution, and allow it to sculpt the nucleus are poorly understood. KATNAL2 is a paralogue of the microtubule (MT) severing enzymes KATNA1 and KATNAL1. Recently we showed that, KATNAL2 and, the katanin regulatory protein, KATNB1 function together to regulate manchette dynamics. Most notably, loss of either KATNAL2 or KATNB1 function results in excessive constriction and elongation of the manchette MTs, accompanied by a lack of manchette movement and delays in its disassembly. This study sought to elucidate how KATNAL2-KATNB1 complexes regulate the manchette. Intriguingly, despite the presence of overt MT defects in knockout mouse models, we show that KATNAL2 does not sever  $\alpha/\beta$  tubulin based MTs. Instead, our data suggests KATNAL2 targets two poorly characterized tubulins,  $\delta$  (TUBD1) and  $\epsilon$  (TUBE1), in addition to modulating  $\gamma$ -tubulin-microtubule interactions. TUBD1 and TUBE1 are predicted to bind laterally to MT polymers, making them attractive candidates as the linker structures that connect manchette MTs to the nucleus and to adjacent MTs. As these links are integral in both the exertion of force on the nucleus and in manchette caudal movement,

we hypothesised that the phenotypes above were due KATNAL2-KATNB1 complexes functioning to disengage these linkers. Here, we show that Tubd1 and Tube1 are expressed in all ages of the mouse postnatal testis and, similar to KATNAL2, both are especially enriched from day 30. Importantly, our data shows both contribute to the manchette structure in spermatids. Further, to ascertain if either TUBD1 or TUBE1 could be the target of KATNAL2 in the manchette, in situ proximity ligation and co-immunoprecipitation assays were performed. We successfully immunoprecipitated both KATNAL2-TUBD1 and KATNAL2-TUBE1 complexes and observed that these complexes localized to the spermatid manchette. Finally, to investigate the origin of the manchette elongation phenotype, we also characterised the expression pattern of the MT nucleator,  $\gamma$ -tubulin, in elongating spermatids. Of note, we found  $\gamma$ -tubulin complexes localised to the caudal tips of the manchette MTs, and in *Katnal2* knockout mice these  $\gamma$ -tubulin foci persisted long after their removal from those in wildtype, suggesting KATNAL2 is required to release manchette MTs from  $\gamma$ -tubulin. Collectively, our data reveals TUBD1 and TUBE1 as new components of the spermiogenesis machinery, and support a model wherein KATNAL2 modulates the association of the manchette MTs with, TUBD1, TUBE1, and  $\gamma$ -tubulin to modulate manchette constriction, movement and length during spermatid remodelling.

**Presence and Potential Function of GPRC6a in Human Trophoblast Cells.** Erin S. McWhorter, Rachel C. West, Jennifer E. Russ, Quinton A. Winger, and Gerrit J. Bouma

Pregnancy disorder such as gestational diabetes and preeclampsia are often associated with placental dysfunction and intrauterine growth restriction, as well as perturbed endocrine signaling. Recent data from our laboratory suggest that androgen signaling maybe important in placental angiogenesis. Androgens signal through androgen receptors (AR), and AR is present in the human, mouse, and sheep placenta. The classical genomic effects of androgens involve translocation of the androgen-AR complex to the nucleus, leading to regulation of gene transcription. However, androgens also have rapid non-genomic effects. Recently, GPRC6A, a G protein-coupled receptor, was reported to be a receptor for testosterone and dihydrotestosterone. Previously, GPRC6A was shown to be involved in binding Osteocalcin (Ocn), an osteoblast-specific hormone that plays a role in bone calcification and calcium ion homeostasis. Ocn also binds GPRC6A in the pancreas, leading to beta cell proliferation and insulin release, as well as stimulating testosterone production by binding Leydig cells in the testes. Furthermore, Ocn levels increase in pregnant women, crossing the placenta to prevent neuronal apoptosis in the growing fetus. We hypothesize that GPRC6A plays a role in mediating non-genomic effects of androgens in trophoblast cells. Studies conducted in our laboratory show the presence of both GPRC6A and AR in the human and mouse placenta. Using the telomerase-immortalized (h-TERT) first trimester human trophoblast cell lines Swan-71 and choriocarcinoma-fused ACH-3P, we identified the presence of both GPRC6A and AR mRNA and protein by quantitative Real-Time PCR, western blot, and immunofluorescence. These findings suggest that androgen signaling in the placenta occurs through both genomic and non-genomic pathways. Current experiments include treatment of Swan-71 and ACH-3P cells with BSA-conjugated testosterone to activate GPRC6A and identifying changes in intracellular calcium, cAMP and trophoblast cell differentiation markers hCG, ERVW-1 and LGALS-13. Ultimately, these findings will lead to better understanding of the role of androgen signaling in placental development and function, which also will provide important insight into mechanisms underlying placental dysfunction and disease.

**New Perspectives on Conceptus Estrogens and Pregnancy Establishment in Pigs.** A. E. Meyer, C. A. Pfeiffer, K. E. Brooks, L. Spate, J. Benne, S. Murphy, R. Cecil, T. E. Spencer, R. S. Prather, and R. D. Geisert

Establishment of pregnancy in pigs involves redirection of prostaglandin F2a (PGF2a) secretion from an endocrine to exocrine manner into the uterine lumen, where it is sequestered to prevent luteolysis after day 15 post-mating. The proposed signal for maternal recognition of pregnancy in pigs is estrogen (E2), produced from the elongating conceptus. Conceptus E2 synthesis is initiated on days 11 to 12 as the conceptus begins to rapidly elongate from a tubular to filamentous form, and E2 increases again from day 15 to 30 which encompasses conceptus attachment and placental development. Production of E2 by the conceptus is dependent on aromatase (CYP19A1). To understand the role of E2 in porcine conceptus elongation and pregnancy establishment, a loss-of-function study was conducted by editing CYP19A1 by using CRISPR/Cas9 technology. Guide RNAs (gRNAs) were designed to create deletions in Exon 2 of the CYP19A1 gene, and fetal fibroblast cells were transfected with a construct expressing Cas9 and the gRNAs. Biallelic deletions in edited cell lines were identified by using PCR genotyping and Sanger Sequencing. Next, Wild-type (WT) and edited (CYP19A1-null) fibroblast cells were used to create embryos through somatic cell nuclear transfer (SCNT) using enucleated oocytes. After in vitro culture, 30 to 50 WT or CYP19A1-null blastocysts were transferred into synchronized recipient gilts. The reproductive tract was collected from recipient gilts on days 14 (n=8) or 17 (n=6) post-estrus. Conceptuses were recovered by flushing the uterine horn with PBS, and the amount of E2, testosterone, and PGs was determined in the uterine luminal flushes (ULF). Elongated and attaching conceptuses were recovered from gilts receiving both WT and CYP19A1-null embryos on day 14 and 17, respectively. Total E2 in the ULF of gilts with CYP19A1-null conceptuses was substantially lower than those with WT conceptuses on day 14 (P 0.10) in the total amount of testosterone, PGF2a, or PGE2 within day 14 and 17 ULF. However, PGs in ULF was lower on day 14 compared to day 17 (P < 0.01). Despite the loss of conceptus E2 production, CYP19A1-null conceptuses were capable of maintaining the corpora lutea (CL). However, gilts gestating CYP19A1-null embryos (n=4) all aborted between days 27 and 31 of gestation. Attempts to rescue the pregnancy of CYP19A1-null embryos with exogenous estrogen or co-transfer with WT embryos failed to rescue the pregnancy. Collectively, these results demonstrate the CYP19A1 is responsible for E2 synthesis by the elongating and developing pig conceptuses. Although E2 has been hypothesized to be the signal for maternal recognition of pregnancy in the pig, intrinsic E2 conceptus production is not essential for pre-implantation development, conceptus elongation, and the early maintenance of CL. However, conceptus E2 during the peri-implantation period plays an essential role in programming endometrial function for maintenance of pregnancy beyond 25 days. Research supported by grant 2017-12211054 from the USDA National Institute of Food and Agriculture.

**Contribution of Follicle Stimulating Hormone to Early Ovarian Recrudescence in Siberian Hamsters.**

Kathleen Leon, Arturo Lopez, and Kelly A. Young

While the contribution of follicle stimulating hormone (FSH) to the process of folliculogenesis has been well studied, the impact of FSH on the photostimulated return to ovarian function in seasonally-breeding species is not fully elucidated. Exposure of adult, female Siberian hamsters (*Phodopus sungorus*) to inhibitory photoperiod reduces plasma FSH and estradiol concentrations, antral follicle development, and ovulation; however, these changes in ovarian function are reversed with subsequent exposure to stimulatory photoperiod exposure. Similar significant photoperiod-mediated changes in LH

are not observed. While FSH is a key mediator in seasonal ovarian function, other laboratories have shown that blocking FSH via the GnRH inhibitor acyline in peri-pubertal females exposed to stimulatory photoperiods failed to generate full ovarian regression. Similarly, administration of FSH to peri-pubertal females exposed to inhibitory photoperiod failed to restore complete ovarian function. While these studies clearly demonstrate the need for factors in addition to FSH for photoperiodic regulation of ovarian activity, the FSH independent/dependent aspects of folliculogenesis resumption during photostimulated recrudescence in adults have not been fully explored. Therefore, we hypothesized that aspects of ovarian recrudescence would be differentially affected by the systemic ablation and replacement of FSH during photostimulation. To address this hypothesis, ovaries were collected from females (n=10 per group, 6 groups total) exposed to 14 weeks of stimulatory long day (LD), inhibitory short days (SD), or 14 weeks of SD + 2 weeks of LD (post transfer groups, PT). The PT females were either treated with acyline (50µg acyline in 5% mannitol injected i.p. every 48h; PTA); acyline +FSH (3IU rhFSH, injected i.p. every 24h, PTAF), mannitol vehicle alone (injected i.p. every 48h, PTV), or no treatment (PT) for the two weeks of photostimulation. As expected, both ovarian and uterine horn mass declined in the SD as compared to LD groups; in contrast, photostimulation in the PT and PTV restored ovarian mass to values no different than LD controls. This restoration of ovarian mass did not occur in females in the PTA group; however, ovarian mass did not differ between the PT group and the FSH-treated PTAF group. As expected, plasma FSH concentrations were significantly higher in the PTAF group as compared to all other groups. When the PTAF group was removed, plasma FSH concentrations were highest in the LD group compared to remaining SD and PT groups, and FSH was reduced in PTA as compared to PT groups. Tertiary follicles were noted in the LD, PT, and PTAF groups, but not in the SD and PTA groups. Inhibin alpha mRNA expression was significantly increased in the PTAF groups as compared to all other groups. FSHR and IGF-1 mRNA expression was not similarly stimulated, with no significant differences noted between the acyline and FSH treated groups; however, the expected decline in FSHR and IGF-1 mRNA expression with SD exposure was noted. These results corroborate previous work suggesting that FSH has a direct stimulatory effect on ovarian recrudescence and imply that factors in addition to FSH may be responsible for aspects of photostimulated return to ovarian function.

**Biological Role of Prostaglandin Synthase 2 (PTGS2) on Early Conceptus Development in Pigs.** C. A. Pfeiffer, A. E. Meyer, L. D. Spate, J. A. Benne, R. F. Cecil, T. E. Spencer, R. S. Prather, and R. D. Geisert

The pig conceptus produces and secretes estrogens, interleukin 1 beta 2 (IL1B2), and prostaglandins (PG) during the establishment of pregnancy. Using gene editing, previous studies established that during the maternal recognition of pregnancy, IL1B2 is essential for rapid conceptus elongation on day 12 of pregnancy (Whyte JJ et al., Proc Natl Acad Sci USA 2018). The role of conceptus-derived PGs during early pregnancy has not been clearly established in pigs. Production of PGs by the embryo and conceptus is dependent on prostaglandin synthase 2 (PTGS2). The long-term goal is to determine the role of conceptus PG production. To achieve this goal, CRISPR/Cas9 gene editing was conducted in porcine fetal fibroblast cells to create loss-of-function deletions in Exon 1 of the PTGS2 gene. Genotyping and sequencing of gene edited fibroblast cell lines was conducted to identify cells with a biallelic mutation. Sanger Sequencing determined the gene edit created a 162 base pair deletion on both alleles in the PTGS2 gene. Next, control wildtype (WT) and edited PTGS2 fibroblast cells were used to create embryos through somatic cell nuclear transfer (SCNT) into enucleated oocytes. The SCNT-

derived embryos were cultured in vitro for 7 days. Resulting blastocyst development rates for WT ranged from 30-40%. Embryos (n=46) with a biallelic edit in PTGS2 had a blastocyst development rate of 48%. Further, day 6 PTGS2 edited blastocysts hatched after addition of 10% fetal bovine serum to the culture medium. These results support the hypothesis that PTGS2 activity, and thus intrinsic PGs, neither inhibits nor plays a critical role in embryo cleavage, blastocyst development, and blastocyst hatching. Future studies will utilize PTGS2 edited embryos as a model to understand the biological role of conceptus-derived PGs in peri-implantation development and establishment of pregnancy. Research supported by grant 2017-12211054 from the USDA National Institute of Food and Agriculture.

**Investigating the Molecular Origins of Mitotic Aneuploidy During Pre-Implantation Development in a Bovine Model.** Brooks K. E. , Daughtry B. L., Fei S. S., Yan M. Y., Davis B., Carbone L., and Chavez S. L.

Whole chromosomal abnormalities (aneuploidy) that arise during pre-implantation embryo development are a major contributor to in vitro fertilization (IVF) failure. It is estimated that ~50-80% of human embryos contain at least one aneuploid cell at the cleavage stage, which can contribute to chromosomal mosaicism detected by pre-implantation genetic screening at the blastocysts stage. In contrast, mouse embryos exhibit only ~1% aneuploidy and infrequent early embryo loss. Previous bovine studies estimate that 32-88% of cleavage stage embryos are aneuploid, advocating cattle as a more physiologically relevant model to study the molecular mechanisms mediating meiotic and/or mitotic aneuploidy. In human embryos, the timing of the first three mitotic divisions in conjunction with assessment of cellular fragmentation, largely distinguishes chromosomally normal and abnormal embryos at the cleavage stage. Interestingly, some cellular fragments contain chromosomal material that likely began as mis-segregated chromosomes which were encapsulated into micronuclei during meiosis and/or mitosis. We hypothesize that cellular fragmentation represents a response to micronucleation that may aid in restoring proper chromosome numbers during early embryo development. To better understand the origin(s) of these abnormalities, bovine pre-implantation embryos were used to investigate micronucleation and fragmentation to identify potential solutions to ameliorate their impact on IVF success using a combination of live-cell imaging, single-cell DNA-sequencing (DNA-seq), whole-embryo RNA-sequencing (RNA-seq), quantitative RT-PCR (qRT-PCR), multi-color confocal microscopy, and morpholino oligonucleotide (MAO) gene knockdown technologies. From the imaging studies, the time interval between the first three mitotic divisions was determined to be similar between bovine and human embryos and able to successfully predict progression to the blastocyst stage (N=84). Bovine embryos frequently contained multi-/micro-nuclei, but underwent cellular fragmentation at a lower incidence than human embryos. Time-lapse imaging followed by DNA-seq of individual bovine blastomeres confirmed that ~50-85% of cleavage stage bovine embryos are aneuploid, which correlated with repeated observations of multi-polar divisions. Analysis of transcriptional differences between fragmented and non-fragmented 2- and 4-cell bovine embryos via RNA-seq identified only a small set of differentially expressed genes between the two groups; suggesting that cellular fragmentation, and by association, aneuploidy, is likely not the result of transcriptional variation during early pre-implantation development. In contrast, single-embryo qRT-PCR of fragmented versus non-fragmented bovine embryos at later developmental stages revealed differences in the expression of BUB1B, a serine/threonine protein kinase that stabilizes kinetochore-microtubule attachments and delays the onset of anaphase until chromosomes are properly aligned. To determine the functional role of BUB1B in normal embryonic development, chromosome segregation, and cellular

fragmentation, a BUB1B MAO was microinjected into bovine zygotes following fertilization (N=44). Unlike controls, BUB1B-injected embryos struggled to divide beyond the 1-cell stage despite the appearance of multiple cleavage furrows. In those that did divide, multi-/micro-nuclei were common as well as blastomeres devoid of nuclei at the 2-cell stage to support the prevalence of abnormal cytokinesis and asymmetrical genome partitioning to daughter cells. This study provides more direct evidence for defective kinetochore checkpoint signaling as an aneuploidy generating mechanism in cleavage stage embryos, and lays the groundwork for translational studies of human infertility treatment.

**Effects of in Vivo Exposure to Di-N-Butyl Phthalate on Ovulation, Antral Follicle Counts, and Serum Progesterone in the Mature Superovulated Mouse.** Lindsay Rasmussen and Zeliann Craig

Phthalates are endocrine-disrupting chemicals (EDCs) that cause reproductive toxicity in both males and females. Phthalate exposure in women has been confirmed by detection of phthalate metabolites in urine and ovarian follicular fluid and, is associated with adverse outcomes such as decreased oocyte retrieval during in vitro fertilization protocols and greater incidence of early pregnancy loss. Di-n-butyl phthalate (DBP) is a member of the phthalate family and is commonly found in many consumer products including: plastics, some beauty products, insecticides, medical devices, and oral medications. According to published DBP exposure estimates, the general population's exposure range is 7-10  $\mu\text{g}/\text{kg}/\text{day}$ , 0.1-76  $\mu\text{g}/\text{kg}/\text{day}$  in occupationally-exposed individuals, and 1-233  $\mu\text{g}/\text{kg}/\text{day}$  in individuals taking DBP coated medications. In comparison to other EDCs, not much is known about the effects of DBP on female reproductive function. Thus, this study was designed to evaluate the effects of environmentally relevant DBP exposures on ovulation rate, antral follicle counts, and serum progesterone concentration. Based on human exposure estimates, we selected DBP exposure levels of 10  $\mu\text{g}/\text{kg}/\text{day}$  (general population exposure) and 100  $\mu\text{g}/\text{kg}/\text{day}$  (occupation and medication exposure) as environmentally relevant for this study. An additional group of mice were treated with DBP at 1000  $\text{mg}/\text{kg}/\text{day}$  as a high dose treatment previously used in classical toxicity studies. Adult CD-1 females (age=67 days old, n=10/treatment) were dosed orally once a day with tocopherol-stripped corn oil (vehicle), 10 or 100  $\mu\text{g}/\text{kg}/\text{day}$ , or 1000  $\text{mg}/\text{kg}/\text{day}$  DBP for 9 consecutive days. Ovulation was induced by exogenous gonadotropin treatment (PMSG/hCG) and females were immediately bred with proven breeder males. Oviducts from each animal were collected at 20 h post-breeding and oocytes and embryos recovered subjected to microscopical examination to determine total number of ovulations. Blood samples were collected to measure circulating levels of progesterone. Both ovaries were collected from animals upon sacrifice, fixed, sectioned, and resulting slides stained with hematoxylin and eosin staining for corpus luteum and antral follicle enumeration. Animals treated with DBP showed no signs of systemic toxicity or disruptions in estrous cyclicity. Ovulation rate, antral follicle count, and serum progesterone concentration were similar between vehicle and DBP-treated animals (n=3-10 mice/treatment; p>0.05). These findings suggest that a short once daily exposure to DBP does not disrupt ovulation, antral follicle counts, or progesterone concentration in adult mice. This work was supported by NIEHS grants R00ES021467 (ZRC) and R01ES026998 (ZRC).

**Sperm-borne Phospholipase C zeta-1 Ensures Monospermic Fertilization in Mice.** Kaori Nozawa, Yuhkoh Satouh, and Masahito Ikawa

During mammalian fertilization, sperm entry into oocytes induces the Ca<sup>2+</sup> oscillations that trigger oocyte activation, consisting of resumption of the meiotic cell cycle and blocking polyspermy. The mechanism of how sperm induces the Ca<sup>2+</sup> changes in oocytes has been investigated for a long time. Here, we found not only phospholipase C zeta 1 (PLCz1) function as a sperm-borne oocyte activation factor (SOAF), but also mammalian spermatozoa have a PLCz1-independent oocyte activation pathway. We generated Plcz1 knockout (KO) mice and found that the KO spermatozoa was defective in inducing Ca<sup>2+</sup> changes in the intracytoplasmic sperm injection (ICSI). However, the KO male mice showed subfertility, and their sperm induced atypical patterns of Ca<sup>2+</sup> changes during in vitro fertilization (IVF). We identified that some oocytes that were fertilized by Plcz1 KO sperm resulted in oocyte activation failure or polyspermy, which was caused by atypical Ca<sup>2+</sup> oscillations. Both of the two major systems for blocking polyspermy, zona pellucida block to polyspermy (ZBPB) and plasma membrane block to polyspermy (PMBP), were delayed in the oocytes fertilized by KO spermatozoa. Furthermore, combined with the analysis of astacin-like metalloendopeptidase (Astl) KO female mice, we found that the PMBP plays a more crucial role than ZBPB in vivo to prevent polyspermic fertilization. At last, we obtained healthy pups from point mutant male mice carrying a human infertile PLCZ1 mutation by a single sperm ICSI supplemented with Plcz1 mRNA. These data suggest that mammalian sperm has a primitive oocyte activation mechanism under physiological conditions, and PLCz1 is important to ensure monospermic fertilization in mammals. Our findings provide insights into details of the oocyte activation mechanism and the development of infertility treatment.

This work was supported by a KAKENHI JP15J03870, JP17K15126, JP17H01394, JP 25112007, Takeda Science Foundation, NIH grant P01HD087157, and R01HD088412.

**Early Embryo Kinetics and Differential Gene Expression of Bovine Embryos Using High and Low in Vitro Fertility Bulls.** Mayra E.O.A Assumpção, Tamie G. Almeida, Letícia S. de Castro, Adriano F.P. Siqueira, Thais R. S. Hamilton, Camilla M. Mendes, Marcelo D. Goissis, Patrícia K. Fontes, Andrea C. Basso, Marcella P. Milazzoto, and Marcelo F. G. Nogueira.

The use of different sires influences in vitro embryo production (IVP) outcome, so understanding why some bulls have higher fertility in vitro is fundamental for bull selection. Paternal effects were already described as determinants for proper embryonic development in vitro, specially during embryonic genome activation (EGA) which is a key step for further blastocyst rates and viability. In this work we characterize the paternal influence on early embryo kinetics (a biomarker of embryo viability) and its effect on mRNA abundance of 96 genes at 8-cell and blastocyst stage. For that, ten bulls were retrospectively selected in high (HF; n=5) and low (LF; n=5) in vitro fertility from a database of approximately 100 bulls used in commercial IVP ranked based on embryo development rate (blastocyst/cleaved rate). IVP embryos from 5 manipulations were classified by their stage of development (2 cell, 3-4 cell, 6 cell, 8 cell), at 24, 36, 48, 60, 72 hpi, to evaluate embryo kinetics. Cleavage rate was assessed at day 3 (D3) of embryonic culture and blastocyst rate (Grade I and II) was assessed at day 7 (D7). Five embryos at 8-cell stage and 5 blastocysts from each bull and each manipulation, totalizing 500 embryonic structures, were collected for RNA extraction (Pico Pure kit®) and cDNA synthesis (Superscript VILO cDNA Synthesis kit) following manufacturer's instructions (Life

Technologies, USA). Transcripts abundance from 96 genes was assessed by Taqman® assays specific for *Bos taurus* by using the Microfluid platform BioMark HD System™ (96.96 Dynamic array). ACTB, HMBS, PPIA and ACTB, HMBS, GAPDH genes were used as endogenous control for 8 cell and blastocyst respectively. Data were analyzed using PROC GLIMMIX of SAS (SAS® 9.3 Institute Inc., USA, 2003). There was no difference in early embryo kinetics ( $p > 0.05$ ), and cleavage rate (HF=86.7%; LF= 84.9%;  $p = 0.2581$ ). As expected, blastocyst rate (HF=29.4%; LF= 16.0%;  $p < 0.0001$ ) and development rate (HF=33.9 % LF= 18.9%;  $p < 0.0001$ ) were higher in the HF group than in the LF. At 8 cell stage, 30 transcripts were differentially represented ( $p < 0.10$ ) between the two groups. Only PGK1, PPIA and TFAM levels were higher in HF group. Stress related genes (9/27, 33%), cell proliferation (8/27, 30%), lipid metabolism genes (6/27, 22%), and other cellular functions (4/27, 15%) were highly expressed on LF embryos. Blastocysts had only 12 differentially represented transcripts ( $p < 0.10$ ); only ACSL3, ELOV1 and IFNT were higher in HF. Lipid metabolism genes (3/9, 33%) and other cellular functions (6/9, 67%) were higher in LF group. Results demonstrate that although there is no paternal effect on early in vitro embryo kinetics, sire in vitro fertility influences the content of transcripts at 8-cell stage and at blastocyst stage, but at a lower extent. An increase in apoptotic and oxidative stress genes at EGA stage suggest that embryo development is impaired in LF group causing reduction of blastocyst rate.

Supported by : In Vitro Brasil (Genus PLC), Coordenação de Aperfeiçoamento de Pessoal de Nível Superior (CAPES).

**Expression and Function of Cation Permeable Channels in Mouse GV Oocytes.** Goli Ardestani, Aujan Mehregan, Andrea Fleig, F. David Horgen, Ingrid Carvacho, and Rafael Fissore

Mammalian oocytes are arrested until the initiation of maturation at the prophase stage of meiosis I, the germinal vesicle (GV) stage. Calcium ( $\text{Ca}^{2+}$ ) influx occurs in GV oocytes causing spontaneous oscillations. During maturation this influx contributes to the increase in internal  $\text{Ca}^{2+}$  stores, which supports the initiation of  $\text{Ca}^{2+}$  oscillations at fertilization. However, the channel(s) that mediate(s) this influx in GVs are not known. Biochemical and functional studies showed that GV oocytes express Cav3.2 (T-type) channels and components of the Store Operated Calcium Entry (SOCE): STIM1, 2 and ORAI1. Remarkably, females null for these channels are fertile, and oocytes display minor to no changes in  $\text{Ca}^{2+}$  homeostasis. To identify other channels, we tested the molecular expression of the Transient Receptor Potential (TRP) family of channels that are non-selective cation-permeable channels. Using RT-PCR, we detected expression of members of this superfamily, including TRPC 1, 3, 5, 6, TRPM 6, 7, TRPV 3, 5 and TRPA1. To determine which of these channels are functional, we tested different divalent cations such as  $\text{Ca}^{2+}$ ,  $\text{Sr}^{2+}$ ,  $\text{Mn}^{2+}$  and  $\text{Ni}^{2+}$ , and techniques such as  $\text{Ca}^{2+}$  imaging, electrophysiology, inhibitors and genetic models. We found that these ions permeate GV oocytes, and whereas  $\text{Ca}^{2+}$  and  $\text{Sr}^{2+}$  induce oscillations in WT GV oocytes,  $\text{Mn}^{2+}$  and  $\text{Ni}^{2+}$  persistently quench fluorescence. We observed that Cav3.2 channels contribute to basal  $\text{Ca}^{2+}$  influx, as oscillations were reduced in null mice. Further, additional external  $\text{Ca}^{2+}$  triggered normal oscillations in Cav3.2 and TrpV3KO oocytes, suggesting  $\text{Ca}^{2+}$  entry through other channels. A candidate for this influx is TRPM7, as its antagonists, NS8593 and waixenicin-A, effectively blocked  $\text{Ca}^{2+}$  oscillations.  $\text{Sr}^{2+}$  influx is almost uniquely dependent on Cav3.2 channels, as oscillations failed to occur in Cav3.2KO oocytes, and were rapidly terminated by inhibitors such as  $\text{Ni}^{2+}$  and Mibefradil. Cav3.2 and TRPM7 channels equally permeated  $\text{Mn}^{2+}$  as Cav3.2KO oocytes showed moderate reduction in  $\text{Mn}^{2+}$  influx, and inhibitors for both channels were equally effective at

terminating the responses. Lastly, Ni<sup>2+</sup> entry depended on TRPM7, as only NS8593 and waixenicin-A prevented its influx. Altogether, our results show that Ca<sup>2+</sup> influx occurs through different channels in GV oocytes highlighting its importance for maturation and fertilization. The expression of channels that permeate Zn<sup>2+</sup> and Mg<sup>2+</sup>, such as TRPM7, supports a key role for these ions in early development. Future studies should reveal the function, signaling mechanisms and stage of development at which these channels impact embryo development and fertility.

**The Use of Microfluidics to Study Stoichiometry, Sensitivity and Tonic Stimulation of Luteinizing Hormone Release From Mouse Pituitary Stimulated with Different Doses Of Buserelin.** Soon Hon Cheong, Zachary Roga, and Mark Roberson

Luteinizing hormone (LH) is secreted by the anterior pituitary in a pulsatile rhythm in response to Gonadotropin-Releasing Hormone (GnRH) or its analogs. Buserelin is a potent GnRH receptor agonist but chronic exposure of pituitary gonadotropes to buserelin can lead to desensitization and fatigue. We hypothesize that the peak and duration of buserelin acetate induced LH pulse release is dose dependent. Microfluidics allows accurate control of media and this technology was used to produce exact pulsatile exposure of pituitary tissues to GnRH analogs. Whole pituitary from bred FVB mice on gestation day 0.5 was inserted into the reaction chamber of the 3D printed microfluidic chip. The programmable microfluidic pumps were set to alternate flow of control media (DMEM, 10% BSA, gentamycin) for 5 minutes, then media with buserelin acetate (17.4 pg/mL, 3.4 pg/mL or 0.8 pg/mL) for 5 minutes followed by control media for the remaining 50 minutes all at a flow rate of 50 μL/min. Media was collected from the outflow every 5 minutes and the concentration of LH was determined using ELISA. The microfluidic chip was previously validated via experiments using dyes and by simulation trials which demonstrated that the device produced consistent mechanical stresses and patterns of fluid flow. In the reaction chamber of the microfluidic chip, the pituitary was exposed to 50% saturation of media within 2 minutes and 89% saturation of media at 5 minutes after the input media is changed. The outflow of media was also validated and the respective media for each time point arrived at the outflow port at 1 minutes with the 50 μL/min flow rate. We found that LH release from the pituitary was constant around 120 ng/mL when exposed to the high buserelin peak concentration of 17.4 pg/mL. At the intermediate buserelin concentration of 3.4 pg/mL, pituitary LH release was pulsatile with a peak at 98.9 ng/mL and dropped to a plateau of 51.4-55.7 ng/mL by 30 minutes. The low buserelin dose of 0.8 pg/mL induced a modest LH peak of 45.6 ng/mL and remained fairly constant between 30.5-39.2 ng/mL. Therefore, exposure to high dose of buserelin even in a pulse pattern results in tonic LH release; moderate buserelin dose is able to induce pulsatile release of LH; and low dose of buserelin failed to result in a robust LH pulse release. This study provides new stoichiometric data on the sensitivity and pattern of the response of pituitaries to the GnRH analog buserelin.

**ATRA Activation of the Akt Pathway in Cumulus Cells and its Effects on Embryo Development Following in Vitro Fertilization in Bovine.** Casey C. Read and Paul W. Dyce

In developing follicles, cellular coupling within cumulus-oocyte-complexes (COCs) creates a functional syncytium allowing the passage of small molecules. Cellular coupling between granulosa cells results from the expression of connexin 43 (CX43 or Gja1) and the formation of gap junctional plaques. All-trans

retinoic acid (ATRA) has been shown to affect CX43 expression in many different cell types. Our lab has previously shown that ATRA treatment increased the expression of CX43 and improved embryo development. We then sought to elucidate the mechanism behind ATRA's effects on CX43 expression. When present in cells, ATRA elicits responses through both genomic and nongenomic pathways. Intracellular ATRA is transported to and binds retinoic acid receptors (RARs) where they travel to the nucleus and bind retinoic acid response elements (RAREs) on the DNA, influencing transcription. CX43 does not possess RAREs in its sequence therefore, our lab investigated potential nongenomic mechanisms behind ATRA's effects on Cx43 expression. ATRA's nongenomic actions vary by cell type and include modification of cellular proteins. Multiple studies have shown a link between ATRA treatment and the phosphorylation of Akt. Additionally, they have shown a link between Akt phosphorylation and CX43 expression. The objectives of this study were to investigate the relationship between Akt and CX43 gap junctional coupling and embryo development and to investigate the effects of ATRA on Akt in bovine cumulus cells. Our lab utilized in vitro fertilization (IVF) to compare COCs treated with ATRA, an inhibitor of Akt phosphorylation (10-NCP), vehicle control, and ATRA + Akt inhibitor. Treatment of COCs with all-trans retinoic acid (ATRA, 10 $\mu$ M) resulted in an increased number of GJA1 gap junctional plaques when compared to the vehicle only control, 2.30 $\pm$ 0.15 vs 1.33 $\pm$ 0.12 plaques/cell ( $p < 0.05$ , t-test). Moreover, the addition of ATRA (10 $\mu$ M) increased the oocyte maturation rate from 78.97 $\pm$ 0.52% to 86.89 $\pm$ 1.74%, cleavage rate from 66.67 $\pm$ 6.12% to 80.27 $\pm$ 4.12%, and blastocyst rate from 19.00 $\pm$ 5.56% to 27.33 $\pm$ 4.51% ( $p < 0.05$ , t-test). Multiple studies have shown that ATRA's effects on Akt phosphorylation happen rapidly. We then performed an experiment where cells were treated with control, 10 $\mu$ M ATRA, 5 $\mu$ M 10-NCP, or 10 $\mu$ M ATRA + 5 $\mu$ M 10-NCP for 0.5 and 3 hours. After 0.5 hours, the ratio of phosphorylated to total Akt was significantly increased in the ATRA treated group (1.63 $\pm$ 0.03 fold) compared to control, 10-NCP, and ATRA + 10-NCP (1.0 $\pm$ 0.0 fold, 0.78 $\pm$ 0.09 fold, and 0.71 $\pm$ 0.1 fold, respectively). After 3 hours, there was a significant difference between control, ATRA, 10-NCP, and ATRA + 10-NCP groups in CX43 levels (1.0 $\pm$ 0.0 fold, 2.12 $\pm$ 0.34 fold, 0.76 $\pm$ 0.13 fold, and 1.3 $\pm$ 0.25 fold, respectively). Our lab is currently investigating the effects of Akt inhibition on CX43 localization and on embryo developmental outcome. ( $n \geq 3$  for all experiments). This research was partially funded by the Alabama Cattleman's Association and the Alabama Agriculture Experiment Station and Hatch program of the National Institute of Food and Agriculture, U.S. Department of Agriculture.

**Signaling of the Pro-Inflammatory Cytokine TNF $\alpha$  through NF $\kappa$ B-p65 Increases Gdf9 and Decreases Figla mRNAs in Oocytes of Primary Follicles.** Kelsey R. Timme, Heidi B. Miller, and Jennifer R. Wood

Female obesity is associated with ovarian inflammation, oxidative stress, and reduced oocyte quality, resulting in reduced embryo development rates. Our previous studies demonstrated that C57BL/6 mice fed a high fat diet (DIO) had increased ovarian expression of Tnfa mRNAs, as well as increased phosphorylation of signal transducer and activator of transcription 3 (STAT3) and NF $\kappa$ B p65. Furthermore, the abundance of developmental pluripotency-associated protein 3 (Dppa3), POU domain class 5 homeobox 1 (Pou5f1), newborn ovary homeobox (Nobox), folliculogenesis specific bHLH transcription factor (Figla), and growth differentiation factor 9 (Gdf9) mRNAs were increased in ovulated, matured oocytes and/or whole ovaries of DIO mice that were effectively depleted of antral follicles. Based on these data, we hypothesized that pro-inflammatory cytokine signaling selectively increases oocyte-specific mRNAs by transcriptional and/or post-transcriptional mechanisms. In the current study, we tested the hypothesis that acute treatment of primary follicles with TNF $\alpha$  would

activate NFkB signaling and alter Dppa3, Pou5f1, Nobox, Figla, and Gdf9 transcript abundance within the growing oocytes. Ovaries were collected from pre-pubertal CD1 mice (12-14 days of age), partially digested in media containing collagenase and DNase I, and primary follicles were isolated. Immunofluorescence studies were initially performed using antibodies against either total STAT3 or total p65 and confirmed that these proteins were expressed in the oocyte of primary follicles. Subsequently, 10 primary follicles were cultured in media containing 0, 1, 10, or 100 ng/ml TNFa for twenty minutes. Western blot analysis demonstrated a dose response effect of TNFa on p65 phosphorylation. Specifically, the band intensity for phosphorylated NFkB p65 was significantly increased in follicles exposed to 10 ng/ml TNFa, with no difference between 0, 1, and 100 ng/ml TNFa treated follicles. Furthermore, there were no observed differences in band intensity for total NFkB p65, phosphorylated or total STAT3, or ACTB. Next, primary follicles were cultured in the absence or presence of 10 ng/ml TNFa for 0, 2, and 8 hours (n=4 per experimental group with 20 pooled follicles per n) and RNA isolated, reverse transcribed, and droplet digital PCR performed using primers against Dppa3, Pou5f1, Gdf9, Figla, Nobox and the housekeeping gene calnexin (Canx). The ratio of Gdf9/Canx was increased two-fold in follicles treated for 8 hours (3.97 +/- 0.35) with TNFa compared to 0 hour (2.01 +/- 0.48) controls (p-value = 0.027); however, there was no significant difference in Gdf9/Canx abundance between 0 hour control and follicles treated 2 hours with TNFa. Conversely, there was a numerical decrease in Figla/Canx mRNA abundance between 0 (0.39 +/- 0.18), 2 (0.26 +/- 0.08), and 8 (0.16 +/- 0.09) hours post-TNFa treatment. There were no significant differences in Dppa3/Canx, Pou5f1/Canx, or Nobox/Canx mRNA abundance at the time-points analyzed. These data show that TNFa activates NFkB p65, which may directly inhibit Figla and stimulate Gdf9 mRNA transcription. Furthermore, obesity-dependent transcriptional or post-transcriptional changes in Dppa3, Pou5f1, and Nobox mRNAs are likely indirectly regulated by TNFa, other inflammatory signaling pathways (e.g. JAK-STAT3), or obesity-induced oxidative stress. Supported by UN Foundation and UN Hatch (NEB26-206, NEB26-231) funds.

### **Transcriptomic Changes in the Endometrium and Chorioallantois During Placental Inflammation in the Mare.** S. C. Loux, P. Dini, K. Wang, D. Baxter, and B. A. Ball

Placental inflammation (placentitis) is one of the leading causes of late-term abortion and preterm birth in both humans and horses, occurring in 1-5% of pregnancies. Despite the prevalence of placentitis, relatively little is known about transcriptional changes occurring in either the endometrium (EN) or chorioallantois (CA) at this time. Therefore, we aimed to characterize the transcriptome in the EN and CA during placentitis. For this study, we induced bacterial ascending placentitis in five mares via transcervical inoculation with 5 x 10<sup>6</sup> CFU of *Streptococcus equi* ssp. *zooeidemicus*. Mares were monitored daily via ultrasound, then euthanized three to six days post-inoculation based on clinical signs of disease. Three un-inoculated, gestationally age-matched mares were used as controls. Matched chorioallantois and endometrium were sampled in 2 locations: 1) main lesion by cervical star, includes separation of the chorioallantois and endometrium; and 2) uterine body 10 cm beyond the inflamed tissue. RNA was extracted using the RNeasy Mini Kit with RNA quality assessed via bioanalyzer. Sequencing was performed on a NextSeq 500 (Illumina), resulting in an average of 12.3 x 10<sup>6</sup> reads/sample. Reads were trimmed for adapters and quality using TrimGalore, then mapped to EquCab2.0 via STAR. Gene expression was quantified using Cufflinks, including a customized transcriptome based on ENSEMBL v.88 to allow for the discovery of novel transcripts. Reads were filtered for highly expressed reads (FPKM > 1), resulting in 16,086 genes analyzed, including 2273 novel genes not identified in the ENSEMBL

annotation. Differentially expressed genes (DEG) were identified using one-way ANOVA with a false-discovery rate  $P < 0.05$  (JMP 12). In total, 3,943 DEG were identified in one or both regions of the CA, while 474 DEG were identified in the EN. To better assess the function of the DEG, the PANTHER statistical overrepresentation test was used (FDR  $P < 0.05$ ). In the CA, the majority of the transcriptional changes represented changes in the immune response, including antigen processing, regulation of neutrophil migration and initiation of chemokine production. Transcriptional changes in the EN were primarily metabolic processes, suggesting that the endometrium is not directly affecting the immune response, but is instead responding to altered energy requirements. Although counterintuitive, this is consistent with the lack of gross inflammation seen in the EN itself compared to the CA. Additionally, we identified several genes which were differentially expressed in three of the four tissue regions analyzed. These included immune modulators such as CD44 and CXCL14; and apoptosis modulators such as dystrobrevin alpha and S29. Characterization of the differentially regulated novel transcripts is currently underway, with preliminary findings showing many lncRNA as well as putative protein coding genes not previously described in the horse. Ultimately, these data provide valuable information into the transcriptional changes of the endometrium and chorioallantois during placentitis in the mare, allowing a better understanding of the physiological changes occurring during disease.

**Acknowledgements:** This work was funded by the Grayson-Jockey Club Research Foundation, the Albert Clay Endowment and the Paul Mellon post-doctoral fellowship. The authors thank Claudia Fernandes for her assistance with the animal work.

**Cross-Talk Between Intraflagellar Transport and Intramanchette Transport, Two Cargo Transport Systems Essential for Mammalian Sperm Flagella Formation.** Zhenyun Wang, Wei Li, Shiyang Zhang, Lin Shi, and Zhibing Zhang

Sperm flagella formation is a complex process that requires cargo transport systems to deliver structural proteins for sperm flagella assembly. Two cargo transport systems, the intramanchette transport (IMT) and intraflagellar transport (IFT), have been shown to be essential for spermatogenesis and sperm flagella formation. IMT exists only in elongating spermatids, and IFT is responsible to deliver cargo proteins in the developing cilia/flagella. Our laboratory discovered that mouse meiosis expressed gene 1 (MEIG1), an essential gene for sperm flagella formation, is present in the cell bodies of spermatocytes and round spermatids, but it is translocated to the manchette. An IFT-B complex component, IFT20, is present in the Golgi bodies of spermatocytes; it is also present in the manchette of the elongating spermatids. Given that both IFT20 and MEIG1 are present in the manchette, and both are essential for normal spermatogenesis and sperm flagella formation, we hypothesize that the two proteins are in the same complex. This is supported the fact that both proteins were co-precipitated from the testis extracts using the specific IFT20 antibody. In the sucrose gradient assay, the two proteins were present in similar fractions. MEIG1 distribution was not changed in the conditional *Ift20* mutant mice; however, IFT20 protein drifted toward lighter fractions in the *Meig1* mutant mice. In the IFT20-deficient mice, MEIG1 was still present in the manchette in the elongating spermatids; however, in the MEIG1-deficient mice, IFT20 was no longer present in the manchette in the elongating spermatids even though it was still present in the Golgi bodies of spermatocytes. Our data suggest a cross-talk between IMT and IFT. Some IFT components, including IFT20 also participates in the IMT process and is MEIG1-dependent.

**Fewer and Dysfunctional Fetal Leydig Cells Produce Less Testosterone and Cause Delayed Testis Descent and Abnormal External Genitalia in Gli3XtJ Mutant Mice.**

Joan S. Jorgensen, Jessica L. Muszynski, Samantha R. Lewis, Elena M. Kaftanovskaya, Emily M. Merton, Alexander I. Agoulnik, Martin J. Cohn, and Anna E. Baines

In humans, Greig cephalopolysyndactyly syndrome (GCPS) is an autosomal dominant disorder linked to craniofacial and limb development, but some male patients are also born exhibiting defects in sex differentiation including cryptorchidism and/or hypospadias. GCPS is caused by a mutation in a Hedgehog pathway mediator, GLI3 that results in a non-functional protein and a phenotype with complete penetrance, but with variable severity across tissues. Whereas it is established that Desert Hedgehog (DHH) signaling via Smo is essential for the onset of androgen synthesis and normal male sex differentiation, elimination of individual downstream mediators, GLI1 or GLI2, had no effect. GLI3 has not been tested; therefore, we hypothesized that GLI3 is required for DHH-mediated androgen synthesis and male sex differentiation. To test this hypothesis, we used the Gli3XtJ mouse model, which faithfully models GCPS. Reminiscent of the variability in GCPS phenotypes, our results showed delayed testis descent in all Gli3XtJ mutants due to failed disintegration of the cranial suspensory ligament, and abnormal external genitalia phenotypes with varying severity. While transcript and immunohistochemical analyses indicated that germ, Sertoli, and peritubular myoid cells of Gli3XtJ testes were not different from wild type, fetal Leydig cell numbers were significantly decreased. Further, after correction for cell number, transcript levels specific to fetal Leydig cell function, including DHH mediators, Sf1, and steroidogenic enzymes were significantly lower in Gli3XtJ testes. Diminished fetal Leydig cell number and function culminated in significantly less testosterone production. Thus, we conclude that variances in the severity of male sex differentiation in Gli3XtJ embryos are caused by disparities in fewer fetal Leydig cells to produce androgens. These findings are important because they represent a genetic component to fluctuant fetal Leydig cell numbers and function that suggests potential thresholds in androgen production requirements for normal differentiation of each male characteristic. Advanced understanding of the concentrations of androgen required for male sex differentiation would impact our ability to discover potential genetic and/or environmental interactions that are associated with the troubling increase in incidence in male birth defects within industrialized nations.

Supported by NIH R01-AR070093 (AIA), NIH R01-DK110408 (MJC), NIH R01-HD075079 (JSJ), NIH R01-HD090660 (JSJ), the University of Wisconsin-Madison (JSJ),

**A Role for CHTF18 in Ovarian Aging.** Karen Berkowitz, Barenya Mukerji, Abigail Harris, Ferdusy Dia, and Tanu Singh

In women, the number and quality of oocytes, as well as the decline in both of these parameters with age, determines reproductive potential. These changes in the oocyte pool lead to infertility and pregnancy loss, yet the underlying mechanisms are not well understood. Previously, we identified roles for CHTF18, the conserved DNA replication protein, in male fertility and gametogenesis. Recently, we revealed that Chtf18-null female mice were subfertile with reduced litter sizes and numbers compared to wild type females. Consistent with these findings, Chtf18-null ovaries were smaller and contained fewer ovarian follicles at all stages of folliculogenesis, and the decreases became more significant as females aged. Chromosomal synapsis was complete but homologs separated prematurely during

prophase I. Meiotic recombination was defective and *Chtf18*-null oocytes possessed fewer DNA crossovers or lacked crossovers. Because DNA crossovers and chromosomal cohesion are both necessary to keep homologs physically joined until anaphase I, we postulated that chromosomal cohesion is deficient in *Chtf18*-null oocytes. To test this hypothesis, we examined localization of cohesin proteins that mediate cohesion, on homologs during meiosis. Preliminary analysis suggests that localization of meiotic cohesins REC8, STAG3, and SMC3 was decreased on homologs during prophase I, while REC8 was almost depleted at metaphase I. Because defective meiotic recombination and crossover formation could compromise oocyte quality and developmental competence, we evaluated the ability of *Chtf18*-null oocytes to progress following meiotic resumption. Only a minority of *Chtf18*-null oocytes reached metaphase II compared to the majority of wild-type oocytes. Given our findings suggestive of impaired meiotic cohesion and lack of meiotic progression consistent with poor oocyte quality, we suspected that *Chtf18*-null oocytes might be aneuploid. We utilized an in situ chromosome counting assay to score numbers of chromosomes in *Chtf18*-null compared to wild type metaphase II oocytes. We found that *Chtf18*-null oocytes were aneuploid and showed the gain or loss of a single sister chromatid or chromosome pair as indicated by unpaired kinetochores, compared to wild type oocytes, which were all euploid with paired kinetochores. Interestingly, sister kinetochore cohesion appeared weakened in *Chtf18*-null oocytes at metaphase II and some *Chtf18*-null oocytes exhibited premature sister chromatid separation. These data support, for the first time, a function for CHTF18 in meiotic cohesion and DNA crossover formation in females. They suggest that CHTF18 prevents aneuploidy during female meiosis, too. Given the decline in both the quantity and quality of oocytes in *Chtf18*-null females, our findings also indicate a role for CHTF18 in ovarian aging. This research was supported by NIH R01GM106262, 2013 ASRM Research grant, 2011 Mary DeWitt Pettit Fellowship Award, and 2009 PA Department of Health (CURE) Award to K.B.

**Investigating L1 Expression and Epigenetic Regulation During Germ Cell Development with LacZ Reporter Mice.** Partha Saha, Karly Ackermann, and Wenfeng An

Long interspersed elements type 1 (L1s) are highly abundant retrotransposons in the human genome. To fully understand the role of L1s during development and disease, it is important to track L1 expression and epigenetic regulation at individual L1 loci throughout development at the cellular level. However, it is extremely technically challenging to monitor transcriptional activities of individual endogenous L1s due to high sequence homology. Toward this goal, we created independent single-copy LacZ transgenic mouse lines, in which the LacZ reporter is regulated by a copy of the endogenous mouse L1 promoter. To control for the effect of gene-body DNA methylation on L1 promoter activity, we also generated independent mouse lines with the CpG-less version of the LacZ, termed LacG. After mapping of the transgene locus in each line, mouse tissues were stained with X-gal to visualize L1 promoter activity at single cell level. Initial screening demonstrated that the LacG reporter system supported robust expression as compared to the LacZ reporter. Interestingly, the frequencies of signal in each tissue were largely conserved across generations for a specific LacG mouse line but varied significantly among reporter lines. Ongoing effort aims to reveal the pattern of these signals in different anatomical regions, which might support L1 retrotransposition in different developmental period in these mouse models. The goal is to provide a comprehensive mapping of L1 promoter activity in a cell dependent and locus dependent manner. Such information will be instrumental in our understanding of L1's involvement in

physiological and pathological conditions, including embryogenesis, gametogenesis, and under environmental stress.

**Absence of YWHAE Protein (14-3-3 Epsilon) Causes Infertility in Male but not in Female Mice.** Alaa Eisa, Alexander Ignatious, Sumit Bhutada, Suranjana Goswami, Souvik Dey, Wesam Nofal, Eva Gilker, Rahul Bhattacharjee, Srinivasan Vijayaraghavan, and Douglas Kline

Gametogenesis involves the interplay of a number of signaling processes and regulatory proteins. YWHA or 14-3-3 proteins are key regulatory proteins found in eukaryotic cells that, among other functions, are central in regulating the cell cycle. The 14-3-3 proteins form homodimers or heterodimers and act as adaptor proteins that affect protein localization, confirmation, stability, or activity. The family of 14-3-3 proteins, encoded by seven different genes, includes YWHAB, YWHAE, YWHAG, YWHAH, YWHAQ, YWHAZ, and SFN). In examining the role of 14-3-3 proteins in gametogenesis we have focused, in part, on YWHAE (14-3-3 Epsilon) utilizing conditional knockout mice that inactivate the gene for YWHAE during in germ cells during spermatogenesis and oogenesis. A portion of the coding region of 14-3-3 epsilon was deleted with Cre-Lox recombination using Stra8 Cre mice for the male germ cell-specific knockout, or Zp3 Cre mice for the oocyte-specific knockout. Confirmation of the transgenic genotypes was accomplished through PCR amplification using specific primers targeted to the coding region. The absence of the protein in sperm and oocytes was confirmed by using both western blot and immunohistochemical staining techniques. In vivo breeding tests and in vitro fertilization indicate that, in the absence of 14-3-3 Epsilon, males are infertile. Sperm from the conditional knockout males are less motile and appear to be produced in fewer number. Analysis suggests changes in other proteins associated with sperm motility and in mitochondrial activity. In contrast, the absence of 14-3-3 Epsilon in females does not appear to alter oogenesis, oocyte maturation or fertility. 14-3-3 proteins often act interchangeable in interacting with target proteins or in forming heterodimers. Here we find that 14-3-3 Epsilon alone may be required for normal sperm function. We suspect that other 14-3-3 isoforms function critically in oogenesis.

**Estrogens Stimulates Rapid H<sub>2</sub>S Production in Human Uterine Artery Endothelial Cells in Vitro via GPER-Mediated Nongenomic Pathways.** Thomas J. Lechuga and Dong-bao Chen

Estrogens are potent vasoactive hormones that stimulate uterine artery (UA) dilation via genomic mechanisms mediated by specific estrogen receptors (ER $\alpha$ / $\beta$ ) and nongenomic pathways via plasma membrane ER including ER $\alpha$ / $\beta$  and G protein-coupled estrogen receptor 1 (GPER). H<sub>2</sub>S is a potent vasodilator primarily synthesized from L-cysteine by cystathionine b-synthase (CBS) and cystathionine gamma-lyase (CSE). Our recent work showed that long-term treatment with estrogens stimulates UA H<sub>2</sub>S production via specific ER-mediated selective upregulation of CBS transcription in UA endothelial cells (UAEC) and smooth muscle cells; however, it is not known if estrogens stimulate rapid H<sub>2</sub>S production in UAEC. This study was aimed to determine if estrogens stimulate rapid UAEC H<sub>2</sub>S production via activation of plasma membrane ER-mediated nongenomic pathways. Primary human UAEC (hUAEC) were isolated by collagenase digestion from primary UAs collected from Cesarean hysterectomies of late pregnant women. The cells were cultured in endothelial cell culture medium for experimental use at passage 3-6. Following treatments with different forms of estrogens in the presence or absence of de

novo protein synthesis inhibitors and ER/GPER agonists and antagonists for various times, cellular H<sub>2</sub>S production was determined by the methylene blue assay or a novel fluorescent H<sub>2</sub>S probe to determine real-time intracellular H<sub>2</sub>S production using fluorescent microscopy. Treatments with 10 nM 17 $\beta$ -estradiol (E2b) or the membrane impermeable E2b-BSA stimulated rapid H<sub>2</sub>S production in hUAEC in a time (0-2 h)-dependent manner, as determined by both the methylene blue assay and the specific fluorescent H<sub>2</sub>S probe. H<sub>2</sub>S production began to increase at 10 min, maximized at 30-40 min, and reached plateau at 60 min after treatments with estrogens. Pretreatment with inhibitors of either CBS or CSE partially inhibited and their combination completely blocked estrogen-stimulated H<sub>2</sub>S production. Treatment with the GPER agonist G1 (10 nM) also stimulated time-dependent H<sub>2</sub>S production similar to E2b in hUAEC. Both treatment with E2b and G1 had greater responses in pregnant vs. nonpregnant hUAEC. Pretreatment with inhibitors of RNA polymerase (Actinomycin, 5  $\mu$ M) or protein synthesis (Cycloheximide, 5  $\mu$ M) did not alter E2b- and G1- stimulated rapid H<sub>2</sub>S production. Pretreatment with the ER antagonist ICI 182,780 and GPER antagonist G15 blocked E2b/E2b-BSA and G1-stimulated H<sub>2</sub>S production, respectively. Thus, estrogens stimulate rapid H<sub>2</sub>S production in hUAEC independent of de novo protein synthesis but mediated by nongenomic pathways involving activation of CBS/CSE and specific ERs localized on the plasma membrane including GPER and possible ER $\alpha$ / $\beta$ . (supported by NIH RO1 HL70562).

#### **Effect of Heat Stress on Corpus Luteum Function and Expression of Microrna During Early Pregnancy in**

**Figs.** R. Blythe Schultz, Katie L. Bidne, Matthew R. Romoser, Malavika K. Adur, Jacob T. Seibert, Lance H. Baumgard, Aileen F. Keating, and Jason W. Ross

Heat stress (HS) compromises swine reproduction, though the mode of action is not well understood. Progesterone, produced by the corpus luteum (CL), is required for pregnancy establishment and maintenance in pigs, and reduction of CL functionality during seasonal HS is a phenotype observed in domestic species. HS also compromises intestinal function resulting in increased circulating lipopolysaccharide, which can be detrimental to the viability and function of the CL. MicroRNA (miRNA) are short, noncoding RNA that regulate a broad range of cellular functions through posttranscriptional activity and contribute to CL development, function, and maintenance during the peri-implantation stage of pregnancy. This study investigated our working hypothesis that HS during the luteal phase adversely affects CL development and function corresponding to an altered CL miRNA profile. Postpubertal gilts (n = 26) were estrus synchronized using oral administration of altrenogest (14 d; 15 mg/d), and upon observation of behavioral estrus, were randomly assigned to diurnal HS (n = 12; 35  $\pm$  1oC for 12h/31.6  $\pm$  1oC for 12h) or thermoneutral (TN; n = 14; 21  $\pm$  1oC) conditions 2 d post estrus (dpe) until 12 dpe. To evaluate the effects of pregnancy status on miRNA profile and CL function, 5 animals from the HS group and 7 animals from the TN group were artificially inseminated before being exposed to thermal treatment. Serum progesterone levels were assessed at 0, 4, 8 and 12 dpe and all animals were euthanized at 12 dpe. CLs were counted and diameter measurements were recorded for one ovary of each animal before the CLs were excised, weighed, and snap frozen for assessment of progesterone levels and miRNA abundance. Heat stress did not affect CL diameter (P = 0.45) in cyclic gilts, but tended (P = 0.07) to reduce CL weight. Interestingly, HS caused a reduction in CL weight (13.3%; P > 0.05). Six miRNAs (miR-21, miR-143, miR-150-5p, miR-196a-5p, miR-378, and let-7i-5p) were analyzed based on previous implications in ovarian function related to oocyte maturation, steroid hormone production, regulation of autophagy, apoptosis and tumor growth, as well as being linked to CL developmental

stages. Following normalization to RNU43, pregnancy status nor thermal treatment influenced the transcript abundance of the targeted miRNAs ( $P \geq 0.18$ ). In summary, HS reduced CL weight, but did not alter circulating progesterone. Although our targeted miRNAs did not correspond to the phenotypic differences in CL weight observed in this study, further work is needed to assess environmental influence on miRNA expression during the luteal phase and to investigate the potential of other molecular regulators involved with CL functionality during HS in swine. This project was supported by the Iowa Pork Producers Association and the Agriculture and Food Research Initiative Competitive Grant no. 2017-67015-26459 from the USDA National Institute of Food and Agriculture.

**Development of Cortical Stroma in the Bovine Fetal Ovary.** Raymond J. Rodgers, Monica D. Hartanti, Katja Hummitzsch, Helen F. Irving-Rodgers, Wendy M. Bonner, and Vivienne E.A. Perry

During formation of the fetal ovary the stroma penetrates from the mesonephros and branches and expands. As it does so it appears to play a role in firstly the formation of ovigerous cords, and then of the ovarian surface epithelium and ovarian follicles [1]. The aim of our study was to morphometrically analyse the development of the bovine ovarian stroma. We collected and weighted 28 ovaries from bovine fetuses, and identified the gender of the small fetuses less than 10 cm by analysing the SRY gene. Across gestation we measured the total volume and relative proportions of cortex and medulla, the proportion and total volume of stroma in the cortex, and the numerical and proliferation index of cells in the stroma of the cortex. The stroma was identified by immunohistochemistry of collagen type I and the Ki67 marker was used to identify proliferating cells. We devised a classification system based upon five identifiable stages of development of the cortex commencing with ovigerous cord formation (stage I), the ovigerous cord breakdown (stage II), follicle formation (stage III), surface epithelium formation (stage IV) and tunica albuginea formation (stage V). These corresponded to averages from 79 days (stage I) and 264 days (stage V). During stages I to III, taking 94 days, versus III to V, taking 91 days, the fold changes in ovarian weight were 4.2 and 4.2 fold, in medullary volume were 6.3 and 7.6 fold and in cortical volume were 6.7 and 2.0 fold, respectively. Thus clearly the rate of expansion of the cortex declined whilst the medulla continued. The proportion of the cortex that was stroma (volume density) and the total stromal volume of cortical stroma increased throughout the gestation. Both were strongly correlated with crown-rump length ( $R^2 = 0.8065$ ,  $P < 0.01$  and  $R^2 = 0.8194$ ,  $P < 0.01$ , respectively). Interestingly, the numerical density of proliferating cells and the proliferation index in cortical stroma decreased throughout development. The numerical density of cells in the stromal cortex did not change throughout gestation. Thus the rate of expansion of cortical stroma is greatest early in development when the stroma penetrates the ovarian primordium from the mesonephros. The expansion of the cortical stroma occurs due to cell proliferation and not a change in cell size or a change in the amount of extracellular space.

1. Hummitzsch, K., et al., A new model of development of the mammalian ovary and follicles. PLoS One, 2013. 8(2): p. e55578.

**RNA-Seq Analysis of Porcine SCNT Blastocysts with High and Low Incidence of Apoptosis.** Laura A. Moley, Roussele Jones, Aaron J. Thomas, Abby D. Benninghoff, and S. Clay Isom

While cloning through somatic cell nuclear transfer (SCNT) has been achieved in a growing number of species, the efficiency of this assisted reproductive technology remains poor. The low efficiency of SCNT

has been attributed to faulty epigenetic reprogramming of SCNT embryos leading to low overall success. We hypothesized that the increased prevalence of faulty epigenetic reprogramming in some SCNT embryos would lead to aberrant gene expression resulting in poor embryo development, elevated apoptosis levels, and eventual failure following embryo transfer. Conversely, embryos that undergo proper epigenetic reprogramming would maintain appropriate gene expression, adequate embryo development, low levels of apoptosis, and increased success following embryo transfer. To test these hypotheses, we utilized a nontoxic, noninvasive caspase activity reporter (SR-FLICA Poly Caspase Assay Kit; Immunochemistry Inc.) to separate SCNT porcine blastocysts exhibiting high or low apoptosis on day 6 of development. Embryos in the top and bottom 20% of detected caspase activity were classified as high and low incidence of apoptosis, respectively (3 replicate cloning sessions, total n=13 embryos). RNA-Seq libraries were prepared from individual blastocysts using the Ovation SoLo RNA-Seq system (NuGEN Technologies). Libraries were sequenced on the Illumina NextSeq sequencing platform using single-end 75bp reads. Reads were aligned to the *Sus scrofa* 11.1 genome and differential gene expression was determined using EdgeR. Preliminary analysis resulted in an average of 4.75 million reads aligned per sample. Comparing high to low apoptosis embryos, 140 genes had decreased expression while 35 genes had increased expression with a fold-change  $\geq 1.5$  and false discovery rate-corrected  $P \leq 0.05$ . This list of differentially-expressed genes was used to perform enrichment analysis to identify over-represented Gene Ontology terms or KEGG pathways (DAVID EASE v. 6.8 against the *Sus scrofa* background genome). However, no significantly enriched GO terms or pathways were identified (all FDR p values  $>0.05$ ). This may suggest that aberrations in genome reprogramming in SCNT embryos may be random in nature, and that the associated transcriptional responses to these programming defects is also widely variable and inconsistent. Additional analysis of DNA methylation from reduced representation bisulfite sequencing libraries of each of these same individual blastocysts is currently in progress, which should expand our understanding of reprogramming in individual embryos and reaffirm the stochastic nature of reprogramming.

#### **Prostaglandin E2 Signaling and Epigenetic Regulation of Proapoptotic miRNA34c in Endometriosis.**

Joe A. Arosh, Jone A. Stanley, Kaylon L. Bruner-Tran, Kevin G. Osteen, and Sakhila K. Banu

Epigenetics plays an important role in the pathogenesis of endometriosis. Recent multi-omics studies indicate that epigenetic silencing of proapoptotic genes and miRNAs is one of the important contributing factors in the survival of chronic inflammatory diseases. In the present study, we investigated the interaction between proinflammatory mediator prostaglandin E2 (PGE2) signaling and epigenetic silencing, restoration, and proapoptotic role of miRNA34c in endometriosis. Peritoneal endometriotic lesions from women with endometriosis (n=6) and endometrial biopsy from age-matched endometriosis-free women (n=6) were obtained during the proliferative phase of the menstrual cycle. Human endometriotic epithelial cells 12Z and stromal cells 22B cells and 12Z/22B-xenograft mice were used as in vitro and in vivo models. Expression and regulation of miR34c was determined by array, qPCR, MS-PCR, bisulphite sequencing, and ChIP-PCR. Expression of miR34c is barely detectable ( $p < 0.05$ ) in the peritoneal endometriotic lesions compared to endometrium in women, which is due to partial DNA methylation. Pharmacological inhibition of PGE2 receptors EP2 and EP4 increases ( $p < 0.05$ ) the expression of miR34c in 12Z and 22B cells in vitro and experimental endometriosis in vivo. Inhibition of EP2/EP4 decreases ( $p < 0.05$ ) enrichment of DNMT3a/3b, MeCP-2, Sin3A, and MBD1 proteins; decreases ( $p < 0.05$ ) the enrichment of H3K9me3, H3K27me3, EZH2 and SUV39H1 proteins; and does

not change the enrichment of H3K4me3, H3K9ac, H3K27ac, and POL II in the regulatory region of miR34c in 12Z and 22B cells. Restoration of miR34c by overexpression induces ( $p < 0.05$ ) apoptosis of 12Z and 22B cells in vitro. Intraperitoneal administration of miRNA34c mimics induces ( $p < 0.05$ ) apoptosis of lesions in experimental endometriosis in vivo. Our new findings suggest that expression of proapoptotic miRNA34c is epigenetically silenced in the endometriotic lesions and inhibition of PGE2-EP2/EP4 signaling restores its expression by modulating DNA methylation and H3 Histone methylation. Targeting proapoptotic miRNA34c could emerge as potential non-steroidal and apoptosis-targeted therapy for endometriosis.

**BODIPY-Cholesterol Can Reliably be Used to Monitor Reverse Cholesterol Transport in Capacitating Mammalian Spermatozoa.** Naomi C. Bernecic, Bart M. Gadella, Jos F.H.M. Brouwers, Jeroen W.A.

Jansen, Ger J.A. Arkesteijn, Simon P. de Graaf, and Tamara Leahy

Reverse cholesterol transport (RCT) from spermatozoa is a crucial event during capacitation. Alongside this process, spermatozoa acquire the ability to bind to the zona pellucida and to undergo the acrosome reaction, both of which are essential for successful fertilisation. We present a novel cholesterol assay for spermatozoa in which a fluorescent BODIPY-cholesterol is used to label spermatozoa and flow cytometry is used to monitor RCT from spermatozoa to albumin after in vitro capacitation. The objectives of this study were to 1) validate the BODIPY-cholesterol results with the detected amount of endogenous sperm cholesterol and 2) compare BODIPY-cholesterol results with the amount and distribution patterns of filipin staining (a fluorescent staining method for endogenous sperm surface cholesterol). Ram and boar spermatozoa were washed via a swim-up or discontinuous Percoll density gradient respectively and then incubated for up to 3h in TALP media either with or without bovine serum albumin (BSA), bicarbonate and cAMP upregulators (1mM dibutyryl cAMP, caffeine and theophylline). RCT was first assessed by quantifying the amount of BODIPY-cholesterol per spermatozoon in both species using flow cytometry. The amount of endogenous cholesterol in ram spermatozoa was quantified after lipid extraction with mass spectrometry. Filipin staining patterns of boar spermatozoa were analysed by confocal fluorescence microscopy and the amount of filipin fluorescent signal per sperm cell was detected with flow cytometry. BODIPY-cholesterol as well as endogenous cholesterol quantification showed that a loss of sterols was detected from ram spermatozoa under full cAMP stimulation in combination with BSA (20-25% for BODIPY-cholesterol and 10-27% for endogenous cholesterol, respectively). When microscopically observed, boar spermatozoa showed a significantly higher percentage of cells with diminished filipin staining when compared to non-capacitating spermatozoa (TALP:  $7.2 \pm 3.9\%$ ; TALP+cAMP up-regulators:  $7.2 \pm 4.0\%$ ; TALP-bicarbonate+cAMP up-regulators:  $11.3 \pm 6.8\%$  versus Control:  $0.6 \pm 0.4\%$ ;  $P < 0.05$ ). Moreover, boar spermatozoa also showed an increase in a filipin-cholesterol pattern indicative of redistributed cholesterol following incubation in capacitating conditions ( $P < 0.01$ ). This pattern was identified as a concentration of filipin-cholesterol at the apical region of the sperm head. In contrast to filipin analysis, the BODIPY-cholesterol assay was able to quantify a significant loss in BODIPY-cholesterol from boar spermatozoa in conditions that support capacitation compared to a non-capacitating control (TALP:  $71.7 \pm 8.1\%$ ; TALP+cAMP up-regulators:  $66.4 \pm 3.6\%$ ; TALP-bicarbonate+cAMP up-regulators:  $68.0 \pm 8.0\%$ , relative values to control values of 100%;  $P < 0.0001$ ). Taken together, these results show that flow cytometric detection of RCT from the sperm surface, during in vitro capacitation, can be reliably monitored after labeling spermatozoa with BODIPY-cholesterol both in the ram and boar. The use of filipin to detect sperm surface cholesterol is less straight forward as this probe complexes to cholesterol

inside the two lipid leaflets of the sperm plasma membrane and this process is not linearly related to the amount of cholesterol present per surface area. However, filipin staining is useful for detecting capacitation-dependent redistribution of endogenous cholesterol and this process appears to correlate - in a yet to be unraveled fashion- to RCT in capacitating spermatozoa.

**PI3K/AKT/PTEN Pathway Involvement in Motility Loss Associated with Prohibitin Downregulation in Sperm from Infertile Men.** Hong Chen, Ranran Chai, Guowu Chen, and Wai-sum O.

Phosphoinositide 3-kinase (PI3K) activity has been reported to be critical to sperm motility and mitochondrial ROS generation while mitochondrial membrane protein Prohibitin (PHB) controls PI3K/AKT pathway in somatic cells by regulating mitochondrial function. Our recent findings showed that sperm PHB expression is significantly decreased in infertile men with poor sperm quality by regulating mitochondrial morphology and function. The objective of this study is to test if PHB expression in sperm is associated with the PI3K/AKT/PTEN pathway. Semen samples from 101 male subjects between 30-40 years old attempting ICSI/IVF were collected and then assayed by semen analysis according to 2010 WHO standards. Contaminating leucocytes are removed from all samples by using magnetic Dynabeads coated with a monoclonal antibody against CD45 and confirmed using a zymosan provocation assay. After then, the localization and the level of expression and phosphorylation of PI3K/AKT/PTEN pathway in sperm was detected using immunofluorescence staining, SDS-PAGE, and Western blot in infertile men with poor sperm motility (asthenospermia, A) and/or low sperm concentrations (oligoasthenospermia, OA). Our results demonstrate a significantly lower expression of P110 catalytic subunit but a higher P85 regulatory subunit of PI3K in sperm from A and OA subjects than that from normospermic (N) subjects. However, the findings of significantly lower level of phosphorylation of P85 regulatory subunit (pTyr199 and pTyr467) of PI3K may result from the significantly lower level of phosphorylation of PTEN (pSer380) in sperm from A and OA subjects. Consequently, the significantly lower phosphorylation of AKT (pSer473 and pThr308) shown in sperm from A and OA subjects, may result from lower phosphorylation of PI3K/PTEN in sperm with a higher level of mitochondrial ROS as reported previously. Collectively, our observations suggest that lower phosphorylation of PI3K/AKT/PTEN pathway shown in infertile men with high mitochondrial ROS generation and poor sperm motility may be associated with decreased PHB expression. (This project was supported by National Natural Science Foundation of China, Grant No. 81270738).

**Homologous mRNA of Equatorin Protein can Predict Boar Fertility.** Won-Ki Pang, Sae-Han Kang, Ki-jin Kwon, Ki-Uk Kim, Kyu-Ho Kang, Do-Yeal Ryu, Won-Hee Song, Md Saidur Rahman, Woo-Sung Kwon, and Myung-Geol Pang

Equatorin (EQTN) is a membrane protein that is specifically localized in the equatorial segment of mammalian spermatozoa. It has been demonstrated that EQTN plays a major role in acrosome reaction, a penultimate steps of fertilization subsequently facilitates sperm-oocyte fusion. Differential expression of this protein was also reported in boar spermatozoa of different fertility. However, due to lack of commercial porcine anti-EQTN antibody, it has not yet been validated whether this protein expression could consider as a biomarker for male fertility. In the present study, we conducted qRT-PCR to measure the levels of homologous mRNA of the EQTN protein in 20 individual boar spermatozoa with different

fertility (litter size ranges from 10.3 – 14.2). Field fertility for the selected boars (litter size) was calculated based on artificial insemination (AI) outcomes (average insemination number was 57) of 668 sows. Simultaneously, motility parameters and capacitation status of spermatozoa were examined by computer-assisted sperm analysis and chlortetracycline/Hoechst 33258 dual staining, respectively. Our data showed a significant positive correlation ( $P < 0.05$ ,  $\rho = 0.513$ ) between EQTN expression (mRNA level) and boar litter size. Further, to assess the utility of the EQTN expression for identifying litter size ( $\geq 13$  or  $< 13$ ), a receiver-operating curves (ROCs) were used. We found that the overall accuracy of EQTN expression for predicting litter size was 80% (sensitivity, specificity, negative predictive value, and positive predictive value were 100.00, 71.43, 100.00, and 60.00%, respectively). Interestingly, using a cut-off value for average litter size, selected boars (average litter size 13.53) represented a significantly increased pups number 1.49 in AI field trial than that of culled boars (average litter size 12.04). In contrast, the EQTN expression level did not show any significant correlation with other parameters, such as motility, motion kinematics, and capacitation state of spermatozoa. Based on this findings, we suggest that homologous mRNA of EQTN could be an alternative of EQTN protein for predicting male fertility. To best of our knowledge, it is the first study to investigate the correspondence relationship of EQTN expression and male fertility. However, further studies are needed to confirm our initial findings.

This work was supported by Korea Institute of Planning and Evaluation for Technology in Food, Agriculture, Forestry, and Fisheries (IPET) through Agri-Bio Industry Technology Development Program, funded by Ministry of Agriculture, Food, and Rural Affairs (MAFRA) (116172-3).

**Role of Connexin Hemichannels and Apoptosis in Vitrification and Warming of Immature Bovine Cumulus-Oocyte-Complexes.** Katarzyna Joanna Szymanska, Nerea Ortiz-Escribano, Etienne Van den Abbeel, Ann Van Soom, and Luc Leybaert

Gap junctions, made of connexin proteins, form open channels between the oocyte and cumulus cells that facilitate their direct coupling, and are required for oocyte growth and maturation. Gap junctions comprise two hemichannels and can exist as single channels that are closed in physiological conditions but may open in response to cellular stress conditions, thereby creating a non-selective leakage pore, which can lead to cell death. Vitrification is a cryopreservation technique where cells are exposed to extremely stressful conditions, which may trigger hemichannel opening and lead to cell death, thereby impairing the functional viability and in vitro maturation rates of oocytes. Cumulus-oocyte-complexes (COCs) were subjected to a vitrification protocol as described in Stoop et al., 2012. We investigated the trigger of the hemichannel opening and the influence of various protocol parameters (equilibration times, temperature, cryoprotectant concentrations and extracellular  $Ca^{2+}$  concentration) on hemichannel opening (assessed via PI-dye uptake assay and exclusion of 10kDa fluorescein-dextran) and apoptotic cell death (via TUNEL assay) in cumulus cells. We tested the duration of the opening and the change in apoptotic cells with time. We optimized the protocol to find conditions associated with minimal hemichannel opening and minimal cell death. Finally, we compared the maturation rates of all protocols (non-vitrified, vitrified with primary protocol, and vitrified with optimized protocols) as well as cleavage and blastocyst formation rates after parthenogenetic activation. We observed that, vitrification and warming triggered significant hemichannel opening (15%) and apoptosis (10%). We found that all tested parameters influenced hemichannel opening activity and cell death. Based on those results we optimized tested conditions and created two distinct protocols with minimal hemichannel opening and

apoptosis after warming. Open hemichannels remained open, up to 6h hour after warming. Interestingly, the highest percentage of apoptosis was detected immediately after warming and was significantly reduced after 1h. Overall, we obtained on average high maturation (57%) and developmental rates (cleavage 60%, blastocyst 11%) after vitrification. All vitrified groups had statistically lower maturation and development rates compared to non-vitrified control. Maturation and blastocyst rates from vitrified groups were not statistically different from each other. However, there was a difference in cleavage rate of one of the optimized protocols. Our results confirm that vitrification/warming triggers hemichannel opening and increases apoptotic cell death in cumulus cells. Protocol modifications that prevent hemichannel opening are a promising strategy to overcome the detrimental effects of vitrification/warming but more work is needed to understand its exact molecular effect on the oocyte and cumulus cells.

**Challenges to Generating Induced Pluripotent Stem Cells From Cattle.** Viju V. Pillai, Tiffany Kei, Shannon Reddy, Moubani Das, and Vimal Selvaraj

Underlying mechanisms that direct reprogramming of somatic cells to induced pluripotent stem cells (iPSCs) are considered highly conserved across all mammalian species studied. Equally, proof of principle that iPSC-like cells can be derived from cattle is indicated in 12 publications till date. Despite these results, there remain inconsistencies, serious gaps in characterization, and inappreciable research progress towards fundamental understanding or commercial application of these cells. In our efforts to derive and study bovine iPSCs, we encountered problems linked to reprogramming and lack of methods for propagation and sustenance of bovine iPSCs. Our results suggest that iPSC protocols optimized for mouse and human cells render bovine somatic cells considerably refractory to reprogramming. Moreover, methods used to improve reprogramming efficiency in mouse and human cells had none to minimal effects on bovine cell reprogramming. This included knockdown of p53 expression, knockdown of MBD3 expression, overexpression of BRD3R, and use of small molecule regulators (SB421542 and PD0325901). Among the different conditions tested, use of bovine genes coding for Oct4, Sox2, Klf4, cMyc and Nanog delivered via retroviruses appeared to produce consistent iPSC-like cells, albeit at very low efficiency. Efficiency observed was relatively higher with use of cells from the Wharton's jelly. Nevertheless, bovine iPSC-like colonies derived from any approach could not be sustained or passaged effectively. Although teratoma formation appears to be a consistent demonstration in previous publications on bovine iPSCs, none have demonstrated that these cells could integrate with the inner cell mass of blastocyst embryos and establish chimeras. Our findings indicate that significant roadblocks exist for reprogramming bovine differentiated somatic cells to iPSCs. These problems could emanate from epigenetic roadblocks leading to incomplete reprogramming, and/or core distinctions in cellular physiology that are simultaneously subject to discordant or inadequate culture conditions during this process. Without necessary knowledge of cell biology linked to bovine pluripotency, this field risks generation of iPSCs with epigenetic aberrations that may preclude beneficial use. Therefore, studies on the core aspects of bovine pluripotency regulation (both transcriptional and signaling) are necessary before iPSC-driven bovine technologies can be realized.

**Macrophage Involvement in Pregnancy-Associated Uterine Apoptotic Cell Clearance in the Rat.** Sarah J. Bacon, Gargi Mishra, Banna Hussein, Eudoria Lee, and Vicky Yau

Maternal immune cells are crucial to uterine remodeling in pregnancy and the puerperium. These cells operate in networks that initiate vascular changes within the placental bed, facilitate cervical softening in late pregnancy, and coordinate the healing and restoration of the postpartum uterus, among other important roles. Many investigators have articulated the way in which uterine Natural Killer cells in particular mediate changes to maternal uterine vasculature in rodents. Yet uterine macrophages, while abundant, are less well characterized. In this study, we use qPCR, immunofluorescence and immunohistochemistry to extend what is known about macrophage functional networks by looking explicitly for indicators of efferocytosis, that is, the phagocytosis of cells that become necrotic or apoptotic in the course of active uterine remodeling in the rat. We hypothesized that macrophages, often found in a secondary ring around the cuff of Natural Killer cells encircling the uterine vasculature, could operate to clear the cell fragments generated in vascular remodeling. We followed the estrous cycle of female rats by daily vaginal lavage, pairing receptive females with experienced males prior to lights out on the day of proestrus. Dams were weighed daily and sacrificed on gestation days 12, 14, or 16 to assess macrophage infiltration of the decidua and metrial gland as well as steady-state levels of mRNA for the pan-macrophage marker CD68, the cytokines TGF $\beta$  and TNF $\alpha$ , and the phosphatidylserine receptor MerTK. Virgin and postpartum uterine tissues were used as negative and positive controls, respectively. Frozen embedded tissues were sliced and stained with fluorescently-labelled antibodies to CD68, MerTK, perforin, and Annexin V (a marker of apoptosis) to identify apoptotic cells. We found that mRNA levels for the pan-macrophage marker CD68 rose throughout mid-pregnancy, consistent with our previous immunohistochemical data from macrophage-specific antibody staining. Steady-state levels of mRNA for TGF $\beta$  in mid-pregnancy metrial gland also rose, while TNF $\alpha$  levels did not rise above background, consistent with the interpretation that macrophages operate within an immunosuppressive network in midpregnancy, suppressing harmful inflammation that could accompany extensive tissue remodeling. We also tested for the presence of MerTK, a receptor that recognizes apoptotic fragments by binding to exposed phosphatidylserine residues. MerTK mRNA was not elevated in midpregnancy in any tissues examined, suggesting that if macrophages are phagocytosing apoptotic cells in the mid-pregnancy uterus, the initial steps may be mediated by another phosphatidylserine receptor. Strikingly, however, MerTK expression was elevated in the uterus in the first week postpartum. Immunofluorescence staining of mid-pregnancy uterine decidua and metrial gland confirms that CD68 positive cells are present, as is MerTK and Annexin V, but there is not extensive coexpression of these molecules on the same cells. Taken together, these data are consistent with an immunomodulatory role for macrophages during pregnancy, and also suggest that there may be multiple mechanisms by which remodeling-associated apoptotic cells are cleared to suppress inflammation in the uterus.

**Investigating the Role of the Cystic Fibrosis Transmembrane Conductance Regulator (CFTR) in the Epithelial Barrier Function of Human Epididymis.** Shih-Hsing Leir, James Browne, Calvin Cotton, Scott Eggener, and Ann Harris

The cystic fibrosis transmembrane conductance regulator (CFTR) is an ATP- and cAMP-dependent chloride channel located in the apical membrane of many epithelial cells. The epididymis plays a key role in sperm maturation, and animal studies using mouse and swine models have shown that CFTR is important for maintaining normal epididymal function. However, the structural and cellular dissimilarities in the epididymis between animals and humans indicate that a human cell model is required to study the role of CFTR in maintaining human epididymis function. We recently established

cultures of human epididymis epithelial (HEE) cells and used these to address CFTR function. Non-cancerous human epididymis tissue was obtained from patients undergoing orchiectomy following a clinical diagnosis of testicular cancer. The tissues were dissected into three different anatomical regions: caput (head), corpus (body) and cauda (tail), digested with collagenase type I, and grown on permeable filter membrane supports to form polarized epithelial layers. Among the three different anatomical regions, the caput had the highest CFTR mRNA expression, followed by the corpus and cauda. HEE cells cultured by this method possess a tight-junction integrity that can be quantified by measuring transepithelial resistance (TER) using a voltohmmeter and fluorescent dextrans. The contribution of CFTR to epididymal epithelial barrier function was assessed using a pharmacological CFTR potentiator (VX-770) and forskolin to increase transepithelial short-circuit current, followed by blocking with CFTR inhibitor. In the absence of androgen treatment, the TER of the caput cultures was maintained at a low value of below 100 ohm-cm<sup>2</sup>. In contrast, the corpus and cauda cultures presented higher TER values of 400 and 1500 ohm-cm<sup>2</sup>, respectively. Exposure of caput HEE cells to physiological concentrations of testosterone (200 nM) or R1881 (1 nM) for 12–16 hrs significantly increased the TER of these cultures ( $P < 0.05$ ). In the corpus and cauda cells, no increase was observed upon androgen treatment. Our results demonstrate that differentiated epithelial cells from the caput, corpus and cauda of the human epididymis displayed different epithelial barrier characteristics. The TER and CFTR expression in caput cells were found to be regulated by androgen. Additionally, these results suggest that tight junctions in corpus and cauda cells are not androgen-regulated. In conclusion, the polarized HEE cultures on membrane inserts provide a useful in vitro model in which to study the roles of ion channels, such as CFTR, in human epididymis. This research was supported by the Cystic Fibrosis Foundation (LEIR17G0).

#### **Interrogating Mechanisms Underlying Uterine Dysfunction in Labour Using a New Mouse Model.**

Helena Parkington, Kelly Walton, Ranga Siriwardhana, Don Conrad, Kenneth Aston, Craig Harrison, Harold Coleman, and Moira O'Bryan

Failure to progress in labour due to poor uterine contractions is the major factor precipitating caesarean delivery at term. A recent study in Denmark followed 2 million individuals from birth to 16 years of age and found that those born by caesarean section had a significantly increased rate of diseases associated with immune dysfunction throughout childhood. For the mother, caesarean section increases the risk of post-partum haemorrhage, and placenta praevia and accreta in subsequent pregnancies. Thus, the rate of caesarean section should be kept to a minimum. Therapeutic options are limited, and even oxytocin can fail to achieve augmentation of contraction. Our efforts to develop effective therapeutic strategies would be enhanced by a model with which to interrogate hypotheses and plug the knowledge gap. A recent serendipitous finding in our lab came when we noticed that female mice with a mutation in the *INHBB* gene (M360T), which causes infertility in men, experienced difficulties in labor. Wildtype (WT) C57Bl6J mice and *INHBB*M360T mutant mice were time mated and continuously monitored via a CCD camera and LifeCam from E17 of pregnancy and through to delivery of all pups or for 12h of labour. A set of animals were euthanized in the middle of labour and contractile activity of uterine muscle (myometrium) was studied. Membrane potential and tension were recorded simultaneously in myometrial strips. In WT mice, pregnancy was  $19.2 \pm 0.1$  (n=6) days in length and this was significantly increased to  $20.7 \pm 0.5$  days (n=7,  $p=0.022$ ) in inhibin mutant mice. The duration of labour was  $1.2 \pm 0.1$  h in WT mice and was increased to  $9.0 \pm 1.5$ h in mutant mice ( $p=0.003$ ). In 2/7 mutant mice, labour failed completely and upon post mortem, although the cervix was fully dilated the uterus had full litters (9 and

7 pups). Strips of laboring myometrium from WT mice contracted spontaneously throughout the 9h of experimentation. Spontaneous contractions in strips from mutant mice ceased after about 1h. The spike of the action potential was some 10mV reduced in myometrial cells from mutant mice. WT myometrium contracted well to oxytocin with an EC<sub>50</sub> of 1.1±0.2pM. Oxytocin at 1nM evoked only a small 4±1mV depolarization and no contraction in strips from mutant mice. In WT tissues, spontaneous action potentials spread from the source of initiation to invade the entire strip. This failed to occur in strips from mutant mice, suggesting poor electrical connectivity. In summary and conclusion, pregnancy was prolonged by 1.5 days in INHBBM360T mutant mice and this is equivalent to about 3 weeks in humans. Labour was markedly prolonged and failed entirely in 2/7 animals. Thus, this mutation provides a useful model with which to study failure to progress in labour. Our evidence suggests an extreme failure of oxytocin, the major agent used to augment failing labour in women. There was also indications of altered calcium ion channel density, which would reduce contractile function, and evidence of disrupted connectivity between smooth muscle bundles, which would blunt contractile power in a manner analogous to fibrillation.

**No difference in the Maturation Capacity, in Vitro Fertilization and Pregnant Rate of Cocyles Obtained by Ultrasound-Guided Ovum Pick-Up From Pregnant Dairy Cows and Heifers.** Gloria Patricia Zavala-González, Yazmín Elizabeth Felipe-Pérez, Luiz Gustavo Pessoa-Rocha, Adrián Nava-Mondragón, Antonio Nogueira, Rafael Cano-Torres, and Nazario Pescador

Several lines of evidence indicate that ovarian dysfunction in dairy cows is attributable to the disparity in fertility between lactating cows and nulliparous heifers. Lactating cows have higher incidence of double ovulation, larger dominant follicles, prolonged dominant follicles, and lower progesterone concentrations than nulliparous heifers. These studies together indicate that the metabolic stress in terms of negative energy balance in lactating cows leads to detrimental microenvironment within ovarian follicles. The consequence is that the oocytes display reduced developmental competence. The present work evaluated the maturation and subsequent embryonic development and pregnancy rate after an ovum pickup technique (OPU), during the spring season in a hot-desert weather location in Mexico. The oocytes were obtained from 112 OPU sessions, from Holstein pregnant cows (n = 112), which were grouped by lactation, oocytes were matured for 24 hours, fertilized and incubated in vitro evaluating number of oocytes obtained and embryo production. In the same way, oocytes obtained from 39 OPU sessions, from Holstein pregnant heifers (n = 39), were exposed to the same protocol as the cows, and compared embryo production. Sexed frozen semen was used for both experiments. The 113 embryos obtained from cows and heifers were transferred, until reaching gestation diagnostic at day 45. Results showed no significant differences in the number of oocytes obtained between cows and heifers, nevertheless between cows of second and third lactation there is a difference (550 vs 338; P < 0.002); however, no difference was shown among the number of embryos produced. While, for development of matured, fertilized and cultured oocytes, there was a significant difference in cows of second lactation, there was not an influence on the pregnancy rates. Although, the cleavage rate was higher for the group of heifers (63.5%), no difference was observed between groups. Also the pregnancy rate of transferred embryos, showed no difference between groups. We conclude that the number of recovered oocytes, the rate of cleavage, oocyte maturation and embryonic development through the OPU technique in pregnant dairy cattle are similar to what is obtained from pregnant heifers.

**Mapping of Metabolic Behaviors in Embryos as a Model for the Improvement of Cell Culture Systems in Vitro.** Camila Bruna de Lima, Érika Cristina dos Santos, Jéssica Ispada, Patrícia Kubo Fontes, Marcelo Fabio Gouveia Nogueira, Charles Morphy Dias dos Santos, and Marcella Pecora Milazzotto

The study of key metabolic processes of the early embryo has been driven by the desire to define requirements for embryo growth and viability. A complimentary aim of such knowledge is related to the similarities between embryonic metabolic behaviors with other rapidly proliferating cells such as cancer and embryonic stem cells. This study was based on a factorial experimental design (2x2x3) created to evaluate glucose and oxidative metabolism patterns on embryos with distinct developmental kinetics. Fast (4 or more cells at 22 hours post insemination) and Slow embryos (2-3 cells) were produced in vitro using standard protocols and cultured in 20% or 5% O<sub>2</sub>, and also in distinct glucose concentrations (0, 2 and 5mM), resulting in 12 groups. Blastocysts were evaluated for 92 characters including 85 genes [control of gene expression (14 genes), lipid metabolism (16), energy metabolism (15), cell death (5), response to oxidative stress (17), other cellular functions (18)]; and 7 biochemical evidences: consumption of glucose, glutamate and pyruvate; production of lactate and ATP; generation of reactive oxygen species (ROS), mitochondrial activity and lipid content by mass spectrometry. Data were normalized and gathered in a matrix that was analyzed under parsimony, with 500 replicates and Tree-Bisection Reconnection as the swapping algorithm (TNT software). All characters were additive and equally weighted. This analysis resulted in a single optimal tree, fully resolved. Results show the groups arranging in two main clusters according to oxygen tension regardless of developmental kinetics and glucose, except the groups cultured in a hyperglycemic environment (5mM) that formed a separate cluster. Next, a correlation attribute evaluation (Weka software) was performed to highlight characters that contributed to differentiate the study groups. We found a total of 33 genes [control of gene expression (8); lipid metabolism (10); cell death (2); response to oxidative stress (10)] as being responsible for the differences between groups cultured in 20% vs. 5% O<sub>2</sub>. Biochemical analysis also showed increased consumption of pyruvate and production of ROS by the groups cultured in 20% O<sub>2</sub>, and together with gene expression data these findings possibly indicate an overall altered metabolism related to the elevated oxygen tension. Based on that information, the initial evidence matrix was divided isolating the oxygen tension. Upon isolation of 5% O<sub>2</sub> factor, which was then considered as a more physiological parameter, groups formed two clusters, this time according to developmental kinetics and independently of glucose concentration in culture media. Correlation of attributes was performed again, now regarding the features that are responsible for separation between fast and slow. Among the genes found with altered expression on these groups, 5 of them are involved with synthesis of fatty acids. In slow groups, the increased production of lactate and the augmented content of fatty acids corroborate our hypothesis that instead of resorting to  $\beta$ -oxidation, these embryos are deflecting energy metabolism towards aerobic glycolysis. Finally, we believe that the lower availability of glucose associated with hypoxic conditions offer the best conditions for fast-kinetics embryos to maintain a physiological metabolism, similar to an in vivo phenotype.

**Paternal High-Fat Diet Alters Metabolism Transgenerationally in Male but Not Female Descendants.** Anne-Sophie Pépin, Christine Lafleur, Vanessa Dumeaux, Deborah M. Sloboda, and Sarah Kimmins

BACKGROUND: There is increasing evidence that the paternal preconception environment can impact the development and health of offspring. However, the specific mechanisms involved in the epigenetic

inheritance of complex diseases remain elusive and the role of histone methylation in sperm in this phenomenon is unknown. We previously established using a transgenic mouse model, that histone methylation in sperm is implicated in transgenerational inheritance (Siklenka et al., 2015). Histone methylation in sperm is sensitive to diets that impact one carbon metabolism and are one means of transmitting paternal environmental information across generations. Using our existing mouse model of epigenetic inheritance that is characterized by a compromised sperm epigenome at the level of histone methylation, we aim to identify epigenetic signatures in sperm that are sensitive to paternal BMI. High-fat diets (HFD) associated with elevated BMI alter the methyl donor pool and have been implicated in metabolic disease transmission across generations. We hypothesize that descendants derived from a paternal line with an altered sperm epigenome will be more sensitized to the detrimental effects of an environmental challenge in the form of a HFD. **METHODS:** Transgenic mice with an altered sperm epigenome were challenged with a high-fat diet for two spermatogenic cycles. In brief, wild-type C57BL6NCrI control (n=14 and 17 per diet), KDM1A transgenic (n=15 and 17) and wild-type littermates (non-transgenic; n=13 and 17) male mice were fed either a low- or high-fat diet (10% and 60%kcal fat ad libitum, respectively) for 10-12 weeks from weaning. To confirm (pre)diabetic status, metabolic function was assessed by intraperitoneal glucose and insulin tolerance tests, and baseline glucose and insulin serum levels. Males were bred to 6-week-old C57BL6NCrI females to generate the F1 generation. F1 and F2 descendants were fed a control chow diet and tested for metabolic function at 5 months of age similar to their F0 sires. All females used for breeding, as well as F1 and F2 descendants, were fed a regular chow diet ad libitum. Male and female offspring were sacrificed at 6-8 months of age and data was analyzed by sex. Sperm was collected for chromatin immunoprecipitation sequencing (ChIP-seq) targeting histone methylation (n=5 per group) and livers were collected at necropsy for RNA sequencing (n=3-6 per group). **RESULTS:** After 10-12 weeks, males on a high-fat diet become obese, insulin resistant and glucose intolerant, with reduced fertility. Sex-specific effects were noted, where none of the female offspring and grand-offspring had altered metabolic response resulting from their (grand)paternal diet, nor genotype. In contrast, male offspring showed changes in their metabolic profile resulting from their father's high-fat diet. Interestingly, these metabolic profiles as well as sex-specific effects persisted in grandoffspring. Preliminary findings suggest the sperm epigenome may serve in the transmission of the next generations' metabolic phenotypes.

### **Frequency of Persistent Müllerian Duct Syndrome (PMDS) Mutations in the General Population.**

Alexandra S. E. Fontaine, Lidija K. Gorsic, and Margrit Urbanek

Persistent Müllerian Duct Syndrome (PMDS) is a rare disorder of male sex differentiation defined by incomplete regression of Müllerian ducts in genetic males (XY) with otherwise complete external virilization. PMDS is inherited as an autosomal recessive trait. Mutations in anti-Müllerian hormone (AMH) and its cognate type 2 receptor (AMHR2) account for ~80% of PMDS cases with roughly equal number of AMH and AMHR2 mutations. AMH is a member of the TGF $\beta$  peptide hormone superfamily. In fetal males, AMH causes regression of the Müllerian ducts preventing their differentiation into the uterus, fallopian tubes, and upper vagina. In adults, AMH inhibits testosterone production, and in women AMH impairs folliculogenesis. Through a genomic screen of women with polycystic ovary syndrome (PCOS), we identified 17 AMH coding mutations with reduced AMH signaling activity. Five of these variants have previously been identified in PMDS; however, in contrast to men with PMDS, PCOS women are heterozygote carriers of PMDS variants. The population prevalence of PCOS in the U.S. is 6-

10% for the NIH consensus criteria of hyperandrogenemia and oligomenorrhea/amenorrhea. The population prevalence of PMDS is unknown. To answer this question, we determined the population frequency of PMDS (homozygote and compound heterozygote carriers of AMH and/or AMHR2 mutations) and the frequency of heterozygous carriers of these mutations from the allele frequency of known PMDS variants (model of PCOS). We assembled a comprehensive list of PMDS mutations identified in AMH and AMHR2 from the literature and mapped those variants onto known genetic variants in dbSNP, a central public repository of genetic variation consisting of 324+ million human variants. Expected frequencies of homozygotes and compound heterozygotes (model of PMDS) and of heterozygote carriers (model of PCOS) of AMH and/or AMHR2 functional variants were calculated from allele frequencies of PMDS mutations in dbSNP. We identified 133 PMDS mutations (69 AMH; 64 AMHR2) in 217 PMDS cases (108 AMH, 109 AMHR2) and were able to assign dbSNP identifiers to 57 of these mutations (26 AMH; 30 AMHR2) accounting for 57% of PMDS cases. Population based allele frequencies from the 57 informative PMDS variants predict a homozygote/compound heterozygote frequency, in AMH and/or AMHR2 (PMDS model), of  $1.63 \times 10^{-5}$  or 5,312 individuals (2,656 males) in the U.S. (estimated 2017 population = 325,719,178). The frequency of heterozygote carriers (PCOS model) of PMDS variants was much higher (frequency = 0.0101; 1,255,169 women in the U.S.) illustrating how causal variants of even very rare recessive disorders can be very prevalent in the heterozygous state. These estimates are likely to be 2-4 fold underestimates of the true frequency of PMDS since 1) we only surveyed published PMDS mutations and therefore did not count undiagnosed and/or uncharacterized cases of PMDS, 2) we were not able to find dbSNP identifiers for ~50% of PMDS mutations, and 3) we do not account for the 20% of PMDS cases without AMH or AMHR2 variants. Using population frequencies of known PMDS mutations, we estimate the incidence of PMDS in the U.S. to be 2,600-10,000 and for AMH/AMHR2 mutations to impact 1-4% of women in the U.S.

**The Effect of Transplanting Germ-cell Depleted Ovaries on Post-Menopausal Health.** Tracy Habermehl, Kyleigh Tyler, McKenna Walters, Kate Parkinson, and Jeffrey Mason

At a young age, females have a measurable health advantage over males. Once women go through menopause, their ovaries become senescent and the risk of health-related diseases increases tremendously. Reproduction has an established influence on health. Our research manipulates reproductive influence to improve the life and health span of aged mice. The transplantation of young, intact ovaries to aged mice showed a tremendous increase in life span. Germ cell depleted ovaries that were transplanted into these geriatric mice had an increase in their life and health span further. We believe that the communication and reprogramming of the somatic cells by the germ cells allows the ovaries to support the organism and increase health. Three different age groups are being used as the controls; aged – 850 days old (n=5), middle-aged – currently 600 days old (age matched controls) n=6, and young – currently 250 days old (n=6). All of which have their original ovaries. The treated group (currently 600 days old) contains 1) middle-aged mice with young transplanted ovaries that contain both germ and somatic cells (n=9) and 2) middle-aged mice with young transplanted ovaries that have been germ cell depleted (no germ cells) n=10. Each mouse is currently going through several health span assays associated with several post-menopausal parameters that decline with age. Data will be analyzed with two-factor ANOVA and a Tukey-Kramer post-hoc test will be used to determine difference between groups. We expect to see changes in metabolism, immunity, musculoskeletal, cardiovascular and cognition between germ cell containing and germ cell depleted ovary recipient mice as well as their

relation to non-transplanted mice of different age groups. The reasoning behind the suggested expectations arise from enhancement of health in germ cell depleted primitive species. The upregulation of Foxo signaling and the preservation of the somatic cells are causative of the improvement of health in those organisms. The Foxo gene plays a role in several cellular pathways, and at the absence of the germ line, Foxo upregulates the pathways needed for survival, improving health in primitive organisms. Therefore, with the absence of the germ cells in the ovaries, Foxo signaling should help to improve those aspects of health influenced by aging. The young germ cell depleted ovaries are hypothesized to increase and return the health of all mentioned aspects compared to young, non-transplanted mice, reflecting the age of the transplanted ovary and not the chronological age of the mouse. Understanding and utilizing the reprogramming and communication between the somatic and germ cells is hoped to restore and improve the health aspects of post-menopausal human women in the future.

**Paternal Folate Deficiency Increases Birth Defect Severity in Offspring Sired by Mice with an Altered Sperm Epigenome.** Ariane Lismer, Christine Lafleur, Keith Siklenka, Vanessa Dumeaux, Romain Lambrot, and Sarah Kimmins

**BACKGROUND:** Every year worldwide, birth defects affect more than 8.14 million infants and are responsible for the death of 303 000 children aged four weeks and under (WHO, 2016). A father's environmental exposures (e.g toxicants and poor diet) can influence disease transmission across generations, potentially through epigenetic inheritance (Lambrot et al., 2015). However, the mechanisms involved in such paternal transmission remain unclear, and whether there can be additive effects on the sperm epigenome is unknown. **HYPOTHESIS:** Environmental stressors alter the sperm epigenome at the level of histone methylation and there can be enhanced effects in cases of pre-existing epigenome damage. **METHODS:** We used a transgenic (TG) mouse model that overexpresses the lysine-specific histone demethylase KDM1A in developing sperm, resulting in an altered sperm epigenome. To elucidate whether there can be cumulative effects of an environmental stressor, adult TG sires with an altered sperm epigenome, or control mice with a normal sperm epigenome, were fed a folate deficient (FD, 0.3 mg/kg) or folate sufficient (FS, 2.0 mg/kg) diet beginning at weaning for a full spermatogenic cycle. The male mice were then bred to control females fed regular chow. A quantitative skeletal analysis was conducted on embryonic day 18.5 mice (n = 2 per litter, with 7 – 10 litters per group) to assess for abnormalities in offspring. To quantify the effect of the FD diet and identify susceptible regions on the sperm epigenome, ChIP-sequencing targeting H3K4me3 was performed (n = 5) followed by analysis using the Bioconductor package csaw (Lun et al., 2016). **RESULTS:** Skeletal analysis at embryonic day E18.5 revealed a significant increase in severe abnormalities in the offspring sired by FD TG. These abnormalities included craniofacial and spinal defects as well as pronounced developmental delays. In addition, preliminary analysis suggests that sires on the FD diet have altered H3K4me3 enrichment in the sperm. **CONCLUSION:** The increased incidence of severe abnormalities in the offspring of TG mice fed a FD diet and the differential H3K4me3 enrichment in the sperm suggest that environmental stressors may act cumulatively to provoke detrimental effects in offspring. These findings may be relevant when considering whether there can be multiple and lasting impacts of environmental stressors.

**Sperm Quality is Affected in Rabbit and Mouse After Exposure to Low Doses of TCDD.** Heba Yehia Anwar Elsayed, Esvieta Tenorio-Borroto, and Nazario Pescador

In the last decade the harm use of dioxin has been demonstrated on the human health and the whole environment. It is well known among scientists as 2, 3, 7, 8-Tetrachloro dibenzo-p-dioxin (TCDD), an endocrine-disrupting environmental pollutant. The aim of the present study was to evaluate the toxicity effect of TCDD on New Zealand male rabbits and CD1 male mice. Three concentrations of TCDD were tested and the effects on sperm cells were assessed at one experimental time points. As bioindicators of TCDD toxicity, a comprehensive analysis of several sperm parameters including motility, vitality, count, morphology and viability were performed, the oral gavage was used to administrate TCDD. Neither mortality or clinical signs of over toxicity were observed in both mice and rabbit. All surviving mice and rabbit showed no differences in reproductive organ weight. The results showed remarkable differences on sperm count (concentrate), percentage of dead sperm, normal morphology, sperm abnormality, and sperm motility between control and treated groups (in both mice and rabbits). Percentages of sperm count and normal sperm morphology were decreased significantly ( $P < 0.05$ ) by 20.6% and 13.4% respectively in exposed mice compared to control. TCDD exposure induced significant changes in sperm motility after 10 days of administration with a significant decrease in the percentage of progressive sperm in mice and rabbit exposed to 1.5  $\mu\text{g}/\text{kgBW}$  and, simultaneously, an increase in the percentage of immotile sperm ( $p < 0.05$ ). For rabbits, a significant decrease in the concentration of sperm cells was found between the control and treated groups ( $p = 0.000$ ) with 18%. We concluded that TCDD affect significantly the spermatozoa motility, morphology and vitality in rabbits and mice.

**Polycystic Ovary Syndrome (PCOS) Associated Functional Rare Variants in the Anti-Müllerian Hormone Pathway.** Margrit Urbanek, Richard S. Legro, M. Geoffrey Hayes, and Lidija K. Gorsic

Polycystic Ovary Syndrome (PCOS) is responsible for the majority of anovulatory infertility cases among women of reproductive age. PCOS is a highly heritable, common endocrine disorder characterized by hyperandrogenism, irregular menses and polycystic ovaries. PCOS is often accompanied by elevated levels of anti-Müllerian hormone (AMH). In the ovary AMH inhibits follicle maturation thus the elevated AMH levels observed in women with PCOS are consistent with the observed arrested folliculogenesis. AMH also inhibits steroidogenesis through transcriptional repression of CYP17a1, which encodes a rate limiting enzyme in steroidogenesis, thus predicting a loss of function of AMH in PCOS, a phenotype of androgen excess. We recently identified 16 rare PCOS-specific pathogenic variants in AMH. All of the variants with altered function were loss of function variants that reduced downstream signaling in vitro (1). We, thus, hypothesized that impaired AMH signaling results in the loss of AMH inhibition on steroidogenesis leading to hyperandrogenemia, a cardinal trait of PCOS. Here, we solidify this hypothesis by expanding our variant analyses the coding region of the AMH-specific type 2 receptor, AMHR2, and potential regulatory regions in AMH and AMHR2. We sequenced the genomic region plus 5 kb upstream and downstream of the AMH and AMHR2 genes in 604 PCOS women and 125 reproductively normal controls. Thirteen PCOS-specific noncoding variants were identified in the 5' UTR and within introns of AMH. Four noncoding AMH variants were not PCOS specific. AMHR2 analyses identified 2 missense variants; 1 PCOS-specific (P30S) and 1 non-PCOS specific that was found in cases and controls (R548Q). Additionally, 53 noncoding variants were identified upstream and within introns of AMHR2 in women with PCOS, while only 5 such variants were found in cases and controls. Four

PCOS-specific and 1 non-PCOS specific variants in the AMH 5' UTR as well as 3 of the PCOS-specific and 1 non-PCOS specific variants upstream of AMHR2 that mapped to genomic regions enriched for epigenetic marks and transcription binding sites were tested for regulatory activity in a dual luciferase assay in Chinese hamster ovary cells. PCOS-specific variants all showed a significant decrease in luciferase activity, while the non-PCOS specific variants had similar regulatory activity as the reference sequence. Missense AMHR2 variant (P30S) found in 1 PCOS case showed impaired AMH signaling, while R548Q found in PCOS and reproductively normal women retained wild-type signaling. In this study, we identified PCOS-associated loss of function variants in AMHR2 and thus expanded the repertoire of genes in the AMH signaling pathway that are mutated in PCOS. These data provide further evidence for an important role for the AMH signaling cascade in steroidogenesis in PCOS. Sources of Research Support: NIH Grants T32 DK007169, RO1 HD057450, P50 HD044405, RO1 HD056510

**Introduction of Novel Female and Male Urine Pheromones Alters Estrous Cycle Length and Synchronizes Estrous Cycles in Captive Female Red River Hogs (*Potamochoerus porcus*) in North American Zoos.** Camille Goblet, Bryce Lewis, Monica Jarboe, Dameriss Silva, Linda Penfold, and Annie Newell-Fugate

Captive red river hogs (RRH) have variable reproductive success yet the potential causes are unknown. We hypothesized that introduction of novel pheromones to nonbreeding male-female pairs of RRH or harem groups of female RRH would improve estrous cyclicity. Estrous cycles and progesterone (P4) concentrations were compared between: 1) same sex housed females (harem (H); n=3); 2) proven-breeder females (control (C); n=3); 3) poor-breeder females repaired with new males (novel male (NM); n=4); 4) poor-breeder females exposed to novel pheromones (novel pheromone (NP); n=3). Fecal samples were collected 3-5 times per week for a year. NP Females had baseline sampling (6 months), followed by a 2.5 month exposure to sow urine, a 2-4 week wash-out, and a 2.5 month exposure to boar urine. Dried fecals were extracted with a 90% ethanol by boiling method and resuspended in an initial 1:10 dilution of ethanol and buffer followed by dilution 1:1000 (C, NM, NP) or 1:3000 (H) in buffer. Average extraction efficiency was over 99%. Extracts were assayed with a P4 mono-clonal ELISA (ISWE mini-kit, Arbor Assays, Ann Arbor, MI). Extracts from H females were assayed with a P4 poly-clonal ELISA (R4859, Coralie Munro). Luteal cycles were considered periods when a peak in P4 concentration was discerned graphically. Results were assessed for normality with PROC GLM (SAS, Cary, N.C.) and non-normal data was transformed prior to analysis with repeated measures ANOVA (P4) or ANOVA (cycles) with a level of significance  $\alpha=0.05$ . Introduction of male pheromones in H females shortened estrous cycle length ( $p < 0.05$ ) and synchronized estrous cycles amongst females. However, in NP females paired with males, there was a trend for estrous cycle length to elongate in response to male pheromones (NP baseline:  $15.7 \pm 1.5$  days; NP post-male:  $19.3 \pm 3.1$  days;  $p = 0.07$ ). Baseline and post-male pheromone estrous cycle lengths in H females were longer than C, NM or NP females ( $p < 0.05$ ). Pregnancies occurred in 2/3 C, 1/4 NM and 0/3 NP females. Pseudopregnancy was noted in 1/3 C and 2/4 NM females. Average gestation length was  $112.8 \pm 5.4$  days (range: 107-120 days; n=4) and average pseudopregnancy length was  $56.7 \pm 15.5$  days (range: 44-74 days; n=3). Average P4 concentration for pregnant C females was over double that for pregnant NM females (C:  $16908.0 \pm 429.0$  ng/g feces; NM:  $7114.6 \pm 618.3$  ng/g feces;  $p < 0.0001$ ). Overall luteal phase P4 concentration was highest in the C females and lowest in the NM females (C:  $9343.7 \pm 360.0$  ng/g feces; NP:  $6213.6 \pm 509.1$  ng/g feces; NM:  $3756.0 \pm 362.7$  ng/g feces;  $p < 0.0001$ ). An interaction between season and treatment group ( $p < 0$

.0001) and acyclicity of females July-November irrespective of group suggest that season may confound our results. Additionally, females housed with pregnant females were either acyclic or pseudopregnant, indicating reproductive suppression may occur in female RRH. In conclusion, urine-derived pheromones may be a cost-effective and efficient means to manipulate estrous cycling in captive RRH. Careful consideration of the number of female RRH in a captive herd is warranted to avoid reproductive suppression unless desired.

**Evaluation of Functional Placenta Capacity via Metabolome Analysis of Fatty Acid Contents and Related Proteins Expression in Mice.** Jong Geol Lee, Globinna Kim, Hyun Ju Yoo, Sang-Yoon Nam, and In-Jeoung Baek

Placenta is an essential organ for survival and growth of the fetus during pregnancy, allowing metabolic component and gas exchange between fetal and maternal circulation. Many studies have been carried out using mice, especially genetically engineered mice (GEM), to find essential genes for placental development. The primitive structure of the mouse placenta is formed at embryonic day (E) 9.0~9.5. It is known that placenta becomes functional around E11.5 (Wu et al., 2003; Nature) when it begins nutrient transport from maternal to fetal side. However, until now, the placental transport function before E11.5 has not been elucidated although nutrient need for embryo development is continuously increasing from initial placenta formation. To confirm the exact functional period of mouse placenta, we investigated the expression of several fatty acid (FA) transport related proteins, such as FA binding protein 3 (Fabp3), Fabp4, FA transport protein 4 (Fatp4), and Fatp6 in the embryo and placenta, respectively. Their mRNA and protein expression in placenta increased generally in a time-dependent manner during embryogenesis (E9.5~18.5). Among them, Fabp3, Fabp4, and Fatp4 were exclusively expressed in the embryo-derived labyrinth fetal endothelial cells, and Fatp6 was expressed in the maternal endothelial cells. Next, through applying gas chromatography coupled with mass spectrometry (GC-MS), we measured embryonic and placental FA contents including essential FA (EFA), because embryonic EFA should be derived from mother and thus can be a useful marker for placental nutrient transport activity. EFAs such as arachidonic acid (AA), linoleic acid (LA), and docosahexaenoic acid (DHA), which are known to accumulate in embryos after mid-gestation period, were detected at E9.5~10.5. All FAs were accumulated in embryo and placenta in a time-dependent manner with its embryonic demands. Here, we revealed when and how placenta becomes functional during pregnancy, on the basis of its capacity of FA transport, and further intended to establish the functional phenotyping platform of placenta in mice. This study will be useful for placenta biology field by providing a practical phenotyping strategy for GEM models.

**Three-dimensional System Applied to In Vitro Maturation of Bovine Oocytes.** Ricarda Santos, Luísa Miglio, Amanda Nonato, Luana Felix Rosa, Deize de Cássia Antonino, Mayara Mafra Soares, Benner Geraldo Alves, Marcelo Emílio Beletti, and Kele Amaral Alves

The in vitro embryo production (PIVE) process is usually made in a conventional two-dimensional (2D) system. On this system, the oocytes adhere to the plate's bottom, which can modify the oocyte morphology and limit the contact with nutrients in the medium. Three-dimensional (3D) culture systems using nanoparticles and magnetic levitation have been used in vitro in different cell types allowing

greater cell-cell interaction, synthesis, and cell viability. The purpose of this study was to evaluate the effect of culture systems (2D vs. 3D) during the in vitro maturation of bovine oocytes with different degrees of quality (good quality vs. bad quality) on the cleavage and blastocysts rates. The oocytes (G1, excellent quality) and G3 (bad quality and discarded in standard routines) were randomly distributed in conventional (2D) and three-dimensional (3D) culture systems with concentrations of 50 and 75  $\mu\text{l}$  of nanoparticles, forming four groups: G1-2D, G3-2D, G1-3D 50, G3-3D 50, G1 3D 75 and G3 3D 75. Then, the oocytes were submitted to maturation (22 hours), fertilization (18 hours) and in vitro culture in an incubator with 5% CO<sub>2</sub>, 38.5 ° C and saturated humidity. The cleavage and blastocyst rates were evaluated 48 hours and seven days after in vitro fertilization respectively. The data were analyzed by the chi-square test with Yates correction and the results considered significant when  $P < 0.05$ ) to the G1-2D and G1-3D groups. Additionally, the rate of blastocysts of G3 3D 75 group was similar to the G1 2D and G1 3D 50 groups. In this way, we demonstrated that the use of the three-dimensional system during in vitro maturation increased the rate of cleavage of inferior bovine oocytes, optimizing their use during PIVE routines.

**Protein Kinase A and AMP-dependent Protein Kinase Signaling Pathways Regulate Steroidogenesis via Opposite Effects on Hormone Sensitive Lipase (HSL) Activity in the Bovine Corpus Luteum.** Emilia Przygodzka, Xiaoying Hou, Michele Plewes, Pan Zhang, Heather Talbot, and John S. Davis

Luteinizing hormone (LH) triggers ovulation and formation of the corpus luteum (CL), which arises from the differentiation of follicular granulosa and theca cells into large and small luteal cells, respectively. The small and large luteal cells produce progesterone, a steroid hormone required for establishment and maintenance of pregnancy. During CL development the large luteal cells acquire sensitivity to the luteolytic action of prostaglandin F<sub>2</sub> $\alpha$  (PGF), a uterine derived hormone that initiates a cascade of events that results in a reduction in progesterone synthesis and the demise of the CL. There is growing body of evidence showing the presence and importance of cytoplasmic lipid droplets (LDs) for appropriate secretory function of the CL. These lipid-rich intracellular organelles store cholesteryl esters which are hydrolyzed by hormone sensitive lipase (HSL, also known as LIPE) releasing cholesterol, the main substrate necessary for progesterone (P<sub>4</sub>) synthesis. Metabolic requirements control lipolysis in adipocytes by phosphorylation of HSL; it is well-documented in adipocytes that protein kinase A (PKA) stimulates HSL via phosphorylation on Ser563 and AMP-activated protein kinase (AMPK) inhibits HSL activity via phosphorylation on Ser565. However, there is scant data on regulation of HSL in bovine luteal cells. Therefore, we hypothesized that regulation of HSL, either by LH (via PKA) or PGF (via AMPK) may control steroidogenesis in bovine luteal cells. To test this hypothesis large (LLC) and small luteal cells (SLC) isolated from mature CL (n=3-5) were cultured in the presence of medium (control), PGF (100 nM), AICAR (1 mM; AMPK activator), LH (10 and 100 ng/ml), forskolin (10  $\mu\text{M}$ ; PKA activator) and LH+AICAR. After 2, 10, 30 minutes and 4 hrs cells and media were collected in order to determine phosphorylation of AMPK (Ser485 and Thr172) as well as HSL (Ser565 and Ser563) and P<sub>4</sub> concentration, respectively. Treatment of SLC with LH or forskolin increased phosphorylation of HSL (Ser563) and P<sub>4</sub>, and reduced activation of AMPK (reduced Thr172 phosphorylation). Treatment of SLC with AICAR to activate AMPK reduced LH-stimulated HSL (Ser563) phosphorylation and P<sub>4</sub>. Treatment of LLC with PGF or AICAR increased AMPK phosphorylation at Ser485 and Thr172 residues as well as phosphorylation of HSL (Ser565) indicating inhibition of HSL. In contrast, treatment of LLC with LH and forskolin reduced phosphorylation of AMPK at position Thr172, increased HSL phosphorylation at Ser563, and enhanced

P4 production. Pretreatment of LLC with AICAR activated AMPK and reduced the stimulatory effect of LH on HSL (Ser563) phosphorylation as well as P4 secretion. The data indicate that LH stimulates the activity of HSL via increased PKA-mediated phosphorylation of HSL and/or reduced activity of AMPK. In contrast, PGF and AICAR stimulate AMPK activity and inhibit HSL. The findings suggest that a lack of luteotrophic support by LH may permit the luteolytic actions of PGF via AMPK activation to inhibit HSL activity and consequently reduce the steroidogenic capacity of luteal cells.

Supported by NIFA USDA grant no. 2017-67015-26450, VA and NIH R01 HD092263.

**Cyclicity Phenotype and Ovarian Cortex Androgen Secretion in Androgen Excess Cows are Predictive of Plasma Steroid and Lipids, Liver Enzymes and Follicular Fluid Cytokines.** Mariah L. Hart, Mohamed A. Abedal-Majed, Renata Spuri-Gomes, Alexandria P. Snider, Scott G. Kurz, Jeff W. Bergman, Renee M. McFee, Carol A. Casey, Caleb O. Lemley, Robert A. Cushman, John S. Davis, Jennifer R. Wood, and Andrea S. Cupp

We have identified a population of cows that produce excess androstenedione (A4; High A4; >40 ng/ml A4; control < 20 ng/ml A4) in follicular fluid of the dominant follicle, secrete excess A4 (43-fold higher) in ovarian cortex cultures, display irregular cyclicity, are often anovulatory, and have reduced fertility. We hypothesized that High A4 cows secreting greater A4 in ovarian cortex cultures would have altered hormone metabolism, plasma hormones, lipids, and greater pro-inflammatory cytokines in follicular fluid compared to controls. Cows (n=17) were synchronized to induce a new follicular wave. Follicle development was monitored and blood collected. Ovariectomies were performed 36-42 hours after PGF2a, and ovarian cortex cultures and liver biopsies were conducted to measure A4 concentrations in media and to determine liver enzyme activity, respectively. High A4 cows were further categorized into: High A4-Irregular, or High A4-Ovulatory based on whether they ovulated or were anovulatory/stimulated to ovulate. High A4-Ovulatory and High A4-Irregular cows produced greater amounts of A4 in the first 3 days of cortex culture when compared to controls (High A4-Ovulatory vs. Controls,  $P < 0.005$ , 72.0-fold increase; High A4-Irregular vs. Controls,  $P < 0.02$ , 53.0-fold increase). High A4-Ovulatory cows tended ( $P < 0.10$ ) to have decreased circulating 17- $\beta$  estradiol (E2; 2.0-fold) compared to controls. There was a tendency ( $P < 0.10$ ;  $R = -0.67$ ;  $R^2 = 0.45$ ) for decreased activity of hepatic P450 3A (RLU/min/mg protein; metabolizes E2) as cortex culture A4 increased. There was a relationship for increased activity ( $P < 0.05$ ;  $R = 0.78$ ;  $R^2 = 0.60$ ) of hepatic P450 2C (RLU/min/mg protein; metabolizes P4) as cortex culture A4 concentrations increased. Circulating triglycerides tended (TG;  $P < 0.06$ ;  $R = -0.60$ ;  $R^2 = 0.36$ ) to decrease as cortex culture A4 concentrations increased. To elucidate differences in pro-inflammatory cytokines and chemokines, we evaluated follicular fluid from cows (High A4: n = 15; Control: n = 15). CXCL9 ( $P < 0.05$ ;  $R = 0.37$ ;  $R^2 = 0.14$ ) concentrations decreased and CXCL10 concentrations tended (pg/ml;  $P < 0.08$ ;  $R = -0.33$ ;  $R^2 = 0.11$ ) to decrease as cortex culture A4 concentrations increased. CD40L ( $P < 0.04$ ;  $R = 0.40$ ;  $R^2 = 0.16$ ) and IL-17A ( $P < 0.04$ ;  $R = 0.38$ ;  $R^2 = 0.15$ ) concentrations increased as cortex culture A4 concentrations increased. These data indicate that amount of A4 secreted from the ovarian cortex can predict differences in liver steroid inactivation enzymes and circulating TGs. Whether High A4 cows are ovulatory or have irregular cyclicity may predict alterations in E2. Furthermore, correlations with chemokines and cytokines and culture A4 suggest that there are alterations in pro-inflammatory cytokines and chemokines as concentrations of A4 increase, which may affect altered cyclicity. Thus, the amount of A4 secreted into media correlates with plasma

metabolites, steroid hormone concentrations, hepatic inactivation enzymes, TGs, and inflammatory markers may contribute to the ovulatory status and infertile phenotype of High A4 cows. This research was funded through USDA grant 2013-67015-20965. USDA is equal opportunity provider and employer.

**Control Mechanisms of Chromosome Segregation in Female Meiosis I.** Martin Anger, Kovacovicova Kristina, Lenka Radonova, Michal Skultety, Michael Hopkins, and Bela Novak

Mammalian oocytes and also embryos are frequently affected by aneuploidy arising during chromosome segregation. The reason why chromosome segregation errors are more frequent in these cells in comparison to somatic cells is still not completely understood. Using micromanipulation and live cell confocal imaging we monitored the activity of Spindle Assembly Checkpoint (SAC) on individual kinetochores and whole cell activity of Anaphase Promoting Complex (APC) and correlated these with chromosome positions, spindle formation and polar body extrusion simultaneously in individual cells progressing through the first meiotic division and approaching anaphase I. Our results show similarities between oocytes and somatic cells in relationship between SAC and APC activity as well as important and unexpected differences. Apart from other valuable insights into function of these two mechanisms in mammalian oocytes, our results also provided quantitative overview of SAC and APC activity in physiological situations as well as in situations when spindle apparatus is assembled improperly. Our results revealed that the checkpoint mechanisms involved in monitoring chromosome segregation and the pathways controlling anaphase entry in oocytes show remarkable functional differences in comparison to their function in somatic cells. This difference might contribute to the high incidence of aneuploidy in these cells. This work was supported by Czech Science Foundation Projects 17-20405S and by the Ministry of Education, Youth, and Sports of the Czech Republic under the project CEITEC 2020 (LQ1601). We acknowledge the core facility Cellular Imaging supported by the MEYS CR (LM2015062 Czech-BioImaging).

**Obese Females Fed a High Fat Diet Containing Virgin Coconut Oil Have Improved Glucose Tolerance and Ovarian Folliculogenesis Despite Visceral Adiposity.** Annie E. Newell-Fugate, Luke Browning, Cassandra Skenandore, Daniel Hernandez, and Camille Goblet

Forty percent of American women are obese, increasing their risk for type II diabetes and infertility. Obesity affects ovarian function and fertility as obese women tend to have poorer response to IVF than lean women due to decreased ovulation rates and difficulty with ovulation induction. Coconut oil improves glucose homeostasis in lean individuals, but few reports have examined its effects in obesity and it is unknown if or how it affects ovarian function. We hypothesized that female Ossabaw pigs fed a high fat diet with 5% virgin coconut oil would exhibit improved glucose homeostasis and ovarian folliculogenesis compared to female Ossabaw pigs fed a high fat diet with 5% lard. We fed female Ossabaw pigs 2200 kcal of control (C; n=6), 6000 kcal of lard high fat (WSD; n=5), or 6000 kcal of coconut oil high fat (COC; n=6) diets for 9 estrous cycles. Fasting blood and ovarian ultrasound images were collected on days 1, 4, 8, 12, 16, 18 and 20 for baseline (C 0), cycle 7 (C 7) and cycle 9 (C 9) and on days 1 and 8 for other cycles. Following C 0, females were transitioned to diets over an estrous cycle (C T). An intravenous glucose tolerance test (IVGTT) was performed after C 7. Females were heat checked daily. Weights and morphometric measurements were taken weekly. Each animal was used as its own control,

comparing baseline to diet-induced parameters within treatment. Data were assessed for normality and transformed if non-normal followed by repeated measures ANOVA (SAS, Cary, NC). WSD females demonstrated an increased estrous cycle length in response to diet (C initial:  $19.3 \pm 0.3$  days; C final:  $19.9 \pm 0.5$  days; WSD initial:  $21.2 \pm 0.3$  days; WSD final:  $22.1 \pm 0.4$ ; COC initial:  $20.4 \pm 0.3$  days; COC final:  $20.6 \pm 0.4$  days;  $p = 0.05$ ). In response to diet, COC females demonstrated increased numbers of ovulatory sized follicles on cycle day 1 (C initial D1:  $6.8 \pm 0.8$  follicles; C final D1:  $6.5 \pm 0.5$  follicles; WSD initial D1:  $6.0 \pm 0.7$  follicles; WSD final D1:  $7.7 \pm 0.4$  follicles; COC initial D1:  $5.5 \pm 0.7$  follicles; COC final D1:  $8.9 \pm 0.4$  follicles;  $p = 0.0009$ ). During the IVGTT, C and COC females had similar glucose tolerance, whereas WSD pigs had higher glucose concentrations than the other groups until 40 minutes post-bolus ( $p < 0.02$ ). In response to diet, C and COC females demonstrated no difference in fasting blood glucose whereas WSD females developed increased fasting blood glucose (C initial:  $56.4 \pm 1.8$  mg/dL; C final:  $56.4 \pm 1.3$  mg/dL; WSD initial:  $55.7 \pm 1.6$  mg/dL; WSD final:  $68.4 \pm 1.1$  mg/dL; COC initial:  $66.1 \pm 1.4$  mg/dL; COC final:  $66.9 \pm 1.1$  mg/dL;  $p < 0.0001$  for WSD). WSD and COC females were both obese with similar weights ( $p = 0.53$ ) and abdominal girths ( $p = 0.2$ ) after diet induction. However, COC females had the largest thoracic girth ( $p = 0.003$ ). These data suggest coconut oil can improve glucose homeostasis and possibly stimulate ovarian folliculogenesis in obese females with visceral adiposity.

**Androgens Impact Theca and Stromal Cell Functions: New Targets That Contribute to Ovarian Dysfunction in Androgen Excess.** Nicholes R. Candelaria, Yi A. Ren, Achuth Padmanabhan, Fabio Stossi, Katharine E. Shelley, and JoAnne S. Richards

Following the organization of the theca cell layer in primary follicles, theca cell production of androgens is regulated not only by pituitary LH but also by the paracrine actions of intra-follicular factors, including estradiol, activin and IGF1 (Young & McNeilly, 2010). Remarkably, disruption of the androgen receptor (Ar) selectively in theca cells does not impair normal fertility or ovarian functions in mice but does prevent a PCOS-like phenotype promoted by excess androgens in a mouse model (Ma et al., 2017). These results suggest that AR is functional in theca cells and contributes to ovarian functions in the presence of androgen excess. Our studies were undertaken to determine the molecular and cellular events that are altered in theca and stromal cells compared to granulosa cells in mice exposed to androgen excess, using the non-aromatizable androgen DHT. Standard molecular and cellular techniques, genome-wide microarray studies, quantitative PCR, western blotting, immunohistochemistry (IHC) and immunofluorescence imaging were utilized to analyze ovarian cell functions prior to and at 1 week and 2 months post-DHT treatment. Females treated for two months develop both cystic and hemorrhagic follicles, recapitulating major facets of human PCOS patients and other mouse models. Changes in ovarian morphology and function were not only observed in follicles, but also in the theca and stromal compartments, the latter of which became hyperplastic. IHC staining showed clear nuclear staining of AR in stromal cells of androgen-treated mice compared to cytoplasmic staining in control mice, indicating they are androgen-responsive. To better understand the changes to the ovarian stroma, we analyzed the IHC staining of the mesenchymal marker vimentin and showed that its levels are reduced and appear more diffuse in androgen treated mice. Subsequent inspection of the stroma cells revealed the accumulation of lipid, an observation confirmed by oil red O, suggesting that pathological ovarian states associated with hyperandrogenic states are linked with substantial stromal changes. Genome-wide microarray analyses documented marked changes in the transcriptome of granulosa cells confirming increased levels of Fshr, a major regulator of granulosa endocrine function

and known androgen target in granulosa cells. Particularly striking was the increased expression of vascular cell adhesion molecule 1 (Vcam1), which we demonstrate is expressed in the theca of growing follicles. VCAM1+ cells are found outside of the theca layer, spread throughout the interstitial stroma of the androgen-treated mice. Theca-specific depletion of AR abrogates DHT-mediated induction of VCAM1 mRNA, demonstrating that androgens (DHT) transmit a signal to upregulate VCAM1 expression through AR. Elevated VCAM1 in the stroma suggests that androgens, via AR, lead to the expansion of theca cells and/or the stimulation of theca-like stem cells within the stroma. Although VCAM1 is most often associated with endothelial cells and the attachment of immune cells, its high levels in the stroma of DHT-treated mice and in adult Leydig cells indicate that there may be other functions for VCAM1 in the reproductive tissues, including the gonads.

**A New Model for Investigating the Processes Leading to Formation of the Ovarian Reserve: The Naked Mole-Rat.** Ned J. Place, Miguel A. Brieño-Enriquez, Paula E. Cohen, Jacob T. Sinopoli, Diana J. Laird, and Melissa M. Holmes

Although mice are the most widely studied mammalian model, their comparatively short lifespan limits their relevance to human biology. Reproductive lifespan in women is ~38 years compared to 1-2 years in mice. By contrast, the Naked Mole-Rat (NMR) lives up to 35 years and females can reproduce throughout their adult lives. Owing to its protracted fertility and small body size, we sought to establish the NMR as a model for investigating the establishment and maintenance of the ovarian reserve. Reproductive lifespan is determined by the size of the ovarian reserve, which is established in the fetus and subsequently eroded by the atresia of oocytes at two points of development: the transition from mitosis to meiosis and the formation of primordial follicles. Whereas these transitions occur synchronously in mice, germ cell development within the human fetal ovary is highly asynchronous, in that oogonial mitosis, the initiation of meiosis and the formation of primordial follicles occur concurrently for several weeks during mid-gestation. Our studies indicate that germ cell development is asynchronous in NMRs, and key developmental processes associated with the establishment of the ovarian reserve occur postnatally, rather than in the fetus as in mice. Surprisingly, NMR ovaries harbor an unusually large number of germ cells at postnatal day 8 (P8), with the vast majority still found in nests and a paucity of primordial follicles. Whereas some P8 germ cells have initiated meiosis, a substantial proportion appear to be pre-meiotic by their expression of pluripotency markers OCT4 and SOX2, and some germ cells along the periphery are immuno-reactive for phosphorylated histone H3, which suggests oogonial mitosis is still occurring. Asynchronous germ cell development persists at NMR P28, with the coexistence of primary follicles, primordial follicles, meiotic and pre-meiotic germ cells. Our preliminary results indicate a scarcity of germ cell apoptosis in NMR ovaries during the initiation of meiosis and during primordial follicle formation, and understanding how germ cell atresia is largely avoided in NMRs could lead to insights on how to protect the ovarian reserve in humans. Overall, the similarities to human germ cell development and long reproductive lifespan make the NMR an ideal laboratory model system for studying the processes that lead to variations in the size of the ovarian reserve in long-lived species like ourselves.

**Sperm Chromatin Structure and Bull Fertility are Influenced by Sperm Histone 4.** Muhammet Rasit Ugur, Naseer Ahmad Kutchy, Erika Bezerra de Menezes, Asma Ul Husna, Abdullah Kaya, Arlindo Moura, and Erdogan Memili

Bull fertility, ability of the sperm to fertilize and activate the egg and support embryo development is vital for cattle reproduction and production. It is known that chromatin remodeling during spermatogenesis results in dynamic changes in sperm chromatin structure through DNA methylation and post-translational modifications (PTM) of sperm histones, which are important for regulation of gene expression. However, amounts of sperm Histone 4 (H4), its acetylated form (H4ac), and to what extent these molecular attributes influence sperm chromatin structure and bull fertility are unknown. These gaps in the knowledge base are important because they are preventing advances in the fundamental science of bovine male gamete and improvement of bull fertility. The objective of the current study was to test the hypothesis that expression dynamics as well as PTM of sperm H4 are associated with bull fertility. Flow cytometry was utilized to quantify H4 and H4ac in sperm from seven high and seven low fertility Holstein bulls. The experiments were repeated three times, and 100,000 spermatozoa/bull were analyzed. The results indicated that the average number of cells with H4 or H4ac expression in high and low fertility bull spermatozoa were  $34.6 \pm 20.4$ ,  $1.88 \pm 1.8$ ,  $15.2 \pm 20.8$ , and  $1.4 \pm 1.2$  respectively. These values, however, were not different ( $p > 0.05$ ). However, combined amounts of cells with of H4 and H4ac were different between high and low fertility groups ( $3.5 \pm 0.6$ ;  $1.8 \pm 0.8$ ;  $P = 0.04$ ). Expression levels of H4 were measured by immunocytochemistry and Western blotting (WB) in sperm from three high and three low fertility bulls. Immunocytochemistry demonstrated that both acetylated and methylated H4 were equally distributed in the sperm head of high and low fertility sires. The results of the WB experiments showed that H4 was detectable in low and high fertile bull spermatozoa. The expression of both H4 and H4ac were not different in high and low fertility bull spermatozoa ( $p > 0.05$ ). Moreover, in high fertility group, H4 intensity was inversely related to bull fertility. In low fertility bulls, as fertility increased, H4 expression levels tended to increase. The results are significant because findings help advance fundamental science of mammalian early development and reproductive biotechnology.

**OptiXcell is a Comparable Animal Protein-Free Alternative to Egg-Yolk Based Extender for Rhinoceros Semen Cryopreservation.** Jessye Wojtusik, Monica A. Stoops, and Terri L. Roth

The effective use of egg-yolk in rhinoceros semen extenders to protect against cryodamage during freezing/thawing is well established. However, egg-yolk composition is variable, it requires refrigeration, and egg-yolk is at risk of pathogenic contamination. OptiXcell® (IMV Technologies USA) is an animal protein-free extender that promoted sperm motility and viability in bulls and buffalo, is at less risk of microbial contamination, and can be transported at room temperature. Additionally, a protocol employing a shortened cooling rate would allow samples to be stored quickly after collection. The goals of this study were to: 1) test OptiXcell as an animal protein-free alternative to egg-yolk based extenders for cryopreservation of rhino semen and 2) evaluate the impact of shorter chilling times during processing on sperm quality post-thaw. Semen was collected via electroejaculation from three managed rhino species (African black rhino (*Diceros bicornis*;  $n=2$ ), African white rhino (*Ceratotherium simum*;  $n=2$ ), Indian rhino (*Rhinoceros unicornis*;  $n=1$ )). Samples were diluted 1:1 with established semen extender (EQ; containing lactose, disodium EDTA, egg yolk, glucose, Equex STM, penicillin, streptomycin)

and cooled to 4-5°C, diluted 1:1 stepwise (25, 25, 50% v/v every 20 min) with extender containing 10% glycerol, and allowed to equilibrate at a final concentration of 5% glycerol for 1 h at 4°C. As OptiXcell contains glycerol, the OptiXcell control sample (OP) was diluted 1:1 and chilled at 4°C for 1h. Additional treatment groups were diluted 1:1 with EQ + 5% glycerol or OptiXcell, accordingly, and cooled at 4°C for 15 min (fast; FEQ and FOP) or not subjected to a chilling period (immediate; IEQ and IOP). All groups were loaded into 0.5 ml straws and lowered into a charged dry shipper for 10 min before being plunged into LN2. Samples thawed for 10s at RT then 37°C for 20s were evaluated for sperm motility, viability, morphology, progression, and acrosomal integrity at 0, 1, 4, and 24h post-thaw. Data were analyzed using repeated measures GLM and presented as means  $\pm$  SD. Post collection motility was  $82.5 \pm 5.0\%$ , progressive status:  $3.9 \pm 0.8$  (scale 0–5), viability:  $88.9 \pm 2.8\%$ , and morphologically normal spermatozoa:  $73.8 \pm 12.3\%$ . Post-thaw motility, progression, and viability decreased ( $P < 0.05$ ). Morphology did not differ post-thaw, among treatments or over time ( $P > 0.05$ ). OptiXcell proves to be a comparable animal-protein-free substitute for traditional egg-yolk based extenders for rhinoceros semen. Furthermore, equilibration time does not significantly impact sperm survival or quality parameters. (Supported by the Coombe Family Fund of the Greater Cincinnati Foundation, Elizabeth Tu Hoffman and an anonymous private donor.)

#### **Distinct Mechanisms Maintain the CL During Early vs Later Pregnancy as Highlighted by Profiles of Prostaglandin F2 Alpha Metabolite in Dairy Cattle During the First and Second Months of Pregnancy.**

Megan A. Mezera, Caleb S. Hamm, Caio A. Gamarra, Rodrigo S. Gennari, Victor E. Gomez-León, Rafael Reis Domingues, Alexandre B. Prata, Mateus Zucato Toledo, and Milo C. Wiltbank

Pulsatile PGF<sub>2</sub> alpha (PGF) release is critical to corpus luteum (CL) regression, while pregnancy requires CL maintenance. It is believed low PGF concentration contributes to pregnancy maintenance in month one, though there is insufficient PGF characterization during consecutive days throughout pregnancy. We hypothesized there would not be PGF pulses in pregnancy, while non-pregnant animals would display pulsatile PGF secretion. To test this hypothesis ovulations were synchronized, and jugular catheterization occurred day 17 of the estrous cycle or pregnancy or during the second month of pregnancy. Blood samples were taken every two hours for 52 hours in second month pregnant animals (group P2, n=8; Days 47-61), and for 74 hours on days 18-21 of pregnancy (group P1, n=5) and the estrous cycle (group NP, n=4; non-pregnant, CL regressed during sampling period). Serum was analyzed for concentration of PGFM (13,14-dihydro-15-keto-PGF<sub>2</sub> alpha), a metabolite of PGF. A pulse was identified if the CV for a sample was greater than 3 times the mean inter-assay CV, and the sample concentration was two times assay sensitivity. No pregnancies were lost during the study. Basal PGFM was low and similar ( $P=0.26$ ) in P1 ( $10.7 \pm 2.6$  pg/mL) and NP ( $13.3 \pm 2.1$  pg/mL) animals, while P2 basal concentrations ( $34.0 \pm 5.3$  pg/mL) were much greater ( $P < 0.001$ ) than all cows days 18-21. On days 18-21, NP had more ( $P < 0.001$ ) PGFM pulses per day, leading to CL regression, ( $1.43 \pm 0.11$  pulses/day; 4/4 with pulses) than P1 ( $0.13 \pm 0.08$  pulses/day in animals with pulses; 2/5 with pulses), and tended ( $P < 0.10$ ) to have more pulses than P2 ( $0.81 \pm 0.19$  pulses/day, 7/8 with pulses). P2 had more PGFM pulses than P1 ( $P < 0.05$ ), yet no P2 aborted. Peak concentration (largest pulse in cows with pulses) was greater ( $P < 0.01$ ) in NP ( $142.9 \pm 21.9$ ) than P1 ( $30.04 \pm 3.3$  pg/mL), and greater ( $P < 0.05$ ) than P2 ( $67.1 \pm 5.0$ ). Peak amplitude (largest pulse in cows with pulses) was greater ( $P \leq 0.05$ ) in NP ( $131.0 \pm 33.3$  pg/ml) than P1 ( $24.09 \pm 2.6$  pg/ml) and P2 ( $44.3 \pm 4.0$ ). Peak amplitude and concentration of PGFM were greater in P2 than in P1 ( $P < 0.05$ ,  $P < 0.01$ ). Thus, CL maintenance during the first month of pregnancy

is related to low PGF concentration and inhibition of PGF pulses. During the second month of pregnancy basal PGF is three times greater than the first month and there are distinct PGF pulses, yet the CL is maintained. This suggests there are different mechanisms involved in CL maintenance during later pregnancy.

### **Enhancer of Zeste Homolog 2 (EZH2) Regulates Uterine Development and Gene Expression in Mice.**

Ana M. Mesa, Manjunatha K. Nanjappa, Theresa I. Medrano, Sergei Tevosian, Wendy Jefferson, Carmen J. Williams, Ellis R. Levin, and Paul S. Cooke

Enhancer of zeste homolog 2 (EZH2) is a rate-limiting catalytic subunit of the histone methyltransferase PRC2. EZH2 plays a critical role in silencing gene activity through trimethylation of the repressive histone mark histone 3 lysine 27 (H2K27me3), and aberrant expression of EZH2 is associated with endometrial cancer, uterine leiomyomas and other uterine pathologies. We previously developed a mouse with conditional uterine knockout of EZH2 (EZH2cKO) using mice with floxed EZH2 and Cre expression driven by the progesterone receptor gene. This mouse shows altered uterine development, cell proliferation and estrogen response. To further investigate EZH2's uterine role, ovariectomized (OVX) adult controls (EZH2flox/flox) and EZH2cKO (EZH2flox/flox, PgrCre/+) mice (n = 4/group) were given either oil or 1 ng/g BW of 17 $\beta$ -estradiol (E2), and 24h later, RNA was extracted and used for RNA-Seq analysis. Data were analyzed using the DESeq2 package in R, and the false discovery rate was adjusted using the Benjamini-Hochberg procedure. Biological relevance was interpreted by analysis of differentially expressed genes (p value  $\leq$  0.05, fold change  $>$  1.5) using Ingenuity Pathway Analysis<sup>®</sup>. H2K27me3 and H3K27 acetylation status was detected by western blot of uterine histone extract. Progesterone (40 mg/g), the anti-estrogen ICI 182,780 (45 mg), or increasing concentrations of E2 (200 pg-10 ng/g BW) were injected into OVX EZH2cKO mice to determine effects on uterine weight and epithelial proliferation. In EZH2 cKO mice, 478 uterine transcripts were upregulated and 187 downregulated compared to WT controls. Major canonical pathways altered in the conditional knockout included genes involved in mitosis, cell cycle check-point regulation, estrogen mediated S-phase entry, and stem cell pluripotency. E2 treatment of EZH2cKO mice upregulated 197 transcripts and downregulated 207 transcripts compared to vehicle-treated EZH2cKO mice. EZH2cKO uteri showed significant decrease (P < 0.001) in H3K27me3 and increase in H3K27ac (P = 0.07) marks compared to WT vehicle-treated mice. Uterine weights of OVX EZH2cKO injected with E2 were higher than those injected with vehicle, ICI or P4 (38  $\pm$  8 mg, 28  $\pm$  6, 26  $\pm$  6, 33  $\pm$  7 mg, respectively; P < 0.001). Epithelial proliferation measured by MKI67 immunostaining was increased by E2, and ICI reduced epithelial proliferation compared to vehicle- and P4-treated mice (84  $\pm$  1% vs. 23  $\pm$  6%, 47  $\pm$  1%, 43  $\pm$  1% P < 0.001). Uterine weight and proliferation index showed dose-responsive increases in both WT and EZH2cKO mice, but E2 responsiveness was greater in EZH2cKO mice. Weights of non-ovx EZH2cKO uteri were recorded at postnatal day 22, 74, 200 and were higher compared to WT at day 22 (6  $\pm$  2 mg vs. 10  $\pm$  3 mg), day 60 (83  $\pm$  40 mg vs 102  $\pm$  52 mg) and day 200 (102  $\pm$  52 mg vs. 276  $\pm$  122 mg, P < 0.0001). Collectively, these results indicate that EZH2 plays a role in regulating uterine chromatin organization and gene expression, and loss of EZH2 increases uterine growth, epithelial proliferation and E2 responsiveness by activating ligand-independent estrogen receptor signaling. Supported by NIH grants HD088006 and HD0875328 to PSC.

**Altered Mitochondrial Dynamics in Oocytes of Pdss2-Deficient Mice is Partially Regulated by Opa1 Processing via Oma1 Activity.** Kyunga (Sally) Kim, Jessica Scott, and Andrea Jurisicova

While it is well established that oocyte quality decreases with increasing age, the mechanism underlying this decline is unclear. We have previously demonstrated that decreased levels of coenzyme Q (coQ), a component of the mitochondrial respiratory chain, may contribute to oocyte aging. mRNA and protein expression levels of coQ biosynthetic enzymes, Pdss2, is decreased in aged oocytes, implying that coQ biosynthesis may be down-regulated with aging. Oocyte specific Pdss2-deficient females have reduced ovarian reserve and poor embryo developmental potential. In order to uncover how oocyte quality declines with age, we further assessed the phenotypes of the Pdss2-deficient females, focusing on the mitochondrial health of their GV and MII oocytes. Our studies showed compromised mitochondrial function and decreased mitochondrial endowment caused by Pdss2-deficiency, as indicated by reduced levels of respiring mitochondria, mitochondrial ROS, mitochondrial DNA (mtDNA) copy number, and ATP. Additionally, quantitation of proteins that regulate mitochondrial fusion and fission (such as Mfn1, Mfn2, Opa1, and Drp1) by western blotting revealed increased processing of the Opa1, mitochondrial fusion protein, in Pdss2-deficient oocytes. Opa1 exists as multiple isoforms with distinct role in regulation of mitochondrial fusion. We identified Oma1, a mitochondrial metallopeptidase, as a potential proteolytic regulator of Opa1 in oocytes and created an Oma1-Pdss2 double knockout mouse line. Our preliminary data indicate that Oma1 deletion may alleviate some of the dysfunction in Pdss2-deficient oocytes, such as reduced ATP levels and decreased ovulation rates. Further analyses of the Opa1 cleavage patterns and assessment of the developmental potential of oocytes from double knockout females is currently underway to determine full impact of rescue. Research is supported by Canadian Institutes of Health Research (CIHR).

**CXCL12 May Function as a Luteotropic Factor by Regulating Inflammatory Cytokine Production in the Corpus Luteum.** Stacia Z Prosser, Kelsey E. Quinn, and Ryan L. Ashley

As sole producer of progesterone during early gestation, the corpus luteum (CL) is paramount to pregnancy maintenance. This transient endocrine gland is characterized by a microenvironment of diverse cells under constant influence by the local cytokine milieu, which modulates luteal structural and functional integrity. Studies of the CL and cytokines/chemokines during gestation are limited, which represents a major barrier to understanding CL lifespan during early pregnancy. C-X-C motif chemokine ligand 12 (CXCL12) signaling through CXCR4 modulates inflammatory cytokine production and enhances cell survival and proliferation in many tissues, and CXCR4 expression in granulosa cells is upregulated by the ovulation-inducing luteinizing hormone surge. Still, the contribution of CXCL12 to CL functional regulation is unknown. Based on this information and previous work in our laboratory, we hypothesized that CXCR4 and CXCL12 synthesis in the CL would increase as early pregnancy progresses, corresponding to an altered inflammatory cytokine milieu. In the present study, corpora lutea were collected from ewes on day 10 of the estrous cycle (cycling) and on three days of early pregnancy: 20, 25, and 30. Abundance of select proteins was detected by western blot and immunofluorescence allowed for protein localization. Compared to non-pregnant ewes, CXCR4 levels increased on day 30 ( $P < 0.05$ ) and large luteal cells, among other cell types, stained positive for CXCR4. Likewise, protein for CXCL12 increased on days 25 and 30 ( $P < 0.05$ ) of gestation, signifying that this pair may be necessary for structural development of the CL. Pro-inflammatory cytokine protein levels were also elevated in CL

during pregnancy, with greater soluble tumor necrosis factor (sTNF;  $P < 0.001$ ) and interferon gamma (IFNG;  $P < 0.001$ ) on days 25 and 30 compared to cycling ewes. Previous reports indicate that treatment with TNF in cattle prolongs CL function, increases production of angiogenic factors in the mid-cycle mare CL, and TNF is elevated in porcine CL on day 17 compared to cycling sows. Elevated levels of pro-inflammatory cytokines as well as the chemokine-receptor pair led us to an additional hypothesis that CXCL12 regulates CL inflammatory cytokine synthesis. To investigate CXCL12 regulation of cytokine synthesis, an in vitro model of steroidogenic granulosa-like cells was used. Greater amounts of sTNF were observed following CXCL12 administration ( $P < 0.01$ ), an effect that was not abrogated by pre-treatment with the CXCR4 inhibitor AMD3100 ( $P < 0.05$ ). While progesterone levels were similar regardless of treatment, CXCL12 may function in a luteotropic manner by activating ACKR3, thus stimulating sTNF synthesis to facilitate structural integrity of the CL. Indeed, TNF mediates angiogenesis and stimulates PGE2 production in vitro and may play a role in luteal vasculogenesis. These novel data add to our previous report of CXCR4 presence in the ovine CL and provide insight as to how luteal function is modulated during gestation. Research supported by the "Partnership for the Advancement of Cancer Research: NMSU/FHCRC", NCI grant U54 CA132383, the New Mexico Agricultural Experiment Station (AES), an AES graduate research award, and an Institutional Development Award (IDeA) from the National Institute of General Medical Sciences of the National Institutes of Health, grant #P20GM103451.

**Aberrant Gene Expression in Transdifferentiated Sertoli-like Cells in The Ovaries of Estrogen Receptor Double Knockout Mice.** April K. Binder, Katherine A. Burns, Karina F. Rodriguez, and Kenneth S. Korach

Normal ovarian function requires estrogen receptor  $\alpha$  and  $\beta$  (ER $\alpha$  and ER $\beta$ ) in distinct cell types within the ovary. ER $\alpha$  (Esr1) is expressed in theca cells while ER $\beta$  (Esr2) is expressed in granulosa cells. Previous characterization of the  $\alpha\beta$ ERKO double mutant ovary demonstrated that loss of both ERs led to the appearance of seminiferous tubule-like structures with Sertoli-like cells which are typically found in the testis that express Sex determining region Y-box 9 (Sox9). This original  $\alpha\beta$ ERKO was made on a 129S6/C57BL/6 mixed genetic background, and the phenotype was lost when backcrossed to C57BL/6. More recently, ER  $\alpha$  and  $\beta$  knockout mouse lines were created by global disruption of exon 3 floxed ER $\alpha$  and ER $\beta$  and then bred to create Ex3 $\alpha\beta$ ERKO animals with a similar mixed genetic background to the former  $\alpha\beta$ ERKOs. The ovaries of the Ex3 $\alpha\beta$ ERKO animals, on a mixed background, display a hemorrhagic phenotype, and as the animals age, the ovaries have dismorphogenic regions that have a mixed population of cells that reduced protein levels of granulosa cell specific Forkhead box L2 (FOXL2) that is followed by an increase in Sertoli cell specific SOX9 protein levels. At the same time, the ovaries have the appearance of seminiferous tubule-like structures in animals aged 6-12 months. These dismorphic regions appear with variable penetrance in the Ex3 $\alpha\beta$ ERKO ovaries and have increased levels of testis specific SOX9 and doublesex and mab-3 related transcription factor 1 (DMRT1) as examined by immunohistochemistry. To examine differences in gene expression, ovarian RNA was isolated, cDNA was synthesized and microarray analysis was performed to compare each single ER knockout ovary with the Ex3 $\alpha\beta$ ERKO. A large number of genes are differentially expressed in each ER knockout model compared to control, with 832 genes differentially expressed in the Ex3 $\alpha$ ERKO, 117 genes in the Ex3 $\beta$ ERKO, and 2,961 genes in the Ex3 $\alpha\beta$ ERKO. Of these genes only 77 are differentially expressed in all three models. To examine genes that may contribute to ovarian transdifferentiation, 2,457 genes specific to the Ex3 $\alpha\beta$ ERKO were compared to the gene list generated using the aromatase knockout model, which also

demonstrates postnatal ovarian transdifferentiation. Comparison of these two models has allowed for identification of 23 genes that show differential expression in the absence of estrogen receptor signaling in the ovary, including several that are involved in testis development including Sox9, Cst9, and Cldn11. To confirm altered gene expression, quantitative real-time PCR was performed using RNA from ER single and double knockout ovaries. Increased expression of Tweety homolog 1 (Ttyh1), a gene essential for brain development, was confirmed to be differentially and specifically increased in the Ex3 $\alpha$ ERKO ovary as a possible candidate for ovarian transdifferentiation. These results suggest that ER signaling is necessary for the maintenance of granulosa cell differentiation and provide a unique model to explore postnatal sex reversal of the ovary. Additionally, these animals may provide insight into the programming of genes important for the maintenance of proper sexual differentiation.

**Tumor Rejection Antigen P1A (TRAP1A) Expression in Murine Pregnancy.** S. K. Kshirsagar, G. Grzesiak, S. H. Ahn, S. L. Nguyen, and M. G. Petroff

**Objective:** The placenta is a specialized fetal organ that not only mediates nutrient and gas exchange between mother and fetus, but also modulates the maternal immune system. Tumor rejection antigens are proteins that are highly expressed in tumor cells and have the ability to promote anti-tumor immunity. These antigens are absent in normal adult tissues, with the intriguing exception that some are highly expressed in the placenta. TRAP1A is thought to be one such antigen, but its spatial and temporal expression patterns are unknown. The objective of this study was to determine whether TRAP1A protein is restricted to the placenta, and to map its temporal expression across pregnancy. We also examined the possibility that central tolerance may be established to TRAP1A by examining its expression in the thymus of pregnant and non-pregnant mice.

**Methods:** Eight- to 12 week old WT Balb/C female mice were bred to WT Balb/c males, and implantation sites/placentas were harvested at gestation day (GD) 7.5-8.5 (pre-placental stage), 10.5-13.5 (placental stage) and 16.5-17.5 (late pregnancy). TRAP1A mRNA expression was analyzed by qRT-PCR, and protein expression was analyzed by western blot. Tissues from non-pregnant Balb/c female mice were used to determine tissue specific expression of TRAP1A.

**Results:** TRAP1A mRNA and protein were highly expressed in the placenta across gestation, with low levels of protein expression in the brain of non-pregnant female mice. Protein was undetectable in liver, uterus, spleen, testis, heart, lung, and small intestine. TRAP1A mRNA expression was near undetectable in the thymus of both non-pregnant and pregnant mice. In pregnant mice, relative quantities of mRNA for TRAP1A revealed low levels of expression in GD7.5-8.5 implantation sites, but progressively higher quantities in the placenta as gestation progressed. Consistent with protein analysis, TRAP1A mRNA was undetectable in kidney and lung.

**Conclusions:** This study reveals the restricted tissue expression of TRAP1A in the placenta of mice. Its absence in the thymus suggests that these animals may not be tolerized to the antigen, raising the possibility that its abundance in the placenta primes maternal immunity to tumor antigens during pregnancy.

**The Role of PTEN and DICER Haploinsufficiency in Endometrial Cancer Development.** X. Wang, S. Khatri, R. Broaddus, F. DeMayo, J. Lydon, R. Emerson, A. Buechlein, D. Rusch, K. So, C. Zhang, and S. M. Hawkins

Endometrial cancer is the most frequent gynecologic malignancy, with 61,380 new cases diagnosed in 2017 in the US. While women with early stage disease are typically cured with simple hysterectomy, the prognosis for women with aggressive forms of the disease (i.e., clear-cell adenocarcinoma or carcinosarcoma) is dismal. To study endometrial cancer in a mouse model, we started with the PgrCre;Ptenf/f mouse (Pten cKO). This mouse model deletes Pten, the most frequently mutated tumor suppressor in women with endometrial cancer, using a conditional allele for the uterus. To this mouse model, we further deleted one or two alleles of Dicer [PgrCre;Ptenf/f;Dicerf/+ (Pten-Dicer het) and PgrCre;Ptenf/f;Dicerf/f (dcKO)]. DICER is a ribonuclease III required for miRNA synthesis, and lowed DICER expression correlates with poor prognosis tumors and recurrent disease in women. Surprisingly, Pten-Dicer het female mice (n = 19) had significantly worse survival than Pten cKO (n = 22) or dcKO (n = 19) [P Müllerian tumor (MMMT). MMTT of the uterus, also known a uterine carcinosarcoma, is an extremely rare and aggressive malignancy in women. Mouse models of endometrial cancer that recapitulate human disease represent translational tools for better understanding of aggressive disease. We anticipate that this model will be highly relevant, not only to study the molecular characteristics of the more rare forms of human endometrial cancer, but also to study the preclinical development of therapeutics for uterus carcinomas.

**Voluntary Sperm Collection From the Critically Endangered Philippine Crocodile (*Crocodylus mindorensis*).** Jason R. Herrick, Teresa Shepard, Andy Reeves, Jonathan Aaltonen, and Jessi Krebs

The Philippine crocodile (*Crocodylus mindorensis*) is a critically endangered species (  $1 \times 10^6$  spermatozoa. Motility was low ( $< 20\%$ ) in all samples, which could be related to the lack of energy substrates in the medium and/or the presence of debris from the cloaca. The large variability in the number of recovered spermatozoa suggests our collection technique needs to be optimized for more consistent recovery of large quantities of spermatozoa. Fortunately, the non-stressful nature of the technique provides numerous opportunities for optimization that are rarely available for large, dangerous wildlife species. Our results represent the first and only information regarding reproduction in this critically endangered species and suggest that sperm production may peak in the spring and summer months.

**Co-Expression of Membrane-Only E-Domain of ESR1 and Nuclear-Only ESR1 Transgenes in Mice Does Not Fully Restore Fertility and Estrogen Responsiveness in Uterus.** Paul S. Cooke, Manjunatha K. Nanjappa, Theresa I. Medrano, Ana M. Mesa, Indrani Bagchi, Athilakshmi Kannan, and Ellis R. Levin

Female and male reproductive development and function are regulated by estrogens acting primarily through estrogen receptor 1 (ESR1 or ER $\alpha$ ). Most ESR1 is nuclear/cytoplasmic, but in addition to nuclear ESR1 (nESR1), 5-10% of cellular ESR1 is membrane ESR1 (mESR1) that signals through pathways distinct from nESR1. Work from our group has shown that adult male or female nuclear-only ESR1 (NOER) mice, which lack mESR1 but retain nESR1, are infertile with reproductive abnormalities. Thus, mESR1 is

essential for normal 17 $\beta$ -estradiol (E2) response. Furthermore, the E-domain of ESR1 alone may be sufficient for normal mESR1 signaling. Cells lacking ESR1 have been transfected with a plasmid encoding a fusion protein (Emem) driven by a cytomegalovirus (CMV) promoter and consisting of the human (h) ESR1 E-domain, the N-terminal 20 amino acids of neuromodulin, and a cyan fluorescent variant of GFP; this restored normal non-genomic rapid activation of protein kinases (MAPK and PI3K) by estrogen. The neuromodulin fragment contains two cysteines that are palmitoylated (the main mechanism by which ESR1 is targeted to cell membranes), resulting in exclusive membrane localization of all protein produced by the Emem transgene. The E-domain of ESR1 contained in Emem retains the ligand-binding domain and also allows ESR1 dimerization, but lacks the DNA binding domain and does not alter transcription. In addition, localization of E2/ESR1 to the pS2 promoter in NOER hepatocytes in vitro was impaired. However, the Emem vector transfected into these hepatocytes restored localization of E2/ESR1 complexes to pS2 promoters and E2-induced pS2 mRNA production to WT levels, suggesting that the E-domain alone restores E2 responses in cells expressing only nESR1. In this study, we produced NOER mice that also expressed Emem (Esr1NOER/NOER, Emem+/-) to determine if this restored normal fertility and estrogen responsiveness and reversed morphological abnormalities. Both adult male NOER and Esr1NOER/NOER, Emem+/- mice were infertile, indicating that the hESR1 E-domain did not restore fertility. Some (2/25) female Esr1NOER/NOER, Emem+/- mice gave birth to viable litters, while viable litters were never produced by NOER females. In E2-treated ovariectomized female Esr1NOER/NOER, Emem+/- mice, both uterine MAPK and PI3K expression (induced through mESR1) was detected. Normal E2 responsiveness was not restored in female Esr1NOER/NOER, Emem+/- mice. Morphological and histological abnormalities in efferent ductules, rete testis and seminiferous tubules and decreases in sperm production seen in NOER mice also occurred in Esr1NOER/NOER, Emem+/- mice. These results indicate that expression of the Emem transgene containing the hESR1 E-domain is insufficient to fully restore fertility or other abnormalities in NOER mice, although female Esr1NOER/NOER, Emem+/- mice showed partial restoration of fertility. This could result from lack of normal physiological control of the expression of the hESR1 E-domain and consequent lack of synchrony with nESR1 in transgenic mice, from the ESR1 E-domain alone being insufficient for mediating all aspects of mESR1 signaling needed for full E2 responses in vivo, despite its mediation of certain E2-induced effects in vitro, or that the Emem transgene is not haplosufficient. Supported by NIH grants HD088006 and HD0875328 to PSC.

**Assessment of Reproductive Hazards of Biocompatible 3D-Printed Resins.** Hunter B. Rogers, Emily Zaniker, Tracy Zhou, Atsuko Kusuhara, Francesca E. Duncan, and Teresa K. Woodruff

With the development of more sophisticated manufacturing techniques, biomaterials are increasingly being implemented in biomedical research. Biomaterials frequently contain plastics or leachates which may be biocompatible with respect to non-reproductive tissues, but may exhibit reproductive toxicity. For example, short-term, low-dose exposure to bisphenol A, a component of many plastics, is an endocrine disruptor and induces meiotic errors and aneuploidy in the mouse oocyte. As 3D-printing has become more accessible and printers have become more advanced, 3D-printing technology is a promising resource for the creation of new biomedical devices. However, the resins currently available for most printers are still limited, with only a few that have been tested for their general biocompatibility. The objective of this study is to test the potential reproductive toxicity of two commercially available 3D-printable dental resins that are currently marketed as biocompatible: Dental SG and Dental LT. Additionally, ozone plasma treatment, a common surface treatment of biomaterials,

of both materials was tested as a method to minimize reproductive toxicity. For this study, mice were hyper-stimulated with pregnant mare serum gonadotropin (PMSG) to obtain a high yield of uniform oocytes from large antral follicles. These oocytes were then matured in vitro for 14-16 hours in defined media in Dental SG, Dental LT, or polystyrene well plates. Meiotic progression was quantified by assessing the meiotic stage (prophase I, prometaphase I/metaphase I, and metaphase II) according to established morphological criteria using light microscopy. In addition, immunocytochemistry and confocal microscopy were performed on resulting metaphase II-arrested eggs to characterize the meiotic spindle, including spindle length and chromosome alignment at the metaphase plate. All oocytes degenerated during in vitro maturation in untreated Dental SG and Dental LT resins. Plasma treatment of Dental SG wells resulted in similar rates of meiotic progression compared to the polystyrene control. However, when comparing the plasma-treated Dental SG condition to the control, increased incidence of chromosomal abnormalities was observed. Plasma treatment of the Dental LT material did not reduce observed reproductive toxicity and all oocytes matured in this material degenerated. As these resins are labeled as biocompatible, it may be tempting for researchers to use them for the development of biomedical devices and/or long term use in oral retainers. However, our results show that these materials should be used cautiously, especially for reproductive medicine applications, due to their potential for reproductive toxicity.

This work was funded by supported by the NIEHS/NIH/NCATS UG3 grant (ES029073-01), the Master of Science in Reproductive Science and Medicine program at Northwestern University, and the Center for Reproductive Health After Disease (P50 HD076188) from the National Centers for Translational Research in Reproduction and Infertility (NCTRI).

#### **Genomic Profile of Human Atypical Meningioma.** Eunhye Kim, Young Seok Park, and Sang-Hwan Hyun

We report the establishment and comparative characterization of patient-derived, spontaneously immortalized cancer stem cell lines derived from atypical meningioma. We performed whole-exome sequencing across blood, tumor, primary cell lines at early and late passage derived from atypical meningioma patient. A total of 184,696 single nucleotide variants (SNVs) were identified through whole-genome sequencing of the meningioma samples, including 12,057 inserted and deleted sequences (indels) and 172,639 single nucleotide polymorphisms (SNPs). Of these SNVs, a high prevalence of C>T base (G>A base in the complementary strand) transversions were observed, comprising an average of 36.82% of the total substitutions in the tumor sample. Also, chromosome 1, 6, 12 and 10 have commonly more SNVs across the individual chromosome. AKT1 and SMO mutations co-occurred with mutations in MYBL2 in this non-NF2-mutant atypical meningioma. These results will help to facilitate more robust and effective genomics-guided personalized therapy in atypical meningioma.

#### **Inhibition of Chemokine Receptor 4 (CXCR4) Signaling at the Fetal-Maternal Interface Alters ROCK1 and Mtor Signaling Pathways During Early Gestation in Sheep.** Cheyenne L. Robinson, Stacia Z. Prosser, Kim K. Kane, and Ryan L. Ashley

During early pregnancy, an intricate communication between fetal extraembryonic membranes and maternal endometrium directs major developmental events including angiogenesis and cell

proliferation, effectively setting the foundation for placentation. Because vascular endothelial growth factor (VEGF) is considered the most potent angiogenic inducer, a greater knowledge of factors regulating VEGF as well as molecular pathways facilitating early vascularization are needed to advance understanding of placental development. We demonstrated chemokine (C-X-C motif) ligand 12 (CXCL12) stimulates VEGF production in trophoblast cells and now extend these findings to ovine endometrial cells. Moreover, we demonstrated that inhibiting the CXCL12 receptor, CXCR4, in vivo at the fetal-maternal interface in sheep results in less hypoxia-inducible factor 1a (HIF1A), VEGF and its receptor fms-like tyrosine kinase 1 (FLT1) in maternal caruncle tissue. Based on our previous data, we hypothesized that inhibiting CXCR4 signaling at the fetal-maternal interface in sheep would affect signaling pathways involved in placental development. The PI3K/AKT/mTOR pathway stimulates cell survival, proliferation, angiogenesis, and migration, yet the functional contributions of CXCL12-induced mTOR signaling during placental vascularization remains to be elucidated. Further, Rho kinase 1 (ROCK1) is a key player in cytoskeleton rearrangement, cell motility, and invasion, which are all central to proper placentation. Our objective was to determine impacts of inhibiting CXCR4 at the fetal-maternal interface on ROCK1 and mTOR signaling pathway in fetal and maternal placenta. To this end, we utilized a CXCR4 antagonist, AMD3100. On day 12 of gestation, mini-osmotic pumps were surgically installed in sheep with a catheter delivering AMD3100 (treatment, n = 5) or PBS (control, n = 6) into the uterine lumen ipsilateral to the corpus luteum for 7 days. On day 20 fetal membrane, caruncle and intercaruncle tissues were collected and factors regulating placental angiogenesis determined by western blotting and immunofluorescence. Production of ROCK1 and mTOR were similar in intercaruncle tissue, regardless of treatment. However, abundance of phosphorylated mTOR decreased ( $P < 0.05$ ) in caruncle and fetal membrane tissues when CXCR4 was inhibited compared to control ewes. Greater ( $P < 0.05$ ) amounts of ROCK1 were observed in caruncle tissue when CXCR4 was impaired compared to control. Similar to our previous reports of altered VEGF production after inhibiting CXCR4, in the current study immunofluorescence analysis revealed less ( $P < 0.05$ ) VEGF in uterine cross sections from AMD3100-infused ewes compared to control. Conversely, immunofluorescence imaging for cluster of differentiation 34 (CD34), was greater ( $P < 0.05$ ) in uterine endometrium from AMD3100-infused ewes compared to control. As CD34 is as common marker for hematopoietic stem and endothelial cells, a vascular rescue mechanism may exist when CXCR4 signaling is compromised. Our results further highlight the importance of CXCL12-CXCR4 signaling at the fetal-maternal interface and its impact on proper placental development. A greater understanding of CXCL12-CXCR4 functions will enhance our comprehension of the mechanisms driving placental growth and vascularization. Research supported by Cowboys for Cancer Research (C4CR) Foundation, NM Agricultural Experiment Station, and an Institutional Development Award (IDeA) from the National Institute of General Medical Sciences of the NIH, grant #P20GM103451.

**Unique Postmating Expression Profiles of *Drosophila melanogaster* Female Reproductive Tract Structures.** Caitlin E. McDonough, Scott Pitnick, and Steve Dorus

The female reproductive environment interacts with the male ejaculate in diverse ways that coordinate reproductive events, bias sperm usage and influence reproductive investment. Female reproductive tract (FRT) structures and secretions have been associated with a variety of functions including lubrication, seminal fluid protein processing, sperm movement and storage, ovulation, re-mating behavior, immune response, and gamete modification. To identify female contributions to these

interactions, we conducted comprehensive transcriptomics on structures of the *Drosophila melanogaster* FRT at virgin, 6 hours, and 24 hours postmating. These structures included the oviduct, bursa (uterus), spermatheca (glandular sperm storage organ), seminal receptacle (epithelial sperm storage organ), parovaria (female accessory gland), and a fat body tightly associated with the FRT. We identified unique expression profiles for these different structures that provide insight into their shared and distinct functions as well as genes involved in specific functions such as sperm storage. Several genes with significantly higher expression in the parovaria (a previously uncharacterized FRT gland) were found clustered on the X chromosome, including genes with unknown functions arising through duplication events during the radiation of the *melanogaster* subgroup. We also identified genes with similar postmating expression patterns in multiple female reproductive structures, indicating a suite of redundant functions spatially distributed throughout the FRT. In addition, many structures shared enriched gene ontology categories of proteases, protease inhibitors and anti-microbial agents supporting established functions of FRT structures in seminal fluid processing and postmating immune response. This system level approach to the FRT creates an atlas of gene expression and predicted functions across the different structures of the FRT throughout mating.

#### **Single Cell RNA-seq of First Trimester Human Chorionic Villi from Healthy Ongoing Pregnancies.**

Tianyanxin Sun, Yizhou Wang, Chintda Santiskulvong, Bora Lee, Tania Gonzalez, Jie Tang, John Williams, III, and Margareta D. Pisarska

The placenta plays a critical role in fetal development, forming the interface between the developing fetus and the mother. It contains different types of trophoblast cells such as cytotrophoblasts, syncytiotrophoblasts, extravillous trophoblasts, as well as other non-trophoblastic cells such as mesenchymal cells, immune cells and vascular cells, all of which are indispensable for placental function throughout pregnancy. The first trimester is when pregnancy associated diseases likely manifest but our understanding of the placenta during this early stage is still very limited. We have previously characterized the first trimester placenta transcriptome at the tissue level and identified sexual dimorphism of the genes that may contribute to different pregnancy outcomes such as lower birth weight in females. In order to better understand the various cell types present in the first trimester placenta, we performed single cell RNA sequencing on tissue from chorionic villi samples (CVS) at 11~13 weeks gestation from 6 healthy singleton pregnancies (3 female, 3 male). We constructed and sequenced single-cell barcoded RNA-seq libraries from these samples using large-scale microfluidic single cell technologies and the latest sequencing platform Novaseq. Over 11,000 cells in total were captured, with an average sequencing depth of 120,000 reads per cell. We identified 8 distinct cell populations based on known cell markers, including cytotrophoblasts, syncytiotrophoblasts, extravillous trophoblasts, endothelial cells, macrophages, dendritic cells, mesenchymal cells and T lymphocytes. We defined new markers for each population and by profiling the transcriptomes within each population, we also identified diverse cellular subtypes within some of these populations, such as macrophages and mesenchymal cells. Though there doesn't appear to be gender specific cell clusters, a number of sexually dimorphic genes were found to only be expressed in some cell types but not others, which strongly suggests their important role in sex differences. To our knowledge, this is the first study to dissect the cellular heterogeneity of the first trimester placenta from more than 11,000 non-marker selected primary chorionic villus cells from healthy ongoing pregnancies with large-scale microfluidic single cell transcriptomic technologies. Further, we defined new cell-type-specific signatures and explored gender-

specific genes at the single cell level. This study is the first step in understanding the interaction of the different cell types that make up the first trimester placenta. This work was supported by NIH/NICHD R01HD074368, R01HD091773.

**Temporal Regulation of AKT, Mtor and Erk Signaling Activity Reveals Differences Between in Vivo and in Vitro Produced Mouse Embryos.** Sandeep K. Rajput, Alison F. Ermisch, Deirdre M. Logsdon, John C. Becker, William B. Schoolcraft, and Rebecca L. Krisher

The ultimate goal of in vitro embryo culture is to produce high quality embryos capable of implantation, successful pregnancy and birth of healthy offspring. We previously demonstrated that in vivo (high quality) and in vitro (poor quality) produced embryos differ metabolically during preimplantation development. However, signaling mechanisms regulating metabolism, cell proliferation and differentiation, and thus embryo quality during preimplantation development remain poorly understood. AKT/mTOR and Erk are key signaling pathways implicated in a variety of cellular processes that regulate metabolism and growth. We hypothesized that the observed differential metabolism of in vivo and in vitro produced embryos is reflected by differential expression and activity of AKT/mTOR and ERK signaling pathways. Our objectives were: 1) to determine temporal regulation of AKT, mTOR and ERK protein expression during early development; and 2) to investigate stage specific differences in AKT, mTOR and ERK signaling activity in both in vivo and in vitro produced embryos. In vivo and in vitro produced mouse embryos were collected after ovarian stimulation at 1-cell (C), 2C, morula and blastocyst stages (n = 20 embryos/stage; 3 replicates/stage) and subjected to Western blot analysis using antibodies specific to phosphorylated (p) AKT, total (t) AKT, p-mTOR, t-mTOR, p-ERK and t-ERK protein. The ratio of phosphorylated and total protein abundance was used to determine the signaling activity of each pathway. mTOR and ERK protein abundance was highest at the 1C stage, was significantly reduced at the 2C and morula stages, and was further decreased at the blastocyst stage in both types of embryos. Expression of AKT in in vivo produced embryos was stable from 1C to morula, followed by a significant reduction at the blastocyst stage. However, in vitro produced embryos showed a significant reduction in AKT abundance at both the morula and blastocyst stages. Activity of mTOR signaling from the 1C to the blastocyst stage, and AKT signaling from the 1C to the morula stage, was significantly higher in in vitro produced embryos compared to those produced in vivo. ERK signaling activity was observed only at the 1C stage regardless of the type of embryo, and was reduced in 1C embryos produced in vitro. Comparative analysis across preimplantation development revealed that the most active pathways by stage were ERK at 1C, AKT at 2C, and mTOR from 2 cell to blastocyst. Our results demonstrate for the first time the temporal regulation of AKT, mTOR and ERK signaling pathway activity during early embryo development. In vitro produced embryos exhibited elevated activity of mTOR and AKT signaling, suggesting their role in up-regulation of metabolism resulting in reduced embryo quality in embryos cultured in vitro, which supports the quiet embryo hypothesis. The absence of ERK signaling activity after the first cleavage division suggests its dispensable role during preimplantation development. Collectively, these results increase our understanding of stage specific metabolic regulation during embryo development, and highlight how these pathways differ in embryos produced in vitro. Designing culture medium to support correct pathway activity will lead to improvement in the quality of embryos produced in vitro.

**Multiple Dominant Follicles are Required for Complete Suppression of Circulating FSH in a High Fecundity Bovine Genotype as Demonstrated with a One-Follicle Model.** Alvaro Garcia-Guerra, Pedro L. J. Monetiro Jr, Caio. A. Gamarra, Emil A. Walleser, Brian W. Kirkpatrick, and Milo C. Wiltbank

A novel high fecundity bovine allele, Trio, was recently discovered. Cattle carrying the Trio allele have multiple ovulations of smaller-sized follicles while half-sibling non-carriers have single ovulations. Our hypothesis is that maintenance of inhibition of FSH to basal concentrations after follicle deviation (selection) is dependent on only a single dominant follicle in non-carriers but requires multiple dominant follicles in Trio carriers. A synchronized follicular wave was induced in Trio carrier (n=19) and non-carrier (n=20) heifers, by follicular ablation with follicle growth in a controlled progesterone (P4) environment (no CL, one intravaginal P4 implant). Five days after synchronization, intravaginal P4 was removed, and heifers within each genotype were randomized to one of two treatments: 1) One-follicle model: removal of all follicles except largest dominant follicle (F1), or 2) Sham-aspiration control. Thus, four groups were analyzed: Trio carrier, one-follicle (TC-OF; n=11); Trio carrier, control (TC-C, n=8); Non-carrier, one-follicle (NC-OF, n=12); and Non-carrier, control (NC-C, n=8). Heifers in OF groups had all follicles  $\geq 4$  mm in diameter, except F1, removed by ultrasound-guided transvaginal follicle aspiration with re-aspiration of any visible, previously-aspirated follicles 12 h later. Heifers in control group underwent a sham aspiration in which no follicles were removed. Blood samples were collected by coccygeal venipuncture every 12h starting 24h before treatment and FSH concentrations were determined by radioimmunoassay. Diameter of F1 at time of treatment was greater (282% greater volume; P 0.10). Removal of all but the F1 follicle in Trio carrier heifers (TC-OF) resulted in increased (P 0.20) from pre-treatment values for heifers in NC-C (89%), NC-OF (108%) and TC-C (91%). Percentage change in FSH at hours 12 and 24 was greater in the TC-OF group than in any of the other groups (P < 0.02). Thus our hypothesis was supported. After selection of the dominant follicle(s), non-carrier controls require only a single dominant follicle to achieve complete suppression of FSH, whereas, Trio carriers require multiple dominant follicles to maintain FSH inhibition, probably due to the differences in F1 size (282% greater volume in non-carriers than Trio carriers) and correspondingly lower secretion of FSH suppressors.

**Non-Steroidal Anti-Inflammatory Drugs Inhibit Multidrug Resistance Like Protein 4 (MRP4) Expression in Porcine Vas Deferens Epithelia.** Bruce D. Schultz, Kelsey Madden, and James D. Lillich

Vas deferens epithelial cells express prostaglandin synthase 2 (PTGS2) upon exposure to testosterone. PVD9902 cells, derived from pig vas deferens epithelia, synthesize and secrete substantial amounts of prostaglandins (PG) E2 and D2. Freshly isolated porcine vas deferens epithelia and PVD9902 cells form highly resistive epithelial barriers in culture and have been employed to show that PGE2, and to a lesser extent PGD2, are secreted or accumulated preferentially in the mucosal compartment. In culture, PG concentrations can become more than twenty-five fold greater in the mucosal compartment than the serosal compartment in a twenty-four hour period. The objective of the current research was to identify a mechanism that can account for this preferential mucosal secretion or accumulation. RT-PCR showed that mRNA coding for MRP4 was expressed in these cells and immunoblots showed immunoreactivity with anti-MRP4 antibodies. Subsequent experiments showed that non-steroidal anti-inflammatory drugs (NSAIDs) including indomethacin, ibuprofen and Celebrex profoundly reduced PGE2 and PGD2 accumulation in the mucosal compartment but had a lesser effect on serosal accumulation. Consistent with this observation, NSAIDs reduced both the amount of mRNA coding for MRP4 and protein

expression as assessed by immunoblot. Taken together, these observations suggest that MRP4 is expressed in the apical membrane of vas deferens epithelia and accounts for the preferential secretion or accumulation of PGs in the reproductive duct lumen. Importantly, the results suggest that NSAIDs, either directly or indirectly, reduce the expression of this multidrug resistance like protein that is known to export therapeutic drugs from cells. (Support: NIH, R15 DK091791, T35OD010979; Kansas State University College of Veterinary Medicine)

### **Mechanisms that Maintain the Corpus Luteum Differ After Day 25 of Pregnancy as Evidenced by Increased Circulating Prostaglandin F-Metabolite (PGFM) Secretion after Oxytocin Challenge in Dairy Cows.**

Jessicá N. Drum, Pedro L. J. Monteiro Jr, Alex B. Prata, Rodrigo S. Gennari, Caio A. Gamarra, Michele Brich, Amanda B. Alvarenga, Aurea M.O. Canavessi, Milo C. Wiltbank, and Roberto Sartori

Our hypothesis was that oxytocin-induced PGFM secretion would be suppressed in pregnant (P) cows, potentially explaining the mechanism that maintains the CL during pregnancy. Effect of an oxytocin challenge on circulating PGFM profile of lactating Holstein cows (n=121) was evaluated throughout the first 2 months of pregnancy. On d11 (n=23), 18 (n=23), and 25 (n=12) after AI, and on d32 (n=13), 39 (n=13), 46 (n=12), 53 (n=13), and 60 (n=12) of pregnancy, cows were challenged with 50 IU oxytocin, i.m. Blood was collected before (0 min), 30, 60, 90, and 120 min after oxytocin challenge for plasma concentrations of PGFM (pg/mL) by ELISA. Ultrasound evaluations were performed for pregnancy diagnosis on d32, 39, and 60 post-breeding and interferon-stimulated genes (ISGs) were evaluated in peripheral blood cells on d18 as marker of an elongating embryo. Analysis of PGFM used only information from non-pregnant (NP) cows on d18, based on ISGs, or cows diagnosed P on d32, using ultrasound. Data were analyzed by PROC MIXED of SAS 9.2. On d11, there was no difference between P and NP, both had low PGFM, and there was no effect of oxytocin on PGFM. On d18, NP tended to have greater basal (prior to oxytocin treatment) PGFM than P ( $16.3 \pm 3.2$  vs.  $9.5 \pm 1.2$ ;  $P = 0.08$ ) and had 3-fold greater PGFM after oxytocin ( $72.9$  vs.  $24.4$ ;  $P < 0.05$ ). Comparing only P cows from d11 to 60, basal PGFM concentrations increased ( $P < 0.0001$ ) as pregnancy progressed, with d11 ( $9.4 \pm 2.3$ ) and d18 ( $9.5 \pm 1.2$ ), lower than all days from d25 to d60 of pregnancy (d25= $22.6 \pm 3.7$ ; d32= $30.5 \pm 4.8$ ; d39= $27.8 \pm 2.7$ ; d46= $22.7 \pm 3.9$ ; d53= $29.0 \pm 4.4$ ; d60= $28.0 \pm 4.2$ ). Overall PGFM increased throughout gestation, and there was an interaction between gestation day and time after challenge ( $P < 0.001$ ). Pregnant cows on d18 had little increase in PGFM following oxytocin but it tended ( $P = 0.06$ ) to be greater compared to the negligible PGFM after oxytocin in P cows on d11. The oxytocin-induced PGFM in P cows on d25 ( $48.3 \pm 8.6$ ) was greater than P cows on d18 ( $16.6 \pm 3.3$ ;  $P = 0.006$ ), especially at 60 min after challenge ( $P = 0.01$ ) when values were 2.9-fold higher on d25. Moreover, PGFM at 90 min after oxytocin treatment was lower ( $P < 0.05$ ) on d25 ( $41.7 \pm 8.1$ ) compared to d53 ( $139.2 \pm 19.7$ ) and d60 ( $120.8 \pm 15.5$ ), with intermediate values on d32 ( $74.8 \pm 14.8$ ), d39 ( $97.5 \pm 26.6$ ), and d46 ( $94.1 \pm 11.6$ ). Thus, consistent with our hypothesis and previous reports, the CL of early pregnancy is maintained due to suppression of PGF secretion likely a result of actions by embryonic interferon-tau. However, our hypothesis was not supported during the second month of pregnancy. Uterine PGF secretion was not suppressed since basal PGFM and oxytocin-induced PGFM secretion were greatly elevated (equal or greater than in d18 NP cows). These results indicate that there are alternative mechanisms for maintenance of the CL during second month of pregnancy that do not involve suppression of uterine PGF secretion. Acknowledgements: FAPESP, CNPQ, CAPES, and WI Experiment Station.

**Epiblast Development During in Vitro Post Implantation Embryo Outgrowth Accurately Predicts the Developmental Potential of Mouse Blastocysts.** Deirdre M. Logsdon, Alison F. Ermisch, Rebecca Kile , William B. Schoolcraft, Rebecca L. Krisher, and Ye Yuan

Embryo transfer is the most direct means to measure the developmental potential of blastocysts. However, it is technically demanding, time-consuming, and may not be readily available in many species. An in vitro model to predict post-implantation developmental potential would be a valuable tool for both research and clinical applications. In this study, we cultured mouse blastocysts from different origins in an in vitro outgrowth system to determine parameters predictive of developmental competence. Embryos of varying quality inferred by the duration of their time in vitro were produced from outbred mice (SW, CF1). In the first group, immature oocytes were collected 48 h post PMSG for in vitro maturation (IVM), followed by fertilization and culture in vitro to produce embryonic day (E) 3.5 blastocysts (SW, n=10). In the second group, E 3.5 blastocysts were produced in vitro from in vivo matured (IVO) oocytes collected following stimulation (CF1, n=24). In the third group, in vivo produced E 3.5 blastocysts were flushed from the uterus after stimulation and mating (CF1 n=32, SW n=43). Embryos with similar morphologies were dezonated and plated onto optical-grade outgrowth plates coated with fibronectin. Embryos were cultured in IVC1 (Cell Guidance Systems) for the first 72 h, followed by culture in IVC2 for an additional 48 h. All embryos attached within 72 h. On E 8.5, embryos were fixed and stained with DAPI and antibodies against F-actin and pluripotency marker Pou5f1 for 3D confocal microscopy. The number of epiblast cells, total volume of outgrowth, and outgrowth area were measured. Embryos produced from SW IVM oocytes had significantly fewer epiblast cells ( $117.7 \pm 32.1$ ) compared to their in vivo produced counterparts ( $338.0 \pm 50.6$ ), although outgrowth area (IVM  $0.34 \pm 0.01$  mm<sup>2</sup>, in vivo  $0.33 \pm 0.03$  mm<sup>2</sup>) and volume (IVM  $1.90 \pm 0.24 \times 10^5$  μm<sup>3</sup>, in vivo  $2.84 \pm 0.30 \times 10^5$  μm<sup>3</sup>) did not differ between the two groups. For CF1 mice, embryos produced from IVO oocytes had significantly fewer epiblast cells (IVO  $109.7 \pm 19.1$ , in vivo  $344.1 \pm 36.8$ ) compared to in vivo developed embryos. However, the outgrowth volume (IVO  $2.33 \pm 0.46 \times 10^5$  μm<sup>3</sup>, in vivo  $2.65 \pm 0.38 \times 10^5$  μm<sup>3</sup>) and area (IVO  $0.66 \pm 0.04$  mm<sup>2</sup>, in vivo  $0.62 \pm 0.05$  mm<sup>2</sup>) were not different. To validate the difference in developmental potential, embryo transfer was also performed with CF1 blastocysts. In vivo developed blastocysts (n=45) yielded 64.4% implantation and 62.2% fetal development, whereas blastocysts produced in vitro from IVO oocytes (n=120) had a 67.5% implantation rate but only 16.7% fetal development. In summary, epiblast development in peri-implantation embryos grown in vitro is a more accurate method to predict the developmental potential of a blastocyst than assessments of blastocyst morphology, outgrowth attachment area and outgrowth volume. This work sets the stage for routine evaluation of embryo quality past the time embryos would normally be transferred, which has not previously been possible. The ability to determine post implantation potential without embryo transfer will greatly improve efforts to culture higher quality embryos in vitro.

**Sperm Epimutation Biomarkers of Obesity and Pathologies following DDT Induced Epigenetic Transgenerational Inheritance of Disease.** Stephanie E. King, Margaux McBirney, Daniel Beck, Ingrid Saddler-Riggleman, Eric Nilsson, and Michael K. Skinner

Dichlorodiphenyltrichloroethane (DDT) has previously been shown to promote the epigenetic transgenerational inheritance of adult onset disease in rats. The current study investigated the potential that sperm epimutation biomarkers can be used to identify ancestral induced transgenerational disease

and associated pathologies. Gestating F0 generational rats were transiently exposed to DDT during fetal gonadal sex determination and the incidence of adult onset pathologies was assessed in the subsequent F1, F2, and F3 generations. In addition, sperm differential DNA methylation regions (DMRs) that were associated with specific pathologies in the F3 generation males were investigated. No pathology was observed in the F1 generation DDT lineage males or females compared with F1 generation controls (vehicle exposure). There was an increase of testis disease and early onset puberty in the F2 generation DDT lineage males. The F3 generation DDT males had significant increases in testis disease, prostate disease, and late onset puberty. The F3 generation DDT females had significant increases in ovarian and kidney disease. Both the F3 generation males and females had significant increases in the frequency of obesity and multiple disease. Germline mediated epigenetic alterations are required for the transgenerational inheritance of disease. The F3 generation sperm was collected to examine differential DNA methylation regions (DMRs) for the ancestrally exposed DDT male populations. Unique sets of sperm DMRs were associated with late onset puberty, prostate disease, kidney disease, testis disease, obesity and multiple disease pathologies. Gene associations with the DMR were also identified. The male germline epigenetic DMR signatures identified for these pathologies provide potential biomarkers/diagnostics for transgenerationally inherited disease susceptibility. Observations demonstrate that DDT can promote the germline mediated epigenetic transgenerational inheritance of reproductive diseases and other pathologies. The DMRs or epimutations observed in the F3 generation sperm provide potential biomarkers for transgenerational disease and ancestral environmental exposures.

**Alterations in Sperm DNA Methylation, Non-Coding RNA and Histone Retention Associate with DDT- and Vinclozolin-Induced Epigenetic Transgenerational Inheritance of Disease.** Millissia Ben Maamar, Ingrid Sadler-Riggelman, Daniel Beck, Eric Nilsson, Margaux McBirney, Rachel Klukovich, Xie Y., Tang C., Wei Yan, and Michael K. Skinner

Epigenetic transgenerational inheritance of disease and phenotypic variation can be induced by several toxicants. A large number of environmental factors have been shown to promote the epigenetic transgenerational inheritance of disease and phenotypic variation. These include the agricultural fungicide vinclozolin and pesticide DDT (dichlorodiphenyltrichloroethane), as well as nutritional caloric restriction or high fat diets, and stress. This epigenetic transgenerational inheritance phenomenon is highly conserved and appears in a wide variety of species including plants, insects, fish, birds and mammals such as humans. This non-genetic form of inheritance requires epigenetic modifications (DNA methylation, non-coding RNA and histone modifications) of the germline (sperm and egg) to transmit an altered epigenome to the early embryo which can impact the epigenetics and transcriptomes of all subsequently derived somatic cells. The current study was designed to investigate the vinclozolin and DDT induced concurrent alterations of a number of different epigenetic processes including DNA methylation and ncRNA, but also the potential role of histones to help mediate the epigenetic transgenerational inheritance. To do so, gestating females were exposed transiently to vinclozolin or DDT during fetal gonadal development. The directly exposed F1 generation, the directly exposed germline F2 generation and the transgenerational F3 generation sperm were studied. DNA methylation and ncRNA were altered in each generation sperm with the direct exposure F1 and F2 generations being distinct from the F3 generation epimutations. For the first time, a reproducible core of histone H3 retention sites was observed using an H3 chromatin immunoprecipitation (ChIP-Seq) analysis in the

control, vinclozolin and DDT lineage F1, F2 and F3 generations. Interestingly, additional differential histone retention sites (DHRs) were only observed in the F3 generation exposure lineage sperm. All three different epimutation types were affected in the DDT and the vinclozolin lineage transgenerational sperm (F3 generation). The direct exposure generations (F1 and F2) epigenetic alterations were distinct from the transgenerational sperm epimutations (F3). Moreover, these epimutations do not overlap between DDT and vinclozolin showing that each chemical has a unique epigenetic signature. The genomic features and gene pathways associated with the epimutations were investigated to help elucidate the integration of these different epigenetic processes. Observations demonstrate that in addition to alterations in sperm DNA methylation and ncRNA previously identified, the induction of DHR sites also appear to be involved and integrated in the mediation of the environmentally induced epigenetic transgenerational inheritance phenomenon.

**The DNA Methylation Status Influences the Kinetics of First Cleavages During in Vitro Development of Embryos.** Jéssica Ispada, Camila Bruna de Lima, Érika Cristina dos Santos, Kelly Annes, Patrícia Kubo Fontes, Marcelo Fabio Gouveia Nogueira, and Marcella Pecora Milazzotto

The timing of the first cleavages has been used, especially in humans, as a biomarker of embryo quality and pregnancy outcome. In bovine, we previously reported that this character influences the not only metabolic features but also the global transcriptome and methylome of blastocysts (Milazzotto et al., 2016 and Ispada et al., 2018). In this work, we investigate the levels of DNA methylation throughout the embryo development and the transcriptional profile of DNA methylation enzymes in blastocysts with different kinetics of first cleavages. Fast (4 or more cells at 40 hours post insemination) and Slow bovine embryos (2-3 cells) were in vitro produced with sexed semen using standard protocols remaining in culture until the blastocyst stage. At 40hpi (CL) and 96hpi (EGA) embryos were collected for DNA methylation analysis and at 168hpi embryos (BL) were collected for both DNA methylation and transcript quantitation analysis. For DNA methylation, embryos (5-10 structures for each stage and group/ 4 replicates) were immunostained with 5 methylcytosine (5mC) antibody. The fluorescence intensity from each nucleus was quantified using ImageJ (17-54 CL, 69-74 EGA and 368-486 BL), normalized by the nucleus area and analyzed by Student's t-test (kinetics) or one-way ANOVA (stage). For transcript quantitation, embryos (4 replicates/ 3 blastocysts per group) were analyzed by BioMark™. PPIA was used as endogenous control for  $\Delta$ Ct calculation and data were submitted to Student's t-test (kinetics). DNA methylation were lower in slow compared to fast embryos in all development stages (FCL 19.561±1895 A.U. vs SCL 2.559±614,2 A.U.; FEGA 39.973±4974 A.U. vs SEGA 9.374±599,8 A.U.; FBL 58.885±1550 A.U. vs SBL 19.199±687,9 A.U.;  $P < 0.0001$ ). It is important to note that DNA methylation status is similar between FCL and SBL groups. An increase in DNA methylation occurred throughout the embryo development for both groups ( $P < 0.0001$ ), except in the transition to SCL to SEGA ( $p=0.06$ ). Regarding the gene expression analysis, there was no difference between the transcription levels of DNMT3a and DNMT3b, mainly involved in de novo DNA methylation. However, the presence of DNMT1 mRNA, required for methylation hemimethylated sites during the cell cycle was higher in FBL than SBL ( $P=0,05$ ). The present study corroborates the previous microarray report from our group in which FBL presented increased number of hypermethylated regions in comparison with SBL. These higher levels of DNA methylation might be due to the increased expression of DNMT1. Despite that, the present data also indicate that the difference between FBL and SBL occurs from earlier stages of development, since the difference between groups was already present in cleavage stage.

### **Alterations in Fetal Organ Haemodynamics in Response to Maternal Nutrient Restriction in the Ewe.**

Colleen Lambo, Elizabeth MacConnell, Shannon Washburn, and M. Carey Satterfield

A nutrient restriction model in gestating ewes has proven valuable for producing small for gestational age (SGA) offspring. This has allowed for research into the impacts of nutritional insults on placental programming and subsequent postnatal health and disease. We have recognized that this highly utilized model does not produce a homogeneously impacted phenotype, as frequently assumed. Nutrient restricted (NR) ewes respond in a spectral manner, with some compensating for the loss of nutrition, and producing fetuses that are comparable in weight to those from control-fed ewes. Our recent studies have focused on comparisons of the range of fetal weights produced by a NR model, seeking to identify factors that could predict or mitigate an extreme reduction in fetal size. Using our established NR model, we hypothesized a reduction in fetal organ blood flow (BF) between control fed (n=5; 100%NRC) and NR (n=32; 50%NRC) ewes having SGA fetuses, but not those having normal weight fetuses. To study fetal BF, catheters were surgically placed into the fetal abdominal aorta and inferior vena cava through insertion into the cranial tibial arteries and saphenous veins on gestational day (GD)117. On GD121, a neutron-activated microsphere suspension (Biopal, Inc) was administered to the fetus through the venous catheter, while a reference sample was continuously drawn from a fetal arterial catheter using a syringe pump (New Era Pump Systems, Inc). Dams were sacrificed, and fetal organs processed for microsphere quantification, and flow calculation. Fetuses from the NR treatment group displayed the expected spectral phenotype where lower quartile fetuses were considered SGA (n=7; NR-SGA;  $2.71 \pm 0.10$  kg), and upper quartile fetuses (n=7; NRnon-SGA;  $3.82 \pm 0.14$ kg) were comparable to control fetal weights ( $3.38 \pm 0.17$ kg). Results showed that fetal cerebral cortex had lower BF/gram in the NR-SGA group than NRnon-SGA or control groups. Pancreatic tissue had lower BF/gram in both NR groups than control and a linear correlation was seen for pancreatic BF/gram and fetal weight across all NR fetuses ( $R^2 = 0.16$ ;  $P < 0.03$ ), such that fetal weight increased in association with greater pancreatic BF. When BF/gram was multiplied by whole organ weight; the thymus and kidney had lower flow per organ in the NR-SGA group than NRnon-SGA or control groups ( $P < 0.05$ ), and the cerebral cortex flow was higher in the NRnon-SGA group than in control and NR-SGA groups. There was also a trend toward significance for the heart, liver, and brown adipose tissue ( $P < 0.1$ ). In cotyledonary tissue, BF/gram was not different between groups, but NR-SGA fetuses had a lower total cotyledonary weight, resulting in lower total cotyledonary BF ( $P < 0.01$ ); regression analyses of cotyledonary mass ( $R^2 = 0.45$ ) and total flow ( $R^2 = 0.23$ ) to fetal weight in the NR group were significant ( $P < 0.01$ ), while a regression of cotyledonary BF/gram was not. With previously described differences in pancreatic weights, and compromised insulin production and function within NR-SGA fetuses, this data extends our current knowledge. Insulin does not cross the ovine placenta, and changes impacting pancreatic size and function, and thus compromising insulin actions have a strong relationship with a compromised fetus.

### **Testis Enriched Actin Related Proteins Mediate Spermatid Specific Cytoskeletal Roles Essential for Spermiogenesis and Male Fertility.** Tracy Clement and Mitch Eddy

Proper spermatid morphogenesis is essential to male fertility. This complex process involves restructuring of essentially all cellular components including intracellular transport mechanisms, chromatin, and cytoskeleton. To better understand how cellular processes are adapted for spermiogenesis, the roles of testis enriched Actin Related Proteins (ARPs) are being investigated. The

ARP family includes somatic proteins with essential roles in intracellular transport, chromatin dynamics, and actin cytoskeleton dynamics. The roles of testis enriched ARPs however were previously unknown. We have shown that ACTL7B is essential specifically for male fertility and serves a key role in spermatid morphogenesis. We now report ACTL7B interactions suggesting a mechanistic role through novel cytoskeletal associations affecting the spermatid specific F-actin containing acroplaxome and the spermatid specific microtubule based organelle called the manchette. The localization of ACTL7B to the developing acrosome suggested a potential role of ACTL7B in regulation of the F-actin component of the acroplaxome of the subacrosomal perinuclear theca. In support of this hypothesis, immune-gold labeling of spermatids visualized by electron microscopy shows a subcellular localization largely to this peri-nuclear acroplaxome region. Furthermore, the F-actin in this region of developing spermatids is disorganized and detaches from the nuclear surface of elongating spermatids. This is at a time when the microtubular manchette forms and is instrumental in the intraspermatid transport pathway and mechanotransduction of force for spermatid elongation. In the ACTL7B-null spermatids, the Manchette is not properly anchored at the peri-nuclear ring region to the acrosome, nuclear or plasma membranes. We found that ACTL7B associates with tubulin and that tubulin post-translational modifications are altered in ACTL7B-null spermatids. This work demonstrates a novel ARP role in male fertility affecting the actin and microtubule cytoskeleton, and a novel ARP-family member role in tubulin regulation.

**The Effect of Thymic Nurse Cell (TNC) Exposure on the Uterus in NZBWF1 Mice.** Eboni Price, Michael Henderson, Maria Martinez, Chastity Bradford, Donuniqua Fine, Terrance Platt, and Olga Bolden-Tiller

Systemic lupus erythematosus (SLE) or lupus is a chronic autoimmune disease that attacks many organs of the body and has been predominately characterized as a female disease, as it is estimated that four to 12 females for every one male is at risk for SLE within the child bearing ages of 15 to 44 in humans with a significance in African-American women. SLE is known to cause considerable damage to the reproductive system in females. Autoimmune oophortitis, a rare cause of primary ovarian insufficiency, has been associated with lupus and estrogen and occurs when the body's immune system attacks the ovaries and uterus causing inflammation, fibrosis, and atrophy. Recent studies suggest that a reduction in the number of TNC correlates with the aggressiveness of SLE reported in the NZBWF1 mice, which displays human like symptoms. We hypothesize that TNC exposure can mitigate the effects of SLE on the female reproductive system. The objective of the current study was to utilize the NZBWF1 mouse model to determine the effect of SLE and the exposure of TNC on the uterus. NZBWF1 mice were assigned to one of the following groups: A = No Treatment (n=6), B = Saline (n=7), and C = TNC Injected (n=9), and BALB/c mice were used as a control (group D; n=8). Groups A and B were pooled for the statistical analysis ANOVA. Animals were treated at 12 weeks of age and sacrificed at 16 weeks at which time the uteri and ovaries were harvested and weighed. The uterine weight for groups A ( $0.095 \pm 0.017g$ ) and group B ( $0.102 \pm 0.106g$ ) were not significantly different, and when pooled, the uterine weights for these animals ( $0.098 \pm 0.008g$ ) were significantly lower (P This research was supported by USDA/NIFA80-22090210 and the NIH RCMI Grant# G12RR003059-21A.

**PAX2 Loss Recapitulates Secretory Cell Outgrowths (SCOUTs), Precursors to High-Grade Serous Ovarian Cancer.** Jose Colina, Subbulakshmi Karthikeyan, Peter Varughese, and Joanna E. Burdette

Ovarian cancer is the most lethal gynecological malignancy and the 5th leading cause of cancer death among women. In 2017 alone, there were predicted be over 14,000 deaths and over 22,000 new cases

of ovarian cancer. The deadliest subtype of disease is called high grade serous ovarian cancer (HGSOC) with an average 5-year survival rate of 29%. The fallopian tube epithelium (FTE) gives rise to pre-cancerous secretory cell outgrowths (SCOUTS), which can then progress to become HGSOC. PAX2 is a transcription factor that, when lost, gives rise to a SCOUT, indicating that loss of PAX2 is an early event in the pathogenesis of ovarian cancer from the FTE. Recent publications, have characterized 2 distinct sub-types of SCOUTS based on histological and microarray analysis of human lesions: type 1 SCOUTs are considered benign while, type 2 SCOUTs display a more dysplastic histology and mRNA expression pattern consistent with pre-malignant and malignant tubal masses. In the present study, we developed PAX2 deficient murine oviductal epithelial (MOE) cell lines (analog of human FTE), to model loss of PAX2 in the development of SCOUTs, and study how it potentiates the FTE for further transformation. We modeled PAX2 deficiency into MOE cells, with either a stable PAX2 shRNA knock down, to explore partial PAX2 loss or, PAX2 CRISPR/CAS9 knockout to study cells with complete loss of PAX2. Loss of PAX2 in MOE cells, regardless of level of PAX2 deficiency, lead to no significant cancer specific phenotypic changes including adhesion, migration, and proliferation; this observation is typical of a benign precursor lesion. However, RNA sequencing of PAX2 shRNA cells revealed a transcriptional overhaul that resulted in an mRNA expression pattern similar to human SCOUTs. Moreover, the RNAseq showed that PAX2 deficient MOE cells more closely matched the unique transcriptional fingerprint of type 2 SCOUTs over type 1 SCOUTs. Further analysis of the RNAseq, revealed that loss of PAX2 potentiated the cells for tumor progression through changes in key pathways. One key pathway identified was AKT signaling where we observed an upregulation in AKT3, PI3K, PIP3, GRB2 and more. Additionally, it has been shown that re-expressing PAX2 in PTEN null FTE tumor models reduces cell survival and reduces tumor burden that may be related to a reduced AKT signaling. Furthermore, cross analysis of our RNAseq data with RNAseq of estrogen stimulated MOE cells revealed remarkable overlap similarly altered genes suggesting that loss of PAX2 regulates hormonal responses. Hormone responsiveness of these cells was investigated using ERE and PRE luciferase assays which revealed higher basal hormone activity and sensitivity to hormone treatment with loss of PAX2. In summary, loss of PAX2 in early lesions does not manifest itself in transformative phenotypes, but rather in potentiating changes in the transcriptome, particularly in key pathways shown to be dysregulated in HGSOC such as AKT, estrogen, and progesterone signaling.

**Methyltestosterone But Not Dihydrotestosterone is Sufficient to Induce Tubular Urethra and Penile Formation in Female Mice.** Shanshan Wang, John Lawless, and Zhengui Zheng

Previous studies suggested that genital tubercle before sexual differentiation had bisexual potential, exposure to androgen especially dihydrotestosterone (DHT) could drive to masculinization and penile formation. To determine whether DHT is sufficient to induce penile formation in females, we compared the effect of DHT and methyltestosterone (MT) on external genital masculinization in female mice, attended to induce penile formation in females and further understand the androgen-controlled masculinization of external genitalia. Prenatally and neonatally DHT (2mg/kg) treated female mice failed to induce tubular urethra and penile formation, same stage MT (2mg/kg) treated all female mice (100%) formed penises with all characteristics the male penis has, including tubular urethra, os-penis with distal cartilage, corpus cavernosum, corpus spongiosum and penis spines at the weaning time. We further revealed that only prenatal MT is required for induction of penis formation in females. As DHT has more potential binding androgen receptors than testosterone, we keep the neonatal treatment dosage the

same and treated prenatal mice with DHT in different concentration groups (50 $\mu$ g/kg, 250 $\mu$ g /kg, 2mg/kg and 5mg/kg, each group minimum 3 litters), the penile development had no obvious effect in F1 males, but enlarged clitoris in F1 females, interestingly, the urethra of all treated F1 females were open and form female hypospadias in all the treatment groups (100%). The developing urethral epithelial and mesenchymal cells in MT, but not DHT treated females also showed similar patterns in cell proliferation, cell death and urethral fusion as control males. In addition, androgen receptor localization and selected downstream genes expression in MT, but not DHT treated females were found similar to control males. We further revealed aromatase was strongly expressed in developing genital tubercle and placenta using aromatase cre tdTomato reporter mice, and MT treatment failed to induce penile formation in aromatase knockout female mice. Our data suggest that prenatal MT but not DHT is sufficient to induce tubular urethra and penile formation in female mice, aromatization and endogenous estrogen at prenatal stage may play a role in MT induced penile formation in females. Research supported by medical school of SIU to ZZ.

**Characterization of ACE 2 in the Testis of a Type 2 Diabetic Mouse Model with Cardiac Ischemia Reperfusion Injury.** DonunIQUE Fine, Mikhail Kolpakov, Abdelkarim Sabri, Chastity Bradford, and Olga Bolden-Tiller

Currently, several assisted reproductive technologies utilize testicular germ cells to investigate infertility. However, to take full advantage of these technologies, it is important to understand molecular mechanisms associated with male reproduction, including spermatogenesis which is hormonally regulated. The National Institute of Diabetes and Digestive and Kidney Diseases reported that 90% of the 10.3 million Americans with diabetes have type 2 diabetics. Further, adults diagnosed with type 2 diabetes are twice as likely to develop coronary artery disease. Chronic diabetes has been shown to promote ischemia and oxidative stress, which can disrupt male reproductive function. Although timely and effective reperfusion rescues ischemic tissue, it exacerbates damage, leading to ischemia reperfusion injury (IRI). The renin-angiotensin system (RAS) is a hormonal signaling pathway that regulates blood pressure and is shown to play a pertinent role in the male reproductive function. Components of RAS, such as angiotensin converting enzyme 1 (ACE1) and angiotensin converting enzyme 2 (ACE2), have been identified in the testes, epididymis, Leydig cells, and spermatozoa and are involved in processes associated with testicular function. However, further research is needed to fully understand the role of RAS in the testes, particularly in type 2 diabetic individuals with cardiac IRI, for which there are no reports. To determine the effect of cardiac IRI on testes of diabetic mice, heterozygous (dB/+) and diabetic (dB/dB) mice were divided into one of four groups (G1-G4). G1 (dB/+ + sham [n=15]) and G2 (dB/dB + sham [n=11]) were controls. The remaining groups, G3 (dB/+ +IRI [n=13]) and G4 (dB/dB + IRI [n=12]), had ischemia induced for 30 minutes followed by reperfusion for eight weeks. Animals were then euthanized; the heart, tibia, and testes were harvested and evaluated. As expected, the fed state blood glucose levels for G1 (137.13 $\pm$ 6.95 mg/dL) and G3 (112.77 $\pm$ 2.77 mg/dL) were lower (P < 0 .05) compared to G2 (491.91 $\pm$ 27.11mg/dL) and G4 (492.58 $\pm$ 20.24 mg/dL). As expected, the body weight for G1 (30.7 $\pm$ 0.53g) and G3 (29.6 $\pm$ 0.51g) were lower (P < 0 .05) compared to G2 (44.0 $\pm$ 2.28g) and G4 (49.3 $\pm$ 1.76g). The body weight/tibia length ratio for G1 (13.93 $\pm$ 0.69g/mm) and G3 (12.38 $\pm$ 0.19g/mm) was lower (P < 0 .05) compared to G2 (19.04 $\pm$ 0.94g/mm) and G4 (21.20 $\pm$ 0.73g/mm). The heart weight/tibia length ratio for dB/+ mice (0.079 $\pm$ 0.006g/mm) was significantly lower (P < 0 .05) compared to dB/dB mice (0.101 $\pm$ 0.012g/mm). Testicular weights of G1

(0.21±0.01g) and G3 (0.18±0.01g) were greater ( $P < 0.05$ ) compared to G2 (0.13±0.01g) and G4 (0.12±0.01g). The seminiferous tubule diameter for G4 (122.87±7.9µm) was significantly lower ( $P < 0.05$ ) compared to G1 (156.63±5.73µm), G2 (149.00±5.88µm) and G3 (140.66±3.75µm). Immunohistochemistry showed no ACE2 expression in G1; however, low intensity ACE2 staining in interstitial cells in G2, G3 and G4 was detected. These data show that the IRI negatively impacts testicular morphology, and that the dB/dB mouse provides a good model to evaluate the impact of comorbid conditions, such as diabetes and cardiovascular disease, on the testes. However, further analysis is needed to discern the molecular mechanisms associated with these observations. Research supported by the State of Alabama/Alabama Agricultural Land Grant Alliance 80-31244155, USDA/NIFA 80-22090210, and American Heart Association 15SDG22650004.

**High-Resolution Transcriptome Analysis of the Primate Testis by Single Cell RNA-Sequencing.** Sarah Munyoki, Adrienne N. Shami, Qianyi Ma, Chris Green, Jun Li, Sue Hammoud, and Kyle Orwig

Cytotoxic treatments for cancer like chemotherapy can damage spermatogonial stem cells (SSCs) in the testes causing permanent infertility. Cryopreserving sperm before treatment is currently the only reliable option for patients to safeguard their fertility. This option is not available to prepubertal boys however, as they have not yet begun producing sperm, the loss of fertility can have devastating effects on their quality of life. Testicular tissue freezing has emerged as an option for these boys, because their testes contain SSCs that can be exploited to potentially restore fertility. This approach has been demonstrated in rodents, where mouse SSCs (mSSCs) were transplanted into the testis of an infertile recipient male, regenerating spermatogenesis. We successfully replicated this technique in Rhesus macaques made infertile by alkylating chemotherapy. These results highlight the potential use of SSC transplantation therapy in the human clinic. However, transplantation efficiency is directly correlated to the quantity of SSCs injected into the testes thus the small biopsies taken from prepubertal boys may not contain sufficient SSCs for transplantation. It may therefore be necessary to first expand the SSCs in vitro, to generate enough cells for robust engraftment. Long-term mSSC culture was achieved by supplementing media with GDNF and bFGF, growth factors produced by the endogenous mSSC niche, that regulate mSSC self-renewal and proliferation. Whether these growth factors are conserved from rodents to humans remains unknown. Additionally, it is not possible to evaluate the spermatogenic potential of in vitro propagated human SSCs by transplantation and production of progeny in the laboratory. We will utilize the nonhuman primate model which closely resembles human testicular biology and is amenable to transplantation. While the basic processes of spermatogenesis are similar among mammals there is some divergence at a genetic and cellular level. Consequently, it is reasonable to presume that primate SSCs have unique growth factor requirements. Identifying these growth factors would allow us to mimic the primate SSC microenvironment in vitro. We have employed Drop-Seq a high throughput microfluidic technique for single-cell RNA-sequencing (scRNA-seq) of the monkey testis. Unlike bulk tissue RNA-seq which has the potential to mask relevant signals from rare cell types, scRNA-seq allows us to generate ~22,440 single cell transcriptomes representing all cell types in the heterogeneous Rhesus testis, including the rare SSCs. Principal component analysis and unsupervised clustering have defined transcriptionally distinct Rhesus testicular cell populations. The expression of well characterized markers for the different testicular cell types were used to identify cell types. Future work will focus on the Rhesus SSC (rhSSC) transcriptome data to determine growth factor receptors they express, as well as their corresponding ligands expressed by the testicular somatic cells that are

important for rhSSC self-renewal and proliferation. The identified ligands will be candidates for testing in Rhesus culture. If successful, the cultured rhSSCs can be functionally evaluated by autologous or homologous transplantation into the testes of infertile Rhesus recipients. This research was supported by NIH/NICHD P01 HD075795, NIH/NICHD R01 HD055475 and NIH/NICHD R01 HD076412.

**The Fluorescence-Based Morphometry Computer-Assisted Sperm Analysis has a Potential to Determine Progeny Sexed Spermatozoa in Both African (*Loxodonta Africana*) and Asian (*Elephas Maximus*) Elephants.** Saroch Kaewmanee, Nithida Boonwittaya, Pattama Nitthaisong, Birendra Mishra, Jamroen Thiengtham, Marnoch Yindee, and Anuchai Pinyopummin

Separation of X- and Y-chromosome bearing sperm has been performed for selection of desired sex of offspring to increase the profit in companion animals, livestock and endangered species.

This study was designed to determine the ability of computer-assisted sperm analysis morphometry (CASA-Morph) with Fluorescence in-situ hybridization (FISH) to discriminate between spermatozoa carrying different sex chromosomes in the elephants.

The experiment was to study the morphometric differences between X- and Y-chromosome-bearing spermatozoa (SX and SY, respectively). Spermatozoa from four bulls (2 from African and 2 from Asian bulls) were processed to assess simultaneously the sex chromosome by FISH and sperm morphometry by fluorescence-based CASA-Morph. SX cells were larger than SY cells on average.

We concluded that the CASA-Morph fluorescence-based method has the potential to find differences between X- and Y-chromosome-bearing spermatozoa in elephant species. More studies are needed to increase the precision of sex determination by this method.

**Modulation of the Developing Male Reproductive Axis by Phthalates: Diethylhexylphthalate and Diisononyl Phthalate Effects in Male Rats.** Rachel Knight, Bamidele Jeminiwa, and Benson T. Akingbemi

Phthalates are used as plasticizers and as solvents in consumer products, including cosmetics and children's toys and in medical tubing and catheters. Increasing public concern has arisen in response to reports that exposures to phthalates may result in abnormalities of the reproductive tract in the human male. Several studies in laboratory species also demonstrated that diethylhexylphthalate (DEHP), the most abundant phthalate in the environment, caused reproductive tract anomalies. Compared to DEHP, some studies suggested that diisononyl phthalate (DINP) had reduced effects on male rat development. DINP is therefore thought to be an environmentally friendly plasticizer that may be used to replace DEHP in the manufacture of consumer products. The pituitary gonadotropins [follicle stimulating hormone (FSH) and luteinizing hormone (LH)] are the primary regulators of gonadal development and function. FSH receptors are exclusively present in Sertoli cells, and LH receptors are localized mostly to Leydig cells. On the other hand, steroid nuclear receptors [androgen and estrogen receptors (ARs and ESRs)] which are present in reproductive tract tissues mediate steroid hormone effects in the hypothalamus and pituitary gland, and thereby regulate pituitary gonadotropin secretion. For these reasons, we have initiated a study to compare DEHP and DINP effects in the developing male reproductive axis. In separate experiments, 21 day-old Long-Evans male rats (n=6) were fed DEHP or DINP in drinking water

ad libitum at 0, 5, 10, 15 and 20 µg/L for 14 days, i. e, from weaning at 21 days until 35 days of age. Chemicals were dissolved in DMSO to achieve solubility and were fed in drinking water to avoid activation of the hypothalamus-pituitary-adrenal axis, a common gavage effect. Chemical exposures were terminated at 35 days of age when animals were sacrificed to collect pituitary glands and testes. Tissues were processed for Western blot analysis to measure pituitary FSH $\beta$  and LH $\beta$  subunit protein and testicular anti-Müllerian hormone (AMH) protein expression levels. Exposure to DEHP increased pituitary FSH $\beta$  protein while DINP caused the opposite effect, and these effects were significant at the highest exposure levels; i.e., 20 µg/L of drinking water ( $P < 0.05$ ). On the other hand, testicular AMH protein was decreased after exposure to DEHP but were increased by DINP ( $P < 0.05$ ). These observations imply that exposures to DEHP and DINP have a similar capacity to interfere with gonadotropin secretion in prepubertal male rats. The possibility that DEHP and DINP-mediated changes in gonadotropin secretion affect testis development will be investigated along with other mechanisms of endocrine disruption that target the steroidogenic machinery in the testis. Understanding the mechanistic basis of endocrine disrupting chemical activity in reproductive tract tissues will facilitate identification of vulnerable segments of the population and facilitate development of strategies to mitigate chemical exposure effects. This study was funded in part by the Animal Health and Disease Research Program of the College of Veterinary Medicine at Auburn University (to BTA).

**Gut Microbiota Drives Progression of Endometriosis.** Sangappa B. Chadchan, Lindsay A. Parnell, Meng Cheng, Yin Yin, Andrew Schriefer, Indira U. Mysorekar, and Ramakrishna Kommagani

Endometriosis, which causes pain in the pelvis and lower abdomen, afflicts up to 10% of women between the ages of 25 and 40 in the United States. Current treatments for endometriosis, such as hormone therapy and surgery, have negative side effects and do not prevent recurrences, so a new approach is needed to reduce the incidence of this disease. A well-accepted theory is that endometriosis occurs when endometrial tissue enters the peritoneal cavity via retrograde menstruation and implants itself onto pelvic organs and peritoneal surfaces. However, whereas up to 90% of women experience retrograde menstruation, only 10% of women develop endometriosis, suggesting that other factors contribute to the development of endometriosis. We hypothesized that one factor promoting endometriosis is the gut microbiome. To test this hypothesis, we surgically induced endometriosis in intact adult female mice and then treated them with either control/vehicle or with the broad-spectrum antibiotics vancomycin, neomycin, metronidazole, and ampicillin (VNMA) for three weeks. We then isolated the eutopic uterus, ectopic endometriotic lesions, and distal colonic tissue. Compared to mice treated with vehicle, mice treated with VNMA had fewer bacteria in the distal colon and smaller ectopic endometriotic lesions ( $p < 0.001$ ) with lower expression of the proliferation marker Ki-67 and the angiogenesis marker CD31. Although we detected no bacteria in endometriotic lesions, we found that mice with endometriotic lesions contained more bacteria in their distal colons than did mice that were not subjected to the endometriosis-inducing surgery. We performed bacterial community profiling (by 16S amplicon next-generation sequencing) on fecal samples and identified one specific phylum enriched in the mice with endometriotic lesions but not in the mice that were not subjected to the surgery or in the VNMA-treated mice that were subjected to the surgery. Collectively, we provide compelling evidence that gut microbiota, and perhaps a particular phylum, promote endometriotic lesion growth. Our findings provide novel mechanistic insight about the causes of endometriosis progression and may lead to the development of microbiota-altering therapeutics to prevent or treat this painful disease.

This research was supported by a National Institutes of Health/National Institute of Child Health and Human Development grant (R00 HD080742).

**The Effects of Testosterone on the Viability of the -TM4 Sertoli Cell Line.** Khalda Fadlalla, Ebony Gilbreath, and Olga Bolden-Tiller

The demand for goat is one of fastest growing segments of livestock production in the United States, which is a reflection of the changing demographics. Nonetheless, the United States goat industry remains in its infancy. Assisted reproductive technologies (ART) have the potential to rapidly propagate superior genetics in goats which could positively impact the goat breeding stock and subsequently the industry. Understanding the molecular mechanisms associated with testicular function and spermatogenesis can lead to the improvement of existing and the development of new ART to help address this issue. Spermatogenesis is highly controlled by endocrine and paracrine factors, such as testosterone, that affect the testicular cell-cell interactions. It has been shown that a number of cytokines, such as interleukin-6 (IL-6), are thought to be involved in the regulation of spermatogenesis. Interleukin-6 (IL-6) is a multifunctional cytokine produced mainly by macrophages in response to foreign antigens, pathogens, and also in chronic inflammation (immunologic activation). Cells of nonimmune cell origin, such as dendritic cells, fibroblasts, endothelial cells, smooth muscle cells, mesangial cells, astrocytes and epithelial cells, also produce IL-6, which has been shown to be regulated by testosterone (T). The binding of IL-6 to gp130 activates the JAK/STAT signal transduction pathway, facilitating proliferation and differentiation. IL-6 and other cytokines have been found in the seminal plasma of fertile and infertile men and associated with germ cell differentiation. Under in vitro conditions, Sertoli cells secrete IL-6 following stimulation with low levels of testosterone and follicle stimulating hormone in mice. Currently, little to no information on IL-6 is available in goats, particularly in the testes. The overall objective of the lab is to characterize IL-6 in goat testes during three life stages: neonatal (0.05), Suggesting that this model is acceptable to evaluate the effect of T on IL-6 in Sertoli cells by enzyme-linked immunosorbent assay. Further, preliminary data from our lab indicate that this model show that IL-6 is detectable by ELISA. This work was supported by Alabama Agriculture Land Grant Alliance #80-31244155, USDA/NIFA #80-22090210 and NIH #31-21130009.

**Structural, Mechanical, and Biochemical Characterization of Ovarian Decellularized Extracellular Matrix Hydrogels.** Emma Gargus and Teresa K. Woodruff

Our group was the first to decellularize an ovary, repopulate it with ovarian cells, and demonstrate that the decellularized ovarian tissue scaffold supported function of ovarian cells in vitro and in vivo. Despite this success, the use of decellularized tissue scaffolds comes with severe limitations; specifically, matrix properties and matrix architectures are “locked in”, and it is very difficult to control the placement and seeding efficiency of different cell types (important for full organ function) within the structure. To overcome these limitations, we processed ovarian decellularized ECM into ovary-specific hydrogels, compatible with follicle encapsulation, micromolding, and direct extrusion 3D printing. Briefly, hydrogels were prepared by digesting milled decellularized ECM powder in acidic pepsin solution and then, the resulting pre-gel solution was cross-linked by neutralizing the pH and incubating at physiologic temperature. The goal of this study was to characterize the structural, mechanical, and biochemical

properties of decellularized ECM hydrogels derived from bovine cortex, medulla, and whole ovary. To analyze structure, 5 mg/mL decellularized ECM hydrogels were fabricated and imaged using scanning electron microscopy. Porosity and fiber organization were analyzed using DiameterJ, a validated nanofiber characterization tool through ImageJ. Percent porosity was similar between cortex-, medulla-, and whole ovary-derived hydrogels (49.76, 48.03, and 44.87% respectively), but fiber orientation in the medulla-derived hydrogels was unique. Whereas medulla- and whole ovary-derived hydrogels showed one or two discrete peaks in orientation angle, the fibers in medulla-derived hydrogels were distributed randomly. Next, the kinetics of gelation and the final mechanical properties (storage & loss modulus) of the resulting hydrogels were measured using rheology. The gel point was reached within two minutes for all formulations, which indicates that the gelation kinetics of ovary-derived ECM hydrogels are compatible with follicle encapsulation. We found that medulla-derived hydrogels were more rigid than either whole ovary- or cortex-derived hydrogels (storage modulus 351.31 vs. 242.50 vs. 151.50 Pa, respectively). Finally, the biochemical composition of the decellularized ECM hydrogels derived from cortex, medulla, and whole ovary were compared. We specifically assayed for collagen (using the hydroxyproline assay) and sulfated proteoglycans and glycosaminoglycans. Due to prior successes using decellularized and collagen hydrogels, decellularized ECM hydrogels will likely support follicle survival, growth, and function in *in vitro* culture. Future work will investigate the tissue- and compartment-specificity of the bioactivity of decellularized ECM hydrogels. For example, we are investigating whether outcomes differ between follicles cultured in ovary-derived ECM hydrogels compared to testis- or other non-matched tissue-derived ECM hydrogels. We will also study whether particular follicle populations (e.g. primordial follicles) prefer particular fractions of ovarian ECM hydrogels (e.g. cortex). This study contributes to a body of work regarding biomaterials for follicle culture and transplantation, with the ultimate goal of developing functional ovarian tissue mimics for *in vitro* analysis or to restore ovarian function *in vivo*, respectively.

This work was supported by the National Institutes of Health National Center for Translational Research in Reproduction and Infertility (NCTRI) Center for Reproductive Health After Disease (P50HD076188).

**Development of a Functional 3D Human Uterine Myometrial Tissue Model.** Heather Burkin, Megan Rulla, Janet Lambert, and Craig Ulrich

Our long-term goal is to understand the molecular pathways that lead to preterm birth and to identify therapeutic methods to prevent or delay spontaneous preterm birth. Progress towards this goal is complicated by the fact that the molecular regulation of human parturition is not fully understood and appears to differ substantially from regulation in animal models. Two-dimensional cell culture models do not always mimic the characteristics of three-dimensional tissue and cannot be used for contractile studies. Contractile and pharmacological experiments require a steady source of human preterm tissue and these samples are relatively difficult to obtain. Our laboratory is seeking ways to maximize the data we can extract from every preterm sample and to share available tissue samples. The objective of this work is to develop and validate a new 3D human myometrial tissue model in which to study uterine contraction. To determine whether synthesized 3D human myometrial tissue responds physiologically to the contractile-agonist oxytocin, term human uterine myometrial tissue was obtained under informed consent. Myometrial cells were mechanically separated, strained, centrifuged, and resuspended in cell culture medium (DMEM) containing 10% serum (FBS), antibiotics, and estrogen and progesterone in

concentrations to mimic third trimester human pregnant plasma concentrations. Isolated cells were allowed to proliferate on cell culture dishes at 37°C, 5% CO<sub>2</sub>. After 3-4 passages, cells were trypsinized, rinsed with calcium-free PBS, and combined with bio-ink. An Aspect Biosystems RX1™ Bioprinter was used to deposit myometrial cells in 12 mm rings in an alginate scaffold containing collagen. Cells within synthesized rings were allowed to proliferate for 24 h and then transferred to DMEM containing 0.1% FBS with estrogen and progesterone and allowed to differentiate and form interconnected networks for 7 days. Rings were incubated with Calcein AM, Hoechst, and propidium iodide to assess cell viability. Contraction was assessed by measuring the change in ring diameter in response to 8 nM oxytocin. Both primary and immortalized human uterine myometrial cells within 3D printed rings displayed >90% viability, and the rings averaged 9% area reduction in response to oxytocin compared to control rings treated with vehicle. These results indicate that cultured uterine myometrial cells retain the ability to contract in response to a physiological agonist and synthesized tissue rings may be developed for future contractile experiments and tocolytic drug screens.

**Characterization of the Endometrial and Vaginal Microbiome in *Capra Hircus*.** S.K. Lewis, W.B. Foxworth, F.R.B. Ribeiro, L.C. Nuti, L.A. Banks, A.J. Ho-Watson, and G.R. Newton

At breeding, seminal fluid recruits macrophage populations into the endometrium and stimulates an inflammatory response to insemination in several species. Leukemia inhibitory factor and interleukin 1 beta secreted by macrophages increases alpha (1-2)-fucosyltransferase (FUT) activity which increases expression of specific adhesion factors by uterine epithelial cells, including alpha (1-2) fucosylated Histo- and Lewis-blood group carbohydrate antigens. Lymphoid cells and commensal bacteria induce intestinal epithelial FUT expression and fucosylation in mice. Rapid fucosylation of intestinal epithelial cells increases availability of L-fucose attached to cell membrane glycoproteins and glycolipids and may create a symbiotic environment that maintains gut epithelial – commensal microbial interactions and protects against infection by pathogens. Our hypothesis is similar mechanisms involving macrophages, commensal bacteria, FUT and uterine epithelial cells may operate in the uterus and help maintain reproductive tract immunity during the estrous cycle and early pregnancy. Therefore, the objective of this study was to determine if bacteria could be detected in the uterus and if bacterial community composition and structure differs between vaginal and endometrial samples. Goats (n=6) were euthanized using captive bolt stunning and exsanguination on Day three of the estrous cycle. Vaginal swabs were taken before reproductive tracts were clamped at the cervix, removed from the goats, placed in plastic bags containing sterile saline + 1% Rocal and transported to a laminar flow hood. One horn was opened and swabs were taken from the uterine horn and the corresponding body of the uterus. Endometrium (500 mg) was collected from the other uterine horn and the corresponding uterine body. DNA was extracted from swabs and tissues, the V4 hypervariable region of the 16S rRNA gene was amplified, and amplicons were sequenced using Illumina MiSeq2x250b technology. Amplicons were detected in all endometrial tissue samples and endometrial and vaginal swabs. Significant differences in alpha diversity at each sampling site were demonstrated through analysis of observed operational taxonomic units ( $P < 0.01$ ) and Shannon diversity indices ( $P < 0.02$ ). Distinct community composition and structural differences were detected between vaginal and endometrial samples using both qualitative- ( $P < 0.01$ ;  $R^2 = 0.411$ ; PC1+2 = 26.17% variation explained) and quantitative- ( $P < 0.01$ ;  $R^2 = 0.307$ ; PC1+2 = 47.20% variation explained) UniFrac analysis, suggesting the upper female reproductive tract (UFRT) contains a unique microbome when compared to the vagina. Eight different

phyla were identified, with Firmicutes (40% relative abundance), Proteobacteria (24% relative abundance), and Bacteroidetes (16% relative abundance) most abundant in both the upper and lower female reproductive tract. The relative abundance of specific genera of bacteria identified in endometrial and vaginal samples also differed. The relative abundance of *Escherichia/shigella* was greatest in endometrial samples, while *Aerococcus* was the more abundant in vaginal samples. Therefore, the UFRT contains microbial communities that are distinct from those found in the vagina on Day three of the estrous cycle. These microbial communities may contribute to normal uterine functions.

**Investigatory Methods to Model the Male Gonad In Vitro.** Maxwell E. Edmonds, Alexandra R. Rashedi, Micah Forshee, Sharon Tam, Hanna Pulaski, Kyle E. Orwig, and Teresa K. Woodruff

The testis is a sophisticated organ with a compartmentalized architecture, responsible for both fertility and reproductive hormone production. Male fertility preservation has only one clinical option, the banking of sperm. Unfortunately, this is not feasible for patients whom cannot provide a semen sample, most pertinently pediatric male patients. Alternatives to animal models, particularly de novo tissue mimics have seen a resurgence in the past few years. Moreover, little is known about sperm development and testicular endocrine function in vitro, which represents a fundamental knowledge gap in the reproductive science field. We hypothesize that a cellular microenvironment mimetic of in vivo conditions is obligatory for functional in vitro modeling of complex tissues. Therefore, we have proposed that microfluidic culture and biomaterial scaffolds will prove permissive and instructive towards in vitro modeling of testicular tissue. To test this hypothesis, we have compared microfluidic explant culture and extracellular matrix (ECM) -based culture approaches, to assess their ability to maintain testicular explants, and recreate de novo testicular tissues, respectively. Beginning with testis explants, we have demonstrated that human testis explants can be maintained in culture for multiple weeks in both static and microfluidic culture settings. These explants respond to gonadotropins (FSH and hCG) throughout culture, with the production of testosterone and inhibin B. However, germ cell presence starkly decreases during culture. In de novo tissue modeling, we have determined that cell aggregation is a prerequisite for compartmentalization of murine testicular cells, and furthermore, that biomimetic ECMs promote aggregation over controls. Among different ECM trials, 3D culture in Matrigel has produced the most robust cellular aggregation, along with testosterone and inhibin B production. We have also successfully grown organoids in the absence of ECM. These organoids produce testosterone and inhibin B in response to gonadotropin stimulation, and are composed of multiple cell types, including Sertoli, germ, peritubular myoid, and Leydig cells. Further work is needed to optimize our microfluidic explant method, and characterize the structure and function of our organoid model. Sources of Support: National Center for Advancing Translational Sciences (NIEHS/NCATS: UH3TR001207) and the Eunice Kennedy Shriver National Institute of Child Health and Human Development (NICHD: F31HD089693) at the National Institute of Health.

**Functional Mapping of the Equine Blastocoel Fluid Secretome.** Soon Hon Cheong, Viju Pillai, Anthony Herren, Brett Phinney, Juan Castillo, Mariana Diel de Amorim, and Vimal Selvaraj

Equine embryos are unique among domestic species as it remains spherical and migrates within the uterine lumen until day 16 during which it undergoes rapid expansion reaching a diameter of over 20

mm and develops a surrounding acellular blastocyst capsule. This large size associated with the early embryonic physiology makes it possible to study the blastocoel fluid composition in early embryos. Although previous studies have identified some of these proteins, knowledge of secreted proteins in the blastocoel fluid remains limited. Through bioinformatics, it is possible to identify secreted proteins by analyzing signal peptide sequences and differentiating them from likely intracellular protein contaminants from ruptured cells and degrading cellular debris. Simultaneous evaluation of the blastocoel fluid proteome and the embryo transcriptome can determine which secreted proteins in blastocoel fluid are likely produced by the embryo itself and also determine the extent to which the external uterine microenvironment contributes to the proteome of the blastocoel fluid. Such a comprehensive dataset may include the signal for maternal recognition as well as the factor for stem cell maintenance in horses. In vivo produced equine embryos (n=7) were collected on day-11 post ovulation via transcervical uterine lavage with Lactated Ringer's solution and washed 25 times in phosphate buffered saline. Blastocoel fluid was collected and shotgun proteomic analysis performed on individual embryo blastocoel fluid samples. Blastocyst transcriptome analysis was also performed on individual embryos. Proteomics and transcriptomic data were evaluated using a previously developed data analysis pipeline to identify secreted proteins (protein-secretome) and transcripts (transcript-secretome). A total of 1,342 proteins were identified from the blastocoel fluid of which 87 were classified as secreted using a bioinformatics sequence prediction algorithm. Pathway analysis was used to group proteins into classes that included growth factors and cytokines, enzymes, extracellular matrix components and metabolic regulatory proteins. Transcriptome sequencing identified a total of 11,012 transcripts which were classified based on abundance. Functional categorization of highly abundant candidates revealed critical information on proteins involved in extracellular matrix formation and reorganization, growth factors and cytokines, adhesion molecules and other structural proteins critical to the embryo during this period. Comparison of the protein-secretome and transcript-secretome suggested that majority of the secreted proteins (91.5%) of the blastocoel fluid is secreted by the cells of the early embryo. Our protein and transcript integrated data on the secretome of the equine embryo highlights the diversity of the regulatory mechanisms that underlie early embryo development. Furthermore, secreted proteins identified from our study could be candidates for further functional studies to understand maternal recognition of pregnancy, equine pluripotency and early embryo development.

**Effects of the Follicular Environment of ART Patients of Endometriosis on in Vitro Maturation of Mouse Oocytes.** Paola Berrío, Ingrid Zorrilla, Ricardo Pella, Francisco Escudero, Patricia Orihuela, Ygor Pérez, Mario García, and Sergio Romero

At our center 20% of patients requiring Assisted Reproductive Technologies (ART) suffer from endometriosis. Oocytes of such patients have been suggested to develop in an environment with oxidative stress. In order to alleviate such condition, patients are administered antioxidant therapy, however there is few evidence that supports the use of such therapies to improve oocyte wellbeing.

Our objective is to evaluate the effect of the follicular environment (follicular fluids, FF) of infertile patients with endometriosis on in vitro maturation (IVM) of mouse oocytes. Moreover, the antioxidant capacity of such follicular fluids was also assessed.

Ninety-Five F1 female mice (C57xBalb-c), aged 23-days, were primed for 48h with eCG in order to induce follicular growth and allow the collection of immature oocytes at the germinal vesicle stage. After collection and selection, mouse cumulus-oocytes complexes (COCs) were divided into 7 groups and subjected to IVM: G0 (Control), G1 (20% CFF + 0.3% BSA), G2 (10% CFF + 0.3% BSA), G3 (5% CFF + 0.3% BSA), G4 (20% EFF + 0.3% BSA), G5 (10% EFF + 0.3% BSA), G6 (5% EFF + 0.3% BSA). Follicular fluids were obtained during follicular aspiration of patients with endometriosis [3 under antioxidant therapy (+AO) and 3 without it (-AO)]. Following collection and selection of mouse cumulus oocytes complexes (COCs), COCs were randomly distributed into 5 groups: Control (without FF), G1 (20% FF), G2 (20% FF + 0.3% Bovine serum albumin, BSA), G3 (10% FF + 0.3% BSA), G4 (5% FF + 0.3% BSA). The same setup was used for both studies (+AO & -AO). In vitro maturation was performed at 37°C, 5%CO<sub>2</sub> in air, for a period of 18h. Oocyte maturation was assessed by the presence of the first polar body.

In +AO group, the maturation rate of G1 (79.3% ± 12.5%), G2 (94% ± 8.9%), G3 (94.6% ± 8.1%) and G4 (90.2% ± 7.2%) was comparable to the control group (90.9% ± 20.3%) (p>0.05). However, in -AO group, maturation rate of G1 (68.5% ± 10.1%), was significantly lower than G3 (57% ± 17.9%) (p < 0 .05) and G4 (89.2% ± 4%) (p < 0 .05). Thus, these results indicate that follicular fluids of infertile patients with endometriosis without antioxidant therapy, affect maturation of mouse oocytes, in vitro. Apart from the effects on oocyte maturation, follicular fluids of infertile patients with endometriosis were analyzed for its antioxidant capacity. FF were subjected to ABTS [2,2'-azino-bis(3-ethylbenzothiazoline-6-sulphonic acid)], FRAP (Ferric reducing ability of plasma) and TBARS (Thiobarbituric acid reactive substances) assays. In the FRAP assay, follicular fluids of infertile patients of endometriosis, administered (or not) with antioxidant therapy, were significantly lower in their antioxidant capacity than the control group (FF of young donors) (p=0.0096; p=0.0442 respectively).

In conclusion, our findings suggest that the antioxidant capacity of follicular fluids in patients with endometriosis (undergoing ART treatments) administered (or not) with antioxidant therapy is lower than the donor follicular fluids; and therefore, are likely to have an effect on oocyte maturation. Since exposure to follicular fluids of such patients may have effects beyond the maturation capacity, the embryony development of in vitro matured eggs remains to be evaluated.

**IUI Success is Associated with Aberrant Sperm DNA Methylation on the H19 Gene.** Mohammad Abbasi, Latoya Williamson, Alan Horsager, and Philip J. Uren.

Intrauterine insemination (IUI) is a widely used fertility treatment. Previous works have studied IUI success rate and its relation to semen analysis parameters (i.e. count, morphology, and motility) and DNA fragmentation. In recent years, the study of the role of DNA methylation in fertility has received much interest and it has been shown that disruption in sperm epigenetic profiles is associated with fertility rates and poor embryo quality in IVF patients. Despite these advancements, the relation between sperm DNA methylation and IUI success rate still remains to be seen. Here we study genome wide association between sperm aberrant DNA methylation and IUI success rates.

Using array technology, we profiled DNA methylation levels at more than 480,000 CpG sites in semen samples from 66 patients. Samples were collected from four major fertility clinics throughout the United States and Canada, from couples undergoing IUI treatment to achieve pregnancy. Data was normalized to correct for potential batch effects. Differentially methylated regions (DMRs) were detected using the

DMRcate package in R while controlling for male age and with a p-value cut-off of 0.05 for statistical significance of probes. Fisher's method with Sidak correction for multiple hypothesis testing was used to determine the p-value for each region.

We did not observe any significant difference in semen analysis parameters or male and female age between the 20 patients who achieved chemical pregnancy through IUI treatment and 46 who did not. In addition, we probed for specific genomic loci showing strong association between methylation level and IUI success. We identified 9 such regions covering 8 genes with a median of 7 probes (average genomic length = 0.6Kbp). The most highly significant region covered 32 probe locations (average increase in methylation = 6%, corrected p-value =  $1.35 \times 10^{-11}$ , genomic length = 1.3Kbp) and was located in the promoter region of the H19 gene. H19 is a genomic imprinted gene and previous studies have shown that aberrant methylation of this gene is associated with idiopathic male infertility. H19 is also known to be a regulator of the expression of the IGF2 gene which has been shown to be a key player in early embryo development.

To our knowledge this is the first study relating IUI success to aberrant sperm DNA methylation. Our results suggest that sperm epigenetic profile disruptions are associated with IUI success. We also conclude that the most significant of these disruptions are located at the genomic imprinted H19 gene which is assumed to have an important role in reproduction. Clinically, these results could help physicians counsel patients to understand the likelihood of IUI success before pursuing treatment.

#### **Nuclear Translocation of Carnitine Acetyltransferase (CrAT) During Spermiogenesis.** Anne Gouraud and Guylain Boissonneault

Spermiogenesis involves the most striking change in chromatin structure known to the eukaryotic domain, where round spermatids undergo chromatin remodeling as well as a morphological change leading to highly differentiated spermatozoa. This transition is critical and essential for proper fertilization and begins with a global hyperacetylation of histones. Acetylation on histone H4 is then recognized by testis-specific protein to allow eviction of histones and their replacement by transition proteins and protamines, coincident with a surge of DNA double-strand breaks. A systematic search of the responsible histone acetyltransferase, by our lab and others, yielded no potential candidate, while histone deacetylases are no longer present at these steps. Because acetyl-CoA is a limiting substrate for acetylation, we investigated the potential role of carnitine acetyltransferase (CrAT) in the process. CrAT is an enzyme, which is known to have a mitochondrial or peroxysomal location and reversibly catalyzes the transformation of acetylcarnitine into acetyl-coenzyme A. Using immunofluorescence and confocal microscopy analysis on murine and human testis sections, we observed the synchronous expression of CrAT to the nucleus with H4 hyperacetylation. In order to determine the origin of CrAT's nuclear addressing, human CrAT splicing variants were cloned with a GFP- or FLAG-tag at both C- or N- terminal and transiently transfected into HeLa cells or human primary fibroblasts. The peroxysomal variant of CrAT (pCrAT) retains a partial intron that introduces an early in-frame stop codon, forcing transcription from a downstream ATG. This variant lacks the mitochondrial targeting signal presents in the other variant (mitochondrial CrAT, mCrAT), leaving a C-terminal peroxysomal targeting signal (PTS). Localisation of CrAT to the nucleus was observed with the peroxysomal variant, when the PTS is hampered by the tag (GFP or FLAG) or deleted. For the functional study of nuclear CrAT, the latter construct was used to generate an inducible, stably transfected HeLa cell line (pCrAT/ $\Delta$ PTS). Nuclear

localization of CrAT in this cell line was confirmed upon doxycycline induction by immunofluorescence. A combination of immunofluorescence, immunoblot, acid urea gels and mass spectrometry studies are underway to establish the impact on the nuclear acetylome. We therefore hypothesize that CrAT can translocate to the nucleus as a result of interference or hindrance of the PTS in vivo. Because CrAT is well-known to regulate the acetyl-CoA pool in the cell, its nuclear localization can impact chromatin structure and the overall process of chromatin remodeling in spermatids. Interestingly, a recent bioinformatics analysis revealed that, among the subset of genes expressing at least one transcript harboring a mitochondrial targeting signal, the testis expresses many variants of these transcripts that lack the MTS as compared to other tissues. Hence, other mitochondrial enzymes may be directed to the spermatid's nucleus to support the controlled apoptosis-like process that is observed in differentiating spermatids. Funded by the Canadian Institute of Health Research (#MOP-136925).

**Computational Modeling of Reproduction in Fathead Minnows (*Pimephales promelas*): the Hypothalamic-Pituitary-Gonadal Axis and Oocyte Growth Dynamics.** Karen H. Watanabe and Kendra D. Conrow

Fathead minnows (*Pimephales promelas*) are a small fish species native to North America and are used by the U.S. Environmental Protection Agency as a small fish model for studies of chemical reproductive toxicity. In a 21-day reproductive toxicity test, changes in apical reproductive endpoints are measured which include fecundity, plasma vitellogenin and steroid hormone concentrations. A wide variety of endocrine active chemicals have been tested in fathead minnows, and data from studies of ethinylestradiol, a synthetic estrogen, and 17 $\beta$ -trenbolone, an androgenic metabolite of a growth promoter were used to develop a mathematical model of the female hypothalamic-pituitary-gonadal (HPG) axis. The HPG axis model predicts changes in apical reproductive endpoints and plasma vitellogenin concentrations for a variety of doses and dosing regimens. An oocyte growth dynamics model was developed to predict effects upon fecundity from measured plasma vitellogenin concentrations treated as a constant over the model simulation period. While this predicted the fecundity well for experimental data, to better model realistic conditions we needed to account for plasma vitellogenin concentrations varying over the course of the model simulation. Thus, a second oocyte growth dynamics model that accepts time-varying plasma vitellogenin concentrations was developed. This poster describes the new version of the oocyte growth dynamics model that can be used with either constant or time-varying plasma vitellogenin concentrations to predict changes in fathead minnow fecundity. Future work with these models include evaluating their capability to predict changes in reproduction due to mixtures of endocrine active chemicals such as estrogens and androgens.

**Atypical Protein Kinase C Iota (PKCi) Function in Trophoblast Progenitors Ensure Post-Implantation Placenta Development and Survival of the Embryo.** Bhaswati Bhattacharya, Pratik Home, Avishek Ganguly, Soma Ray, and Soumen Paul

One of the most important causes for early pregnancy failure is defective placentation. However, the molecular mechanisms underlying proper placentation during early post-implantation development are poorly understood. We studied importance of a conserved Protein Kinase C family member, Atypical

Protein Kinase C iota (PKCi), in the early post-implantation placenta development. PKCi is essential for survival of mouse embryos after implantation. Gene knockout studies in mice have shown that loss of Prkci gene, encoding PKCi, causes embryonic lethality prior to embryonic day (E) 9.5, a developmental stage equivalent to first trimester in humans. We have observed that PKCi is predominantly expressed in the trophoblast stem and progenitor cells (TSPCs) during early stages of mouse and human placentation. However, PKCi signaling in TSPCs and its importance in the context of early post-implantation placenta development has never been studied. In this study, we found that post-implantation placental development is impaired in Prkci<sup>-/-</sup> mouse embryos, with a major defect in labyrinth zone formation. Prkci<sup>-/-</sup> embryos show lack of expression of labyrinth trophoblast (LTP) markers like Gcm1 and Dlx3. We have also found that Gdf6, also known as Bmp13, along with several other differentiation factors are significantly upregulated upon PKCi depletion using transcriptomic analysis in trophoblast stem cells. Furthermore, our study with PKCi-depleted TSPCs reveals that PKCi is essential to establish the trophoblast stem state-specific gene expression program. PKCi-depleted TSPCs show reduced LTP marker expression upon induction of differentiation. Our study discovers novel trophoblast-specific function of PKCi in successful progression of pregnancy.

**GATA Switch Regulates FLK1 Transcription During Erythroid Differentiation.** Avishek Ganguly, Pratik Home, Bhaswati Bhattacharya, Soma Ray, and Soumen Paul

Vascular endothelial growth factor A receptor or Flk1 is receptor tyrosine kinase expressed in lateral mesodermal progenitor that give rise to hematopoietic and vascular endothelial cell lineages. Gene targeting studies revealed severe defect in both the hematopoietic and endothelial lineage in the mice lacking this receptor. Although the role of Flk1 is well established in context of endothelial cell biology but the relation of Flk1 with hematopoietic differentiation is poorly understood. Therefore, present study explores the temporal regulation of Flk1 expression in hematopoietic differentiation. A quantitative RT PCR analysis showed that Flk1 expression is hugely down regulated in a terminally differentiated hematopoietic cell as opposed CD34<sup>+</sup> progenitor cell. Moreover, Flk1 expression was significantly up regulated in EB (D4) as compared to ES cell. We have identified a region at -88Kb upstream of Flk1 gene as a repressor element with a GATA factor binding motif and disruption of GATA motif abolished the repression of Flk1 promoter activity. Conditional GATA1 induction resulted in a temporal-sensitive repression of Flk1 with the concomitant binding of GATA1 at -88kb region of Flk1 locus during erythroid differentiation. Conversely, genetic knockout study demonstrated that GATA2 was essential for Flk1 expression. Quantitative ChIP analysis revealed that GATA2 to GATA1 switch at -88kb region represses Flk1 expression during erythroid differentiation. Furthermore, ex vivo analysis of erythroid cell from mouse fetal liver showed that GATA2 occupancy at -88kb region of Flk1 locus in erythroid precursor cell whereas GATA1 occupancy at same locus of terminally differentiated erythroid population substantiate GATA switching at -88kb distal repressor of Flk1 gene. Moreover, 3c analysis demonstrated that -88kb regulatory region physically interact with the Flk1 promoter to repress the Flk1 expression. Therefore, this study uncovers the underline mechanism of flk1 gene repression by a novel distal regulatory element.

**Expression and Localization of Extracellular Vesicles Biogenesis Pathway Elements in the Porcine Endometrium and Conceptuses.** Guzewska Maria M., Heifetz Yael, and Kaczmarek Monika M.

Establishment of pregnancy in the pig involves activation of numerous cellular processes, mediated by a plethora of molecular pathways. Recent studies have highlighted the importance of the endometrial function regulation without involvement of the transcription and translation processes. The main role in this phenomenon is assigned to the extracellular vesicles (EVs), which are double membrane covered vesicles released by cells. To date, EVs were shown to have an effect on fundamental biological and molecular processes by delivering effectors, such as transcription factors, proteins and non-coding RNAs to recipient cells. Based on our previous data showing the presence of EVs carrying miRNAs in the uterine lumen during pregnancy (Krawczynski et al., BOR 2015), we decided to investigate the expression profile and localize molecules involved in EVs biogenesis and transport pathways in the porcine endometrium and conceptuses.

To this end, we collected samples from crossbred gilts on 11-12 days [D] and 15-16 of either the estrous cycle or pregnancy (n=5-13/day/status). Next we performed immunofluorescent staining and real-time PCR analysis. We decided to focus on two groups of genes belonging to: 1) the endosomal sorting complex required for transport (ESCRT), involved in cargo sorting and biogenesis of vesicles and 2) the Rab family of proteins, involved in vesicle transport pathway. In addition, transmission electron microscopy (TEM) was used to image EVs in endometrial and trophoblast cells. Rab proteins (RAB11 and RAB27) and component of ESCRT complex (VPS37B) were detected in luminal and glandular epithelial cells. In parallel, presence of EVs in the lumen of uterine glands and multivesicular bodies located in epithelial and trophoblast cells was confirmed using TEM. Among ESCRT genes expressed in endometrium five of them (VPS25, VPS22, VPS36, PDCD6IP, VPS4A) were affected by status and the day ( $p < 0.05$ ). Among Rab genes only RAB27A and RAB7B showed different patterns of expression between pregnancy and the estrous cycle ( $p \leq 0.0005$ ). On days 11-12, RAB11A, VPS4 and VPS37B expression was significantly increased in conceptuses (vs. 15-16D;  $p < 0.05$ ).

In summary, different patterns of EVs biogenesis pathway gene expression between endometrium and conceptus were observed at the most critical moment for successful establishment of pregnancy in pigs (days 11-12, maternal recognition of pregnancy). Increased expression of ESCRT components in conceptus suggest that it is more prone to release EVs than endometrium, giving an impetus to further large scale functional analysis.

#### **Oxidative Stress Affects SUMO Specific Protease 1 (SEN1) During Oocyte Maturation.** Patricia L. Morris and Weber B. Feitosa

During oocyte maturation, meiotic arrest at prophase I is released, allowing cell cycle resumption through metaphase II. This process involves a dynamic network of microtubules and associated proteins that are essential for proper spindle organization and chromosome segregation. For proper microtubule networks, spatial and temporal post-translational protein modifications by Small Ubiquitin-Like Modifiers (SUMOylation) as well de-SUMOylation by SUMO-specific isopeptidases (SEN1) are essential for proper spindle organization and chromosome segregation. SUMO-modified pathways are involved in cellular stress and inflammatory responses. Oocytes are very sensitive to oxidative stress; under various types of stressors, the mammalian oocyte is highly prone to errors in spindle organization and meiotic chromosome segregation, resulting in aneuploid gametes. Herein, we evaluated SEN1 dynamics during mouse oocyte maturation, as well as the effect of oxidative stress on spindle organization, chromosomal alignment and SEN1 localization in MII oocytes. Oocytes matured in vitro were employed as an

experimental paradigm. Using high-resolution bioimaging and immunodetection, SENP1 was demonstrated to be both cytoplasmic and nuclear, with largest expression at the nuclear membrane in germinal vesicle (GV). After GV breakdown (GVBD), SENP1 was coincident with  $\alpha$ -tubulin at the organizing spindle. At metaphase I (MI), SENP1 was localized with  $\alpha$ -tubulin over the spindle. Similarly, at anaphase, telophase and metaphase II (MII), SENP1 was coincident with  $\alpha$ -tubulin over the spindle. SENP 1 was seen with a marked intensity at the spindle poles and at the microtubule organizing center (MTOC). These findings are consistent with de-SUMOylation processing by SENP1 of essential proteins for spindle assembly. To further evaluate the correlation between SENP1 with microtubule dynamics, in vivo matured oocytes at MII stage were treated with Taxol, a microtubule-stabilizing drug (10  $\mu$ M, 30 min). Taxol-induced formation of numerous cytoplasmic MTOC. Interestingly, at the center of the MTOC, SENP1 was coincident with  $\alpha$ -tubulin. To ascertain the effect of oxidative stress on SENP1, in vivo matured oocyte were treated with H<sub>2</sub>O<sub>2</sub> (1  $\mu$ M, 30 min) or with the inflammatory cytokine interleukin 6 (IL6). H<sub>2</sub>O<sub>2</sub>-induced stress significantly increased the percentage of oocytes displaying microtubule and chromosomal alignment defects. Following spindle disruption by H<sub>2</sub>O<sub>2</sub>, the percentage of oocytes with SENP1 localized over the spindle decreased approximately 4-fold. Similar results were observed following IL6 treatment. IL6 increased the percentage of microtubule and chromosomal alignment defects and decreased intensity of SENP1 over the spindle, without affecting the intensity of  $\alpha$ -tubulin. To evaluate the relationship between SUMOylation and de-SUMOylation by SENP1, in vivo-matured MII oocytes were treated with SUMO inhibitor Ginkgolic Acid (GA, 100  $\mu$ M; 1h). GA inhibition decreased spindle  $\alpha$ -tubulin intensity without affecting SENP1 intensity. Taken together, these findings are consistent with the proposal that SENP1 is involved in spindle organization. Additionally, SENP localization can be affected by oxidative stress, but de-SUMOylation is not strictly temporally correlated with concurrent SUMOylation.

Research supported, in part, by NICHD, Population Council, F. M. Kirby Foundation and The Fred H. Bixby Foundation.

**Identification of Potential Novel Protein Coding Genes in the Post-Meiotic Male Germ Cell.** Elizabeth Snyder, Jaya Gamble, Steve Gygi, and Robert Braun

The male germ cell has one of the most complex transcriptomes in the mammalian body, yet only limited descriptions of the male germ cell transcriptome have been reported and very little work has addressed whether germ cell transcriptome complexity impacts proteome diversity. Using a set of novel analysis tools, RNA-sequencing (RNA-seq) data from late juvenile testis was used to define a complete testis transcriptome. This transcriptome was compared to the annotated mouse transcriptome and found to include a large number of unannotated transcripts, from both known and novel loci. Extensive molecular confirmation demonstrated the efficacy of the transcript-building pipeline for both unannotated transcript types. This analysis further found many novel transcripts were testis specific or enriched. Additionally, RNA-seq data suggested most were expressed primarily in meiotic and post-meiotic germ cells. In silico coding potential analysis identified a subset of novel transcripts with high protein coding potential (putative mRNAs - pmRNAs), suggesting that germ cell transcriptome complexity might indeed increase proteome complexity. The majority of pmRNAs examined showed testis enriched or specific expression similar to other novel transcripts. Nearly all pmRNAs were associated, to some degree, with actively translating ribosomes and a number were found to have non-

mouse homologs with known or provisional protein-coding status. To test whether pmRNAs could be generating protein, FACs isolated post-meiotic germ cells were analyzed by LC-MS/MS. This analysis identified a large number of peptides that could be derived exclusively from pmRNAs, further supporting the idea that pmRNAs represent genuine protein coding transcripts. Surprisingly, the LC-MS/MS analysis also identified a set of peptides that appeared to be derived from annotated long non-coding RNAs (lncRNAs). Ongoing and future efforts will focus on molecular confirmation of peptides generated from pmRNAs and protein coding lncRNAs.

**Changes in Vaginal Cytology, Fecal Steroids, and Serum Progesterone During the Estrous Cycle of the African Giant Pouched Rat (*Cricetomys ansorgei*).** Jeremy J. Allen, Bryant S. Blank, Bhupinder Singh, Dean Jeffery, Soon Hon Cheong, and Alex G. Ophir

African giant pouched rats (*Cricetomys ansorgei*) can be trained to detect land mines and even tuberculosis. Due to their utility and restrictions on importing animals from Africa, establishing captive breeding colonies in the United States is of practical interest. However, the inception of efficient breeding programs is currently limited by an incomplete understanding of the reproductive physiology of female pouched rats. Previous studies with different species of pouched rats disagree on the length of the estrous cycle, and no studies have measured concentrations of steroid hormones during the cycle. To begin to characterize the morphological, cytological, and hormonal changes that occur during the estrous cycle of captive pouched rats, we collected physical measurements, vaginal cytology samples, feces, and blood from 6 females every day for 14 consecutive days. Cytology samples were collected by vaginal lavage and the stage of the cycle (estrus, metestrus, diestrus, or proestrus) was determined based on proportions of cell types (parabasal, nucleated epithelial, anucleate epithelial, and neutrophil) present in the sample. Concentrations of fecal estrogens and progestins were measured by enzyme immunoassay, and serum progesterone was measured by radioimmunoassay. Data were analyzed by ANOVA and post-hoc comparisons made using Tukey's test. One female remained in anestrus (i.e., failed to cycle) for the duration of the study and was excluded from the analyses. Only 1 female showed consistent and repetitive cycles lasting 5 days, whereas most females had longer cycles lasting 10 or more days. Length of estrus (1 to 9+ days) and diestrus (1 to 14+ days) varied among females, but proestrus remained consistent at 1-2 days. Metestrus was short ( $\leq 1$  day) and rarely observed. Baseline concentrations of fecal estrogens averaged 30 pg/mg, and fecal estrogens were significantly higher during proestrus (40 pg/mg) and estrus (33 pg/mg) than in diestrus (27 pg/mg). Interestingly, there was a negative relationship between fecal estrogen concentrations and anogenital distance ( $P < 0.05$ ), suggesting that females with longer anogenital distances (i.e., masculinized) produce less estrogen than those with shorter distances. Baseline concentrations of fecal progestins averaged 29.7 pg/mg, but there was no significant relationship between fecal progestins and stage of cycle. Baseline serum progesterone averaged 2.5 ng/ml and serum progesterone concentrations were significantly higher during diestrus (3 ng/ml) than estrus (1.9 ng/ml). Baseline steroid concentrations were different among females; compared to others, the female that showed repetitive cycles had the highest baseline concentrations of all steroids measured and the shortest anogenital distance ( $P < 0.05$ ). These results show for the first time that concentrations of fecal estrogens and serum progesterone in female pouched rats are significantly different during estrus and diestrus, which corroborates studies with other mammals. Our vaginal cytology results complement those of previous studies and suggest that the length of the estrous cycle in pouched rats is highly variable, at least in captivity. The ability to

synchronize or induce cyclicity in female pouched rats can improve breeding efficiency and is the focus of ongoing research. This research was supported by the Army Research Office (ARO) and DAPRA under award number 65344-LS.

**Mechanism of Diverse Progesterone Receptor Function in Reproductive Tissues.** Darryl L. Russell, Doan Thao Dinh, Jimmy Breen, and Rebecca L. Robker

Progesterone (P4) is an essential reproductive hormone produced by the ovarian follicle immediately prior to ovulation and maintained at high levels post-ovulation by the corpus luteum. P4 has diverse pleiotropic roles in all aspects of female reproduction from differentiation of the endometrium in preparation for embryo implantation to proliferation and differentiation of milk producing cells in the mammary gland and P4 plays a key role as the essential mediator of ovulation of the oocyte. These actions of P4 all involve direct binding to the nuclear progesterone receptor (PGR) which binds to PGR Response Elements (PRE) in chromatin and acts as a transcriptional regulator.

PGR plays diverse important roles in regulating large suites of genes in many reproductive tissues, yet relatively few genes are regulated in the same manner between different tissues, suggesting the regulatory effect of PGR is highly tissue-specific. We used a combination of genomics technologies to investigate the unique molecular mechanism of PGR action in the ovary in contrast to other reproductive organs. We performed microarray analysis of PRKO granulosa cells and oviducts to identify for the first time the full PGR dependent transcriptome in these tissues. Using PGR ChIP-Seq we defined the PGR chromatin binding cistrome in periovulatory granulosa cells and combine these datasets in bioinformatics analyses to characterise PGR interaction at its target genes. A further layer of analysis combining our transcriptome and PGR cistrome datasets with similar published studies in the uterus defined the extremely diverse response to PGR in these distinct but highly related target organs. In granulosa cells the binding of PGR was remarkably enriched in very proximal regions (< 3 kb) of gene promoters, while in the uterus PGR binding was preferentially in intergenic enhancer regions. Furthermore, the PGR-binding sites throughout the genomes of granulosa cells vs uterine cells showed only around 10% overlap, and motif enrichment analysis at the PGR cistromes in each tissue indicate the specific mode of action in each target organs is driven by PGR interaction with defined tissue specific accessory transcription factors and cofactors that interact with PGR and modulate the specificity of chromatin binding. This study illustrates the multiple facets of PGR mechanism in the reproductive tract showing that PGR is responsible for the regulation of tissue-specific group of genes through the novel interactions with accessory factors and coregulators not previously described.

**Naringenin Restores Impaired Sertoli Cell Function and Antioxidant Activity Following Use of Antiretrovirals.** Misturah Yetunde Adana, Edidiong Nanso Akang, Edwin Coleridge Stephen Naidu, John Miller Basgen, and Onyemaechi Okpara Azu

Whilst infection with Human Immuno-deficiency Virus depresses the health status of men, it however does not eliminate the desire for procreation especially with the roll-out of Highly Active Antiretroviral Therapy (HAART). Unfortunately, testicular toxicity has been associated with HAART linked to increased activity of reactive oxygen species that ultimately overwhelms the tissue's total antioxidant balance.

This study investigated testicular ultrastructural changes and antioxidant enzyme activity following use of antiretroviral therapy and naringenin, a bioactive flavonoid in Sprague-Dawley rats (SD) rats. Thirty male SD rats weighing 200–220g, were randomly assigned into groups; viz DW: Distilled water, H: HAART, N40: Naringenin, 40 mg/kg, N80: Naringenin, 80 mg/kg, HN40: HAART+Naringenin, 40 mg/kg and HN80: HAART+Naringenin, 80 mg/kg. Oxidative enzyme activities were assayed using enzyme linked immunoassay and testicular ultrastructural changes were noted via electron microscopy. Results revealed significantly increased activities of testicular catalase and levels of glutathione peroxidase in N80 group compared with DW ( $p=0.024$ ) and H ( $p=0.003$ ) mirroring elevation in caspase levels in HAART group ( $P=0.05$ ). Ultrastructural distortions in HAART-treated groups revealed thickened basal laminae, myoid cell hypertrophy with atrophied spermatogenic cells in the basal compartment. Naringenin treatment (alone and adjuvant with HAART) restored most structural alterations in the sections as well as the altered antioxidant activity. This suggests that HAART has deleterious effects on testicular cytoarchitecture and oxidant balance with the potential for Naringenin as a useful adjuvant in this model. Funding: UKZN is acknowledged for support to MYA, AEA and ECSN. South African NRF is acknowledged for grant U99053 to OOA.

**Human IVF Embryo Secretions Regulate Endometrial Adhesion via The Lncrna, PTENP1's Sponge Effect on Endometrial MicroRNA.** Masashi Takamura, Kate Rainczuk, Carly Cuman, Luk Rombauts, and Eva Dimitriadis

Embryo implantation failure is a major cause of infertility. We have previously demonstrated that human blastocyst secretions (BCM) influence endometrial epithelial cell adhesion, the initiating event of implantation. The role of long non-coding (lnc) RNA in embryo implantation is poorly defined, and there are no studies investigating the role of human embryo secretions on endometrial lncRNA expression. We hypothesised that human embryos regulate embryo implantation via altering lncRNA and aimed to determine the role of human embryo secretions on endometrial lncRNA expression and the functional and mechanistic effects in endometrial receptivity and implantation. We used array analysis to determine the expression of lncRNA in endometrial epithelial cells treated with human IVF embryo secretions from embryos that implanted compared to embryos that did not implant. lncRNA was localised in endometrium throughout the menstrual cycle in fertile women and women with primary infertility by in situ hybridization and expression levels determined by qRT-PCR. The effect of endometrial lncRNA on sponging endometrial microRNA was determined by array and confirmed by fluidigm analysis. To determine the effect of lncRNA on endometrial epithelial cell adhesive capacity we used a co-culture adhesion model of trophoblast cell line (HTR8 cells) spheroids and primary human endometrial epithelial cells. We identified that the lncRNA PTENP1 (Phosphatase-And-Tensin-Homolog-Pseudogene-1) was reduced in primary human endometrial epithelial cells (HEEC) treated with BCM from embryos that did not implant after IVF. PTENP1 and PTEN expression in endometrial tissue across the menstrual cycle ( $N = 8/gp$ ) did change across the cycle or with fertility status. PTENP1 localized in human endometrial epithelium and maximally in luminal epithelium (site of blastocyst attachment) in the receptive phase. siRNA knockdown of PTENP1 in HEEC blocked HTR8 spheroid adhesion to HEEC (reduced by  $21\pm 4.0\%$ ,  $p < 0.001$ ) and reduced several microRNA. Specifically, miR-590-3p was augmented after PTENP1 knockdown ( $2.28\pm 0.23$  fold,  $p < 0.05$ ) suggesting a 'sponging' effect. miR-590-3p mimic reduced adhesion of HEEC ( $p < 0.001$ ) via LIF, RHOA and ALCAM. In conclusion, this data show for the first time that human embryos regulate their destiny to implant via regulating endometrial

lncRNAs and have important implications in developing novel therapeutics to facilitate implantation in women with implantation failure/infertility.

**SOX17 Regulates Leukemia Inhibitory Factor to Promote Female Fertility during the Window of Implantation.** Xiaoqiu Wang, Nuria Balaguer, Tianyuan Wang, San-Pin Wu, Carlos Simón, and Francesco J. DeMayo

Mammalian pregnancy is dependent on the ability of uterus to support embryo implantation. During the window of implantation, the epithelial cells must cease proliferation and become permissive for embryo, while the stromal cells undergo mesenchymal-to-epithelioid transformation to form the decidua in support of subsequent embryo development. The ovarian steroids Estrogen (E2) and Progesterone (P4) govern these processes via their nuclear receptors, the estrogen receptor (ESR1), and progesterone receptor (PGR). Recent studies have identified the Sox17 gene as a novel target PGR regulation. Ablation of Sox17 specifically in murine uterine epithelium results in altered uterine epithelial cell proliferation, uterine gland development and embryo implantation, thereby causing infertility. Analyses the mRNA of the uteri of mice with uterine epithelial ablation of Sox17 showed that leukemia inhibitory factor (LIF), a pleiotropic cytokine required for the successful implantation, was reduced at gestational day 3.5 (GD3.5). ChIP-seq analysis of murine uteri at GD3.5 demonstrated SOX17 binds to regions 3kb (mLif3), 6kb (mLif6) and 9kb (mLif9) 5' to and 4kb (mLif4) 3' to the Lif locus, respectively. Comparison with other ChIP-seq datasets revealed that the SOX17 binding peaks at mLif6 and mLif9 also bound by ESR and PGR. In silico analysis further revealed that the SOX17 binding peaks at mLif3, mLif6 and mLif9 contained binding sites of GATA2, FOSL2, FOXA2, FOXO1, RUNX1, CEBPA and CEBPB, as well as perfect half sites of ERE. Each of these SOX17 binding peaks (mLif3, mLif6, mLif9 and mLif4) were cloned in pGL3 with TK promoter, resulting in plasmids pmLif3-luc, pmLif6-luc, pmLif9-luc and pmLif4-luc. The role of Sox17 in regulation of these binding sites were analyzed by co-transfection with a SOX17 expression plasmid into HeLa cells. The co-transfection analysis revealed that SOX17 repressed luciferase activity ( $P < 0.05$ ) in pmLif6-luc and pmLif9-luc, but induced ( $P < 0.05$ ) luciferase activity in pmLif3-luc. SOX17 had no impact on luciferase activity from pmLif4-luc. This analysis identified SOX17 as a potential positive and/or negative regulator of Lif expression. Further in vivo analysis by gene editing approaches are necessary to identify the function of these enhancer/silencer regions.

**3-Hydroxy Fatty Acids Induce Placental Trophoblast Necroptosis During Acute Fatty Liver of Pregnancy.** Prakash Kumar Sahoo, Philma Glora Muthuraj, Ezhumalai Muthukrishnan, and Sathish Kumar Natarajan

Mitochondrial beta-oxidation is one of the major energy-producing mechanisms in the human placenta, which supports growth and development of both the placenta and the fetus; therefore, dysfunctions in this pathway has severe consequences on both maternal and fetal health. Fetus with homozygous in the enzyme Long-chain 3-hydroxy acyl-CoA dehydrogenase (LCHAD) is highly associated with the development of Acute Fatty Liver of Pregnancy (AFLP). AFLP is a maternal liver injury marked by microvesicular steatosis and acute liver failure that develops in the last trimester of pregnancy. The mutation in the enzyme LCHAD results in the accumulation of 3-hydroxy fatty acids and subsequently infiltrates to the liver from the placenta through maternal circulation. In this study, we aim to

understand the molecular mechanisms underlying 3-hydroxy fatty acid-induced lipotoxicity in placental trophoblast cells. **Methods:** Human choriocarcinoma-derived trophoblast cells (JEG-3 and JAR) were treated with various concentrations (100-200  $\mu\text{M}$ ) of 3-hydroxy myristic acid (3-HMA) for 16hr. Cell death was assessed by characteristic nuclear morphology changes and Caspase 3/7 activity. Mitochondrial bioenergetics were assessed using Seahorse XF24 Extracellular Flux Analyzer. **Results:** We observed that placental trophoblast cells treated with increasing concentration of 3-HMA showed enhanced biochemical characteristic nuclear morphological changes of cell death; however, there was no caspase 3/7 activation. These results suggest that 3-HMA induces caspase-independent cell death. Further, 3-HMA-induced cell death was prevented with the inhibition of receptor interacting protein kinase 1 (RIPK1), using necrostatin suggesting necroptosis as a mechanism of cell death. We also observed that treatment of 3-HMA to placental trophoblast cells showed mitochondrial dysfunction altering its bioenergetics as evidenced by a dramatic decrease in mitochondrial spare respiratory capacity compared to controls. In conclusion, 3-hydroxy fatty acids induce mitochondrial dysfunction and placental trophoblast necroptosis. Further studies are underway to characterize the signaling mechanism of 3-HMA-induced placental trophoblast necroptosis.

**Stearoyl-CoA Desaturase Essential for Lipid Droplet Formation During Porcine Early Embryo Development.** Dong-Kyung Lee, Jae Yeon Hwang, Kwang-Hwan Choi, Seung-Hun Kim, Jong-Nam Oh, Mingyun Lee, and Chang-Kyu Lee

Lipid droplets (LDs) provides a source of energy and its importance during embryogenesis is being increasingly recognized. Especially, pig has large amounts of intercellular lipid bilayers in embryo than other species that represent porcine embryo were more dependent on lipid metabolic pathway. In transcriptome analysis, in vivo embryos, we found several genes were increasing before and after maternal zygotic transition stage which interactions were mapped and given a significance score. Among these genes, stearoyl-coenzyme A desaturase 1 (SCD1) gene were significantly increased during 8cell to blastocyst stage. SCD1 mRNA expression, however, was significantly higher at 4cell than other stages of in vitro produced embryos. Aim of this study was to detect the effect of SCD1 on LDs formation and associate with the mRNA abundance of LD formation related genes (LSD1, SREBP, PLD1, COPI, ERK2) in porcine in vitro produced embryos. To determine the effect of SCD1 on LD formation and related genes, we investigating SCD inhibition assay by CAY10566 (SCD inhibitor) on parthenogenetic embryos. CAY 10566 downregulate mRNA levels of LD formation related genes, LD density and embryo development. These results revealed a function of SCD1 on regulation of LD formation via phospholipid formation and LD effect on embryo development.

**Efcab9 Is a pH-Dependent  $\text{Ca}^{2+}$  Sensor That Regulates CatSper Channel Activity and Sperm Motility.** Jae Yeon Hwang, Nadja Mannowez, Yongdeng Zhang, Joerg Bewersdorf, Polina V. Lishko, and Jean-Ju Chung

CatSper is the weakly voltage dependent, pH-activated calcium channel in sperm cells, where it mediates  $\text{Ca}^{2+}$ -entry required for hyperactivated motility and male fertility. CatSper channels exist as a multi-subunit complex that organize linear  $\text{Ca}^{2+}$ -signaling nanodomains in the flagellar membrane along the sperm tail. However, the cytoplasmic machinery modulating the channel activity and the domain

organization remains largely unknown. We sought to find modulators of CatSper channel using proteomic and comparative genomic screens and identified a novel EF-hand protein, EFCAB9. We show that EFCAB9 interacts directly with CATSPERZ that dissociates at elevated pH and Ca<sup>2+</sup> concentrations. Studies using knockout mice created by CRISPR/Cas9 show that EFCAB9 in complex with CATSPERZ confers pH-dependent activation of CatSper channel. In the absence of Efcab9, sperm motility and fertility is compromised and the linear arrangement of the Ca<sup>2+</sup> signaling domains is disrupted. These observations suggest that EFCAB9 is pH-dependent Ca<sup>2+</sup>-sensor from the cytoplasmic mouth of CatSper channels and transduce signals to regulate motility.

### **Gene Expression Profiling Of The Canine Placenta During Normal And Antigestagen-Induced**

**Luteolysis: Preliminary Data.** Marta Nowak, Hubert Rehrauer, Alois Boos, and Mariusz P. Kowalewski

Reproductive functions in the domestic dog are regulated by endocrine mechanisms distinctly different from those known in other domestic animals. Thus, e.g., the canine placenta is devoid of steroidogenic ability, rendering the corpus luteum as the exclusive provider of progesterone (P4). Furthermore, secretion profiles of P4 are nearly identical in pregnant and non-pregnant bitches, except for the rapid P4 decline during parturition luteolysis. There is no parturition increase of estrogens, and cortisol is only sporadically observed in the maternal circulation. The parturition drop in P4 coincides with elevated PGF<sub>2</sub>α levels in the maternal blood. The latter originates in the fetal part of the placenta (trophoblast) and is also initiated by treatment with antigestagens, e.g., aglepristone, interfering with nuclear P4 receptors (PGR) localized solely in maternal decidual cells. Concomitantly, diminishing effects of the parturition endocrine milieu on VEGFA in utero-placental units is observed, together with PGF<sub>2</sub>α-driven vasoconstriction mediated through endothelin receptor A (ETA). Consequently, a functional interplay between placenta materna and fetalis is implied during initiation of the luteolytic cascade. Therefore, by applying next-generation sequencing (RNA-seq), we aim to investigate the underlying molecular events characteristic of the canine placenta during parturition and/or abortion. Here, results from our pilot experiments are presented. For this exploratory study, samples from nine dogs were used (n=3/group) at mid-gestation, parturition luteolysis and induced luteolysis (mid-gestation, aglepristone-treatment, Alizine®; 10mg/kg bw, 2x/24h apart, samples collected 24h after treatment). Following RNA isolation, libraries were prepared based on polyA-selection strategy. Sequencing was performed on the Illumina HiSeq 4000. First datasets were analyzed using SUSHI, a data analysis framework developed by FGCZ ETH/UZH. The transcriptomes of placentae from parturition or induced luteolysis were compared to mid-gestation. Over 1900 differentially expressed genes (DEG) were found during parturition luteolysis. Genes overrepresented during parturition luteolysis mapped mostly with functional terms associated with the following gene ontologies (GOs): apoptosis, increased cell communication and cholesterol transport, suppression of cell growth and division. Downstream analysis implied activation of cytokine pathways, e.g., IL-3- and -8 or TGFβ, indicating involvement of the immune system. When compared with mid-term placentae, antigestagen treatment revealed over 100 highly regulated DEG, potentially involved in the luteolytic cascade and showing similar GOs and expression patterns as during natural luteolysis. Generally, as indicated by our preliminary analysis, functional changes appear to be more pronounced during normal parturition luteolysis, indicating possible time- and/or signaling cascade-related effects. Interestingly, aglepristone-treatment seemed to be more strongly associated with modulation of the immune system. Our preliminary data indicate potential involvement of P4-dependent genes in luteolysis, including, e.g., some metalloproteinases, IGF1 or HSD11B2.

Downregulation of HSD11B2 implies local involvement of increased availability of cortisol at premature and physiological termination of pregnancy. In conclusion, based on our previous observations and current preliminary analyses, it appears that both natural and induced P4 withdrawal may be associated with disruption of the feto-maternal interface, leading to impaired vascular functions and apoptosis. The time-related maturation of the feto-maternal interface needs to be considered further, as it may be clinically relevant.

**Microphysiologic Modeling of Human Ectocervical Tissue with Endocrine Support Reveals Distinct Follicular and Luteal Phase Gene Expression Profiles.** Kelly E. McKinnon, Rhitwika Sensharma, Chloe Williams, Jovanka Ravix, Spiro Getsios, and Teresa K. Woodruff

There is a shortage of research models that accurately represent the unique mucosal environment of human ectocervical tissue, which has limited the development of new vaccines and therapies for treating infection or cancer. We developed three distinct microphysiologic human ectocervical tissue models to study hormone action, viral infection and oncogenic transformation. First, we reconstructed ectocervical tissue using decellularized extracellular matrix as a scaffold, which supported epithelial and stromal cell integration and could be useful clinically. Secondly, we generated an organotypic static culture system that consisted of ectocervical explants, with endocrine support provided through co-culture with hormone-secreting murine ovaries or step-wise exogenous hormone treatments to mimic the human menstrual cycle. These cultures remained viable and hormone-responsive for at least 28 days in vitro. And finally, we engineered a cervical tissue model that consisted of a stromal-equivalent and fully differentiated epithelium. These microphysiologic culture systems mimicked many aspects of in vivo physiology, including squamous maturation, hormone response, and mucin production, which are important components of barrier defense. There is increasing evidence that many barrier and immune properties in ectocervical tissue are mediated directly or indirectly through hormone action of ovarian steroid hormones estradiol and progesterone, suggesting potential vulnerability to pathogenic infection based on menstrual cycle phase. To identify transcriptional differences between follicular and luteal phase hormone action, we analyzed RNA sequence data from engineered cervical tissue exposed to follicular and luteal phase treatments and compared each with corresponding no-treatment controls. An unsupervised cluster analysis grouped significant differentially expressed genes into two distinct profiles for follicular and luteal phase treatments and gene ontology and pathway analysis revealed follicular phase genes were associated with proliferation, cell cycle, transcription, cell adhesion and communication, while luteal phase samples were associated with inflammation, immune response, signaling and translation. This supports the hypothesis that changes occurring in barrier and immune properties during the menstrual cycle may increase susceptibility to infection during the luteal phase. Additionally, we have identified the differentiation-dependent localization of ectocervical mucins in both native and engineered tissue, which will allow increased efficiency in targeting mucins for vaccine development and drug delivery. Moreover, this is the first time that gene expression in human ectocervical tissue has been characterized with physiological endocrine function across the menstrual cycle during homeostasis and increases our understanding of hormone-mediated events that could potentially be targeted for preventative or therapeutic treatments. In summary, we have developed three microphysiologic human ectocervical tissue models, and determined hormone-response profiles for follicular and luteal phase hormones that will be useful for a variety of research applications, such as drug development and toxicology studies, development of preventative and therapeutic treatments,

and basic research on hormone action in a critical reproductive tissue for women's health that has been historically understudied.

### **PTHLH Affects Preimplantation Embryonic Development via Akt/Cyclin D1 Pathway in Mouse.**

Zhiming Han, Yuanyuan Li, Lei Guo, Hui Li, and Shengsheng Lu

Parathyroid hormone-like hormone (PTHLH), also known as Parathyroid hormone-related protein (PTHrP), is expressed in adult and fetal tissues in many species and has multiple physiological functions, including the regulation of morphogenesis, cell proliferation and differentiation, and transplacental calcium transport. Our previous study determined that PTHLH influenced the blastocyst formation, the expression of the pluripotency-related genes *Nanog* and *Pou5f1*, and the histone acetylation pattern in mouse preimplantation embryos. To clarify the mechanism of the regulation of PTHLH on the expression of the pluripotency-related genes and histone acetylation patterns, the expression of *Wnt/β-catenin*, *Runx2*, *ERK/MAPK*, *Akt* and *Cyclin D1* during mouse preimplantation embryonic development was further investigated in this study. The *Pthlh* knockdown was performed by the siRNA-mediated *Pthlh* depletion at the 1-cell stage embryos and the effects were examined by Western blot, Immunofluorescence, Quantitative real-time PCR, etc. with at least three replicates per experiment. The results of Western blot and Immunofluorescent staining showed that the protein level of p-Akt1/2/3 and Cyclin D1 significantly decreased in the *Pthlh* depletion groups compared with the control groups at the stage of 2-cell, 4-cell, 8-cell and morula. Western blot results showed that the protein level of p-ERK1/2 was low in the preimplantation embryos, and there were no difference between the *Pthlh* depletion groups and the control groups. There were also no significant difference in the protein level of the PTHLH related genes *β-catenin* and *Runx2* between the *Pthlh* depletion groups and the control groups. These results suggest that the effects of *Pthlh* depletion on preimplantation embryonic development act via Akt/Cyclin D1 pathway. This study was supported by the National Natural Science Foundation of China (31372144, 31572226) to Z.H.

### **MicroRNA Profiles Comparison of Testicular Tissues Derived From Successful and Unsuccessful Micro-TESE Retrieval in NOA Patients.** Xunbin Huang, Na Fang, Congcong Cao, Yujiao Wen, Xiaoli Wang, and Shuiqiao Yuan

Non-obstructive azoospermia (NOA) has been considered as a main symptom of male infertility in clinical diagnosis. Although most of NOA cases could retrieve sperm by micro-dissection testicular sperm extraction (micro-TESE) to fertilize eggs through intracytoplasmic sperm injection (ICSI), there still lacks of the potential biomarkers for non-invasive diagnosis before micro-TESE surgery currently. To seek the predictive biomarkers for sperm successful retrieval before micro-TESE, in this study, we tried to determine whether microRNAs(miRNAs) were differentially expressed in testicular tissues derived from successful sperm retrieval NOA patients (SSR) and unsuccessful sperm retrieval patients (USR) by next generation small RNA sequencing (RNA-Seq). As indeed, we totally identified 180 miRNAs in which expression levels were significantly changed between SSR and USR testicular tissues. Among them, the expression levels of 13 miRNAs were up-regulated and 167 miRNAs were down-regulated in USR groups compared to that of SSR group, respectively. Unexpectedly, 86 testicular miRNAs were found completely absent in USR but showing higher expression level in SSR group, which suggest that those miRNAs might

serve as biomarkers for microTESE application and play essential role in spermatogenesis as well. Moreover, top 20 significantly changed miRNAs were selected to validate the RNA-Seq data by RT-qPCR and thus revealed that those miRNAs showing a promising signature for NOA diagnosis biomarker candidates. Of which, 3 differential miRNAs were found highly expressed in seminal plasma of human semen, suggesting non-invasive biomarker potentialities for micro-TESE outcome prediction. Further GO term and KEGG pathway analyses indicated that those significantly changed miRNAs between USR and SSR groups were involved in apoptosis, cell proliferation and differentiation which were of great importance during spermatogenesis. Bioinformatics combined with gene target analyses revealed that Prnd is predicted to be a putative target gene of hsa-miR-34c-5p, the one of most significant changed miRNA, and validated by Dual-luciferase reporter assay. In summary, our study identified a panel of miRNAs that highly expressed in NOA patient testicular tissues with successful sperm retrieval yet not in unsuccessful sperm retrieval, which provided new insights into specific miRNAs that may play important roles on epigenetic regulation during spermatogenesis. Our finding provide a useful resource to further elucidate the regulatory role of miRNAs in spermatogenesis and a profound clue to identify useful biomarkers for predicting residual spermatogenic loci in NOA patients during assisted reproductive treatment.

**Interactions Between Estradiol, Progesterone and Insulin Regulate Uterine Glycogen Metabolism in the American Mink.** Ayokunle Hodonu, Jason Hunt, Logan Beach, Mario Escobar, and Jack Rose

The mammalian uterus produces and mobilizes glycogen in a reproductive-cycle-dependent pattern that supports the energy requirements of pre-embryonic development before implantation. We show here for the first time that the mink uterus expresses insulin and insulin-like growth factor-1 receptor (INSR & IGFR1) mRNA and protein; the levels of which peak during peri-implantation. While estradiol (E2) or progesterone (P4) did not increase glycogen content of immortalized mink uterine epithelial cells (GMMe), insulin alone significantly increased glycogen concentrations. Treatment with insulin + E2, resulted in glycogen concentrations that were higher than for cells receiving insulin only. Treatment of cells with insulin + P4, or insulin-pretreatment followed by P4, resulted in glycogen levels not different from controls. Even when cells were primed with E2 followed by P4 (with or without insulin), glycogen concentrations did not differ from controls. We conclude that E2 – induced glycogen synthesis, requires the concomitant actions of insulin and that E2 increases the uterine response to insulin. After ovulation, P4 from the corpus luteum, promotes glycogen mobilization to completion before implantation. Even though glycogen reserves are depleted, increased uterine sensitivity to insulin at this time may be requisite to an adequate level of glucose uptake, promoting pre-embryonic development, invasion into the endometrium and placental formation.

**From Flies to Mammals: Developing and Validating a Mouse Follicle Rupture Assay to Test Potential Female Contraceptive Candidates identified in a Drosophila Ovulation Model.** Jiyang Zhang, Sharon Tam, Sarah Wagner, Jianjun Sun, and Teresa Woodruff

Mouse follicles cultured in an encapsulated system (in vitro Follicle Growth (eIVFG) culture) preserves 3D follicular structure and is a good tool for basic research on follicle function and is amenable to drug testing and toxicology screening. In contrast to earlier contraceptive screening tools that have largely relied on rupture of the follicle, our eIVFG system provides a rapidly assayable rupture endpoint and further enables assessment of the transition of the follicle structure from estrogen- to progesterone-

producing. This additional step ensures that drug candidates could be viable in vivo drugs. In our eIVFG system, multi-layered secondary follicles (150-180  $\mu\text{m}$  in diameter) were isolated from PD16-18 mouse ovaries and encapsulated in 0.5% alginate. After 7 days culture, follicles were removed from alginate and follicle rupture was induced by incubating in maturation media containing human chorionic gonadotrophin (hCG) with or without the drug candidates for 16 hours. Follicle rupture rate was assayed visually, and oocytes were scored into three categories: degenerated, metaphase II(MII) and germinal vesicle break down (GVBD). After ovulation, follicles were kept for 7 more days culture, with media sampled every other day. The progesterone level was measured in collected media by enzyme-linked immune assay (ELISA) to evaluate granulosa cell survival and luteal transition. Here we test the ability of the system to serve as a robust screen for follicle-targeted contraceptives. The drug candidates tested in this screen were identified in a novel ex vivo *Drosophila* follicle rupture model. Similar to mammalian follicles, this rupture process in *Drosophila* also depends on proteases to break down follicle walls. This simple and reliable ex vivo assay permits screening of large numbers of compounds for further testing in the mammalian system. Among the 5 drug candidates tested in our eIVFG system, we found 2 of them promising: chlorpromazine and amitriptyline. They inhibited the follicle rupture rate to less than 50% while maintaining a normal progesterone profile. Another strong candidate based on the *Drosophila* model, niclosamide, dramatically inhibited ovulation effect (less than 10% of follicles rupture), but the follicles did not transition to progesterone production. In the future, the eIVFG mouse follicle rupture assay will be combined with robotic liquid handling and image software systems that can be customized to differentiate rupture and un-ruptured follicles automatically to create a high-throughput system for the screening of contraceptive compounds from *Drosophila* models and elsewhere. This study was funded by Bill & Melinda Gates Grand Challenges Explorations award number OPP1161206.

**A Subset of Germ Cells Controls Cyp26b1 Expression by Sertoli Cells.** Parag Parekh, Thomas Garcia, Reham Waheeb, Vivek Jain, Pooja Gandhi, Gunapala Shetty, Marvin Meistrich, and Marie-Claude Hofmann

Cytochrome P45026B1 (CYP26B1) is an enzyme that degrades all-trans-retinoic acid (RA). It therefore plays a key role in preventing germ cell differentiation by controlling local distribution of RA. Interestingly, little is known about the mechanisms of Cyp26b1 gene regulation. In Sertoli cells, Cyp26b1 expression is maintained by SF1 and SOX9 during gonad development, but inhibitory mechanisms that would downregulate its expression after birth to increase RA availability are not known. Our previous data indicated that expression of Cyp26b1 is inversely correlated to NOTCH pathway activity. We hypothesized that 1) Cyp26b1 downregulation after birth is directly dependent on canonical NOTCH signaling; 2) A subset of premeiotic germ cells might be responsible for Cyp26b1 downregulation through the NOTCH ligand JAG1. Flow cytometry experiments demonstrated that JAG1 is mainly expressed by Aundiff spermatogonia. Further, JAG1 increased expression of the transcriptional repressors and canonical NOTCH target genes Hes1 and Hey1 in cultured primary Sertoli cells. This upregulation of Hes/Hey gene expression was associated with significant decreases in Cyp26b1 expression, while simultaneous downregulation of Hes/Hey by RNAi led to significant increases. Further, Luciferase and CHIP-PCR assays demonstrated that only HEY1 directly binds to the Cyp26b1 promoter to downregulate its expression. To elucidate which germ cells activate NOTCH signaling in adult Sertoli cells in vivo, we performed germ cell depletion experiments using a single moderate dose of busulfan (20 mg/kg), and assessed the composition of the remaining germ cell population at day 8 after injection. The

number of germ cells in each stage of the seminiferous epithelium was counted and normalized to Sertoli cells. Germ cells and Sertoli cell markers were assessed in parallel by qRT-PCR. We found that that stem cells are present but there is a major decrease in Aaligned through zygotene spermatocytes, while Hey1 mRNA is reduced by 30% and Cyp26b1 expression is up 2.5-fold. Therefore, NOTCH signaling in Sertoli cells is activated by progenitors and more differentiated cells, not by the stem cells or pachytene spermatocytes. In conclusion, our data indicates that an expanding pool of JAG1-expressing germ cells control and maintain their own differentiation by downregulating Cyp26b1 through NOTCH signaling in Sertoli cells after birth.

Supported by NIH R01HD081244

### **In Utero and Lactational Exposure of DEHP Increases the Susceptibility of Prostate Carcinogenesis in Male Offspring Through PSCA Hypomethylation.** Yunhui Zhang and Huijing Shi

As an ubiquitous environmental endocrine disruptor, di(2-ethylhexyl) phthalate (DEHP) has been shown to interfere with the development of reproductive organs and induce pathological changes in prostate. Our previous finding showed that in utero and lactational (IUL) DEHP exposure could disrupt the balance of testosterone and estrogen and increase the susceptibility of prostate carcinogenesis. The purpose of this study is to investigate whether the early-life specific epigenetic modifications could mediate the effect of DEHP exposure on prostate carcinogenesis in rodents, for epigenetic modifications play important roles in regulating prostate carcinogenesis. The pregnant rats were treated with corn oil (negative control) or DEHP at 0.01, 0.1 and 1 mg/kg BW/day from GD7 to PND21. On PND21, the expression and DNA methylation change of six prostate carcinogenesis-related genes (ESR2/ GSTP1/ NKX3.1/ PSCA/ PTGS2/ Rassf1a) were assessed through SYBR-Green real-time PCR combined with pyrosequencing assay in F1 male offspring. On PND196, the relationship between these genes' expression and prostate carcinogenesis parameters (including prostate/body weight ratio, PIN scores, Gleason scores, and serum PSA concentrations) were evaluated. Results showed that IUL exposure to DEHP significantly increased the expression of GSTP1, PSCA and PTGS2 in a dose-dependent manner, which were positively correlated with PIN scores, Gleason scores, serum PSA concentrations and negatively correlated with prostate/body weight ratio on PND196. Meanwhile, 1mg/kg BW/day DEHP markedly reduced DNA methylation level of PSCA in all studied CpG sites. Significant inverse correlations between methylation levels of the promoter CpG site and PSCA mRNA expression were observed. These results indicated that transcriptional changes of GSTP1, PSCA and PTGS2 induced by DEHP exposure might be contribute to the increasing susceptibility of prostate carcinogenesis in late life. Moreover, hypomethylation of PSCA could mediate the effect of DEHP on prostate carcinogenesis in rats.

### **The Sphingosine Kinase Regulates Hormone-Induced Oocyte Meiotic Resumption in Mouse.** Meijia Zhang, Xiaoqiong Hao, and Feifei Yuan

In preovulatory ovarian follicles, oocyte is maintained in meiotic prophase arrest by natriuretic peptide type C (NPPC) and its receptor guanylyl cyclase-linked natriuretic peptide receptor 2 (NPR2). The activation of epidermal growth factor (EGF) receptor increases calcium levels of cumulus cells resulting in the inactivation of NPR2 that promotes resumption of meiotic. Here, we investigated the regulatory mechanism of EGF receptor signaling in calcium levels in cumulus cells. Cumulus cell-oocyte complex was cultured in the medium with 30 nM NPPC. In this system, EGF could stimulate oocyte meiotic

resumption, which could completely be reversed by sphingosine kinase (SphK) inhibitor SKI- II . SphK catalyze the phosphorylation of sphingosine to generate sphingosine 1-phosphate (S1P). We also found that the levels of S1P in COCs increased when they were treated with EGF, and this effect was reversed by SKI-II. Future study demonstrated that U0126 could decrease S1P levels caused by EGF, suggesting that EGF-mediated MAPK3/1 signaling pathway results in the activation of SphK. After that, we found that S1P has the same effect of EGF on elevating calcium levels in cumulus cells, as well as the decrease of the binding affinity of NPR2 for NPPC. SKI-II could reverse the EGF-induced the elevation of calcium and the decrease of the binding affinity of NPR2 for NPPC. In addition, we studied the effect of SphK on oocyte meiotic resumption. Compared with wild type, SphK1-/-; SphK2f/f; FshR-cre mice had low rates of maturation, ovulation and birth. These results indicate that SphK, by increasing S1P and calcium levels, plays an important role in oocyte meiotic resumption in mouse. Research supported by National Natural Science Foundation of China.

**Perinatal Exposure to Endometriosis Modifies H3K27me2 in the Adult Testes and Alters Genes Important for Spermatogenesis.** Henda Nabli and Kathy L. Sharpe-Timms

Infertility is a worldwide problem that affects 15% of couples with approximately one third of cases attributed to male factor alone, but the causes are poorly understood. There is very little published research addressing the impact of prenatal exposure to endometriosis on male fertility. We hypothesize that the inflammatory peritoneal environment in endometriosis affects the testes development and function. Our research used a well-established surgical model of endometriosis to generate Endo (induced endometriosis) and Sham (surgery control) female rats. Endo and Sham rats were bred with normal proven breeder males and data was collected from their sexually mature male offspring. We previously reported that males born from females with endometriosis had smaller litter sizes, early testicular descent, reduced sperm density, and decreased testicular H3K27me2 histone modifications; all indicators of possible testicular dysfunction, alterations in spermatogenesis, and/or epigenetic related infertility. The objective of this study was to characterize the differences in the genomic distribution of H3K27me2 between Endo and Sham rat testes. H3K27me2 chromatin immunoprecipitation followed by high-throughput sequencing (ChIP-Seq) was performed on snap frozen testes from 32 week old male Endo (n = 3) and Sham (n = 3). Comparison of ChIP-Seq profiles between Endo and Sham revealed a total of 90 genes displaying reduced H3K27me2 levels in Endo and 13 genes with increased levels (fold change  $\geq 1.5$   $P < 0.05$ ). Genes involved in networks regulating morphology of reproductive system (Abca1, Bmyc, Cadm1, Ctcfl, Slca25, Wnt9b, Wnt7a, Loxl1, Lef1, Lbh, Itgb8, and E2f3), cell viability of sperm (Cadm1), maturation of sperm (Cadm1), and arrest in spermatogenesis of spermatids (Cadm1) were identified by the Ingenuity Pathway Analysis (IPA) software. Abca1, Bmyc, Cadm1, Ctcfl, Slca25, and Wnt9b were selected for further validation by RT-qPCR. We conclude that embryonic and fetal exposure to endometriosis may have induced epigenetic reprogramming in the developing testes, leading to modification of H3K27me2 and affecting genes important for spermatogenesis and sperm development. Targeting these novel dysregulated genes may generate novel gene therapy methods to treat male factor infertility.

This research was supported by the NICHD (R21HD080763 to KST) and an MU System Research Board Grant (to KST).

### **Access and Utilization of Fertility Preservation Services based on Medical and Elective Indications.**

Audrey Kindsfather, Hanna Valli-Pulaski, Kyle E. Orwig, and Marie Menke

The number of women undergoing fertility preservation (FP) for both elective and medical reasons has been increasing over the last several years. Patients pursuing elective FP are generally seeking to bypass age-related fertility decline. In contrast, medical FP patients often have an underlying urgency requiring expedited care. Reasons for medical FP include malignant and benign conditions that require surgery, chemotherapy, or radiotherapy that have a chance to induce premature ovarian insufficiency. Rate of referral of young female patients to reproductive specialists for medical FP and follow-through with FP have consistently low rates. Once referred, little is known regarding the timing and access to expedited care for medical FP patients. Our objective was to examine differences in access to care between patients with elective versus medical indications for fertility preservation (FP). A retrospective chart review was conducted of female patients who contacted the Center for Fertility and Reproductive Endocrinology (CFRE) at Magee-Womens Hospital in Pittsburgh, PA with an interest in FP services between January 2014 and April 2017. Patients were divided into those with an underlying medical condition that increased their risk of fertility loss versus those seeking FP electively. Dates of the first contact with CFRE (e.g. scheduling, fertility preservation information office), first in-person appointment with CFRE, and FP start date were recorded, along with factors related to pre-treatment testing. A total of 203 patients expressed interest in FP services. Medical FP patients were significantly younger (28.9 years, 95%CI [26.2, 31.5]) compared to those seeking care electively (34.6 years, 95%CI [32.0,37.3];  $p < 0.01$ ). The two groups did not differ with respect to marital status and history of prior conception. Average time was shorter for medical FP patients than elective FP patients with regards to first contact to appointment date ( $0.5 \pm 0.6$  versus  $2.2 \pm 2.0$  days;  $p < 0.05$ ) and first appointment date to FP cycle start ( $6.4 \pm 18.6$  versus  $34.6 \pm 24.3$  days;  $p < 0.01$ ). Medical FP patients had more screening tests ordered (14.1, 95%CI [10.8,17.3], versus elective FP 7.8, 95%CI [5.1,10.5] tests;  $p < 0.001$ ) and completed (11.1, 95%CI [8.5,13.6], versus elective FP 6.7, 95%CI [4.6,8.8] tests;  $p < 0.01$ ) at their initial appointment. Total medication doses did not differ between the two groups. In conclusion, access to care was enhanced for patients wishing to undergo FP for medical reasons. Medical FP patients were more likely to receive earlier appointments, completion of screening tests, and initiation of care compared to patients seeking care electively. Once referred, timing and access to expedited services for medical FP patients should not be considered a barrier to FP care. This research was supported by Magee-Womens Hospital and Research Institute and the Howard Hughes Medical Institute Medical Fellows Research Program.

### **Single Cell Profiling of the Human Ovarian Cortex; Defining The Ovarian Stroma.** Mikaela A. Therrie, Devin K. Porter, Emmett Hedblom, Angela L. Cuenca, Yvonne A. White, and James Lillie

Studies of the ovarian cortex primarily focus on the oocytes and granulosa cells and/or the importance of their interactions. The ovarian stroma, which constitutes the largest proportion of the cortex is understood to play an important role in ovarian function and remodeling, however it remains largely understudied. Very little is known about the non-follicular support cells that make up the ovarian cortex and their roles in the changing microenvironment in which early follicles rest, become activated, grow,

undergo atresia or ultimately are selected for ovulation. The aim of this study is to define more specifically the populations of cells and support creating an atlas of the human ovarian cortex.

Single-Cell RNA Sequencing on three individual human cortex samples was performed using 10x Genomics 3' v2 Chemistry, under manufacturer's protocol. In brief, three 6x6x1mm samples were obtained from each donor aged 24, 29 and 36 (post mortem; PMI < 24hrs) and slow frozen. Samples were thawed, dissociated using enzymatic and mechanical dissociation and pooled by donor. For each donor sample, 6000 cells were analyzed at a sequencing saturation of 75% to ensure maximum sensitivity of detection. Iterations of T-SNE analysis followed by clustering with a graph-based clustering algorithm of the three samples yielded 15 distinct clusters. Based on gene expression signatures, major clusters of cells were tentatively assigned as granulosa cells (AMHR2+/ FOXL2+), mural granulosa cells (FSHR+/CYP19A1+/AMH+), thecal cells (INSL3+/CYP17A1+), endothelial cells (CD34+/PECAM1+), smooth muscle cells (MYH11+/PLN+), mesothelial cells (UPK3B+/LRRN4+), cumulus cells (HAS2+/TNFAIP6+/SFRP2+), and hematopoietic cells (PTPRC+). Complementary samples from each donor were collected for histological analysis.

The cluster of cells assigned as granulosa cells (defined as AMHR2+/FOXL2+) were also positive for STAR. Surprisingly, these clusters also contained cells with mRNAs previously associated with ovarian "stroma", including ECEL1, ARX, PROK1 and SIGLEC11. In contrast, putative cumulus cells expressing HAS2, TNFAIP6 and SFRP2 expressed much lower levels of these four genes. Given the broad expression of ECEL1, ARX, PROK1 and SIGLEC11 in the ovarian cortex, either the ovarian "stroma" contains many granulosa-like cells not associated with follicles, or AMHR2, FOXL2 are STAR are expressed in cells other than granulosa cells. Protein expression analysis to support localization of these markers is underway.

Overall profiles of the three donors presented with unique characteristics. Increasing the sample cohort to evaluate the impact of age-related and physiological (i.e cycle phase, birth control) changes within the ovarian cortex will be imperative in generating a complete global picture of the human ovarian cortex.

We believe that this and further studies will make an important contribution towards creating an atlas of the human ovarian cortex and prompt more research into defining (or characterizing) the roles of all cells comprising the peripheral ovarian cortex. This research should lead to an enhanced understanding of normal and dysfunctional ovarian physiology.

Author disclosures: This research was supported by OvaScience.

### **The Effects of Phthalate Metabolites on Expression of Genes Important for Estradiol Synthesis and Degradation in Antral Follicles.** Daryl D. Meling, Liying Gao, Genoa R. Warner, and Jodi A. Flaws

Phthalates are used as solvents and plasticizers in a wide variety of consumer products. Most people are exposed to phthalates as parent compounds through ingestion, inhalation, and dermal contact. However, these parent compounds are quickly metabolized to more active compounds in several tissues. Although studies indicate that the phthalate metabolites reach the ovary, little is known about whether they are ovarian toxicants. Thus, this study tested the hypothesis that phthalate metabolites influence the expression of genes involved in the synthesis and degradation of estradiol by mouse antral follicles in vitro. The selected metabolite mixture was based on concentrations in urine of pregnant

women in the I-Kids study in Illinois; it included 36% monoethyl phthalate, 19% mono(2-ethylhexyl) phthalate, 15% monobutyl phthalate, 10% monoisononyl phthalate, 10% monoisobutyl phthalate, and 8% monobenzyl phthalate. Antral follicles from adult CD-1 mice (32-40 days) were cultured in groups of 10-12 follicles for 96 hours with vehicle control (DMSO) or metabolite mixtures (0.1-500 mg/ml). Growth of follicles in culture was monitored every 24 hours. Following culture, total RNA was extracted and reverse transcribed. Real-time PCR was then performed for Cyp19A1, which is required for estradiol synthesis, and for Cyp1A1 and Cyp1B1, which are capable of metabolizing estradiol. The higher doses of phthalate mixture inhibited follicle growth compared to controls. The results also show that higher doses of the mixture decrease expression of Cyp19A1 and Cyp1B1, whereas they increase expression of Cyp1A1 compared to control. In addition, the highest doses of the mixture increased the ratio of Cyp1A1/Cyp1B1 expression greater than 10-fold compared to control. Collectively, these data suggest that the phthalate metabolite mixture impacts ovarian expression of key genes in the estradiol synthesis and degradation pathway. Supported by R56 ES 025147.

**The Identification and Characterization of the Novel Sperm Gene, Family with Sequence Similarity 205 Member C (Fam205c), in The Testis.** Theodore R. Chauvin and Kenneth P. Roberts

Fertilization of an egg requires sperm capable of progressive motility, and with the ability to undergo an induced acrosome reaction upon contact with the egg. Defects in either of these two sperm functions contribute significantly to male infertility. Multiple proteins or protein isoforms expressed specifically in the male germ cell have been described and shown to be necessary for normal sperm function; examples include the Catsper ion channels and the sperm-specific isoforms of PGK and LDH. Previously, our lab performed a large proteomic project with sperm isolated from the mouse cauda epididymis. A small number of undescribed, sperm-specific proteins were discovered among the 2850 proteins identified in these cells. One such protein was Family with sequence similarity 205, member C (Fam205c), which is novel and unannotated, and appears to be highly enriched in sperm.

We have characterized the mRNA expression level of Fam205c, finding that it is highly expressed in the testis compared to other tissues, which is consistent with EST abundance data published by NCBI. Furthermore, we have performed a developmental expression analysis on the gene, which showed that expression of Fam205c begins around day 21. This onset of expressions suggests expression in germ cells (late spermatocytes and/or early spermatids), as they begin to proliferate at this time. This data is consistent with germ cell-specific expression during spermatogenesis, and the presence of this protein in sperm, at relatively high levels, leads us to hypothesize that this protein is necessary for proper sperm function. In addition to these expression studies, we transfected a plasmid containing the full sequence of Fam205c that was linked to recombinant green fluorescent protein (GFP) into heterologous Chinese hamster ovary (CHO) cells. The GFP expression appears to be nuclear in nature, with GFP expression at the nuclear membrane. Analysis of the amino acid sequence suggests that there is a nuclear transmembrane domain, as well as a domain of unknown function; both of these domains are present in all mammals investigated, and the amino acid sequence also appears to be highly conserved across many different species. All of this data warrants further studies to investigate which specific cells express the Fam205c protein, and to localize the protein in testicular germ cells.

**C-Type Natriuretic Peptide Stimulates the Function of Rat Sertoli Cells via Activation of NPR-B/Cgmp/PKG Signaling Pathway.** Yuejin Yu, Chunlei Mei, Na Lia, and Donghui Huang

C-type natriuretic peptide (CNP) is a key regulator of male reproductive process. Our previous investigations showed that CNP can significantly stimulate the mRNA expression of androgen-binding protein (ABP) and transferrin (TRF) in rat Sertoli cells, but the pathways responsible for this process remain to be elucidated. We assume that CNP bind natriuretic peptide receptor B (NPR-B) to regulate the expression of ABP and TRF gene through the cGMP pathway. To address this question, in this study we firstly confirm the expression and localization of CNP and NPR-B in rat testis by immunohistochemistry and western blotting. And then, ELISA and real-time PCR were performed to investigate signaling pathway of CNP on Sertoli cells of rat testis. Our results showed that CNP was mainly localized in germ cells and Leydig cells, and its receptor NPR-B was mostly expressed in Sertoli cells and vascular endothelial cells. Supplementation of CNP in Sertoli cell medium was accompanied by elevations in the amount of intracellular cGMP and the production of ABP and TRF mRNA, whereas inhibition of PKG with KT5823 led to a decrease in the expression of ABP and TRF mRNA. Moreover, ABP and TRF mRNA were no longer elevated when we use liposome-mediated RNA interference technology to silence NPR-B gene in a rat Sertoli cell line (TM4). These results suggest that CNP contributes to the regulation of ABP and TRF in rat Sertoli cells through NPR-B/cGMP/PKG signaling pathways.

**The Stk35 Locus Contributes to Normal Gametogenesis and Encodes a Lncrna Responsive to Oxidative Stress.** Yoichi Miyamoto, Penny A.F. Whiley, Hoey Y. Goh, Chin Wong, and Kate L. Loveland

Serine/threonine kinase 35 (STK35) is a recently identified human kinase with an autophosphorylation function, linked functionally to actin stress fibers, cell cycle progression and survival. Synthesis of the Stk35 transcript can be mediated by importin  $\alpha$ 2, a nucleocytoplasmic transport protein, that becomes nuclear-localized under stress conditions and at specific spermatogenic stages in mice and human. In adult tissues, STK35 transcript levels are highest in the testis. Our analysis of transcripts from this locus, available from existing databases and publications identified 2 coding mRNA isoforms and 1 potential long non-coding RNA (lncRNA). In situ hybridisation analysis of these three transcripts in fixed mouse testis sections revealed there is progressive expression of each of these transcripts from the Stk35 locus in mouse testis during spermatogenesis, indicating their tightly controlled synthesis. The lncRNA appeared to be most abundant in the spermatogenic stages when germ cells are fully surrounded by Sertoli cells (spermatocytes). Using RT-qPCR analysis of mouse and human germ cell lines, we demonstrated that lncRNA, but not the mRNA, levels were rapidly and transiently increased by exposure to oxidative stress. We created a Stk35 knock out (KO) mouse model that lacks all 3 RNAs. KO mice are born at sub-Mendelian frequency, and adults manifest both male and female germline deficiency. KO males exhibit no or partial spermatogenesis in most testis tubule cross-sections, while KO ovaries are smaller and contain fewer follicles. The eyes of KO mice sporadically display phenotypes ranging from gross deformity to mild goniodysgenesis or iridocorneal angle malformation, to overtly normal. These findings demonstrate the central importance of the Stk35 allele for fertility, and provide evidence that tight regulation of transcription from this locus may be mediated in part by local changes in the environment, including oxidative stress. We propose that nuclear-localized importin proteins influence gene expression in male germ cells, with Stk35 one important target for their action.

**Investigating the Role of Long Non-Coding RNA 483Rik During Mouse Placental Development.** Laramie Pence, Jessica Martin, and Bhanu Telugu

The placenta is a distinguishing feature of mammals and is essential for normal embryonic development and a successful pregnancy. During pregnancy, the placenta serves as the interface between the fetus and the mother to facilitate nutrient, gas, and waste exchange. Many unsuccessful pregnancies are the result of abnormal placental development, therefore it is important to identify the genes and mechanisms that control the normal state of development. Our hypothesis is that long non-coding RNAs (lncRNAs) that are expressed uniquely in the placenta play an essential role in the development of this organ, and when dysregulated will perturb normal embryonic development. Extensive transcriptomic analysis has now confirmed that 70-90% of the genome is transcribed, yet only 1-2% codes for proteins, therefore a large portion of the genome is non-coding. These non-coding regions were once thought of as junk, but non-coding transcripts such as lncRNAs are now known to be involved in important regulatory networks that drive developmental programs. It is the goal of this study to identify lncRNAs that are important for placental organ development. In this study transcriptomic analysis of E7.5 mouse embryonic tissues has identified several embryonic and placental-specific lncRNAs. From this data one placental-specific lncRNA in particular, designated as 483Rik, was selected for further study. RT-PCR analysis has revealed specific expression of 483Rik in the placenta at multiple time points during development. Furthermore, in situ hybridization has revealed expression in the labyrinthine region of the placenta, where exchange between the maternal and fetal circulatory systems occurs. To understand the function of this lncRNA in the placenta, 483Rik knock-out mice have been generated using the CRISPR/Cas system. Analysis of Mendelian ratios has revealed that 483Rik null mice have an embryonic lethal phenotype and fewer heterozygous mice than expected were obtained at weaning. Currently, timed heterozygous intercrosses have been initiated in order to determine the stage at which null embryos die in utero. Morphological and histological analysis will be performed in order to determine the cause of death. In future studies RNA immunoprecipitation will be used to reveal 483Rik binding partners to further elucidate the mechanism behind 483Rik's function in the placenta. The placenta is arguably the most important organ for early mammalian growth, yet is the least understood. Identifying genes that are essential for normal developmental processes is the first step in understanding the causes for abnormal development. This study is expected to expand our current understanding of the role of lncRNAs in reproductive health and early pregnancy loss as it relates to placental development.

**Prefoldin-5 is a Novel Regulator of C-Myc Expression in Endometriotic Epithelial Cells Whose Expression Correlates with That Of RPLP1 and Cell Proliferation.** Zahraa Alali, Fatimah Aljubran, Amanda Graham, and Warren B. Nothnick

**INTRODUCTION:** Endometriosis is a common disease in women of reproductive age in which endometrial tissue establishes and survives in ectopic locations, yet its pathogenesis is poorly understood. MYC regulates numerous targets associated with endometriotic cell survival including RPLP1. Recently, we discovered an increase in endometriotic tissue and epithelial cell expression of pre-foldin-5 (PFDN5) which correlates with endometriotic cell proliferation. PFDN5 is a tumor suppressor, which inhibits the transcriptional activity of MYC, thus blocking its action. If PFDN5 functions in a similar manner in endometriotic tissue and cells is unknown. The objective of the current study was to examine

if endometriotic epithelial cell expression of PFDN5 regulates MYC expression and in turn cell proliferation.

**METHODS:** To test our hypothesis, endometriotic epithelial (12Z) cells were transfected with a scrambled siRNA (control-transfected) or siRNA to PFDN5 (siRNA SMARTPool; 50 nM final concentration; N=3 experiments). Cells were harvested at 24 and 48h post-transfection and mRNA and protein expression were examined by qRT-PCR and Western blot analysis, respectively.

**RESULTS:** PFDN5 knockdown was confirmed by qRT-PCR and Western blot analysis. PFDN5 knockdown was associated with increased RPLP1 (2.1-fold increase) and MYC expression (1.7-fold increase) at 24h, which returned to near baseline levels by 48h. Alterations to cellular proliferation were further confirmed by assessing cyclin E (CCNE) expression in 12Z cells. PFDN5 knockdown was associated with increased CCNE1 transcript (2.7-fold increase compared to control-transfected cells).

**CONCLUSIONS:** PFDN5 is expressed in endometriotic epithelial cells and its expression is correlated with cell proliferation. We conclude that this regulatory pathway involves PFDN5 regulation of MYC which modulates expression of known MYC targets such as RPLP1 and CCNE1 and in turn cell proliferation. Enhancing our understanding on the role of PFDN5 in the pathophysiology of endometriosis may lead to novel approaches to curtail endometriotic lesion survival and development of novel therapeutic approaches for treating this debilitating disease.

**Calcium Dynamics in Intact Ovarian Follicles.** Jeremy R. Egbert, Paul G. Fahey, Jacob Reimer, Russell S. Ray, Andreas S. Tolia, and Laurinda A. Jaffe

In mammalian ovaries, follicle-stimulating hormone (FSH) induces granulosa cell differentiation and follicle maturation, including the upregulation of the luteinizing hormone (LH) receptor in preovulatory follicles. During each reproductive cycle, the surge of LH then acts on preovulatory follicles to trigger oocyte meiotic resumption, ovulation, and luteinization of granulosa cells. Although both FSH and LH receptors primarily signal through cAMP/PKA, both FSH and LH have been shown to increase intracellular calcium concentrations in a subpopulation of isolated porcine granulosa cells. However, calcium dynamics in response to FSH and LH have not been investigated in intact follicles. Here we examine the spatial and temporal dynamics of calcium in follicles from mice that ubiquitously express one of two highly sensitive calcium indicators: the FRET sensor Twitch-2B (Kd ~200 nM), or the single fluorophore GCaMP6s (Kd ~140 nM). In the outer granulosa cells of preantral follicles (150-200  $\mu$ m in diameter) and small antral follicles (220-270  $\mu$ m in diameter) from mice expressing Twitch-2B, FSH (1 nM) slowly increased the YFP/CFP emission ratio to a peak before decreasing at a similar rate, indicating a transient increase in free calcium. The peak FRET ratio occurred an average ( $\pm$  sem) of  $11 \pm 1$  min (n = 6) following FSH treatment, and was  $70 \pm 13\%$  higher than the baseline ratio (p < 0.05 by paired t-test). Similar results were obtained for both preantral and small antral follicles. When 10 nM LH was applied to intact preovulatory follicles, there was a small but significant increase in Twitch-2B FRET ratio within the outer mural cells. Following treatment with a saturating concentration of LH (300 nM), the FRET ratio in the outer mural cells peaked at  $90 \pm 7\%$  (n = 16) above baseline. With the Twitch-2B sensor, it was not practical to evaluate whether all cells responded to LH with an increase in calcium, or only a subset of cells. In order to visualize calcium changes within individual granulosa cells, we used preovulatory follicles from mice expressing the GCaMP6s sensor, which increases in brightness as

calcium increases. We found that some, but not all, granulosa cells near the basal lamina respond to 10 nM LH with oscillations in intracellular calcium. These oscillations were variable in their amplitude and latency of onset after LH treatment, even within a single follicle. There was no evidence of calcium “waves” between many granulosa cells, even though they are connected by gap junctions. Instead, oscillations appeared to be isolated to single cells or asynchronous between adjacent cells. In response to 300 nM LH, calcium rapidly increased in most outer mural cells, but the oscillations were less distinct compared to 10 nM LH. The physiological significance of these gonadotropin-induced calcium increases remains to be determined. Supported by NIH grant R37HD014939 to L.A.J.

**Microbiome Profile of Mouse Female Reproductive Tract During Embryo Implantation.** Yuehuan Li, Christian Lee Andersen, Zidao Wang, and Xiaoqin Ye

Emerging clinical studies have implicated altered distribution of bacteria within women’s reproductive tract in reproductive diseases, such as miscarriage and infertility. The microbiome in the female reproductive tract can potentially be used to predict the overall health status of the female reproductive tract. Because of ethical issues, mouse models have been widely used in vivo models for studying mechanisms involving physiology (e.g., embryo implantation) and pathology (e.g., embryo implantation failure) of the female reproductive system. Embryo implantation is a critical step in mammalian reproduction. It initiates around gestation day 4.0 (D4.0) in mice. There is a lack of information available about the microbiome in the mouse female reproductive tract during embryo implantation. We hypothesize that the microbiome profile in the female reproductive tract undergoes changes to facilitate embryo implantation and mouse models with defective embryo implantation have altered microbiome profiles in their reproductive tracts. To test this hypothesis, we will determine the whole microbiome profiles in different parts (vagina, uterus, and oviduct) of the female reproductive tract at different time points of early pregnancy leading to embryo implantation, from D0.5 to D4.5. We have collected vaginal, uterine, oviductal, and uterine flush samples from the wild type mice on D0.5, D2.5, D3.5, and D4.5, and are collecting comparable samples from our mouse models with defective embryo implantation. Preliminary quantitative PCR data from wild type uterine samples suggest differential expression of *Lactobacillus* genus during early pregnancy. Our ongoing study will determine the spatiotemporal microbiome composition and distribution in the mouse female reproductive tract with normal or failed embryo implantation. The obtained data will provide valuable information for future investigation on the functions of female reproductive tract microbiome in embryo implantation.

**Inhibitor of Apoptotic Pathway Protects Ovarian Reserve From Cyclophosphamide.** Yi Luan, Teresa K Woodruff, and So-Youn Kim

Cancer therapy can cause off-target effects including ovarian damage, which may result in premature ovarian insufficiency (POI) in prepubertal to premenopausal women. Loss of ovarian follicles leads to ovarian endocrine dysfunction and further affects fertility. Cyclophosphamide (CPA), a commonly used chemotherapeutic and immunosuppressant agent, is known to be a high level gonadotoxic agent that destroys ovarian cells by crosslinking with DNA. To protect against CPA damage to the ovarian reserve, it

is necessary to precisely map the mechanism responsible for ovarian reserve depletion by CPA treatment. Our results showed that CPA depletes ovarian follicles, specifically primordial follicles in all tested strains (CD-1, C57BL/6J and BALB/c). Contrary to previous reports, our data showed that the number of primary and secondary follicles did not increase in any of the CPA conditions, implying that CPA does not induce the follicle growth through an activation pathway. In accordance with the in vivo data, in vitro testing with 1  $\mu$ M 4-hydroxyperoxycyclophosphamide (4-HC), a metabolite of CPA, showed that it destroys primordial oocytes without affecting the number of primary and secondary follicles. This suggests that CPA first targets primordial germ cells in the ovarian reserve and destroys through DNA damage, which supports the rationale underlying early menopause in CPA-treated premenopausal women. Interestingly, p-AKT, a marker for primordial follicle activation through the PI3K-p-AKT-FOXO3 pathway, appeared in primordial oocytes 3 days post injection of CPA. These same p-AKT positive primordial oocytes co-expressed apoptotic signals of cleaved PARP in the nucleus 3 days after injection. Two apoptosis pathway inhibitors, ETP46464 and CHEK2 inhibitors, protected primordial follicles from apoptosis after 4-HC treatment in vitro. This study will help establish the molecular basis for ovarian reserve loss and, further, create an opportunity for the feasible clinical application of fertility-preserving adjuvants against gonadotoxic cancer treatments.

This work was funded by Center for Reproductive Health After Disease (P50HD076188) from the National Institutes of Health National Center for Translational Research in Reproduction and Infertility (NCTRI).

**Adverse Transgenerational Effects of Paternal Exposure to Environmental Contaminants are Palliated by Folic Acid.** Janice L. Bailey, Maryse Lessard, Phanie Charest, Pauline Mathilde Herst, and Mathieu Dalvai

Recent reports indicate that the effects of environmental exposures can be transmitted to future generations via fathers. Persistent Organic Pollutants (POPs) are transported to the north via natural weather currents, contaminating the Arctic food chain. Inuit populations, therefore, have high POPs body burdens. There is a major health discrepancy between Inuit people and non-Aboriginal Canadians. The risks of infant death are substantially elevated among Inuit and are attributed to poor foetal growth, placental disorders, and congenital disorders. We hypothesized that paternal exposure to Arctic contaminants induces epimutations in the sperm that are transgenerationally-transmitted through the paternal lineage, thereby inducing developmental complications in subsequent generations. A therapeutic strategy to reduce the impact of POPs is desirable to improve the health of exposed populations. Therefore, we further hypothesized that dietary folic acid (FA), which is well-known to reduce congenital anomalies, mitigates the effects of POPs. Four groups of Sprague-Dawley F0 founder females (n = 6) were gavaged with an environmentally-relevant mixture of Arctic POPs (500 $\mu$ g/kg) or corn oil (Control) and received either 1X or 3X FA representing intake from fortified foods or a daily multivitamin containing FA. F0 females were treated for 5 wks then mated to untreated males. POPs and FA treatments continued until weaning of the F1 litters. Only F0 females received POPs or 3X FA. Unexpectedly, 100% of the foetal congenital anomalies observed across the 4 generations were in the 3X FA lineage. F1 foetus:placenta weight was lower in the POPs lineage indicating a less effective placenta, but was palliated by 3X FA. Foetus:placenta weight were also affected in F2 and F4 generations. Prenatal POPs exposure decreased sperm function parameters and were partly rescued by

3X FA. Adverse reproductive effects of POPs persisted as sperm viability and sperm count were reduced in F2 males, while fertility of F3 males appeared to be impaired even with 3X FA. Hemoglobin, hematocrit and platelets levels were reduced in F1 due to POPs and 3X FA improved values to approach controls. In contrast, the 3X FA lineage had reduced hemoglobin and mean corpuscle volume in the F4. POPs exposure reduced miRNA expression in F1 sperm. This pattern dilutes from F2 until F4. Forty-seven differentially-expressed miRNAs, due to POPs exposure, were conserved in F1 and F2 sperm, of which 4 miRNAs were conserved until F3. Conserved miRNAs are indirectly involved in reproductive structure development, developmental growth and pathways in cancer. Combining POPs + 3X FA resulted in fewer differentially regulated miRNAs in F1-F4 compared to POPs exposure. Although fewer differentially-expressed miRNAs (23) were conserved due to POPs+ 3X FA, there were still 5 miRNAs conserved until F3. FA alone affected miRNA expression until F2 and no transgenerational effect was observed. In conclusion, sperm miRNA expression is perturbed transgenerationally due to paternal POPs exposure with a moderating effect of 3X FA and may be partly responsible for the foetal and adult phenotypes observed in four generations of rats. Funded by FRQNT, CIHR and NSERC.

**Auxin-Inducible Protein Degradation as a Novel Approach for Protein Depletion and Reverse Genetics Discoveries in Oocytes.** Nicole J. Camlin and Janice P. Evans

RNAi and gene knockout are traditionally used to investigate protein function in oocytes. However, these methods have major limitations. Most notably, if a protein is indispensable at an early time point, then its role at a later time point is unable to be investigated (e.g., if a protein is essential for meiosis I completion, then knockout and/or knockdown cannot be used to elucidate the protein's function(s) in meiosis II). Auxin Inducible Degradation is a powerful new approach that overcomes these limitations through the use of inducible protein degradation. This method takes advantage of the fact that SCF E3 ubiquitin ligases are conserved across all eukaryotes; these are heterotrimeric complexes with Skp, Cullin, and F-Box proteins. F-Box proteins dictate the substrates of each SCF E3 ligase, and the Auxin Inducible Degradation system utilizes the F-Box dependent specificity and conserved nature of SCF E3 ligases. TIR1 is a plant-specific F-Box protein that can combine with endogenous Skp and Cullin proteins to form a functional E3 ubiquitin ligase. TIR1 also dictates ligase specificity through its recognition of a specific degron sequence (the Auxin Inducible Degron; AID), and only in the presence of the plant hormone auxin. Thus, Auxin Inducible Degradation system leverages all these components. Through expression of TIR1 and AID-tagged proteins in cells, the addition of auxin can lead to precisely timed and highly specific depletion of the AID-tagged target, via proteasomal degradation of the AID-tagged proteins. In yeast and mammalian cultured cells, almost complete loss of an AID-tagged protein is observed in 30-90 minutes after auxin treatment. The aim of this study is to determine if Auxin Inducible Degradation can be used in mammalian oocytes. To test the AID system, oocytes were microinjected with cRNAs encoding TIR1 and AID-EGFP. Oocytes expressing TIR1 and AID-EGFP were tested at three different stages of meiosis – prophase I, prometaphase I (3 hr after release from prophase I arrest), and metaphase II. Treatment of oocytes with auxin at each of these stages led to loss of EGFP signal. A similar loss is not observed in the absence of auxin. Together this data highlights the utility of auxin inducible protein degradation system to study protein function throughout oocyte meiosis.

**Engineering a Synthetic Hydrogel Based Matrix to Confine Cancer Cells and Prevent their Reintroduction Following Ovarian Tissue Autotransplantation.** Anu David, James Day, Catherine Long, and Ariella Shikanov

In the last two decades improved chemo- and/or radio-therapeutic treatments have led to an increase in the number of young women surviving cancer. However, such treatments have impaired the patient's reproductive function, causing primary ovarian insufficiency. Autotransplantation of cryopreserved ovarian tissue can restore ovarian endocrine function and fertility. However, in women with blood-borne cancers, such as leukemia, ovarian tissue may harbor cancer cells and present the risks of transferring cancer following transplantation. To minimize the risk of reintroducing cancer cells harbored in the ovarian tissue we propose to encapsulate the tissue in an immuno-isolating device. The core of the device is designed with a degradable synthetic poly (ethylene glycol)-vinyl sulfone (PEG-VS) hydrogel-based matrix that promotes ovarian tissue survival and the non-degradable shell made with the same material prevents cancer cells evasion into the host. To test our hypothesis and the design of the immuno-isolating device we encapsulated 4T1 breast cancer cells at a concentration of (i) 250000 cells/mL and (ii) 2500000 cells/mL in the degradable core surrounded by one or two non-degradable shells. This matrix was designed by varying the photo-crosslinked non-degradable hydrogel shell thickness to prevent any cancer cell escape and the composition of the enzymatically degradable core hydrogel to allow for cellular proliferation and development. The engineered multilayered hydrogel matrix allowed proliferation of cancer cells but prevented it from escaping the matrix up to 34 days in vitro in addition to follicular development without compromising the diffusion properties of the hydrogel. Non-encapsulated 4T1 cells injected subcutaneously on the dorsal side of BALB/c mice developed into a tumor within seven days. By day 14 the cells had metastasized to the liver and the spleen was enlarged, Cancer cells encapsulated in the immuno-isolating capsule remained contained and did not metastasize to any of the organs. To summarize, PEG-VS based hydrogel capsule successfully retained cancer cells and facilitated follicular growth. Our results demonstrate the increasing prospect of utilizing PEG-VS hydrogels as an encapsulating matrix to allow for safe transplantation of ovarian tissue possibly contaminated with cancer cells for fertility and ovarian endocrine function restoration.

This research was supported by the National Institute of Biomedical Imaging and Bioengineering to AS (R01 EB022033) and National Science Foundation Graduate Research Fellowship to JD (DGE 1256260).

**Influence of MicroRNA 21 Inhibition on Pig Oocyte Maturation and Embryo Development.** Yunsheng Li, Malavika Adur, Aileen F. Keating, and Jason W. Ross

MicroRNA (miRNA), small non-coding RNA molecules critical for regulating cellular function, are abundant in the maturing pig oocyte and developing embryo. However, the function of miRNA during oocyte maturation in pigs remains ill-defined. The objective of this study was to assess the role of miRNA-21 (miR21) during pig oocyte maturation and subsequent implications for embryonic development. Follicular fluid from 3-6 mm diameter ovarian follicles was aspirated and intact cumulus-oocyte-complexes (COCs) were selected for maturation or microinjection. Germinal vesicle (GV) and metaphase II (MII) stage COCs were denuded using 0.1% hyaluronidase and held in microinjection operating medium (TCM199 supplemented with 2% FBS and 7.5 µg/mL cytochalasin B). Either GV or MII-arrested oocytes were injected with 100 nm miR21 inhibitor (miR21-I) or negative control (NC) oligonucleotides using an Eppendorf FemtoJet microinjector. Non-injected COCs were utilized for

assessing miR21 abundance at different stages of oocyte maturation and embryo development. Following microinjection GV stage oocytes were incubated in maturation medium for 42 hours at 38.5°C in 5% CO<sub>2</sub>. Upon maturation, indicated by first polar body extrusion, oocytes were parthenogenetically activated (PA) and presumptive zygotes were washed and cultured in porcine zygote media 3 (PZM3) for 7 days at 38.5°C in 5% CO<sub>2</sub>. Oocyte maturation rate, cleavage rate, blastocyst rate, and blastocyst cell number were recorded for a minimum of three independent replications. The proportion of oocytes achieving MII arrest, identified by polar body extrusion, was decreased ( $P = 0.01$ ) in the miR21-I group ( $n = 760$ ;  $80.1 \pm 1.5\%$ ) compared to the NC group ( $n = 622$ ;  $87.0 \pm 2.0\%$ ). Following PA, cleavage rate at 48 hours in the miR21-I group ( $n = 184$ ;  $80.6 \pm 0.5\%$ ) was decreased ( $P < 0.01$ ) as compared to NC group ( $n = 199$ ;  $92.3 \pm 1.2\%$ ). The blastocyst rate was numerically reduced ( $P = 0.1$ ;  $27.2 \pm 3.5\%$  and  $35.8 \pm 2.6\%$  for miR21-I and NC, respectively) and blastocyst cell number did not differ ( $36.8 \pm 4.3$  and  $36.5 \pm 2.9$  for miR21-I and NC, respectively). No differences were observed between miR21-I ( $n = 269$ ) and NC ( $n = 254$ ) treatment groups for oocytes injected at MII arrest after in vitro maturation, with respect to cleavage rate ( $81.6 \pm 6.7\%$  vs  $79.8 \pm 4.5\%$ ), blastocyst rate ( $55.7 \pm 2.6\%$  vs  $53.2 \pm 5.0\%$ ) and blastocyst cell number ( $39.2 \pm 4.0$  vs  $36.9 \pm 2.8$ ). MiR21 oocyte expression was also assessed at different stages of oocyte maturation and embryo development and was increased ( $P < 0.01$ ) from GV to MII stage. Following activation of MII-arrested oocytes, 2- and 4-cell stage embryos had reduced ( $P < 0.05$ ) abundance of miR21 compared to MII-arrested oocytes. These data highlight the importance of miR21 during oocyte maturation and early development in the pig, and illustrate the temporal nature of miR21 regulation. This project was supported by Agriculture and Food Research Initiative Competitive Grant no. 2017-67015-26459 from the USDA National Institute of Food and Agriculture.

**New Mechanistic Insights on Egg Formation in the Oviduct of Laying Hens.** Birendra Mishra, Nirvay Sah, Donna K. Lee, Sanjeev Wasti, Vedbar Khadka, and Rajesh Jha

The oviduct of a laying hen provides a conducive biological environment for the formation and potential fertilization of the egg. Besides environmental, nutritional, and pathological conditions, oviductal functions also govern the egg quality. During the egg formation, albumen is synthesized and deposited around the yolk in the magnum, and eggshell is materialized around the egg in the uterus. However, the involvement of cellular processes and biological pathways in the albumen synthesis and eggshell formation are not clearly understood. The objectives of this study were to 1) identify the differentially expressed genes (DEGs) in the shell gland (laying vs non-laying), and 2) validate the identified novel genes in the laying (3 h and 15-20 h postovulation), non-laying, and molter hens. Segments of oviducts were collected from laying hens at 3h postovulation (p.o., egg present in magnum) and 15-20 h p.o. (egg present in uteri), molter (reproductive rest), and non-laying (no growing ovarian follicles) hens. Total RNAs were isolated from magnum and uteri ( $n=6$ /group). To delineate the transcriptomic profile involved in the albumen synthesis and eggshell formation, total RNAs from the magnum of laying hens at 3 h p.o. vs non-laying hens ( $n=3$ /group), and total RNAs from the uteri of laying hens at 15-20 h p.o. vs non-laying hens ( $n=3$ /group), respectively, were subjected to RNA-Sequencing. The mapped genes with FDR adjusted P-value  $\geq 2$  were considered as differentially expressed. Highly up-regulated genes from the RNA-seq data were further validated in all the experimental groups using real-time PCR. Among the up-regulated genes in the magnum, MMP1 (degrades collagen), MMP9 (degrades gelatin), CGN (Cingulin; regulates endothelial tight junctions and vascular permeability) were significantly higher in the magnum only at 3 h p.o. (during albumen synthesis). L-serine biosynthetic process was the most-enriched Gene

Ontology (GO) biological process while “glycine, serine, and threonine metabolism” was the most enriched KEGG pathway among the up-regulated DEGs. GO enrichment analysis of the DEGs further indicated the importance of solute carrier genes in molecule transport during albumen syntheses, such as SLC25A4, SLC51B, SLC17A9, SLC2A1, SLC1A4, and SLC6A1. Among the up-regulated genes in the uterus, Otopetrin 2 (modulator of calcium influx) and Calcitonin (bone mineralization), Stanniocalcin 2 (biomineralization), Plasma membrane Ca<sup>2+</sup> transporting 2 (calcium transporter), and Follistatin (uterine glands morphogenesis) had the highest expression ( $P < 0.05$ ) in the uteri of layers at 15-20 h p.o. (around eggshell formation). KEGG pathway analysis showed that the up-regulated genes belonged to the enriched calcium signaling pathway. GO enrichment analysis revealed that the biological processes for sodium and potassium ion-transport were significantly enriched ( $P < 0.05$ ) due to the up-regulated genes. Identified novel genes from uterus may increase the bioavailability, mineralization, and remodeling of calcium for the eggshell formation. In conclusion, this study for the first time identified the novel genes and biological pathways involved in the albumen synthesis and eggshell formation, and can potentially be used to enhance the egg production traits in chickens. (Supported by USDA Multistate Fund, CTAHR, UH Manoa to BM).